Convention on Long-range Transboundary Air Pollution

emep

Co-operative programme for monitoring and evaluation of the long-range transmission of air pollutants in Europe

STATUS REPORT 1/2023

Transboundary particulate matter, photo-oxidants, acidifying and eutrophying components

Status Report 1/2023

msc-w & ccc & ceip & ciam

EMEP Report 1/2023
Date: August 23, 2023

METEOROLOGISK INSTITUTT
Norwegian Meteorological Institute

Transboundary particulate matter, photo-oxidants, acidifying and eutrophying components

EMEP/MSC-W:	Hilde Fagerli, Anna Benedictow, Willem van Caspel, Michael Gauss, Yao Ge, Jan Eiof Jonson, Heiko Klein, Ágnes Nyíri, David Simpson, Svetlana Tsyro, Álvaro Valdebenito, Peter Wind
EMEP/CCC:	Wenche Aas, Anne Hjellbrekke, Sverre Solberg, Kjetil Tørseth, Karl Espen Yttri
EMEP/CEIP:	Bradley Matthews, Sabine Schindlbacher, Bernhard Ullrich, Robert Wankmüller
EMEP/CIAM:	Zbigniew Klimont
CCE/UBA:	Thomas Scheuschner
TNO:	Jeroen J.P. Kuenen
FMI:	Heidi Hellén
IGE:	Jean-Luc Jaffrezo, Dielleza Tusha
TROPOS:	Falk Mothes
IMT Nord:	Therese Salameh
IDAEA-CSIC:	Barend L. van Drooge
FZJV:	Robert Wegener

EMEP Status Report 2023; August 23, 2023

ISSN 1504-6109 (print)
ISSN 1504-6192 (on-line)

Executive Summary

This report presents the EMEP activities in 2022 and 2023 in relation to transboundary fluxes of particulate matter, photo-oxidants, acidifying and eutrophying components, with a focus on results for 2021. It presents major results of the activities related to emission inventories, observations and modelling. This year, special attention has been given to ozone: we present first results from the EMEP Intensive Measurement Period (IMP) on ozone episodes, conducted in July 2022. The impact of CH_4 and regional and global non-CH_4 emission reductions on European O_3 are analyzed. In addition, we present for the first time source receptor matrices for ozone using the Local Fractions method.

Measurements and model results for 2021

EMEP MSC-W model simulations and EMEP observations for 2021 show a general increase in the annual mean of regional background PM_{10} and $PM_{2.5}$ over land from north to south, with PM_{10} concentrations being below 2-5 µg m^{-3} in northern parts of Europe and Russia, going up to 5-15 µg m^{-3} in the mid-latitudes, and to 20 µg m^{-3} and above further south. $PM_{2.5}$ follows in general the same spatial pattern, with somewhat lower concentration levels than PM_{10}.

Annual mean PM_{10} concentrations (modelled and observed) were below the EU limit value of 40 µg m^{-3} for all of Europe in 2021. The modelled annual mean PM_{10} is mostly below those specified in the WHO Air Quality Guidelines Global Update 2021 (AQG-2021), while EMEP observations registered PM_{10} exceedances of AQG-2021 at 8 sites (out of 66). For daily PM_{10}, exceedances of EU limit value were observed at 38 sites, but on fewer than 35 days (required by EU Directive 2008/50/EC). WHO AQG-2021 were exceeded at 51 sites, and 26 sites had more than 3 exceedance days.

Modelled and observed annual mean $PM_{2.5}$ concentrations in 2021 were mostly below the EU limit value of 20 µg m^{-3}, except in the Po Valley according to the model. However, there were observed cases of $PM_{2.5}$ exceedances of WHO AQG-2021 levels at 40 sites (out of 50). Daily $PM_{2.5}$ concentrations exceeded AQG-2021 recommended limit of 15 µg m^{-3} at 47 sites, out of which 45 sites had more than 3 exceedance days.

There were several ozone episodes in 2021, the most prominent on 17-20th June. During this period the weather situation was dominated by an extensive blocking high pressure system centered around the southern parts of the Baltic Sea, and a low pressure system in the near

Atlantic ocean, with southerly winds prevailing in Central Europe. In addition there were several ozone episodes strongly affected by wildfires. The new long-term air quality guideline for ozone exposure from WHO (peak season MDA8[1] > 60 µg m^{-3}) is exceeded over the whole domain. Also the UN-ECE limit for forests (EU-AOT40f) is exceeded over large regions although not to the same extent as the WHO guideline.

Exceedances of critical loads

Model calculations suggest that the critical loads (CLs) for eutrophication are exceeded in practically all countries in 2021. The share of ecosystems where the critical load for eutrophication is exceeded is 61 % in 2021. The European average accumulated exceedance (AAE) in the year 2021 is about 260 eq ha^{-1} yr^{-1}. The highest exceedances of CLs are found in the Po Valley in Italy, the Dutch-German-Danish border areas and in north-eastern Spain. By contrast, critical loads of acidity are exceeded in a much smaller area. Hot spots of exceedances can be found in the Netherlands and its border areas to Germany and Belgium, with some smaller maxima in southern Germany and Czechia, whereas for most of Europe no exceedances are simulated. Acidity exceedances in the year 2021 occur on around 4% of the ecosystem area, and the European average AAE is about 28 eq ha^{-1} yr^{-1}.

Monitoring programme

Altogether 31 Parties reported measurement data for 2021, from 167 sites in total. Of these, 135 sites reported measurements of inorganic ions in precipitation and/or main components in air; 73 of these sites had co-located measurements in both air and precipitation. The ozone network consisted of 138 sites. Particulate matter was measured at 77 sites. In addition, 57 sites from 20 Parties reported at least one of the aerosol components required in the advanced EMEP measurement program (level 2), while 19 sites from 10 Parties measured volatile organic compounds (VOCs), though only 4 sites with both hydrocarbons and carbonyls. Since 2010, 37% of the Parties have improved their monitoring programme for level 1 parameters, while 35% have reduced their monitoring. For level 2 there is a general increase in the number of sites and components measured.

Status of emission reporting

In 2023, 46 out of 51 Parties (90%) submitted emission inventories to the EMEP Centre on Emission Inventories and Projections (CEIP), and 40 Parties reported black carbon (BC) emissions. In general, the number of timely submissions has increased over time. Reporting of gridded emissions in $0.1°\times 0.1°$ longitude/latitude resolution increased in 2021 compared to 2017, and some additional gridded data were reported in 2023, despite 2023 not being an obligatory reporting year for gridded emissions. In spite of these positive trends in terms of reporting, reporting is not yet complete, and missing emissions are gap-filled and spatially distributed using expert estimates.

Estimates of particulate matter emissions, as currently provided by Parties, have a number of major uncertainties, and there is a clear need for clarification and standardisation of the

[1] MDA8 is maximum daily 8-hour mean ozone concentrations. Peak season MDA8 is here calculated as April to September average of MDA8

methods used to define and report PM emissions, especially with respect to whether the condensable component has been included in the reported estimates. In 2022, CEIP organised an ad hoc review dedicated to the topic on condensables, which resulted in a list of Parties where it could be assumed with a good degree of certainty that the condensable component is mostly included in PM emissions for GNFR sector C (small-scale combustion). This list was updated based on recalculations, comparison with the data from TNO Ref2 and information provided by Parties in their informative inventory reports in 2023. For these Parties the reported PM emissions were used, while for other Parties updated TNO Ref2 (version v2.1) emission data were used. If no TNO Ref2 estimates were available, gap-filled data by CEIP was used for GNFR sector C. The resulting GNFR C dataset was combined with official EMEP emissions into the so-called EMEPwRef2_v2.1C emission dataset. This emission dataset has been used in the assessment of the air quality situation in Europe and the source receptor calculations for 2021 made this year.

Based on the compiled datasets in 2023, it can be concluded that emissions from the land areas have decreased for most pollutants except for PM_{coarse} and NH_3 from 2000 to 2021. In addition to these long term trends, the emissions of almost all pollutants for the EMEP domain demonstrated discrete decreases between 2019 and 2020 due to the COVID-19 pandemic impacts on socio-economic activity. For almost all pollutants and regions, emissions in 2021 tended to increase compared to 2020, due to the partial resumption of normal activity and easing of the pandemic-related restrictions.

The amended Protocol to Abate Acidification, Eutrophication and Ground-level Ozone (Gothenburg Protocol) entered into force on 7 October 2019 and sets out the emission reduction commitments for SO_x, NO_x, NH_3, NMVOCs and $PM_{2.5}$ for 2020 and beyond, expressed as percentage reductions from the 2005 emission level. In 2021 emissions from the following countries were above their respective Gothenburg Protocol requirements: NO_x: Lithuania and Romania; NMVOC: Lithuania, Luxembourg and the Netherlands; SO_x: Cyprus ; NH_3: Bulgaria, Denmark, Latvia, Lithuania, Luxembourg, Norway, Portugal and Sweden; $PM_{2.5}$: Romania, the United Kingdom and the United States.

In 2021 there was a long lasting volcanic eruption at Mt. Fagradalsfjall in Iceland. There was no significant amount of ash released in the eruption, but a total of 967 kt of SO_2 were emitted into the atmosphere between 19 March and 18 September 2021, as reported by Iceland in 2023. Gas emissions from Fagradalsfjall mainly affected lower altitudes and the transport of SO_2 influenced air quality mainly in Iceland, with limited effects on Scandinavia, Ireland and the United Kingdom.

Impact of background CH_4 and regional and global non-CH_4 emission reductions on European O_3

The importance of reducing CH_4 in order to reduce surface O_3 concentrations in Europe has been investigated using the EMEP MSC-W model. For this, the impact of background CH_4 reductions have been compared with the impact of other emission reductions, both within and outside of Europe. The emissions and CH_4 projections followed a current legislation (CLE) and a reduced emission (LOW) scenario up to the year 2050. Notably, the LOW scenario included a 50% CH_4 emission reduction by 2050 relative to 2015, broadly following the guidelines set by the Methane Pledge for 2030 and the Global Methane Assessment for 2050.

The impact of background CH_4 changes and of emission reductions were compared against the 2015 baseline year, as well as between the CLE and LOW scenarios by 2050. Relative to 2015, CH_4 changes were found to have only a small contribution to the peak season MDA8 changes, almost an order of magnitude smaller than those achieved through the reduced non-CH_4 emissions. However, between the 2050 CLE and LOW scenarios, the CH_4 reduction achieved in the LOW scenario accounted for roughly a third of the total peak season MDA8 reduction in Europe. The non-CH_4 LOW emission reductions outside and inside of the EMEP domain accounted for another one-third of the total O_3 reductions each.

Our work further illustrates that the relative importance of CH_4 and non-CH_4 emission changes varies considerably between the different ozone indicators (e.g. peak season MDA8, O_3 mean, 4th highest MDA8 and SOMO35). For instance, the relative importance of CH_4 was largest for annual mean O_3, amounting to 27% of the reductions achieved by non-CH_4 emissions in the LOW 2050 scenario relative to 2015 (compared to 13% for peak season MDA8).

Considering that WHO guidelines for surface ozone exposure are not met by 2050 in the CLE scenario, and that CH_4 mitigation efforts can be relatively cost-efficient, this highlights the importance of CH_4 as an O_3 precursor. Reducing CH_4 concentrations furthermore has the benefit of limiting its role as a greenhouse gas.

The Local Fractions method and its application to ozone

For several decades, country-to-country source receptor matrices in EMEP have been calculated using the so-called brute force method (BF, also referred to as the 'perturbation method'). The main disadvantage of the BF method is that it is computationally demanding.

The Local Fractions method (LF) allows to track a large number of sources in a single simulation. It has been further developed to allow the treatment of non-linear species such as ozone, including the detailed interactions through the full chemistry. The result is the sensibility to (small) changes in emissions. The contributions from all countries are obtained in a single simulation, in contrast to the BF method where estimation of the contribution from each country necessitates a separate simulation.

For linear species, BF and LF do in principle give identical results. For non-linear species differences should be expected as the LF method gives the effect of very small emission changes, while the traditional brute force method (BF) is obtained by reducing emissions from one country by a larger amount, e.g. 15% (and gives the average response to 15% emission changes). Some other less important effects are also treated differently in the two approaches. Despite these methodological differences, direct comparisons of BF and LF results for country-to-country blame matrices for peak season MDA8 for ozone show that the differences are small, in general within 10%.

This opens for alternative ways to compute source receptor relationships. Since the method is much simpler to manage and computationally cheaper, it would for example be feasible to compute source receptor relationships for multiple emission backgrounds or scenarios.

EMEP intensive measurement period on ozone episodes summer 2022

To better understand the formation of ozone during heat waves, an intensive measurement period (IMP) was conducted between 12th-19th July 2022. The IMP included measurements of more than 120 different VOC compounds emitted from a range of sources, as well as tracers for biogenic secondary aerosols (SOAs). In total, 27 sites participated.

The relative contribution of different VOC types does not vary very much between the sites; all are dominated by oxygenated VOCs and non-methane hydrocarbons (NMHCs). However, there are individual differences depending on their nearby environment, e.g. Madrid has the highest relative influence of aromatic species, whereas the forest site in Belgium has a relatively large contribution of monoterpenes. In Madrid, NMHCs concentrations are high in the beginning of the IMP week and low in the end, whilst in Norway they go from low to high. This agrees with the general movement of the episode across the European continent.

Up to 80% of organic aerosol during the IMP was attributed to SOA, which is somewhat higher than the long-term (2010 - 2020) mean of the SOA/OA fraction in July. Approximately one-third of SOA originated from α-pinene oxidation, a biogenic VOC (BVOC), and accounted for around 20% of organic aerosol. To improve the understanding of SOA, we will look more closely into the part of SOA originating from isoprene oxidation. This is a part of our ongoing work with the IMP Summer 2022 data.

The initial inter-laboratory comparison (ILC) on biogenic SOA tracers, including 3-MBTCA from α-pinene oxidation and 2-methyltetrols from isoprene oxidation, conducted during IMP Summer 2022, showcased promising outcomes. For harmonization and comparability of biogenic SOA tracers, accessible quantification standards and authentic isotope-labeled standards are vital. We propose an imminent ILC encompassing prominent organic tracers like 3-MBTCA and 2-methyltetrols to be initiated.

Comparisons of modelled versus observed NMVOC, 2018 and IMP period

A comprehensive spatial and temporal comparison of EMEP MSC-W model output with VOC measurements from the EMEP network was carried out for the year 2018, and for the IMP campaign in summer 2022. Both CEIP and Copernicus Atmosphere Monitoring Service (CAMS) emission inventories were utilized, along with two different chemistry mechanisms. For this study, we have developed a detailed VOC emission speciation for all GNFR sectors based on data sourced from the UK National Atmospheric Emissions Inventory (NAEI), European Environment Agency (EEA) emission inventory guidebook, and several academic studies.

The degree to which the modelled and measured VOCs agree varies depending on the specific species. For the alkane species, the model successfully captures the overall spatial variation of the annual concentrations of especially n-butane, but less so for i-butane and propane. The annual concentrations of ethene and isoprene show better model-measurement agreement than propene and acetylene. The three aromatic species showed good model-measurement agreements. Formaldehyde and methyl glyoxal demonstrate reasonably good agreement between modelled and measured time series throughout the year 2018 simulations, though both are underestimated in the IMP campaign.

Although the results are preliminary, this evaluation study indicates potential issues pertaining to certain VOC emissions and to the model setup. The comparisons will be repeated with improved boundary conditions and after further reviews of VOC speciation.

EMEP MSC-W Model Improvements

Version v5.0 of the EMEP MSC-W model, as used for this report, has had a number of significant changes made since v4.45 used for EMEP Report 1/2022. Most notably, the photolysis schemes have been completely revised (see Cloud-J section, below), but numerous other improvements have been made. The thermodynamic module ISORROPIA-lite was implemented, and the alternative EQSAM module upgraded. Upgrades were made in treatment of cloud liquid water, AOD calculation, soil NO emissions, time-factors, boundary conditions, wildfire emissions (see below) and dispersion. The Local Fractions capabilities were upgraded (as noted above), with ozone included for the first time. In addition, a new country-variable (CV) format was introduced to simplify the netcdf files used for emissions. However, despite the number of changes, and improvements in the scientific basis of several datasets and formulations, the overall model performance is rather similar to that found in earlier years.

Updated photolysis rate calculations using Cloud-J v7.3e

Photolysis reactions are driven by the absorption of sunlight by molecules, and play an essential role in the production and loss mechanisms of atmospheric pollutants such as ozone, oxidized nitrogen, and volatile organic compounds. Photolysis reactions and their associated reaction rates (J-values) are therefore an essential part of any chemical transport model.

In the EMEP model, the old tabulated photolysis rate system has been replaced by the now default Cloud-J v7.3e scheme. One major advantage over the old system is that Cloud-J incorporates the instantaneous radiative impact of the modelled abundance of ozone and of biomass burning, sulphate, dust, and sea salt aerosols. The representation of the radiative impact of clouds is also considerably improved. For the EMEP MSC-W model implementation, the Cloud-J photolysis rates are shown to compare favourably against a large number of surface and aerial photolysis rate measurements. In the global EMEP model configuration, surface ozone concentrations are increased by around 10%, while surface nitrogen dioxide concentrations are reduced by around 5-10%. However, compared to the ozone results presented in previous years (e.g. in EMEP Status Report 1/2022), ozone increased just a couple of percent due to other compensating effects.

Modelling effects of wildfires in the EMEP MSC-W model

Wildfires are an important source of air pollution globally, and also in Europe. This year, a new method to disperse forest fires has been introduced in the EMEP MSC-W model, and the default emission inventories for forest fires have been updated to FINNv2.5.

In this report we focus on two wildfire events in 2021: the fire in southern Italy, lasting for several weeks in late July and August, and the intense fire in central Spain in mid August lasting only a few days. Those wildfires resulted in a marked increase in model calculated air pollution levels. EMEP MSC-W model calculations with and without wildfire emissions showed that in central Spain, a spike in measured ozone levels of more than 10 ppb could only be reproduced by the EMEP model with wildfire emissions included.

Acknowledgments

This work has been funded by the EMEP Trust Fund.

The development of the EMEP MSC-W model has also been supported by the Nordic Council of Ministers, the Norwegian Space Centre, the Norwegian Ministry of Climate and Environment and Copernicus Atmosphere Monitoring Service (CAMS) projects.

The work of TNO was partly funded by the Nordic Council of Ministers and partly by the Copernicus Atmosphere Monitoring Service (CAMS), in particular the Contracts on emissions (CAMS2_61) and policy products (CAMS2_71).

The work presented in this report has benefited largely from the work carried out under the four EMEP Task Forces and in particular under TFMM.

A large number of co-workers in participating countries have contributed in submitting quality assured data. The EMEP Centers would like to express their gratitude for continued good co-operation and effort. The institutes and persons providing data are listed in the EMEP/CCC's data report and identified together with the data sets in the EBAS database. Further, many has contributed to the intensive measurement period in the summer 2022, both in the planning and in the operational work in the field and in the laboratories. Their co-operation and commitment to this work is very much appreciated. In addition, the European Solvents Industry Group (ESIG) sponsored a substantial part of the cost of transport of samples and for the analysis. The campaign would not have been possible without this engagement.

For developing standardized methods, harmonization of measurements and improving the reporting guidelines and tools, the close co-operations with participants in the European Research Infrastructure for the observation of Aerosol, Clouds, and Trace gases (ACTRIS) as well as with the Scientific Advisory Groups (SAGs) in WMO/GAW are especially appreciated.

For the Cloud-J photolysis work, we acknowledge all researchers and supporting personnel who participated in the ChArMEx 2013 campaign. We are also grateful for the code and measurement data availability from the ATom-1 campaign.

Chris Heyes, Gregor Kiesewetter and colleagues from EMEP CIAM/IIASA are acknowledged for provision of emission data and helpful discussions and advice.

Melissa Anne Pfeffer from the volcanic hazard team at the Icelandic Met Office is acknowledged for kindly providing us with the time series of plume height observations and the SO_2 emission rate measurements from the Fagradalsfjall eruption.

Marc Guevara from the Barcelona Supercomputing Center is acknowledged for provision of emission time-factors (CAMS-REG-TEMPO v3.2 and v4.1) and helpful discussions and advice.

Thanks are due to Athanasios Nenes (Institute of Chemical Engineering Sciences, Foundation for Research and Technology Hellas, Patras, Greece; School of Architecture, Civil and Environmental Engineering, École Polytechnique Fédérale de Lausanne (EPFL), Switzerland) and Swen Metzger (ResearchConcepts io GmbH, Germany) for valuable aid in the implementation and discussion of ISORROPIA-lite and EQSAM v11, respectively.

We extend our sincere gratitude to the UK National Atmospheric Emissions Inventory (NAEI) team for providing the speciated NMVOC emissions data, which was instrumental for our model-measurement comparison work of non-methane volatile organic compounds (NMVOCs).

The Working Group on Effects and its ICPs and Task Forces are acknowledged for their assistance in determining the risk of damage from air pollution.

IT infrastructure in general was available through the Norwegian Meteorological Institute (MET Norway). Furthermore, the CPU time granted on the supercomputers owned by MET Norway has been of crucial importance for this year's source-receptor matrices and long-term calculations. Some computations were performed on resources provided by UNINETT Sigma2 - the National Infrastructure for High Performance Computing and Data Storage in Norway (grant NN2890k and NS9005k). The CPU time made available by ECMWF has been important both for generation of meteorology used as input for the EMEP MSC-W model as well as source-receptor and status calculations in this year's report.

Contents

CHAPTER 1

Introduction

1.1 Purpose and structure of this report

The mandate of the European Monitoring and Evaluation Programme (EMEP) is to provide sound scientific support to the Convention on Long-range Transboundary Air Pollution (LRTAP), particularly in the areas of atmospheric monitoring and modelling, emission inventories, emission projections and integrated assessment. Each year EMEP provides information on transboundary pollution fluxes inside the EMEP area, relying on information on emission sources and monitoring results provided by the Parties to the LRTAP Convention.

The purpose of the annual EMEP status reports is to provide an overview of the status of transboundary air pollution in Europe, tracing progress towards existing emission control Protocols and supporting the design of new protocols, when necessary. An additional purpose of these reports is to identify problem areas, new aspects and findings that are relevant to the Convention.

This year, special attention has been given to the EMEP Intensive Monitoring period performed in summer 2022. We present a first analysis of the observations available from the campaign and compare the observations to EMEP MSC-W modelling results. In addition, we present some work that has been done to support the review of the Gothenburg Protocol - analyzing the importance of mitigation of CH_4 emissions for ozone in future scenarios.

The present report is divided into four parts. Part I presents the status of transboundary air pollution with respect to acidification, eutrophication, ground level ozone and particulate matter in Europe in 2021. The impact of the COVID-19 restrictions have been included (through total and temporal distribution of emissions), however, we do not attempt a major analysis of how the situation in 2021 would have been without COVID-19. Part II summarizes research activities of relevance to the EMEP Programme, while Part III deals with technical developments going on within the centres.

Appendix A in Part IV contains information on the national total emissions of main pollutants and primary particles for 2021, while Appendix B shows the emission time series for the period of 1990-2021. Country-to-country source-receptor matrices with calculations of the transboundary contributions to pollution in different countries for 2021 are presented in

Appendix C. Appendix D summarizes common statistical measures of model performance for 2021 with respect to EMEP observations, while model evaluation against all EMEP observations is visualized online at https://aeroval.met.no/evaluation.php?project=emep&exp_name=2023-reporting. Appendices E-G contain supplementary information to the chapters in Part I - Part III, while Appendix H describes the country reports which are issued as a supplement to the EMEP status reports.

The present report and the model evaluation web interface are complemented by numerical fields and other information on the EMEP website. The reader is encouraged to visit the website, http://www.emep.int, to access this additional information.

1.2 Definitions, statistics used

For sulfur and nitrogen compounds, the basic units used throughout this report are μg (S or N)/m^3 for air concentrations and mg (S or N)/m^2 for depositions. Emission data, in particular in some of the Appendices, is given in Gg (SO_2) and Gg (NO_2) in order to keep consistency with reported values.

For ozone, the basic units used throughout this report are ppb (1 ppb = 1 part per billion by volume) or ppm (1 ppm = 1000 ppb). At 20° C and 1013 mb pressure, 1 ppb ozone is equivalent to 2.00 µg m^{-3}. A complicating factor is that various threshold values are given in µg m^{-3} such as in the EU directive and the WHO recommendations, and furthermore, the standard ozone unit in various databases is also µg m^{-3}. However, today all surface ozone measurements are done with UV-monitors that give the mixing ratios of ozone in ppb. In order to evaluate the exceedances of the various thresholds, these values are then converted to a proxy µg m^{-3} when imported to the databases using a fixed constant. Both the EU directive and the WHO recommendation uses the factor 2 as mentioned above corresponding to 20° C and 1013 mb pressure. This conversion is crucial to keep in mind when comparing the measured data (in proxy µg m^{-3}) with the model results that provides ozone in mixing ratio (ppb).

A number of statistics have been used to describe the distribution of ozone within each grid square:

MDmaxO3 - Mean of Daily Max. Ozone. - First we evaluate the maximum modelled concentration for each day, then we take either 6-monthly (1 April - 30 September) or annual averages of these values.

SOMO35 - The Sum of Ozone Means Over 35 ppb is the indicator for health impact assessment recommended by WHO. It is defined as the yearly sum of the daily maximum of 8-hour running average over 35 ppb. For each day the maximum of the running 8-hours average for O_3 is selected and the values over 35 ppb are summed over the whole year.

If we let A_8^d denote the maximum 8-hourly average ozone on day d, during a year with N_y days (N_y = 365 or 366), then SOMO35 can be defined as:

$$SOMO35 = \sum_{d=1}^{d=N_y} \max\left(A_8^d - 35 \text{ ppb}, 0.0\right)$$

where the `max` function evaluates $\max(A - B, 0)$ to $A - B$ for $A > B$, or zero if $A \leq B$, ensuring that only A_8^d values exceeding 35 ppb are included. The corresponding unit is ppb.days.

MDA8 - Maximum daily 8-hour mean ozone concentrations.

MDA8$_{\mathrm{AS}}$ - April to September average of MDA8. This corresponds to the peak season ozone level specified by WHO(WHO 2021). The 2021 WHO AQG (Air Quality Guideline) gives a target level of 60 µg m^{-3} for MDA8$_{\mathrm{AS}}$ as well as interim targets of 100 µg m^{-3} and 70 µg m^{-3}. In addition to these long-term exposure levels, WHO recommends a short-term AQG of 100 µg m^{-3} and interim targets of 160 µg m^{-3} and 120 µg m^{-3}, all referring to the 99-percentile of all MDA8 values through the year.

POD$_Y$ - Phyto-toxic ozone dose, is the accumulated stomatal ozone flux over a threshold Y, i.e.:

$$\mathrm{POD}_Y = \int \max(F_{st} - Y, 0)\, dt \tag{1.1}$$

where stomatal flux F_{st}, and threshold, Y, are in nmol m^{-2} s^{-1}. This integral is evaluated over time, from the start of the growing season (SGS) to the end (EGS).

In this report we work with the POD values which are intended for large-scale 'Integrated Assessment Modelling' (IAM), whereby generic crop, forest and other semi-natural species, and their characteristics, are as specified in the ICP-Vegetation Mapping Manual (LRTAP 2017). See also Mills et al. (2011a,b, 2018), and LRTAP (2017).

AOT40 - is the accumulated amount of ozone over the threshold value of 40 ppb, i.e..

$AOT40 = \int \max(O_3 - 40 \text{ ppb}, 0.0)\, dt$

where the `max` function ensures that only ozone values exceeding 40 ppb are included. The integral is taken over time, namely the relevant growing season for the vegetation concerned, and in some daytime period. The corresponding unit are ppb.hours (abbreviated to ppb.h). The usage and definitions of AOT40 have changed over the years though, and also differ between UNECE and the EU. LRTAP (2017) give the latest definitions for UNECE work, and describes carefully how AOT40 values are best estimated for local conditions (using information on real growing seasons for example), and specific types of vegetation. In the EU approaches, O_3 concentrations are taken directly from observations (at typically ca. 3 m height), or grid-average 3 m modelled values. In the Mapping Manual (LRTAP 2009) approaches, there is a strong emphasis on estimating AOT40 using ozone levels at the top of the vegetation canopy. Since O_3 concentrations can have strong vertical gradients, this approach leads to lower AOT40 estimates than with the EU approach.

The EMEP MSC-W model now generates a number of AOT-related outputs,and in this report we will use:

EU-AOT40c - AOT40 calculated using EU criteria, from modelled (3 m) or observed ozone, for the assumed crop growing season of May–July. Here we use the EU definitions of day hours as 08:00–20:00.

EU-AOT40f - AOT40 calculated using EU criteria from modelled 3 m ozone, or observed ozone, for the assumed forest growing season of April–September. Here we use the EU definitions of day hours as 08:00–20:00.

MM-AOT40f - AOT40 calculated for forests using estimates of O_3 at forest-top. This AOT40 is that defined for forests by LRTAP (2017), but using a default growing season of April-September.

MM-AOT40c - AOT40 calculated for agricultural crops using estimates of O_3 at the top of the crop. This AOT40 is close to that defined for agricultural crops by LRTAP (2017), but using a default growing season of May-July, and a default crop-height of 1 m.

For MM-AOT40f and MM-AOT40c only daylight hours are included, and for practical reasons we define daylight in the model outputs as the time when the solar zenith angle is equal to or less than 89°. (The proper UNECE definition uses clear-sky global radiation exceeding 50 W m^{-2} to define daylight).

In practice, it is very difficult to convert measured O_3 from an EMEP observation site to the MM-AOT40 values, since there are no data with which is to estimate the vertical gradient to get to upper-canopy O_3. Therefore, in the comparison of modelled and observed AOT40s in Ch 2, we have used the EU AOT definitions, since this approach is readily applicable to observed as well as modelled values. We do, however, present source-receptor calculations for the UNECE metrics MM-AOT40f and MM-AOT40c in Appendix C.

The AOT40 levels reflect interest in long-term ozone exposure which is considered important for vegetation - critical levels of 3 000 ppb.h have been suggested for agricultural crops (MM-AOT40c) and natural vegetation, and 5 000 ppb.h for forests (MM-AOT40f) (LRTAP 2017). Note that the UNECE/ICP-vegetation recommendations are that AOT40 concepts are replaced by ozone flux estimates for crops and forests (see also LRTAP 2017).

Furthermore, this report includes concentrations of particulate matter (PM). The basic units throughout this report are µg m^{-3} for PM concentrations and the following acronyms are used for different components to PM:

POA - primary organic aerosol - which is the organic component of the PPM emissions (defined below). (POA is in this report assumed to be entirely in the particle phase, see Fagerli et al. (2020).)

SOA - secondary organic aerosol, defined as the aerosol mass arising from the oxidation products of gas-phase organic species.

SIA - secondary inorganic aerosols, defined as the sum of sulfate (SO_4^{2-}), nitrate (NO_3^-) and ammonium (NH_4^+). In the EMEP MSC-W model SIA is calculated as the sum: SIA= SO_4^{2-} + NO_3^-(fine) + NO_3^-(coarse) + NH_4^+.

SS - sea salt.

MinDust - mineral dust.

PPM - primary particulate matter, originating directly from anthropogenic emissions. One usually distinguishes between fine primary particulate matter, $PPM_{2.5}$, with aerosol diameters below 2.5 μm and coarse primary particulate matter, PPM_{coarse} with aerosol diameters between 2.5 μm and 10 μm.

$PM_{2.5}$ - particulate matter with aerodynamic diameter up to 2.5 μm. In the EMEP MSC-W model, $PM_{2.5}$ is calculated as $PM_{2.5}$ = SO_4^{2-} + NO_3^-(fine) + NH_4^+ + $SS_{2.5}$ + MinDust(fine) + SOA(fine) + $PPM_{2.5}$ + 0.2 · NO_3^-(coarse) + PM25water. (PM25water = PM associated water).

PM_{coarse} - coarse particulate matter with aerodynamic diameter between 2.5μm and 10μm. In the EMEP MSC-W model PM_{coarse} is calculated as PM_{coarse} = 0.80 · NO_3^-(coarse)+ SS(coarse) + MinDust(coarse) + PPM_{coarse}.

PM_{10} - particulate matter with aerodynamic diameter up to 10 μm. In the EMEP MSC-W model PM_{10} is calculated as PM_{10} = $PM_{2.5}$ + PM_{coarse}.

SS_{10} - sea salt aerosol with diameter up to 10 μm.

$SS_{2.5}$ - sea salt aerosol with diameter up to 2.5 μm.

In addition to bias, correlation and root mean square the statistical parameter, index of agreement, are used to judge the model's agreement with measurements:

IOA - The index of agreement (IOA) is defined as follows (Willmott 1981, 1982):

$$IOA = 1 - \frac{\sum_{i=1}^{N}(m_i - o_i)^2}{\sum_{i=1}^{N}(|m_i - \bar{o}| + |o_i - \bar{o}|)^2} \tag{1.2}$$

where $\bar{o}$ is the average observed value. Similarly to correlation, IOA can be used to assess agreement either spatially or temporally. When IOA is used in a spatial sense, N denotes the number of stations with measurements at one specific point in time, and m_i and o_i are the modelled and observed values at station i. For temporal IOA, N denotes the number of time steps with measurements, while m_i and o_i are the modelled and observed value at time step i. IOA varies between 0 and 1. A value of 1 corresponds to perfect agreement between model and observations, and 0 is the theoretical minimum.

Finally, Table 1.1 details the 19 emission sectors incorporated in the model, which comprise 13 GNFR sectors and additional 6 subsectors as defined by the CAMS emission inventory. CEIP provides emission data from these 13 GNFR sectors, treating sectors A and F collectively (i.e., without individual data for subsectors A1, A2, F1, F2, F3, F4). By contrast, CAMS reports emissions from the same 13 GNFR sectors, but it divides the emissions from sectors A and F into their respective subsectors.

Table 1.1: Relations between EMEP, GNFR_CAMS and SNAP sectors

EMEP code	SNAP	GNFR_CAMS code	Source
1	1	A	Public Power
2	3	B	Industry
3	2	C	Other Stationary Combustion
4	5	D	Fugitive
5	6	E	Solvents
6	7	F	Road Transport
7	8	G	Shipping
8	8	H	Aviation
9	8	I	Offroad
10	9	J	Waste
11	10	K	Agri - Livestock
12	10	L	Agri - Other
13	3	M	Other
14	1	A1	PublicPower & Point
15	1	A2	PublicPower & Area
16	7	F1	Road Transport Exhaust - Gasoline
17	7	F2	Road Transport Exhaust - Diesel
18	7	F3	Road Transport Exhaust - LPG
19	7	F4	Road Transport Non-Exhaust

Notes: The EMEP codes 1–19 are used in the EMEP model. The SNAP codes 1–11 are from the earlier EMEP model version.

1.3 The EMEP grid

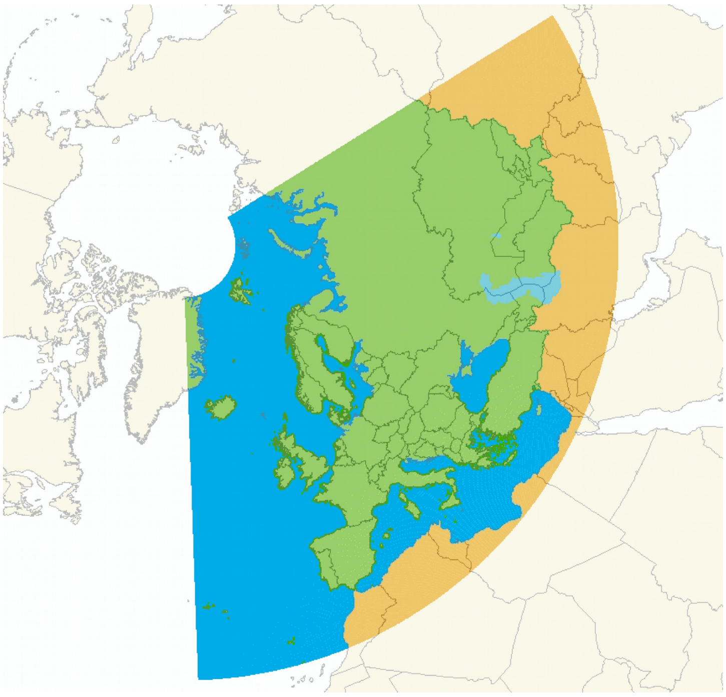

Figure 1.1: The EMEP domain covering the geographic area between 30° N-82° N latitude and 30° W-90° E longitude.

At the 36^{th} session of the EMEP Steering Body the EMEP Centres suggested to increase spatial resolution and projection of reported emissions from 50×50 km^2 polar stereographic grid to 0.1° ×0.1° longitude-latitude grid in a geographic coordinate system (WGS84). The EMEP domain shown in Figure 1.1 covers the geographic area between 30° N-82° N latitude and 30° W-90° E longitude. This domain represents a balance between political needs, scientific needs and technical feasibility. Parties are obliged to report gridded emissions in this grid resolution from year 2017.

The higher resolution means an increase of grid cells from approximately 21500 cells in the 50×50 km^2 grid to 624000 cells in the 0.1° ×0.1° longitude-latitude grid.

1.3.1 The reduced grid: EMEP0302

For practical purposes, a coarser grid has also been defined. The EMEP0302 grid covers the same region as the 0.1° ×0.1° longitude-latitude EMEP domain (Figure 1.1), but the spatial resolution is 0.3° in the longitude direction and 0.2° in the latitude direction. Each grid cell from the EMEP0302 grid covers exactly 6 grid cells from the 0.1° ×0.1° official grid.

1.4 Country codes

Several tables and graphs in this report make use of codes to denote countries and regions in the EMEP area. Table 1.2 provides an overview of these codes and lists the countries and regions included.

Table 1.2: Country/region codes used throughout this report.

Code	Country/Region/Source	Code	Country/Region/Source
AL	Albania	IS	Iceland
AM	Armenia	IT	Italy
AST	Asian areas	KG	Kyrgyzstan
AT	Austria	KZ	Kazakhstan
ATL	N.-E. Atlantic Ocean	LI	Liechtenstein
AZ	Azerbaijan	LT	Lithuania
BA	Bosnia and Herzegovina	LU	Luxembourg
BAS	Baltic Sea	LV	Latvia
BE	Belgium	MC	Monaco
BG	Bulgaria	MD	Moldova
BIC	Boundary/Initial Conditions	ME	Montenegro
BLS	Black Sea	MED	Mediterranean Sea
BY	Belarus	MK	North Macedonia
CH	Switzerland	MT	Malta
CY	Cyprus	NL	Netherlands
CZ	Czechia	NO	Norway
DE	Germany	NOA	North Africa
DK	Denmark	NOS	North Sea
DMS	Dimethyl sulfate (marine)	PL	Poland
EE	Estonia	PT	Portugal
ES	Spain	RO	Romania
EU	European Union (EU27)	RS	Serbia
EXC	EMEP land areas	RU	Russian Federation
FI	Finland	SE	Sweden
FR	France	SI	Slovenia
GB	United Kingdom	SK	Slovakia
GE	Georgia	TJ	Tajikistan
GL	Greenland	TM	Turkmenistan
GR	Greece	TR	Türkiye
HR	Croatia	UA	Ukraine
HU	Hungary	UZ	Uzbekistan
IE	Ireland	VOL	Volcanic emissions

All 51 Parties to the LRTAP Convention, except two, are included in the analysis presented in this report. The Parties that are excluded of the analysis are Canada and the United States of America, because they lie outside the EMEP domain.

1.5 Other publications

A list of all associated technical reports and notes by the EMEP centres in 2023 (relevant for transboundary acidification, eutrophication, ozone and particulate matter) follows at the end of this section.

Peer-reviewed publications in 2022

The following scientific papers of relevance to transboundary acidification, eutrophication, ground level ozone and particulate matter, involving EMEP/MSC-W and EMEP/CCC staff, have become available in 2022:

Bessagnet, Bertrand; Allemand, Nadine; Putaud, Jean-Philippe; Couvidat, Florian; André, Jean-Marc; Simpson, David; Pisoni, Enrico; Murphy, Benjamin N.; Thunis, Philippe. Emissions of Carbonaceous Particulate Matter and Ultrafine Particles from Vehicles - A Scientific Review in a Cross-Cutting Context of Air Pollution and Climate Change. Applied Sciences ; 2022; 12. (7) DOI: https://doi.org/10.3390/app12073623

Ge, Yao; Vieno, Massimo; Stevenson, David S.; Wind, Peter; Heal, Mathew R.. A new assessment of global and regional budgets, fluxes, and lifetimes of atmospheric reactive N and S gases and aerosols. Atmospheric Chemistry and Physics (ACP) 2022 ; 22. (12) p. 8343-8368 DOI: https://doi.org/10.5194/acp-22-8343-2022

Jonson, Jan Eiof; Fagerli, Hilde; Scheuschner, Thomas; Tsyro, Svetlana. Modelling changes in secondary inorganic aerosol formation and nitrogen deposition in Europe from 2005 to 2030. Atmospheric Chemistry and Physics (ACP) ; 2022; 22 . (2) p. 1311-1331 DOI: https://doi.org/10.5194/-acp-22-1311-2022

Mu, Qing; Denby, Bruce; Wærsted, Eivind Grøtting; Fagerli, Hilde. Downscaling of air pollutants in Europe using uEMEP_v6. Geoscientific Model Development ; 2022; 15. p. 449-465 DOI: https://doi.org/10.5194/gmd-15-449-2022

Quaas, Johannes; Jia, Hailing; Smith, Chris; Albright, Anna Lea; Aas, Wenche; Bellouin, Nicolas; Boucher, Olivier; Doutriaux-Boucher, Marie; Forster, Piers M.; Grosvenor, Daniel; Jenkins, Stuart; Klimont, Zbigniew; Loeb, Norman G.; Ma, Xiaoyan; Naik, Vaishali; Paulot, Fabien; Stier, Philip; Wild, Martin; Myhre, Gunnar; Schulz, Michael. Robust evidence for reversal of the trend in aerosol effective climate forcing. Atmospheric Chemistry and Physics (ACP) 2022 ; 22. p. 12221-12239 DOI: https://doi.org/10.5194/acp-22-12221-2022

Sindelarova, Katerina; Markova, Jana; Simpson, David; Huszar, Peter; Karlicky, Jan; Darras, Sabine; Granier, Claire. High-resolution biogenic global emission inventory for the time period 2000–2019 for air quality modelling. Earth System Science Data 2022; 14 p. 251-270 DOI: https://doi.org/10-.5194/essd-14-251-2022

Tsyro, Svetlana; Aas, Wenche; Colette, Augustin; Andersson, Camilla; Bessagnet, Bertrand; Ciarelli, Giancarlo; Couvidat, Florian; Cuvelier, Kees; Manders, Astrid; Mar, Kathleen; Mircea, Mihaela; Otero, Noelia; Pay, Maria-Teresa; Raffort, Valentin; Roustan, Yelva; Theobald, Mark, R.; Vivanco, Marta García; Fagerli, Hilde; Wind, Peter; Briganti, Gino; Cappelletti, Andrea; D'Isidoro, Massimo; Adani, Mario. Eurodelta multi-model simulated and observed particulate matter trends in Europe in the period of 1990–2010. Atmospheric Chemistry and Physics (ACP) ; 2022; 22. p. 7207-7257 DOI: https://doi.org/10.5194/acp-22-7207-2022

von Salzen, Knut; Whaley, Cynthia; Anenberg, Susan C.; Van Dingenen, Rita; Klimont, Zbigniew; Flanner, Mark G.; Mahmood, Rashed; Arnold, Stephen R.; Beagley, Stephen; Chien, Rong-You; Christensen, Jesper H.; Eckhardt, Sabine; Ekman, Annica M. L.; Evangeliou, Nikolaos; Faluvegi, Greg; Fu, Joshua S.; Gauss, Michael; Gong, Wanmin; Hjorth, Jens; Im, Ulas; Krishnan, Srinath; Kupiainen, Kaarle; Kuhn, Thomas; Langner, Joakim; Law, Kathy S.; Marelle, Louis; Olivié, Dirk Jan Leo; Onishi, Tatsuo; Oshima, Naga; Paunu, Ville-Veikko; Peng, Yiran; Plummer, David; Pozzoli, Luca; Rao, Shilpa; Raut, Jean-Christophe; Sand, Maria; Schmale, Julia; Sigmond, Michael;

Thomas, Manu Anna; Tsigaridis, Kostas; Tsyro, Svetlana; Turnock, Steven T.; Wang, Minqi; Winter, Barbara. Clean air policies are key for successfully mitigating Arctic warming. Communications Earth & Environment 2022 ; 3. Art, 222 DOI: https://doi.org/10.1038/s43247-022-00555-x

Whaley, Cynthia; Mahmood, Rashed; von Salzen, Knut; Winter, Barbara; Eckhardt, Sabine; Arnold, Stephen R.; Beagley, Stephen; Becagli, Silvia; Chien, Rong-You; Christensen, Jesper; Damani, Sujay Manish; Dong, Xinyi; Eleftheriadis, Konstantinos; Evangeliou, Nikolaos; Faluvegi, Gregory; Flanner, Mark G.; Fu, Joshua S.; Gauss, Michael; Giardi, Fabio; Gong, Wanmin; Hjorth, Jens Liengaard; Huang, Lin; Im, Ulas; Kanaya, Yugo; Srinath, Krishnan; Klimont, Zbigniew; Kuhn, Thomas; Langner, Joakim; Law, Kathy S.; Marelle, Louis; Massling, Andreas; Oliviè, Dirk Jan Leo; Onishi, Tatsuo; Oshima, Naga; Peng, Yiran; Plummer, David A.; Pozzoli, Luca; Popovicheva, Olga; Raut, Jean Christophe; Sand, Maria; Saunders, Laura; Schmale, Julia; Sharma, Sangeeta; Skeie, Ragnhild Bieltvedt; Skov, Henrik; Taketani, Fumikazu; Thomas, Manu Anna; Traversi, Rita; Tsigaridis, Kostas; Tsyro, Svetlana; Turnock, Steven T; Vitale, Vito; Walker, Kaley A.; Wang, Minqi; Watson-Parris, Duncan; Weiss-Gibbons, Tahya. Model evaluation of short-lived climate forcers for the Arctic Monitoring and Assessment Programme: a multi-species, multi-model study. Atmospheric Chemistry and Physics (ACP) ; 2022; 22. p. 5775-5828 DOI: https://doi.org/10.5194/acp-22-5775-2022

Wærsted, Eivind Grøtting; Sundvor, Ingrid; Denby, Bruce; Mu, Qing. Quantification of temperature dependence of NOx emissions from road traffic in Norway using air quality modelling and monitoring data. Atmospheric Environment: X ; 2022; 13. DOI: https://doi.org/10.1016/j.aeaoa.2022.100160

Zhong, Qirui; Schutgens, Nick; Van Der Werf, Guido; Van Noije, Twan; Tsigaridis, Kostas; Bauer, Susanne E.; Mielonen, Tero; Kirkevåg, Alf; Seland, Øyvind; Kokkola, Harri; Checa-Garcia, Ramiro; Neubauer, David; Kipling, Zak; Matsui, Hitoshi; Ginoux, Paul; Takemura, Toshihiko; Le Sager, Philippe; Rémy, Samuel; Bian, Huisheng; Chin, Mian; Zhang, Kai; Zhu, Jialei; Tsyro, Svetlana; Curci, Gabriele; Protonotariou, Anna; Johnson, Ben; Penner, Joyce E.; Bellouin, Nicolas; Skeie, Ragnhild Bieltvedt; Myhre, Gunnar. Satellite-based evaluation of AeroCom model bias in biomass burning regions. Atmospheric Chemistry and Physics (ACP) 2022 ; 22. (17) p. 11009-11032 DOI: https://doi.org/10.5194/acp-22-11009-2022

Groot Zwaaftink, C. D., Aas, W., Eckhardt, S., Evangeliou, N., Hamer, P., Johnsrud, M., Kylling, A., Platt, S. M., Stebel, K., Uggerud, H., and Yttri, K. E.: What caused a record high PM10 episode in northern Europe in October 2020?, Atmos. Chem. Phys., 22, 3789–3810, https://doi.org/10.5194/acp-22-3789-2022, 2022.

Platt, S. M., Hov, Ø., Berg, T., Breivik, K., Eckhardt, S., Eleftheriadis, K., Evangeliou, N., Fiebig, M., Fisher, R., Hansen, G., Hansson, H.-C., Heintzenberg, J., Hermansen, O., Heslin-Rees, D., Holmén, K., Hudson, S., Kallenborn, R., Krejci, R., Krognes, T., Larssen, S., Lowry, D., Lund Myhre, C., Lunder, C., Nisbet, E., Nizzetto, P. B., Park, K.-T., Pedersen, C. A., Aspmo Pfaffhuber, K., Röckmann, T., Schmidbauer, N., Solberg, S., Stohl, A., Ström, J., Svendby, T., Tunved, P., Tørnkvist, K., van der Veen, C., Vratolis, S., Yoon, Y. J., Yttri, K. E., Zieger, P., Aas, W., and Tørseth, K.: Atmospheric composition in the European Arctic and 30 years of the Zeppelin Observatory, Ny-Ålesund, Atmos. Chem. Phys., 22, 3321–3369, https://doi.org/10.5194/acp-22-3321-2022, 2022.

Moschos, Vaios; Schmale, Julia; Aas, Wenche; Becagli, Silvia; Calzolai, Giulia; Eleftheriadis, Konstantinos; Moffett, Claire E.; Schnelle-Kreis, Jürgen; Severi, Mirko; Sharma, Sangeeta; Skov, Henrik; Vestenius, Mika; Zhang, Wendy; Hakola, Hannele; Hellén, Heidi; Huang, Lin; Jaffrezo, Jean-Luc; Massling, Andreas; Nøjgaard, Jacob Klenø; Petäjä, Tuukka; Popovicheva, Olga; Sheesley, Rebecca J.; Traversi, Rita; Yttri, Karl Espen; Prévôt, André S. H.; Baltensperger, Urs; El Haddad,

Imad: Elucidating the present-day chemical composition, seasonality and source regions of climate-relevant aerosols across the Arctic land surface. Environ. Res. Lett. 17 (2022) doi.org/10.1088/1748-9326/ac444b

Moschos, Vaios; Dzepina, Katja; Bhattu, Deepika; Lamkaddam, Houssni; Casotto, Roberto; Daellenbach, Kaspar R.; Canonaco, Francesco; Rai, Pragati; Aas, Wenche; Becagli, Silvia; Calzolai, Giulia; Eleftheriadis, Konstantinos; Moffett, Claire E.; Schnelle-Kreis, Jürgen; Seviri, Mirko; Sharma, Sangeeta; Skov, Henrik; Vestenius, Mika; Zhang, Wendy; Hakola, Hannele; Hellén, Heidi; Huang, Lin; Jaffrezo, Jean-Luc; Massling, Andreas; Nøjgaard, Jacob Klenø; Petäjä, Tuukka; Popovicheva, Olga; Sheesley, Rebecca J.; Traversi, Rita; Yttri, Karl Espen; Schmale, Julia; Prévôt, André S. H.; Baltensperger, Urs; El Haddad, Imad: Equal abundance of summertime natural and wintertime anthropogenic Arctic organic aerosols. Nat. Geosci. 15, 196–202 (2022). https://doi.org/10.1038/s41561-021-00891-1

Gang Chen, Francesco Canonaco, Anna Tobler, Wenche Aas, Andres Alastuey, James Allan, Samira Atabakhsh, Minna Aurela, Urs Baltensperger, Aikaterini Bougiatioti, Joel F. De Brito, Darius Ceburnis, Benjamin Chazeau, Hasna Chebaicheb, Kaspar R. Daellenbach, Mikael Ehn, Imad El Haddad, Konstantinos Eleftheriadis, Olivier Favez, Harald Flentje, Anna Font, Kirsten Fossum, Evelyn Freney, Maria Gini, David C Green, Liine Heikkinen, Hartmut Herrmann, Athina-Cerise Kalogridis, Hannes Keernik, Radek Lhotka, Chunshui Lin, Chris Lunder, Marek Maasikmets, Manousos I. Manousakas, Nicolas Marchand, Cristina Marin, Luminita Marmureanu, Nikolaos Mihalopoulos, Griša Močnik, Jaroslaw Nęcki, Colin O'Dowd, Jurgita Ovadnevaite, Thomas Peter, Jean-Eudes Petit, Michael Pikridas, Stephen Matthew Platt, Petra Pokorná, Laurent Poulain, Max Priestman, Véronique Riffault, Matteo Rinaldi, Kazimierz Różański, Jaroslav Schwarz, Jean Sciare, Leïla Simon, Alicja Skiba, Jay G. Slowik, Yulia Sosedova, Iasonas Stavroulas, Katarzyna Styszko, Erik Teinemaa, Hilkka Timonen, Anja Tremper, Jeni Vasilescu, Marta Via, Petr Vodička, Alfred Wiedensohler, Olga Zografou, María Cruz Minguillón, André S.H. Prevôt: European aerosol phenomenology – 8: source apportionment of organic aerosol using 22 Year-long ACSM/AMS datasets, Environment International, 166, 2022. https://doi.org/10.1016/j.envint.2022.107325.

Associated EMEP reports and notes in 2023

Joint reports

Transboundary particulate matter, photo-oxidants, acidification and eutrophication components. Joint MSC-W & CCC & CEIP Report. EMEP Status Report 1/2023

CEIP Technical and Data reports

Sabine Schindlbacher and Merlin Mayer (CEIP), Kristina Saarinen (SYKE), Jeroen Kuenen (TNO), Ben Richmond (Ricardo). Summary of the Stage 3 ad-hoc review 2022 of emission inventories submitted under the UNECE LRTAP Convention. Technical Report CEIP 1/2023

Bradley Matthews, Robert Wankmüller. Methodologies applied to the CEIP GNFR gap-filling 2023 Part I: Main Pollutants (NO_x, NMVOCs, SO_x, NH_3, CO), Particulate Matter ($PM_{2.5}$, PM_{10}, PM_{coarse}) and Black Carbon (BC) for the years 1990 to 2021. Technical Report CEIP 2/2023

Stephan Poupa. Methodologies applied to the CEIP GNFR gap-filling 2023 Part II: Heavy Metals and POPs (Pb, Cd, Hg, Benzo(a)pyrene, Benzo(b)fluoranthene, Benzo(k)fluoranthene, Indeno(1,2,3-cd)pyrene, Total polycyclic aromatic hydrocarbons, Dioxin and Furan, Hexachlorobenzene, Polychlorinated biphenyls).Technical Report CEIP 3/2023

Sabine Schindlbacher, Bernhard Ullrich, Robert Wankmüller. Inventory review 2023. Review of emission data reported under the LRTAP Convention. Stage 1 and 2 review. Status of gridded and LPS data. Technical Report CEIP 4/2023

Sabine Schindlbacher, Robert Wankmüller: Methodologies applied to the technical review of emission data 2023. Technical Report CEIP 05/2023

CCC Technical and Data reports

Anne-Gunn Hjellbrekke. Data Report 2021: Particulate matter, carbonaceous and inorganic compounds. EMEP/CCC Report 1/2023

Anne-Gunn Hjellbrekke and Sverre Solberg. Ozone measurements 2021. EMEP/CCC Report 2/2023

Wenche Aas, William Frederik Hartz, Katrine Aspmo Pfaffhuber, Helene Lunder Halvorsen and Nora Yttri. Heavy metals and POP measurements 2021. EMEP/CCC Report 3/2023

Sverre Solberg, Anja Claude, Stefan Reimann and Stéphane Sauvage. VOC measurements 2021. EMEP/CCC Report 4/2023

MSC-W Technical and Data reports

Heiko Klein, Michael Gauss, Svetlana Tsyro and Ágnes Nyíri. Transboundary air pollution by sulfur, nitrogen, ozone and particulate matter in 2021, Country Reports. EMEP/MSC-W Data Note 1/2023

NMR reports

Simpson, D., Kuenen, J., Fagerli, H., Heinesen, D., Benedictow, A., Denier van der Gon, H., Visschedijk, A., Klimont, Z., Aas, W., Lin, Y., Yttri, K.E., Paunu, V.-V. Revising $PM_{2.5}$ emissions from residential combustion, 2005–2019. Implications for air quality concentrations and trends, 2022, Nordic Council of Ministers, Nordic Council of Ministers, TemaNord Report 2022:540, issn 0908-6692, https://pub.norden.org/temanord2022-540, doi:10.6027/temanord2022-540.

References

Fagerli, H., Simpson, D., Wind, P., Tsyro, S., Nyíri, Á., and Klein, H.: Condensable organics; model evaluation and source receptor matrices for 2018, in: Transboundary particulate matter, photo-oxidants, acidifying and eutrophying components. EMEP Status Report 1/2020, pp. 83–97, The Norwegian Meteorological Institute, Oslo, Norway, 2020.

LRTAP: Mapping critical levels for vegetation, in: Manual on Methodologies and Criteria for Mapping Critical Loads and Levels and Air Pollution Effects, Risks and Trends. Revision of 2009, edited by Mills, G., UNECE Convention on Long-range Transboundary Air Pollution. International Cooperative Programme on Effects of Air Pollution on Natural Vegetation and Crops, updated version available at www.icpmapping.com/, 2009.

LRTAP: Mapping Critical Levels for Vegetation, in: Manual for modelling and mapping critical loads and levels, chap. 3, p. 66, UNECE Convention on Long-range Transboundary Air Pollution. International Cooperative Programme on Effects of Air Pollution on Natural Vegetation and Crops, URL icpvegetation.ceh.ac.uk/get-involved/manuals/mapping-manual, 2017.

Mills, G., Hayes, F., Simpson, D., Emberson, L., Norris, D., Harmens, H., and Büker, P.: Evidence of widespread effects of ozone on crops and (semi-)natural vegetation in Europe (1990-2006) in relation to AOT40- and flux-based risk maps, Global Change Biol., 17, 592–613, doi:10.1111/j.1365-2486.2010.02217.x, 2011a.

Mills, G., Pleijel, H., Braun, S., Büker, P., Bermejo, V., Calvo, E., Danielsson, H., Emberson, L., Grünhage, L., Fernández, I. G., Harmens, H., Hayes, F., Karlsson, P.-E., and Simpson, D.: New stomatal flux-based critical levels for ozone effects on vegetation, Atmos. Environ., 45, 5064 – 5068, doi:10.1016/j.atmosenv.2011.06.009, 2011b.

Mills, G., Sharps, K., Simpson, D., Pleijel, H., Broberg, M., Uddling, J., Jaramillo, F., Davies, William, J., Dentener, F., Berg, M., Agrawal, M., Agrawal, S., Ainsworth, E. A., Büker, P., Emberson, L., Feng, Z., Harmens, H., Hayes, F., Kobayashi, K., Paoletti, E., and Dingenen, R.: Ozone pollution will compromise efforts to increase global wheat production, Global Change Biol., 24, 3560–3574, doi:10.1111/gcb.14157, URL https://onlinelibrary.wiley.com/doi/abs/10.1111/gcb.14157, 2018.

WHO: WHO global air quality guidelines. Particulate matter ($PM_{2.5}$ and PM_{10}), ozone, nitrogen dioxide, sulfur dioxide and carbon monoxide., URL https://www.who.int/publications/i/item/9789240034228, World Health Organisation, European Centre for Environment and Health Bonn Office, ISBN 978-92-4-003422-8 (electronic version), 2021.

Willmott, C. J.: On the validation of models, Physical Geography, 2, 184–194, 1981.

Willmott, C. J.: Some Comments on the Evaluation of Model Performance, Bulletin American Meteorological Society, 63, 1309–1313, doi:10.1175/1520-0477(1982)063<1309:SCOTEO>2.0.CO;2, 1982.

Part I

Status of air pollution

CHAPTER 2

Status of transboundary air pollution in 2021

Svetlana Tsyro, Wenche Aas, Sverre Solberg, Anna Benedictow, Hilde Fagerli, Jan Eiof Jonson and Ágnes Nyíri

This chapter describes the status of transboundary air pollution in 2021. A short summary of the meteorological conditions is presented, the EMEP network of measurements and the EMEP MSC-W model set up is briefly described. Thereafter, the status of air pollution in 2021 is discussed.

2.1 Meteorological conditions in 2021

Air pollution is significantly influenced by both emissions and weather conditions. Temperature and precipitation are particularly important factors. A short summary describing the situation in 2021 with respect to these two parameters, based on NWP model results and as reported by the meteorological institutes in European and EECCA countries, is given below.

The meteorological data to drive the EMEP MSC-W air quality model have been generated by the Integrated Forecast System (IFS) model of the European Centre for Medium-Range Weather Forecasts (ECMWF), hereafter referred to as the ECMWF-IFS model. In the meteorological community, the ECMWF-IFS model is considered to be state-of-the-art, and MSC-W has been using this model in hindcast mode to generate meteorological reanalyses for the year to be studied. IFS Cycle 46r1 is the version used for the year 2021 model runs. In the following section, temperature and precipitation in 2021 are compared to the 2000-2020 average based on the same ECMWF-IFS model setup (i.e. with the same horisontal resolution). Meteorological data for the years 2000 to 2018 have been derived from the IFS Cycle 40r1 version and 2019 to 2021 from IFS Cycle 46r1.

2.1.1 Temperature and precipitation

Globally, 2021 was reported by the World Meteorological Organisation (WMO 2022) to be placed between the fifth and seventh warmest years on record. The annual temperature for Europe in 2021 was ranked just outside the top ten warmest on record according to Copernicus European State of the Climate 2021[1] and for Arctic land areas, October 2020 to September 2021 was the seventh warmest period of the last century (Arctic Report Card 2021 Ballinger et al. 2021.

Global monitoring products reported in BAMS State of the climate 2021 (Global climate, Dunn et al. 2022) indicate that global mean precipitation over land was just below average. Precipitation amounts across Europe were near normal, however, with some seasonal local/regional extreme precipitation events or deficit as reported in the Copernicus and the BAMS climate reports. WMO also reported seasonal snow cover deficit in late spring and summer of 2021, with third lowest Northern Hemisphere snow cover in May since 1970. Particularly the Eurasian Arctic snow extent in May 2021 was the fifth and in June the third lowest on record since 1967.

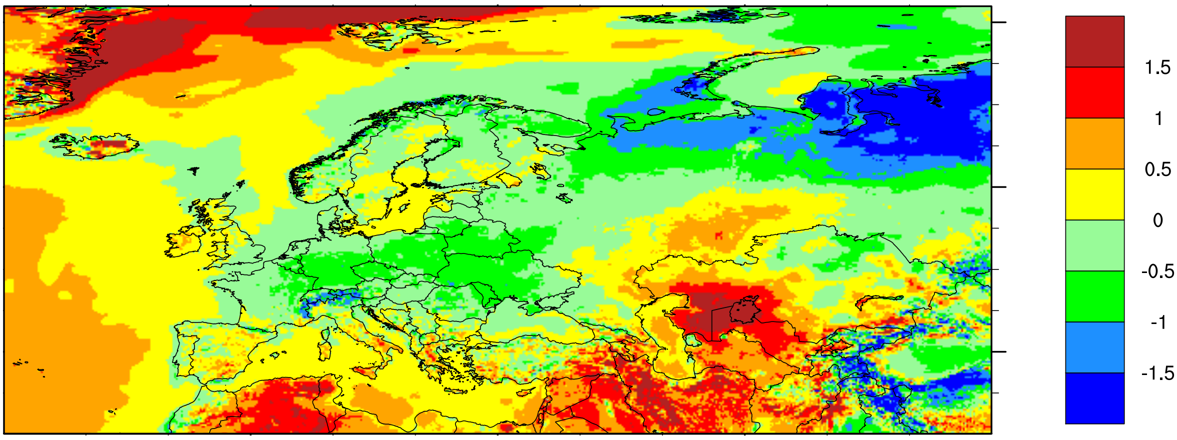

(a) Δtemperature at 2m (2021-climavg)

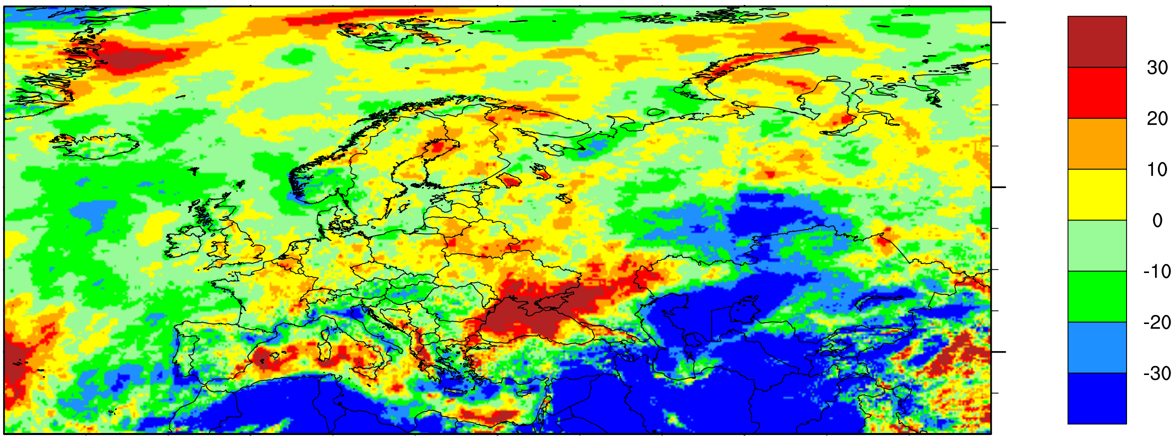

(b) Δprecipitation (2021-climavg)

Figure 2.1: Meteorological conditions in 2021 compared to the 2000-2020 average (climavg) for: a) Annual mean temperature at 2m [K] and b) Annual precipitation [%]. The meteorological data have been calculated with the ECMWF-IFS model.

[1] https://climate.copernicus.eu/esotc/2021

Overall lower temperatures in 2021 compared to the 2000-2020 average are seen in Figure 2.1a over Europe and European Russia, with particularly low temperatures in northern European Russia, northern Scandinavia, Central and eastern Europe. However high temperatures were found in south-eastern European Russia, west Kazakhstan, Türkiye, Greece and Italy. Based on measurements, Armenia reported its 3rd warmest year on record, Türkiye and Greece their 4th and west Kazakhstan its 5th.

Compared to the 2000-2020 average, precipitation in 2021 (Figure 2.1b) shows higher amounts than normal in Belgium, eastern France, Albania, eastern Europe and southern European Russia. On the other hand, there were less than normal precipitation amounts in southern Norway, western and northeastern Spain, northern Italy and western Kazakhstan. Belgium observed its 3rd wettest year on record (since 1991) and European Russia its 6th wettest, while west Kazakhstan reported 2021 to be the 3rd driest.

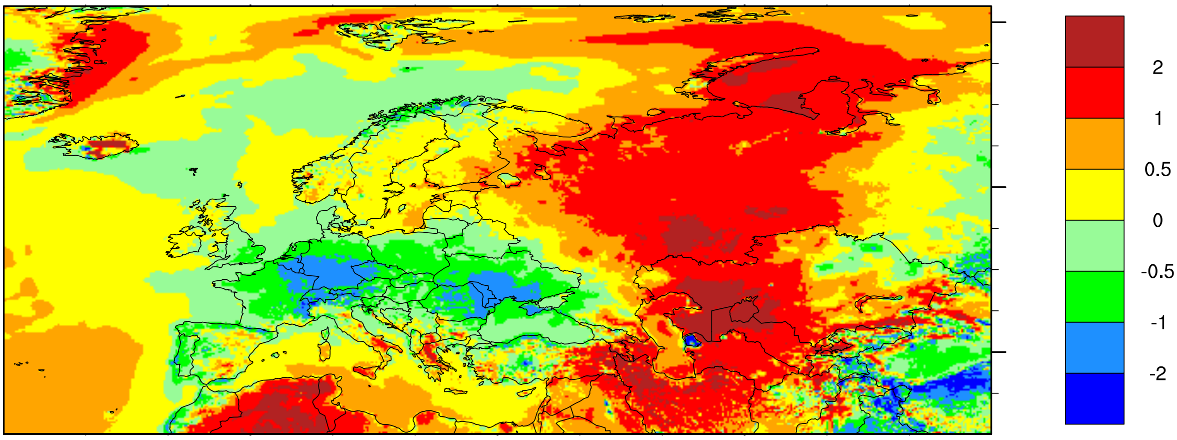

(a) Δtemperature at 2m (AprSep 2021-climavg)

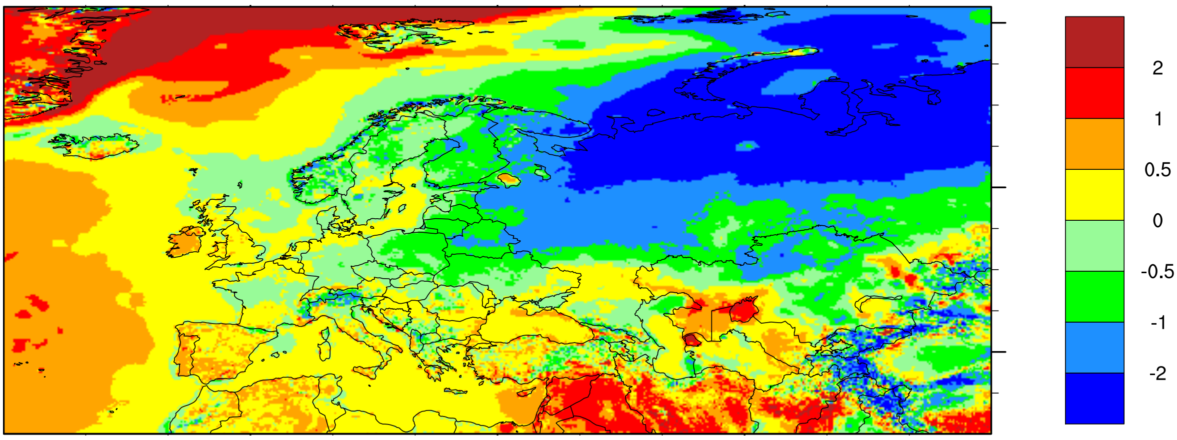

(b) Δtemperature at 2m (OctMar 2021-climavg)

Figure 2.2: Meteorological conditions in 2021 compared to the 2000-2020 average (climavg) for: a) Summer (April-September) temperature [K], b) Winter (January-March and October-December) temperature [K]. The meteorological data have been calculated with the ECMWF-IFS model.

Figure 2.2 shows the temperatures in 2021 compared to the 2000-2020 average in Europe for the summer months (April through September) and the winter months (October through December and January through March). Lower temperatures than normal is shown in Figure 2.2a for Central Europe, but higher for northeastern Iceland, South Finland, southeastern

Spain, South Italy, Greece, eastern Türkiye, Aserbajdsjan, western Kazakhstan and northern European Russia. The summer of 2021 was reported as the warmest on record for Europe and Armenia, second warmest for Finland, Greece, Belarus and European Russia, though April and May was record cold in UK, Benelux and Switzerland. Particularly for Benelux, records of lowest temperatures in April were broken for the Netherlands, Belgium (coldest since 1986) and Luxembourg. On the other hand, the Netherlands had its warmest and Belgium 3rd warmest June on record. Also after a cold spring in Hungary, Poland and Austria, June was the 2nd warmest month on record in Poland and 3rd in Austria (since 1767) and Hungary (since 1901). West Kazakhstan measured their 3rd warmest spring on record, and May was warmest on record in Armenia and in 50 years in Türkiye. For the early autumn, the coldest August since 2014 was observed in Austria, while Greece and North Macedonia had their warmest August on record. September was 2nd warmest month on record for UK and Malta, 3rd warmest for France in 50 years and 4th in Italy, but unusually cold in Belarus.

As shown in Figure 2.2b winter temperatures were lower than the 2000-2020 average in virtually all of Europe, particularly in northern and eastern Europe including Russia and Kazakhstan. For the first months of 2021 northern Europe observed rather cold temperatures and warmer towards the south; Romania, Greece and Bulgaria recorded their 2nd warmest winter and Serbia its 3rd warmest. The year ends with rather cold temperatures in Scandinavian and Baltic countries, but warmer in western European countries. Belarus reported its 5th warmest November on record and Iberia its 4th warmest December.

For April through September Figure 2.3a shows that Central Europe and western EECCA in general had much more precipitation in 2021 than the 2000-2020 average, except for Hungary, southern Europe, Türkiye, Armenia, Azerbaijan and Central Asia. April was reported as the driest month on record in Romania, and spring was the 3rd driest in West Kazakhstan and 4th driest on record in Spain. In May, Central Europe, Latvia, Estonia, Slovenia, Belarus, Ukraine, Moldova, European Russia and Romania was wetter than normal, while western Kazakhstan was very dry. Summer was drier than normal in Armenia (droughts observed in June), United Kingdom, Italy, Slovenia, Croatia, North Macedonia, Bosnia-Herzegovina and West Kazakhstan. June was the 2nd driest since 1917 in Hungary, and also drier than normal in Croatia, Sicily and Malta. July was the wettest since 1864 in Switzerland and since 1991 in Belgium, 2nd wettest in Luxembourg and 3rd since 1955 in France. In August, Finland, Estonia and Sweden was wetter than normal and 2nd wettest in Poland, while September was driest since 1975 in Austria.

As shown in Figure 2.3b the 2021 winter months (January-March and October-December) were wetter than the 2000-2020 average in northwestern and southeastern Europe, and close to normal in Central Europe. Regardless of that, the winter 2020/21 was reported as near normal over most of Europe. The Nordic (except Sweden) and Baltic countries observed a deficit of precipitation, while Serbia and Bulgaria reported their 4th wettest winter. Western Austria and North Macedonia measured record high amounts of precipitation in January, but also Bulgaria, Serbia, Albania and northern Greece was abnormally wet. February was the 3rd wettest since 2000 in Portugal and the 5th on record in European Russia, but Latvia registered its 5th driest since 1924. Observed autumn precipitation was below normal in most of Central Europe, and in particular Moldova received much less than normal precipitation. October was especially dry across Germany, Czechia, South Belarus, Ukraine, Moldova, southern European Russia and the driest on record for Slovakia, on the other hand, much wetter than normal in Azerbaijan, Greece, North Macedonia, Bulgaria (4th wettest on record) and 3rd for Finland. Measured precipitation was also highly variable throughout Europe and the EECCA countries towards the end of the year. Italy, Croatia, Bosnia-Herzegovina and northern European Russia reported above normal precipitation in November, while it was drier than usual in Georgia, Armenia, Azerbaijan and Portugal (3rd driest on record), and at last December with above normal precipitation amounts in Romania, Moldova and Ukraine.

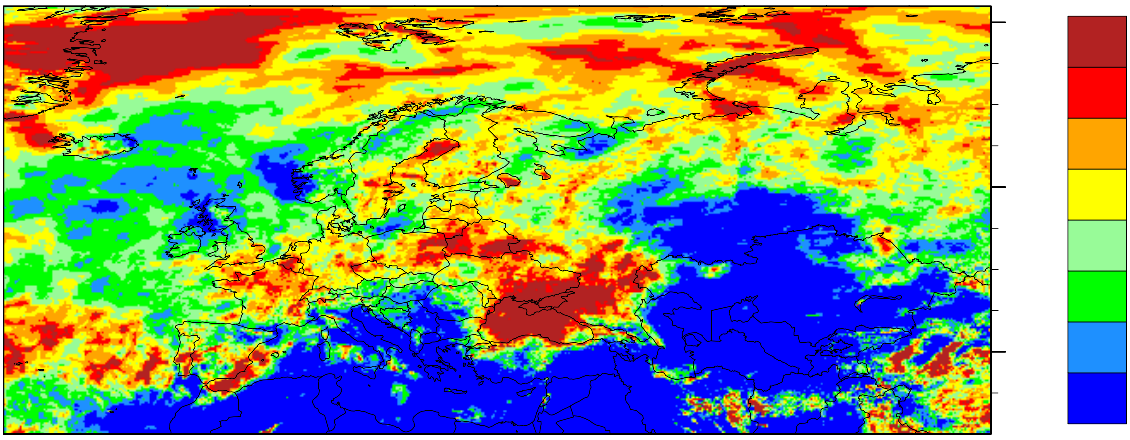

(a) Δprecipitation (AprSep 2021-climavg)

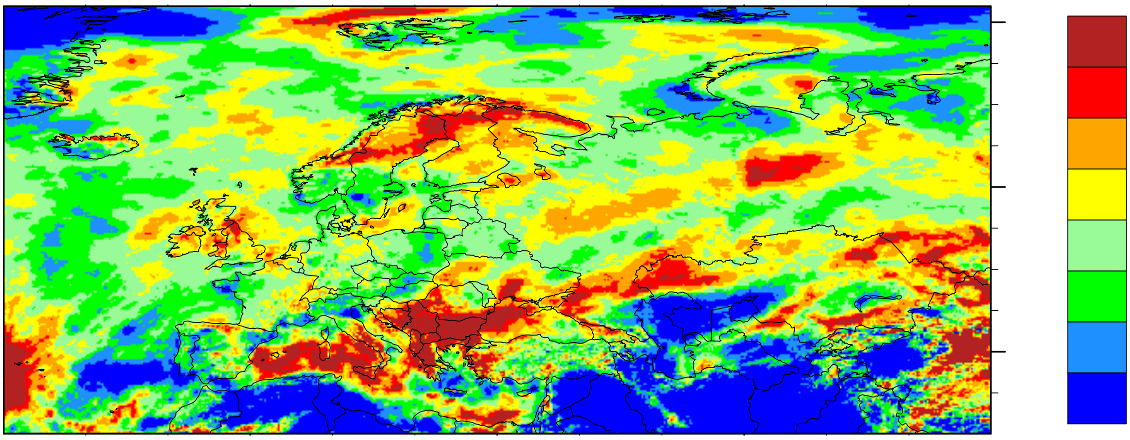

(b) Δprecipitation (OctMar 2021-climavg)

Figure 2.3: Meteorological conditions in 2021 compared to the 2000-2020 average (climavg) for: a) summer (April-September) precipitation [%], b) winter (January-March and October-December) precipitation [%]. The meteorological data have been calculated with the ECMWF-IFS model.

2.2 Measurement network 2021

In 2021, a total of 31 Parties reported measurement data of inorganic components, particulate matter and/or ozone to EMEP from altogether 167 sites. All the data are available from the EBAS database (`http://ebas.nilu.no/`) and are also reported separately in technical reports by EMEP/CCC (Hjellbrekke 2023, Hjellbrekke and Solberg 2023). Figure 2.4 shows an overview of the spatial distribution of the sites reporting data for inorganic ions in air and precipitation, particulate matter and ozone in 2021.

135 sites reported measurements of inorganic ions in precipitation and/or main components in air. However, not all of these measurements were co-located, as illustrated in Fig-

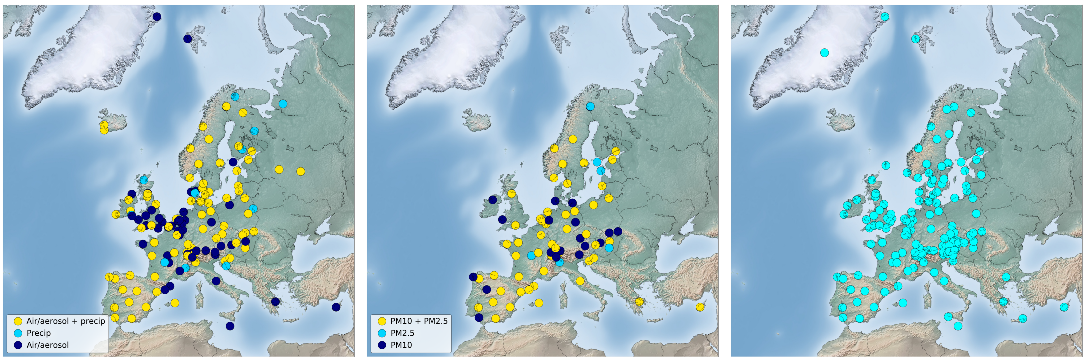

(a) Inorganic compounds (b) PM mass concentration (c) Ozone

Figure 2.4: EMEP measurement network for level 1 components in 2021.

ure 2.4. There were 76 sites with measurements in both air and precipitation. Ozone was measured at 138 EMEP sites.

There were 77 sites measuring either PM_{10} or $PM_{2.5}$ mass. 50 of these sites measured both size fractions, as recommended in the EMEP Monitoring strategy (UNECE 2019) at EMEP level 1 sites. The stations measuring EMEP level 2 variables are shown in Figure 11.2 in Ch 11.1, along with a discussion on compliance with the monitoring obligations and the development of the programme during the last decade.

2.3 Setup for EMEP MSC-W model runs

The EMEP MSC-W model version rv5.0 has been used for the 2021 assessment and source-receptor runs. The horizontal resolution is $0.1° \times 0.1°$, with 20 vertical layers (the lowest with a height of approximately 50 meters).

Meteorology, emissions, boundary conditions and forest fires for 2021 have been used as input. Meteorological data have been derived from ECMWF-IFS Cycle 46r1 simulations (see Ch 2.1). The emission data set EMEPwRef2_v2.1C have been used in the model simulations for 2021 for pollution assessments and the source-receptor runs included in this report. The land-based emissions have been derived from the 2023 official data submissions to UNECE CLRTAP (Schindlbacher et al. 2023), as documented in Ch 3. The officially submitted PM_{10} and $PM_{2.5}$ emissions from residential combustion (GNFR sector C) have been used for the countries which emissions seemed to include condensable organics. For other countries, updated TNO Ref2_v2.1 emission data (or gap-filled data by CEIP) was used, as described in Ch 3.3 (for more details see Simpson et al. (2022)).

Emissions from international shipping within the EMEP domain for 2021 are derived from the CAMS global shipping emissions (CAMS-GLOB-SHIP v3.2) (Granier et al. 2019), developed by the Finnish Meteorological Institute (FMI).

The forest fires emissions are taken from the Fire INventory from NCAR (FINN) (Wiedinmyer et al. 2011), version FINN2.5, based on MODIS data (9.2.1). For more details on the emissions for the 2021 model runs see Ch 3 and Appendix A.

The effects of socio-economic activity restrictions due to the COVID-19 pandemic on emission temporal profiles for 2020 were estimated in Guevara et al. (2022). Following the same methodology, the authors also created daily adjustment factors to the 2021 emissions and combined them with CAMS-REG-TEMPO v3.2 temporal profiles (Guevara et al. 2021) in order to estimate temporal profiles for year 2021. For non-livestock agricultural emissions (GNFR Sector L) the monthly factors from CAMS-REG-TEMPO v4.1 were used. The provided temporal profiles were a combination of monthly, day-of-the-week and day-of-the-year factors, which have been used to create a full set of day-of-the-year emission time factors for 2021, applicable on a country and activity sector basis for each individual pollutant. For more details see Appendix G. The resulting day-of-the-year time profiles, accounting for COVID-19 effects, were used in status and source-receptor runs for 2021.

2.4 Air pollution in 2021

2.4.1 Particulate Matter

Maps of annual mean concentrations of PM_{10} and $PM_{2.5}$ in 2021, simulated by the EMEP MSC-W model, are presented in Figure 2.5. The figures also show annual mean PM_{10} and $PM_{2.5}$ concentrations observed at the EMEP monitoring network, which are represented by colour triangles overlaying the contours of the modelled concentration fields.

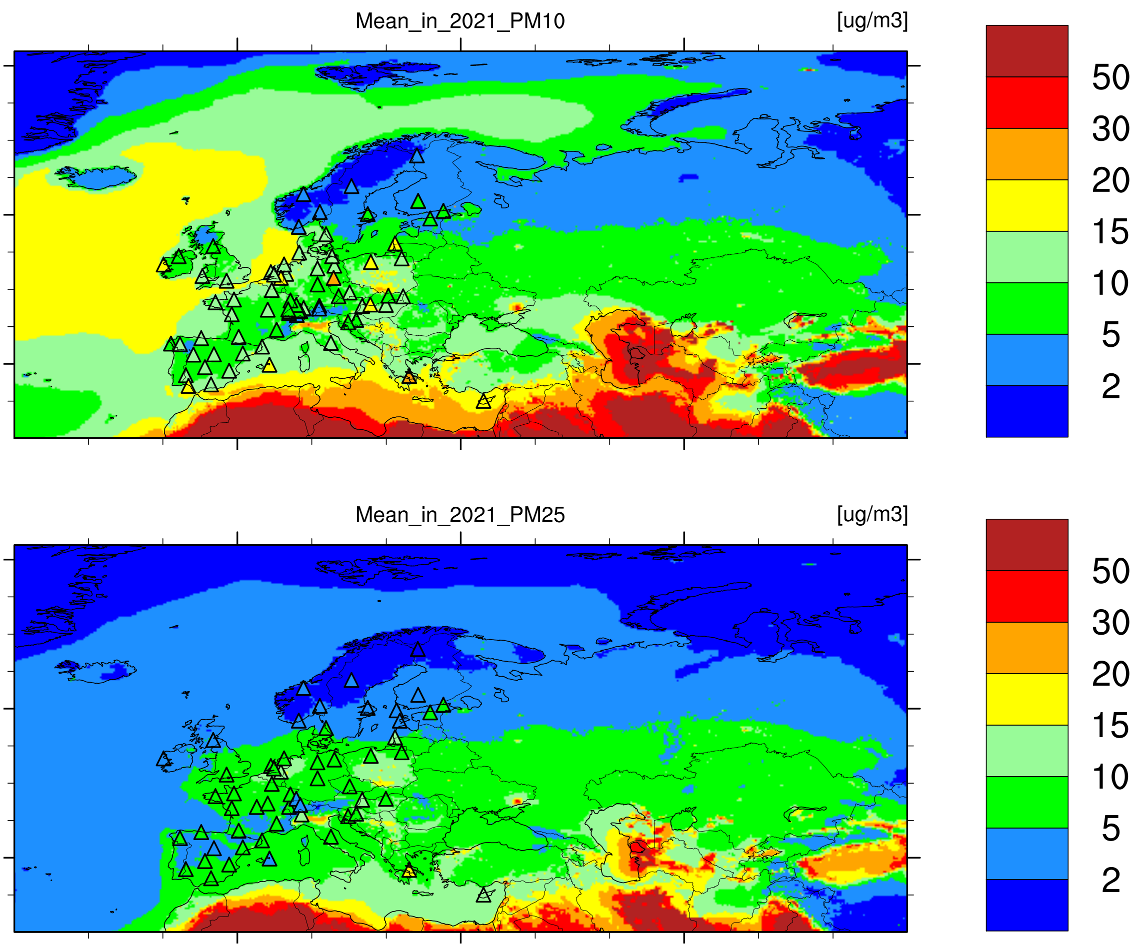

Figure 2.5: Annual mean concentrations of PM_{10} and $PM_{2.5}$ in 2021: simulated by the EMEP MSC-W model (colour contours) and observed at EMEP monitoring network sites (colour triangles).

The maps show a general increase of the annual mean of regional background PM_{10} and

$PM_{2.5}$ over land from north to south, with PM_{10} concentrations being below 2-5 µg m^{-3} in northern parts of Europe and Russia, going up to 5-15 µg m^{-3} in the mid-latitudes, and to 20 µg m^{-3} and above further south. On the other hand, PM_{10} are fairly homogeneous in terms of zonal distribution. $PM_{2.5}$ follows in general the same spatial pattern, with somewhat lower concentration levels with respect to PM_{10}. The EMEP model and the observations are in a quite good agreement regarding PM spatial distribution.

The highest annual mean PM_{10} of 21.1 µg m^{-3} was observed at Melpitz (DE0044), followed by 19.9 µg m^{-3} at Agia Marina (CY0002) and 18.4 µg m^{-3} at Rucava (LV0010). The EMEP model simulated PM_{10} in excess of 20 µg m^{-3} for limited areas in Central Europe, i.e. in the Po Valley and in southern Poland. The highest annual mean $PM_{2.5}$ concentrations of 11.6 µg m^{-3} was observed at Ispra (IT0004), and $PM_{2.5}$ above 10 µg m^{-3} was registered at four more sites (LV0010, NL0010, AT0002, and CY0002). Model simulated $PM_{2.5}$ concentrations are below 10 µg m^{-3} over most of the European EMEP domain, except for Poland, Hungary and Benelux (with $PM_{2.5}$ between 10 and 15 µg m^{-3}), and a hot spot above 20 µg m^{-3} in the Po Valley.

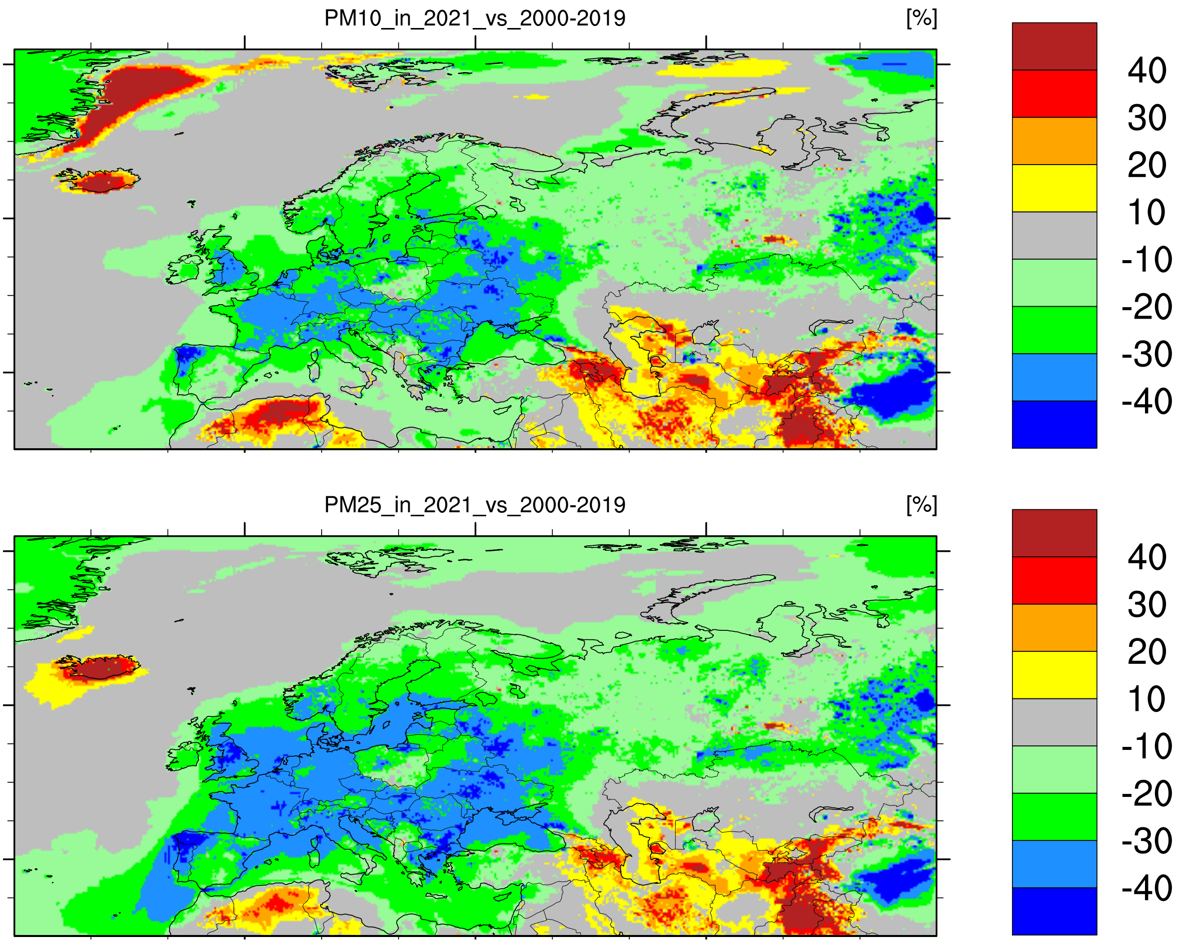

Figure 2.6: Relative differences in annual mean PM_{10} and $PM_{2.5}$ concentrations in 2021 with respect to the 2000-2019 average.

Furthermore, the model simulates high PM for the regions east of the Caspian Sea (parts of Kazakhstan, Uzbekistan, Turkmenistan) and over the southern Mediterranean, with annual mean concentrations of 30-50 µg m^{-3} and higher. These high PM concentrations are due to windblown dust from the arid soils and deserts of Central Asia, though the precision of the calculated values still cannot be verified due to the lack of observations in these regions.

There is a good agreement between the modelled and EMEP observed distributions of annual mean PM_{10} and $PM_{2.5}$, with spatial correlation coefficients of 0.74 and 0.68, respectively. Overall, the model underestimates the observed annual mean of PM_{10} by 25% and $PM_{2.5}$ by 12%. A more detailed comparison between model and measurements for the year 2021 can be found at https://aeroval.met.no/evaluation.php?project=emep&exp_name=2023-reporting.

Relative to the 20-year average (2000-2019), derived from the trend runs with consistent model version (as described in Ch 2.3), PM pollution appears to be quite moderate in 2021 (Figure 2.6). The simulated annual mean PM_{10} concentrations for 2021 are lower than the 2000-2019 average by 30-40% in large parts of western/central/southeastern Europe, by 20-30% in the rest of Europe (including Fennoscandia, parts of eastern Europe and western parts of Russia), and by 10-20% in the rest of Russia. Similar pattern can be seen for annual mean $PM_{2.5}$, which concentrations are even lower with respect to the 20-year average. Only on Iceland, in the Caucasus and in parts of Central Asia, PM_{10} and $PM_{2.5}$ appear higher in 2021 than the 2000-2019 average by as much as 30-40%. The differences in PM levels in 2021 compared to the 20-year average are both due to the changes in emissions and meteorological variability. The year 2020 has been excluded from the 'reference' average of 2005-2019 since the pollution in 2020 was affected by COVID related activity reductions.

Exceedances of EU limit values and WHO Air Quality Guidelines in 2021

In this section, we present a brief discussion of the status of European air quality in 2021 for PM_{10} and $PM_{2.5}$ with respect to EU critical limits and WHO Air Quality Guidelines. Our assessment is based on PM concentrations from EMEP MSC-W model simulations and observations at EMEP sites, both being representative of regional background. In addition to WHO AQG Global Update 2005 (AQG-2005) (WHO 2005), we compare the modelled and observed PM with lately updated AQG, i.e. Global Update 2021 (AQG-2021) (WHO 2021). The WHO AQG offer health-based recommendations for air quality management, i.e. the lowest levels of exposure for which there is evidence of adverse health effects. Though not being legally binding standards, these guidelines provide WHO Member States with a valuable evidence-informed tool that they can use to inform legislation and policy. Table 2.1 summarizes EU and WHO AQG limit values for PM_{10} and $PM_{2.5}$, relevant for air quality assessment for the year 2021.

Table 2.1: EU limit values and WHO Air Quality Guidelines Global Update 2005 (AQG-2005) and Global Update 2021 (AQG-2021) for PM_{10} and $PM_{2.5}$.

Limits	PM_{10} ($\mu g\ m^{-3}$)		$PM_{2.5}$ ($\mu g\ m^{-3}$)	
	Year	24-hour	Year	24-hour
EU	40	50[a]	20	-
AQG-2005	20	50[b]	10	25[b]
AQG-2021	15	45[c]	5	15[c]

[a] not more than 35 days per year

[b] 99th percentile (i.e. 3–4 exceedance days per year)

The EU limit values for protection of human health from particulate matter pollution and the WHO AQG for PM should apply to concentrations for zones or agglomerations, in rural and urban areas, which are representative for exposure of the general population. PM_{10} and $PM_{2.5}$ concentrations calculated with the EMEP MSC-W model on the 0.1°× 0.1° grid cannot reproduce urban hotspot levels, but give a reasonable representation of PM levels occurring in rural and, to some extend, in urban background areas.

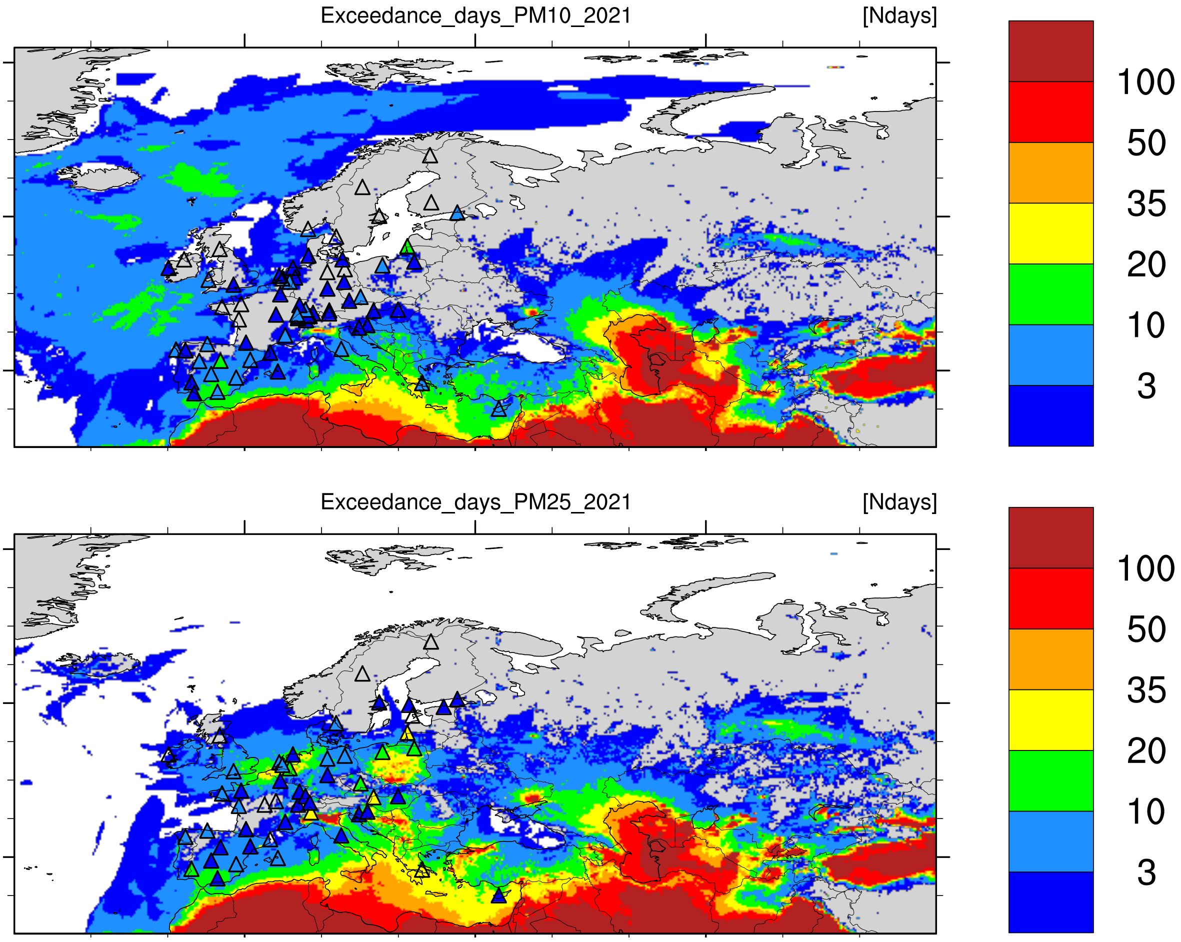

Figure 2.7: Modelled and observed (triangles) number of days with exceedances in 2021: PM_{10} exceeding 50 µg m^{-3} (upper) and $PM_{2.5}$ exceeding 25 µg m^{-3} (lower panel). *Note: The EU Directive requires no more than 35 days with exceedances for PM_{10}, whereas WHO Global Update 2005 recommended no more than 3 days with exceedances for PM_{10} and $PM_{2.5}$ per calendar year.*

Model results and EMEP observational data show that the annual mean PM_{10} concentrations were below the EU limit value of 40 µg m^{-3} for all of Europe in 2021 (Figure 2.5). The model calculated annual mean PM_{10} is mostly below WHO AQG-2005 and AQG-2021 recommended levels, except for small areas in the Po Valley, Poland, Benelux, Serbia, Türkiye and Central Asia. The highest observed annual mean PM_{10} concentrations, exceeding the AQG-2005 of 20 µg m^{-3}, were registered at the Greek site GR0001 (22 µg m^{-3}, 57% data coverage only) and at the German site DE0044 (21 µg m^{-3}), whereas AQG-2021 were exceeded at 8 sites. Further, the observations and model results show that annual mean $PM_{2.5}$ concentrations (Figure 2.5) in 2021 were mostly below the EU limit value of 20 µg m^{-3} (from 01.01.2020), except in the Po Valley, according to the model. However, there were observed

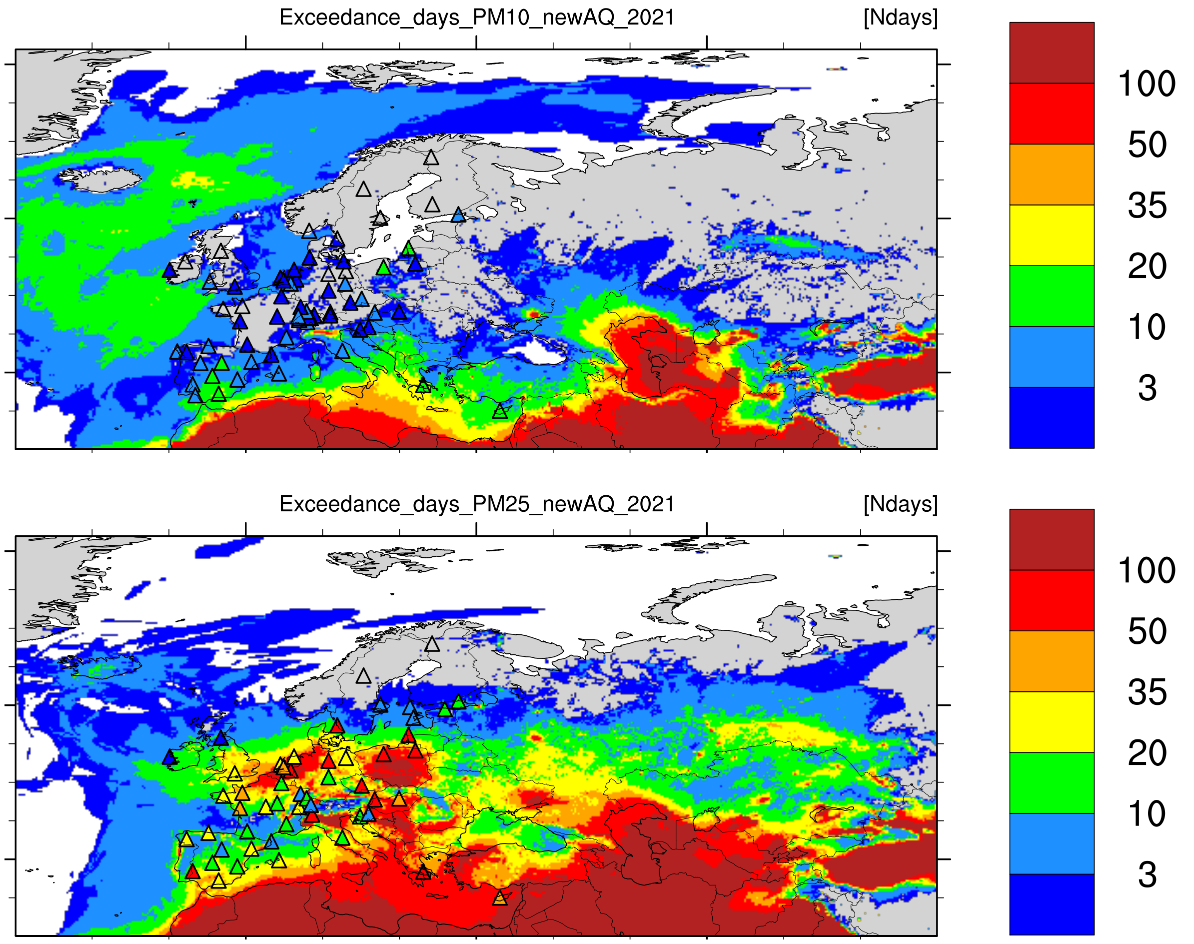

Figure 2.8: Modelled and observed (triangles) number of days with exceedances in 2021: PM_{10} exceeding 45 µg m^{-3} (upper) and $PM_{2.5}$ exceeding 15 µg m^{-3} (lower panel). *Note: WHO AQG Global Update 2021 recommends no more than 3-4 days with exceedances for PM_{10} and $PM_{2.5}$ per calendar year.*

cases of exceedances by annual mean $PM_{2.5}$ of WHO AQG-2005 and AQG-2021 levels at 5 and 40 sites, respectively.

The maps in Figure 2.7 and 2.8 show the number of days with PM_{10} and $PM_{2.5}$ exceedances in 2021 with respect to the limit values recommended by WHO AQG Global Update 2005 and Global Update 2021 respectively, according to EMEP MSC-W model simulations (colour contours) and EMEP observations (triangles). Out of 65 sites with daily or hourly PM_{10} measurements with data coverage above 75%, exceedance days were observed at 4 sites. No exceedances of the PM_{10} EU limit value (more than 35 exceedance days) were observed. Still, 20 sites had more than 3 exceedance days, as recommended by the WHO AQG, Global Update 2005. AQG from WHO Global Update 2021, were exceeded at 51 sites, and 26 sites had more than 3 exceedance days. The highest number of days with PM_{10} exceedances of the EU limit and AQG-2021, i.e. 15 and 16 respectively, was registered at ES0009.

Out of 50 sites with required data coverage in 2021, $PM_{2.5}$ concentrations exceeded AQG-2005 recommended limit of 25 µg m^{-3} at 40 sites, with more than 3 days with exceedances registered at 18 sites. The more stringent AQG-2021 limit of 15 µg m^{-3} was exceeded at 47 sites (45 sites with more than 3 $PM_{2.5}$ exceedance days). The largest number of exceedance days with respect to AQG-2005 and AQG-2021 (33 and 87 respectively) was registered at the Greek site GR0001 (though the data capture was only 55%) and at LV0010 (31 and 9 respectively).

In general, there is a fair correspondence between modelled and observed numbers of days with PM_{10} exceeding the EU limit value of 50 µg m^{-3}. Similar to the observations, the modelled calculated number of exceedance days is below the required limit of 35 days for 2021 at any site. The model under-counts the cases with exceedances for some sites, but the only considerable underestimations of observed exceedance days are for LV0010 and PL0009, for which the model does not calculate any exceedance days while there were registered 13 and 7 days with PM_{10} above 50 µg m^{-3}, respectively); and also for ES0009 (5 calculated vs. 15 observed). For some sites (e.g. CY0002, ES0007, ES0017, HR0002, SI0008), the model slightly overestimates the occurrence of exceedance days compared to observations. Similar model performance compared to observations can be seen for PM_{10} exceedance days with respect to the AQG-2021 limit value of 45 µg m^{-3}.

For $PM_{2.5}$, the model simulates exceedances of AQG-2021 limit value of 15 µg m^{-3} on more than 3 days practically for all sites, except for 7. The largest numbers of $PM_{2.5}$ exceedance days are calculated for IT0004 (126 days vs. 74 observed), HR0002 (94 vs. 7) and NL0008 and NL0644 (87 and 81 vs. 65 and 38 days respectively), whereas the modelled number of exceedance days for GR0001 and LV0010 is much lower than observed, namely 29 and 15, respectively.

2.4.2 Ozone

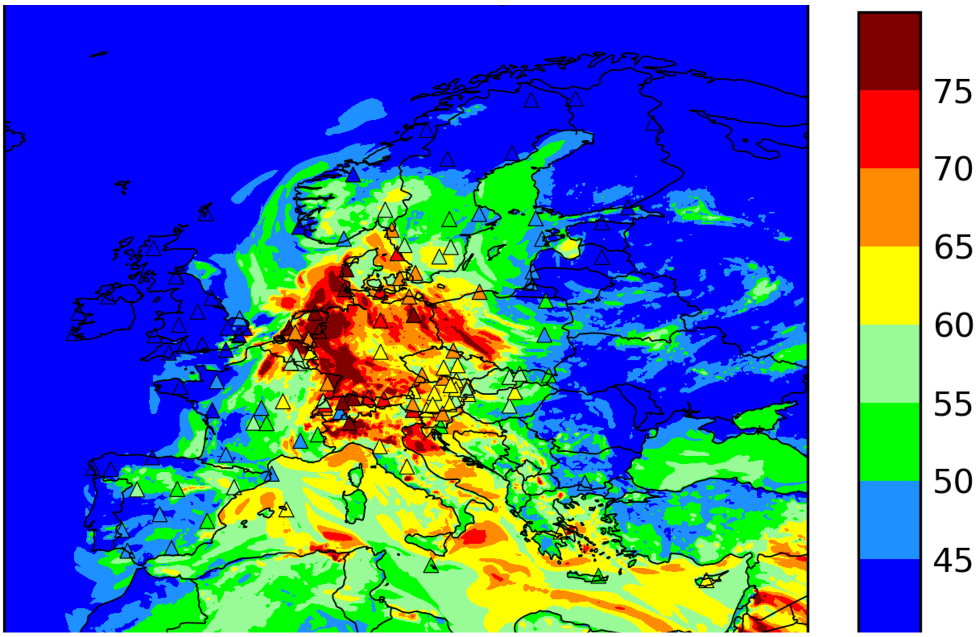

Figure 2.9: Modelled and measured daily maximum ozone [ppb] 17 June 2021.

The ozone observed at a surface station is the net result of various physio-chemical processes: surface dry deposition and uptake in vegetation, titration by nearby NO_x emissions, regional photochemical ozone formation and atmospheric transport of background ozone levels, each of which may have seasonal and diurnal systematic variations. Episodes with elevated levels of ozone are mainly observed during the summer half year when certain meteorological situations (dry, sunny, cyclonic stable weather) promote the formation of ozone over the

European continent. In particular there is a clear link between the increase in frequency and intensity of heatwaves in Europe and peak levels of surface ozone. Peak ozone episodes are now more frequent than in an otherwise stable climate (Solberg et al. 2008, Otero et al. 2016, Zhang et al. 2018).

In Europe there were several ozone episodes in 2021. The June 17 to June 20 episode stands out having a large number of exceedances of the 120 μgm^{-3} (or 60 ppb) EU limit. In particular on 17 June (Figure 2.9) there was a large number of measured exceedances (34). During this period the weather situation was dominated by an extensive blocking high centered around the southern parts of the Baltic Sea, and a low pressure system in the near Atlantic ocean, with southerly winds prevailing in Central Europe.

In addition, there were several ozone episodes strongly affected by wildfires. One major wildfire was centered around southern Italy in late July to the middle of August. A second episode occurred in central Spain in the middle of August where both measured and model calculated ozone levels reached about 90 ppb. These two episodes are described in Ch 9.4.

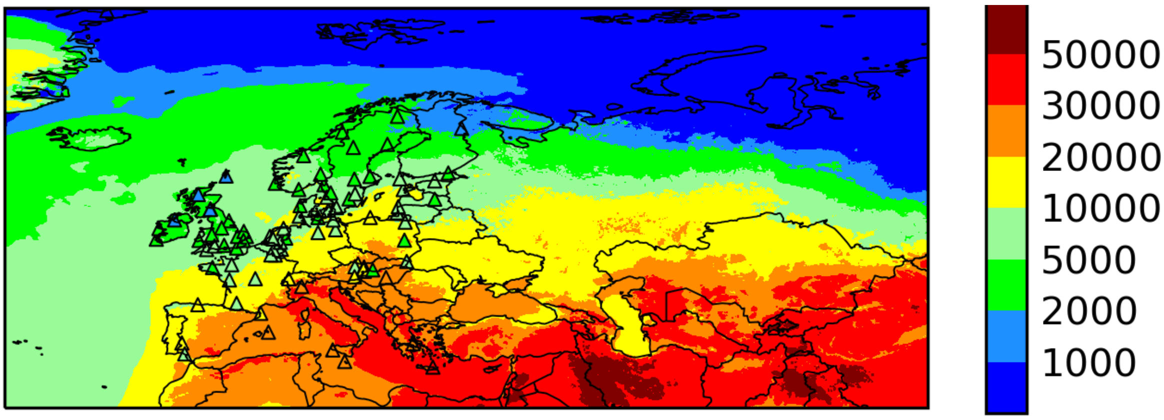

(a) EU_AOT40f

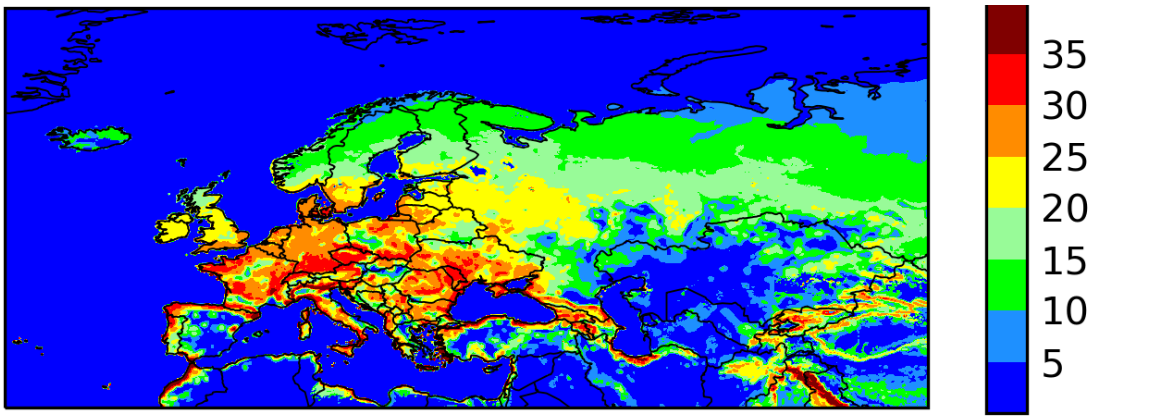

(b) POD_1

Figure 2.10: Year 2021 model results for (a) EU-AOT40f (*ppb.h*) In addition, EMEP stations are shown as triangles, showing only data from measurement sites below 500 m a.s.l. (b) Model calculated POD_1 in nmol m^{-2} s^{-1}.

The ozone metrics discussed below and shown in Figures 2.10 and 2.11 are defined in Ch 1.2.

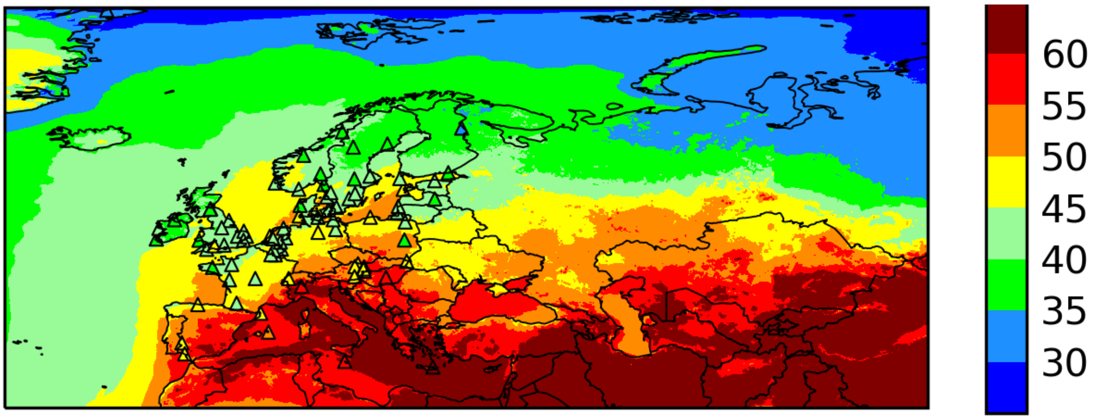

(a) MDmaxO3

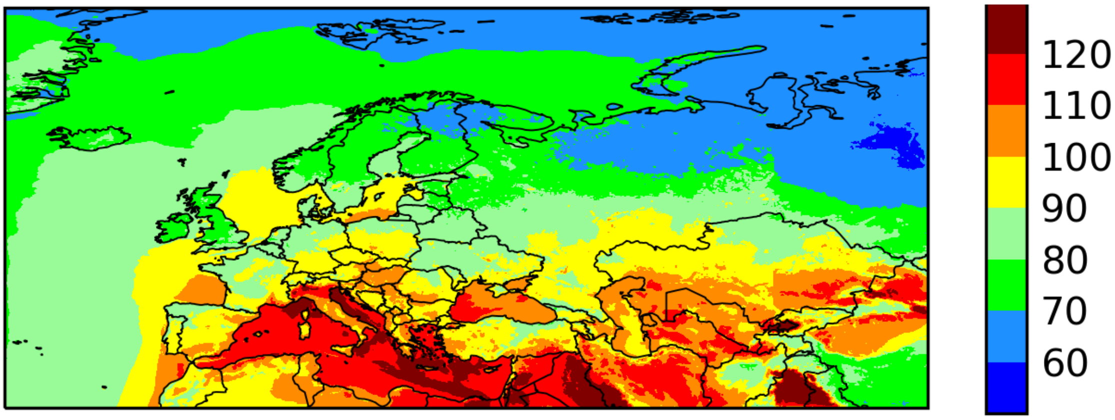

(b) $MDA8_{AS}$

Figure 2.11: Year 2021 April–September model results for: (a) MDmaxO3 (ppb). In addition EMEP stations are shown as triangles, showing only data from measurement sites below 500 m a.s.l. (b) $MDA8_{AS}$ (µg m^{-3})

Figure 2.10 shows EU-AOT40f (top) and POD_1 where EU-AOT40f is the AOT40 for forests calculated using EU definitions, and POD_1 is the phyto-toxic ozone dose. For EU-AOT40f the corresponding measured values (from the EMEP measurement sites) are plotted on top of the modelled data as triangles. Only measurement sites located below 500 metres above sea level are included, in order to avoid uncertainties related to the extraction of model data in regions with complex topography. As shown in Figure 2.10, the agreement between modelled and measured ozone metrics is generally good.

AOT40 (especially using the Mapping Manual definition) has been used as an indicator of ozone damage to vegetation in the past. A clear advantage of this metric is that model calculated levels can be be compared to measurements. However, this parameter does not necessarily reflect the actual damage to crops. As a result, the preferred metric in recent years has been phyto-toxic ozone dose, POD. For POD_1 the limit value depends on the species. For the generic IAM_DF ecosystem used here, the critical level is 5.7 mmole O_3 m^{-2} (PLA) s^{-1}, and this is exceeded almost everywhere. POD calculates the actual flux of ozone into the plants, by taking into account soil moisture deficit and other environmental factors. To control their water balance, plants regulate their stomata opening depending on the soil moisture. In dry conditions the plants tend to close the stomata opening, effectively also limiting the uptake of ozone. This is believed to give a more accurate description of how and when plants are damaged by ozone (Simpson et al. 2007, Mills et al. 2011, 2018). A disadvantage of POD is that it cannot be verified by routine measurements.

Whereas EU-AOT40f shows an increasing gradient from north to south, the pattern for POD is mixed, reflecting that POD levels depend on the additional parameters described above in addition to the ozone levels.

Figure 2.11 shows MDmaxO3 (top) and $MDA8_{AS}$ (bottom) where MDmaxO3 is the mean of the daily max ozone concentration and $MDA8_{AS}$ is the mean of the maximum daily 8-hour mean ozone concentrations, both for the 6-month period April-September. Model calculated MDmaxO3 have been supplemented by measurements at EMEP stations, shown as triangles, including only data from measurement sites below 500 m above sea level. The agreement between modelled and measured MDmaxO3 is generally good. For both MDmaxO3 and $MDA8_{AS}$ there are marked gradients from north to south as expected, which reflects the strong dependency between surface ozone, temperature and solar radiation.

The parameter $MDA8_{AS}$ is linked to the air quality recommendations set by WHO (WHO 2021). WHO's Air Quality Guideline (AQG) for long-term ozone exposure is set at 60 µg m^{-3}, and Figure 2.11 indicates that the AQG was broken over the entire domain in 2021. It should be said that the AQG is very low compared to other guideline values and close to the levels seen in truly remote areas. Evaluations have shown that it is not likely that the AQG will be met unless very strict emission abatement regimes are introduced globally. This was discussed in a presentation by Dick Derwent at the 2023 TFMM (see `https://projects.nilu.no/ccc/tfmm/`). Thus European emission abatement alone is probably not sufficient to meet this criteria. In addition to this long-term target, WHO has introduced interim and target values for the short-term exposure that are linked to the annual 99 percentile of MDA8. These values are, however, not discussed here.

2.4.3 Deposition of sulfur and nitrogen

Modelled total depositions of sulfur and oxidised and reduced nitrogen are presented in Figure 2.12. For sulfur, many hot spots are found in the south-eastern part of the domain. In addition, volcanic emissions of SO_2 lead to high depositions in and around Sicily, and the Fagradalsfjall eruption in 2021 in Iceland (see Ch 3.6) resulted in high SO_2 emissions and depositions especially in and around Iceland.

Oxidised nitrogen depositions are highest in northern Germany, the Netherlands, Belgium, Poland and northern Italy. These countries also have high depositions of reduced nitrogen, as do parts of the United Kingdom, France and Belgium in western Europe, and Türkiye, Georgia, Armenia, Azerbaijan and Kyrgyzstan in the east.

In Figure 2.13 wet depositions of nitrogen and sulfur compounds are compared to measurements at EMEP sites for 2021. Overall, the bias of the model with respect to measurements of wet depositions are around -30% to +15% (see Appendix D), but higher for individual sites. A more detailed comparison between model and measurements for the year 2021 can be found at `https://aeroval.met.no/evaluation.php?project=emep&exp_name=2023-reporting`.

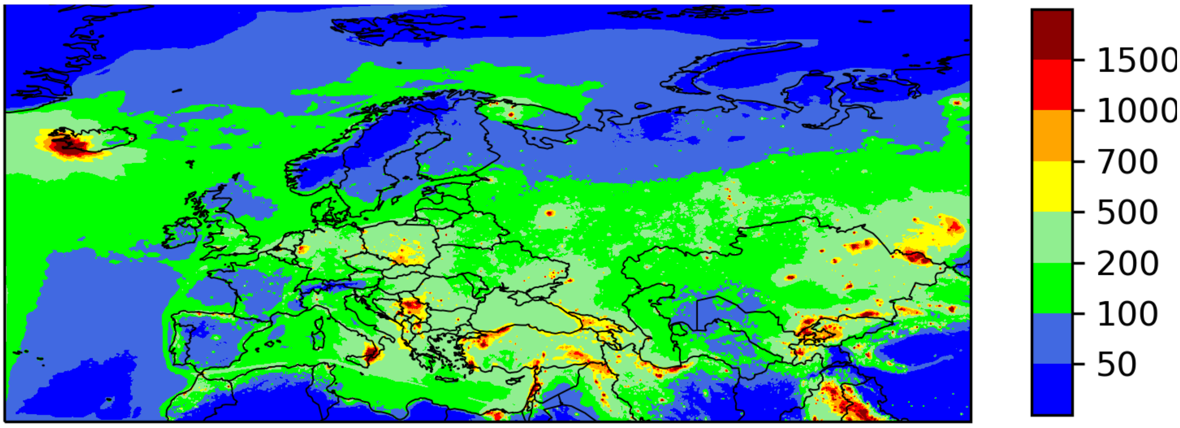

(a) oxidized S

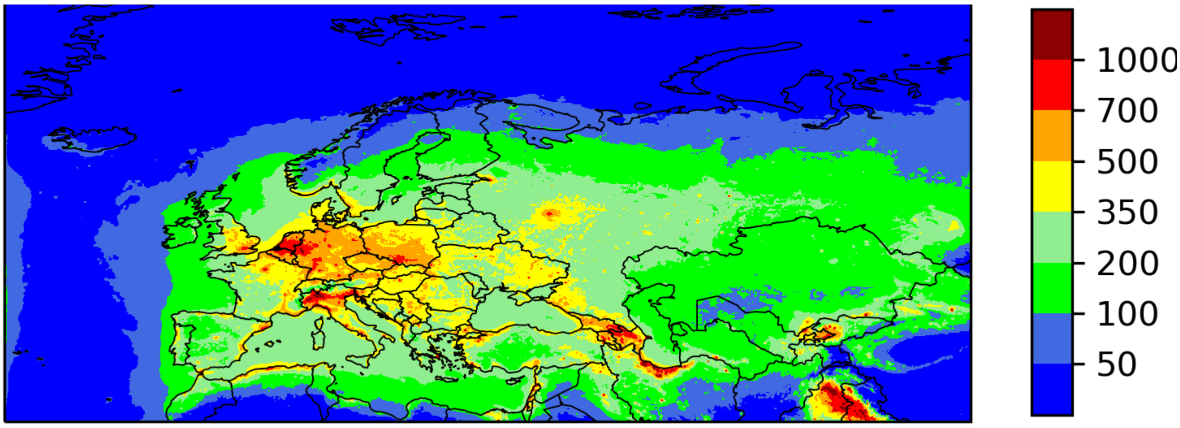

(b) oxidized N

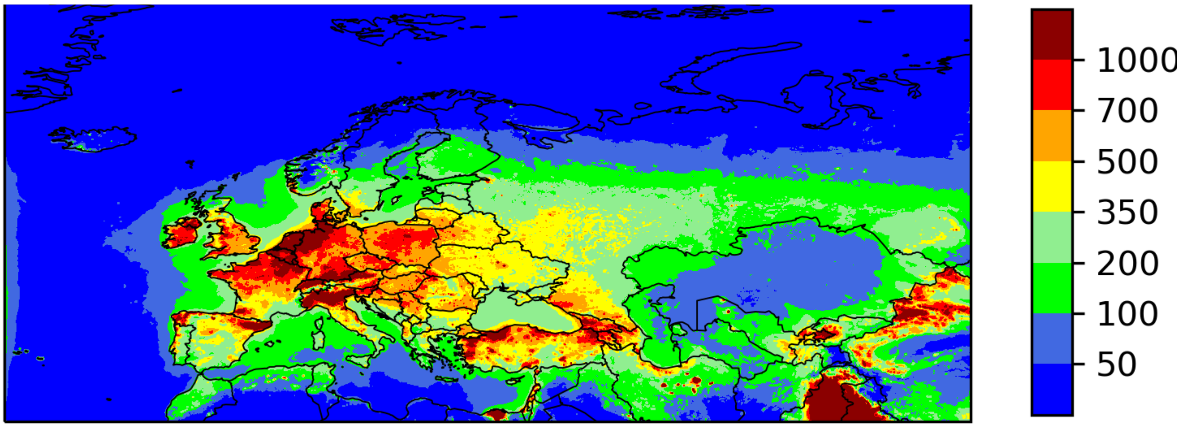

(c) Reduced N

Figure 2.12: Deposition of sulfur and nitrogen (mg(S)m^{-2}, mg(N)m^{-2}) in 2021.

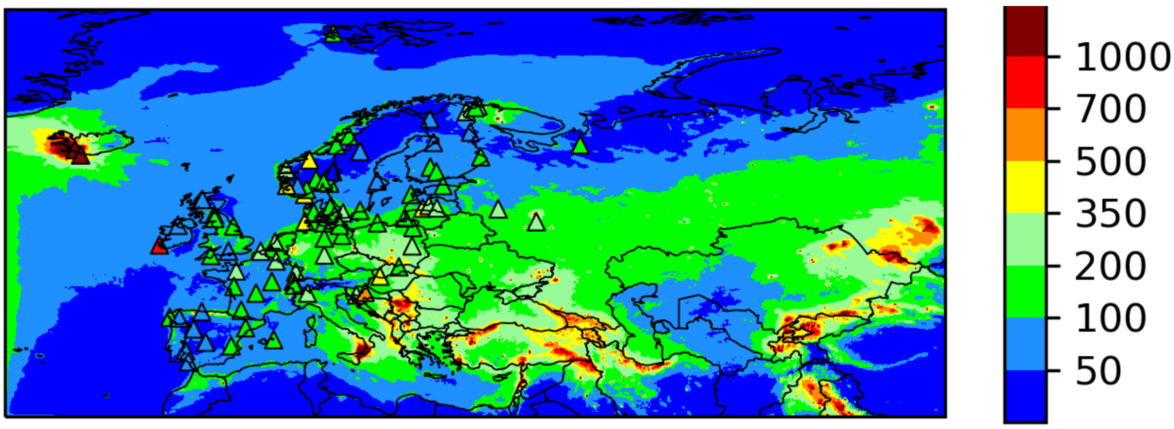

(a) oxidized S

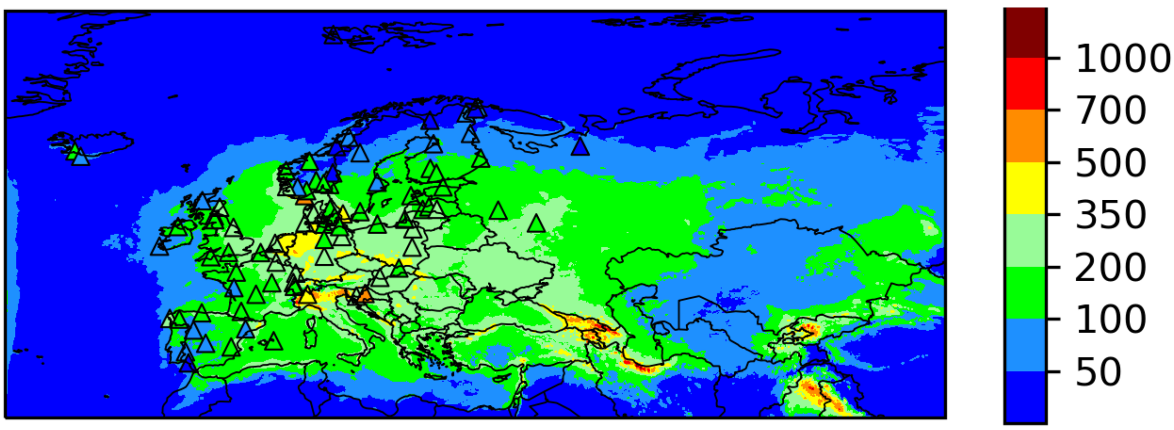

(b) oxidized N

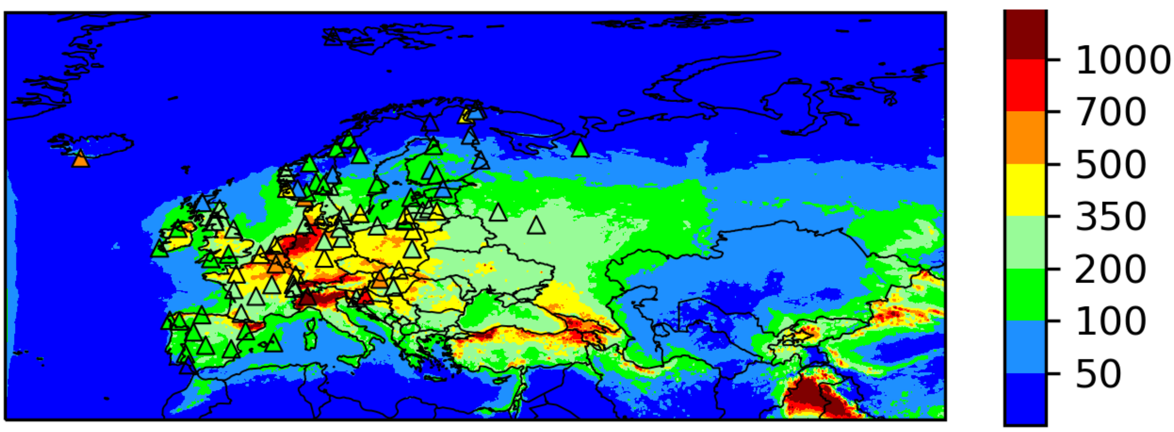

(c) Reduced N

Figure 2.13: Modelled wet deposition of sulfur and nitrogen (mg(S)m^{-2}, mg(N)m^{-2}) in 2021, with EMEP observations on top (marked by triangles).

2.4.4 Exceedances of critical loads of acidification and eutrophication

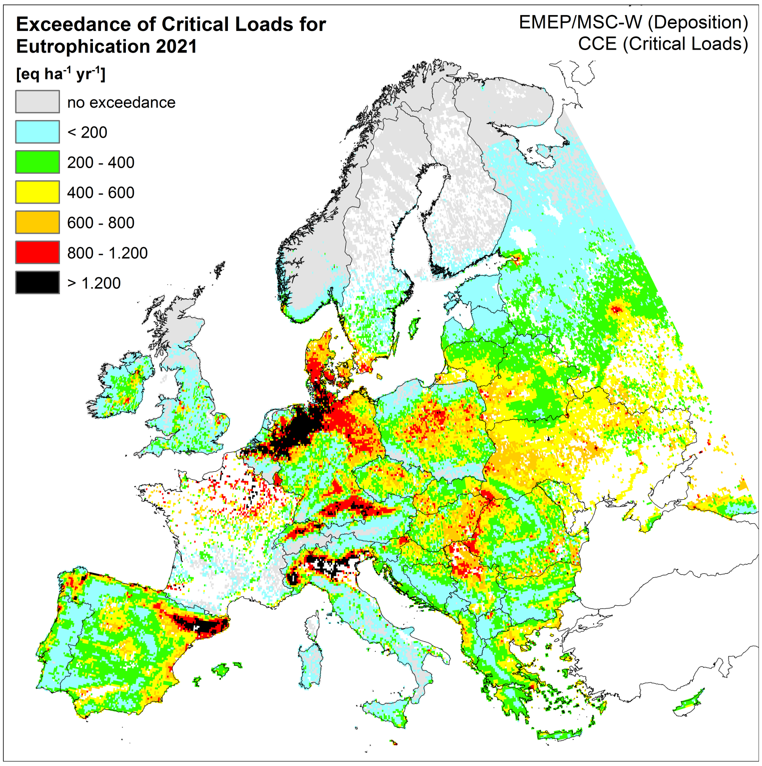

Figure 2.14: Exceedance of Critical Load for Eutrophication for the year 2021.

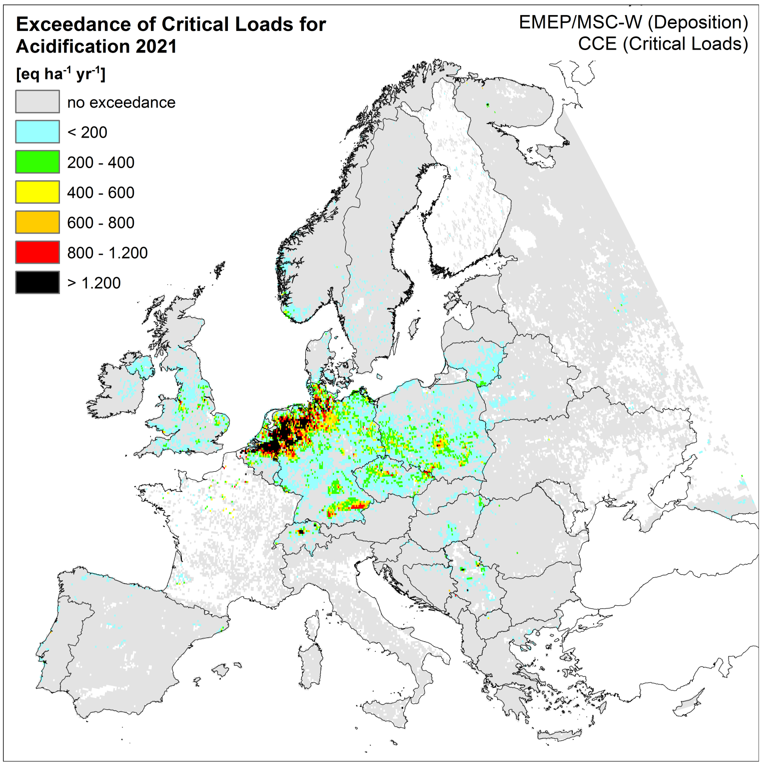

Figure 2.15: Exceedance of Critical Load for Acidification for the year 2021.

The exceedances of European critical loads (CLs) are computed for the total nitrogen (N) and sulphur (S) depositions modelled on the 0.1°× 0.1° longitude-latitude grid (approx. 11.12 x 5.56 km^2 at 60°N). Exceedances are calculated for the European critical loads documented in Geupel et al. (2022), while a description of the methods is given in De Vries et al. (2015). The critical loads data for eutrophication by N (CL eut N) and for acidification by N and S (CL acid) are also used by the EMEP Centre CIAM (located at IIASA) in their integrated assessment modelling. The exceedance in a grid cell is the so-called 'average accumulated exceedance' (AAE), which is calculated as the area-weighted average of the exceedances of the critical loads of all ecosystems in this grid cell. The units for critical loads and their exceedances are equivalents (eq; same as *moles of charge*, molc) per area and time, making S and N depositions comparable on their impacts, which is important for acidity CLs.

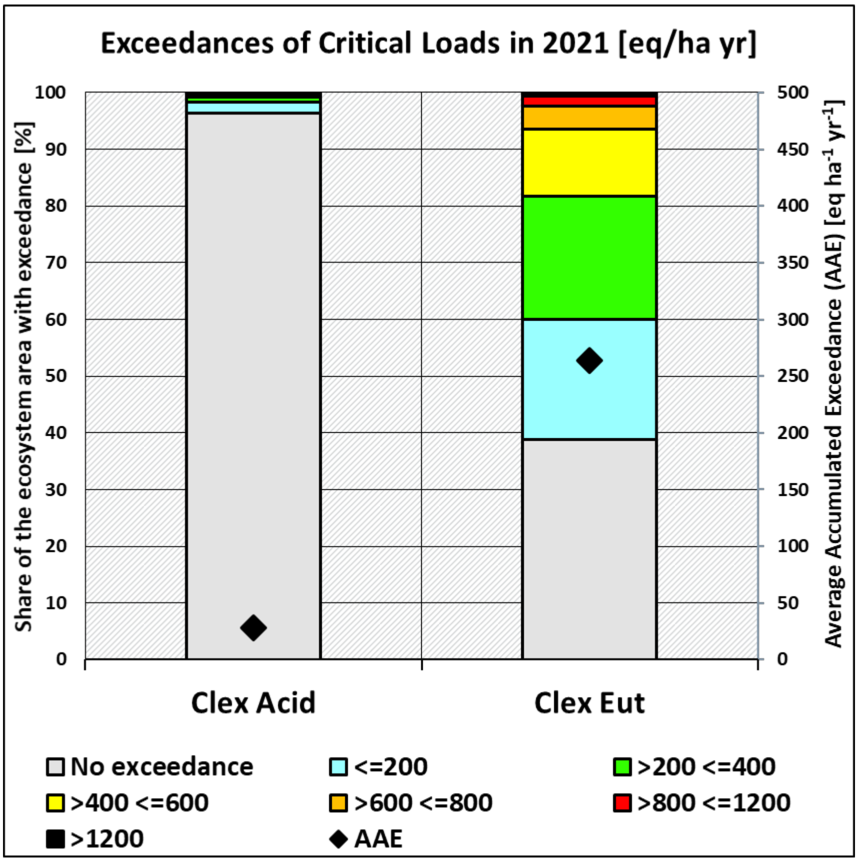

Figure 2.16: Overall statistics for Exceedance of Critical Load for Eutrophication (CLex Eut) and Acidification (CLex Acid).

Critical loads are available for about 4 million ecosystems in Europe covering an area of about 3 million km^2 (west of 42°E). The exceedances (AAE) of those critical loads are computed on a 0.1°× 0.1° longitude-latitude grid, and maps for these exceedances based on the modelled deposition in the year 2021 are shown in Figures 2.14 and 2.15. As indicated in the maps, the critical loads for eutrophication are exceeded in practically all countries. The share of ecosystems where the critical load for eutrophication is exceeded is 61.2% in 2021. European average AAE in the year 2021 is about 264 eq ha^{-1} yr^{-1}. The highest exceedances of CLs are found in the Po Valley in Italy, the Dutch-German-Danish border areas and in north-eastern Spain. By contrast, critical loads of acidity are exceeded in a much smaller area.

Hot spots of exceedances can be found in the Netherlands and its border areas to Germany and Belgium, and some smaller maxima in southern Germany and Czechia, whereas most of Europe is not exceeded (grey areas). Acidity exceedances in the year 2021 occur on 3.6% of the ecosystem area, and the European average AAE is about 28 eq ha^{-1} yr^{-1}. Overall statistics for the share of critical load exceedance and European average of AAE are shown in Figure 2.16.

2.4.5 Model calculations for 2022

Preliminary model calculations for 2022 have been performed. The meteorological data for the 2022 model run has been generated by the ECMWF-IFS model, using the IFS Cycle 48r1 version, which is a newer version compared to the one used in the 2021 model runs (as described in Ch 2.1). The emission data from anthropogenic sources is the same as in the 2021 status run (EMEPwRef2_v2.1C). For forest fires monthly averages for the period 2010-2020 were calculated using FINN version 2.5, based on MODIS data (see Ch 9.2.1). The EMEP MSC-W model version is the same as used for 2021 runs (rv5.0).
The model results are available the EMEP webpage (`http://www.emep.int`). No analysis of the 2022 results has been attempted here, as the EMEP measurement data are not available until spring 2024.

2.4.6 Model calculations for 1990–2021

A trend simulation has been performed for the 32-year period 1990–2021. The run for the year 2021 is identical to this year's status run (Ch 2.3). For more details on the trend simulation see Appendix F).

References

Ballinger, T. J., Overland, J. E., Wang, M., Bhatt, U. S., Brettschneider, B., Hanna, E., Hanssen-Bauer, I., Kim, S. J., Thoman, R. L., and Walsh, J. E.: Surface Air Temperature, in Arctic Report Card 2021, NOAA, NOAA Arctic Report Card 2021, DOI: 10.25923/53xd-9k68, 2021.

De Vries, W., Hettelingh, J.-P., and Posch, M.: Critical Loads and Dynamic Risk Assessments: Nitrogen, Acidity and Metals in Terrestrial and Aquatic Ecosystems, doi:10.1007/978-94-017-9508-1, Environmental Pollution Series Vol. 25, Springer, Dordrecht, xxviii+662 pp.; ISBN 978-94-017-9507-4, 2015.

Dunn, R. J. H., Aldred, F., Gobron, N., Miller, J. B., and K. M. Willett, E.: Global Climate [in “State of the Climate in 2021“]., 2022.

Geupel, M., Loran, C., Scheuschner, T., and Wohlgemuth, L.: CCE Status Report, URL https://www.umweltbundesamt.de/en/publikationen/cce-status-report-2022, 2022.

Granier, C., Darras, S., Denier van der Gon, H., Doubalova, J., Elguindi, N., Galle, B., Gauss, M., Guevara, M., Jalkanen, J.-P., Kuenen, J., Liousse, C., Quack, B., Simpson, D., and Sindelarova, K.: The Copernicus Atmosphere Monitoring Service global and regional emissions (April 2019 version), doi:10.24380/d0bn-kx16, URL https://atmosphere.copernicus.eu/sites/default/files/2019-06/cams_emissions_general_document_apr2019_v7.pdf, 2019.

Guevara, M., Jorba, O., Tena, C., Denier van der Gon, H., Kuenen, J., Elguindi, N., Darras, S., Granier, C., and Pérez García-Pando, C.: Copernicus Atmosphere Monitoring Service TEMPOral profiles (CAMS-TEMPO): global and European emission temporal profile maps for atmospheric chemistry modelling, Earth System Science Data, 13, 367–404, doi:10.5194/essd-13-367-2021, URL https://essd.copernicus.org/articles/13/367/2021/, 2021.

Guevara, M., Petetin, H., Jorba, O., Denier van der Gon, H., Kuenen, J., Super, I., Jalkanen, J.-P., Majamäki, E., Johansson, L., Peuch, V.-H., and Pérez García-Pando, C.: European primary emissions of criteria pollutants and greenhouse gases in 2020 modulated by the COVID-19 pandemic disruptions, Earth System Science Data, 14, 2521–2552, doi:10.5194/essd-14-2521-2022, URL https://essd.copernicus.org/articles/14/2521/2022/, 2022.

Hjellbrekke, A.-G.: Data Report 2021 Particulate matter, carbonaceous and inorganic compounds, Tech. Rep. EMEP/CCC Report 1/2023, NILU, Kjeller, Norway, 2023.

Hjellbrekke, A.-G. and Solberg, S.: Ozone measurements 2021, Tech. Rep. EMEP/CCC Report 2/2023, NILU, Kjeller, Norway, 2023.

Mills, G., Pleijel, H., Braun, S., Büker, P., Bermejo, V., Calvo, E., Danielsson, H., Emberson, L., Grünhage, L., Fernández, I. G., Harmens, H., Hayes, F., Karlsson, P.-E., and Simpson, D.: New stomatal flux-based critical levels for ozone effects on vegetation, Atmos. Environ., 45, 5064 – 5068, doi:10.1016/j.atmosenv.2011.06.009, 2011.

Mills, G., Sharps, K., Simpson, D., Pleijel, H., Broberg, M., Uddling, J., Jaramillo, F., Davies, William, J., Dentener, F., Berg, M., Agrawal, M., Agrawal, S., Ainsworth, E. A., Büker, P., Emberson, L., Feng, Z., Harmens, H., Hayes, F., Kobayashi, K., Paoletti, E., and Dingenen, R.: Ozone pollution will compromise efforts to increase global wheat production, Global Change Biol., 24, 3560–3574, doi:10.1111/gcb.14157, URL https://onlinelibrary.wiley.com/doi/abs/10.1111/gcb.14157, 2018.

Otero, N., Sillmann, J., Schnell, J. L., Rust, H. W., and Butler, T.: Synoptic and meteorological drivers of extreme ozone concentrations over Europe, Environmental Research Letters, 11, 024 005, doi:10.1088/1748-9326/11/2/024005, URL https://doi.org/10.1088/1748-9326/11/2/024005, 2016.

Schindlbacher, S., Ullrich, B., and Wankmüller, R.: Inventory review 2023. Review of emission data reported under the LRTAP Convention. Stage 1 and 2 review. Status of gridded and LPS data, EMEP/CEIP Technical Report 4/2023, CEIP Vienna, 2023.

Simpson, D., Emberson, L., Ashmore, M., and Tuovinen, J.: A comparison of two different approaches for mapping potential ozone damage to vegetation. A model study, Environ. Poll., 146, 715–725, doi:10.1016/j.envpol.2006.04.013, 2007.

Simpson, D., Kuenen, J., Fagerli, H., Heinesen, D., Benedictow, A., Denier van der Gon, H., Visschedijk, A., Klimont, Z., Aas, W., Lin, Y., Yttri, K. E., and Paunu, V.-V.: Revising $PM_{2.5}$ emissions from residential combustion, 2005–2019. Implications for air quality concentrations and trends, Temanord 2022:540, Nordic Council of Ministers, doi:10.6027/temanord2022-540, URL https://pub.norden.org/temanord2022-540, 2022.

Solberg, S., Hov, Ø., Søvde, A., Isaksen, I. S. A., Coddeville, P., De Backer, H., Forster, C., Orsolini, Y., and Uhse, K.: European surface ozone in the extreme summer 2003, Journal of Geophysical Research: Atmospheres, 113, doi:https://doi.org/10.1029/2007JD009098, URL https://agupubs.onlinelibrary.wiley.com/doi/abs/10.1029/2007JD009098, 2008.

UNECE: Monitoring strategy for the Cooperative Programme for Monitoring and Evaluation of the Long-range Transmission of Air Pollutants in Europe for the period 2020–2029, Tech. Rep. ECE/EB.AIR/144/Add.1, UNECE, URL https://www.unece.org/fileadmin/DAM/env/documents/2019/AIR/EB_Decisions/Decision_2019_1.pdf, 2019.

WHO: Air quality guidelines. Global update 2005. Particulate matter, ozone, nitrogen dioxide and sulfur dioxide, URL http://www.who.int/phe/health_topics/outdoorair/outdoorair_aqg/en/, World Health Organisation, European Centre for Environment and Health Bonn Office, ISBN 92 890 2192, 2005.

WHO: WHO global air quality guidelines. Particulate matter ($PM_{2.5}$ and PM_{10}), ozone, nitrogen dioxide, sulfur dioxide and carbon monoxide., URL https://www.who.int/publications/i/item/9789240034228, World Health Organisation, European Centre for Environment and Health Bonn Office, ISBN 978-92-4-003422-8 (electronic version), 2021.

Wiedinmyer, C., Akagi, S. K., Yokelson, R. J., Emmons, L. K., Al-Saadi, J. A., Orlando, J. J., and Soja, A. J.: The Fire INventory from NCAR (FINN): a high resolution global model to estimate the emissions from open burning, Geoscientific Model Dev., 4, 625–641, doi:10.5194/gmd-4-625-2011, 2011.

WMO: WMO Statement on the State of the Global Climate in 2021, WMO-No. 1290, https://public.wmo.int/en/resources/library, ISBN 978-92-63-11290-3, 2022.

Zhang, J., Gao, Y., Luo, K., Leung, L. R., Zhang, Y., Wang, K., and Fan, J.: Impacts of compound extreme weather events on ozone in the present and future, Atmospheric Chemistry and Physics, 18, 9861–9877, doi:10.5194/acp-18-9861-2018, URL https://acp.copernicus.org/articles/18/9861/2018/, 2018.

CHAPTER 3

Emissions for 2021

Bradley Matthews, Sabine Schindlbacher, Bernhard Ullrich, Robert Wankmüller (CEIP/ Umweltbundesamt Austria), Jeroen Kuenen (TNO) and Ágnes Nyíri (MSC-W)

In addition to meteorological variability, changes in the emissions affect the inter-annual variability and trends of air pollution, deposition and transboundary transport. The main changes in emissions in 2020 with respect to previous years are documented in the following sections.

The EMEP Reporting guidelines (UNECE 2014) requests all Parties to the Unece Air Convention to annually report emissions of air pollutants (SO_x[1], NO_2[2], CO, NMVOCs[3], NH_3, HMs, POPs, PM[4] and voluntary BC) and associated activity data. Projection data, gridded data and information on large point sources (LPS) have to be reported to the EMEP Centre on Emission Inventories and Projections (CEIP) every four years. Note that the recent 2022 adoption of the updated Guidelines for Reporting Emissions and Projections Data under the Convention on Long-range Transboundary Air Pollution (Executive Body Decisions 2022/1 and 2022/2) will be relevant for reporting in the years from 2024 onwards.

[1]"sulfur oxides (SO_x)" means all sulfur compounds, expressed as sulfur dioxide (SO_2), including sulfur trioxide (SO_3), sulfuric acid (H_2SO_4), and reduced sulfur compounds, such as hydrogen sulfide (H_2S), mercaptans and dimethyl sulfides, etc.

[2]"Nitrogen oxides (NO_x)" means nitric oxide and nitrogen dioxide, expressed as nitrogen dioxide (NO_2).

[3]"Non-methane volatile organic compounds" (NMVOCs) means all organic compounds of an anthropogenic nature, other than methane, that are capable of producing photochemical oxidants by reaction with nitrogen oxides in the presence of sunlight.

[4]"Particulate matter" (PM) is an air pollutant consisting of a mixture of particles suspended in the air. These particles differ in their physical properties (such as size and shape) and chemical composition. Particulate matter refers to:
(i) "$PM_{2.5}$", or particles with an aerodynamic diameter equal to or less than 2.5 micrometers (μm);
(ii) "PM_{10}", or particles with an aerodynamic diameter equal to or less than 10 μm.

3.1 Reporting of emission inventories in 2023

Completeness and consistency of submitted data have improved significantly since EMEP started collecting information on emissions. Data of at least 46 Parties each year were submitted to CEIP since 2016 (see Figure 3.1). In 2023 (as of 1 June 2023), 46 Parties (90%) submitted inventories[5], five Parties[6] did not submit any data and 40 Parties reported black carbon (BC) emissions for at least one year in the time series (see Ch 3.2). While the number of timely submissions has been increasing, it is worth noting the small, yet recent increase in missing submissions (five missing submissions in 2023 compared to three missing submissions in 2021). The year 2023 is not an obligatory reporting year for large point sources (LPS) and gridded emissions. Nevertheless, three Parties reported information on LPS and four Parties reported gridded data (Schindlbacher et al. 2023).

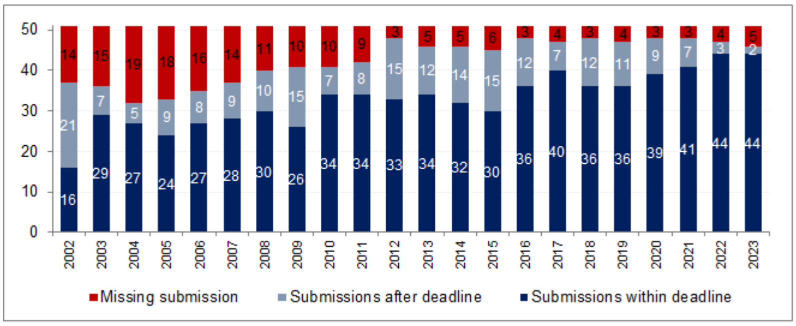

Figure 3.1: Parties reporting emission data to EMEP since 2002, as of 1 June 2023.

The quality of the submitted data across countries differs quite significantly. By compiling the inventories, countries have to use the newest available version of the *EMEP/EEA air pollutant emission inventory guidebook*, currently the 2019 version (EMEP/EEA 2019), which most countries do for most emission sources. As analysed in a technical report (Schindlbacher et al. 2021), uncertainty of the reported data (national totals, sectoral data) is relatively high, e.g. the reported uncertainty estimates range from 6.9% to 56% for NO_x emissions reported in 2020. Furthermore, the completeness, accuracy and comparability issues continue to be identified in the annual reviews.

More detailed information on recalculations, completeness and key categories, plus additional review findings can be found in the annual CEIP review reports[7].

Indeed, the issue of recalculations is highly relevant to users of EMEP emissions data sets. The aforementioned CEIP report on uncertainties in reported emissions highlighted how time series of reported emissions can vary significantly over subsequent rounds of submissions due to, inter alia, revisions in activity data, updates of methods and emissions factors and/or inclusion of previously overlooked sources of emissions (Schindlbacher et al. 2021).

The following sections summarise the inventory submissions in terms of three topics that are currently of high interest within the Convention:

- Reporting of black carbon emissions (Ch 3.2)

[5]The original submissions from the Parties can be accessed via the CEIP homepage on https://www.ceip.at/status-of-reporting-and-review-results/2023-submissions.

[6]Azerbaijan, Bosnia and Herzegovina, Croatia, Kyrgyzstan and Republic of Moldova

[7]https://www.ceip.at/review-of-emission-inventories/technical-review-reports

- Inclusion of the condensable component in particulate matter emissions (Ch 3.3)

- Comparison of reported Party emissions to respective reduction targets set out in the Gothenburg Protocol (Ch 3.4)

3.2 Black Carbon (BC) emissions

Over the last decade, black carbon (BC) has emerged as an important air pollutant in terms of both climate change and air quality.

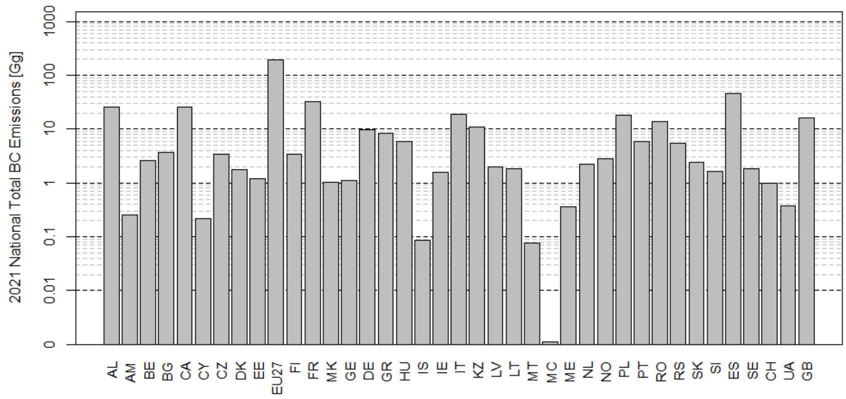

Figure 3.2: Black carbon emissions for the year 2021 as reported by CLRTAP Parties.

The emerging significance of BC is mirrored in developments in the international policy arena with respect to emissions reporting. Since the Executive Body Decision 2013/04, Parties to the LRTAP Convention have been formally encouraged to submit inventory estimates of their national BC emissions, and in 2015 the reporting templates were updated to include BC data emissions.

While BC is not a mandatory pollutant to be reported under the Convention, CEIP continues to monitor and review the level of BC reporting by the Convention's Parties. A brief overview of BC emissions estimates submitted by Parties in 2023 is given below.

Since enabling the reporting of BC, a total of 45 CLRTAP Parties have reported BC emissions estimates[8]. In this round of reporting, 29 CLRTAP Parties submitted a complete time series of national total BC emissions (1990-2020), while 37 CLRTAP Parties submitted a complete time series from 2000 onwards. Furthermore, 39 EMEP Parties have provided national total BC emissions estimates for the year 2021 (see Figure 3.2), while 420 Parties provided a national total emissions estimate for at least one year of the time series.

For more detailed information on BC one can consult the annual CEIP technical inventory review report (Schindlbacher et al. 2023).

[8]As of 1 June 2023 Austria, Bosnia and Herzegovina, Liechtenstein, Luxembourg, Russia and Türkiye have yet to report estimates of national BC emissions.

3.3 Inclusion of the condensable component in reported PM emissions

The condensable component of particulate matter is a class of organic compounds of low volatility that may exist in equilibrium between the gas and particle phase. It is probably the biggest single source of uncertainty in PM emissions. For more background information see Simpson et al. (2020). Currently the condensable component is not included or excluded consistently in PM emissions reported by Parties of the LRTAP Convention. Also in the EMEP/EEA Guidebook (EMEP/EEA 2019) the condensable fraction is not consistently included or excluded in the emission factors; however, much improvement has been made in the last update of the Guidebook. Various EMEP centres and task forces and other stakeholders jointly discuss the topic and work on progress in this area. An important activity in 2020 was the workshop organised by MSC-W that resulted in a comprehensive report by Simpson et al. (2020). However, at the moment PM emissions reported by Parties to the LRTAP Convention are not directly comparable, which has implications on the modeling of overall exposure to PM.

Small scale combustion sources make a notable contribution to total PM emissions. For all Parties that reported $PM_{2.5}$ emissions for "1A4bi Residential: Stationary" for the year 2021 the average contribution to the national total $PM_{2.5}$ emissions from this source category was 47%. Small-scale combustion is one of the sources where the inclusion of the condensable component has the largest impact on the emission factor. For example, for conventional woodstoves, one of the most important categories in Europe, the emission factors excluding and including the condensable fractions may differ by up to a factor of five (Denier van der Gon et al. 2015). To improve the quality of the input data for air quality models, and following a decision of UNECE (2020), the group of experts that met at the workshop organised by MSC-W agreed on the following approach (for more details see Simpson et al. (2020)):

- In year one (which was 2020) the Ref2 emission data provided by TNO, which include condensable organics, are used in an initial estimate for residential combustion emissions.

- In subsequent years these top-down estimates should be increasingly replaced by national estimates once procedures for quantifying condensables in a more harmonized way are agreed on and implemented. Also, where replacement is necessary, the latest available version of the Ref2 type estimates should be used.

In 2022, CEIP organised an ad hoc review dedicated to the topic "condensable component of PM emissions". Twenty-one experts participated in this review. For all Parties that had provided an informative inventory report, the residential heating and road transport sectors were reviewed, with a special focus on the condensable component of particulate matter (PM) emissions. Based on the outcome of the review a list of Parties was prepared, where the conclusion was that the PM emission data reported by the Party should be used as the condensable component seemed to be included for $PM_{2.5}$ emissions from GNFR sector C. This list was updated based on recalculations, comparison with the data from TNO Ref2 and information provided by Parties in their informative inventory reports in 2023. For other Parties updated TNO Ref2 emission data was used, or if no TNO Ref2 estimates were available, gap-filled data by CEIP was used (see Table 3.1).

Table 3.1: Data source for PM emissions in GNFR C used in the EMEP status runs and source-receptor calculations in 2023 (EMEPwRef2_v2.1C data set).

Party Name	Data source for PM emission in GNFR C	Party Name	Data source for PM emission in GNFR C
Albania	CEIP - gap-filled	Latvia	CEIP - reported by Party
Armenia	CEIP - gap-filled	Liechtenstein	CEIP - gap-filled
Austria	REF2	Lithuania	REF2
Azerbaijan	CEIP - gap-filled	Luxembourg	REF2
Belarus	REF2	Malta	CEIP - reported by Party
Belgium	CEIP - reported by Party	Monaco	CEIP - reported by Party
Bosnia and Herzegovina	REF2	Montenegro	REF2
Bulgaria	CEIP - reported by Party	Netherlands	CEIP - reported by Party
Croatia	CEIP - gap-filled	North Macedonia	CEIP - reported by Party
Cyprus	CEIP - reported by Party	Norway	CEIP - reported by Party
Czechia	CEIP - reported by Party	Poland	CEIP - reported by Party
Denmark	CEIP - reported by Party	Portugal	CEIP - reported by Party
Estonia	REF2	Republic of Moldova	REF2
Finland	CEIP - reported by Party	Romania	CEIP - reported by Party
France	CEIP - reported by Party	Russian Federation	REF2/CEIP
Georgia	REF2	Serbia	CEIP - reported by Party
Germany	REF2	Slovakia	CEIP - reported by Party
Greece	CEIP - reported by Party	Slovenia	CEIP - reported by Party
Hungary	CEIP - reported by Party	Spain	CEIP - reported by Party
Iceland	CEIP - reported by Party	Sweden	CEIP - reported by Party
Ireland	CEIP - reported by Party	Switzerland	REF2
Italy	CEIP - reported by Party	Türkiye	CEIP - gap-filled
Kazakhstan	REF2/CEIP	Ukraine	REF2
Kyrgyzstan	CEIP - gap-filled	United Kingdom	CEIP - reported by Party

The Ref2 data set which was used in 2023 is described in Section 3.3.1. In this report, the emission data set which combines Ref2 (version v2.1) estimates for $PM_{2.5}$ from GNFR C with EMEP estimates is referred to as the EMEPwRef2_v2.1C data set (see Appendix A).

3.3.1 Ref2 emissions and changes compared to last year's Ref2 data

The Ref2 emission inventory provides a bottom-up database of PM emissions (both PM_{10} and $PM_{2.5}$) from small combustion activities (GNFR category C), taking into account activity data and consistent emission factors that include condensables, for both wood and solid fuel combustion. It was originally developed for the year 2010 (Denier van der Gon et al. 2015) and updated in full in 2022 (Simpson et al. 2022). Residential emissions vary from year to year, because of technological developments in the sector (replacement of stoves and boilers) but also because of changes in heating demand due to fluctuating temperatures.

The most recent Ref2 emission data set as described in Simpson et al. (2022) covers the years 2005-2019 but it has recently been extrapolated to cover also the year 2021 and 2022 in the framework of the Copernicus Atmospheric Monitoring Service (CAMS), in order to provide the air quality forecasting services provided in CAMS with the most up-to-date emissions available. This data set is referred to as Ref2_v2.1 in this report.

The methodology for extrapolating the emissions to 2021/2022 include:

- Activity data are collected which can be used to represent the trend in the activity (e.g. energy consumption), if not available an alternative data set is used for which the trend is expected to be representative for the trend in activity data.

- For the most important sources, trends in emissions and activity are compared, from which trends in emission factors are derived.

For small combustion, the methodology uses heating degree days to predict the activity data (heating demand) for the year 2021. By comparing historical trends in heating degree days and emissions, a trend in the emission factor is derived which is extrapolated to 2021. This trend is a slightly decreasing one, representing the renewal of the fleet of stoves and boilers, where newer ones typically have lower emissions.

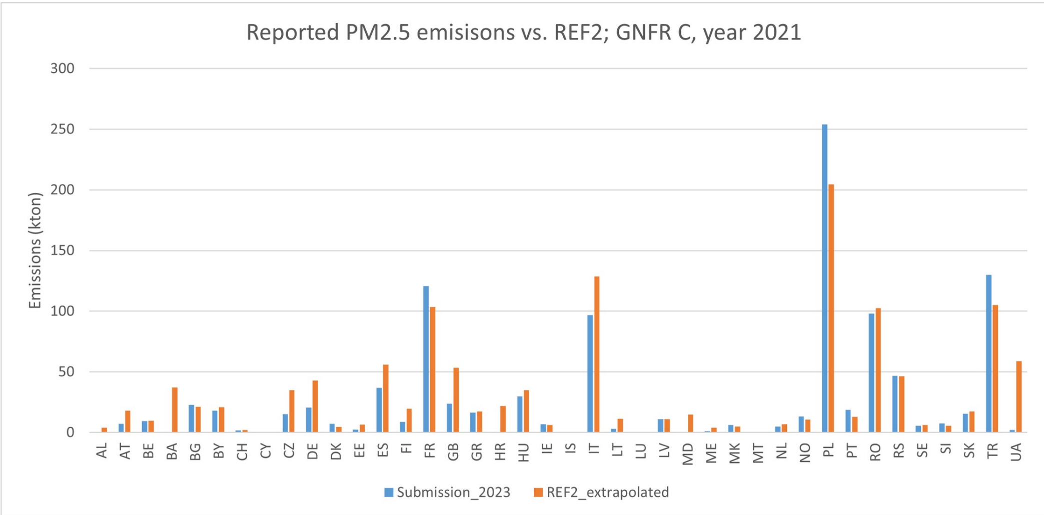

Figure 3.3: $PM_{2.5}$ emissions reported by Parties compared to the $PM_{2.5}$ emisisons as estimated in the extrapolated Ref2_v2.1 inventory for 2021 (GNFR C sector only).

Figure 3.3 shows a comparison between the extrapolated Ref2_v2.1 emissions for 2021 and the official reported emissions for each Party, for $PM_{2.5}$ emissions from GNFR category C. While for some countries the two inventories match well, for others the differences are large. These differences are mostly related to the inclusion of condensables, however since Ref2_v2.1 is an independent bottom-up emission inventory there are also other differences (e.g. fuel use, appliance types, emission factors).

3.4 Gothenburg Protocol targets

The amended Protocol to Abate Acidification, Eutrophication and Ground-level Ozone (Gothenburg Protocol) entered into force on 7 October 2019. Tables 2–6 of Annex II to the amended Protocol[9] set out the emission reduction commitments for SO_x, NO_x, NH_3, NMVOCs and $PM_{2.5}$ for 2020 and beyond, expressed as percentage reductions from the 2005 emission level. Of the thirty-four Parties that are currently listed in Tables 2–6, twenty-seven

[9] https://unece.org/sites/default/files/2021-10/Annex_II_and_III_updated_clean.pdf

have already ratified the amended Gothenburg Protocol. Greece ratified the Gothenburg Protocol in 2023.

In 2012, the Executive Body of the LRTAP Convention decided that adjustments to inventories may be applied in some circumstances (UNECE (2012)). In 2023, Denmark, France, the Netherlands and the United Kingdom have submitted adjustment applications, which had been accepted by the expert review teams in 2022. These adjustments were subtracted for the respective countries when compared with the targets in the figure below.

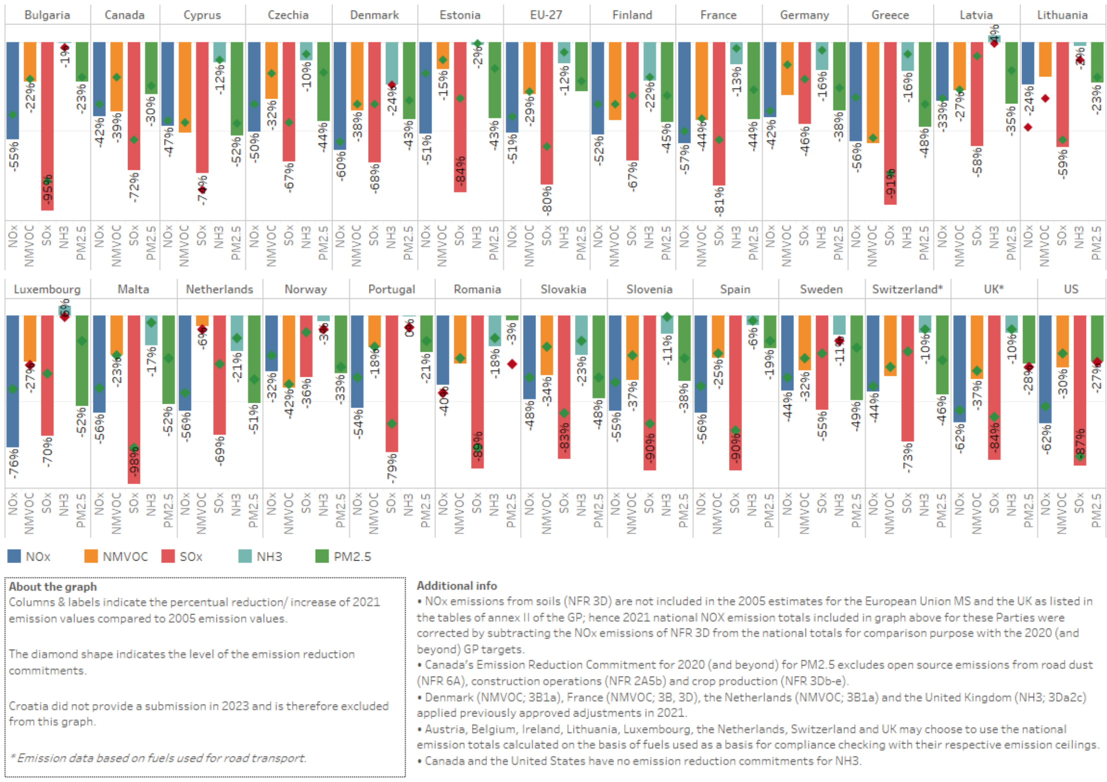

Figure 3.4: National total emissions vs emission reduction commitments for the year 2021 (based on data reported in 2023). Only Parties that have ratified the Gothenburg Protocol and have submitted the required data are included.

Further, The Reporting Guidelines (UNECE (2014)) specify, that some Parties within the EMEP region (i.e. Austria, Belgium, Ireland, Lithuania, Luxembourg, the Netherlands, Switzerland and the United Kingdom of Great Britain and Northern Ireland) *may choose to use the national emission total calculated on the basis of fuels used* in the geographic area of the Party as a basis for compliance with their respective emission reduction commitments. In 2023, Belgium, Switzerland and the United Kingdom used fuel used in the geographic area of the Party as a basis for compliance with their respective emission ceilings.

Figure 3.4 indicates that in the year 2021 Lithuania and Romania could not reduce their NO_x emissions below their respective Gothenburg Protocol requirements. For NMVOC, Lithuania, Luxembourg and the Netherlands were not able to achieve a reduction below the commitment level, whilst Cyprus could not reach the target for SO_x. Bulgaria, Denmark, Latvia, Lithuania, Luxembourg, Norway, Portugal and Sweden are above their emission reduction commitments concerning NH_3. For $PM_{2.5}$, Romania, the United Kingdom and the United States could not reduce the emissions below the reduction commitment level.

3.5 Data sets for modellers 2023

Under the Convention, CEIP is responsible for synthesizing the reported emissions data of the EMEP countries into complete gridded emissions data sets for the EMEP domain (covering the geographic area between 30° N-82° N latitude and 30° W-90° E longitude. These data are mainly used for modelling of air pollutant concentrations and depositions.

To compile these data sets each year, CEIP synthesizes and evaluates the most recent national sectoral emissions estimates and national gridded emissions data reported by the EMEP countries. CEIP strives to include, to the largest possible extent, the reported emissions data it receives from EMEP countries. However, due to cases of non-reporting or identified quality issues in the reported data, emissions need to be gap-filled or replaced. Furthermore, it should be noted how gridded and sectoral emissions totals are combined in compiling these data sets. National gridded emissions data, even if reported annually, are not directly utilized but are rather used to map out relative emissions, with which national sector emission totals are spatially distributed. If for a given year both national sector emissions totals and gridded estimates reported by a given country pass through the CEIP QA/QC checks, the generated gridded emissions will be identical to the gridded emissions reported by the country. The following subchapters describe important aspects of the 2023 EMEP data sets, summarising:

- The status of reporting of national gridded emissions data and the extent to which these are used to distribute emissions spatially (Ch 3.5.1)
- The extent to which sectoral emissions were gap-filled or replaced (Ch 3.5.2)
- The sectoral contributions (Ch 3.5.3) and temporal trends (Ch 3.5.4) in the emissions of carbon monoxide, nitrogen oxides, sulfur oxides, ammonia, non-methane volatile organic carbons, and particulate matter including black carbon. Trends in shipping emissions are discussed separately (Ch 3.5.5).

3.5.1 Reporting of gridded data

After the first round of submissions in 2017, 2021 was the second year for which EMEP countries were obliged to report gridded emissions in the grid resolution of $0.1^\circ \times 0.1^\circ$ longitude/latitude. As of June 2023, 37 of the 48 countries which are considered to be part of the EMEP area reported sectoral gridded emissions in this resolution.

The majority of gridded sectoral emissions in $0.1^\circ \times 0.1^\circ$ longitude/latitude resolution have been reported for the year 2019 (34 countries) and for 2015 (33 countries). For 2016, 2017 and 2020 by five countries, for 2018 by four countries and for 2021 by three countries. Comparing to reporting in 2017, reported gridded data are available for 13 more countries in 2021. In 2022 one additional country and in 2023 no additional country was added.

Fifteen countries reported gridded emissions additionally for previous years (one country for the whole time series from 1980 to 2021; one country for the time series from 1990 to 2021; seven countries for the years 1990, 1995, 2000, 2005 and 2010; one country for the years 1990, 2000, 2005 and 2010; one country for the years 2000, 2005 and 2010; one country for the year 2005; one country for the year 2010; and three countries for the year 2014).

Reported gridded sectoral data in $0.1^\circ \times 0.1^\circ$ longitude/latitude resolution, which can be used for the preparation of gridded emissions for modelers, covers less than 25% of the cells within the geographic EMEP area. For the remaining areas (or for EMEP countries that have no reported gridded data) missing emissions are gap-filled and spatially distributed using independent estimates from global and regional emissions data sets. Reported grid data can be downloaded from the CEIP website[10]. The gap-filled gridded emissions are also available there[11].

An overview of gridded data in 0.1°×0.1° longitude/latitude resolution reported in 2017, 2021 and 2023 is provided in Table 3.2.

For compiling the 2023 EMEP emissions data set, reported gridded data in 0.1°×0.1° longitude-latitude resolution was used from the following EMEP countries: Austria, Belgium, Bulgaria, Croatia, Cyprus, Czechia, Denmark, Estonia, Finland, France, Georgia, Germany, Greece, Hungary, Ireland, Latvia, Luxembourg, Malta, Monaco, Netherlands, North Macedonia, Norway, Poland, Portugal, Romania, Slovakia, Slovenia, Spain, Sweden, Switzerland and United Kingdom.

3.5.2 Gap-filling of reported data in 2023

As described above, sectoral emissions reported by the EMEP countries are used, to the largest extent possible, to compile the gridded EMEP data sets. Each year the reported source-sector level data (NFR level) are aggregated into the 13 GNFR sectors and are then evaluated to identify countries for which emissions have not been reported or appear to exhibit implausible emission levels and/or trends. Based on this assessment, a procedure is then implemented to gap-fill missing emissions data and to replace data that have been identified as implausible. The sectoral emissions are then distributed spatially using, where available (and appropriate), the reported national gridded emissions as relative spatial proxies, or other independent data sets of spatial proxies.

Given the end of May deadline for compiling EMEP data sets, a cut-off date for incorporating reported emissions has to be set to allow necessary time for evaluating the reported emissions and implementing the gap-filling procedure. This year, the sectoral emissions data reported by 17 April 2023 were evaluated and considered for use in the compilation of the 2023 EMEP data sets of gridded emissions.

The Parties for which data were (partly) replaced, corrected or gap-filled in 2023 are: Albania, Armenia, Austria, Azerbaijan, Belarus, Belgium, Bosnia and Herzegovina, Bulgaria, Croatia, Cyprus, Denmark, Estonia, Georgia, Germany, Greece, Hungary, Italy, Kazakhstan, Kyrgyzstan, Liechtenstein, Lithuania, Luxembourg, Montenegro, the Republic of Moldova, the Russian Federation, Serbia, Slovenia, Spain, Sweden, Türkiye and the Ukraine. More Parties were gap-filled these last two years compared to the previous years due to the request for EMEP emission grids starting in 1990. For many countries, the complete reported time series of particulate matter emissions begin with the year 2000. The results of the quality control and gap-filling procedures are described in detail in the CEIP gap-filling report (Matthews and Wankmüller 2023).

Finally, it should be noted that the gap-filling and replacement procedure has been updated since last year. The gap-filling/replacement of EMEP country emissions remains based on the independent estimates from the ECLIPSE v6b[12] data set that has been compiled by IIASA

[10] https://www.ceip.at/status-of-reporting-and-review-results

[11] https://www.ceip.at/webdab-emission-database/emissions-as-used-in-emep-models

[12] https://iiasa.ac.at/web/home/research/researchPrograms/air/ECLIPSEv6.html

Table 3.2: Gridded emissions in $0.1° \times 0.1°$ longitude/latitude resolution reported until 2017, 2021 and 2023.

Country	2017	2021	2023	Comments
	Gridded data available for the years…	Gridded data available for the years…	Gridded data available for the years…	
Austria	2015	2000, 2005, 2010, 2015, 2019	2000, 2005,2010, 2015, 2019	
Belgium	2015	2015, 2019	2015, 2019	
Bulgaria	2015	2015, 2019	2015, 2019	
Croatia	1990, 1995, 2000, 2005, 2010, 2015	1990, 1995, 2000, 2005, 2010, 2015, 2019	1990, 1995, 2000, 2005, 2010, 2015, 2019	
Cyprus		1990, 1995, 2000, 2005, 2010, 2015, 2019	1990, 1995, 2000, 2005, 2010, 2015, 2019	For 1990 and 1995 no PM grid reporting
Czechia	2015	2015, 2019	2015, 2019	
Denmark	2015	2015, 2019	2015, 2019	
Estonia		1990, 1995, 2000, 2005, 2010, 2015, 2019	1990, 1995, 2000, 2005, 2010, 2015, 2019	For 1990 and 1995 no PM grid reporting
Finland	2014, 2015	1990, 1995, 2000, 2005, 2010, 2015, 2016, 2017, 2019	1990, 1995, 2000, 2005, 2010, 2015, 2016, 2017, 2019, 2020	
France		2015, 2019	2015, 2019	
North Macedonia		2015, 2019	2015, 2019	
Georgia		2015	2015	
Germany	1990, 1995, 2000, 2005, 2010, 2015	1990, 1995, 2000, 2005, 2010, 2015, 2017, 2019	1990, 1995, 2000, 2005, 2010, 2015, 2017, 2019	For 1990 no PM grid reporting
Greece		2015, 2019	2015, 2019	
Hungary	2015	2015	2015	
Iceland		2019, 2019	2015, 2019	Gridded data only for POPs
Ireland	2015	2015, 2019	2015, 2019	
Italy		2015,[(d)] 2019[(d)]	2015,[(d)] 2019[(d)]	(d) Reported gridded data was replaced by CAMS proxies
Kyrgyzstan		2019	2019	Reported gridded data was replaced by EDGAR proxies
Latvia	2015	2015, 2019	2015, 2019	
Lithuania	2015[(e)]	2015[(f)], 2019[(f)]	2015[(f)], 2019[(f)]	(e) Reported gridded emissions only on national total level f) Reported gridded data was replaced by CAMS proxies
Luxembourg	2015	2015, 2019	2015, 2019	
Malta		2016, 2019	2016, 2019	Grid reporting not in the defined 0.1°x0.1° coordinates
Monaco	2014, 2015	2014-2019	2014-2021	
Netherlands		1990, 1995, 2000, 2005, 2010, 2015, 2019	1990, 1995, 2000, 2005, 2010, 2015, 2019	
Norway	1990, 1995, 2000, 2005, 2010, 2015	1990, 1995, 2000, 2005, 2010, 2015, 2019	1990, 1995, 2000, 2005, 2010, 2015, 2019	
Poland	2014, 2015	2014, 2015, 2018, 2019	2014, 2015, 2018, 2019	
Portugal	2015	2015, 2019	2015, 2019	The spatial disaggregation of sector 'F – Road Transport' was replaced by CAMS proxies
Romania	2005	2005, 2015	2005, 2015	Gridded data for 2005 was reported only for Hms and POPs
Slovakia	2015	2015, 2019	2015, 2019	
Slovenia	2015	2015, 2019	2015, 2019	
Serbia			2020	Reported gridded data was replaced by CAMS proxies
Spain	1990-2015	1990-2019	1990-2021	For 1990-1999 no PM grid reporting. The spatial disaggregation of sector 'F – Road Transport' was replaced by CAMS proxies
Sweden		1990, 2000, 2005, 2010, 2015, 2019	1990, 2000, 2005, 2010, 2015, 2019	
Switzerland	1980-2015	1980-2019	1980-2021	
United Kingdom	2010, 2015	2010, 2015, 2019	2010, 2015, 2019	Gridded data for 2010 was reported only for POPs
Russian Federation		2019	2019	Reported gridded data was replaced by EDGAR proxies

using their GAINS model (Amann et al. 2011). However, the emissions for the areas 'North Africa', 'remaining Asian areas', and the part of Russia within the EMEP domain for which Russia does not report emissions (referred to as 'Russian Federation Asian part' further in this chapter), are now based on the updated EDGAR v6.1[13] data set (Crippa et al. 2022) that was generated by the European Commission's Joint Research Centre (JRC). Previously, the emissions for these areas were based on a previous version (EDGAR v5.0) of the data set (Crippa et al. 2019). Furthermore, gap-filling and/or replacement of 2020 emissions is often based on a 2020 projection from the ECLIPSE v6b data set and represents a business as usual scenario and does not consider the impact of the COVID-19 pandemic on 2020 emissions. Where 2020 emissions of all or single sectors were replaced/gap-filled with the 2020 projections of GAINS, the emission value was corrected using pollutant- and GNFR sector-specific adjustment factors (Guevara et al. 2022). For 2021 emissions, no COVID-19 adjustment factors were implemented. Here, the linear trend between the 2015 estimate and the 2020 business as usual scenario was extrapolated to 2021. More details can be found in the CEIP gap-filling report (Matthews and Wankmüller 2023).

3.5.3 Contribution of GNFR sectors to total EMEP emissions

Figure 3.5 shows the contribution of each GNFR sector to the total emissions of individual air pollutants (SO_x, NO_x, CO, NMVOC, NH_3, $PM_{2.5}$, PM_{10}, PM_{coarse} and BC) in 2021. To clarify, the reader is reminded that these analyses are based on the emission data in the EMEP data sets for modellers i.e. data based largely on reported emissions, but also compiled with independent emissions estimates for countries and regions where data are not reported or the reported data have been omitted due to quality issues. The sea regions were excluded for this sectoral analysis.

It is evident that the combustion of fossil fuels is responsible for a significant part of all emissions. For NO_x emissions, the largest contributions come from transport (sector F, 36%) and from large power plants (sector A, 20%).

NMVOC sources are distributed more evenly among the different sectors, such as 'E - Emissions from solvents' (25%), 'F - Road transport' (16%), 'D - Fugitive Emissions' (18%), 'B - Industry combustion' (8%), 'K - Manure management' (10%) and 'C - Other stationary combustion' (14%).

The main source of SO_x emissions are large point sources from combustion in energy and transformation industries (sector A, 50% and sector B, 28%).

Ammonia arises mainly from agricultural activities; about 93% combined contribution from sectors K and L. Emissions of CO originate primarily from 'F - Road transport' (33%) and 'C - Other stationary combustion' (34%).

The main sources of primary PM_{10} and $PM_{2.5}$ emissions are industry (23% and 20%) and other stationary combustion processes (40% and 47%). Due to the higher agricultural emissions of PM_{10} versus $PM_{2.5}$, sectors K and L make a much larger relative contribution to PM_{coarse} emissions (30% combined) together with significant contributions from 'B - industry combustion' (27%) and 'C - Other stationary combustion' (27%).

Finally, the most important contributors to BC emissions are 'F - Road transport' (16%) and 'C - Other stationary combustion' (58%).

Figure 3.6 illustrates the sector contributions to the total emissions in the EMEP West

[13] https://edgar.jrc.ec.europa.eu/index.php/dataset_ap61

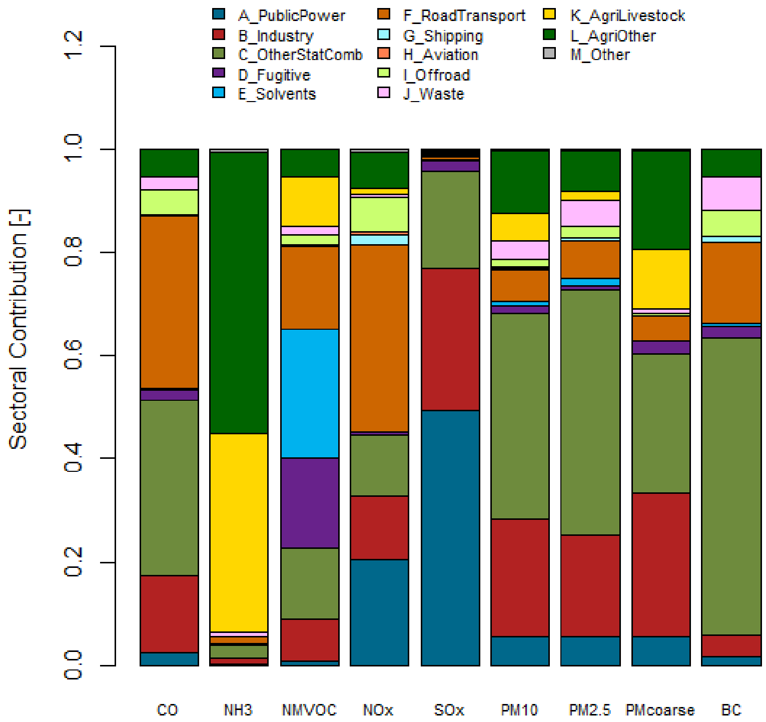

Figure 3.5: GNFR sector contribution to national total emissions in 2021 for the EMEP domain apart from the sea regions.

region and the EMEP East region, respectively. The split between the EMEP West and EMEP East regions is according to https://www.ceip.at/countries (sea regions, North Africa and the remaining Asian areas are excluded). The comparison of both graphs highlights some significant differences between West and East.

For NO_x in both the EMEP West and EMEP East regions the most important sector is 'F - Road transport emissions' (35% in both), although it is worth noting the higher contribution from 'A - Public electricity and heat production' in the East region (19% vs 12% in the West).

For NMVOC in the EMEP West region the most relevant sector is 'E - Emissions from solvents' with a share of 37%. In the EMEP East region the same sector has a considerable lower share (13%), whilst the sector 'F - Road transport' is of high importance (31%).

The main source of SO_x are 'A - Public electricity and heat production' and 'B - Industry combustion'. These two sectors together contribute to 76% and 83% of the SO_x emissions within the EMEP West and EMEP East areas, respectively.

The main sources of NH_3 emissions for both EMEP West and EMEP East are the agricultural sectors (K and L) with 93% and 94%, respectively.

CO emissions arise mainly from 'F - Road transport emissions' (58%) in EMEP East. In the EMEP West region the main sector is 'C - Other stationary combustion' (45%).

For $PM_{2.5}$ and PM_{10} 'C - Other stationary combustion' holds a significant share of the total emissions in the EMEP West area (62% and 43%), compared to the EMEP East area (17% and 13%). For the EMEP East area sector 'B - Industry combustion' is of higher importance. For PM_{coarse} it is worth mentioning the higher contributions from agriculture in the EMEP East area (43%). Finally, it is interesting to note the significant contribution to BC emissions in the EMEP East area from fugitive emissions (11% in EMEP East versus 1% in EMEP West).

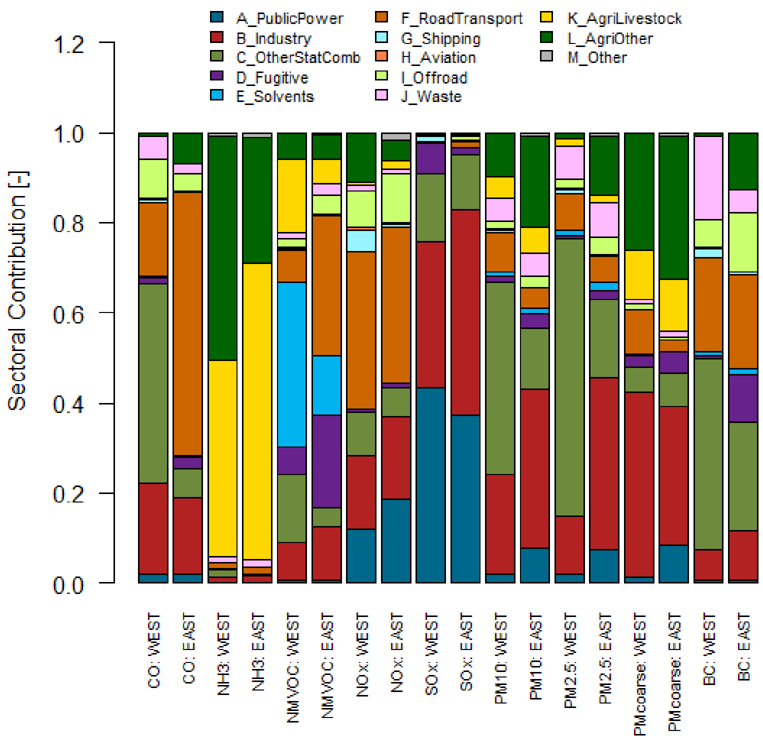

Figure 3.6: GNFR sector contribution to national total emissions in 2021 for the EMEP West and EMEP East areas. Asian areas, North Africa and the sea regions are not included.

3.5.4 Trends in emissions in the geographic EMEP domain

The following trend analyses are based on the emissions data in the EMEP data sets for modellers, i.e. data based largely on reported emissions, but also compiled with independent emissions estimates for countries and regions where data are not reported or the reported data have been omitted due to quality issues.

Excluding shipping emissions in the sea regions (these are summarised in Section 3.5.5), the trend analyses of total emissions from the non-sea areas in the EMEP domain[14] in Figure 3.7 shows that emissions of seven of the nine pollutants have decreased overall since 2000. Only the 2020 PM_{coarse} and NH_3 emissions have increased (by 1 and 9%, respectively) since 2000. The 2020 emissions of SO_x are 57% of the respective 2000 emissions. While the 2020 emissions of CO, NMVOC, NO_x, $PM_{2.5}$, PM_{10} and BC are all lower than respective emissions in 2000 (5-25% lower), it is interesting to note that emissions of these pollutants have been increasing between 2014 and 2019. However, between 2019 and 2020, emissions of most pollutants, particularly NO_x, declined due to the COVID-19 pandemic and the resulting restrictions on socio-economic activity. On the other hand, between 2020 and 2021 emissions of all pollutants increased.

Despite these overall trends, the regional emission developments seem to follow strongly different patterns (Figure 3.8). While emissions of all the pollutants in the EMEP West countries are clearly decreasing, emissions of all pollutants in the EMEP East countries of the EMEP domain have been somewhat stable (albeit gradually decreasing for most pollutants) over the 2000-2019 period. Drops in emissions between 2019 and 2020 due to the COVID-

[14]The EMEP domain covers the geographic area between 30° N-82° N latitude and 30°W-90° E longitude.

Table 3.3: Differences between emissions for 2000 and 2021 (based on gap-filled data as used in EMEP models). Negative values mean that 2021 emissions were lower than 2000 emissions. Red/blue coloured data indicates that 2021 emissions were higher/lower than 2000 emissions. Furthermore, the symbol in parentheses indicate whether the emissions times series are completely based on reported data (R), are partially based on reported data (r), or have been completely replaced/gap-filled (-).

Country	CO	NH3	NMVOC	NOx	SOx	PM10	PM2.5	PMcoarse	BC
Albania	1.7 (-)	20 (-)	8.3 (-)	42.5 (-)	-20.2 (-)	46.6 (-)	46.4 (-)	47.3 (-)	5.4 (-)
Armenia	-58.3 (-)	65.2 (-)	-29.6 (-)	159.8 (-)	673.6 (-)	59.7 (-)	57.6 (-)	65.9 (-)	302.3 (-)
Asian Areas	22.7 (-)	42.4 (-)	39.4 (-)	81.9 (-)	54.4 (-)	59.5 (-)	56 (-)	64.8 (-)	37.9 (-)
Austria	-28.3 (R)	2.7 (R)	-38.9 (R)	-42.3 (R)	-65.5 (R)	-30.5 (r)	-42.7 (r)	-11.8 (-)	-50.3 (-)
Azerbaijan	97 (-)	62.7 (r)	225.3 (-)	254 (-)	-60 (-)	167 (-)	179.2 (-)	127.1 (-)	306.2 (-)
Belarus	-45.4 (-)	13.4 (-)	-28.9 (-)	-21.4 (-)	-56.7 (-)	-10.6 (-)	-5.6 (-)	-23.8 (-)	-9.2 (-)
Belgium	-70.9 (R)	-29.1 (r)	-48.3 (R)	-60.4 (R)	-86.3 (R)	-49.8 (r)	-54.3 (r)	-37.8 (-)	-70.4 (r)
Bosnia and Herzegovina	34.8 (-)	63.7 (-)	57 (-)	18 (-)	-103.5 (-)	33.6 (-)	107.1 (-)	-57.2 (-)	159.1 (-)
Bulgaria	-35.3 (r)	-3.3 (R)	-35.3 (R)	-42.7 (R)	-95.4 (R)	-31.2 (R)	-13.4 (R)	-54 (-)	26.3 (R)
Croatia	-54.2 (r)	-19.5 (r)	-32.6 (r)	-48 (r)	-89.8 (r)	7.8 (r)	-20.6 (r)	93.8 (-)	-31.5 (r)
Cyprus	-65.3 (R)	-10.9 (R)	-42.6 (R)	-45.5 (R)	-79.2 (R)	-58.7 (r)	-59.9 (r)	-57.4 (-)	-63.9 (r)
Czech Republic	-28.4 (R)	-17 (R)	-41.3 (R)	-48.8 (R)	-70.4 (R)	-47.7 (R)	-51.4 (R)	-38.5 (-)	-48.1 (R)
Denmark	-59.3 (R)	-31.9 (R)	-41.1 (R)	-59 (R)	-73.7 (R)	-31.2 (R)	-41.2 (R)	-14.4 (-)	-55.6 (r)
Estonia	-39.6 (R)	18.8 (R)	-24.7 (R)	-49.3 (R)	-87.8 (R)	-55.6 (r)	-55.2 (r)	-55.8 (-)	-42 (r)
Finland	-43.1 (R)	-14.5 (R)	-53.8 (R)	-56.4 (R)	-71.5 (R)	-34.6 (R)	-44.9 (R)	-18.4 (-)	-47.8 (R)
France	-59.7 (R)	-18.2 (R)	-45.8 (R)	-58.4 (R)	-85.6 (R)	-43.8 (R)	-49.7 (R)	-22.6 (-)	-58.8 (R)
Georgia	-9.6 (R)	-23.3 (r)	9.5 (R)	67.9 (r)	152.1 (-)	-21 (-)	-27.3 (-)	34.6 (-)	82.5 (-)
Germany	-49.6 (R)	-18.5 (R)	-42.4 (R)	-48.1 (R)	-60.4 (R)	-39.3 (r)	-49.6 (r)	-26.9 (-)	-74 (r)
Greece	-57.8 (R)	-17.9 (R)	-53.5 (R)	-48.4 (R)	-91.6 (R)	-55.1 (r)	-46.3 (r)	-64.6 (-)	-25.2 (R)
Hungary	-59.7 (R)	-11.5 (R)	-40.2 (R)	-41.8 (R)	-96.7 (R)	-26.3 (r)	-21.7 (r)	-35.8 (-)	-28.4 (r)
Iceland	97.2 (R)	-4.3 (R)	-32.5 (R)	-36.3 (R)	71.2 (R)	-34.2 (R)	-32.6 (R)	-35.7 (-)	-64.1 (R)
Ireland	-61.9 (R)	3.3 (R)	-7.6 (R)	-44.8 (R)	-91.8 (R)	-21.8 (R)	-34.5 (R)	-9.4 (-)	-58.9 (R)
Italy	-56.8 (R)	-23.1 (R)	-46.6 (R)	-59.4 (R)	-89.6 (R)	-31.9 (R)	-27.2 (R)	-42.8 (-)	-57.3 (R)
Kazakhstan	-13.1 (-)	43.9 (-)	55.6 (-)	37.5 (r)	49.7 (-)	12.2 (-)	8.5 (-)	19.2 (-)	-33.6 (-)
Kyrgyzstan	23 (-)	36.7 (-)	45.9 (-)	97.8 (-)	21 (-)	51.4 (-)	56.2 (-)	40.5 (-)	-12.3 (-)
Latvia	-57.4 (R)	15.1 (R)	-31.3 (R)	-22.1 (R)	-79.4 (R)	-7.9 (R)	-34.5 (R)	149.2 (-)	-40.2 (R)
Liechtenstein	-51.6 (R)	12.1 (R)	-46.2 (R)	-59 (R)	-89.1 (R)	-42.7 (R)	-53.1 (R)	-18.9 (-)	-70.1 (-)
Lithuania	-38.9 (R)	10.5 (R)	-22.8 (R)	-17.7 (R)	-71.4 (R)	-7.4 (r)	-23.1 (r)	1 (-)	-3.7 (-)
Luxembourg	-58.1 (R)	-1.8 (R)	-31 (R)	-65.4 (R)	-78.1 (R)	-41.5 (R)	-50.5 (R)	-3.6 (-)	-76.6 (-)
Malta	-71.9 (R)	-34.3 (R)	-36.5 (R)	-49 (R)	-97.2 (R)	23.6 (R)	-48.1 (R)	153.1 (-)	-51.8 (R)
Monaco	-60.4 (R)	-80.9 (R)	-46.5 (R)	-75 (R)	-87.9 (R)	-49.5 (R)	-70.9 (R)	-1.6 (-)	-84.4 (R)
Montenegro	258.7 (-)	-46.5 (R)	285.1 (-)	586 (-)	16.2 (R)	234.2 (-)	297.5 (-)	51.7 (-)	475.7 (-)
Netherlands	-43.3 (R)	-29.7 (R)	-18 (R)	-57.5 (R)	-73.6 (R)	-47.5 (R)	-59.2 (R)	-20.6 (-)	-78.7 (R)
North Africa	-17.2 (-)	30.8 (-)	-27.4 (-)	94.2 (-)	21 (-)	28.5 (-)	22 (-)	39.7 (-)	37.9 (-)
Norway	-27.6 (R)	2.1 (R)	-64.9 (R)	-34.3 (R)	-45.3 (R)	-33.9 (R)	-41.2 (R)	-3.2 (-)	-41.2 (R)
Poland	-24.9 (R)	-17.4 (R)	-13.4 (R)	-31.9 (R)	-70.4 (R)	-4.5 (R)	1.3 (R)	-19.7 (-)	-10.7 (R)
Portugal	-57.5 (R)	-16.2 (R)	-34.5 (R)	-54.5 (R)	-86.7 (R)	-30.2 (R)	-31.2 (R)	-26.6 (-)	-48.3 (R)
Republic of Moldova	101 (r)	-15.9 (r)	83.3 (r)	61 (r)	-5.9 (r)	273.6 (r)	338.7 (r)	151.6 (-)	442.1 (-)
Romania	-8.9 (R)	-9.9 (R)	-23.4 (R)	-32.3 (R)	-86.5 (R)	13 (R)	9.2 (R)	25.1 (-)	9.6 (R)
Russian Federation (European part)	0.2 (r)	1.1 (r)	2.2 (r)	-10.1 (r)	-55 (r)	-29 (r)	-40.7 (r)	-19.1 (-)	-42.7 (-)
Russian Federation (Asian part)	-10.1 (-)	21.6 (-)	1.1 (-)	-17.5 (-)	-36.6 (-)	3.5 (-)	-7.3 (-)	27 (-)	-28.3 (-)
Serbia	-9.1 (R)	-32.4 (R)	-9.9 (R)	19.3 (R)	-18.3 (R)	40.2 (R)	46.9 (R)	21.1 (-)	59.4 (-)
Slovakia	-38.2 (R)	-24.3 (R)	-35.9 (R)	-46.9 (R)	-87.9 (R)	-54.3 (R)	-57.4 (R)	-41.5 (-)	-38.4 (R)
Slovenia	-57.1 (R)	-16.9 (R)	-45 (R)	-56 (R)	-95.6 (R)	-20.9 (r)	-29 (r)	10.5 (-)	-35.4 (r)
Spain	-37.7 (R)	-16.5 (R)	-38.1 (R)	-53.5 (R)	-91.1 (R)	-27.1 (r)	-27.2 (r)	-27 (-)	-12.8 (r)
Sweden	-57 (R)	-14.5 (R)	-37.7 (R)	-48.2 (R)	-64.9 (R)	-34.2 (R)	-52.7 (R)	-1.5 (-)	-65.8 (r)
Switzerland	-63.8 (R)	-13.5 (R)	-52.7 (R)	-50.3 (R)	-77.1 (R)	-29.4 (R)	-51.1 (R)	5.1 (-)	-74.8 (R)
Tajikistan	275.4 (-)	72.6 (-)	254.1 (-)	716.1 (-)	1356.8 (-)	512.3 (-)	532 (-)	453.9 (-)	461.6 (-)
The former Yugoslav Republic of Macedonia	-63.7 (R)	-39.1 (R)	-53.8 (R)	-51.2 (R)	-16.6 (R)	-69.9 (R)	-71 (R)	-67.4 (-)	-62.4 (R)

Table 3.3 cont. Differences between emissions for 2000 and 2021 (based on gap–filled data as used in EMEP models).

Country	CO	NH3	NMVOC	NOx	SOx	PM10	PM2.5	PMcoarse	BC
Türkiye	-42.4 (-)	44.1 (R)	-55.8 (-)	-19.9 (-)	-47.1 (-)	6.8 (-)	-2.6 (-)	36.3 (-)	-48.2 (-)
Turkmenistan	115.7 (-)	41 (-)	112.8 (-)	106.1 (-)	84 (-)	24.7 (-)	28.7 (-)	12.8 (-)	14.4 (-)
Ukraine	-20.4 (-)	-8.5 (-)	-41.7 (-)	-42.2 (-)	-85.3 (r)	-29.4 (-)	-28.6 (-)	-31 (-)	-32 (-)
United Kingdom	-75.4 (R)	-10.5 (R)	-55.6 (R)	-67 (R)	-90.3 (R)	-38.7 (R)	-43 (R)	-31.8 (-)	-57.4 (R)
Uzbekistan	54.7 (-)	75.8 (-)	83.5 (-)	-16 (-)	2.2 (-)	17.7 (-)	21.4 (-)	6.4 (-)	7.9 (-)
Increase (no. countries/areas)	12	22	14	14	11	19	16	23	15
Decrease (no. countries/areas)	42	32	40	40	43	35	38	31	39

19 pandemic are nonetheless visible for both the EMEP West and EMEP East regions. For the Other Land Areas (North Africa and the remaining Asian areas), emissions are clearly on the rise, albeit slowing between 2019 and 2020 as a result of the impacts of the COVID-19 pandemic.

Of course it is not just the emission trends that separate the three land regions. Whereas the emission trends of the EMEP West countries are based to a very large extent on the official national inventories reported to CEIP, the countries of the Other Land Areas within the EMEP domain (North Africa, remaining Asian areas) are not Parties to the Convention and thus are not obliged to report their emissions. For these regions, emissions are based completely on the independent gridded emission estimates of the EDGAR v6.1 data set (Crippa et al. 2022) that was generated by the European Commission's Joint Research Centre (JRC). Furthermore, the recent trends should be viewed with caution as the last available year in the EDGAR v6.1 data set is 2018 and emissions between 2019 and 2021 has to be extrapolated based on economic trends. In EMEP East region not all countries are Parties to the Convention (such as Turkmenistan, Tajikistan and Uzbekistan) and the reported Russian emissions do not cover

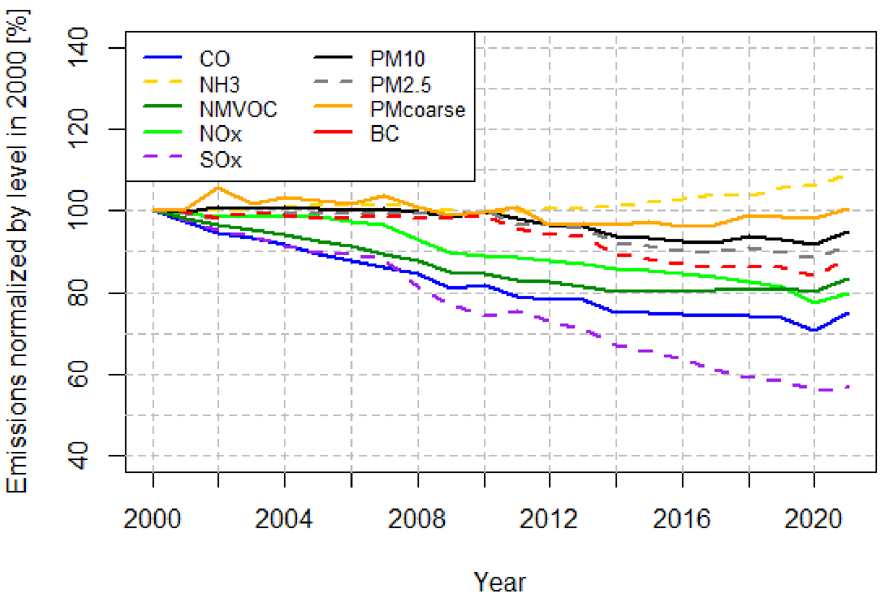

Figure 3.7: Emissions during the 2000–2021 period in the geographic EMEP area (emissions from international shipping in the sea regions are excluded).

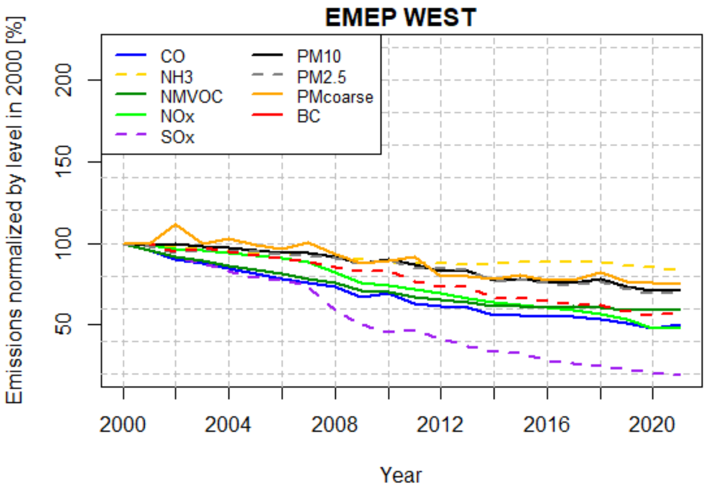

(a) EMEP West

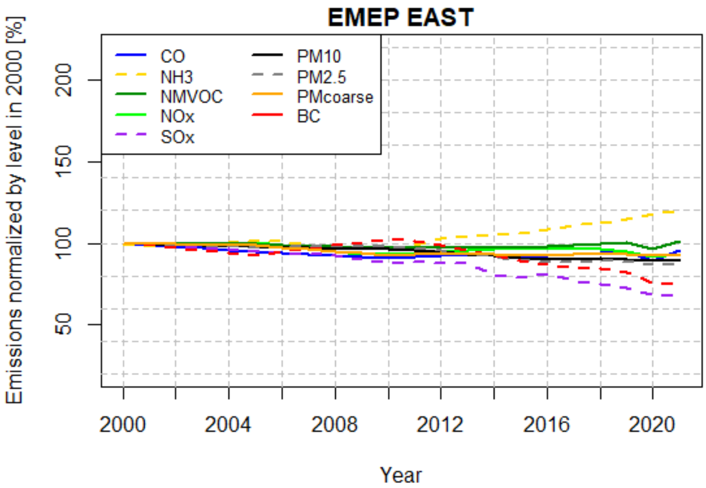

(b) EMEP East

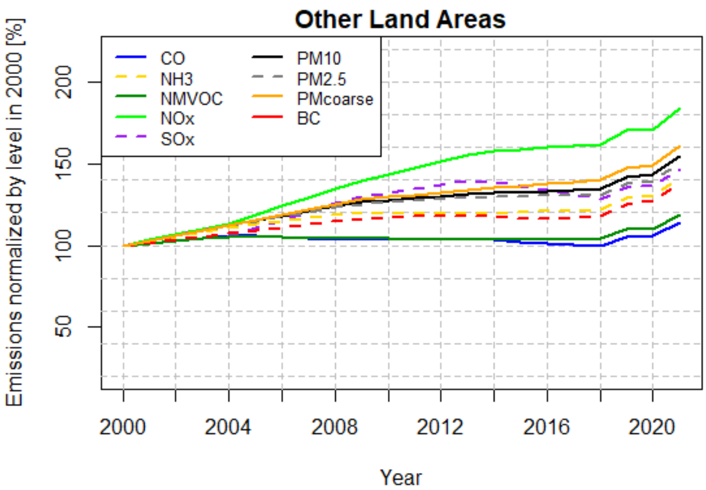

(c) Other Land Areas

Figure 3.8: Emissions during the 2000–2021 period in the geographic EMEP domain (emissions from international shipping in the sea regions are excluded) divided into three areas: 'EMEP West' (top), 'EMEP East' (middle) and 'Other Land Areas' (bottom), that include the emissions from North Africa and the remaining Asian areas.

the region of Russia within the EMEP domain that is ca. east of the Urals. The emissions for the eastern part of Russia have also been gap-filled using the independent gridded emission estimates of the EDGAR v6.1 data set. Finally, it should be noted that many of the emissions time series for the EMEP East countries that are Parties to the Convention have been partially or fully replaced with independent estimates from the ECLIPSE v6b[15] data set that has been compiled by IIASA using their GAINS model (Amann et al. 2011).

Non-sea emission levels in the geographic EMEP domain for 2021 of the individual countries and areas are compared to 2000 emission levels for each pollutant (see Tables 3.3-3.3 cont.). Again, the reader is reminded that the following trend analyses are based on the emissions data in the EMEP data sets for modellers, i.e. the data based largely on reported emissions, but also compiled with independent emissions estimates for countries and regions where data are not reported or the reported data have been omitted due to quality issues. Overview tables with reported emission trends for individual countries have been published on the CEIP website[16]. Detailed information on the sectoral level can also be accessed in WebDab[17].

The assessment of emission levels in individual countries and areas shows an increase of emissions in 2021 compared to 2000 emission levels in several countries or areas.

In case of PM emissions, 23 countries/areas have higher PM_{coarse} emissions in 2020 than in 2000, while PM_{10} and $PM_{2.5}$ emissions increased in 19 and 16 countries/areas, respectively. In case of NO_x there are 14 countries/areas, for SO_x 11, NMVOC 14, NH_3 22 and CO 12 countries/areas with higher emissions in 2021 than in year 2000. Detailed explanatory information on emission trends for the reporting countries should be provided in the respective informative inventory reports (IIRs). Tables 3.3-3.3 cont. indicates whether the emissions were based completely (R) or partially (r) on reported data, or whether the data have been completely gap-filled/replaced (-).

3.5.5 Trends in emissions from international shipping

International shipping emissions are not reported by Parties. Gridded emissions for the sea regions (European part of the North Atlantic, Baltic Sea, Black Sea, Mediterranean Sea and North Sea) were calculated using the CAMS global shipping data set (CAMS-GLOB-SHIP v3.2) (Granier et al. 2019) developed by the Finnish Meteorological Institute (FMI) for the years 2000 to 2021 (Figure 3.9) and provided via ECCAD[18] (ECCAD 2019).

According to FMI the reason for the high emission reduction between 2019 and 2020 for PM and SO_x is the global reduction of maximum sulphur content in ship fuels from 3.5% to 0.5%[19]. This impacts directly the SO_x and particulate SO_4 emissions. The COVID-19 pandemic led to a reduction of shipping activity and emissions in 2020, but the global sulphur cap impacted PM and SO_x emissions even more. The 2021 resumption of normal shipping activity, despite the ongoing pandemic at the time, is reflected in the increase in shipping emissions of all the presented air pollutants from 2020 to 2021.

[15] https://iiasa.ac.at/web/home/research/researchPrograms/air/ECLIPSEv6.html
[16] https://www.ceip.at/webdab-emission-database/reported-emissiondata
[17] https://www.ceip.at/webdab-emission-database/emissions-as-used-in-emep-models and/or https://www.ceip.at/webdab-emission-database/reported-emissiondata
[18] https://eccad.aeris-data.fr
[19] https://www.imo.org/en/MediaCentre/HotTopics/Pages/Sulphur-2020.aspx

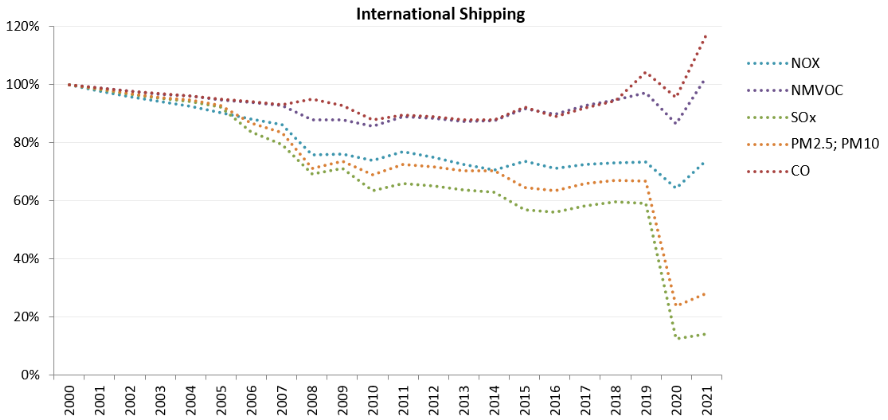

Figure 3.9: International shipping emissions during the 2000–2021 period in the EMEP area, extracted from the CAMS global shipping emission data set developed by by the Finnish Meteorological Institute (FMI) via ECCAD (CAMS_GLOB_SHIP). These are the emissions which have been used for the most recent trend calculations with the EMEP model.

3.6 SO_2 emissions from the Fagradalsfjall eruption in 2021

A basaltic effusive eruption started at Mt. Fagradalsfjall along a fissure on 19 March 2021 and lasted until 18 September 2021. This eruption ended a 781-year dormancy on the Reykjanes peninsula in the southwest of Iceland. This peninsula is an onshore continuation of the Mid-Atlantic plate boundary and has volcanic systems consisting of 10-40 km long NE-SW-trending fissure swarms and geothermal areas. However, Fagradalsfjall is the least active volcanic system of the peninsula. The March-September mean bulk effusion rate was 9.5 $\pm$0.2 m^3/s, ranging between 1 and 8 m^3/s in March- April and increasing to 9-13 m^3/s in May-September (Keller et al. 2023). Measurements of SO_2 emissions were done by the IMO in the following way: the flux of SO_2 was measured with ground-based UV spectrometers. A three-instrument network of DOAS instruments (10 km NNW of the eruption site, 6 km to the NW, and 4.5 km to the SW) was augmented by traverses directly under the eruption cloud which were primarily car-borne, but a few measurements were also made by foot and by aircraft. These measurements are used together with plume height and meteorological conditions to calculate the emission rate of SO_2. The scanning instruments measured the SO_2 flux 4,900 times over the duration of the eruption. Additionally, 148 traverse measurements were made. The traverse calculations attempt to include the uncertainty related to wind properties to have the true measurement uncertainty represented in the results. The total SO_2 emissions are estimated to be 967$\pm$538 kt. The reported emission total for SO_2 from the eruption is 967kt, and this value was used in the EMEP model calculations.

For transport modelling, however, more detailed information about the source term of the eruption, that is, emission rates as a function of altitude and time is needed.

Time series of plume height observations/measurements and the time series of the measured SO_2 emission rates have been kindly provided by Melissa Anne Pfeffer from the volcanic hazard team at the Icelandic Met Office with permission to use the information for input data in the EMEP/MSC-W model simulation. There was high variability of the emission rates and plume heights on very short time scales, which made it difficult to fill in missing data between measurements. In addition to the detailed measurement data, the start and end dates for each eruption phase along with the amount of total emitted SO_2 during the different phases were provided by IMO, and were fully consistent with the reported emission total for SO_2. This additional information about the eruption phases made it possible to calculate the average fluxes for each phase. It is a simplified approach for modelling the eruption, but still includes time variation in the emission strength, while also reproduces the reported emission total.

3.7 Summary

This chapter summarises the status of emissions reported by LRTAP Convention Parties and the extent to which these data have been incorporated into the 2023 EMEP emissions data sets for modellers. The chapter documents the historical improvement in reporting over time, noting the increasing extent of reporting emissions inventories for the mandatory pollutants and black carbon. Generally the number of timely submissions have increased over time, however, the small recent increase in missing submissions since 2021 should be noted (five missing submissions in 2023 compared to three in 2021). An increased reporting of gridded emissions in 2021 compared to 2017 is also noted, as well as some additional gridded data that was reported in 2023. Despite these positive trends in terms of reporting, reporting is not yet complete. For some parties, emissions inventories and gridded data are not reported (or are reported late and/or incomplete). There is further room for improvement on the reporting of particulate matter emissions with respect to whether the condensable component has been included in the reported estimates.

The 2023 EMEP emissions data sets for modellers therefore need to be complied carefully and this chapter documents for which countries and pollutants the time series have been based fully or partially on reported inventories and gridded data, and for which countries and regions the data sets have been built using independent emissions data products.

Based on the complied data sets in 2023, it is worth noting that emissions from the land areas have decreased from 2000 to 2021 for most pollutants except for PM_{coarse} and NH_3. This appears to be driven by the emission changes in the EMEP West countries, for which the time series are based almost completely on reported data. For EMEP West, emissions of all pollutants have decreased since 2000, with the strongest and weakest declines observed for SO_x and NH_3, respectively. In contrast, EMEP East as whole shows much weaker declines in emissions (emissions based partially on reported data), although NH_3 emissions with an increase of 20% since 2000 are worth highlighting. Notable emission increases are shown for the 'Other areas' (based completely on independent estimates). In addition to these long term trends, it should also be noted that the emissions of almost all pollutants for the EMEP domain as a whole (and the EMEP West, EMEP East and 'Other areas', respectively) demonstrated irregular decreases between 2019 and 2020 due to the COVID-19 pandemic impacts on socio-economic activity. An abrupt decrease in international shipping emissions has also been identified (Section 3.5.5). However, in the case of PM and SO_x from international shipping, the much larger reductions were driven not only by the pandemic, but mainly by the introduction of the global sulphur cap on ship fuels. For almost all pollutants and regions (including shipping emissions), emissions in 2021 tended to increase compared to 2020, due to the partial resumption of normal activity and easing of the pandemic-related restrictions.

In 2021 there was a long lasting volcanic eruption at Mt. Fagradalsfjall in Iceland. There was no significant amount of ash released in the eruption, but a total of 967 kt of SO_2 were emitted into the atmosphere between 19 March and 18 September 2021, as reported by Iceland in 2023. Gas emissions from Fagradalsfjall mainly affected lower altitudes and the transport of SO_2 influenced air quality mainly in Iceland, with limited effect on Scandinavia, Ireland and the United Kingdom.

References

Amann, M., Bertok, I., Borken-Kleefeld, J., Cofala, J., Heyes, C., Hoeglund-Isaksson, L., Klimont, Z., Nguyen, B., Posch, M., Rafaj, P., Sandler, R., Schoepp, W., Wagner, F., and Winiwarter, W.: Cost-effective control of air quality and greenhouse gases in Europe: Modeling and policy applications, Environmental Modelling & Software, 26, 1489–1501, doi:10.1016/j.envsoft.2011.07.012, 2011.

Crippa, M., Guizzardi, D., Muntean, M., and Schaaf, E.: EDGAR v5.0 Global Air Pollutant Emissions (Dataset), european Commission, Joint Research Centre (JRC), 2019.

Crippa, M., Guizzardi, D., Muntean, M., and Schaaf, E.: EDGAR v6.1 Global Air Pollutant Emissions (Dataset), european Commission, Joint Research Centre (JRC), 2022.

Denier van der Gon, H. A. C., Bergström, R., Fountoukis, C., Johansson, C., Pandis, S. N., Simpson, D., and Visschedijk, A. J. H.: Particulate emissions from residential wood combustion in Europe - revised estimates and an evaluation, Atmos. Chem. Physics, pp. 6503–6519, doi:doi:10.5194/acp-15-6503-2015, URL http://www.atmos-chem-phys.net/15/6503/2015/, 2015.

ECCAD: Emissions of atmospheric Compounds and Compilation of Ancillary Data, URL https://eccad.aeris-data.fr, 2019.

EMEP/EEA: EMEP/EEA air pollutant emission inventory guidebook - 2019, Technical report 13/2019, European Environment Agency, EEA, URL https://www.eea.europa.eu/publications/emep-eea-guidebook-2019, 2019.

Granier, C., Darras, S., Denier van der Gon, H., Doubalova, J., Elguindi, N., Galle, B., Gauss, M., Guevara, M., Jalkanen, J.-P., Kuenen, J., Liousse, C., Quack, B., Simpson, D., and Sindelarova, K.: The Copernicus Atmosphere Monitoring Service global and regional emissions (April 2019 version), doi:10.24380/d0bn-kx16, URL https://atmosphere.copernicus.eu/sites/default/files/2019-06/cams_emissions_general_document_apr2019_v7.pdf, 2019.

Guevara, M., Petetin, H., Jorba, O., Denier van der Gon, H. A. C., Kuenen, J., Super, I., Jalkanen, J.-P., Majamäki, E., Johansson, L., Peuch, V.-H., , and Pérez García-Pando, C.: European primary emissions of criteria pollutants and greenhouse gases in 2020 modulated by the COVID-19 pandemic disruptions, Earth Syst. Sci. Data, preprint, in review, doi:10.5194/essd-2022-31, URL https://doi.org/10.5194/essd-2022-31, 2022.

Keller, N., Barr, B. C., Asgeirsson, B. U., Einarsdottir, S. R., Helgadottir, Helgason, R., K., A., Helgadottir, D., Helgadottir, I. N., Jonsdottir Thianthong, C., and Hilmarssin, K. M.: Informative Inventory Report, Emissions of Air Pollutants in Iceland from 1990 to 2021, Tech. rep., URL https://webdab01.umweltbundesamt.at/download/submissions2023/IS_IIR2023.zip, 2023.

Matthews, B. and Wankmüller, R.: Methodologies applied to the CEIP GNFR gap-filling 2023 Part I: Main Pollutants (NO_x, NMVOCs, SO_x, NH_3, CO), Particulate Matter ($PM_{2.5}$, PM_{10}, PM_{coarse}) and Black Carbon (BC) for the years 1990 to 2021., EMEP/CEIP Technical Report 2/2023, CEIP Vienna, 2023.

Schindlbacher, S., Matthews, B., and Ullrich, B.: Uncertainties and recalculations of emission inventories submitted under CLRTAP, EMEP/CEIP Technical Report 1/2021, CEIP Vienna, https://www.ceip.at/fileadmin/inhalte/ceip/00_pdf_other/2021/uncertainties_and_recalculations_of_emission_inventories_submitted_under_clrtap.pdf, 2021.

Schindlbacher, S., Ullrich, B., and Wankmüller, R.: Inventory review 2023. Review of emission data reported under the LRTAP Convention. Stage 1 and 2 review. Status of gridded and LPS data, EMEP/CEIP Technical Report 4/2023, CEIP Vienna, 2023.

Simpson, D., Fagerli, H., Colette, A., Denier van der Gon, H., Dore, C., Hallquist, M., Hansson, H. C., Maas, R., Rouil, L., Allemand, N., Bergström, R., Bessagnet, B., Couvidat, F., El Haddad, I., Safont, J. G., Goile, F., Grieshop, A., Fraboulet, I., Hallquist, Å., Hamilton, J., Juhrich, K., Klimont, Z., Kregar, Z., Mawdsely, I., Megaritis, A., Ntziachristos, L., Pandis, S., Prévôt, A. S. H., Schindlbacher, S., Seljeskog, M., Sirina-Leboine, N., Sommers, J., and Åström, S.: How should condensables be included in PM emission inventories reported to EMEP/CLRTAP? Report of the expert workshop on condensable organics organised by MSC-W, Gothenburg, 17-19th March 2020, EMEP Technical Report MSC-W 4/2020, ISSN 1504-6206, 2020.

Simpson, D., Kuenen, J., Fagerli, H., Heinesen, D., Benedictow, A., Denier van der Gon, H., Visschedijk, A., Klimont, Z., Aas, W., Lin, Y., Yttri, K. E., and Paunu, V.-V.: Revising $PM_{2.5}$ emissions from residential combustion, 2005–2019. Implications for air quality concentrations and trends, Temanord 2022:540, Nordic Council of Ministers, doi:10.6027/temanord2022-540, URL https://pub.norden.org/temanord2022-540, 2022.

UNECE: Decision 2012/3: Adjustments under the Gothenburg Protocol to emission reduction commitments or to inventories for the purposes of comparing total national emissions with them, Tech. Rep. ECE/EB.AIR/111, UNECE, URL https://www.unece.org/fileadmin/DAM/env/documents/2013/air/ECE_EB.AIR_111_Add.1__ENG_DECISION_3.pdf, 2012.

UNECE: Guidelines for reporting emission data under the Convention on Long-range Transboundary Air Pollution, Tech. Rep. ECE/EB.AIR/130, UNECE, URL https://www.ceip.at/fileadmin/inhalte/emep/2014_Guidelines/ece.eb.air.125_ADVANCE_VERSION_reporting_guidelines_2013.pdf, 2014.

UNECE: Activities of the Bureaux of the Steering Body to the Cooperative Programme for Monitoring and Evaluation of the Long-range Transmission of Air Pollutants in Europe and the Working Group on Effects, Tech. Rep. ECE/EB.AIR/GE.1/2020/9, UNECE, URL https://www.unece.org/fileadmin/DAM/env/documents/2020/AIR/EMEP_WGE_Joint_Session/ECE_EB.AIR_GE.1_2020_9-2009233E.pdf, 2020.

Part II

Assessment and Research Activities

CHAPTER 4

Impact of background CH_4 and regional and global emission reductions on European O_3

Willem van Caspel, Hilde Fagerli and Zbigniew Klimont

The air pollution (reduction) potential of methane (CH_4) has received considerable attention in recent years, in part due to its strong synergies with the need to reduce CH_4 as a greenhouse gas. In this chapter we investigate the importance of reducing CH_4 in order to reduce surface O_3, and we compare results of CH_4 mitigation efforts with results of other ozone precursor mitigation efforts within and outside Europe.

CH_4 is a relatively long lived and well-mixed gas, with an atmospheric half-life of around 8 years. CH_4 emissions from any given country therefore impact surface O_3 on a global scale, making CH_4 reduction policies also a global effort. Anthropogenic CH_4 emissions account for about one half to one third of the total annual emissions, with natural emissions also being likely to change due to climate change (Guo et al. 2023).

In the following, global anthropogenic emission scenarios from CIAM/IIASA are used to calculate background CH_4 concentrations up to the year 2050 using a box-model. The resulting CH_4 projections are then used in the EMEP model, in conjunction with the full scenario emissions, to simulate the impact on surface ozone. While emphasis is placed on the importance of CH_4 as an ozone precursor, for the 2050 projections the relative importance of emission reductions inside and outside of the EMEP domain are also discussed. Moreover, in addition to peak season MDA8, the relative importance of CH_4 is also discussed for the annual mean O_3, 4th highest MDA8 and SOMO35 ozone indicators.

4.1 Description of the experiments

4.1.1 Emission scenarios

The global anthropogenic emissions of methane (CH_4) and other relevant species, including nitrogen oxides (NOx), non-methane volatile organic compounds (VOC), and carbon monoxide (CO) were developed with the IIASA's GAINS model (Amann et al. 2011)[1] and provided by CIAM/IIASA[2]. The respective emission datasets consist of 5-yearly global annual emissions for the period 2015 to 2050 and include two scenarios: (i) a baseline that is referred to as current legislation case (CLE) and (ii) a scenario that assumes strong mitigation of all species (LOW).

The **current legislation scenario (CLE)** assumes implementation and effective enforcement of all committed energy and environmental policies affecting emissions of air pollutants and greenhouse gases. CIAM has undertaken a review and update of historical data (up to 2020) driving emissions of all species in the GAINS model, drawing on the statistical information from EUROSTAT, International Energy Agency (IEA), UN Food and Agriculture Organization (FAO), as well as reporting of data and emissions to the Center on Emission Inventories and Projections (CEIP[3]). For the EU27, the energy and agriculture projections are consistent with the objectives of the European Green Deal and Fit for 55 package making EU carbon neutral by 2050; these are consistent with the projections used in the EU 3rd Clean Air Outlook[4]. For West Balkan, Republic of Moldova, Georgia, and Ukraine, a similar set of modelling tools was used as for the EU developing a new consistent set of projections. For the rest of the world, the GAINS model downscales projections from IEA and FAO (Alexandratos and Bruinsma 2016, IEA 2018) and updating the air pollution legislation from national and international sources (e.g. DieselNet (n.d.), He et al. (2021), Zhang (2018)), including EU legislation and their implementation in consultations with the EU Member States. Note that the baseline used in this work does not include any recent shock events, i.e., these scenarios were developed before the Ukraine war. Global emissions of CH_4 in the CLE scenario increase by nearly 30% by 2050 compared to 2015 (Table 4.1), while in the EU27 they are expected to decline by nearly 50% owing to the Green Deal assumptions. While European, North American, and Chinese NOx are estimated to continue to decline, which is consistent with other estimates for recent years (McDuffie et al. 2020, Zheng et al. 2018), at the global level no significant trend is visible (Table 4.1) owing to strong growth of emissions in several regions, especially South Asia. Similarly, global VOC emissions remain rather stable, although there are differences in regional trends. Decline in CO of about 20% by 2050 is mainly due to introduction of policies in the transport sector and increasing access to clean energy for cooking.

The **mitigation scenario (LOW)** includes several additional policies and assumes implementation of further emission reduction options, exploiting the proven technical mitigation potential as embedded in the GAINS model for air pollutants (Amann et al. 2020, 2013, Rafaj et al. 2018) and methane (Gomez Sanabria et al. 2022, Höglund-Isaksson 2012, Höglund-Isaksson et al. 2020). While for the EU27 the LOW scenario has the same energy projections as for the CLE (the Green Deal), the rest of the world includes climate policies compatible with Paris Agreement goals resulting in global decline of fossil fuel use and therefore also lower CH_4 emissions. Furthermore, additional assumptions about significant transformation in the agricultural sector are included, leading to strong reduction of livestock numbers, especially cattle and pigs; this brings significant additional reductions of methane. The latter is

[1] https://gains.iiasa.ac.at/models/gains_models4.html

[2] Center for Integrated Assessment Modelling (CIAM) hosted by the International Institute for Applied Systems Analysis (IIASA), Laxenburg, Austria (https://iiasa.ac.at/policy/applications/centre-for-integrated-assessment- modelling-ciam)

[3] www.ceip.at

[4] https://environment.ec.europa.eu/topics/air/clean-air-outlook_en

Table 4.1: Global emission totals for the CLE and LOW emission scenarios in units of Tg yr^{-1}.

Species	Scenario	2015	2020	2025	2030	2035	2040	2045	2050
NOx	CLE	117	108	103	100	98	100	101	103
NOx	LOW			97	72	50	31	28	25
VOC	CLE	110	109	108	106	106	106	107	108
VOC	LOW			97	72	50	31	28	25
CO	CLE	521	478	453	431	423	417	414	412
CO	LOW			312	203	163	112	109	106
CH_4	CLE	338	349	363	375	388	405	420	431
CH_4	LOW			231	219	208	203	196	169

based on the scenarios from the 'Growing Better report 2019' (The Food and Land Use Coalition 2019) and other studies considering ambitious improvements in nitrogen use efficiency and addressing healthy dietary requirements (Kanter et al. 2020, The EAT-Lancet Commission 2019) as used earlier in scenarios for the global air pollution study (Amann et al. 2020).

Global emissions of all species decline strongly in the LOW scenario (Table 4.1). By 2050, global anthropogenic air pollutant (NOx, VOC, CO) emissions decline by about 80% compared to 2015. These reductions are driven by rapid introduction of stringent emission limit values for stationary and mobile sources, strong decline in fossil fuels use and access to clean energy for cooking. Global CH_4 emission decline by about 50%, which is comparable to the estimates in the Global Methane Assessment (GMA 2021) and broadly follows the Methane Pledge for 2030 (30% reduction, Malley et al. 2023). Key factors determining reductions include a mix of technological options increasing utilization of methane losses from production and distribution of fossil fuels, improved waste management, strong decline in fossil fuel use as well as declining livestock numbers due to the transformational changes in agriculture.

4.1.2 Box-model CH_4

In general, the species listed in Table 4.1 act either as sources (NOx) or sinks (VOC, CO) of hydroxyl (OH), affecting the lifetime of CH_4 through its loss against oxidation. The emissions are combined with the direct CH_4 emissions in the chemistry box-model from Olivié et al. (2021), to calculate the time-development of background CH_4 concentrations. To this end, the CLE and LOW emission budgets are linearly interpolated to annual mean values from 2020 onward.

The CLE emissions are first used to tune the modeled CH_4 concentrations to observation between the years 2015-2019. This is done to estimate the natural background CH_4 source strength, which by this method is estimated at 240 Tg/year. The CH_4 concentrations are then calculated up to the year 2050 using the different scenario emissions, as shown in Fig. 4.1, assuming a constant natural emission strength. In the CLE and LOW scenarios, the resulting CH_4 background concentrations are 2215 and 1431 ppb by 2050, respectively, against a baseline concentration of 1834 ppb in 2015. For reference, Fig. 4.1 also includes the projected CH_4 concentrations for a selection of Representative Concentration Pathway (RCP) and Climate scenarios from the Coupled Model Intercomparison Project Phase (CMIP) scenarios. The AGAGE curve shows measurement-based concentrations from the Advanced Global Atmospheric Gases Experiment.

Fig. 4.1 also shows the projected CH_4 concentrations between 2050 and 2070, where the

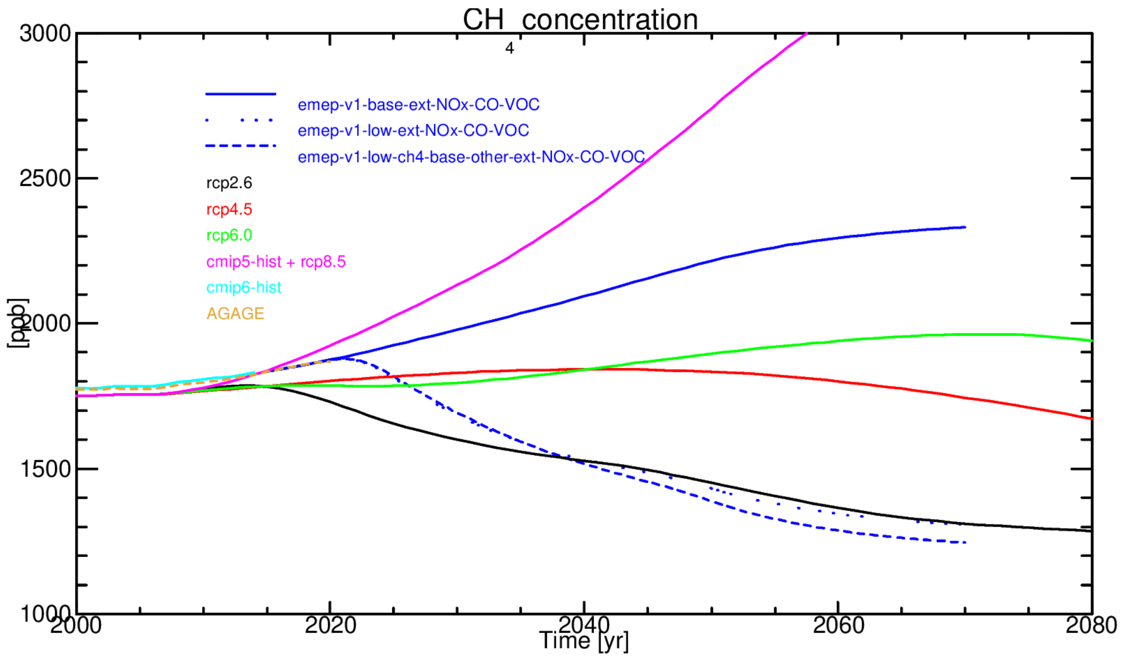

Figure 4.1: Projected background CH_4 concentrations up to 2070 under the range of emission scenarios described in the text. Note that the 'emep-v1-base-ext' experiment refers to the CLE scenario, the 'emep-v1-low-ext' to the LOW scenario, and 'emep-v1-low-ch4-base-other-ext' LOW CH_4 emission scenarios described in the text.

emissions of the respective emission scenarios are kept constant from 2050 onward. This illustrates that background CH_4 concentrations have not yet adjusted entirely to the 2050 emissions, i.e. loss and production terms are not yet in equilibrium, as CH_4 concentrations increase (decrease) by around 10% in the CLE (LOW) scenarios also after 2050. In addition, Fig. 4.1 includes a box-model experiment where the CH_4 emissions follow the LOW scenario, whereas the other emissions follow the CLE scenario ('emep-v1-low-ch4-base-other-ext'). Given the similarity between this curve (1388 ppb by 2050) and that of the full LOW scenario (1431 ppb by 2050), the background CH_4 changes result almost entirely from the changes in the direct emissions of CH_4. Changes in the species affecting the life-time of CH_4 are therefore of secondary importance.

4.1.3 EMEP model setup

In the following, EMEP simulations are performed using the background CH_4 concentrations for 2015 and for the 2050 CLE and LOW scenarios, where the CH_4 concentrations are fixed on an annual mean basis in the EmChem19rc chemistry (as discussed in Section 10.2). For the EMEP model setup, regional 0.1 by 0.1 degree EMEP domain simulations are combined with boundary and initial conditions from global 0.5 by 0.5 degree simulations. The EMEP model version used is rv4.51, employing 19 vertical layers for the global simulations and 20 for the (nested) regional simulations. The meteorological data are derived from ECMWF-IFS Cycle 40r1.

To investigate the impact of background CH_4 changes and emission changes separately, simulations are performed where either the (non-CH_4) emissions or CH_4 concentrations are changed. This is done both relative to the baseline 2015 year and relative to the 2050 CLE

Table 4.2: EMEP model configurations for the experiments described in Section 4.2.

Experiment long-name	short-name	Reg. emis	ROW emis	CH_4 ppb
Baseline 2015	bs15_bs15ch4	2015 base	2015 base	1834
Global 2050 CLE	cle50_cle50ch4	2050 CLE	2050 CLE	2215
Global 2050 LOW	low50_low50ch4	2050 LOW	2050 LOW	1431
Global 2050 CLE emis	cle50_bs15ch4	2050 CLE	2050 CLE	1834
Global 2050 LOW emis	low50_bs15ch4	2050 LOW	2050 LOW	1834
ROW 2050 LOW emis	rolow50_cle50ch4	2050 CLE	2050 LOW	2215
Global 2050 LOW emis 50ch4	low50_cle50ch4	2050 LOW	2050 LOW	2215

scenario. For the comparison against 2050 CLE, additional simulations are performed where the boundary conditions follow the LOW rest-of-world (ROW) emissions, while the regional domain follows that of the CLE scenario. Together with simulations where only the regional emissions are changed to LOW, and where only CH_4 is changed, we can then quantify the relative importance of regional and ROW emission changes and of CH_4 changes relative to the 2050 CLE scenario. The full list of simulations described in the following analysis is given in Table 4.2.

4.2 Results

4.2.1 Baseline 2015 versus 2050 CLE and LOW

In this section, we analyze how ozone in Europe will change assuming that no further policies are implemented (baseline/CLE) or if substantially more ambitious policies are implemented (LOW). To that end, simulations for the 2050 CLE and LOW scenarios are compared against the 2015 baseline.

Fig. 4.2a shows the difference in peak season MDA8 across Europe between the 2015 baseline simulation and a simulation with 2050 CLE emissions. Here the difference is calculated as the baseline minus the 2050 CLE run, indicating that concentrations are reduced by 10-20 µg m^{-3} over much of central Europe. Fig. 4.2b shows the difference between the 2050 CLE emissions run and a run where in addition the background CH_4 concentration is changed from the 2015 baseline value (1834 ppb) to that of the 2050 CLE scenario (2215 ppb). This shows that the impact of CH_4 in the 2050 CLE scenario is to increase concentrations by 3-4 µg m^{-3} over land, while the increase can be as large as 6 µg m^{-3} nearer to ship tracks.

Fig. 4.2c-d are similar to panels a-b, but instead show the results for the LOW scenario. Here the concentration change due to emission reductions is nearer to 25-35 µg m^{-3} over central Europe. The impact of the reduced CH_4 concentrations (1431 ppb) is to reduce peak season MDA8 concentrations by 3-4 µg m^{-3} over land.

4.2.2 2050 CLE versus LOW

In the previous section, we analyzed how ozone could change in the future assuming either a current legislation scenario (CLE) or a substantially more ambitious scenario (LOW) for 2050. In this section, we quantify how much more you can achieve in 2050 when implementing the

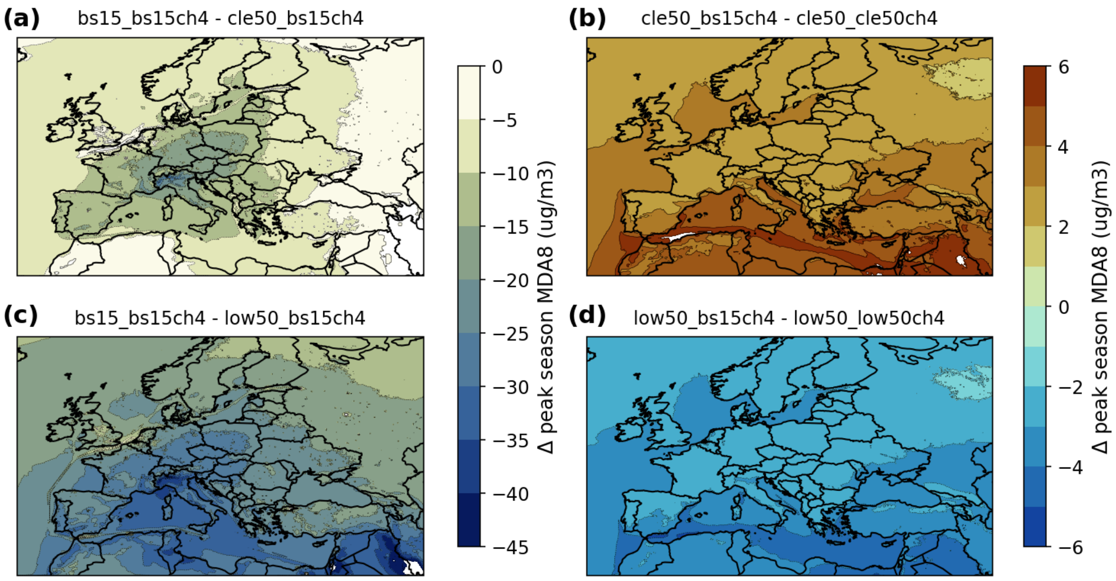

Figure 4.2: Peak season MDA8 change relative to the 2015 baseline year due to 2050 CLE and LOW emissions are shown in panel **(a)** and **(c)**, respectively. Panels **(b)** and **(d)** show the corresponding impacts of the 2050 CLE (2215 ppb) and LOW (1431 ppb) background CH_4 concentrations relative to the 2015 concentration (1834 ppb). Plot titles refer to the experiments listed in Table 4.2.

ambitious scenario (LOW) compared to current policies (CLE). Considering that air quality guidelines are not met in the CLE scenario (and not in the LOW scenario either, as will be discussed in Section 4.3), this addresses a policy-relevant question. Another policy-relevant question is how much that could be achieved by reducing emissions only within the EMEP domain and how much could be achieved by also reducing emissions in the rest of the world (ROW).

To first quantify the total reduction in peak season MDA8 between the 2050 CLE and LOW scenarios, Fig. 4.3a shows the combined impact of the global emission reductions and reduced background CH_4 concentrations (2215 to 1431 ppb). This panel shows that net concentrations are reduced by around 10-15 µg m^{-3} over land in the LOW scenario relative to the CLE scenario.

To quantify the impact of ROW emission reductions from the LOW scenario, the 2050 CLE simulation is repeated using boundary conditions from a global simulation with LOW emissions. The difference between these simulations is shown in Fig. 4.3b, and indicates that the ROW LOW emission reductions lead to a ∼5 µg m^{-3} peak season MDA8 reduction broadly in the western parts of Europe. In Fig. 4.3c, the difference between the simulation with ROW LOW boundary conditions and a simulation where the regional emissions also follow the LOW scenario is shown. This experiment isolates the impact of the regional LOW emissions, with reductions now falling around 5-10 µg m^{-3} over much of Europe. Fig. 4.3d shows the difference between the full LOW emission simulation and a simulation where the background CH_4 concentrations are changed from the CLE (2215 ppb) to that of the LOW (1431 ppb) scenario. This shows that the impact of CH_4 reductions is now to reduce peak season MDA8 by about 5 µg m^{-3} across Europe.

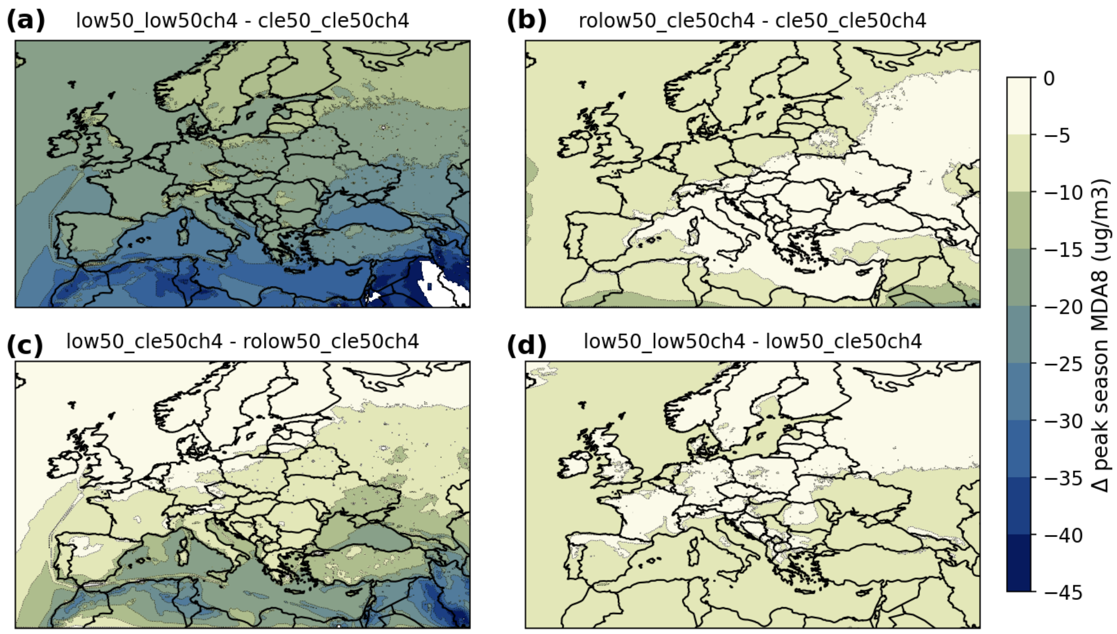

Figure 4.3: Peak season MDA8 changes between the LOW and CLE scenarios in 2050 are shown in panel **(a)**. Panel **(b)** shows the change due to emission reductions outside of the EMEP domain, panel **(c)** the change due to emission reductions inside the EMEP domain, and panel **(d)** the reductions due to the difference in background CH_4 concentrations between the two emission scenarios. Plot titles refer to the experiments listed in Table 4.2.

4.2.3 Population weighted results

This section analyzes the simulation results from the previous section on a population weighted basis. This is done for the EU27 countries, as well as for the population within the EMEP land area (i.e., land area of the EMEP countries within the regional EMEP 0.1 by 0.1 degree domain). In addition, for the EU27 average the number of ozone metrics is also extended to include annual mean O_3, the 4th highest annual MDA8 value, and SOMO35.

For the population distribution, gridded data (3 arcsec resolution) from the Global Human Settlement Layer project (GHSL, European Commission and Joint Research Centre 2023) is aggregated onto the 0.1 by 0.1 degree EMEP grid. Since the CLE and LOW scenario emissions are all gridded to the EMEP spatial distribution for 2019, the population map for 2020 is also used for the 2050 scenario comparisons. We note that the 2020 population map is the nearest available year to 2019 from the GHSL data set.

Baseline 2015 versus 2050 CLE and LOW

Fig. 4.4 repeats the results from Fig. 4.2, but now for each individual population weighted EU27 country, in addition to the EU27 and EMEP regional averages. This figure illustrates that for some countries, such as IE, LU, LV, and BE, the reduction in peak season MDA8 in the 2050 CLE scenario with respect to 2015 is largely outweighed by the increase due to CH_4. The figure also illustrates that, relative to the 2015 baseline, the LOW emission reductions have a far greater impact than the associated CH_4 reductions. For example, the EU27 average reduction due to the LOW emissions is 21.6 μg m^{-3}, whereas the reduction due to the lowered CH_4 concentrations is 2.8 μg m^{-3}. For the CLE scenario, the EU27 average reduction due to

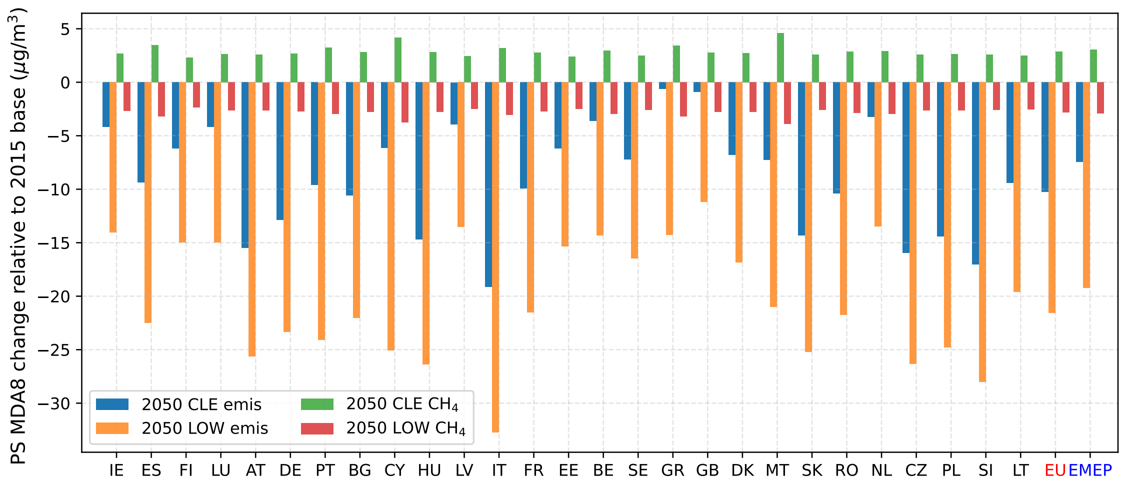

Figure 4.4: Population weighted country average peak season MDA8 (μg m^{-3}) changes due to emission reductions relative to the 2015 baseline in the CLE (blue) and LOW (orange) scenarios by 2050, and due to the corresponding CLE (green) and LOW (red) CH_4 changes. The EU27 and EMEP population weighted averages are marked in blue and red on the x-axis.

emission changes are 10.3 μg m^{-3}, while CH_4 leads to an increase of 2.9 μg m^{-3}.

Fig. 4.5 shows the population weighted results for the EU27 average for the peak season MDA8, annual mean O_3, 4th highest MDA8 and SOMO35 ozone indicators. This figure illustrates that the impact of emission changes can differ considerably between the different indicators, with the sign of the changes due to the CLE 2050 emissions even being opposite for O_3 mean. Moreover, the relative importance of CH_4 is considerably smaller for the 4th highest MDA8 and SOMO35 indicators than it is for peak season MDA8 and O_3 mean. The relative importance of CH_4 is comparatively the largest for annual mean O_3, amounting to 27% of the reductions achieved by non-CH_4 emissions in the LOW 2050 scenario relative to 2015 (compared to 13% for peak season MDA8). The comparatively large CH_4 impact is probably due to the relatively small impact of emission reductions caused by competing NOx titration (winter) and production (summer) effects over the course of a year.

2050 CLE versus LOW

In Fig. 4.6 the 'ROW LOW emis', 'Regional LOW emis' and 'LOW CH_4' bars correspond to the results shown in Fig. 4.3 panels b, c, and d, respectively. These bars illustrate that the impact of CH_4 is generally comparable to the impact of ROW LOW and regional LOW emission reductions, with the exception for Cyprus (CY), where the regional emissions have a considerably larger impact. For Ireland, ROW emission reductions are much more important than regional and CH_4, possibly due to its proximity to the Atlantic air masses. In general, the net difference between the CLE and LOW scenarios by 2050 is split almost evenly between the impact of ROW emission reductions, regional emission reductions, and CH_4 reductions.

Fig. 4.7 shows the EU27 average results for the different ozone metrics. This shows that for annual mean O_3, the ROW emission reductions are comparatively more important, while for the 4th highest MDA8 indicator, the regional emission reductions are more important. For SOMO35, the impact of CH_4 is comparatively small, while the emission impact is split almost evenly between ROW and regional reductions.

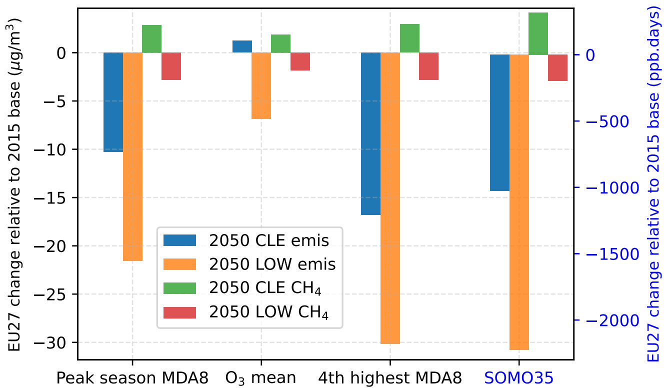

Figure 4.5: EU27 population weighted average changes due to emission changes relative to the 2015 baseline in the CLE (blue) and LOW (orange) scenarios by 2050, and due to the corresponding CLE (green) and LOW (red) CH_4 changes. Changes are shown for the peak season MDA8, annual mean O_3, annual 4th highest MDA8, and SOMO35 ozone indicators. Note the difference in y-axis scaling for the SOMO35 indicator.

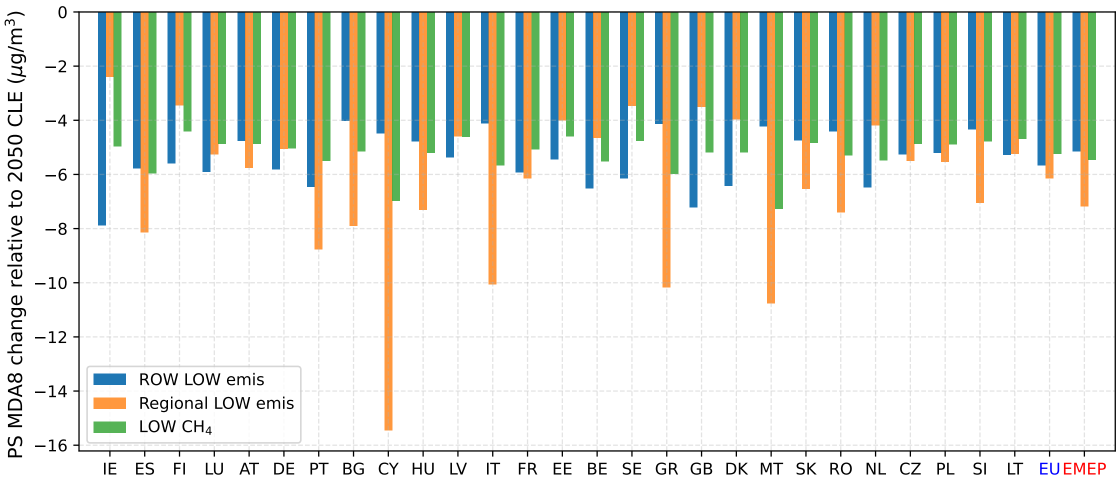

Figure 4.6: Population weighted country average peak season MDA8 (µg m^{-3}) changes in the 2050 LOW scenario relative to 2050 CLE due to emission reductions outside of the EMEP domain (ROW, blue), emission reductions inside the EMEP domain (regional, orange), the difference in background CH_4 between the two scenarios (green). The EU27 and EMEP population weighted averages are marked in blue and red on the x-axis.

4.3 Conclusion

This work investigates the impact of background CH_4 and emission changes on European ozone, both relative to the 2015 baseline year and relative to the 2050 CLE scenario.

We find that in the LOW scenario the impact of a 50% anthropogenic CH_4 emission reduction by 2050 relative to 2015 has a much smaller impact on surface O_3 than the impact of other emission reductions, when comparing against the 2015 baseline. In the LOW emission scenario, the peak season MDA8 reductions due to non-CH_4 emission reductions are almost an order of magnitude larger than those achieved through the reduced background CH_4 concentrations. One reason for this is that the 50% anthropogenic CH_4 emission reduction leads to only a 22% reduction in background CH_4 concentrations, in part due to the influence of

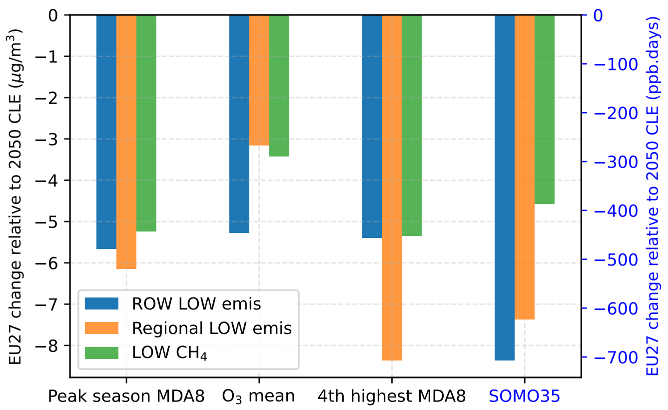

Figure 4.7: EU27 population weighted regional average changes in the 2050 LOW scenario relative to 2050 CLE due to emission reductions outside of the EMEP domain (ROW, blue), emission reductions inside the EMEP domain (regional, orange), the difference in background CH_4 between the two scenarios (green). Changes are shown for the peak season MDA8, annual mean O_3, annual 4th highest MDA8, and SOMO35 ozone indicators. Note the difference in y-axis scaling for the SOMO35 indicator.

natural CH_4 emissions and the relatively long life-time of CH_4.

However, when considering the difference between the 2050 CLE and LOW scenarios, the relative importance of CH_4 is considerably greater. For peak season MDA8, the net reductions between the CLE and LOW scenarios are split almost evenly between emission reductions inside the EMEP domain, outside the EMEP domain, and the associated background CH_4 reduction (2215 to 1431 ppb). This highlights an important role of CH_4, as the CLE emission reductions are not sufficient to achieve WHO peak season MDA8 guidelines (60 µg m^{-3}) across Europe, such that further reductions are required. Indeed, not even the LOW scenario is sufficient to reach the WHO guidelines, as illustrated in Fig. 4.8. CH_4 can therefore play an important role in achieving the further O_3 reductions required to meet WHO guidelines, also considering that CH_4 abatement policies are relatively cost-efficient (Höglund-Isaksson et al. 2020, GMA 2021).

Our work further illustrates that the relative importance of emission and CH_4 changes varies considerably between the peak season MDA8, O_3 mean, 4th highest MDA8, and SOMO35 ozone indicators. This may complicate establishing a clear picture of which emission reductions (i.e., CH_4 or non-CH_4) to prioritize in order to achieve air quality targets.

In this work we have only analyzed results for the CLE and the LOW scenario for 2050. The LOW scenario is a very ambitious scenario that goes beyond the maximum technical feasible (MFR) scenario in that it includes climate policies compatible with Paris goals and developments in the agricultural sector. As a part of the work for the Gothenburg Protocol Review, global MFR scenarios were also developed. We plan to include model simulations using the MFR scenarios in our future work. Future work will also use the box-model to also estimate the impact of biogenic CH_4 emission changes. Furthermore, simulated peak season MDA8 concentrations will be compared to observations, while also investigating the impact of using different meteorological reference years.

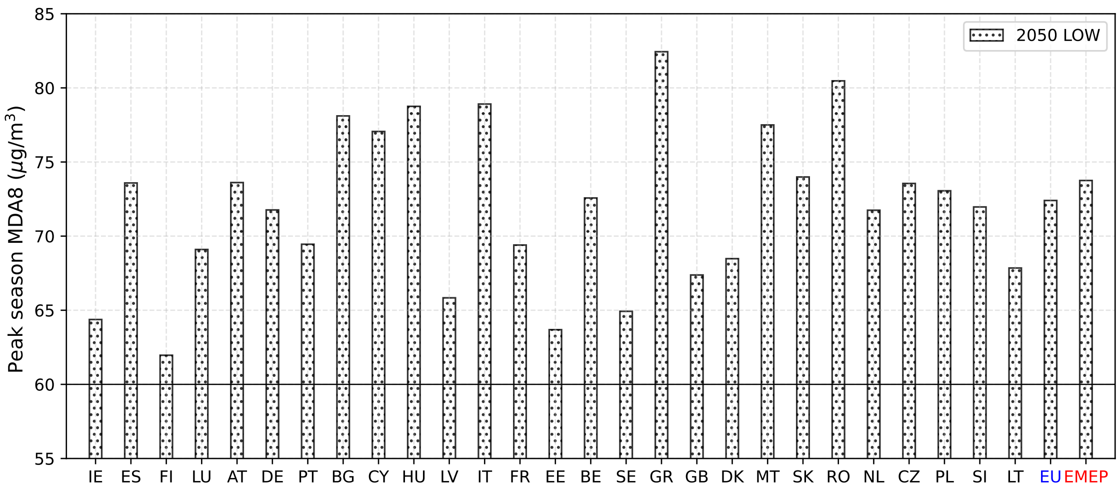

Figure 4.8: Population weighted country average peak season MDA8 (μg m^{-3}) in the 2050 LOW scenario. The horizontal line marks the air quality guideline set by the WHO. The EU27 and EMEP population weighted averages are marked in blue and red on the x-axis.

References

United Nations Environment Programme and Climate and Clean Air Coalition. Global Methane Assessment: Benefits and Costs of Mitigating Methane Emissions. Nairobi: United Nations Environment Programme., Tech. rep., 2021.

Alexandratos, N. and Bruinsma, J.: World agriculture towards 2030/2050: the 2012 revision, Working paper Rome, FAO., 2016.

Amann, M., Bertok, I., Borken-Kleefeld, J., Cofala, J., Heyes, C., Hoeglund-Isaksson, L., Klimont, Z., Nguyen, B., Posch, M., Rafaj, P., Sandler, R., Schoepp, W., Wagner, F., and Winiwarter, W.: Cost-effective control of air quality and greenhouse gases in Europe: Modeling and policy applications, Environmental Modelling & Software, 26, 1489–1501, doi:10.1016/j.envsoft.2011.07.012, 2011.

Amann, M., Klimont, Z., and Wagner, F.: Regional and Global Emissions of Air Pollutants: Recent Trends and Future Scenarios, Annual Review of Environment and Resources, 38, 31–55, doi:10.1146/annurev-environ-052912-173303, 2013.

Amann, M., Kiesewetter, G., Schöpp, W., Klimont, Z., Winiwarter, W., Cofala, J., Rafaj, P., Höglund-Isaksson, L., Gomez-Sabriana, A., Heyes, C., Purohit, P., Borken-Kleefeld, J., Wagner, F., Sander, R., Fagerli, H., Nyiri, A., Cozzi, L., and Pavarini, C.: Reducing global air pollution: the scope for further policy interventions, Philosophical transactions. Series A, Mathematical, physical, and engineering sciences, 378, 20190 331, doi:10.1098/rsta.2019.0331, URL https://europepmc.org/articles/PMC7536039, 2020.

DieselNet: DieselNet: Diesel Exhaust Emission Standards [WWW Document], URL http://www.dieselnet.com/standards/(accessed3.15.14), n.d.

European Commission and Joint Research Centre: GHSL data package 2023, Publications Office of the European Union, doi:doi/10.2760/098587, 2023.

Gomez Sanabria, A., Kiesewetter, G., Klimont, Z., Schoepp, W., and Haberl, H.: Potential for future reductions of global GHG and air pollutants from circular waste management systems, Nature Communication, 13, doi:10.1038/s41467-021-27624-7, 2022.

Guo, J., Feng, H., Peng, C., Chen, H., Xu, X., Ma, X., Li, L., Kneeshaw, D., Ruan, H., Yang, H., and Wang, W.: Global Climate Change Increases Terrestrial Soil CH4 Emissions, Global Biogeochemical Cycles, 37, e2021GB007 255, doi:https://doi.org/10.1029/2021GB007255, 2023.

He, X., Shen, W., Wallington, T., Zhang, S., Wu, X., Bao, Z., and Wu, Y.: Asia Pacific road transportation emissions, 1900–2050, Faraday Discuss., 226, 2021.

Höglund-Isaksson, L.: Global anthropogenic methane emissions 2005-2030: technical mitigation potentials and costs, Atmos. Chem. Phys. Discuss., p. 11275–11315, 2012.

Höglund-Isaksson, L., Gómez-Sanabria, A., Klimont, Z., Rafaj, P., and Schöpp, W.: Technical potentials and costs for reducing global anthropogenic methane emissions in the 2050 timeframe –results from the GAINS model, Environmental Research Communications, 2, 025 004, doi:10.1088/2515-7620/ab7457, 2020.

IEA: World Energy Outlook 2018, 2018.

Kanter, D., Winiwarter, W., Bodirsky, B., Bouwman, L., and Boyer, K.: Nitrogen futures in the shared socioeconomic pathways, Glob. Environ. Change, 61, doi:10.1016/j.gloenvcha.2019, 2020.

Malley, C. S., Borgford-Parnell, N., Haeussling, S., Howard, I. C., Lefèvre, E. N., and Kuylenstierna, J. C. I.: A roadmap to achieve the global methane pledge, Environmental Research: Climate, 2, 011 003, doi:10.1088/2752-5295/acb4b4, 2023.

McDuffie, E. E., Smith, S. J., O'Rourke, P., Tibrewal, K., Venkataraman, C., Marais, E. A., Zheng, B., Crippa, M., Brauer, M., and Martin, R. V.: A global anthropogenic emission inventory of atmospheric pollutants from sector- and fuel-specific sources (1970–2017): an application of the Community Emissions Data System (CEDS), Earth System Sci. Data., 12, 3413–3442, doi:10.5194/essd-12-3413-2020, URL `https://essd.copernicus.org/articles/12/3413/2020/`, 2020.

Olivié, D., Höglund-Isaksson, L., Klimont, Z., and von Salzen, K.: Calculation of future CH 4 mixing ratios for the ECLIPSE-v6b emission scenarios, Tech. rep., 2021.

Rafaj, P., Kiesewetter, G., Gül, T., Schöpp, W., Cofala, J., Klimont, Z., Purohit, P., Heyes, C., Amann, M., B.-K., and J., Cozzi, L.: Outlook for clean air in the context of sustainable development goals, Glob. Environ. Change, 53, 1–11, doi:https://doi.org/10.1016/j.gloenvcha.2018.08.008, 2018.

The EAT-Lancet Commission: Healthy Diets From Sustainable Food Systems, 2019.

The Food and Land Use Coalition: Growing Better: Ten Critical Transitions to Transform Food and Land Use, URL `https://www.foodandlandusecoalition.org/`, 2019.

Zhang, X.: Emission standards and control of PM2.5 from coal power plant, 2018.

Zheng, B., Tong, D., Li, M., Liu, F., Hong, C., Geng, G., Li, H., Li, X., Peng, L., Qi, J., Yan, L., Zhang, Y., Zhao, H., Zheng, Y., He, K., and Zhang, Q.: Trends in China's anthropogenic emissions since 2010 as the consequence of clean air actions, Atmos. Chem. Physics, doi:10.5194/acp-2018-374, 2018.

CHAPTER 5

The Local Fractions method and its application to ozone

Peter Wind and Willem van Caspel

5.1 Introduction

The Local Fractions (LF) method was originally developed as a practical method to give the fraction of pollutants that have a local origin (Wind et al. 2020). It has since been developed and can now efficiently track pollutants from a large number of sources, over large distances.

In its first formulation, the method could only be applied to inert pollutants. Also pollutants that have a non-linear dependence on emission intensity could be described, as long as the non-linear dependency can be neglected in a first approximation. This allowed for example the study of long term trends of reduced nitrogen in the atmosphere (see EMEP Status Report 1/2022).

Many important pollutants have a non-linear dependency on emissions. The LF method has now been developed to allow to track such pollutants through the full complexity of the chemical processes, allowing a description of fundamentally non-linear species such as ozone (O_3).

For non-linear species, the fraction of pollutants from a specific source is not uniquely defined, since the total concentration cannot be expressed as a linear combination of individual contributions without further assumptions. However, for small changes of emissions, the response in for example ozone will be linear: a small change in ozone concentrations can be expressed as a linear combination of different emission changes, as long as those emission changes are small enough.

The original interpretation of LF as the fraction of pollutant from a specific source is no longer valid. Instead, the sensitivity to emission changes are defined (sensibilities). This approach allows for a mathematically well-defined description of non-linear transformations. The sensitivities obtained through the Local Fraction method define the changes in pollutant concentrations that would result from small changes in emissions. By "small", we mean that the method mathematically calculates the tangent of concentrations expressed as a function of emission intensity.

Since the emission of a specie will affect an entire group of species through chemical reactions, the sensibilities of all species that are directly or indirectly involved in the chemical processes must be tracked simultaneously for each source.

5.1.1 Local Fractions as sensibility to emission changes

We can define a generalized local fraction as the sensibility to changes in emissions from a specific source E_k:

$$S(c_i, E_k) = \frac{\partial c_i}{\partial E_k} E_k \tag{5.1}$$

Where c_i is the concentration of pollutant i. The last factor E_k is the rate of emission of source k, to get dimensionless emissions.

The original local fractions was a dimensionless fraction. The generalized definition has units of concentrations. It is equivalent to the original LF definition, only multiplied by the pollutant concentration. The original interpretation (the fraction of pollutant originating from a specific source) cannot be used anymore, however, the equations and code valid for the original local fractions can still be used: simply multiply or divide by the pollutant concentration in order to switch from one representation to the other.

5.1.2 Chemistry

In Wind et al. (2020), we showed how the local fractions are transformed during advection and other linear processes. In this section we will show how non-linear chemical transformations can be taken into account.

Given the local fractions at time t, we want to compute the new local fractions after that the concentrations have been updated through the chemical module. We denote the values obtained after the chemical module by the time $t + \Delta t$. We will assume (as is the case in our model code), that the species emitted by the emission sources are included as an additional term in the chemistry module.

The concentrations c_j at time $t+\Delta t$, can be expressed as a general function of all the input parameters, concentrations and emissions at time t. Only the parameters that are affected by the sources are written explicitly; Δt, temperature, humidity, air density etc. are not modified by a change in emission in our model.

$$c_i(t + \Delta t) = f_i(c_1, c_2...cn, E_1, E_2, E_3...)(t) \tag{5.2}$$

where all concentrations on the right hand side are at time t and E_j are a set of emitted species.

If we derive the equation with respect to E_k we get:

$$\frac{\partial c_i}{\partial E_k}(t + \Delta t) = \sum_{E_j} \frac{\partial f_i}{\partial E_j} \frac{\partial E_j}{\partial E_k} + \sum_{c_j} \frac{\partial f_i}{\partial c_j} (\frac{\partial c_j}{\partial E_k}(t)) \tag{5.3}$$

where $\frac{\partial f_i}{\partial c_j}$ is the Jacobian of the transformation.

We assume that f_i and its partial derivatives are continuous functions. $\frac{\partial f_i}{\partial E_j}$ represents the change in the concentration c_i due to the emissions E_j during Δt. (Note that the method does not assume that Δt is small).

$\frac{\partial E_j}{\partial E_k}$ shows the dependence of emitted species j to the source k. Typically this could be 1 within a country referenced by k and zero outside of the country, or it could be some other fraction if one considers more complex situations such as sector specific emissions.

The $\frac{\partial c_j}{\partial E_k}(t)$ terms are the values of the sensibilities at time t. To use this formula, we need to determine the values of the Jacobian matrix. This is the most time-consuming part of the process, as discussed in the next section.

5.1.3 Computational cost

The calculation of the Jacobian matrix is done by numerical derivatives: for each derivative j we compute a new set of concentrations obtained by changing slightly the concentration of pollutant j. That means that the entire chemical computations are performed independently for as many pollutants as the number of pollutants involved in the ozone chemistry (54 in our case). However, since exactly the same mathematical transformations are applied each time, this can be done relatively efficiently by so-called vectorization of the computer code.

A LF run giving contributions for 55 source countries and NO_x and VOC emission reductions, takes less than 10 hours (wall time) on a supercomputer (2048 cores). This can be compared to about 2.5 hours on 512 cores for a single brute force (BF) simulation, where emissions of one pollutant are reduced in one source country. In terms of CPU hours, the LF runs presented in this report are approximately 16 times more expensive than a single BF run, but gives results equivalent to 111 BF simulations. In the future we expect the method still to allow for improved efficiency.

5.2 Comparison of the brute force (BF) and local fraction (LF) methods

Source receptor calculations are performed for EMEP every year (for the year with recently reported emissions, e.g. for the year 2021 in 2023). The source receptor matrices are generated using the so-called brute force method (BF, also referred to as the ”perturbation method”). As discussed in the previous section, the LF method is far more efficient and could represent a new way of calculating the source receptor matrices for EMEP. As a first step, we want to compare the LF results to the BF results for model runs with exactly the same setup. Note however that the brute force and LF methods are not expected to give the exact same results:

- The brute forces method reduces emissions by 15%, while the LF method extrapolates the derivatives calculated at total emissions to a 15% reduction. Therefore, the BF method will include some non-linearities.

- The LF method uses a different advection scheme in the horizontal direction; the BF method performs two runs, where the concentrations in the run with reduced emissions, will result in a different flux pattern. This is because in the advection scheme used (fourth order Bott (1989)), the fraction of pollutants transported from one grid-cell to a neighboring grid-cell does not only depend on the wind fields, but also on the distribution of pollutants. The sensibilities obtained by the LF method only uses the fluxes from the total emission run and assumes that the flux intensity is not emission dependent.

- Some secondary processes are not taken fully into account in the LF method. For example, some reaction rates will change according to the surface of the aerosols present. The effect of the changes of those reaction rates due to emission changes is not (yet) implemented in the LF model. Also, the photolysis rate will be dependent on the pollutant concentrations in Cloud-J (see Section 8).

The differences between the two methods are secondary in the sense that the fundamental chemical mechanisms are taken into account identically in both methods.

The model version and input data used in this chapter are identical to what was used for computing the source receptor relationships in this the report (Appendix C).

5.2.1 Comparison with BF for peak season MDA8

In order to verify that the code actually gives the correct values for the sensitivities, we compare to the BF method for standard source receptor matrices for peak season MDA8 for a subset of countries (EU27). Peak season MDA8 ($MDA8_{AS}$) is the O_3 metric recently proposed by the WHO (2021), and is calculated as the April to September average of daily maximum 8-hour running averages of hourly O_3 concentrations. For the BF case, a separate run is required for each country and pollutant reduction to calculate the impact on $MDA8_{AS}$. In the LF case, values for all countries and for NOx and VOC reductions are obtained in a single run.

Figure 5.1 shows an example of maps obtained with both methods for Germany (DE), for a 15% NOx reduction. The two methods give very similar geographical distributions, with the same regions showing positive and negative effects. From the figure alone, it is hard to see any differences in the results.

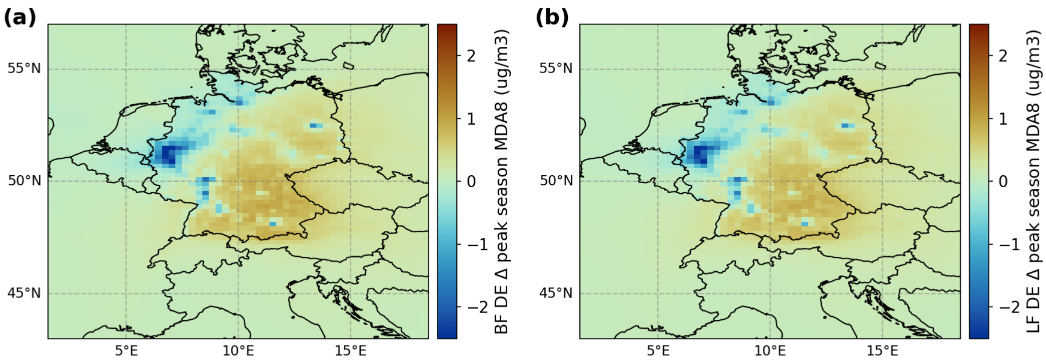

Figure 5.1: Comparison of the impact of a 15% NOx emission reduction from Germany (DE) on peak season MDA8 calculated using the BF **(a)** and LF **(b)** methods.

The total country-to-itself contributions are compared in Figure 5.2 for a set of countries. In blue we show the BF results and in orange the corresponding LF results obtained using the total emissions. In order to gain insight into the magnitude of the non-linearities included in the BF 15% reductions, we performed an additional LF run for a scenario where all NOx emissions are reduced by 15% (P15, in green). The impact of a 15% emission reduction is then calculated by extrapolating the derivatives from the 15% reduced emission scenario up

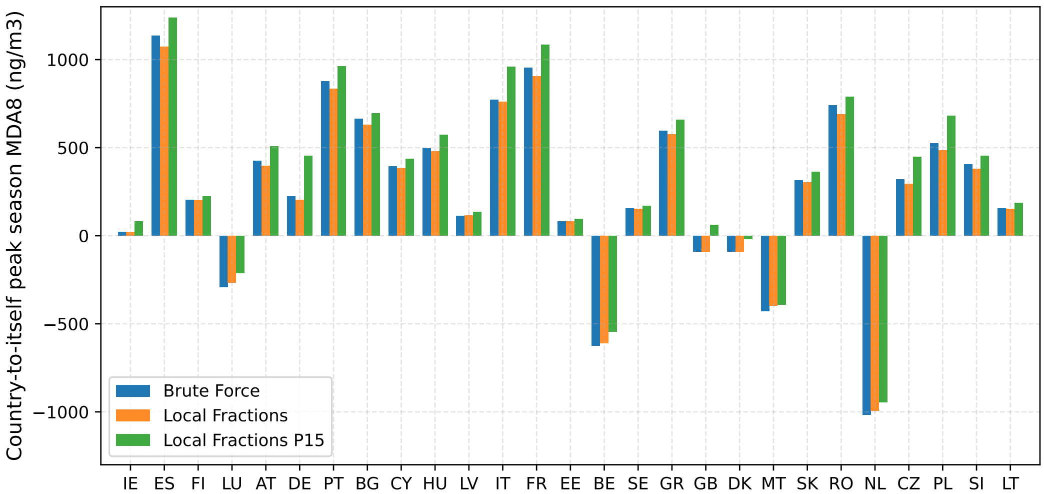

Figure 5.2: EU27 country-to-itself contribution to peak season MDA8 in 2021 for a 15% NO_x emission reduction, based on the brute force (blue) and Local Fractions methods. The local fraction contributions are calculated from a simulation with full emissions (orange) and from a simulation where a 15% emission reduction is applied to all countries (P15, green). Negative numbers imply that peak season MDA8 concentrations are increased when emissions inside the corresponding country are reduced.

to 100% emissions. Note that this is not directly comparable to the BF reductions, where only one country at a time has reduced emissions. Furthermore, the results using the BF method represent the average response to a 15% emission reduction, while LF P15 calculates the tangent at 15%. The difference between the orange (LF) and green (LF P15) bars, is an indicator of the magnitude of the non-linear effects that can be expected for a 15% emission change.

The overall picture is that the two methods (BF and LF) show similar results, with discrepancies usually smaller than the differences due to non-linearities. This is also what is expected from the methodological differences.

To show the consistency of the LF method across the larger source-receptor domain, Figure 5.3 shows the “blame matrix” calculated for the EU27 countries. In this figure, the values calculated using the BF method (ng/m^3) are shown in each of the source-receptor combinations, while the percentage difference between the LF and BF results are overlaid as colours. The figure indicates that the LF differences generally fall between $\pm$10% of the BF values. The results for the German (DE) emission reductions show the largest percentage differences, which will be explored in more detail in the following section. We note, however, that the large percentage differences correspond to absolute differences only on the order of tens of nanograms per cubic meter.

5.2.2 Quantification of discrepancies between BF and LF for DE

In order to get more detailed insight in the reasons for the discrepancies between the BF and LF methods, we have performed additional NOx emission reduction test runs for Germany (DE):

- A brute force run with 1% reduction in emissions, to quantify the non-linear contribution to the BF 15% results (BF1).

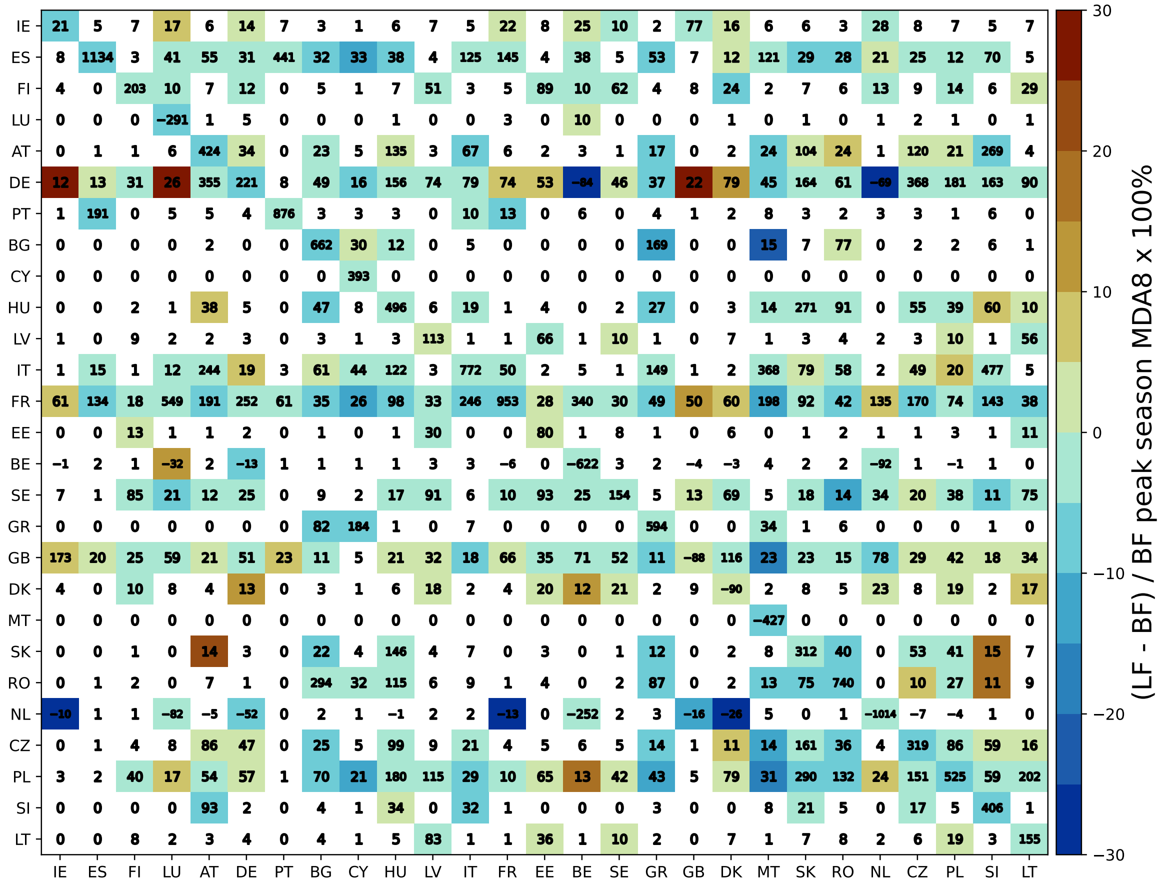

Figure 5.3: EU27 "blame matrix" showing the country-to-country contributions to peak season MDA8 in 2021 for a 15% NO_x emission reduction. Values calculated using the BF method are shown in each of the cells, while the colors indicate the percentage difference between the LF and BF calculations. Percentage differences are only shown for absolute BF changes greater than 10 ng/m^3. Rows and columns correspond to the emitter and receptor countries, respectively.

- Both BF and LF runs with a simplified zero-order advection scheme, where the fluxes are only dependent on the wind fields (BF1 0adv).
- In addition to the simplified advection, the Cloud-J photolysis rates are replaced by tabulated rates computed by a scheme where the rates are independent on the pollutant concentrations (climatological) (BF1 0adv clj).
- In addition to the simplified advection, the dependence on the surface of the aerosols is removed for the part of aerosols which are not inert (BF1 0adv surf).
- In addition to the simplified advection, both the simplified photolysis rates and the dependence on the surface of the aerosols is applied (BF1 0adv clj surf).

The results of these experiments, expressed as the difference between the baseline BF and LF simulations for each of the DE receptor countries, are shown in Fig. 5.4. In this figure, the results for all of the experiments are scaled to 15%, to make the 15% and 1% emission reduction experiments more comparable.

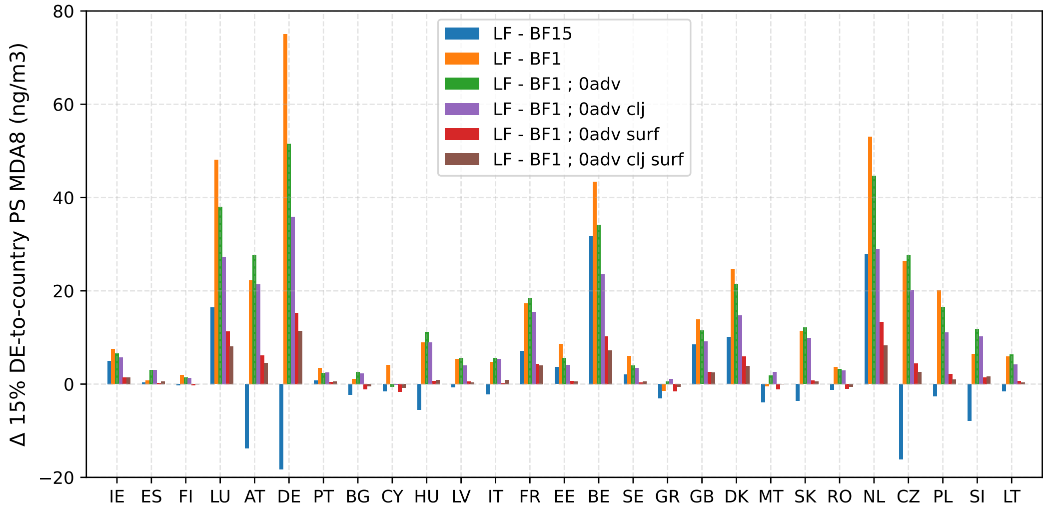

Figure 5.4: Absolute differences between the BF and LF country average peak season MDA8 values calculated for the DE NOx emission reduction experiments described in the text. The emission reduction impacts are scaled to 15% for all experiments.

It should be noted that the effect of NOx emission changes in Germany will reduce $MDA8_{AS}$ in some regions and increase $MDA8_{AS}$ in others (see Fig. 5.1). The net effect is therefore relatively small, and the relative errors as presented in Fig. 5.3 can be misleading. Fig. 5.4 shows that the overall absolute differences between the two methods are small (<80 ng m^{-3}). After the different corrections in methodology are applied, the remaining differences are smaller than 10 ng m^{-3}. The changes caused by reducing emissions by 15% or 1% in the BF method, increases the MDA8 value from DE to itself, and apparently increases the discrepancy between the BF and LF methods. The other corrections (adv0, surf, clj) have an opposite sign, reducing the the discrepancy between the BF and LF methods when combined with the BF1 run.

5.3 Conclusions

We have shown that the LF method can produce source receptor matrices which have similar quality as using the brute force method (BF). There are discrepancies, but those can be understood and explained.

The BF method has been used for decades to produce SR relationships. The main inconvenience of the method is that it is computationally demanding, as several hundreds separate simulations have to be handled to produce the SR tables shown in this report. The 15% reduction associated with them is somewhat arbitrary, and the non-linear contributions due to this finite reduction is not quantified.

The LF run is more computationally expensive than a single BF run, but still much cheaper and simpler to handle than the full range of simulations for all countries. It becomes practically possible to produce full SR relationships for several background emissions or scenarios, giving also insight in the non-linear dependence of the pollutants.

The LF method for Secondary Inorganic Aerosols are not presented in this report, but are also available in an experimental setting. Moreover, additional tests and a detailed description of the methodology will be presented in a separate publication.

References

Bott, A.: A positive definite advection scheme obtained by non-linear re-normalization of the advection fluxes, Mon. Weather Rev., 117, 1006–1015, 1989.

WHO: WHO global air quality guidelines. Particulate matter ($PM_{2.5}$ and PM_{10}), ozone, nitrogen dioxide, sulfur dioxide and carbon monoxide., URL https://www.who.int/publications/i/item/9789240034228, World Health Organisation, European Centre for Environment and Health Bonn Office, ISBN 978-92-4-003422-8 (electronic version), 2021.

Wind, P., Rolstad Denby, B., and Gauss, M.: Local fractions – a method for the calculation of local source contributions to air pollution, illustrated by examples using the EMEP MSC-W model (rv4_33), Geoscientific Model Dev., 13, 1623–1634, doi:10.5194/gmd-13-1623-2020, URL https://www.geosci-model-dev.net/13/1623/2020/, 2020.

CHAPTER 6

EMEP intensive measurement period on ozone episodes in summer 2022

Wenche Aas, Yao Ge, Heidi Hellén, Jean-luc Jaffrezo, Falk Mothes, Therese Salameh, Sverre Solberg, Diellëza Tusha, Barend L. van Drooge, Robert Wegener, Karl Espen Yttri

6.1 Introduction and setup of the campaign

Tropospheric ozone is an adverse environmental and health problem in Europe, and it is of great concern that high ozone episodes typically are underpredicted by atmospheric transport models. It is not clear if this relates to underestimation of emissions of ozone precursors during these episodes or if it reflects deficiencies in the parametrisation of the physio-chemical processes e.g. linked to ozone formation or dry deposition that might differ in these episodes compared to normal conditions. Secondary organic aerosol (SOA) generated by gas-phase oxidation of volatile organic compounds (VOCs) is another major pollutant of concern during extreme ozone episodes that has proven difficult to reproduce by models and which contributes to the adverse health effects caused by secondary air pollutants.

The EMEP monitoring programme of VOCs (Solberg et al. 2021) is not targeted particularly for the ozone episodes for two reasons: 1) Few sites measure a complete VOC programme, it is particularly challenging that only a few sites are measuring oxygenated VOCs (OVOCs), and terpenes have traditionally not been part of the EMEP VOC programme (but in GAW). Terpenes are especially important precursors for SOA. 2) The traditional EMEP monitoring of OVOCs by manual sampling (and NMHC at some sites) includes only 1-2 samples per week, thus not fit for evaluating temporal variations at the scale needed to follow an ozone episode.

To better understand the formations of ozone during heat waves, the EMEP Task Force on Measurement and Modelling (TFMM) organized an intensive measurement period (IMP) in summer 2022. One week of observations of VOCs relevant as ozone precursors was conducted between 12-19 July 2022. The IMP was conducted in close cooperation with the European infrastructures ACTRIS and RI-Urbans.

The campaign was partly supported by the European Solvents Industry Group (ESIG), and it was coordinated by the TFMM. A meteorological team studied the weather situation and the forecasts in the summer season prior to the episode, and when this strong episode was evident from the forecasts the campaign was initiated and a large number of samplers and other equipment was shipped to labs and institutions all over Europe. It turned out that the episode was very well predicted by the forecasts, daily values of MDA8 as extracted from EEA's measurement data of rural, regional, and remote sites are given in Figure 6.1. A unique dataset for surface ozone and hundreds of various VOCs were measured on a pan-European basis during the episode.

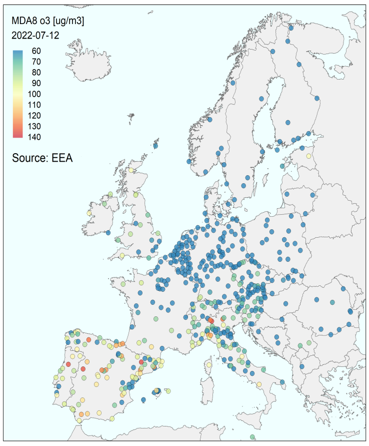

(a) MDA8 12 July

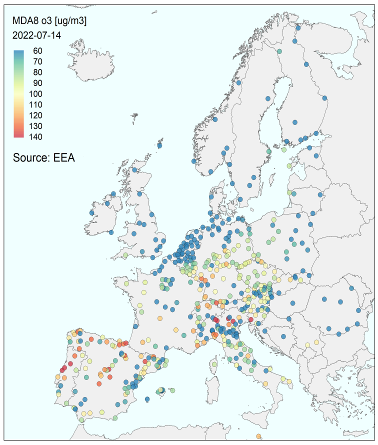

(b) MDA8 14 July

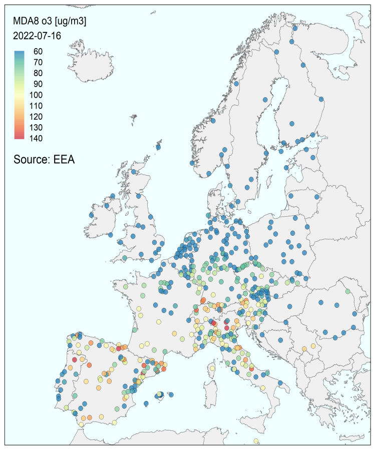

(c) MDA8 16 July

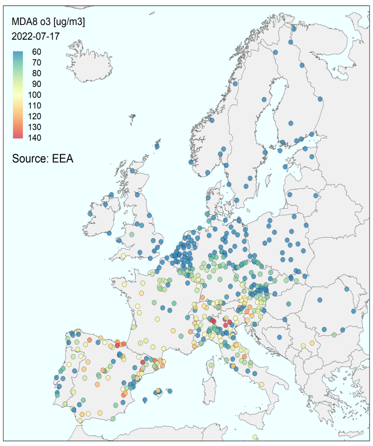

(d) MDA8 17 July

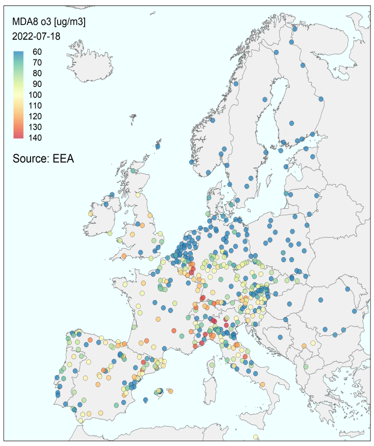

(e) MDA8 18 July

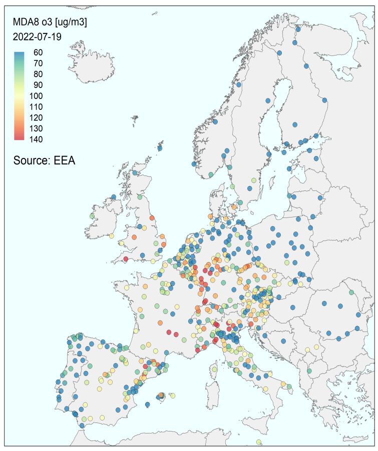

(f) MDA8 19 July

Figure 6.1: Ozone (MDA8) 12-19 July 2022 based on data from rural, regional and remote EEA sites.

The participants of the campaign supplemented their regular EMEP/ACTRIS observations (if they had) to include all relevant VOCs. At those sites where there was not regular monitoring, or there was a lack of some component groups, manual devices for VOC sampling were distributed and subsequently analysed at centralized laboratories. Further, aliquots of OC/EC filters were taken for analysis of selected tracers for biogenic SOA. The different devices and analysis which was performed at the central laboratories:

- Canister air sampler: non-methane hydrocarbons (NMHC) at Forschungszentrum Jülich (FZJV) GmbH, Germany
- DNPH cartridge: Oxygentated VOCs (OVOCs) at the Institut Mines Télécom (IMT) Nord Europe, France
- Tenax tubes: monoterpenes at Finnish Meteorological Institute (FMI), Finland
- SOA tracer analyses from part of EC/OC filters at the Institut des Géosciences de l'Environnement (IGE), CNRS, Grenoble, France

Even though the different laboratories and sampling devices have specific target compounds they measure, there is an overlap between them, i.e the analyses at Jülich also includes some terpenes and O-VOCs and the analyses at FMI includes some NMHCs. Table E:1 in the Appendix E gives an overview of which compounds were measured where.

In total 27 sites participated (Figure 6.2), whereof 17 sites had some or all their VOC analyses done at central lab(s). Additionally, 3 sites participated with organic tracer analyses only (Table E:1). More than 120 different VOCs were measured (see Table E:2 in the Appendix). In addition to the analyses done by the central laboratories, there were several national contributions using other type of sampling procedures and analytical techniques, i.e. monitors (PTR-MS and GC/MS). Several of the methods include analyses of the same VOC species, but the methods are not necessarily fully comparable. The data are available and can be downloaded from the EBAS database (http://ebas.nilu.no/).

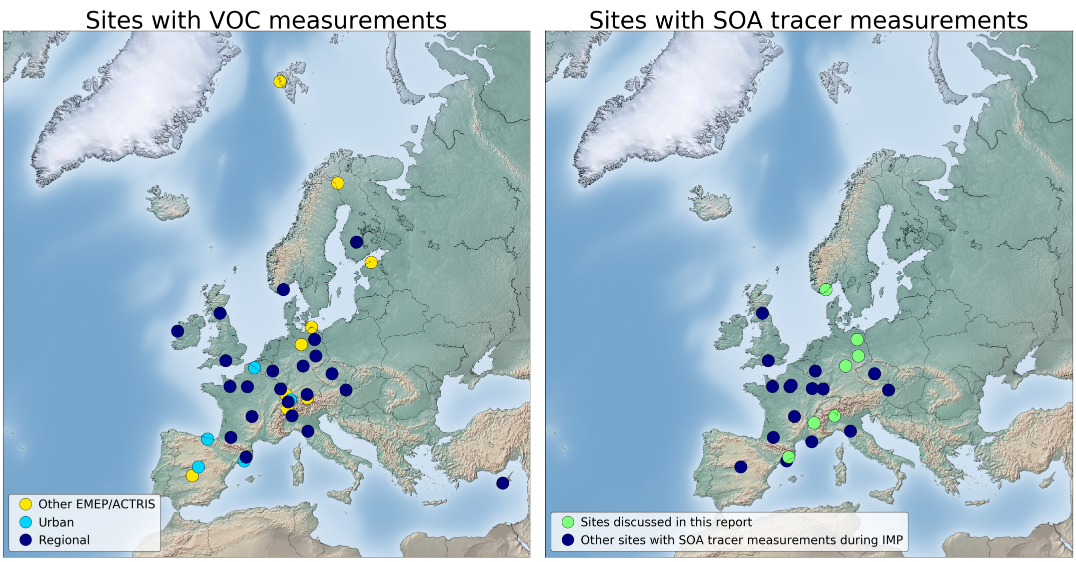

Figure 6.2: Sites participating in EIMP Summer 2022. Left map shows the sites participating with VOC measurements differentiated between urban (light blue) and regional environment (dark blue). Sites which were not part of the campaign, but do report some VOCs to EMEP or ACTRIS, are marked in yellow. The right map shows those sites with tracer analyses for different secondary organic aerosols (SOAs), the seven sites discussed in Chapter 6.4 are marked in green.

6.2 Ozone and NO_2

The ozone episode in July coinciding with the measurement campaign was linked to an extended European heat wave with record-high temperatures and wildfires. In the first days of the period, southwest parts of Europe was under influence of a persistent high pressure system whereas the northeastern part was dominated by inflow of Atlantic air masses from NW leading to somewhat elevated ozone at the Iberian peninsula and parts of France while BeNeLux, UK and Scandinavia experienced clean, marine air masses. In the following days, the high pressure system moved slowly into central Europe while a cold front swept across the area setting up southerly winds that brought hot, polluted air masses to northwest Europe.

On 15 July the Met Office in the UK declared a national emergency, and on 19 July soaring temperatures exceeding 40 °C was recorded in the UK, the highest temperature ever seen in that country. Very high temperatures were experienced also in Norway as a fringe of the heat wave touched southern parts of the country and a peak ozone level of 177 µg m^{-3} was measured at Sandve, the highest annual maximum since 2006 and close to EU's information threshold of 180 µg m^{-3}.

In order to investigate the cause of high ozone episodes during this summertime campaign, we first present some results for ozone and NO_2. An extensive effort has also been made concerning modelled versus observed VOC concentrations, but this is presented in Chapter 7. The model simulation presented in this chapter employs the CRIv2R5Em chemistry mechanism (Bergström et al. 2022), an EMEP adaptation of the Common Representative Intermediates (CRI) v2-R5 mechanism (Watson et al. 2008). The simulation utilises 2019 CEIP emission inventories (since 2022 emissions were unavailable) alongside 2022 meteorology with a grid resolution of $0.1^\circ \times 0.1^\circ$ longitude/latitude.

6.2.1 Results, O_3 and NO_2

Figure 6.3 compares campaign-average modelled and observed concentrations of O_3 and NO_2. It can be noted that certain stations for NO_2 report data measured by multiple instruments or recorded at varying temporal frequencies, resulting in more than one data point for some stations (e.g. AT0002R, Illmitz) in Fig. 6.3.

For ozone, the model captures well the spatial variations, evidenced by a strong linear correlation coefficient of 0.94. Meanwhile, the model overestimates at certain stations and underestimates at others. Nonetheless, most stations are closely aligned with the 1:1 line and span a concentration range of 20-60 ppb, indicating the deviations are not extensive. It should be noted that these are daily mean O_3 values though, so some sites will be affected by nocturnal O_3 depletion.

Also for NO_2, a good linear correlation is also observed, with a correlation coefficient of 0.86. The linear regression line approximates the 1:1 line, having a slope of 1.08. Both the model and measurements reveal large NO_2 concentrations at the FR0027U Villeneuve d'Ascq (France) and the CH0010U Zürich-Kaserne (Switzerland) stations, while the remaining stations record average concentrations below 3 ppb.

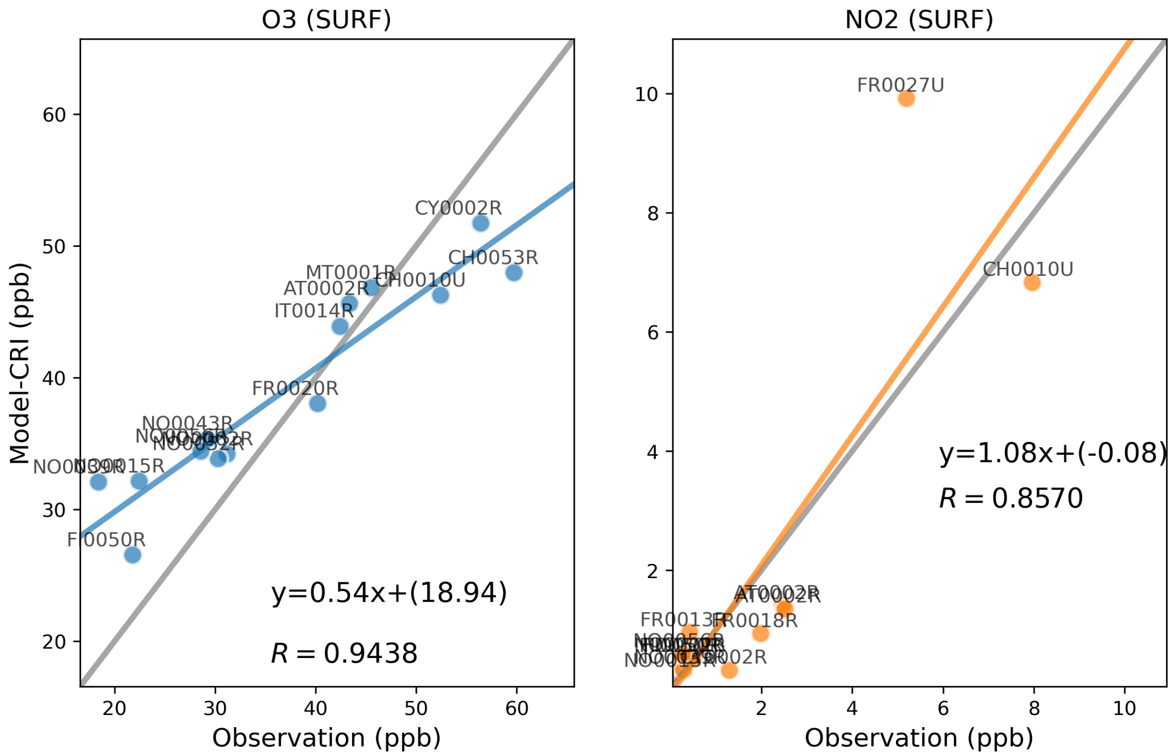

Figure 6.3: Scatter plots of average modelled and measured ozone and nitrogen dioxide concentrations over the campaign period. The term 'SURF' and 'CRI' indicate that the data is from model surface outputs using the CRIv2R5Em mechanism. In each plot, the grey line is the 1:1 line, and another coloured line is the least-squares regression line.

The time series comparisons at stations with both O_3 and NO_2 measurements have also been conducted, with the results being illustrated in Figure 6.4, which provide examples from the Zürich and Illmitz stations.

At the urban Zürich station, on several days, the measured maximum ozone concentrations reached approximately 80 ppb. The modelled O_3 concentrations are in good agreement with the measured values throughout the period, even though the model underestimates the peak concentrations on a daily basis. For NO_2, the model and measurements exhibit similar temporal variations and concentration ranges; however, the modelled NO_2 concentrations are lower than the measured values most of the time, except for two peaks on the 14th and 16th of July.

In contrast, the rural Illmitz station presents a slightly different pattern, with the modelled peak O_3 concentrations exceeding the measured values, particularly on the first half of the campaign period. Both the modelled and measured ozone concentrations display very similar diurnal variations, with peak concentrations reaching around 70 ppb. Also for NO_2, the model data is generally lower than the measurements, particularly towards the end of the campaign period. Nevertheless, the model's NO_2 concentrations show peaks and troughs at similar times to those observed in the measurement data. This pattern demonstrates the model's ability to capture essential temporal characteristics, even when discrepancies in absolute concentrations are present.

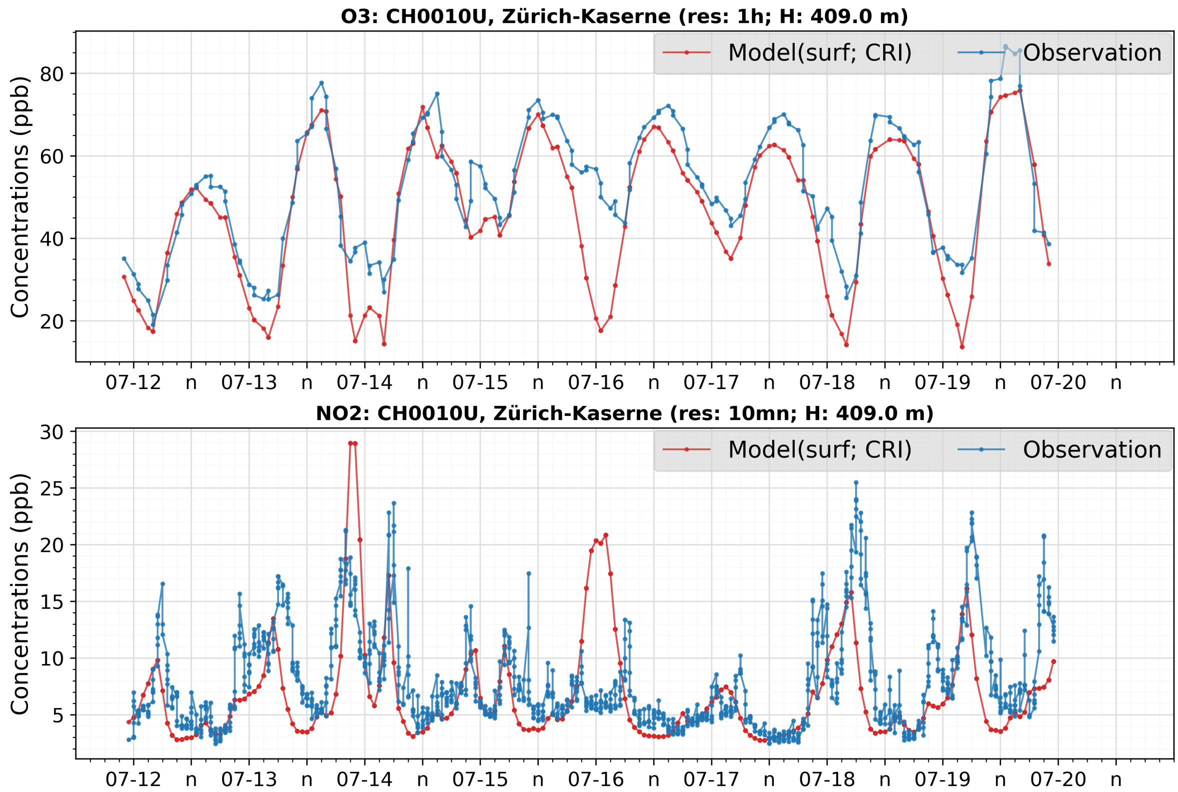

(a) Zurich

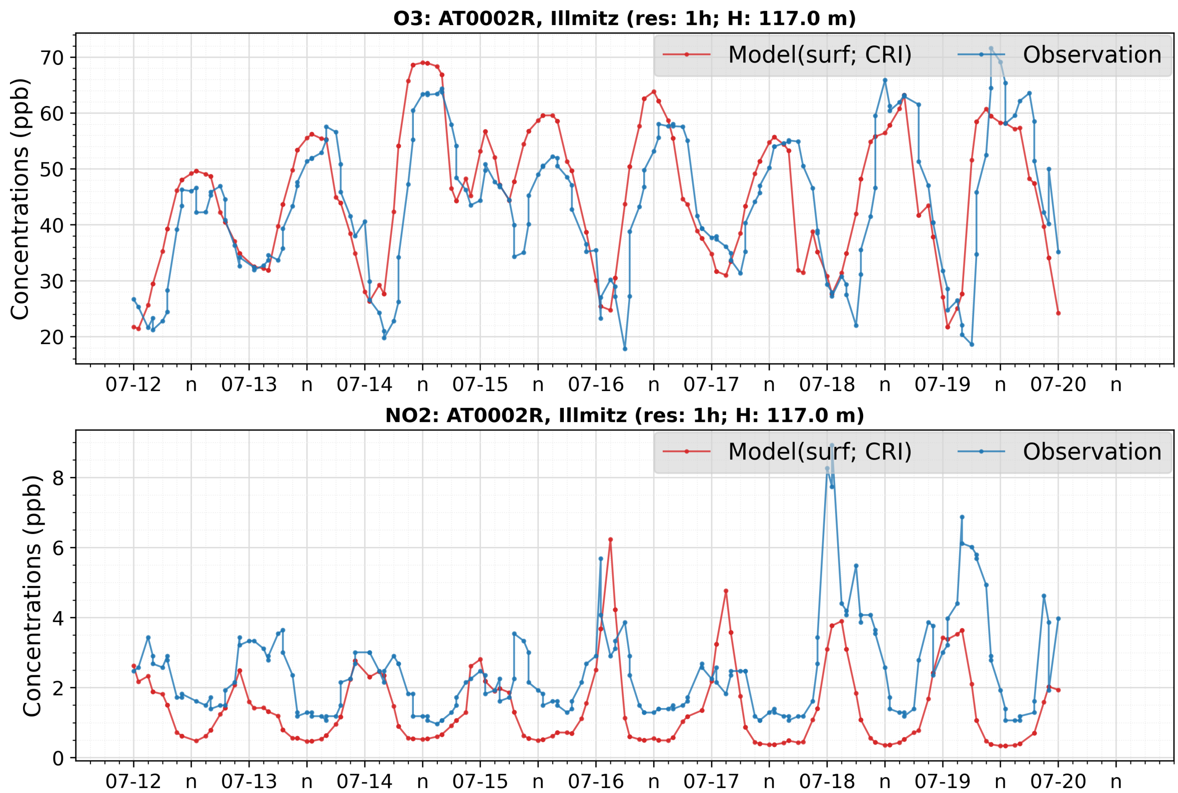

(b) Illmitz

Figure 6.4: Time series comparisons of O_3 and NO_2 concentrations in ppb at the (a) Zürich and (b) Illmitz station. The term 'n' indicates 12 noon. The term 'surf' and 'CRI' indicate that the data is from model surface outputs using the CRIv2R5Em mechanism. The term 'res' denotes the resolution of the measurement. For example, 'res: 1h' means that the measurements are conducted every hour. The term 'H' denotes the site altitude.

6.3 VOCs

6.3.1 Results VOC

More than 120 different VOC components were measured during the campaign (Table E:2), Figure 6.5 shows the relative contribution of different VOCs component groups to the total VOCs at six selected sites. In this Figure the species were merged into 7 groups: isoprene, C2-C5 NMHC, C6-C12 NMHC, OVOCs, aromatics, monoterpenes and sesquiterpenes. Only sites that have analyses of all the samples at the central laboratories have been selected to ensure comparability between sites. All the sites are dominated by OVOCs and C2-C5 NMHCs, and their relative contribution does not vary very much between the sites even though they are situated in quite different environments, except at Illmitz (AT0002R) that has a larger fraction of C6-C12 NMHCs. Madrid (ES0021U) has the highest relative influence of aromatic VOCs which is reasonable when considering nearby emission sources. Viesalam (BE0007R) is situated in a forest and has relatively large contribution of monoterpenes, this is also reflected in Figure 6.6 and Figure 6.7(c).

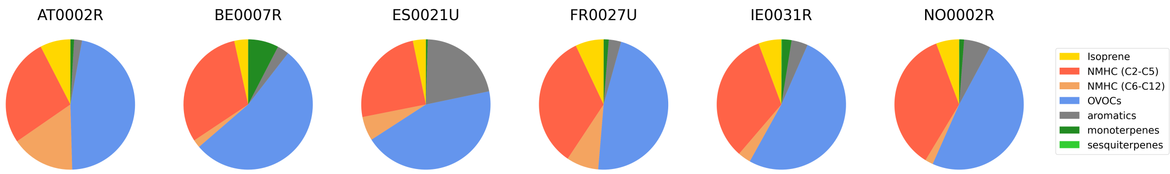

Figure 6.5: Distribution of different VOC groups at selected sites where all the components are measured with comparable methods (central analysis) The groups sums of the average concentration between 12-19 July 2022 of all the relevant components at the different sites.

Figure 6.6 shows stacked bar plots of NMHC, OVOC, and monoterpenes day by day during the campaign for three stations (ES0021U, BE0007R, and NO0002R).The plot for NMHC shows a very different temporal variation from Spain to Norway. The opposite temporal variation at ES0021U (going from high to low) vs that seen in the north (low to high) agrees with the general development of the episode moving across the continent as seen in Figure 6.1. Furthermore, the absolute levels reflect the station type from ES0021U located in an urban background area compared to NO0002R at a clean, rural location. The relative fraction of the NMHC corresponds to this with a much higher fraction of the long-lived species like ethane at NO0002R and a higher fraction of reactive NMHC at ES0021U and BE0007R. On the contrary, the relative distribution of the OVOC is strikingly similar for the three stations although the temporal development agrees with what is seen from the NMHC levels. The bar plots for the monoterpenes differ from what is seen for NMHC and OVOC with no clear patterns except that α-pinene is the most abundant species at all sites.

The finding of similar relative distributions of the OVOCs is also seen in Figure 6.7, showing the mean concentrations during the campaign at 16 sites. This is a rather surprising finding given the large spread in the stations both with respect to the geographical location and type of station. For monoterpenes, a large spread in the mean concentrations is seen among the sites, reflecting the surrounding biogenic environment with highest levels at BE0007R and FR0008R. When compared to the mean levels of NMHC, it is seen that there is no clear links between these high monoterpene sites and isoprene. BE0007R is the peak site for monoterpenes while the isoprene levels are not particularly high. FR0008R, on the other side, shows both high monoterpene and isoprene levels.

It is difficult to compare the VOC levels observed during this intensive summer week in 2022 with earlier years since few of the sites have similar comparable monitoring prior to 2022 and therefore not possible to get a general comparison over Europe especially for other species than NMHC. Looking at those few observations available it does not seem like July 2022 differ much from what is seen in July the last five years, but further assessment is needed to evaluate this.

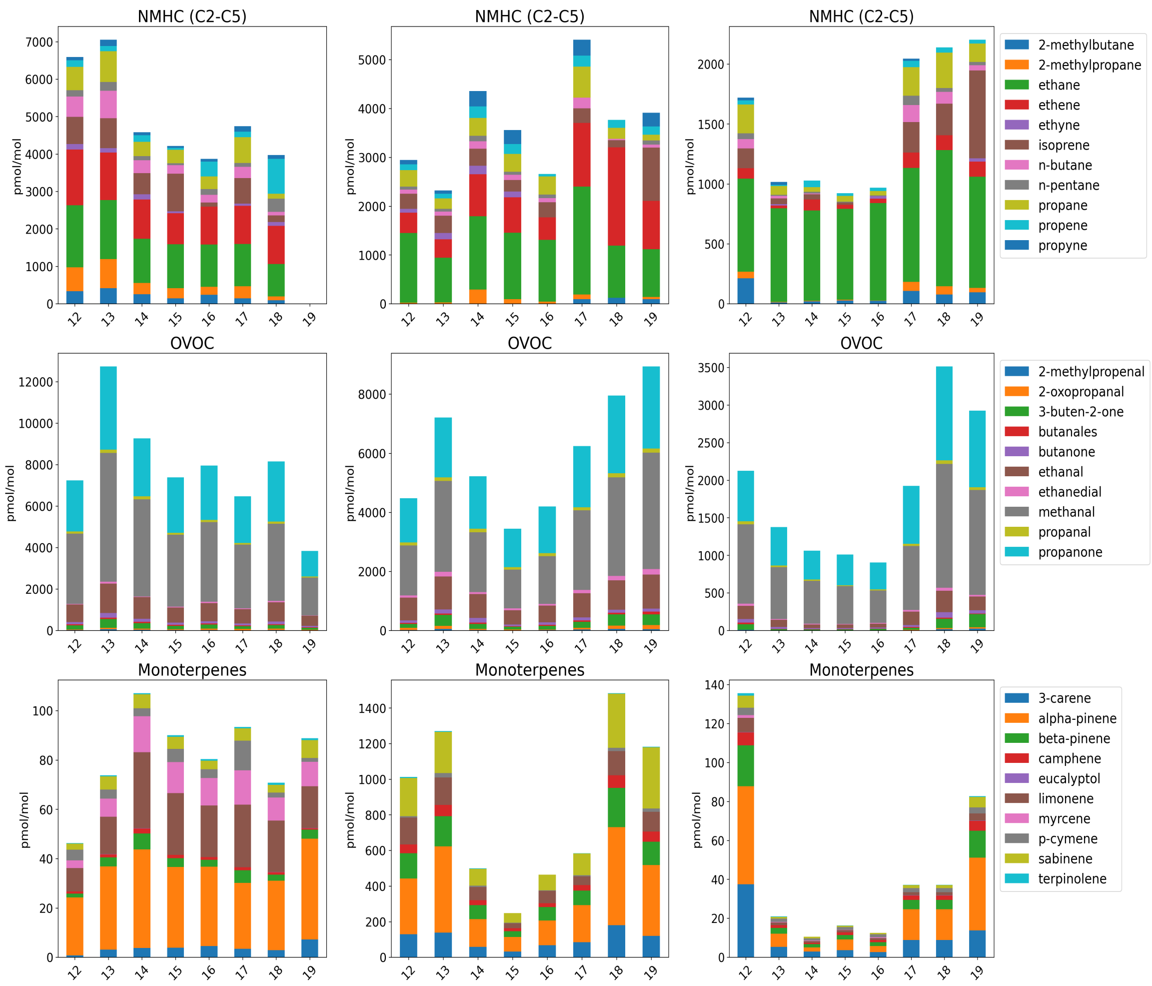

(a) ES0021U (b) BE0007R (c) NO0002R

Figure 6.6: Chemical composition of the different VOC groups (NMHCs (C2-C5), OVOC and monoterpenes) at selected sites (ES0012U, BE0007R and NO0002R) where all the components are measured with comparable methods (central analysis) during 12-19 July 2022. The observations which were reported in mass units were converted to pmol/mol.

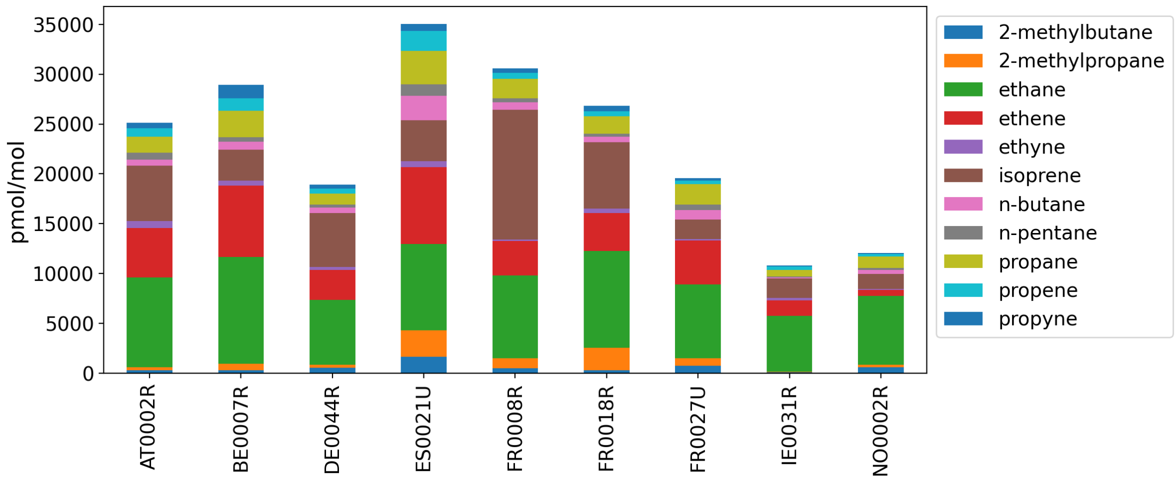

(a) NMHCs (C2-C5)

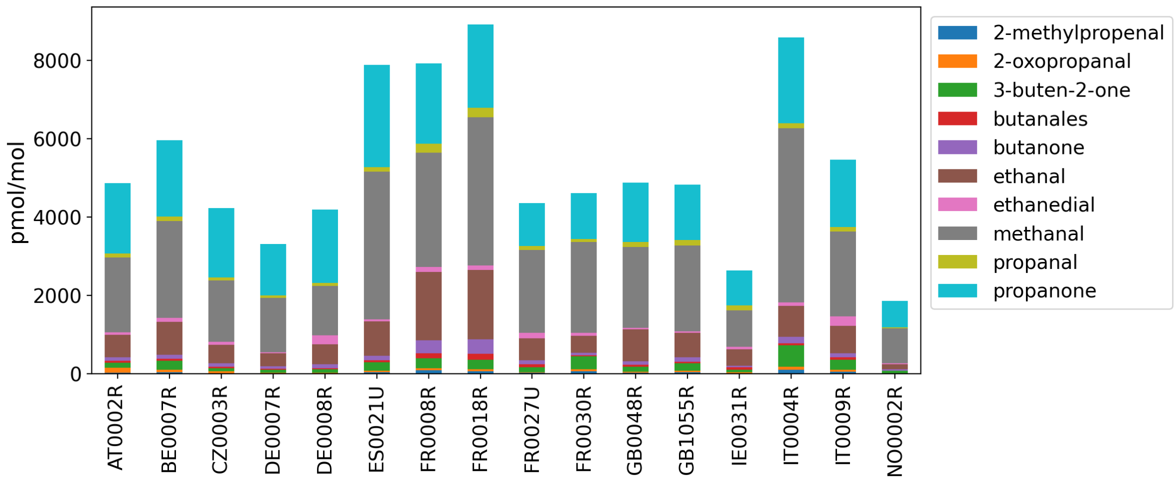

(b) OVOCs

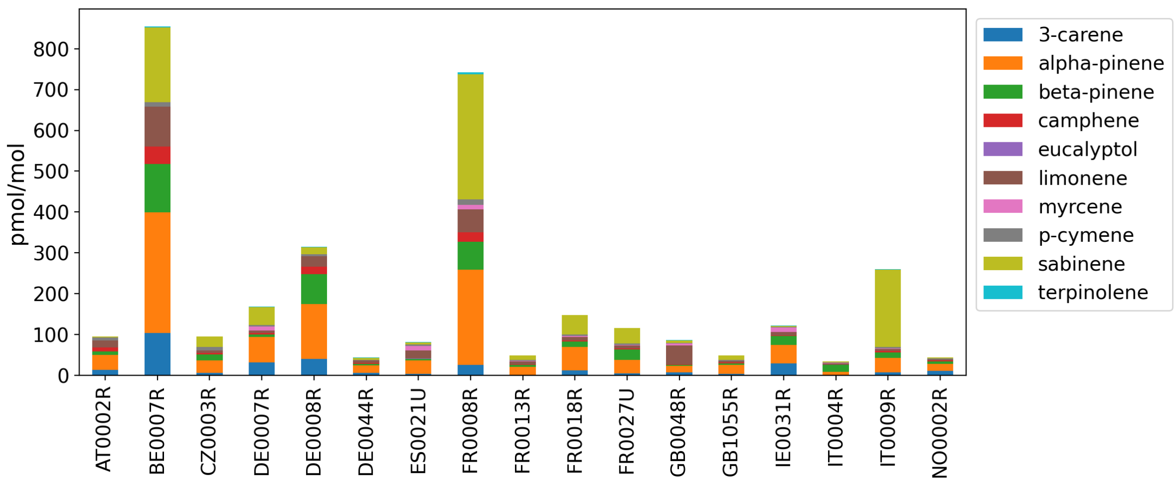

(c) Monoterpenes

Figure 6.7: Average concentrations of the measurement period (12-19 July 2022) of different NMHCs (a), OVOCs (b) and monoterpenes (c) for the sites with central analysis.

6.3.2 Quality assurance and reporting

The PTR-MS measurements are relatively new observations to be reported to EMEP, and the naming-convention of the species detected with these instruments was not properly defined prior to the IMP, nor which metadata should be included with the data. Consequently, reporting guidelines for these measurements have been developed, in close cooperation with the ACTRIS Centre for Reactive Trace Gases In Situ Measurements (CiGas) and other experts.

The principle of the PTR-MS method is a chemical ionization of water vapor followed by a proton-transfer reactions from H_3O^+ to a wide variety of VOCs, creating protonated VOC ions that can be detected and identified by their molecular mass. There are two categories of the PTR-MS instruments, one with a time-of-flight mass spectrometer (PTR-ToF-MS) and one with a quadrupole mass spetrometer (PTR-QMS). The PTR-ToF-MS measures the time it takes for ions generated from the sample to reach a detector based on their mass-to-charge ratios. This allows for high-resolution analysis of a wide range of VOCs, while the PTR-QMS selectively filter ions based on their mass-to-charge ratios. The identification of the VOCs are challenging when there are several species with the same mass, e.g. at unit mass (m/z) 61, there are several organic compounds that potentially can be detected: acetic acid, hydroxyethanal, n-propanol and 2-Propanol. These have either chemical composition $C_2H_4O_2H^+$ (with m/z: 61.028)) or $C_3H_8OH^+$ (with m/z: 61.033). The PTR-ToF-MS can distinguish between these two different mass units while the PTR-QMS not. Therefore, three different component names have been defined: mass_ 61 organic_compounds to be used for PTR-QMS and mass_61.028_organic_compounds and mass_61.033_organic_compounds for PTR-ToF-MS. Table E:2 gives an overview of which species and component groups that have been reported with PTR-MS.

Isoprene is detected by the PTR-MS, but for PTR-QMS isoprene is detected together with furan (both with m/z 69), while PTR-ToF-MS can separate between these two compounds. Another complicating factor is the possible interference from fragments of VOCs with higher masses. The potential for interference from fragments varies, e.g for toluene the contributions of those compounds is expected to be less than 10% (Ambrose et al. 2010). At BE0007R a PTR-ToF-MS was measuring alongside the manual sampling shown in Figure 6.6 and a comparison of isoprene shows an overestimation of 35% for the PTR-ToF-MS, but there are too few data points to draw any conclusions.

Several species were sampled with different methods and/or analysed at different laboratories (Table E:2). α-pinene and limonene were sampled with both canisters and Tenax tubes at 9 sites, analysed at FZJV and FMI respectively. The observations sampled with canisters show on average higher concentrations than from Tenax, two times higher for α-pinene and three times higher for limonene. The differences can be due to issues with sampling (efficiency of ozone scrubber, absorption, sampling interval and more) or analytical (different GC columns and extraction techniques). Further investigations are needed to understand these differences.

6.4 Organic aerosols

In addition to the measurements of volatile organic compounds (VOCs), we assessed the formation of secondary organic aerosol (SOA) during these high ozone episodes, as SOA form from oxidation of VOCs and is a major fraction of secondary pollution contributing to poor air quality. Our focus is on SOA from biogenic precursors (BSOA) and addressed primarily by organic tracer analysis. Here, we present a snapshot of carbonaceous aerosol measurements performed during EIMP Summer 2022, focusing on measurements conducted at seven sites (Figure 6.2 (right); Table 6.1) along a South to North transect, of which six are rural background sites and one is an urban background site.

Table 6.1: Location of the six rural background sites and one urban background site discussed in the present chapter.

Site	Coordinates	Altitude (m asl)	PM cut-off size
Montseny (ES1778R)	41° 46’ 0” N, 2° 21’ 0” E	700	PM_{10}
Grenoble (FR0038U)	45° 18’ 85” N, 5° 72’ 45” E	212	PM_{10}
Ispra (IT0004R)	45° 48’ 0” N, 8° 38’ 0” E	209	$PM_{2.5}$
Schmücke (DE0008R)	50° 39’ 0” N, 10° 46’ 0” E	937	$PM_{2.5}$
Melpitz (DE0044R))	51° 31’ 48” N, 12° 55’ 48” E	86	PM_{10}
Neuglobsow (DE0007R))	53° 10’ 0” N, 13° 2’ 0” E	62	$PM_{2.5}$
Birkenes Observatory (NO0002R)	58° 23’ 18” N, 8° 15’ 7” E	219	PM_{10}

6.4.1 Methodology

Concentrations of organic carbon (OC) and elemental carbon (EC) observed at seven of the sites involved in EIMP Summer 2022 are listed in Table 6.2. These measurements were compared to a reference period encompassing all OC and EC observations for the month of July from 2010 to 2020 and for Grenoble and Ispra, results are shown in panels a and b of Figure 6.8, respectively. All measurements were conducted according to the EUSAAR-2 protocol (Cavalli et al. 2010), including those of the reference periods. Here we see the benefit of a unified and widespread analytical method for OC and EC, where the analyses were performed by individual laboratories across Europe that regularly participate in OC/EC inter laboratory comparisons.

We used the EC tracer method (e.g. Turpin and Huntzicker (1995); Day et al. (2015)) to estimate the SOA fraction for samples collected at the sites Grenoble (Figure 6.8, panel c) and Ispra (Figure 6.8, panel d).

$$POA = (OC/EC)_{Primary} \times [EC] \tag{6.1}$$

$$SOA = [OC] - POA - PBAP \tag{6.2}$$

The EC tracer method requires that:

1. There are periods in the data set when anthropogenic primary OC (POA) from combustion dominates.

2. The $(OC/EC)_{Primary}$ ratio is constant.

Ispra is in the Po valley, one of Europe’s most polluted regions, and is significantly influenced by anthropogenic emissions, as shown by Henne et al. (2010). Consequently, Ispra is more likely to meet the specified criteria of the EC tracer method compared to other rural background sites, which are less influenced by anthropogenic emissions. Opposite to the other six sites, Grenoble is an urban background site, and thus influenced both by biogenic and anthropogenic emissions of OC in summer (Borlaza et al. 2021, Srivastava et al. 2018)

To calculate POA, we utilized $(OC/EC)_{Primary}$ ratios of 2.1 (Ispra) and 2.0 (Grenoble) corresponding to the 1st percentile of the OC/EC ratio observed in samples collected in the reference period (July 2010 - 2020). These ratios aligns well with the range of OC/EC slopes (0.85 - 2.7) observed in five major American cities, as demonstrated by Day et al. (2015). The higher OC/EC ratios (6.7 - 9.0) at our other sites suggest a minor influence from local combustion sources and indicate that most OA have undergone aging processes, which would lead to an underestimation of SOA following from Eq. 6.1 and Eq. 6.2.

PBAP refers to a class of primary particles that are not from combustion sources, but it should nevertheless be accounted for to obtain a more correct estimate of SOA in Eq. 6.2. OC associated with PBAP (OC_{PBAP}) was calculated using Eq. 6.3, which involved the sum of four PBAP tracers (arabitol, mannitol, glucose, and trehalose) included in our data set, and the OC to $PBAP_{\mathrm{Tracers}}$ ratio (14.6) reported by Groot Zwaaftink et al. (2022). Notably, such a ratio is site specific, and likely also with respect to the size fraction measured, thus applying it to several different sites across Europe will inevitably cause additional uncertainty.

$$OC_{\mathrm{PBAP}} = PBAP_{\mathrm{Tracers}} \times 14.6 \tag{6.3}$$

To ensure comparability amongst sites, the analysis of BSOA, BB and PBAP tracers was conducted at a centralized laboratory. Some of these species underwent a pilot inter-laboratory comparison (ILC) and selected results from this ILC are presented in 6.5. Figure 6.9 displays the mean concentrations of the BSOA tracers 3-MBTCA (3-Methylbutane-1,2,3-tricarboxylic acid) and 2-MT (sum of 2-methylerythritol and 2-methylthreitol) (panel a), which are oxidation products of α-pinene and isoprene (BVOCs), respectively; the biomass burning tracer levoglucosan is shown in panel b for the seven selected sites. The 3-MBTCA to 2-MT ratio for all sites is shown in Figure 6.10. Long-term or full year data for these organic tracers are only available for a few sites in Europe (e.g. Yttri et al. (2023), Yttri et al. (2021), Borlaza et al. (2021)) and for only two of the sites (Birkenes and Grenoble) participating in EIMP Summer 2022. We calculated OC associated with BSOA from oxidation of α-pinene ($OC_{\mathrm{BSOA}\alpha-\mathrm{pinene}}$) and BB ($OC_{\mathrm{BB}}$) using Eq. 6.4 and Eq. 6.5, respectively.

$$OC_{\mathrm{BSOA}\alpha-\mathrm{pinene}} = [\text{3-MBTCA}] \times 57 \tag{6.4}$$

$$OC_{\mathrm{BB}} = [\text{Levoglucosan}] \times (\text{4.6 to 8.9}) \tag{6.5}$$

We utilized concentrations of 3-MBTCA for calculation of $OC_{\mathrm{BSOA}\alpha-\mathrm{pinene}}$). The 3-MBTCA to OC ratio (57) was derived from a BSOA factor obtained through a PMF (Positive Matrix Factorization) source apportionment study conducted by Borlaza et al. (2021). No 2-MT to OC ratio was available for calculation of BSOA from oxidation of isoprene. Note that we cannot ascertain whether this PMF factor from which the 3-MBTCA to OC ratio was derived encompasses BSOA from precursors other than α-pinene, such as isoprene. Notably, a high correlation between 3-MBTCA and 2-MT was only found for a few sites participating in EIMP Summer 2022, like Neuglobsow (R^2 = 0.972). Hence, we emphasize that our calculations provide coarse estimates only and that they are likely to be highly conservative in terms of OC_{BSOA} and in the upper end for $OC_{\mathrm{BSOA}\alpha-\mathrm{pinene}}$). As for the OC to $PBAB_{Tracer}$ ratio, the OC to 3-MBTCA ratio is likely also quite site-specific, thus additional uncertainty must be expected when used for different sites.

To calculate OC from biomass burning (OC_{BB}), we relied on the measured concentrations of the biomass burning tracer levoglucosan (Simoneit et al. 1999). We utilized OC to levoglucosan ratios ranging from 4.6 to 8.9 (Yttri et al. 2022). It is important to note that these ratios are derived from residential wood combustion (RWC) emissions, whereas the samples collected during EIMP Summer 2022 were influenced by wildfires (WF) to an unknown extent. We did not differentiate between secondary and primary OC for the BB source.

6.4.2 Results and discussion

The concentrations of both OC and EC during the EIMP Summer 2022 were within the range of the reference period (Table 6.2). For Grenoble and Ispra, these results are shown in Figure 6.8 in panel a and b, respectively.

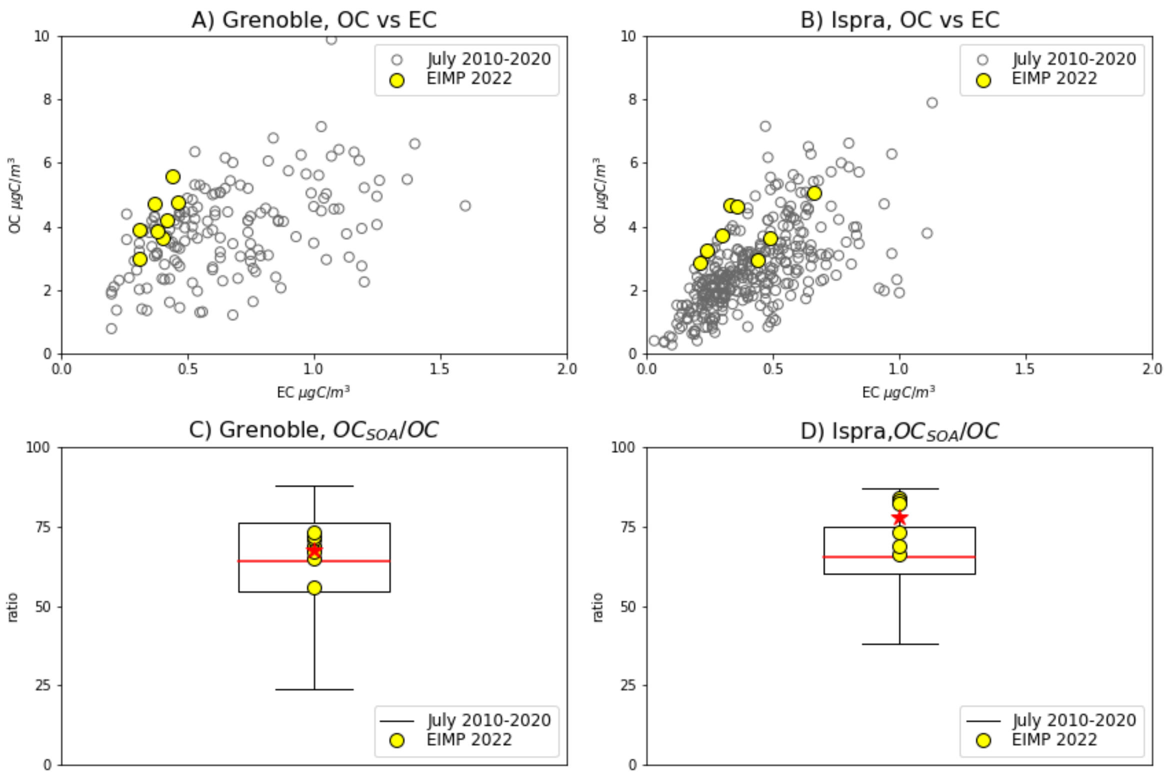

Figure 6.8: Concentrations of OC vs. concentrations of EC for EIMP Summer 2022 (12-20 July) and for the reference period July (2010 - 2020) for Grenoble (panel a) and Ispra (panel b). The OC_{SOA}/OC fraction for EIMP Summer 2022 and for the reference period is shown for Grenoble (panel c) and Ispra (panel d). The box shows the interquartile range, whereas the top horizontal bar is $Q3 + IQR \times 1.5$ (maximum) and the lower horizontal bar is $Q1 - IQR \times 1.5$ (minimum). The red horizontal bar is the mean of the reference period, whereas the red star is the mean of the EIMP Summer 2022.

Table 6.2: Mean concentration of OC and EC during EIMP Summer 2022 and its corresponding percentile of the long term mean for July 2010/13 - 2020. [a]Measurements from 2013-2020.

Site	OC (EIMP) Mean (percentile)	OC July (2010 - 2020) Mean (min - max)	EC (EIMP) Mean (percentile)	EC July (2010 - 2020) Mean (min - max)
Montseny	3.7 (95)	2.6 (1.5-4.7)	0.26 (77)	0.22 (0.07-0.49)
Grenoble	4.2 (60)	3.8 (0.8-9.9)	0.39 (18)	0.65 (0.14-1.7)
Ispra	3.9 (83)	2.7 (0.28-7.9)	0.39 (47)	0.18 (0.03-1.1)
Schmücke	2.0 (59)	1.9 (0.36-5.8)	0.13 (53)	0.13 (0.04-0.40)
Melpitz[a]	3.0 (32)	4.2 (1.2-12.8)	0.16 (26)	0.22 (0.05-0.71)
Neuglobsow	1.7 (43)	2.2 (0.65-6.4)	0.11 (28)	0.15 (0.04-0.39)
Birkenes	0.8 (33)	1.1 (0.48-2.8)	0.06 (50)	0.06 (0.01-0.14)

Among the sites, Montseny and Ispra exhibited particularly high OC levels, corresponding to the 95th and 83rd percentiles of the long-term mean, respectively. Consistent with previous findings (Yttri et al. 2007), mean OC and EC concentrations decreased along the South to North transect, with levels at the three southernmost sites being 5 - 6 times higher compared to the northernmost site. Birkenes was the only site where the level of EC during EIMP Summer 2022 corresponded to a higher percentile (50%) of the long term mean than for OC (33%) (Table 6.2). The mean EC/TC ratio varied from 5% (Melpitz) to 9% (Ispra), indicating a minor influence of primary organic aerosol (OA) from combustion sources and a predominant contribution of SOA, along with some influence of primary biological aerosol particles (PBAP).

Estimates of the secondary organic aerosol (SOA) concentration were provided for Grenoble and Ispra for EIMP Summer 2022 using the EC tracer method. In Grenoble (Figure 6.8, panel c), $68 \pm 5.4\%$ of OC was attributed to OC_{SOA}, slightly higher than the long-term mean of $64 \pm 16\%$. In Ispra (panel d), the estimated contribution of OC_{SOA} was $78 \pm 7.3\%$, which falls within the upper range of the long-term mean of $65 \pm 15\%$. It is important to note that the OC_{SOA} calculated for the reference period does not account for the contribution of PBAP and therefore overestimates the OC_{SOA} fraction. The impact of accounting for PBAP can be assessed for EIMP Summer 2022. In Ispra, the inclusion of OC_{PBAP} reduced the OC_{SOA} estimate from $80 \pm 6.8\%$ to $78 \pm 7.3\%$, suggesting a marginal decrease in the long-term mean OC_{SOA} fraction. This supports the conclusion that OA is predominantly formed through secondary processes in summer. In Grenoble, accounting for OC_{PBAP} decreased the OC_{SOA} estimate from $81 \pm 2.5\%$ to $68 \pm 5.4\%$. This suggests that the long-term mean OC_{SOA} fraction should be significantly lower, indicating a relatively higher importance of OC_{SOA} during EIMP Summer 2022.

Levels of the BSOA tracers 3-MBTCA and 2-MT decreased along the South to North transect (Figure 6.9, panel a; Figure 6.10) as OC and EC, reflecting that BVOC emissions decrease pole wards from the equator. Long-term measurements were only available for Birkenes where the 2-MT level was relatively low, corresponding to the 22nd percentile of the reference period (July 2017 - 2019) and more alike levels observed in August than in July (Yttri et al. 2021, 2011a).

Figure 6.10 (left) shows how mean 2-MT concentrations were equally high or higher than mean 3-MBTCA concentrations at most (16/23) sites across Europe and that this feature was particularly pronounced for western Europe. This does not necessarily imply that BSOA from oxidation of isoprene was higher than BSOA from oxidation of α-pinene, as there are multiple

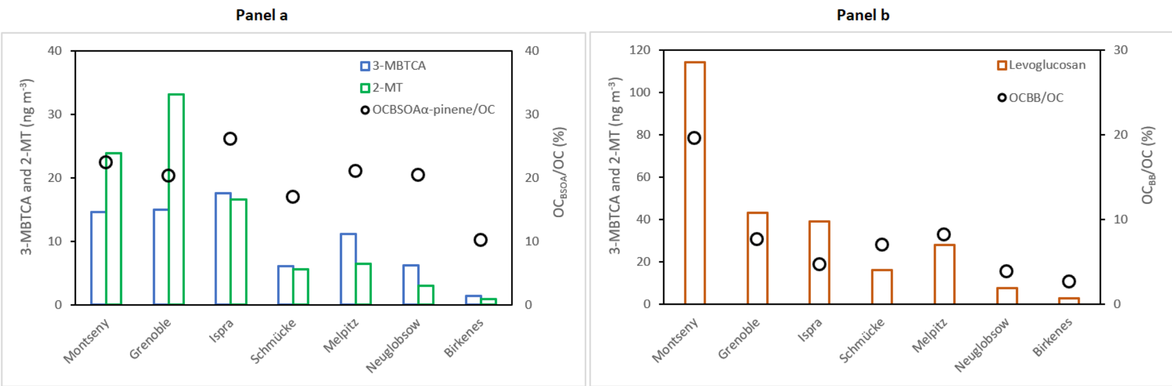

Figure 6.9: Mean concentrations of 3-MBTCA and 2-MT (panel a) and levoglucosan (panel b) observed at six rural background sites and one urban background site during EIMP Summer 2022. OC_{BSOA} and OC_{BB} are calculated as described in Eq. 6.4 and Eq. 6.5 , respectively. The sites are arranged from South to North going from left to right.

factors such as emission, yield, formation pathways, atmospheric lifetime, PAR, and ambient temperature influencing the observed concentrations (El Haddad et al. 2011). However, the results clearly show a spatial variability in the BSOA composition across Europe during EIMP Summer 2022. Daily variability in the 3-MBTCA/2-MT ratio was observed, but at most sites one of the two species dominated. In Illmitz, there was a stepwise transition from 3-MBTCA dominance to 2-MT dominance, unlike at the other sites.

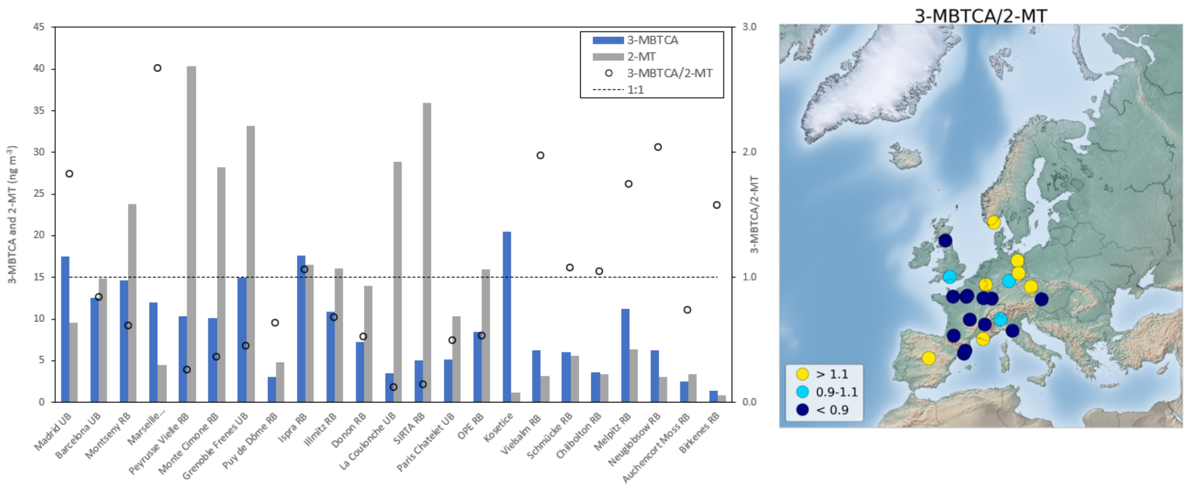

Figure 6.10: Concentrations of 3-MBTCA and 2-methyltetrols and the 3-MBTCA/2-MT ratio during EIMP Summer 2022 listed from South to North going from left to right (left figure), and the spatial pattern of the 3-MBTCA/2-MT ratio across Europe during EIMP Summer 2022 (right).

We estimate that $OC_{BSOA\alpha-\text{pinene}}$ contributed 20 - 26% to OC at the three southernmost sites, 17 - 21% at three sites in Central Europe and 10% at the Nordic site. These estimates are all substantially lower than results obtained by Gelencsér et al. (2007) (63 - 76%), Gilardoni et al. (2011) (50 ± 7%), Yttri et al. (2011b) (56 - 71%) and Yttri et al. (2011a) (48 - 57%) for European rural background sites in summer. These studies used measurements of ^{14}C and organic tracers to calculate OC_{BSOA} from all precursors and related to TC not OC, whereas we largely accounted for BSOA from oxidation of α-pinene. Conversely, source apportionment studies of carbonaceous aerosol combining measurements of ^{14}C and organic tracers are shown to overestimate BSOA at the expense of PBAP (Yttri et al. 2021). This bias is considered more pronounced for PM_{10} than for $PM_{2.5}$, as PBAP reside in the coarse fraction of PM_{10}.

As for the variables discussed above, concentrations of levoglucosan decreases from South to North (Figure 6.10). The rather high mean concentration at the southernmost site Montseny (120 ng m^{-3}) was caused by one sample (647 ng m^{-3}), which otherwise would have a mean concentration comparable to Ispra (39 ng m^{-3}). OC_{BB} made a minor (3 - 8%) contribution to OC, except at Montseny (20%).

A more detailed daily apportionment of OA was attempted for Grenoble and Ispra (see Figure 6.11), separating OC_{POA} into OC_{BB} and OC_{FF} (fossil fuel sources), and OC_{SOA} into $OC_{BSOA\alpha-pinene}$ and OC_{SOA} from other sources, primarliy for oxidation isoprene and anthropogenic emissions ($OC_{BSOAIsoprene+ASOA}$. Additionally, the contribution of OC_{PBAP} was considered.

With about one third of OC_{SOA} attributed to oxidation of α-pinene both in Grenoble and Ispra, oxidation products of isoprene and anthropogenic emissions dominated, constituting around half of total OC. Apportionment of OC_{SOA} from isoprene oxidation done in a similar way as for α-pinene ought to be possible soon (studies in progress). The OC_{FF} fraction was found to be larger than OC_{BB} both in Grenoble (13% vs. 6%) and in Ispra (14% vs. 6%), which is consistent with findings from other studies (e.g., Gilardoni et al., 2011). In Grenoble, OC_{PBAP} contributed equally to OC as OC_{FF}, accounting for 13% of OC, while in Ispra, its contribution was negligible (2%), due to the difference in particle cut-off size (PM_{10} for Grenoble and $PM_{2.5}$ for Ispra).

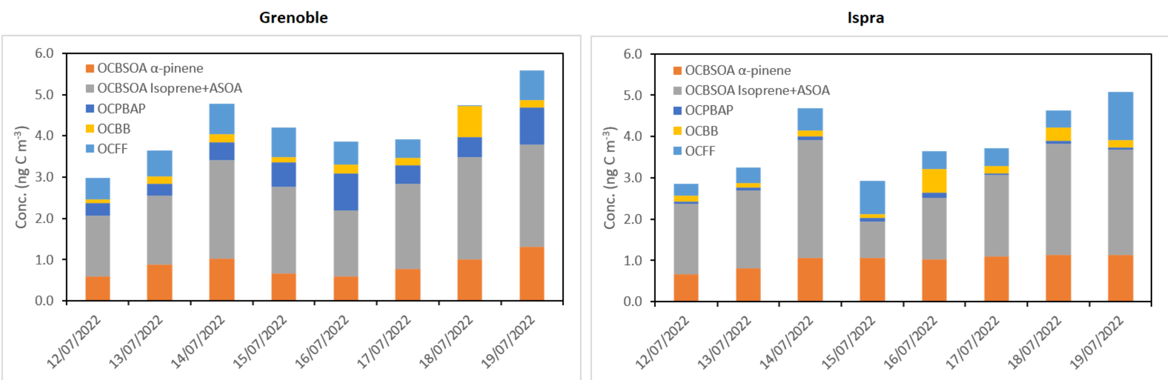

Figure 6.11: Organic aerosol apportioned into secondary and primary categories for the Grenoble (left) and Ispra (right) sites.

6.5 Inter-laboratory comparison on organic tracers

Organic tracers are used to identify the emission of aerosol particles from specific sources or their formation in the atmosphere (Cass 1998). Integrating organic tracers into Positive Matrix Factorization (PMF) has expanded the range and distinctiveness of PMF factors (referred to as aerosol sources), enabling quantitative estimates of aerosol sources that are otherwise challenging to quantify, such as biogenic secondary organic aerosol (BSOA) and primary biological aerosol particles (PBAP) (Waked et al. 2014, Srivastava et al. 2021, Yttri et al. 2021).

The value of organic tracers for source identification and apportionment is widely recognized in scientific research, and they are an integral part of the EMEP monitoring strategy (UNECE 2019) and the ACTRIS infrastructure (Wandinger and others. 2018)

In the 2014 EMEP Status Report, we emphasized that:

- “Measurements of source specific organic tracers at rural background sites should be more widespread.”

- “Organic tracer time series intending to span several decades should be initiated.”

- “Inter laboratory comparisons (ILC) of the most used tracers should be conducted to ensure high quality data and should follow from a more widespread use.”

While organic tracers have been included in EIMP 2008/2009 (Yttri et al. 2019), EIMP 2017/2018 (Platt et al. in prep.), and here in the EIMP 2022 (Aas et al. in prep.), only two sites consistently report organic tracers to EBAS. One site (Birkenes Observatory) has been reporting since 2008 (Yttri et al. 2021), while the other (Zeppelin Observatory) began reporting in 2017 (Yttri et al. 2023). Amongst the tracers reported are the biomass burning tracer levoglucosan, arabitol and mannitol, which are associated with fungal spores, and 2-methyltetrols, which are oxidation products of isoprene. Levoglucosan, a widely used organic tracer for assessing the impact of biomass burning emissions, underwent the first major inter-laboratory comparison (ILC) over a decade ago (Yttri et al. 2015). However, there have been no subsequent ILCs for other organic tracers.

During EIMP Summer 2022, the analysis of organic tracers for all sites was conducted by a centralized laboratory to ensure comparability. Notably, two different analytical methods (IGE-1 and IGE-2) were used by the centralized laboratory to cover the wide range of species. To ensure quality assurance and quality control, the performance of these analytical methods was compared to two different methods used by other labs. While the centralized laboratory analyzed several organic tracers, we will focus on comparing a few of them here: the well-known BSOA tracers of isoprene oxidation (2-methyltetrols; 2-methylerythritol and 2-methylthreitol) and α-pinene oxidation (3-methylbutane-1,2,3-tricarboxylic acid; short form: 3-MBTCA). These tracers were chosen due to the focus on secondary aerosol during EIMP Summer 2022. Additionally, levoglucosan was included in the comparison due to its extensive and long-standing use as a tracer, providing significant scientific and analytical experience.

The comparison was based on a total of nine aerosol filter samples collected from three different locations: the rural background site Observatoire Pérenne de l’Environnement (OPE) in France, the urban background site Marseille Longchamp (also in France), and the rural background site Melpitz in Germany. Aliquots of these filter samples were distributed among the participating laboratories for analysis. The four analytical methods used are listed and described in Table 6.3 and Table 6.4. For an extensive description of the analytical methods, please have a look at the references provided in Table 6.4.

Table 6.3: Overview of laboratories and the analytical methods used to analyze 2-methylterols, 3-MBTCA and levoglucosan

Lab	Species	Separation/Detection	Extraction	Column
IGE-1	3-MBTCA	IC-MS	H_2O, Mechanical	AG11-HC Thermo Fischer
IGE-2	2-Methyltetrols Levoglucosan	UPLC-MS/MS (ESI-)	H_2O, Mechanical	2.1 x 150 mm, 3 μm, Luna Omega Sugars
NILU	2-Methyltetrols Levoglucosan	UPLC Orbitrap Q-Exactive Plus (ESI-)	C_4H_8O, Ultrasonic	3.0 x 150 mm, 1.8 μm,, HSS T3 Waters Inc
IDAEA-CSIC	3-MBTCA 2-Methyltetrols Levoglucosan	GC-MS	CH_2Cl_2 + CH_3OH, Ultrasonic	60 m HP-5MS

Table 6.4: Overview of laboratories and the analytical methods used to analyze 2-methylterols, 3-MBTCA and levoglucosan.

Lab	Internal std/Recovery std	Quant. standards	Derivatization	References
IGE-1	3-MBTCA:		No	Glojeck et al. (in prep.)
IGE-2	2-Methyltetrols: $^{13}C_6$-Levoglucosan Levoglucosan: $^{13}C_6$-Levoglucosan	2-methyltetrols Levoglucosan	No	Glojeck et al. (in prep.)
NILU	Levoglucosan: $^{13}C_6$-Levoglucosan 2-Methyltetrols: $^{13}C_6$-Levoglucosan	Levoglucosan 2-methyltetrols	No	Yttri et al. (2021), Yttri et al. (2023)
IDAEA-CSIC	3-MBTCA: $^2H_4$-succinic acid 2-Methyltetrols: $^2H_7$-Levoglucosan Levoglucosan : $^2H_7$-Levoglucosan	Succinic acid Levoglucosan Levoglucosan	BSTFA, Pyridine	Alier et al. (2013), Fontal et al. (2015)

6.5.1 Results

2-Methyltetrols

The method employed by the centralized lab (IGE-2) for analyzing 2-methyltetrols showed very good agreement with the NILU lab, with a mean percentage difference (PD) of 20 $\pm$ 16% ($\pm$ SD) and an R^2 value of 0.885 (Figure 6.12; Table 6.5). Although the correlation (R^2 = 0.792) remained relatively high, the PD between IGE-2 and IDAEA-CSIC was substantial at 83 $\pm$ 43%. The PD between NILU and IDAEA-CSIC was in the same order as between IGE-2 and IDAEA-CSIC, but the correlation was higher (R^2 = 0.971).

The PD calculated using Eq. 6.6 represents the percentage difference between concentrations C1 and C2.

$$PD = |C1 - C2| \times 100/((C1 + C2)/2) \tag{6.6}$$

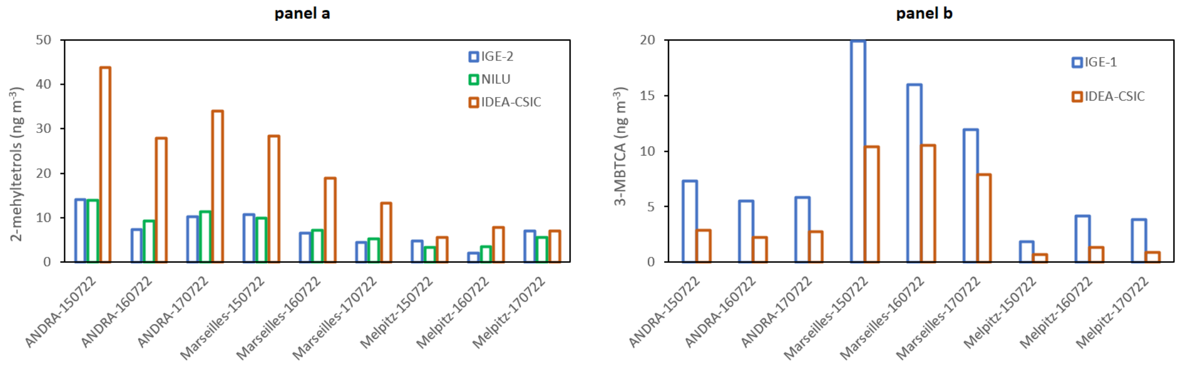

Figure 6.12: Results obtained for 2-methyltetrols (panel a) and 3-Methylbutane-1,2,3-tricarboxylic acid (panel b) by the three methods intercompared.

Despite providing detailed descriptions of the analytical methods, it is challenging to determine the exact reasons why IGE-2 and NILU yielded highly comparable results while IGE-2 and IDAEA-CSIC did not. IGE and NILU used liquid chromatography while IDAEA-CSIC used gas chromatography for the analysis of the compounds. It is worth noting that commercially available quantification standards for 2-methyltetrols are lacking, and IGE and NILU got their standards synthesized in separate laboratories, while IDAEA-CSIC used levoglucosan for quantification. Additionally, due to the unavailability of isotope-labeled internal standards for 2-methyltetrols, non-authentic standards were employed, each differing from one another (Table 6.4). Therefore, it is both surprising and encouraging to observe such a high level of comparability between IGE-2 and NILU. At the same time, it is speculated that the absence of synthesized quantification standards may account for the significant discrepancy observed with IDAEA-CSIC.

Notably, the PD was lower for the samples collected at Melpitz (44 ± 63%) than for the two French sites (102 ± 9.1%) when comparing IGE-2 and IDAEA-CSIC, whereas it was the other way around when comparing IGE-2 and NILU, with 37 ± 13% for Melpitz and 11 ± 7.5% for the French sites. This observation might indicate that the aerosol matrix plays a role, including both the collection location and the aerosol cut-off size. The Melpitz samples had a PM_{10} cut-off, while the French sites had a $PM_{2.5}$ cut-off.

Table 6.5: Calculated mean percentage difference (PD) for the three methods analyzing concentrations of 2-methyltetrols, 3-Methylbutane-1,2,3-tricarboxylic acid, and levoglucosan in the pilot ILC.

	All sites		**French sites**		**Melpitz**	
	PD (Mean ±SD) (%)	R^2	PD (Mean ±SD) (%)	R^2	PD (Mean ±SD) (%)	R^2
2-methyltetrols						
IGE-2 vs. NILU	20 ±16	0.885	11 ±7.5	0.927	37 ±13	
IGE-2 vs. IDAEA-CSIC	83 ±43	0.792	102 ±9.1	0.905	44 ±63	
NILU vs. IDAEA-CSIC	81 ±27	0.971	96 ±6.3	0.995	51 ±25	
3-MBTCA						
IGE-1 vs. IDAEA-CSIC	79 ±28	0.952	65 ±21	0.928	106 ±18	
Levoglucosan						
IGE-2 vs. NILU	32 ±43	0.95	6.8 ±3.8	0.999	83 ±38	
IGE-2 vs. IDAEA-CSIC	39 ±44	0.953	12 ±7.5	0.999	92 ±33	
NILU vs. IDAEA-CSIC	8.1 ±5.3	0.999	6.4 ±3.5	0.999	11 ±7.4	

3-MBTCA

The PD between the two methods, IGE-1 and IDAEA-CSIC, measuring 3-MBTCA was relatively high at 79 ± 28%, but with a high correlation (R^2 = 0.952). In contrast to 2-methyltetrols, commercially available quantification standards exist for 3-MBTCA, although isotope-labeled internal standards are not available. IGE-1 and IDAEA-CSIC used both different quantification and internal standards for 3-MBTCA analysis. The availability and widespread use of authentic isotope-labeled internal standards for commonly used organic tracers would be a crucial step towards harmonization and comparability of such measurements. Similar to 2-methyltetrols, significant differences in PD were observed between sites for 3-MBTCA as well (Table 6.5).

Levoglucosan

As anticipated, the overall comparability between methods was higher for levoglucosan compared to 2-methyltetrols and 3-MBTCA. This can be attributed to laboratories having more extensive experience in analyzing levoglucosan, and the availability of quantification standards and isotope-labeled standards. The mean PD (percentage difference) was quite similar between IGE-2 and NILU (32 ± 43%) and between IGE-2 and IDAEA-CSIC (39 ± 44%), while it was significantly lower between NILU and IDAEA-CSIC (8.1 ± 5.3%). When excluding the samples collected at Melpitz, the PD remained consistently low (ranging from 6.4% to 12%) between all methods. In the inter-laboratory comparison (ILC) on levoglucosan conducted by Yttri et al. (2014), the accuracy, represented by the mean percentage error (PE) for each participating laboratory, varied from -63% to 20%. However, most laboratories (85%) achieved accuracy within the range of ± 20%. We consider the results presented here to be comparable to those of Yttri et al. (2014). Note that the ILC conducted by Yttri et al. (2014)) focused on filter samples influenced by emissions from residential wood combustion (RWC), while the samples used in the present study were collected in summer when concentrations of levoglucosan typically are much lower and the aerosol matrix is different than in winter, and levoglucosan might originate from wild and agricultural fires in addition to RWC.

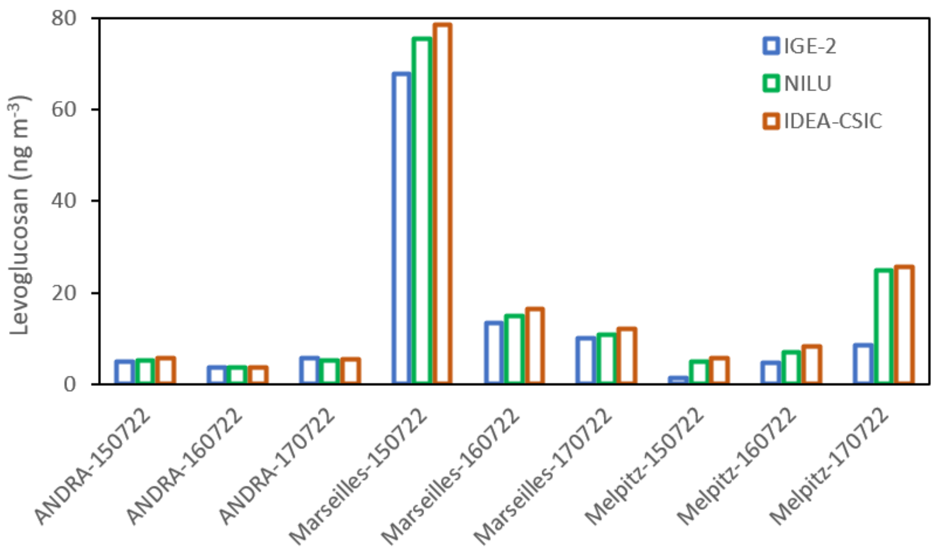

Figure 6.13: Results obtained for levoglucosan by the three methods intercompared.

The correlation coefficients (ranging from 0.953 to 0.999) were remarkably high for all comparisons conducted. However, no correlation was determined for the population consisting solely of samples from Melpitz due to the limited number of samples available (n = 3)

6.5.2 Conclusions

The correlation coefficients between concentrations of organic tracers obtained by different methods were consistently high, ranging from 0.792 to 0.999. However, there was significant variability in the ability of the methods to produce comparable concentrations of organic tracers. This might partly be attributed to challenges associated with the aerosol matrix. The reproducibility was better for the biomass burning tracer levoglucosan compared to the BSOA tracers 2-methyltetrols and 3-MBTCA. This can be attributed to laboratories practices, the availability of quantification standards and isotope-labeled standards. The results presented are encouraging, but this study involved only a few analytical methods and a limited number of samples, and it is evident that efforts are needed to improve the comparability of analytical methods for the tested BSOA tracers. A crucial first step towards harmonization and comparability is the availability of quantification standards and authentic isotope-labeled standards. An ILC for the most used organic tracers, including 2-methyltetrols and 3-MBTCA is long overdue and should be conducted in the near future, as previously done for levoglucosan.

References

Aas, W. et al.: Extensive measurement campaign of ozone, VOCs and BSOAs during the European heat wave, July 2022, in prep.

Alier, M., van Drooge, B. L., Dall'Osto, M., Querol, X., Grimalt, J. O., and Tauler, R.: Source apportionment of submicron organic aerosol at an urban background and a road site in Barcelona (Spain) during SAPUSS, Atmospheric Chemistry and Physics, 13, 10 353–10 371, doi:10.5194/acp-13-10353-2013, URL https://acp.copernicus.org/articles/13/10353/2013/, 2013.

Ambrose, J. L., Haase, K., Russo, R. S., Zhou, Y., White, M. L., Frinak, E. K., Jordan, C., Mayne, H. R., Talbot, R., and Sive, B. C.: A comparison of GC-FID and PTR-MS toluene measurements in ambient air under conditions of enhanced monoterpene loading, Atmospheric Measurement Techniques, 3, 959–980, doi:10.5194/amt-3-959-2010, URL https://amt.copernicus.org/articles/3/959/2010/, 2010.

Bergström, R., Hayman, G. D., Jenkin, M. E., and Simpson, D.: Update and comparison of atmospheric chemistry mechanisms for the EMEP MSC-W model system — EmChem19a, EmChem19X, CRIv2R5Em, CB6r2Em, and MCMv3.3Em, EMEP Technical Report 1/2022, The Norwegian Meteorological Institute, Oslo, Norway, 2022.

Borlaza, L. J. S., Weber, S., Uzu, G., Jacob, V., Cañete, T., Micallef, S., Trébuchon, C., Slama, R., Favez, O., and Jaffrezo, J.-L.: Disparities in particulate matter (PM_{10}) origins and oxidative potential at a city scale (Grenoble, France) – Part 1: Source apportionment at three neighbouring sites, Atmospheric Chemistry and Physics, 21, 5415–5437, doi:10.5194/acp-21-5415-2021, URL https://acp.copernicus.org/articles/21/5415/2021/, 2021.

Cass, G. R.: Organic molecular tracers for particulate air pollution sources, TrAC Trends in Analytical Chemistry, 17, 356–366, doi:https://doi.org/10.1016/S0165-9936(98)00040-5, URL https://www.sciencedirect.com/science/article/pii/S0165993698000405, 1998.

Cavalli, F., Viana, M., Yttri, K. E., Genberg, J., and Putaud, J.-P.: Toward a standardised thermal-optical protocol for measuring atmospheric organic and elemental carbon: the EUSAAR protocol, Atmos. Measurement Techniques, 3, 79–89, doi:10.5194/amt-3-79-2010, URL http://www.atmos-meas-tech.net/3/79/2010/, 2010.

Day, M. C., Zhang, M., and Pandis, S. N.: Evaluation of the ability of the EC tracer method to estimate secondary organic carbon, Atmospheric Environment, 112, 317–325, doi:https://doi.org/10.1016/j.atmosenv.2015.04.044, URL https://www.sciencedirect.com/science/article/pii/S1352231015300479, 2015.

El Haddad, I., Marchand, N., Temime-Roussel, B., Wortham, H., Piot, C., Besombes, J.-L., Baduel, C., Voisin, D., Armengaud, A., and Jaffrezo, J.-L.: Insights into the secondary fraction of the organic aerosol in a Mediterranean urban area: Marseille, Atmospheric Chemistry and Physics, 11, 2059–2079, doi:10.5194/acp-11-2059-2011, URL https://acp.copernicus.org/articles/11/2059/2011/, 2011.

Fontal, M., van Drooge, B. L., López, J. F., Fernández, P., and Grimalt, J. O.: Broad spectrum analysis of polar and apolar organic compounds in submicron atmospheric particles, Journal of Chromatography A, 1404, 28–38, doi:https://doi.org/10.1016/j.chroma.2015.05.042, URL https://www.sciencedirect.com/science/article/pii/S0021967315007529, 2015.

Gelencsér, A., May, B., Simpson, D., Sánchez-Ochoa, A., Kasper-Giebl, A., Puxbaum, H., Caseiro, A., Pio, C., and Legrand, M.: Source apportionment of $PM_{2.5}$ organic aerosol over Europe: primary/secondary, natural/anthropogenic, fossil/biogenic origin, J. Geophys. Res., 112, D23S04, doi:10.1029/2006JD008094, 2007.

Gilardoni, S., Vignati, E., Cavalli, F., Putaud, J. P., Larsen, B. R., Karl, M., Stenström, K., Genberg, J., Henne, S., and Dentener, F.: Better constraints on sources of carbonaceous aerosols using a combined ^{14}C – macro tracer analysis in a European rural background site, Atmospheric Chemistry and Physics, 11, 5685–5700, doi:10.5194/acp-11-5685-2011, URL https://acp.copernicus.org/articles/11/5685/2011/, 2011.

Glojeck, K. et al.: Sources apportionment of PM10 in an alpine valley with impacts of biomass burning, traffic, and industrial emissions: a study with advanced chemical characterization, in prep.

Groot Zwaaftink, C. D., Aas, W., Eckhardt, S., Evangeliou, N., Hamer, P., Johnsrud, M., Kylling, A., Platt, S. M., Stebel, K., Uggerud, H., and Yttri, K. E.: What caused a record high PM_{10} episode in northern Europe in October 2020?, Atmospheric Chemistry and Physics, 22, 3789–3810, doi:10.5194/acp-22-3789-2022, URL https://acp.copernicus.org/articles/22/3789/2022/, 2022.

Henne, S., Brunner, D., Folini, D., Solberg, S., Klausen, J., and Buchmann, B.: Assessment of parameters describing representativeness of air quality in-situ measurement sites, Atmospheric Chemistry and Physics, 10, 3561–3581, doi:10.5194/acp-10-3561-2010, URL https://acp.copernicus.org/articles/10/3561/2010/, 2010.

Platt, S. et al.: Source apportionment of equivalent black carbon from the winter 2017–2018 EMEP intensive measurement campaign using PMF, in prep.

Simoneit, B. R. T., Schauer, J. J., Nolte, C. G., Oros, D. R., Elias, V. O., Fraser, M. P., Rogge, W. F., and Cass, G. R.: Levoglucosan, a tracer for cellulose in biomass burning and atmospheric particles, Atmos. Environ., 33, 173–182, 1999.

Solberg, S., Claude, A., Reimann, S., Sauvage, S., and Walker, S.-E.: VOC measurements 2020, Tech. Rep. EMEP/CCC Report 4/2022, NILU -Norwegian Institute for Air Research, Kjeller, Norway, URL https://projects.nilu.no/ccc/reports/EMEP_CCC-Report_4_2022_VOC_measurements_2020.pdf, 2021.

Srivastava, D., Tomaz, S., Favez, O., Lanzafame, G. M., Golly, B., Besombes, J.-L., Alleman, L. Y., Jaffrezo, J.-L., Jacob, V., Perraudin, E., Villenave, E., and Albinet, A.: Speciation of organic fraction does matter for source apportionment. Part 1: A one-year campaign in Grenoble (France), Science of The Total Environment, 624, 1598–1611, doi:https://doi.org/10.1016/j.scitotenv.2017.12.135, URL https://www.sciencedirect.com/science/article/pii/S0048969717335593, 2018.

Srivastava, D., Xu, J., Vu, T. V., Liu, D., Li, L., Fu, P., Hou, S., Moreno Palmerola, N., Shi, Z., and Harrison, R. M.: Insight into $PM_{2.5}$ sources by applying positive matrix factorization (PMF) at urban and rural sites of Beijing, Atmospheric Chemistry and Physics, 21, 14 703–14 724, doi:10.5194/acp-21-14703-2021, URL https://acp.copernicus.org/articles/21/14703/2021/, 2021.

Turpin, B. J. and Huntzicker, J. J.: Identification of secondary organic aerosol episodes and quantitation of primary and secondary organic aerosol concentrations during SCAQS, Atmospheric Environment, 29, 3527–3544, doi:https://doi.org/10.1016/1352-2310(94)00276-Q, URL https://www.sciencedirect.com/science/article/pii/135223109400276Q, 1995.

UNECE: Monitoring strategy for the Cooperative Programme for Monitoring and Evaluation of the Long-range Transmission of Air Pollutants in Europe for the period 2020–2029, Tech. Rep. ECE/EB.AIR/144/Add.1, UNECE, URL https://www.unece.org/fileadmin/DAM/env/documents/2019/AIR/EB_Decisions/Decision_2019_1.pdf, 2019.

Waked, A., Favez, O., Alleman, L. Y., Piot, C., Petit, J.-E., Delaunay, T., Verlinden, E., Golly, B., Besombes, J.-L., Jaffrezo, J.-L., and Leoz-Garziandia, E.: Source apportionment of PM_{10} in a north-western Europe regional urban background site (Lens, France) using positive matrix factorization and including primary biogenic emissions, Atmospheric Chemistry and Physics, 14, 3325–3346, doi:10.5194/acp-14-3325-2014, URL https://acp.copernicus.org/articles/14/3325/2014/, 2014.

Wandinger, U. and others.: Deliverable D5.1: Documentation on technical concepts and requirements for ACTRIS Observational Platforms, URL https://www.actris.eu/sites/default/files/Documents/ACTRIS%20PPP/Deliverables/ACTRIS%20PPP_WP5_D5%201_Documentation%20on%20technical%20concepts%20and%20requirements%20for%20ACTRIS%20observational%20platforms.pdf, aCTRIS PPP. WP5, 2018.

Watson, L. A., Shallcross, D. E., Utembe, S. R., and Jenkin, M. E.: A Common Representative Intermediates (CRI) mechanism for VOC degradation. Part 2: Gas phase mechanism reduction, Atmos. Environ., 42, 7196–7204, doi:10.1016/j.atmosenv.2008.07.034, 2008.

Yttri, K., Platt, S., and Aas, W.: Relative contribution of biomass burning to TC across Europe - The 2017/2018 winter intensive measurement period, in: Transboundary particulate matter, photo-oxidants, acidifying and eutrophying components. EMEP Status Report 1/2022, pp. 113–122, The Norwegian Meteorological Institute, Oslo, Norway, 2022.

Yttri, K. E., Aas, W., Bjerke, A., Cape, J. N., Cavalli, F., Ceburnis, D., Dye, C., Emblico, L., Facchini, M. C., Forster, C., Hanssen, J. E., Hansson, H. C., Jennings, S. G., Maenhaut, W., Putaud, J. P., and Tørseth, K.: Elemental and organic carbon in PM_{10}: a one year measurement campaign within the European Monitoring and Evaluation Programme EMEP, Atmospheric Chemistry and Physics, 7, 5711–5725, doi:10.5194/acp-7-5711-2007, URL https://acp.copernicus.org/articles/7/5711/2007/, 2007.

Yttri, K. E., Simpson, D., Nøjgaard, J. K., Kristensen, K., Genberg, J., Stenström, K., Swietlicki, E., Hillamo, R., Aurela, M., Bauer, H., Offenberg, J. H., Jaoui, M., Dye, C., Eckhardt, S., Burkhart, J. F., Stohl, A., and Glasius, M.: Source apportionment of the summer time carbonaceous aerosol at Nordic rural background sites, Atmospheric Chemistry and Physics, 11, 13 339–13 357, doi:10.5194/acp-11-13339-2011, URL https://www.atmos-chem-phys.net/11/13339/2011/, 2011a.

Yttri, K. E., Simpson, D., Stenström, K., Puxbaum, H., and Svendby, T.: Source apportionment of the carbonaceous aerosol in Norway -quantitative estimates based on ^{14}C, thermal-optical and organic tracer analysis, Atmospheric Chemistry and Physics, 11, 9375–9394, doi:10.5194/acp-11-9375-2011, URL https://acp.copernicus.org/articles/11/9375/2011/, 2011b.

Yttri, K. E., Tsyro, S., Solberg, S., Alastuey, A., and Aas, W.: Improved source understanding., in: Transboundary particulate matter, photo-oxidants, acidifying and eutrophying components (EMEP Status Report, 1/2014), pp. pp. 83–104), The Norwegian Meteorological Institute, Oslo, Norway, 2014.

Yttri, K. E., Schnelle-Kreis, J., Maenhaut, W., Abbaszade, G., Alves, C., Bjerke, A., Bonnier, N., Bossi, R., Claeys, M., Dye, C., Evtyugina, M., García-Gacio, D., Hillamo, R., Hoffer, A., Hyder, M., Iinuma, Y., Jaffrezo, J.-L., Kasper-Giebl, A., Kiss, G., López-Mahia, P. L., Pio, C., Piot, C., Ramirez-Santa-Cruz, C., Sciare, J., Teinilä, K., Vermeylen, R., Vicente, A., and Zimmermann, R.: An intercomparison study of analytical methods used for quantification of levoglucosan in ambient aerosol filter samples, Atmospheric Measurement Techniques, 8, 125–147, doi:10.5194/amt-8-125-2015, URL https://amt.copernicus.org/articles/8/125/2015/, 2015.

Yttri, K. E., Simpson, D., Bergstrom, R., Kiss, G., Szidat, S., Ceburnis, D., Eckhardt, S., Hueglin, C., Nojgaard, J. K., Perrino, C., Pisso, I., Prevot, A. S. H., Putaud, J.-P., Spindler, G., Vana, M., Zhang, Y.-L., and Aas, W.: The EMEP Intensive Measurement Period campaign, 2008-2009: characterizing carbonaceous aerosol at nine rural sites in Europe, Atmos. Chem. Physics, 19, 4211–4233, doi:10.5194/acp-19-4211-2019, 2019.

Yttri, K. E., Canonaco, F., Eckhardt, S., Evangeliou, N., Fiebig, M., Gundersen, H., Hjellbrekke, A.-G., Lund Myhre, C., Platt, S. M., Prévôt, A. S. H., Simpson, D., Solberg, S., Surratt, J., Tørseth, K., Uggerud, H., Vadset, M., Wan, X., and Aas, W.: Trends, composition, and sources of carbonaceous aerosol at the Birkenes Observatory, northern Europe, 2001–2018, Atmos. Chem. Physics, 21, 7149–7170, doi:10.5194/acp-21-7149-2021, URL https://acp.copernicus.org/articles/21/7149/2021/, 2021.

Yttri, K. E., Bäcklund, A., Conen, F., Eckhardt, S., Evangeliou, N., Fiebig, M., Kasper-Giebl, A., Gold, A., Gundersen, H., Myhre, C. L., Platt, S. M., Simpson, D., Surratt, J. D., Szidat, S., Rauber, M., Tørseth, K., Ytre-Eide, M. A., Zhang, Z., and Aas, W.: Composition and sources of carbonaceous aerosol in the European Arctic at Zeppelin Observatory, Svalbard, EGUsphere, 2023, 1–49, doi:10.5194/egusphere-2023-615, URL https://egusphere.copernicus.org/preprints/2023/egusphere-2023-615/, 2023.

CHAPTER 7

Comparisons of modelled versus observed NMVOC, 2018 and IMP periods

Yao Ge, David Simpson and Sverre Solberg

7.1 Introduction

The spatial and temporal distributions and concentrations of non-methane volatile organic compounds (NMVOCs) are shaped by a range of atmospheric processes. These include primary emissions from a number of sources, chemical transformations, regional transport, and variations in meteorological conditions. As a result, difficulties in emissions estimation and model parameterisation of these processes, combined with technical challenges in accurately measuring ambient VOC levels, often leads to varying agreements between model and measurement (Pfister et al. 2008, Veefkind et al. 2012, Huang et al. 2017, Dalsøren et al. 2018, Bray et al. 2019, Solberg et al. 2001, von Schneidemesser et al. 2023).

Comparison of modelled VOC results with observations presents a number of challenges beyond those of other compounds such as NOx, CO or NH_3. In particular, emissions are input to the model as total NMVOC, but these emissions then need to be converted to inputs of specific species (C_2H_6, C_3H_8 etc), and few data are available to support this speciation. Thus, results from models can diverge significantly based on different VOC emission profiles used. Also, the lifetime of many of the VOCs is so short that a sound comparison of measured and modelled levels is difficult. Moreover, a particular monitoring site's representativeness of its surrounding air, and the quality of its measurement data, can also vary dramatically. In response to these challenges, continuous efforts have been invested in enhancing the chemistry mechanisms in the EMEP model and implementing long-term VOC measurements across Europe in recent years.

Further, real-world NMVOCs comprise many 1000s of species, but chemical transport model schemes can only cope with a much smaller number of compounds, typically in the

100s. In the standard chemistry mechanisms, EmChem19a (Simpson et al. 2020, Bergström et al. 2022), and the update, EmChem19rc, (Sect. 10.2), most emitted VOCs are lumped into different groups (e.g. most alkanes are treated as n-butane), with only a select few VOC species having explicit emissions and chemistry. This approach offers the dual benefit of maintaining an accurate description of ozone generation and promoting computational efficiency. However, it presents challenges when attempting to produce specific VOC concentrations for comparison with observation data. Given the substantial shifts in real-world VOC emission profiles and the significant advancements in the EMEP model physical and chemical formulation since the last model evaluation studies of VOCs in the 1990s (Hov et al. 1997, Solberg et al. 2001), it is imperative to update our understanding of the current model's performance and the factors that affect it.

The research project detailed herein aims to augment the VOC species set in the EMEP model with tracers for individual NMVOC compounds, thereby enabling a more comprehensive comparison of VOCs between the EMEP model and ambient measurements. For this purpose, we deployed a 'tracer' method, which allows us to input explicit emissions into the model and compute concentrations of individual VOCs. This tracer method has been used for whole-year comparisons (for 2018) of NMVOC as described in Sect. 7.6 and for comparisons during the 2022 EMEP intensive measurement period (IMP) as presented in Sect. 7.7. The methodology behind both studies is described in Sect. 7.2.

It is important to note that the work here is preliminary, and the work will be updated in future once we have made further modifications to the model setup (especially concerning boundary conditions and handling of some tracer species), and have further analysed the NMVOC speciation.

7.2 Methods

7.2.1 Chemistry mechanisms

Two chemistry mechanisms, EmChem19rc and CRIv2R5Em, have been utilised to develop VOC tracers. EmChem19rc (see Sect. 10.2,10) is the default chemical mechanism used in v5.0 of the EMEP model. It typically employs primary emissions from 16 VOC surrogates (14 anthropogenic and 2 biogenic) to stand for a wide variety of VOCs that are actually emitted into the atmosphere (Bergström et al. 2022). For instance, n-butane (nC4H10) is utilised to represent alkanes that contain more than three carbon atoms, alongside a handful of other species with similar Photochemical Ozone Creation Potentials (POCP) (Derwent and Jenkin 1991, Jenkin et al. 2017). In a similar vein, aromatic VOCs include explicit benzene and toluene species, but then o-xylene is used as a surrogate for itself and all other aromatic VOCs having more than seven carbon atoms.

The CRIv2R5Em chemical mechanism is an EMEP adaptation (Bergström et al. 2022) of the Common Representative Intermediates (CRI) v2-R5 mechanism (Watson et al. 2008). This mechanism is the simplest variant of CRI v2, considered suitable as a reference mechanism in large-scale chemistry-transport models. A selection of 27 (24 anthropogenic and 3 biogenic) emitted species are chosen as VOC surrogates to represent all non-methane VOCs emitted in CRIv2R5Em, based on their POCP, abundance, and simplicity of mechanism. This EMEP adaptation (derived from a version based on CRIv2.1), CRIv2R5Em, was created prior to the release of the latest CRI v2.2, hence it slightly differs from the official CRIv2R5 version.

In order to obtain VOC concentration outputs from the model that are directly comparable with measurements, without affecting the computational efficiency and the mechanism's innate capability for ozone production, we employ a 'tracer' method. This method retains the normal EmChem19 mechanisms for the calculation of photochemistry (and hence OH, O_3 and NO_3 radical concentrations), but additionally introduces individual VOC tracers (denoted by the suffix "_T") that take explicit emissions from a certain species and follow species-specific loss and production processes to yield precise concentrations of that species. These tracers neither consume any actual atmospheric oxidants, like the OH radical, nor generate any actual products; they are created solely to track VOC concentrations. For example, although emissions of iso-butane (iC_4H_{10}) are lumped with those of other heavy alkanes into the surrogate nC_4H_{10} species for the standard photochemical calculations, we also track the emissions and losses (using explicit OH + iC_4H_{10} reaction rates) for the tracer species iC4H10_T. This procedure should give the best estimate of its concentrations, assuming that the standard EmChem19 model concentrations of OH are reasonable – something which was demonstrated by Bergström et al. (2022).

Table 7.1 summarises available VOC species in the adapted EmChem19rc mechanism. Based on chemical species and reactions in CRIv2R5Em, eleven new species (coloured in blue in Table 7.1) are added to EmChem19rc as VOC tracers, which not only enable a comparison with CRIv2R5Em, but also with more measurements. Alongside these new species, additional tracers have also been created for existing lumped surrogates such as NC4H10_T, OXYL_T, and others.

Table 7.1: Summary of current primary VOC species in EmChem19rc. Species coloured in blue are newly added VOC tracers. N-PrOH_T and I-PrOH_T represent 1-propanol and 2-propanol respectively; MEK represents methyl ethyl ketone.

Groups	Species			
Alkane	C2H6	C3H8_T	NC4H10	IC4H10_T
Alkene	C2H4	C3H6	C4H8_T	
Alkyne	C2H2_T			
Aromatics	C6H6	C6H5CH3	C6H4(CH3)2	
Alcohol	CH3OH	C2H5OH	N-PrOH_T	I-PrOH_T
Aldehyde	HCHO	CH3CHO	C2H5CHO_T	
Dialdehyde	OCHCHO	CH3COCHO		
Ketone	CH3COCH3_T	MEK		
Carboxylic acid	HCOOH_T	CH3COOH_T		
Biogenic VOC	C5H8	α-Pinene	β-Pinene_T	
Rest†	Oth_alkane_T			

Notes †: Rest includes alkane and some other species.

7.3 Emission sources

VOC emissions in the EMEP model consist of biogenic VOC (BVOC) which are calculated online from temperature, radiation and land-cover data (Simpson et al. 1999, 2012), biomass-burning emissions from Fire INventory from NCAR (FINN) v2.5 (Wiedinmyer et al. 2023, Ch. 9), and gridded anthropogenic VOC (AVOC) sources which are provided annually from

CEIP, or through the CAMS projects Kuenen et al. (2021), Granier et al. (2019). (Here we used the dataset CAMS-REG-v5.1.)

Of the BVOC emissions, isoprene is an explicit species (i.e. not a surrogate species), but monoterpenes and sesquiterpenes are lumped surrogate compounds. The biomass-burning emissions are discussed in Sect. 7.3.3. The other AVOC emissions are provided by CEIP or CAMS as sector-specific totals (e.g. VOC from solvents or road traffic sectors), and are the main focus of this study.

For this project, the primary source of AVOC emission profiles is the UK National Atmospheric Emission Inventory (UK NAEI), provided by the NAEI team upon email request in 2022. The key advantage of this inventory is its extensive coverage: it offers emissions data for 664 VOC species across 249 sectors, spanning the period from 1990 to 2019. Despite being based on a somewhat dated speciation profile developed in the early 2000s (Passant 2002), this inventory is highly valuable. As there appears to be a scarcity of national speciated VOC emission inventories reported by other European countries, the UK NAEI remains a robust reference source.

7.3.1 Emissions sector mapping

This study utilizes two European emission inventories, namely CEIP and CAMS. Emission sectors in the UK NAEI are mapped to the 19 EMEP sectors as shown in Table 1.1. Given that most activities in the UK NAEI are classified into various NFR sectors, this mapping is achieved using a cross-walk between NFR and GNFR sectors as detailed in Matthews and Wankmüller (2021). Most sources in the UK NAEI have corresponding emission profiles, with the exception of activities falling under sectors K (Agri-Livestock), L (Agri-Other), and F3 (Road Transport Exhaust - LPG). Emission profiles reported by the EEA emission inventory guidebook Chapter 3.B Manure management[1] serve as a reference for activities relating to poultry, cattle, and pigs. Additionally, Hobbs et al. (2004) reported speciated VOC emissions from sheep. By combining data from these two sources, we have established VOC speciation for sector K.

Sector L, Agri-Other, encompasses activities (e.g., the application of animal manure to soils, cultivated crops, and field burning of agricultural residues, etc.) which can have vastly different emission profiles. The primary issue is the lack of publicly available, speciated emission data for these activities. Consequently, we have temporarily assigned sector L the same profile as sector K, and plan to revisit this decision when relevant data becomes available in the future. For sector F3, the VOC speciation for LPG exhaust is derived from the EMEP/CORINAIR Emission Inventory Guidebook[2].

7.3.2 Emissions species mapping

The reference species mapping was developed by Garry D. Hayman[3] as part of the study that was eventually published as Bergström et al. (2022)). This mapping was based on an older version of the UK NAEI for EmChem19rc species and for SNAP sectors, which serves as the starting point for the VOC speciation described here. Figure 7.1 illustrates the mapping

[1] https://www.eea.europa.eu/publications/emep-eea-guidebook-2019/part-b-sectoral-guidance-chapters/4-agriculture/3-b-manure-management/view

[2] https://www.eea.europa.eu/publications/EMEPCORINAIR5/B710vs6.0.pdf/view

[3] now at UK Centre for Ecology and Hydrology

process from NAEI's speciated VOC emissions to EMEP VOCs (EV) within EMEP sectors (ES). Utilising raw data from the NAEI for a selected year, the total emissions for EMEP sector i, denoted as ES_i, are calculated as follows:

$$ES_i = \sum_{j=1}^{n} EV_{j,1} + EV_{j,2} + \cdots + EV_{j,28}$$

where j is the corresponding NAEI sector, n is the total number of NAEI sectors that belong to i, and $EV_{j,1}$ to $EV_{j,28}$ represent emitted masses of 28 EMEP VOCs. In the EMEP sector i, the percentage of the EMEP VOC x, $P_{i,x}$, is calculated as follows:

$$P_{i,x} = \frac{\sum_{j=1}^{n} EV_{j,x}}{ES_i} \times 100\%$$

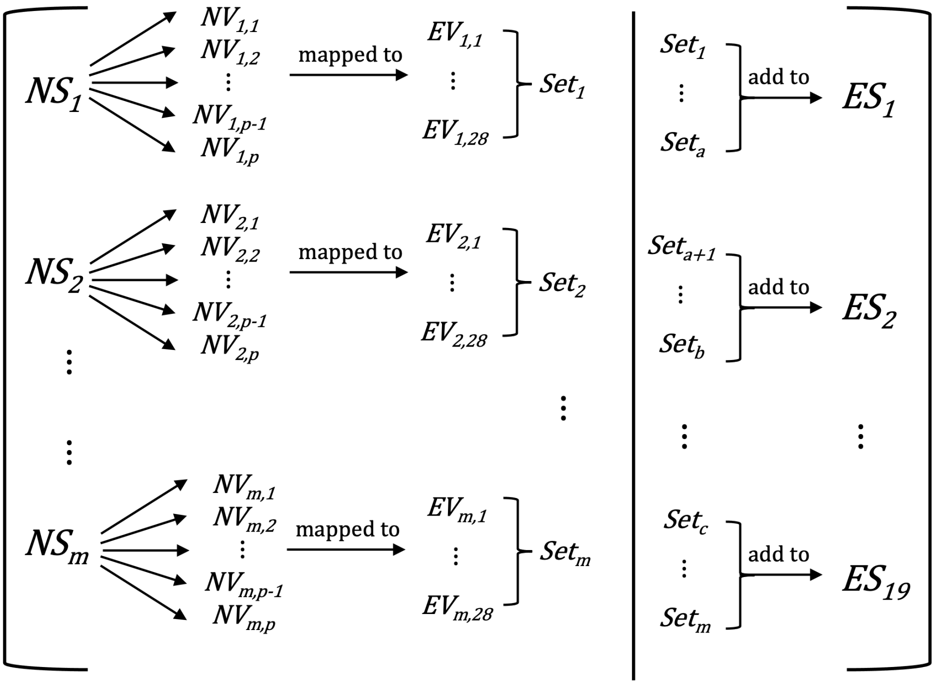

Figure 7.1: The emission mapping of NAEI VOCs (NV) from NAEI sectors (NS) to EMEP VOCs (EV, 28 species in total) and EMEP sectors (ES, 19 sectors in total). The total number of NS is denoted by m; the total number of NV is denoted by p.

Figure 7.2 presents the annual total NMVOC emissions for individual EMEP sectors in both inventories, as well as each sector's emission profiles implemented in the model. The CAMS inventory, with its smaller domain, generally reports lower sector totals than the CEIP inventory. As mentioned in Section 7.3.1, in the CAMS inventory, emissions from the Road Transport (RT) sector are reported in four subsectors (i.e., F1=RT-Gasoline, F2=RT-Diesel, F3=RT-LPG, and F4=RT-Non-exhaust), and thus its total is shown as the sum of emissions from these subsectors. In contrast, the CEIP inventory reports emissions only the Road Transport sector, while emissions for its subsectors are all set to zero (hence, emission profiles for these subsectors are not used in actual model simulation). The same logic applies to the usage of emission profiles of the Public Power sector and its subsectors when utilising different inventories. Apart from these differences, both inventories indicate that the significant VOC emitting sectors include Industry, Other Combustion, Fugitive, Solvents, Road Transport, and Agri-Livestock.

Utilizing 2018 anthropogenic emissions data, 664 VOCs from the NAEI, in addition to 5 other VOCs from the EEA emission inventory guidebook, are mapped to 28 EMEP species or groups (which includes OTH_ALKANE). Figure 7.2 illustrates the 19 most substantially emitted species or groups, with the lesser-emitted VOCs incorporated into the REST group.

It is worth noting that anthropogenic emissions of traditionally recognised biogenic VOCs do exist, as represented by the BVOC group in Fig. 7.2. This group represents anthropogenic emissions of isoprene, α-pinene, β-pinene, and some terpene species. Anthropogenic emissions of the BVOC group only become visible in the Industry sector and are considerably smaller compared to their biogenic emissions.

The OTH_ALKANE group signifies emissions of higher alkanes with more than four carbon atoms, as well as some other complex VOCs. The UNREAC group represents emissions of species with low or no reactivity. Considering both sector totals and sector speciation, the most substantial VOC emissions from the largest emitting sectors are C2H5OH, C2H4, C2H6, C3H8, NC4H10, OTH_ALKANE, BENZENE, OXYL, and TOLUENE.

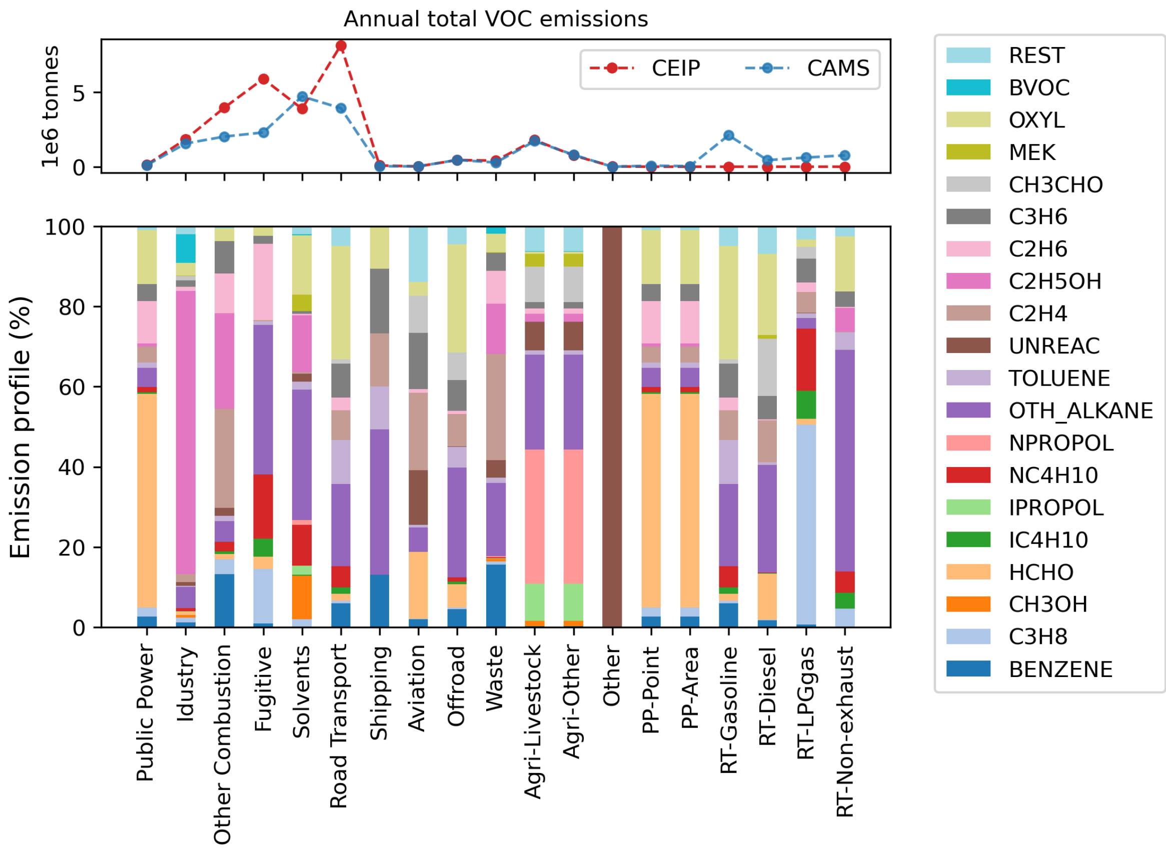

Figure 7.2: Annual total emissions (upper panel) and VOC profiles (lower panel) of individual EMEP sectors from CEIP and CAMS-REG emission inventories in 2018. Among the last 6 subsectors, PP stands for Public Power, RT stands for Road Transport. Note that CEIP do not provide data for the last six sectors (A1,A2,F1–F4), so zero emissions shown.

7.3.3 Speciation of biomass burning emissions

Table 7.2 displays the emission splitting factors used in the EMEP model for biomass burning species in the FINN inventory. While FINN typically provides emissions data for individual species, it only offers a combined emission for butane species. Consequently, the VOC speciation data derived from Andreae (2019) is employed to determine the ratios of n-butane to i-butane.

Table 7.2: The mapping between biomass burning species in the FINN inventory and species in the EMEP model

FINN species	model species	Factor
C2H6	C2H6_T	1
C3H8	C3H8_T	1
ALK4	NC4H10_T	0.6255
ALK4	IC4H10_T	0.3745
C2H4	C2H4_T	1
PRPE	C3H6_T	1
XYLE	OXYL_T	1
BENZ	BENZENE	1
TOLU	TOLUENE	1
CH2O	HCHO	1
ALD2	CH3CHO_T	1
MGLY	MGLYOX	1
ACET	CH3COCH3_T	1
MEK	MEK_T	1

7.4 Measurements

Ambient measurement data are compiled from the Ebas platform (`ebas-data.nilu.no`) developed by EMEP/CCC. The regular EMEP VOC measurement data are documented in the EMEP annual VOC reports (e.g. Solberg et al. 2020, 2022) and references therein. Table 7.3 presents a summary of the codes, names, and altitudes of all stations referenced in this chapter, including both the 2018 and 2022 IMP campaign comparisons. Stations situated above 800m in altitude are omitted from all analyses, as the concentrations measured at these locations are unsuitable for comparison with modeled surface concentrations.

7.5 Model experiments

The VOC tracers and their related code are integrated into the EMEP model via the GenChem system (Simpson et al. 2020). It utilises a chemical pre-processor GenChem.py to convert chemical equations into differential form and generate the corresponding FORTRAN code for use in the EMEP model. Four model simulations (Table 7.4) were carried out at a grid resolution of $0.1° \times 0.1°$ over the Europe domain for 2018 to test the tracer method with both EmChem19rc and CRIv2R5Em mechanisms and both CEIP and CAMS emission inventories.

Table 7.3: Codes, names, and altitudes (m) of stations involved in this chapter (for both the whole year of 2018 and 2022 IMP campaign).

Code	Name	Country	Altitude/m	Code	Name	Country	Altitude/m
AT0002R	Illmitz	Austria	117	FR0027U	Villeneuve d'Ascq	France	70
BE0007R	TMNT09 Vielsalm	Belgium	496	GB0048R	Auchencorth Moss	UK	260
CH0053R	Beromünster	Switzerland	797	GB1055R	Chilbolton Observatory	UK	78
CY0002R	Cyprus Atmospheric Observatory	Cyprus	520	IE0031R	Mace Head	Ireland	5
CZ0003R	Kosetice (NAOK)	Czechia	535	IT0004R	Ispra	Italy	209
DE0007R	Neuglobsow	Germany	62	IT0014R	Capo Granitola	Italy	5
DE0044R	Melpitz	Germany	86	MT0001R	Giordan Lighthouse	Malta	167
ES0019U	Barcelona (Palau Reial)	Spain	80	NO0002R	Birkenes II	Norway	219
ES0021U	Madrid (CIEMAT)	Spain	669	NO0015R	Tustervatn	Norway	439
FI0050R	Hyytiälä	Finland	181	NO0039R	Kårvatn	Norway	210
FR0008R	Donon	France	775	NO0043R	Prestebakke	Norway	160
FR0013R	Peyrusse Vieille	France	200	NO0052R	Sandve	Norway	15
FR0018R	La Coulonche	France	309	NO0056R	Hurdal	Norway	300
FR0020R	SIRTA Atmospheric Research Observatory	France	162				

For the 2022 campaign comparisons, the model simulation uses the CRIv2R5Em chemistry mechanism, 2019 CEIP emission inventories (since 2022 emissions were unavailable) and 2022 meteorology.

Table 7.4: Configuration of 4 model simulations.

Simulation	Mechanism	Emission
Em-CEIP	EmChem19rc	CEIP
Em-CAMS	EmChem19rc	CAMS-REG-v5.1
CRI-CEIP	CRIv2R5Em	CEIP
CRI-CAMS	CRIv2R5Em	CAMS-REG-v5.1

The boundary conditions (BC) for n-butane and i-butane employed in this study are derived from the average concentrations from a five-year dataset of high-frequency, in-situ VOC measurements taken at Mace Head, Ireland, as documented by Grant et al. (2011). Table 7.5 displays the mapping between the default boundary condition species and the EMEP model species. A numerical factor is used to partition the boundary condition of the lumped species C4H10 into three VOC tracers: NC4H10_T, IC4H10_T, and OTH_ALKANE_T. Unfortunately, time did not allow the implementation of BCs for some species, e.g. for propane or acetylene. According to Grant et al. (2011) the annual mean baseline concentration of propane should be around 260 ppt. Year to year variation is large, however, with e.g. 476 ppt in 2005 but 227 ppt in 2009. These BCs will be revised and improved for the next round of modelling.

Other aspects of the model setup are the usual defaults.

Table 7.5: The boundary conditions for VOC species in the EMEP model. For each species, 'Surf' gives mean surface BC values; 'Dmax' gives the day number of the maximum value in a year (e.g., for C4H10, 45 means the maximum appears in mid-February).

BC species	model species	Surf/ppb	Dmax	Factor
C2H6	C2H6_T	2.0	75	1
C4H10	NC4H10_T	2.0	45	0.0547
C4H10	IC4H10_T	2.0	45	0.0253
C4H10	OTH_ALKANE_T	2.0	45	0.9199
HCHO	HCHO	0.7	180	1

7.6 Results, 2018

This section provides a comparative analysis between modelled and measured VOCs for the full year 2018, using measurements from the standard EMEP monitoring network (Solberg et al. 2020). This process is complicated by the fact that the number of monitoring sites differs among species and there are differences in the frequency and duration of sampling across stations. For this work we have matched the hourly model outputs with valid measurements at their native temporal resolution. Consequently, the annual mean concentrations discussed in this section are derived from hours with valid measurements, and where the sites have at least 75% data capture in the year 2018.

The model evaluation is undertaken for all model experiments, using the model surface outputs. The comparisons for the 4 model simulations show similar characteristics. To avoid repetition, all figures in this section are derived from the model simulation utilising the EmChem19rc mechanism and the CAMS inventory.

7.6.1 Alkane species, 2018

Scatter plots comparing the modelled and measured annual mean concentrations of three alkane species (C_3H_8, nC_4H_{10}, iC_4H_{10}) from the Em-CAMS runs are depicted in Fig. 7.3. An overview of the evaluation statistics for each model simulation is provided in Table 7.6.

Both the model and measurements suggest that propane (Mean of observations, Mean_O = 0.664 ppb), has the highest concentrations of these alkanes, followed by n-butane (0.252 ppb), and i-butane (0.154 ppb). (Note that we exclude C_2H_6 from this analysis even though concentrations are even higher, at just under 2 ppb. These concentrations are simply a reflection of boundary conditions (Tab. 7.5) combined with the long lifetime of this species, and statistics were dominated by the effects of one outlier site and by large spikes in daily data.)

Model performance is seen to vary markedly across the species, with significant underpredictions for propane (NMB of -81%) and i-butane (-45%), but overprediction (+36%) for n-butane. The scatter is also significantly larger for propane and i-propane than for n-butane. The underprediction of propane is at least partly due to the omission of boundary conditions for this species, as noted in Sect. 7.5, so better model performance can be expected in the next round of modelling. Another possible problem is simply an underprediction of propane emissions. Dalsøren et al. (2018) found much better agreement between modelled and observed propane when updated emissions from both natural and anthropogenic sources were included in place of their base CEDS emissions (Hoesly et al. 2018); it is not clear if the European

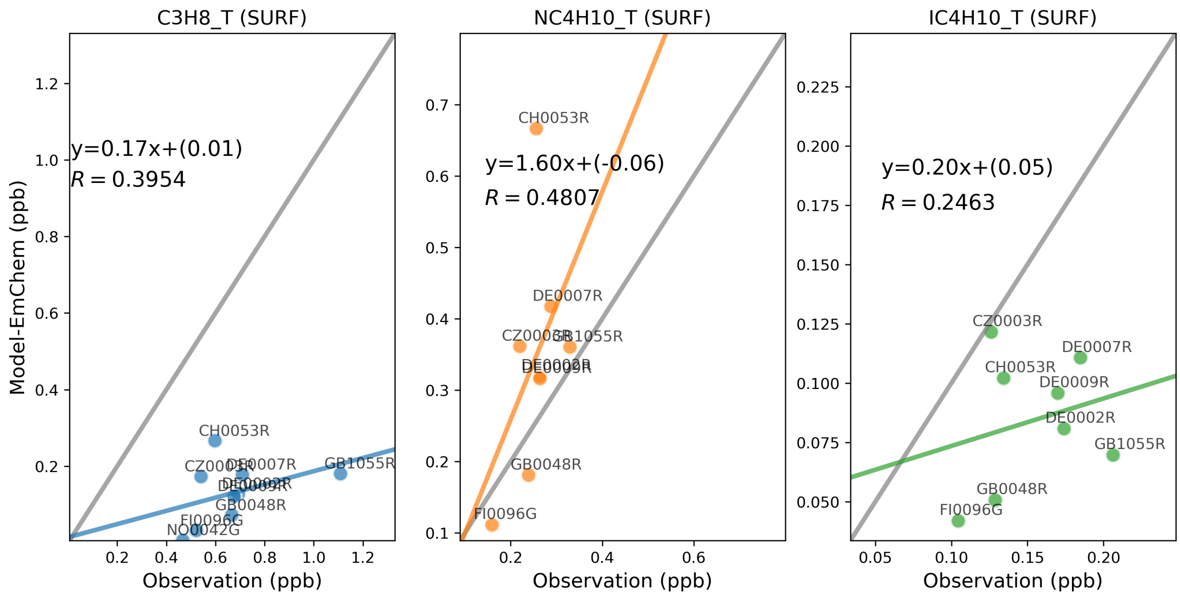

Figure 7.3: Scatter plots of annual mean modelled and measured alkane species concentrations from the Em-CAMS simulation. The terms 'SURF' and 'EmChem' indicate that the data is from model surface outputs using the EmChem19rc mechanism. In each plot, the grey line is the 1:1 line, and another coloured line is the least-squares regression line.

Table 7.6: Summary of the comparison statistics between the model (M) and observation (O) for alkane species. N is the number of sites. R is the Pearson's correlation coefficient. Mean_O and Mean_M refer to the annual average concentrations (in ppb) of O and M, respectively. NMB is the Normalised Mean Bias, and NME is the Normalised Mean Error.

C3H8_T	**N**	**R**	**Mean_O**	**Mean_M**	**NMB**	**NME**
Em-CEIP	9	0.38	0.664	0.122	-82%	82%
Em-CAMS	9	0.4	0.664	0.129	-81%	81%
CRI-CEIP	9	0.38	0.664	0.124	-81%	81%
CRI-CAMS	9	0.39	0.664	0.131	-80%	80%
NC4H10_T	**N**	**R**	**Mean_O**	**Mean_M**	**NMB**	**NME**
Em-CEIP	8	0.48	0.252	0.346	37%	47%
Em-CAMS	8	0.48	0.252	0.342	36%	46%
CRI-CEIP	8	0.47	0.252	0.356	41%	50%
CRI-CAMS	8	0.48	0.252	0.351	39%	49%
IC4H10_T	**N**	**R**	**Mean_O**	**Mean_M**	**NMB**	**NME**
Em-CEIP	8	0.24	0.154	0.083	-46%	46%
Em-CAMS	8	0.25	0.154	0.084	-45%	45%
CRI-CEIP	8	0.24	0.154	0.086	-44%	44%
CRI-CAMS	8	0.25	0.154	0.087	-43%	43%

EMEP emissions suffer from similar underestimates.

Simulations using the four model setups produce rather similar statistical results for each alkane (Table 7.6). When ranking the model performances between different model simulations, those utilizing the CAMS inventory display marginally better comparison results than those utilizing the CEIP inventory. For example, the simulation of n-butane in CRI-CAMS shows a higher R value and a lower NMB, compared to that in CRI-CEIP, but only from 0.47 to 0.48 and from 41% to 39%, respectively. Possible reasons for improvement include the inclusion of more detail in the road traffic emissions sectors (F1–F4) in CAMS, and differences in absolute amounts and spatial distributions of the emissions, but the modelled results for alkanes are obviously not so sensitive to these differences.

As n-butane and i-butane have rather similar chemical loss rates (with lifetimes of ca. 1 day at typical temperatures and OH=5.0×10^6 molec $\cdot$ cm^3), one would expect rather good correlation between the two. Indeed correlations between individual observed n- and i-butane samples are very good (e.g. R=0.97 at the UK site Chilbolton, c.f. Fig.7.4, with consistent ratios of n-butane/i-butane of ca. 2:1 (e.g. 1.56 for Chilbolton, Fig. 7.4, or 1.79 for the German site Neuglobsow, not shown). The equivalent modelled ratios do show a reasonable correlation (R=0.85 for Chilbolton), but the ratio is much higher: 4.64 for this site. Modelled ratios at other sites (e.g. Neuglobsow) can show lower ratios on average, but more scatter, and examination of daily data suggests that a few peak episodes with low ratios control the annual average ratios. These differences point to issues related to the ratio of n-butane to i-butane in either anthropogenic or biomass burning emissions, or possibly both. For example, Fig. 7.5 which shows that the ratios for industrial emissions (GNFR B) and solvent emissions (GNFR E) far exceed those of other sectors, and so the modelled ratios will depend critically on the source sector contributions. From Table 7.2 we can also calculate an n- to i-butane ratio in wildfire emissions of 1.67, so wildfires episodes would lower the ratio. Still, the lack of variability in the observed samples suggests that the emission speciation used for modelling has inaccurate n- to i- ratios.

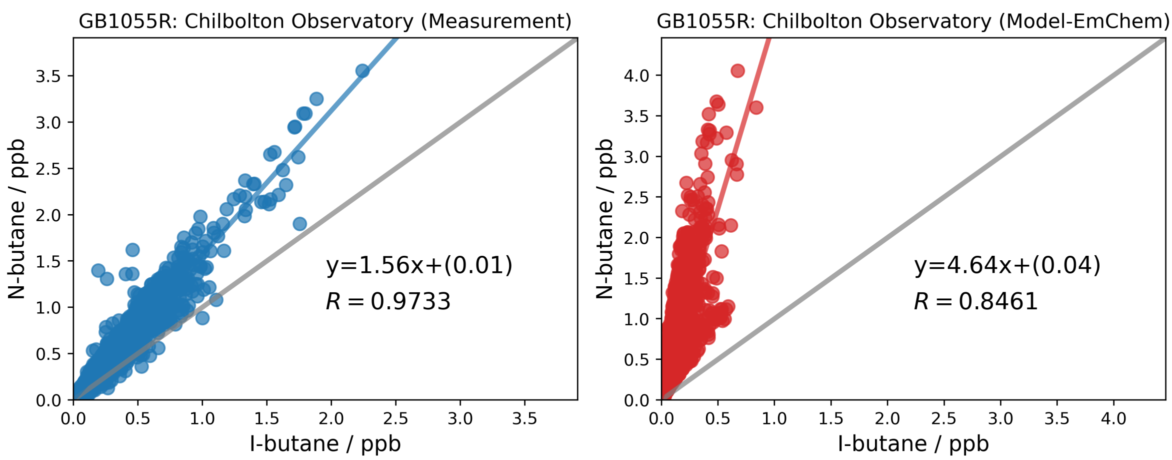

Figure 7.4: Linear correlations between n-butane and i-butane for measurement data (left panel) and model data (right panel) at GB1055R station (Chilbolton), 2018 samples.

7.6.2 Unsaturated NMHCs, 2018

Figure 7.6 compares annual mean data for ethene, propene, acetylene, and isoprene. The comparison statistics are summarised in Table 7.7. Results are very mixed, with rather good results for ethene and isoprene, but very poor results for propene and acetylene.

A detailed time series comparison of acetylene at example stations is illustrated in Figure 7.7. The modelled concentrations are significantly lower and display little seasonal variations,

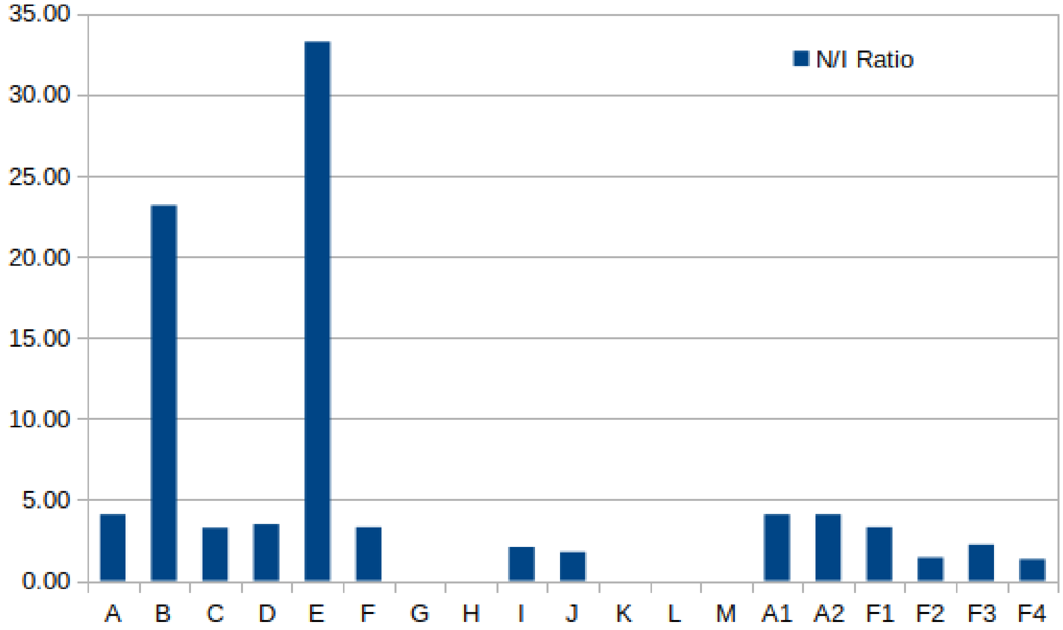

Figure 7.5: Ratios of n-butane to i-butane for GNFR sectors in NAEI-based emission inventory.

whereas the measured values are substantially higher, with multiple concentration peaks occurring during winter. Given that acetylene is commonly regarded as a purely anthropogenic VOC, and often used as a tracer of anthropogenic emissions (e.g. von Schneidemesser et al. 2023), this discrepancy is important. Possible reasons for this discrepancy could be the underestimation of either acetylene emissions from sectors such as road transport or other combustion sources, or from boundary conditions.

Large issues are also found for propene, though we can note that the concentrations are so low that measurements may even be affected by the detection limits. In contrast the results for ethene are much better in terms of both correlations (0.64) and bias (NMB -36%).

The isoprene results show the highest correlation (0.94), and best NMB values (-23%). Isoprene is one of the most important biogenic VOCs, with emissions largely arising from biogenic sources (Guenther et al. 2012, Simpson et al. 1999). Traffic related sources can also be important in wintertime (Reimann et al. 2000, Borbon et al. 2001). The good comparisons for this species are somewhat surprising due to both the difficulties associated with estimating the magnitude and spatial distribution of such emissions (Simpson et al. 1999) and the short life-time.

When comparing the performance of the model across different simulations (Table 7.7), the comparison statistics appear again quite similar. For ethene and propene, simulations that use CAMS emissions shows slightly better R than those using CEIP emissions. For acetylene and isoprene, changing inventories has almost no effect on R. Similarly, altering the chemistry mechanisms barely influences the results for any of the four species.

7.6.3 Aromatic species, 2018

Figure 7.8 presents the comparisons of benzene, toluene, and o-xylene concentrations. Both the model and the measurements indicate that the concentrations of benzene and toluene are an order of magnitude higher than those of o-xylene. All three aromatic species demonstrate

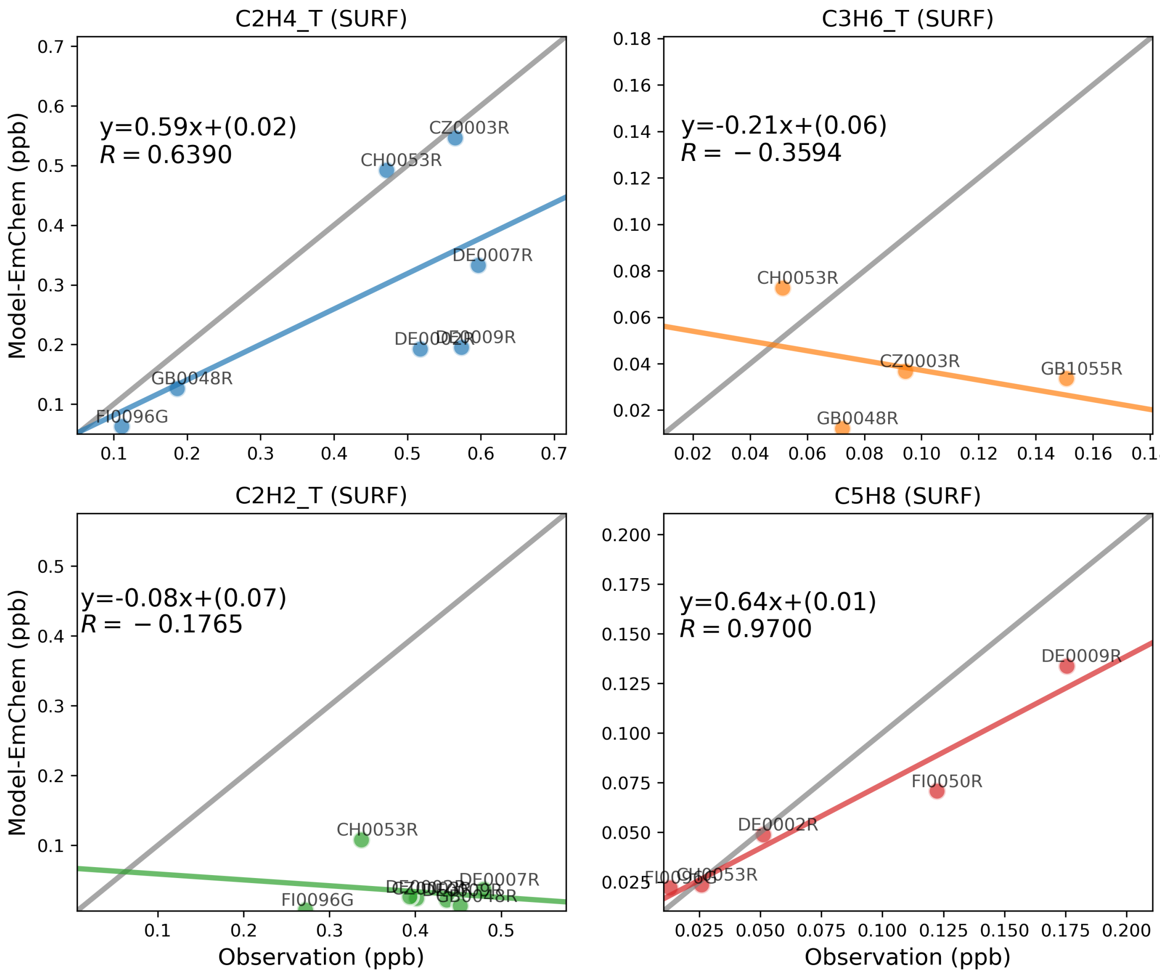

Figure 7.6: As Fig. 7.3, but for unsaturated VOC species concentrations.

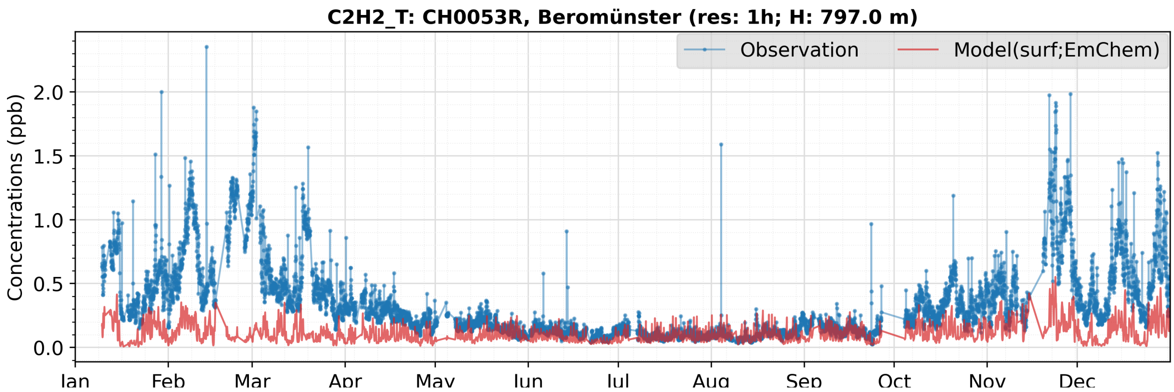

Figure 7.7: Time series of modelled and measured acetylene concentrations in ppb at the Beromünster (Switzerland) Measurements are conducted every hour. The term 'H' denotes the site altitude.

good model-measurement agreements, with correlation coefficients (R) ranging from 0.71 to 0.83. The model accurately simulates the spatial variations of benzene concentrations, exhibiting a slight underestimation of only 22% compared to the measurements. In contrast, the model significantly underestimates toluene concentrations by 51%. Despite the low concentration, the model's performance for o-xylene sits between that of benzene and toluene, ex-

Table 7.7: As Table 7.6, but for unsaturated NMVOCs.

C2H4_T	**N**	**R**	**Mean_O**	**Mean_M**	**NMB**	**NME**
Em-CEIP	7	0.61	0.432	0.275	-36%	39%
Em-CAMS	7	0.64	0.432	0.278	-36%	37%
CRI-CEIP	7	0.62	0.432	0.292	-32%	39%
CRI-CAMS	7	0.65	0.432	0.294	-32%	35%
C3H6_T	**N**	**R**	**Mean_O**	**Mean_M**	**NMB**	**NME**
Em-CEIP	4	-0.31	0.092	0.037	-59%	66%
Em-CAMS	4	-0.36	0.092	0.039	-58%	69%
CRI-CEIP	4	-0.33	0.092	0.04	-56%	66%
CRI-CAMS	4	-0.37	0.092	0.041	-55%	69%
C2H2_T	**N**	**R**	**Mean_O**	**Mean_M**	**NMB**	**NME**
Em-CEIP	7	-0.14	0.396	0.043	-89%	89%
Em-CAMS	7	-0.18	0.396	0.034	-91%	91%
CRI-CEIP	7	-0.14	0.396	0.044	-89%	89%
CRI-CAMS	7	-0.18	0.396	0.035	-91%	91%
C5H8	**N**	**R**	**Mean_O**	**Mean_M**	**NMB**	**NME**
Em-CEIP	5	0.97	0.078	0.059	-24%	28%
Em-CAMS	5	0.97	0.078	0.06	-23%	28%
CRI-CEIP	5	0.98	0.078	0.065	-16%	24%
CRI-CAMS	5	0.98	0.078	0.066	-15%	24%

hibiting both a consistent spatial variation (R = 0.80) and a moderate underestimation (NMB = 40%).

Model simulations employing different emissions and mechanisms yield slightly varied results, yet the comparison statistics remain similar for all three aromatic species, as presented in Table 7.8. Model simulations utilising CAMS emissions display slightly larger R and smaller NME for benzene compared to those using CEIP emissions. However, the impact on toluene results is inverse when emissions are altered. When comparing this to the effect of altering mechanisms, it becomes clear that the latter induces an even smaller change in the model's performance.

7.6.4 Aldehydes and dialdehydes, 2018

Comparing modelled and measured aldehyde species is complicated by the fact that the sample duration of aldehyde measurements varies across different stations. For instance, at the ES0001R station, each formaldehyde sample is taken over a 7-hour period, as evidenced by the start and end times specified in the raw data. On the other hand, the FR0013R station conducts sampling over a shorter span of 4 hours. As a result, to facilitate a fair comparison with the measured data, the hourly model output at a specific station is averaged over the corresponding sampling duration.

Figure 7.9 illustrates the comparisons for formaldehyde measurements at three distinct stations. The model successfully captures the temporal fluctuations of formaldehyde at the ES0001R and FR0015R stations through the year, and at the FR0013R station in the winter months. Generally, it tends to underestimate the peak concentrations during summer, particularly at the FR0013 and FR0015R stations. However, the overall pattern and the concentration range of the model data aligns reasonably well with the measurements, suggesting that

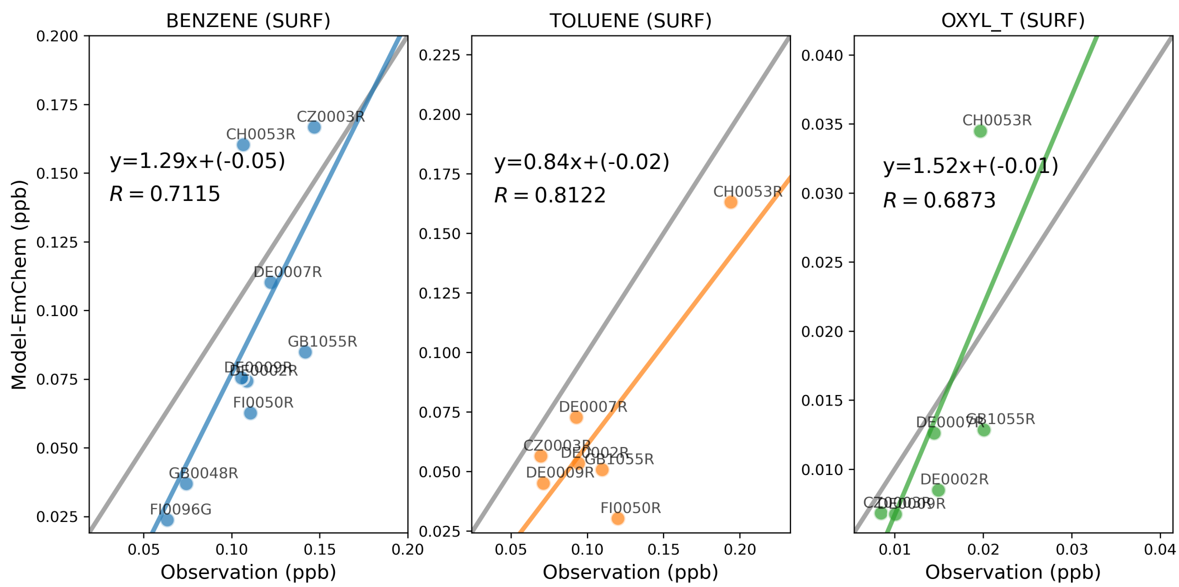

Figure 7.8: As Fig. 7.3, but for aromatic VOC species concentrations.

Table 7.8: As Table 7.6, but for aromatic NMVOCs.

Benzene	**N**	**R**	**Mean_O**	**Mean_M**	**NMB**	**NME**
Em-CEIP	9	0.69	0.109	0.093	-14%	35%
Em-CAMS	9	0.71	0.109	0.088	-19%	34%
CRI-CEIP	9	0.69	0.109	0.095	-13%	35%
CRI-CAMS	9	0.71	0.109	0.09	-18%	34%
Toluene	**N**	**R**	**Mean_O**	**Mean_M**	**NMB**	**NME**
Em-CEIP	7	0.83	0.107	0.073	-32%	32%
Em-CAMS	7	0.81	0.107	0.067	-37%	37%
CRI-CEIP	7	0.83	0.107	0.077	-29%	29%
CRI-CAMS	7	0.81	0.107	0.07	-34%	34%
O-xylene	**N**	**R**	**Mean_O**	**Mean_M**	**NMB**	**NME**
Em-CEIP	6	0.72	0.015	0.013	-10%	33%
Em-CAMS	6	0.69	0.015	0.014	-6%	40%
CRI-CEIP	6	0.71	0.015	0.014	-4%	31%
CRI-CAMS	6	0.68	0.015	0.014	-1%	39%

the chemistry (and precursor emissions) associated with formaldehyde are reasonably well-represented in the model.

Five stations offer acetaldehyde measurements. Figure 7.10 provides a comparison example for one of these stations, Beromünster. The measurements display higher concentrations during the summer, whereas the model reveals peak concentrations in the winter at all stations. Similar results were found at other sites (not shown).

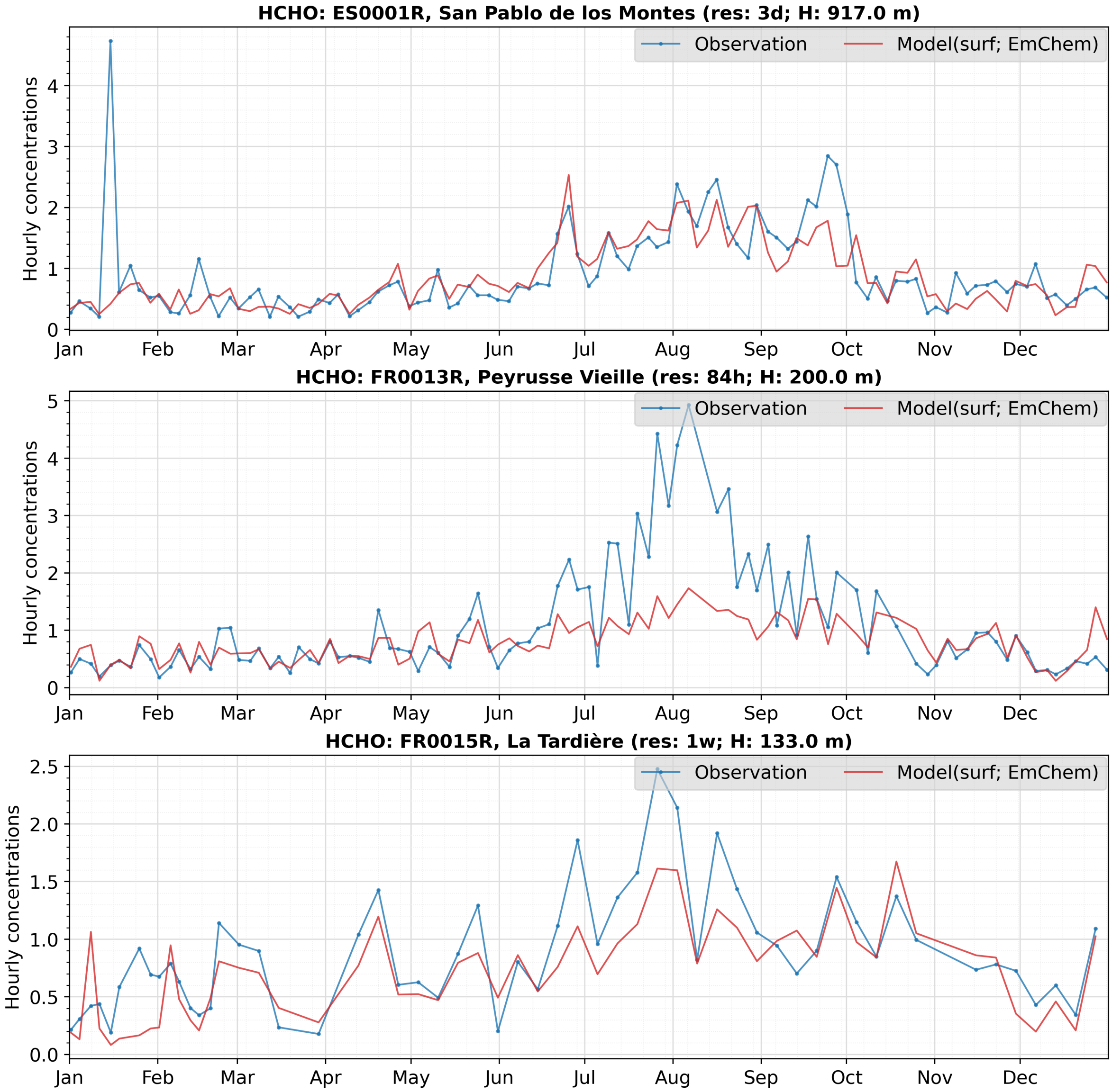

Figure 7.9: Time series of formaldehyde concentrations in ppb at three available monitoring sites in 2018. 'res:' denotes time-resolution; e.g. 'res: 3d' means that the measurements are conducted every three days (1w: one week). The term 'H' denotes the site altitude.

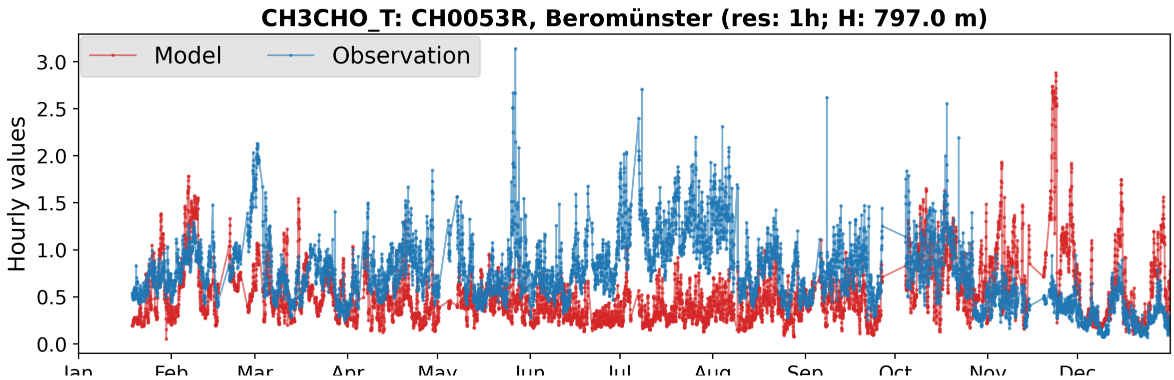

Figure 7.10: Time series of acetyldehyde concentrations in ppb at the Beromünster site in 2018.

Finally for 2018, Fig. 7.11 illustrates the model comparison for methyl glyoxal (a product of e.g. isoprene chemistry) at two French stations. The model successfully captures the summer concentration peaks at both stations. However, it overestimates the methyl glyoxal concentrations throughout the rest of the year when compared to the measurements.

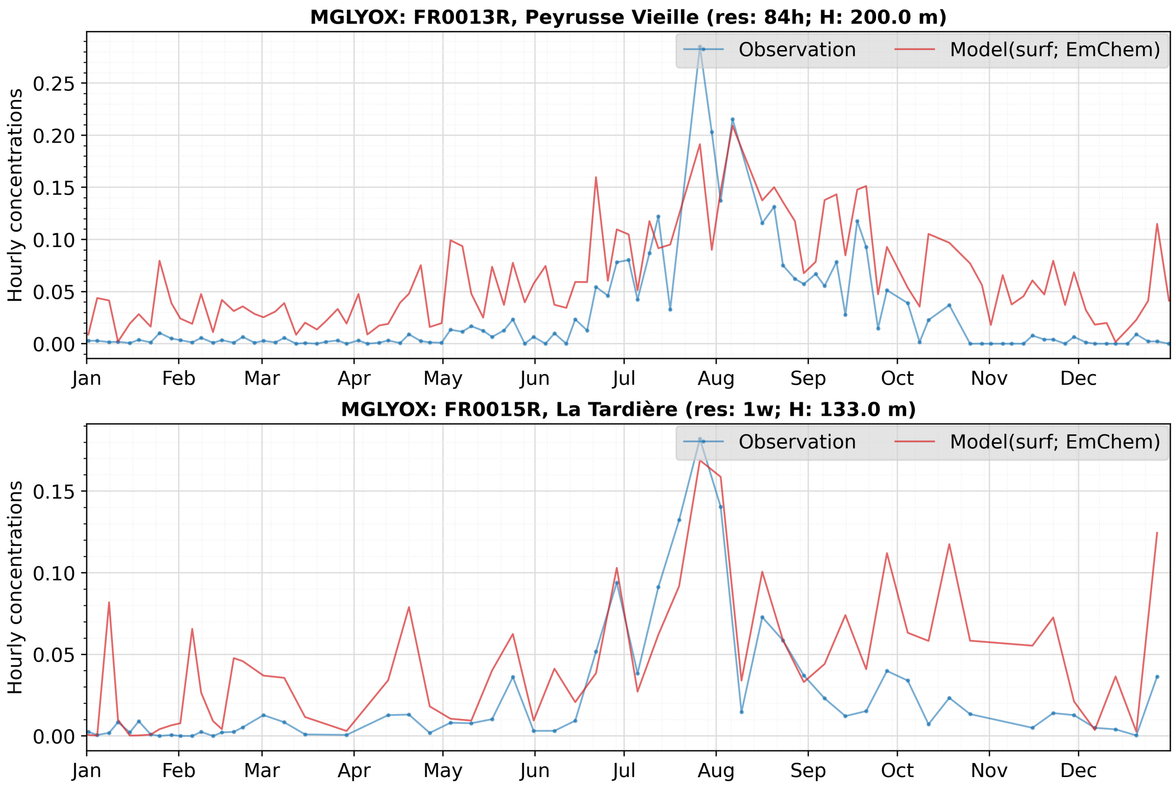

Figure 7.11: Time series of methyl glyoxal concentrations in ppb at two available monitoring sites in 2018.

7.7 Results, IMP campaign

In order to investigate the cause of high ozone episodes during the heatwaves, with a specific focus on the role of VOCs in such episodes, an EMEP intensive measurement period (IMP) of VOCs was conducted between 12-19 July 2022. Detailed information of this campaign, along with comparisons for O_3 and NO_2 from this NMVOC exercise, are presented in Ch. 6. The following sections detail the comparisons between model simulations (using the CRIv2R5Em mechanism and the CEIP emission inventory) and ambient measurements during this specific temporal frame, providing an overview of the model's performance.

The model's outputs have been selected to correspond with the native temporal resolution of the measurement data.

Given the short span of this campaign, lasting only one week, and the many uncertainties in NMVOC emission inventories discussed above, the data may not be sufficiently representative to derive any definitive conclusions from the model-measurement comparisons. However, for VOC species where hourly measurements are available, the comparison of time series between the model and the measurements at corresponding sites may yet yield valuable insights. Specifically, these comparisons can illuminate the model's performance on a high resolution temporal scale, and/or issues with the underlying emissions data.

7.7.1 Anthropogenic VOCs, IMP

Figure 7.12 shows the modelled and measured concentrations of n-butane at two stations which had hourly measurements. The modelled concentrations of n-butane agree well with the measured values in terms of temporal variations during the campaign period. Additionally, both the model and the measurements reveal higher concentrations at the urban Zürich station, (model mean $\overline{M}$: 0.863 ppb, measurement mean $\overline{O}$: 0.749 ppb; similarly, hereinafter) relative to those at the rural Beromünster station ($\overline{M}$: 0.392 ppb, $\overline{O}$: 0.212 ppb). However, the model exhibits larger concentration peaks at certain times compared to the measurements. This is consistent with the general model overestimation of n-butane, as has been noted in the long-term data presented in Sect. 7.6.1.

The time series comparisons of o-xylene at same stations are depicted in Fig.7.13. O-xylene represents one of the common aromatic species present in the atmosphere, with its primary emission sources being the Solvent and Road Transport sectors. Both the model and measurement indicate larger concentrations at the Zürich station, with an average concentration of 0.047 ppb for the model and 0.065 ppb for the measurement. In contrast, the concentrations of o-xylene at the Beromünster station are at lower levels, averaging at 0.019 ppb and 0.014 ppb for the model and measurement, respectively. The modelled time-series exhibit consistent temporal variations with the measurement in most times except for a few exceptions. At the Zürich station, the measurement shows concentration spikes at 19th and 20th of July, while the model displays pronounced peaks on the 13th and 19th of July at the Beromünster station.

As noted in Sect. 7.6.2 the model had severe problems with acetylene over the 2018 period. Figure 7.14 for this campaign period shows similar issues, with modelled concentrations being systematically smaller than the measured values. While the model successfully replicates the timing of some concentration peaks, many other peaks are missed.

In contrast to NMHCs, the measurement of oxygenated VOCs (OVOCs) is conducted on a less frequent temporal scale. The majority of OVOCs are measured only once per day,

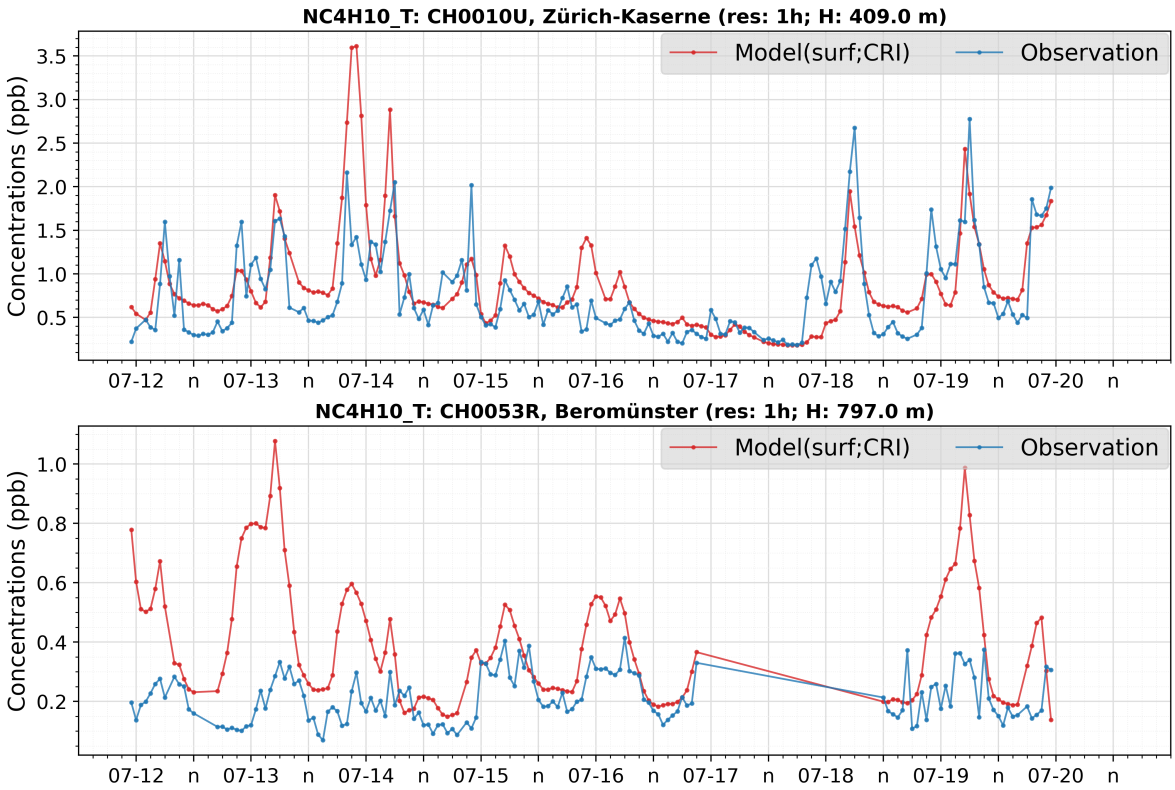

Figure 7.12: Time series comparisons of n-butane concentrations in ppb at Zürich (Switzerland) and Beromünster (Switzerland) stations, from the CRI-CEIP simulations for the IMP campaign. The term 'n' indicates 12 noon.

and at inconsistent times across different stations. Consequently, there are at most 7 data points available for a particular OVOC at a specific station, although in many instances, the availability is further reduced to 3-5 data points due to the presence of invalid measurements. To accommodate this limitation, average concentrations over the campaign period have been utilised to conduct linear correlation analyses between corresponding model and measurement data.

Figure 7.15 shows the linear correlation relationships between modelled and measured concentrations of formaldehyde and methylglyoxal, provided as representative examples. The modelled formaldehyde concentrations align reasonably well with the measured values, yielding a correlation coefficient (R) of 0.89, despite a moderate model underestimation.

The model's performance worsens in the case of methylglyoxal, showing a smaller R value of 0.48 and a larger model underestimation. Atmospheric sources of methylglyoxal are complicated and include direct emissions from primary sources (e.g., industrial emissions, vehicle exhausts, biomass burning) and secondary formations caused by the oxidation of biogenic and anthropogenic precursors (e.g., isoprene, aromatics) (Stavrakou et al. 2009, Rodigast et al. 2016, Li et al. 2022). In contrast to the model's overestimation observed in the long-term 2018 comparisons (Sect. 7.6.4), its underestimation of methylglyoxal during this campaign period likely indicates a relatively larger chemical production and/or primary emissions of this species during this specific period in reality.

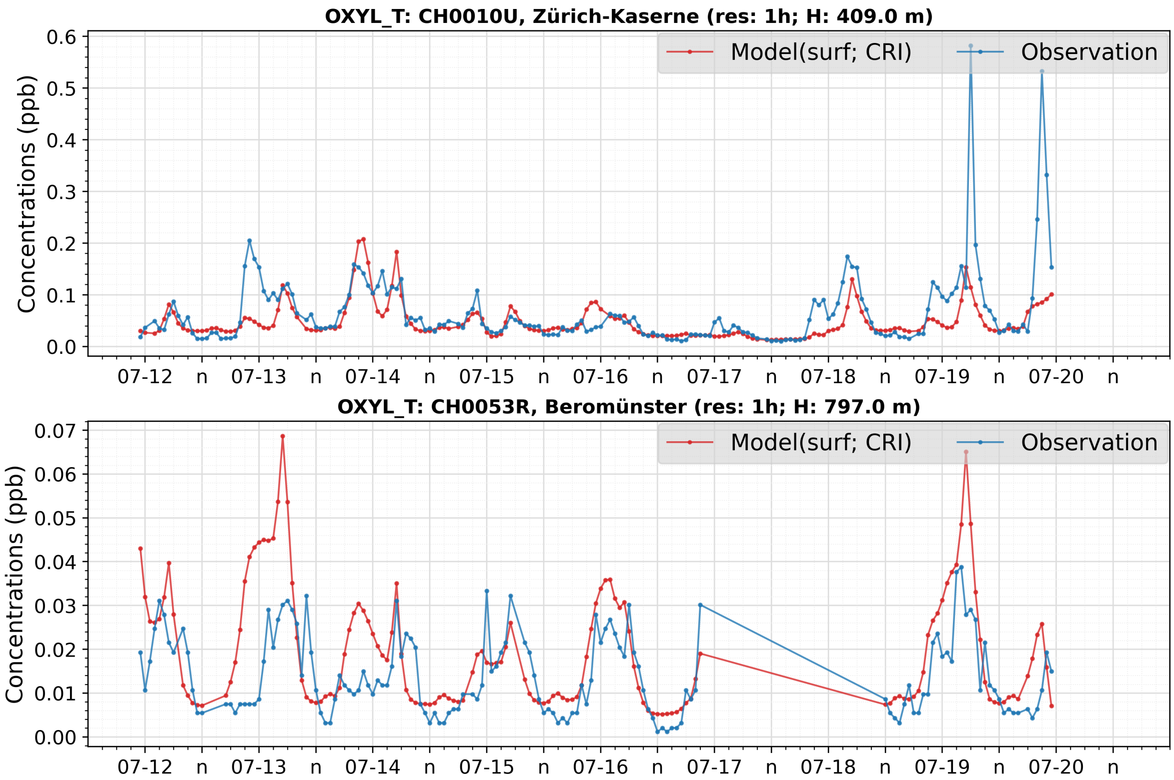

Figure 7.13: Time series comparisons of o-xylene concentrations in ppb at Zürich (Switzerland) and Beromünster (Switzerland) stations for the IMP campaign, CRI-CEIP run.

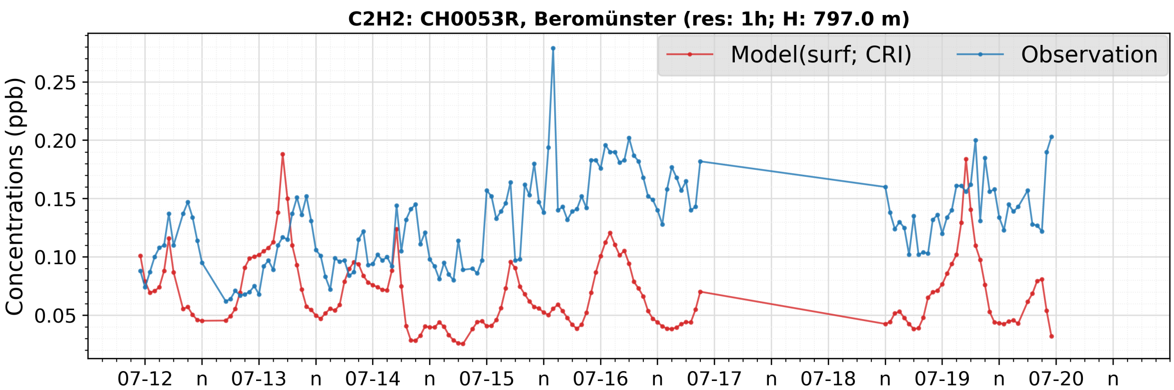

Figure 7.14: Time series comparisons of acetylene concentrations in ppb at the Beromünster station for the IMP campaign, CRI-CEIP run.

7.7.2 Isoprene

Figure 7.16 presents the time series comparisons of isoprene at the site Beromünster. The model captures the overall diurnal fluctuations and many of the concentration peaks found in the measurement data, but shows an earlier rise in C_5H_8 levels than seen in the measurements. As with the 2018 results discussed above (Sect. 7.6.2), there are many issues in modelling isoprene due to the difficulties associated with estimating the magnitude and spatial distribution of such emissions and the short life-time, but again the model seems to get the levels about right.

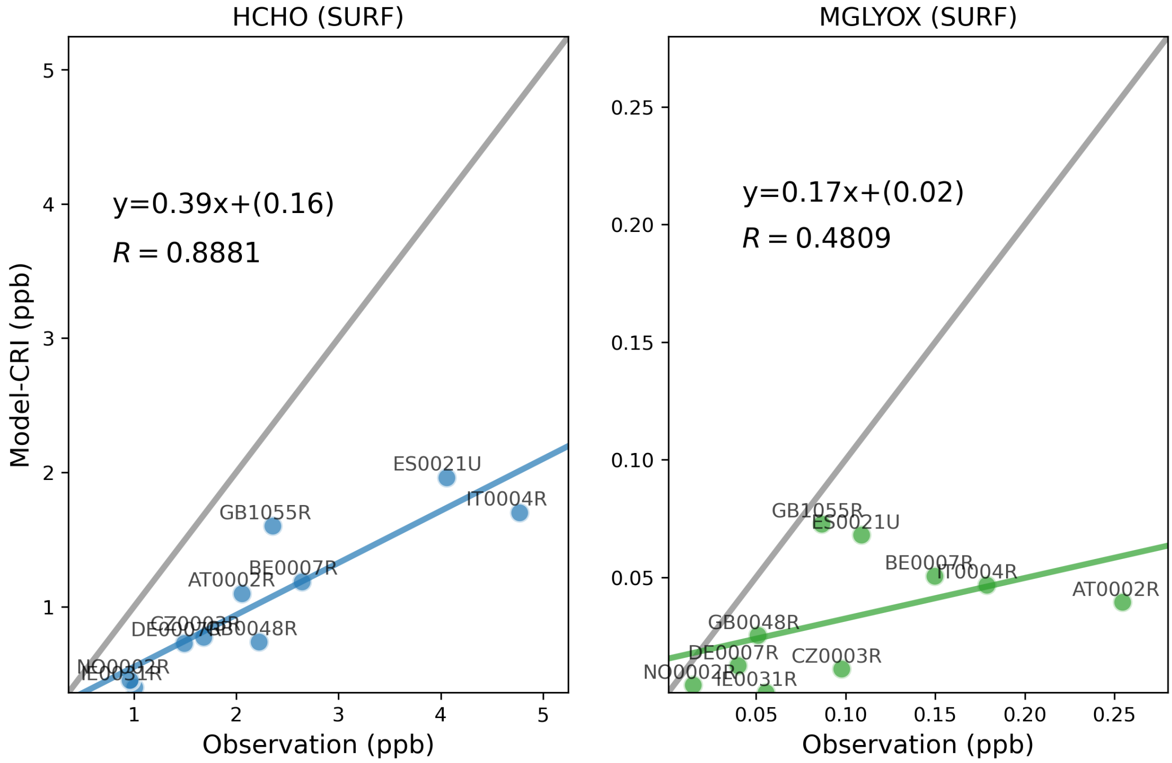

Figure 7.15: Scatter plots of average modelled and measured formaldehyde and methyl glyoxal concentrations for the IMP, from the CRI-CEIP run.

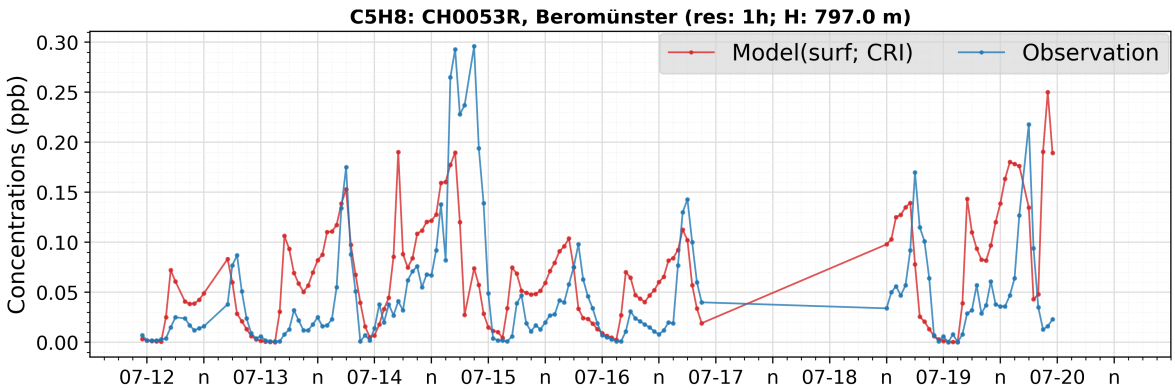

Figure 7.16: Time series comparisons of isoprene concentrations in ppb at the Beromünster site station for the IMP campaign, CRI-CEIP run.

7.8 Summary

This model evaluation study is the first intensive comparison of VOCs between the EMEP model and measurements for many years. We are keen to know how well the model's VOC concentrations and relative speciations agree with measured values. To address these research questions, a comprehensive spatial and temporal comparison of model output with VOC measurements from the EMEP/CCC network was carried out for the year 2018, and for the IMP campaign in summer 2020. Both CEIP and CAMS emission inventories were utilized, along with two different chemistry mechanisms—EmChem19rc and CRIv2R5Em. To model pure

VOC concentrations for comparison with measurement data, we have developed a detailed VOC emission speciation for all EMEP sectors based on data sourced from the UK NAEI, EEA emission inventory guidebook, and several academic studies.

The degree to which the modelled and measured VOCs agree varies depending on the specific species. For the alkane species, the model successfully captures the overall spatial variation of the annual concentrations of especially n-butane, but less so for i-butane and propane. Interestingly, the model overestimates n-butane while underestimating i-butane, which implies potential issues related to the speciation of butane emissions, the boundary conditions, or a combination of both.

As for unsaturated NMVOCs, annual concentrations of ethene and isoprene show better model-measurement linear correlations than propene and acetylene. Notably, the modelled acetylene concentrations are significantly lower than the measured values, which likely suggests an underestimated emission. Somewhat surprisingly (given the difficulties of estimating biogenic emissions), the best results were found for isoprene. All three aromatic species show strong model-measurement agreements, with correlation coefficients R at 0.71 for benzene, 0.81 for toluene, and 0.69 for o-xylene. Formaldehyde, and methyl glyoxal demonstrate reasonably good agreement between modelled and measured time series throughout the year 2018 simulations, though both are underestimated in the IMP campaign. In summary, the model seems to do a reasonable job of capturing spatial patterns of some VOC species (e.g. n-butane, aromatics, HCHO, isoprene), but performs less well for others (e.g. propane, acetylene, i-butane).

This model evaluation study indicates potential issues pertaining to certain VOC emissions and to the model setup. As noted in the introduction, this exercise and the results shown are preliminary, and the comparisons will be repeated with improved boundary conditions and after further reviews of VOC speciation. Further investigations into the VOC speciation and model experiments involving data from different years would also give a more comprehensive understanding of the model-measurement discrepancies observed in this study.

It would be beneficial to engage in further discussions with the measurement team to possibly incorporate insights from measurement data to refine the emission speciation applied in the model. Despite certain limitations in model-measurement comparisons, the detailed evaluations in this study support the use of the EMEP model for analysing the significance of different types of VOCs to ozone formation, and illustrate the benefits of the VOC data for model and emissions evaluation.

References

Andreae, M. O.: Emission of trace gases and aerosols from biomass burning – an updated assessment, Atmospheric Chemistry and Physics, 19, 8523–8546, doi:10.5194/acp-19-8523-2019, URL https://acp.copernicus.org/articles/19/8523/2019/, 2019.

Bergström, R., Hayman, G. D., Jenkin, M. E., and Simpson, D.: Update and comparison of atmospheric chemistry mechanisms for the EMEP MSC-W model system — EmChem19a, EmChem19X, CRIv2R5Em, CB6r2Em, and MCMv3.3Em, EMEP Technical Report 1/2022, The Norwegian Meteorological Institute, Oslo, Norway, 2022.

Borbon, A., Fontaine, H., Veillerot, M., Locoge, N., Galloo, J. C., and Guillermo, R.: An investigation into the traffic-related fraction of isoprene at an urban location, Atmos. Environ., 35, 3749–3760, doi:10.1016/S1352-2310(01)00170-4, 2001.

Bray, C. D., Strum, M., Simon, H., Riddick, L., Kosusko, M., Menetrez, M., Hays, M. D., and Rao, V.: An assessment of important SPECIATE profiles in the EPA emissions modeling platform and current data gaps, Atmos. Environ., 207, 93 – 104, doi:https://doi.org/10.1016/j.atmosenv.2019.03.013, URL http://www.sciencedirect.com/science/article/pii/S135223101930175X, 2019.

Dalsøren, S., Myhre, G., Hodnebrog, Ø., Myhre, C., Stohl, A., Pisso, I., Schwietzke, S., Höglund-Isaksson, L., Helmig, D., Reimann, S., Sauvage, S., Schmidbauer, N., Read, K., Carpenter, L., Lewis, A., Punjabi, S., and Wallasch, M.: Discrepancy between simulated and observed ethane and propane levels explained by underestimated fossil emissions, Nature Geoscience, 11, 178–184, doi:10.1038/s41561-018-0073-0, 2018.

Derwent, R. G. and Jenkin, M. E.: Hydrocarbons and the long-range transport of ozone and pan across Europe, Atmospheric Environment. Part A. General Topics, 25, 1661–1678, 1991.

Granier, C., Darras, S., Denier van der Gon, H., Doubalova, J., Elguindi, N., Galle, B., Gauss, M., Guevara, M., Jalkanen, J.-P., Kuenen, J., Liousse, C., Quack, B., Simpson, D., and Sindelarova, K.: The Copernicus Atmosphere Monitoring Service global and regional emissions (April 2019 version), doi:10.24380/d0bn-kx16, URL https://atmosphere.copernicus.eu/sites/default/files/2019-06/cams_emissions_general_document_apr2019_v7.pdf, 2019.

Grant, A., Yates, E. L., Simmonds, P. G., Derwent, R. G., Manning, A. J., Young, D., Shallcross, D. E., and O'Doherty, S.: A five year record of high-frequency in situ measurements of non-methane hydrocarbons at Mace Head, Ireland, Atmospheric Measurement Techniques, 4, 955–964, doi:10.5194/amt-4-955-2011, URL https://amt.copernicus.org/articles/4/955/2011/, 2011.

Guenther, A. B., Jiang, X., Heald, C. L., Sakulyanontvittaya, T., Duhl, T., Emmons, L. K., and Wang, X.: The Model of Emissions of Gases and Aerosols from Nature version 2.1 (MEGAN2.1): an extended and updated framework for modeling biogenic emissions, Geoscientific Model Dev., 5, 1471–1492, doi:10.5194/gmd-5-1471-2012, URL http://www.geosci-model-dev.net/5/1471/2012/, 2012.

Hobbs, P., Webb, J., Mottram, T., Grant, B., and Misselbrook, T.: Emissions of volatile organic compounds originating from UK livestock agriculture, Journal of the Science of Food and Agriculture, 84, 1414–1420, doi:https://doi.org/10.1002/jsfa.1810, URL https://onlinelibrary.wiley.com/doi/abs/10.1002/jsfa.1810, 2004.

Hoesly, R. M., Smith, S. J., Feng, L., Klimont, Z., Janssens-Maenhout, G., Pitkanen, T., Seibert, J. J., Vu, L., Andres, R. J., Bolt, R. M., Bond, T. C., Dawidowski, L., Kholod, N., Kurokawa, J.-I., Li, M., Liu, L., Lu, Z., Moura, M. C. P., O'Rourke, P. R., and Zhang, Q.: Historical (1750–2014) anthropogenic emissions of reactive gases and aerosols from the Community Emissions Data System (CEDS), Geoscientific Model Dev., 11, 369–408, doi:10.5194/gmd-11-369-2018, URL https://www.geosci-model-dev.net/11/369/2018/, 2018.

Hov, Ø., Sorteberg, A., Schmidbauer, N., Solberg, S., Stordal, F., Simpson, D., Lindskog, A., Areskoug, H., Pedro, O., Lätilä, H., and Heidam, N. Z.: European VOC Emission Estimates Evaluated by Measurements and Model Calculations, J. Atmos. Chem., 28, 173–193, 1997.

Huang, G., Brook, R., Crippa, M., Janssens-Maenhout, G., Schieberle, C., Dore, C., Guizzardi, D., Muntean, M., Schaaf, E., and Friedrich, R.: Speciation of anthropogenic emissions of non-methane volatile organic compounds: a global gridded data set for 1970–2012, Atmos. Chem. Physics, 17, 7683–7701, doi:10.5194/acp-17-7683-2017, URL https://acp.copernicus.org/articles/17/7683/2017/, 2017.

Jenkin, M., Derwent, R., and Wallington, T.: Photochemical ozone creation potentials for volatile organic compounds: Rationalization and estimation, Atmospheric Environment, 163, 128 – 137, doi:https://doi.org/10.1016/j.atmosenv.2017.05.024, URL http://www.sciencedirect.com/science/article/pii/S1352231017303254, 2017.

Kuenen, J., Dellaert, S., Visschedijk, A., Jalkanen, J., and Denier van der Gon, H. A. C.: CAMS -REG-v4: a state-of-the-art high-resolution European emission inventory for air quality modelling, Earth System Sci. Data., In preparation, 2021.

Li, Q., Gong, D., Wang, H., Wang, Y., Han, S., Wu, G., Deng, S., Yu, P., Wang, W., and Wang, B.: Rapid increase in atmospheric glyoxal and methylglyoxal concentrations in Lhasa, Tibetan Plateau: Potential sources and implications, Science of The Total Environment, 824, 153 782, doi:https://doi.org/10.1016/j.scitotenv.2022.153782, URL https://www.sciencedirect.com/science/article/pii/S0048969722008749, 2022.

Matthews, B. and Wankmüller, R.: Methodologies applied to the CEIP GNFR gap-filling 2021 Part I: Main Pollutants (NO_x, NMVOCs, SO_x, NH_3, CO), Particulate Matter ($PM_{2.5}$, PM_{10}, PM_{coarse}) and Black Carbon (BC) for the years 2000 to 2019., EMEP/CEIP Technical Report 2/2021, CEIP Vienna, URL https://www.ceip.at/fileadmin/inhalte/ceip/00_pdf_other/2021/main_pm_bc_gap-filling_documentation_2021_final.pdf, 2021.

Passant, N.: Speciation of UK emissions of non-methane volatile organic compounds, Report ENV-0545 ENV-0545, AEA Technology, Culham, Abingdon, United Kingdom, 2002.

Pfister, G. G., Emmons, L. K., Hess, P. G., Lamarque, J. F., Orlando, J. J., Walters, S., Guenther, A., Palmer, P. I., and Lawrence, P. J.: Contribution of isoprene to chemical budgets:

A model tracer study with the NCAR CTM MOZART-4, J. Geophys. Res., 113, D05 308, 2008.

Reimann, S., Calanca, P., and Hofer, P.: The anthropogenic contribution to isoprene concentrations in a rural atmosphere, Atmos. Environ., 34, 109 – 115, doi:10.1016/S1352-2310(99)00285-X, 2000.

Rodigast, M., Mutzel, A., Schindelka, J., and Herrmann, H.: A new source of methylglyoxal in the aqueous phase, Atmospheric Chemistry and Physics, 16, 2689–2702, doi:10.5194/acp-16-2689-2016, URL https://acp.copernicus.org/articles/16/2689/2016/, 2016.

Simpson, D., Winiwarter, W., Börjesson, G., Cinderby, S., Ferreiro, A., Guenther, A., Hewitt, C. N., Janson, R., Khalil, M. A. K., Owen, S., Pierce, T. E., Puxbaum, H., Shearer, M., Skiba, U., Steinbrecher, R., Tarrasón, L., and Öquist, M. G.: Inventorying emissions from Nature in Europe, J. Geophys. Res., 104, 8113–8152, 1999.

Simpson, D., Benedictow, A., Berge, H., Bergström, R., Emberson, L. D., Fagerli, H., Hayman, G. D., Gauss, M., Jonson, J. E., Jenkin, M. E., Nyíri, A., Richter, C., Semeena, V. S., Tsyro, S., Tuovinen, J.-P., Valdebenito, A., and Wind, P.: The EMEP MSC-W chemical transport model – technical description, Atmos. Chem. Physics, 12, 7825–7865, doi:10.5194/acp-12-7825-2012, 2012.

Simpson, D., Bergström, R., Briolat, A., Imhof, H., Johansson, J., Priestley, M., and Valdebenito, A.: GenChem v1.0 – a chemical pre-processing and testing system for atmospheric modelling, Geoscientific Model Dev., 13, 6447–6465, doi:10.5194/gmd-13-6447-2020, URL https://gmd.copernicus.org/articles/13/6447/2020/, 2020.

Solberg, S., Dye, C., Walker, S., and Simpson, D.: Long-term measurements and model calculations of formaldehyde at rural European monitoring sites, Atmos. Environ., 35, 195–207, 2001.

Solberg, S., Claude, A., Reimann, S., and Sauvage, S.: VOC measurements 2018, EMEP/CCC-Report 4/2020, Norwegian Institute for Air Research, URL projects.nilu.no/ccc/reports/cccr4-2020_VOC_2018.pdf, 2020.

Solberg, S., Claude, A., Reimann, S., Sauvage, S., and Walker, S.-E.: VOC measurements 2020, EMEP/CCC-Report 4/2022, Norwegian Institute for Air Research, URL projects.nilu.no/ccc/reports/EMEP_CCC-Report_4_2022_VOC_measurements_2020.pdf, 2022.

Stavrakou, T., Müller, J.-F., De Smedt, I., Van Roozendael, M., Kanakidou, M., Vrekoussis, M., Wittrock, F., Richter, A., and Burrows, J. P.: The continental source of glyoxal estimated by the synergistic use of spaceborne measurements and inverse modelling, Atmospheric Chemistry and Physics, 9, 8431–8446, doi:10.5194/acp-9-8431-2009, URL https://acp.copernicus.org/articles/9/8431/2009/, 2009.

Veefkind, J., Aben, I., McMullan, K., Förster, H., de Vries, J., Otter, G., Claas, J., Eskes, H., de Haan, J., Kleipool, Q., van Weele, M., Hasekamp, O., Hoogeveen, R., Landgraf, J., Snel, R., Tol, P., Ingmann, P., Voors, R., Kruizinga, B., Vink, R., Visser, H., and Levelt, P.:

TROPOMI on the ESA Sentinel-5 Precursor: A GMES mission for global observations of the atmospheric composition for climate, air quality and ozone layer applications, Remote Sensing of Environment, 120, 70–83, doi:https://doi.org/10.1016/j.rse.2011.09.027, URL https://www.sciencedirect.com/science/article/pii/S0034425712000661, the Sentinel Missions - New Opportunities for Science, 2012.

von Schneidemesser, E., McDonald, B. C., Denier van der Gon, H., Crippa, M., Guizzardi, D., Borbon, A., Dominutti, P., Huang, G., Jansens-Maenhout, G., Li, M., Ou-Yang, C.-F., Tisinai, S., and Wang, J.-L.: Comparing Urban Anthropogenic NMVOC Measurements With Representation in Emission Inventories—A Global Perspective, J. Geophys. Res., 128, e2022JD037 906, doi:https://doi.org/10.1029/2022JD037906, URL https://agupubs.onlinelibrary.wiley.com/doi/abs/10.1029/2022JD037906, e2022JD037906 2022JD037906, 2023.

Watson, L. A., Shallcross, D. E., Utembe, S. R., and Jenkin, M. E.: A Common Representative Intermediates (CRI) mechanism for VOC degradation. Part 2: Gas phase mechanism reduction, Atmos. Environ., 42, 7196–7204, doi:10.1016/j.atmosenv.2008.07.034, 2008.

Wiedinmyer, C., Kimura, Y., McDonald-Buller, E. C., Emmons, L. K., Buchholz, R. R., Tang, W., Seto, K., Joseph, M. B., Barsanti, K. C., Carlton, A. G., and Yokelson, R.: The Fire Inventory from NCAR version 2.5: an updated global fire emissions model for climate and chemistry applications, Geoscientific Model Development, 16, 3873–3891, doi:10.5194/gmd-16-3873-2023, URL https://gmd.copernicus.org/articles/16/3873/2023/, 2023.

CHAPTER 8

Updated photolysis rate calculations using Cloud-J v7.3e

Willem van Caspel

8.1 Introduction

This chapter describes the recent update to the photolysis rate calculation scheme in the EMEP model. Photolysis reactions are driven by the absorption of sunlight by molecules, and play an essential role in the production and loss mechanisms of atmospheric pollutants such as O_3, NOx, and VOCs (Mellouki et al. 2015, Sillman 1999). Important factors impacting the photolysis rates (often referred to as J-values) are the solar zenith angle, ultraviolet absorption by stratospheric O_3, and radiative scattering and absorption by cloud and aerosol particles (Real and Sartelet 2011, Voulgarakis et al. 2009). The representation of these effects is therefore an essential part of any chemical transport model.

This chapter briefly summarises the work undertaken as part of the photolysis rate update in the EMEP model; details can be found in van Caspel et al. (2023). For this work, the old tabulated photolysis rate system has been replaced by the now default Cloud-J v7.3e scheme. One major advantage over the old tabulated system is that Cloud-J incorporates the instantaneous modeled abundance of O_3, and biomass burning, sulphate, dust, and sea salt aerosols in its photolysis rate calculations. The radiative impact of clouds is also taken into account, now based on both the cloud cover and cloud liquid and ice water fields from the input meteorology. In contrast, the tabulated system used pre-calculated clear-sky values, linearly combined with photolysis rates pre-calculated for two idealized cloud-fields at 50°N based only on the meteorological cloud cover field. A brief overview the Cloud-J implementation and evaluation is provided in the following, including a description of how the model results are affected. As mentioned above, a detailed description of the old tabulated system and Cloud-J implementation and evaluation can be found in van Caspel et al. (2023) and references therein.

8.2 Implementation

The Cloud-J code is an 8-stream radiative transfer model, optimized for use in chemical transport models and earth system models (Prather 2015). The code is flexible, in that it requires only the cross-section and quantum-yield data as a function of wavelength for any particular photolysis reaction to calculate its associated J-value at model run-time. The radiative transfer code calculates the changes in the radiation spectrum as radiation is absorbed and scattered throughout the atmospheric column, which determines the flux of radiation (actinic flux) available for photolysis at any given altitude.

Absorption of UV-radiation by stratospheric O_3 strongly impacts the actinic flux available for O_3 photolysis in the troposphere. To accurately describe the absorption of UV-radiation by O_3, stratospheric O_3 observations are included in the Cloud-J calculations, for altitudes above the EMEP model top (100 hPa). To this end, monthly mean gridded (10° by 10° lat-lon) observations up to 50 km altitude from the MErged GRIdded Dataset of Ozone Profiles (MEGRIDOP) (Sofieva et al. 2021) dataset are used. The MEGRIDOP data are available between the years 2002-2021, which are also used to construct monthly climatology files. These climatologies are used by default in the EMEP Cloud-J calculations, to avoid any possible 'jumps' when performing long-term trend analysis. For example, when the trend analysis covers years outside of the range of available MEGRIDOP data. Diagnostic analysis finds that using the year to year monthly files induces surface O_3 variations on the order of 0.5-1.0 ppb over simulations with the climatological files.

Aerosol radiative scattering and absorption effects, often referred to as the aerosol direct effect, are taken into account for biomass burning, sea salt, sulphate (SO_4), and dust aerosols. The biomass burning aerosol in the EMEP model originate from the FINN2.5 fire emission inventory (Section 10.7), while the sea salt and dust aerosol are generated by the model as a function of input meteorology and land cover types. For sea salt, the aerosol mass is calculated as a function of relative humidity using the equations of Gerber (1985) for the mass median diameter and geometric standard deviation growth.

8.3 Evaluation

To ensure that Cloud-J represent an improvement over the old tabulated system, the newly calculated photolysis rates have been compared against number of observational data sets. These data comprise aerial observations from the first NASA Atmospheric Tomography (ATom-1) campaign over the Pacific Ocean (Wofsy et al. 2021), and surface observations made in Europe on the Islands of Lampedusa, Cyprus, and in Chilbolton, England. While van Caspel et al. (2023) provide a detailed description of the model to measurement comparisons, a selection of the results for the ATom-1 and Lampedusa comparisons are highlighted here.

8.3.1 ATom-1 aerial campaign

During the ATom-1 campaign in 2016, irradiance measurements made using the Charged-coupled Actinic Flux Spectroradiometer (CAFS) instrument onboard a series of 10 flights were used to construct climatological vertical profiles of measurement-derived J-O1D and J-NO_2 photolysis rates over the northern and tropical Pacific Ocean blocks. J-O1D refers to the rate of the photolysis pathway of O_3 which produces oxygen atoms in the excited O(1D)

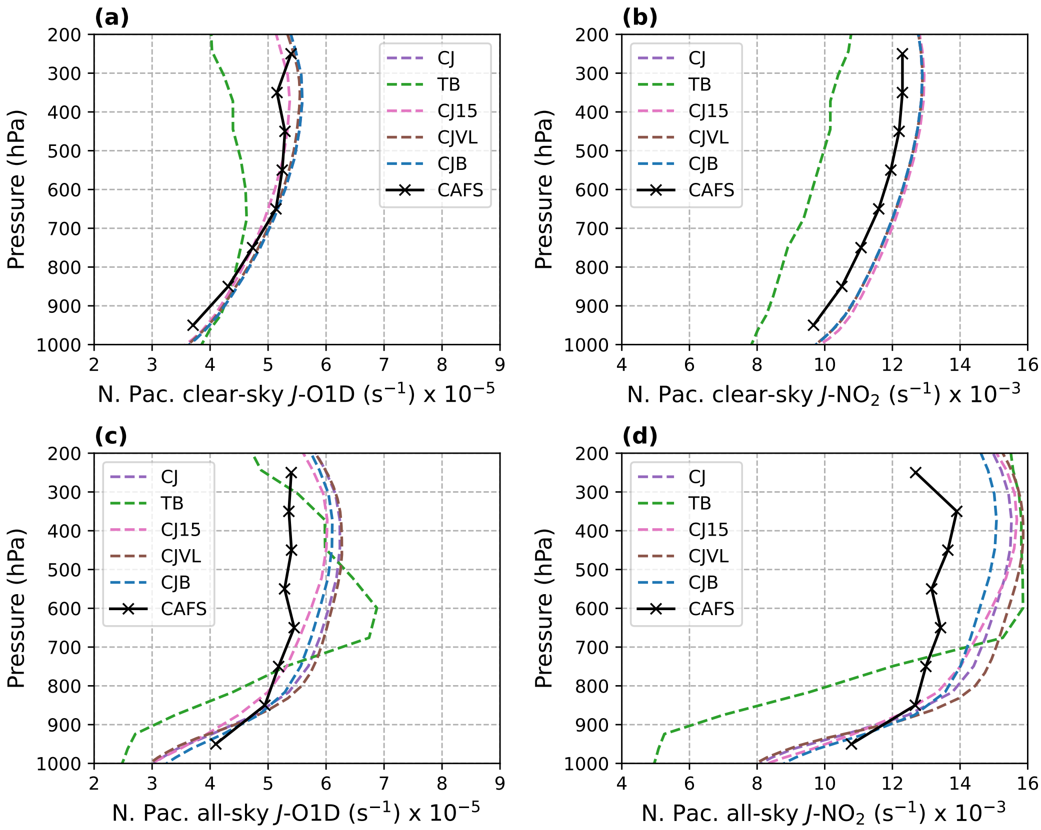

Figure 8.1: Measurement and model derived J-O1D and J-NO_2 vertical profiles over the tropical and North pacific blocks for the summer of 2016. The CAFS values are based on a series of flights from the ATom-1 campaign between the 29th of July to the 23rd of August, while the EMEP model configurations are sampled during day-time for the 16th of August. Legend labels are explained in the text. Note that the x-axis does not start at zero.

state), and J-NO_2 to the photolysis pathway producing NO and the excited O(3P) oxygen state. The J-O1D and J-NO_2 J-values together represent the most important tropospheric photolysis reaction rates. In addition to the measured all-sky values, a commensurate data set of artificially cleared clear-sky photolysis rates was also constructed. To compare simulations to observations, Hall et al. (2018) developed a methodology where a single day of hourly photolysis rate output is used to construct a 'climatology' over the geographic regions and altitude range spanned by the CAFS observations. The Hall et al. (2018) methodology was applied in van Caspel et al. (2023) to compare against photolysis rates calculated by a range of EMEP model configurations, using the 16th of August 2016 as the base-line day. Those simulations that were based on the IFS meteorology are briefly discussed here.

Fig. 8.1 shows the comparison of the observed J-values against EMEP model configurations with the Cloud-J scheme using the default setup (CJ), with a two-fold increase in the number of vertical levels (CJVL), using meteorology for the 16th of August 2015 (CJ15), and using the less computationally expensive Briegleb cloud effect scheme (CJB). The model version running with the tabulated scheme (TB) is also included. The simulation and observation results discussed here focus on the clear-sky and all-sky results for the Northern Pacific block, spanning 20-50°N and 170-225°E.

Fig. 8.1a and b show the J-O1D and J-NO_2 all-sky photolysis rates, respectively. While the Cloud-J based rates closely follow observation for all model configurations, the tabulated rates show considerable deviations. In particular, the upper tropospheric tabulated J-O1D rates are underestimated, while the J-NO_2 rates are underestimated throughout the tropospheric column. The results for the all-sky J-values show that clouds have the general tendency to increase photolysis rates in the above-cloud layer due to upward scattering of radiation, and diminish them in the below-cloud layer due to shadowing effects. This is especially pronounced for the tabulated J-NO_2 values, which are increased by a factor of 1.4-1.7 between 200-700 hPa and reduced by a factor of 0.6-0.7 below 900 hPa. The Cloud-J based all-sky profiles show closer agreement with observation, even though the impact of clouds is overestimated in the middle and upper troposphere. The largest variations between the different model configurations occur for the CJVL and CJB all-sky rates. These differences are nevertheless small compared to the difference with the tabulated scheme, with the latter clearly overestimating the radiative impact of clouds. We note that van Caspel et al. (2023) also include ATom-1 comparisons against EMEP model configurations running with meteorology from the Weather Research and Forecast model (WRF) version 4.4.2.

8.3.2 Lampedusa surface observations

Fig. 8.2 shows the model to measurement comparison for hourly J-O1D and J-NO_2 values at the Lampedusa site between day-of-year (DOY) 160-167 for 2014. The Lampedusa measurements were made as part of the ChArMEx 2013 campaign (Mallet et al. 2016). Since the instrument used to measure the irradiance used a 2-π quartz dome placed at the surface, the measurement-derived photolysis rates represent only the contribution from the downward surface actinic flux. That is, radiation reflected by Earth's surface does not contribute to 'surface' photolysis rates. In the EMEP model, however, this surface reflection component is normally considered in the surface photolysis rate calculations. To closer match the EMEP model with the observational setup, the EMEP-A_0 configuration uses Cloud-J with the surface albedo set to zero, eliminating the surface reflection component.

From the highly repeatable diurnal cycles shown in Fig. 8.2, it becomes apparent that the prevailing meteorological conditions were clear-sky during this period. Focusing first on the Cloud-J based simulations, Fig. 8.2 shows that the EMEP-A_0 results are in close agreement with observation. Furthermore, the EMEP-CJ simulation shows that the surface reflection increases the total surface photolysis rate by about 15%. Since the surface albedo can not be set to zero in the tabulated scheme, the EMEP-TB simulation is most directly comparable to EMEP-CJ. For J-O1D the tabulated scheme clearly overestimates the measured rates. For J-NO_2, however, the EMEP-TB rates closely match observation. But since EMEP-TB includes the effect of surface reflected radiation, the photolysis based on the downward actinic flux component is in fact underestimated.

8.4 Model Results

The results discussed here are derived for Europe using global EMEP model simulations. Since the global simulations do not use boundary conditions, the impact of the photolysis rate update on regional simulations may be smaller. Nevertheless, as discussed in van Caspel et al. (2023), the simulated surface pollutants generally impacted most strongly by the photolysis rate update are NO_2 and O_3. Broadly speaking, in global EMEP-CJ simulations surface NO_2

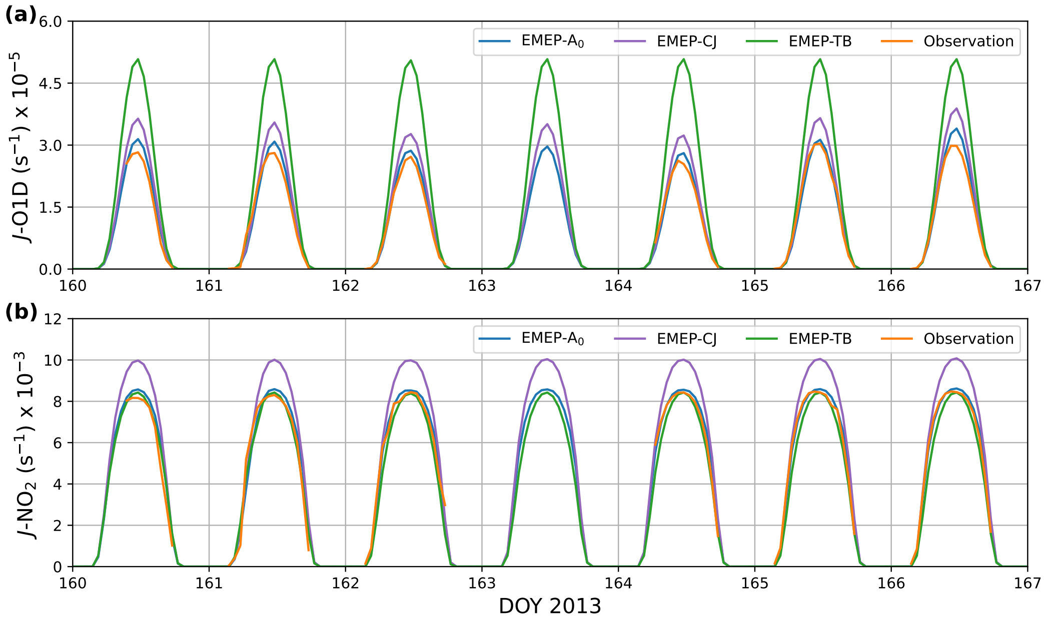

Figure 8.2: Hourly mean J-O1D **(a)** and J-NO_2 **(b)** photolysis rates observed at the Lampedusa site and simulated by EMEP-CJ and EMEP-TB model configurations between DOY 160 and 167 for the year 2013. The EMEP-A_0 simulation includes only the contribution from the downwelling surface actinic flux.

concentrations are reduced by around 10%, while O_3 concentrations are increased by around 10%. However, as shown in the comparison against EBAS for stations across Europe in Table 8.1, the impact of Cloud-J is strongest during spring (March-April-May). During spring, the NO_2 bias changes from -7.1% in EMEP-TB to -19.6%, while the bias of O_3 changes from -4.4% to 6.6%. During summer (June-July-August), the correlation coefficients are considerably increased, with the exception of NO_2. We note that the results shown in Table 8.1 are nearly independent of running Cloud-J with a comparatively cheap cloud effect scheme (Briegleb averaging), in combination with hourly rather than instantaneous photolysis rate updates. With this less computationally expensive approach, the NMB values shown in Table 8.1 change by no more than 0.8%, while the correlation coefficient is only changed by +0.01 for O_3max in summer (van Caspel et al. 2023, supplementary material). With the model time-step and more expensive cloud effect scheme calculations, the EMEP model run-time is increased by $\sim$250%, while in the less expensive configuration this is at most 10%.

To highlight the impact of Cloud-J on the spatial distribution of O_3, the change in the bias of the commonly used metric of daily maximum concentrations (O_3max) is shown in Fig. 8.3. In this figure, the absolute change in the bias (%) is shown for the annual mean simulated O_3max, relative to surface measurement across Europe from the EBAS data base. The general increase in the bias error along the western coast of Europe, together with the general tendency for EMEP-TB to already have a positive bias there, indicate that the overestimation of the inflow of O_3 across the Atlantic Ocean by the surface Westerlies is further increased. However, the bias is considerably improved (10-20% bias reduction) over large parts of Central Europe.

Following the approach of Bian et al. (2003), the change in O_3 concentrations at 250 and 2800 meters altitude in January and July due to aerosol scattering and absorption, is used as a marker for the aerosol direct effect. The impact of aerosols is calculated by running a control

Table 8.1: NMB (%) and correlation coefficients for EMEP-CJ and EMEP-TB (brackets) against surface observations from the EBAS database in Europe. Statistics are based on daily values, and are shown for the four seasons as well as for the yearly average.

Species [ppb]	Stats	DJF	MAM	JJA	SON	Yearly
O_3max	NMB	2.4 (-8.7)	6.0 (-6.2)	0.0 (-10.2)	7.9 (-6.6)	3.9 (-7.9)
	r	0.58 (0.60)	0.62 (0.62)	0.79 (0.77)	0.80 (0.79)	0.80 (0.79)
O_3	NMB	5.3 (-7.7)	10.4 (-3.0)	6.6 (-4.4)	15.0 (-0.9)	9.2 (-3.9)
	r	0.64 (0.65)	0.54 (0.56)	0.73 (0.70)	0.72 (0.73)	0.74 (0.74)
NO_2	NMB	3.5 (12.2)	-19.6 (-7.1)	-14.4 (-3.4)	-11.8 (-2.4)	-9.8 (0.4)
	r	0.63 (0.64)	0.68 (0.69)	0.62 (0.63)	0.72 (0.73)	0.67 (0.68)
CO	NMB	-9.5 (-3.4)	-8.8 (3.4)	-9.4 (4.0)	-4.7 (3.3)	-8.1 (1.5)
	r	0.64 (0.64)	0.67 (0.64)	0.72 (0.71)	0.72 (0.72)	0.70 (0.70)

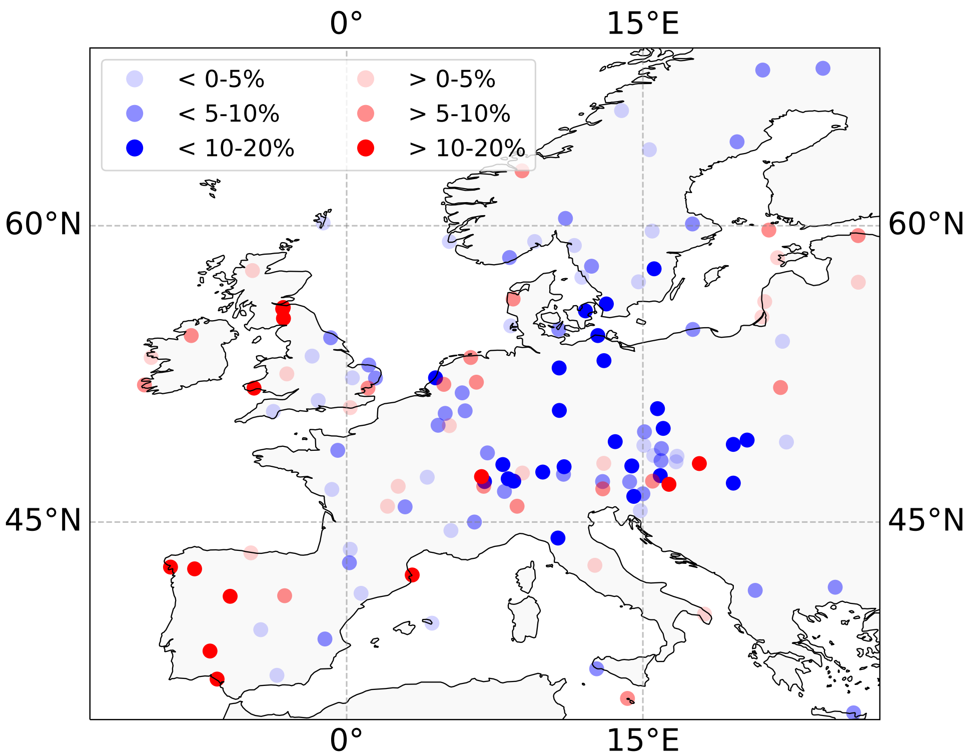

Figure 8.3: Difference in the absolute yearly mean O_3max NMB (%) between the EMEP-CJ and EMEP-TB simulations relative to surface observations from the EBAS database. Blue dots indicate that the average simulated value is closer to observation in EMEP-CJ than in EMEP-TB, and vice versa for the red dots.

EMEP-CJ simulation without aerosol radiative effects included, with the difference between the control run and the EMEP-CJ with aerosol effects included being shown in Fig. 8.4. The O_3 perturbation due to aerosols is largest over the tropical biomass burning regions, reducing O_3 concentrations by as much as 12-16 ppb over central Africa in July. The impact of sea-salt and dust impact is less than 1-2 ppb, indicating that their radiative effects are of secondary importance. Note that this refers to the radiative impact on the photolysis rates, and not necessarily on the energy budget of the atmosphere. Also note that the results of Fig. 8.4 are

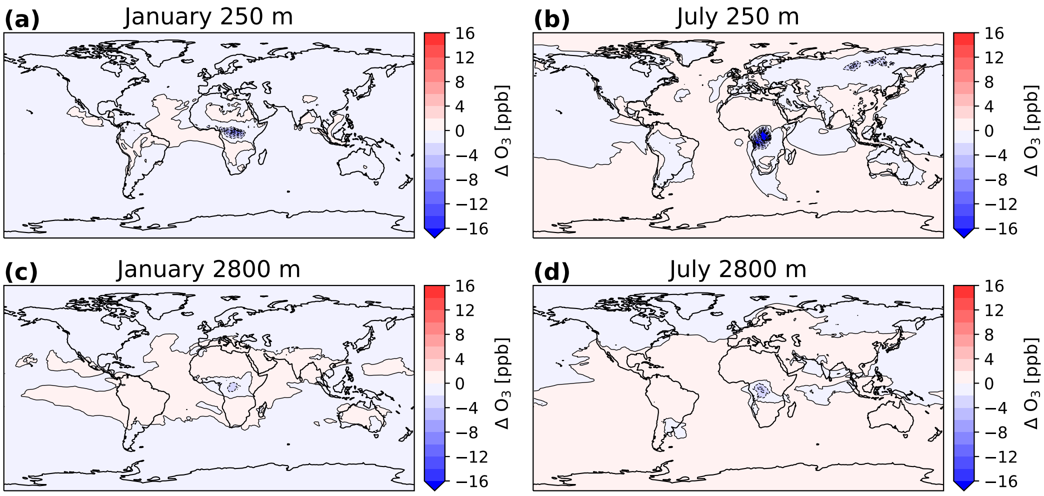

Figure 8.4: Change in monthly mean O_3 concentrations at 250 and 2800 meters altitude in January **(a,b)** and July **(c,d)** 2018 due to aerosol radiative effects.

based on a simulation for the year 2018. Spatial patterns in the impact of biomass burning may therefore be different for other years, depending on where large scale wild fire events occur.

8.5 Conclusion

The aim of this study was to update the old tabulated photolysis rate system, which overestimated the radiative impact of clouds and was not designed for use for latitudes between 30°S-30°N. By using Cloud-J, photolysis rates are now calculated on a global scale at model runtime, incorporating the instantaneous radiative effects of aerosol and O_3 variations. Cloud-J is found to perform favourably in comparison against a range of observations, while also being comparatively insensitive to the EMEP model spatial resolution and choice of cloud effect scheme. The use of Cloud-J leads to a general increase in the model performance to predict O_3 and CO, while simulated NO_2 concentrations are worsened. The general tendency for O_3 concentrations to be increased while NO_2 is decreased, is indicative of a shift of Ox (=O_3 + NO_2) towards the O_3 component. The use of Cloud-J is now used by default in the EMEP model, configured with the Briegleb averaging cloud scheme together with hourly photolysis rate updates. In this configuration, the use of Cloud-J slows down the EMEP model by no more than 10%. Additional practical information about running the EMEP model with Cloud-J is given in Section 10.2.

References

Bian, H., Prather, M. J., and Takemura, T.: Tropospheric aerosol impacts on trace gas budgets through photolysis, Journal of Geophysical Research: Atmospheres, 108, doi:doi.org/10.1029/2002JD002743, 2003.

Gerber, H. E.: Relative-Humidity Parameterization of the Navy Aerosol Model (NAM), NRL Report 8956, Naval Research Laboratory, Washington, DC, 1985.

Hall, S. R., Ullmann, K., Prather, M. J., Flynn, C. M., Murray, L. T., Fiore, A. M., Correa, G., Strode, S. A., Steenrod, S. D., Lamarque, J.-F., Guth, J., Josse, B., Flemming, J., Huijnen, V., Abraham, N. L., and Archibald, A. T.: Cloud impacts on photochemistry: building a climatology of photolysis rates from the Atmospheric Tomography mission, Atmospheric Chemistry and Physics, 18, 16 809–16 828, doi:10.5194/acp-18-16809-2018, 2018.

Mallet, M., Dulac, F., Formenti, P., Nabat, P., Sciare, J., Roberts, G., Pelon, J., Ancellet, G., Tanré, D., Parol, F., Denjean, C., Brogniez, G., di Sarra, A., Alados-Arboledas, L., Arndt, J., Auriol, F., Blarel, L., Bourrianne, T., Chazette, P., Chevaillier, S., Claeys, M., D'Anna, B., Derimian, Y., Desboeufs, K., Di Iorio, T., Doussin, J.-F., Durand, P., Féron, A., Freney, E., Gaimoz, C., Goloub, P., Gómez-Amo, J. L., Granados-Muñoz, M. J., Grand, N., Hamonou, E., Jankowiak, I., Jeannot, M., Léon, J.-F., Maillé, M., Mailler, S., Meloni, D., Menut, L., Momboisse, G., Nicolas, J., Podvin, T., Pont, V., Rea, G., Renard, J.-B., Roblou, L., Schepanski, K., Schwarzenboeck, A., Sellegri, K., Sicard, M., Solmon, F., Somot, S., Torres, B., Totems, J., Triquet, S., Verdier, N., Verwaerde, C., Waquet, F., Wenger, J., and Zapf, P.: Overview of the Chemistry-Aerosol Mediterranean Experiment/Aerosol Direct Radiative Forcing on the Mediterranean Climate (ChArMEx/ADRIMED) summer 2013 campaign, Atmospheric Chemistry and Physics, 16, 455–504, doi:10.5194/acp-16-455-2016, 2016.

Mellouki, A., Wallington, T., and Chen, J.: Atmospheric chemistry of oxygenated volatile organic compounds: impacts on air quality and climate, Chemical reviews, 115, 3984–4014, doi:10.1021/cr500549n, 2015.

Prather, M. J.: Photolysis rates in correlated overlapping cloud fields: Cloud-J 7.3c, Geoscientific Model Development, 8, 2587–2595, doi:10.5194/gmd-8-2587-2015, 2015.

Real, E. and Sartelet, K.: Modeling of photolysis rates over Europe: impact on chemical gaseous species and aerosols, Atmospheric Chemistry and Physics, 11, 1711–1727, doi:10.5194/acp-11-1711-2011, 2011.

Sillman, S.: The relation between ozone, NOx and hydrocarbons in urban and polluted rural environments, Atmospheric Environment, 33, 1821–1845, doi:10.1016/S1352-2310(98)00345-8, 1999.

Sofieva, V. F., Szeląg, M., Tamminen, J., Kyrölä, E., Degenstein, D., Roth, C., Zawada, D., Rozanov, A., Arosio, C., Burrows, J. P., Weber, M., Laeng, A., Stiller, G. P., von Clarmann, T., Froidevaux, L., Livesey, N., van Roozendael, M., and Retscher, C.: Measurement report: regional trends of stratospheric ozone evaluated using the MErged GRIdded Dataset of Ozone Profiles (MEGRIDOP), Atmospheric Chemistry and Physics, 21, 6707–6720, doi:10.5194/acp-21-6707-2021, 2021.

van Caspel, W. E., Simpson, D., Jonson, J. E., Benedictow, A. M. K., Ge, Y., di Sarra, A., Pace, G., Vieno, M., Walker, H., and Heal, M.: Implementation and evaluation of updated photolysis rates in the EMEP MSC-W chemical transport model using Cloud-J v7.3e, Geophysical Model Development, 2023.

Voulgarakis, A., Wild, O., Savage, N. H., Carver, G. D., and Pyle, J. A.: Clouds, photolysis and regional tropospheric ozone budgets, Atmospheric Chemistry and Physics, 9, 8235–8246, doi:10.5194/acp-9-8235-2009, URL `acp.copernicus.org/articles/9/8235/2009/`, 2009.

Wofsy, S., Afshar, S., Allen, H., Apel, E., Asher, E., Barletta, B., Bent, J., Bian, H., Biggs, B., Blake, D., Blake, N., Bourgeois, I., Brock, C., Brune, W., Budney, J., Bui, T., Butler, A., Campuzano-Jost, P., Chang, C., Chin, M., Commane, R., Correa, G., Crounse, J., Cullis, P. D., Daube, B., Day, D., Dean-Day, J., Dibb, J., DiGangi, J., Diskin, G., Dollner, M., Elkins, J., Erdesz, F., Fiore, A., Flynn, C., Froyd, K., Gesler, D., Hall, S., Hanisco, T., Hannun, R., Hills, A., Hintsa, E., Hoffman, A., Hornbrook, R., Huey, L., Hughes, S., Jimenez, J., Johnson, B., Katich, J., Keeling, R., Kim, M., Kupc, A., Lait, L., McKain, K., Mclaughlin, R., Meinardi, S., Miller, D., Montzka, S., Moore, F., Morgan, E., Murphy, D., Murray, L., Nault, B., Neuman, J., Newman, P., Nicely, J., Pan, X., Paplawsky, W., Peischl, J., Prather, M., Price, D., Ray, E., Reeves, J., Richardson, M., Rollins, A., Rosenlof, K., Ryerson, T., Scheuer, E., Schill, G., Schroder, J., Schwarz, J., St.Clair, J., Steenrod, S., Stephens, B., Strode, S., Sweeney, C., Tanner, D., Teng, A., Thames, A., Thompson, C., Ullmann, K., Veres, P., Wagner, N., Watt, A., Weber, R., Weinzierl, B., Wennberg, P., Williamson, C., Wilson, J., Wolfe, G., Woods, C., Zeng, L., and Vieznor, N.: ATom: Merged Atmospheric Chemistry, Trace Gases, and Aerosols, Version 2, doi:10.3334/ORNLDAAC/1925, 2021.

CHAPTER 9

The effects of wildfires

Jan Eiof Jonson

9.1 Introduction

Wildfires, hereafter fires, are an important source of air pollution globally, and also in Europe. In the European Union and its neighbour countries, over 5 500 km^2 of land were burned in 2021 – more than twice the size of Luxembourg, with over 1 000 km^2 within protected areas of Europe's Natura 2000 network, the EU's reservoirs of biodiversity (San-Miguel-Ayanz et al. 2022). The term "wildfires" may actually be misleading, given that in the same report it is estimated that that around 96% of wildfires, at least in the European Union, are caused by human actions. Furthermore, there is an unprecedented increasing trend in not only the number of fires, but also the expansion of the affected areas and the duration of the fire season. The increasing trend is observed not only in Europe, Middle East and North Africa, but in many regions across the globe, e.g. California, Australia, South America, etc. (San-Miguel-Ayanz et al. 2022). This is despite a slight downward trend in total burned area globally. The global decrease in burned area is mostly driven by less fires in savannahs and grasslands, mainly in Africa, outweighing the increase in burned area seen in other parts of the world (Jones et al. 2022).

9.2 Fire emission datasets

The emissions from fires are included in the EMEP model calculations. As of v5.0, used for this report, the default fire inventory is the FINN2.5 emissions (Sect. 9.2.1), but there are also options for including fire emissions from GFAS (Sect. 9.2.2) and the older FINN1.5 (Wiedinmyer et al. 2011) dataset.

9.2.1 FINN2.5

The FINN2.5 fire emission data are freely available from NCAR (https://rda.ucar.edu/datasets/ds312.9/), as described by Wiedinmyer et al. (2023). Data for a full calendar year are usually made available the following summer, so that fire emission data for 2021 were available, whereas 2022 data were not yet available at the time of writing this report. The generation of the FINNv2.5 dataset starts by determining the burned area due to active fires from daily satellite detections using MODIS (nominal 1 km^2 resolution). FINN2.5 datasets using MODIS (hereafter FINN2.5mod) are available from year 2002. In the same resolution FINN2.5 also offer an additional fire emission dataset using also observations from VIIRS (the Visible Infrared Imaging Radiometer Suite onboard of Suomi NPP and NOAA-20 satellites) (hereafter FINN2.5modvrs). The advantage of adding VIIRS data is that this product better captures small fires. The EMEP model can use either FINN2.5mod or FINN2.5modvrs, with the former used by default (especially for trend runs) since the VIIRS data are only available from year 2012.

9.2.2 GFAS

The GFAS fire emissions are described in Rémy et al. (2017). These emissions are derived from the observations of Fire Radiative Power (FRP) from the MODIS instrument on board the National Aeronautics and Space Administration (NASA) Terra and Aqua satellites. The generation of the data is described in Rémy et al. (2017) and references therein. The GFAS emission inventory covers the period from 1 January 2003 to the present (2021). It has been extended to early 2000 using bias-corrected observations from MODIS on board Terra only. The output from GFAS is regularly validated in the framework of the CAMS project (https://atmosphere.copernicus.eu/).

Table 9.1: Number of fire days and emissions of some key species summed up globally and over the EMEP model domain as defined in chapter 1.3. The daily number of fire days summed up over the 0.1 × 0.1 degrees grid for year 2021.

	Global			EMEP		
	FINN2.5		GFAS	FINN2.5		GFAS
	mod	modvrs		mod	modvrs	
Nr. fire days†	24.60	59.91	23.57	0.70	2.95	1.32
	Emissions in Gg					
CO (as CO)	244038	617719	362376	7263	20977	15557
NO (as NO)	3758	9524		146	424	
NO_2 (as NO_2)	9266	23328	9247*	268	780	290‡
$PM_{2.5}$	27094	68613	29013	744	2140	1039

† *Devided by 10^5*
‡ *NO_x as NO_2*

9.2.3 Comparison of the emission datasets

As noted above, the FINN2.5 "mod" data-set is the default option for the EMEP model. Even though the "modvrs" data-set including the VIIRS data represents a clear improvement, it is available for only last 10 years, therefore the MODIS only data-set is used in model trend simulations and for consistency also in the status run for this report. The GFAS fire emissions are not used in this report, but are used in forecast mode as used within CAMS `https://regional.atmosphere.copernicus.eu/`. At first sight, the location of the fires are similar in FINN2.5mod, FINN2.5modvrs and GFAS, see Figure 9.1. However, there are substantial differences between the datasets when it comes to both the number of fires and emitted mass. Table 9.1 lists the number of fire days and the mass of key species emitted for FINN2.5mod, FINN2.5modvrs and GFAS, both globally and within the EMEP model domain (c.f. Sect. 1.3) for the year 2021.

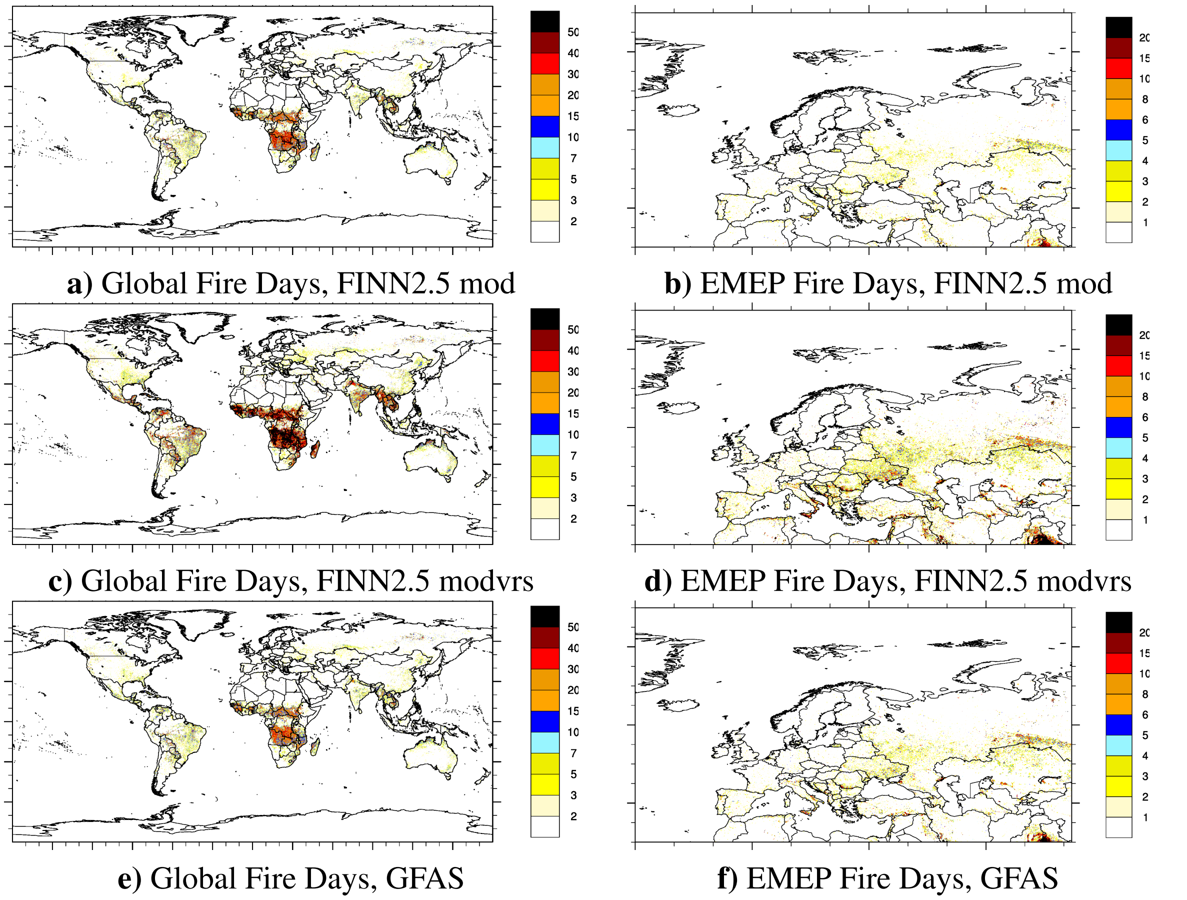

a) Global Fire Days, FINN2.5 mod **b)** EMEP Fire Days, FINN2.5 mod

c) Global Fire Days, FINN2.5 modvrs **d)** EMEP Fire Days, FINN2.5 modvrs

e) Global Fire Days, GFAS **f)** EMEP Fire Days, GFAS

Figure 9.1: Number of fire emission days in the year 2021, summed up over the $0.1^\circ \times 0.1^\circ$ grid: global (left panels) and within the EMEP domain as defined in chapter 1.3. (right panels). The top two panels show the fire counts from FINN2.5mod, the middle panels from FINN2.5modvrs, and the bottom panels the fire counts from GFAS.

The number of fires are summed up over the 0.1×0.1 degrees grid for a full year. Globally the number of fire days is about a factor of 2.4 higher in the FINN2.5modvrs compared to FINN2.5mod, and more than a factor of 4 higher within the EMEP model domain. Compared to the global domain, the large difference between FINN2.5mod versus FINN2.5modvrs in the EMEP domain is probably caused by a relatively larger number of small fires that are not detected by MODIS (see 9.2.1). Globally the difference in emitted mass between FINN2.5modvrs and FINN2.5mod is about the same as for the number of fire days (about a factor of 2.5), In the EMEP domain this factor is only marginally larger than in the global domain (2.8), suggesting that in this region the much larger number of small fires in FINN2.5modvrs do not contribute a lot to the total emitted mass.

Globally, the number of fires in GFAS is similar to FINN2.5mod, whereas in the EMEP domain the number in GFAS is about half way between FINN2.5mod and FINN2.5modvrs. In GFAS the emitted mass is larger than FINN2.5mod, but smaller than in FINN2.5modvrs both globally and within the EMEP model domain.

9.3 Vertical dispersion of wildfire emissions

Information on emission injection heights is available in different forms, depending on the emission data source. For FINN2.5 emission, monthly averaged injection height profiles are available, but only for a limited number of years (Val Martin and Toska 2018). The GFAS data (Sect. 9.2.2) includes daily information on injection heights, and also FRP (Fire Radiative Power) that can be used for the calculation of fire injection heights. However in GFAS, about two thirds of the recorded fires emit only at the surface. Furthermore, a large portion of the material emitted from the remaining fires is injected within the boundary layer.

Although the number of fires injecting material into the free troposphere is low, it will potentially affect a larger area, but when GFAS FRP data are plotted against emission height, there is little or no correlation between FRP and emission height; it is clearly difficult to reproduce such high injection height events. In order to determine the injection height FRP must be supplemented by additional information such as type of material burned and meteorological parameters. Unfortunately FRP is included in the GFAS data, but not in FINN2.5.

In previous versions of the EMEP model, emissions were distributed vertically up to 800 hPa (ca. 2 km), but given the above findings, a new system was introduced for v5.0. In the new system, emissions from fires are distributed evenly within the boundary layer, up to the mixing height. Model tests have shown that this change had only marginal effects on model results, but the new system should better represent the dispersion in the majority of cases.

9.4 Model calculations

EMEP model calculations have been made on the EMEP grid using both FINN2.5mod and FINN2.5modvrs. In addition, a model run has been made excluding fire emissions. Figure 9.2 shows the differences in annual levels of MDmaxO3 (see section 1.2) and $PM_{2.5}$ levels calculated with and without fire emissions. For both FINN2.5mod and FINN2.5modvrs, the largest difference in MDmaxO3 and $PM_{2.5}$ levels are calculated in the eastern parts of the model domain, including parts of Russia and Kazakhstan. However for large parts of Europe, the calculated effects of fire emissions are small to moderate. The exception is the northeastern parts of the Mediterranean region, where the calculated effects of fire emissions are large (Figure 9.2b) for calculations using FINN2.5modvrs, but much smaller for the calculations using FINN2.5mod.

9.4.1 Two European fire episodes in 2021

There were several wildfires in Europe in 2021. Two of the most prominent fires this year occurred in southern Italy and in central Spain.

A substantial portion of the fire emissions in southern Italy occurred in late July to mid August. The extensive fires in this period are described in San-Miguel-Ayanz et al. (2022). Similar to Figure 9.2, Figure 9.3 shows the difference in pollutant concentrations for August

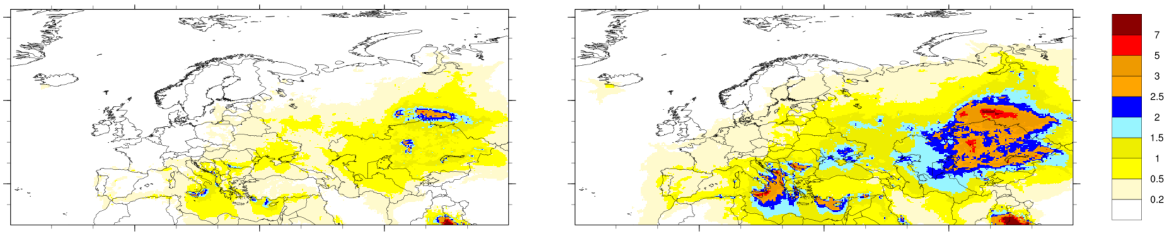

a) DMaxO3, FINN2.5mod **b)** DMaxO3, FINN2.5modvrs

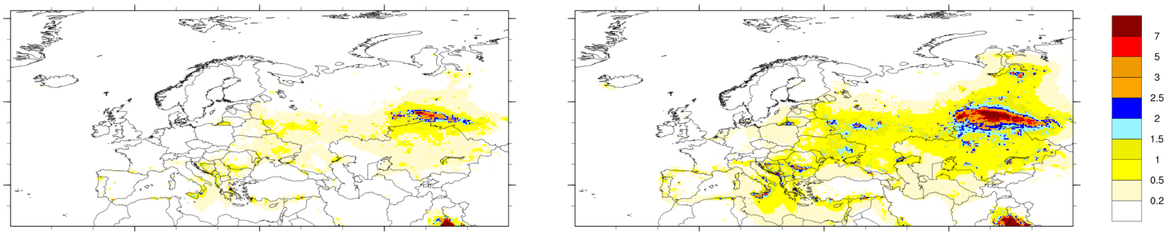

c) $PM_{2.5}$, FINN2.5mod **d)** $PM_{2.5}$, FINN2.5modvrs

Figure 9.2: The top panels show the annual average difference in daily maximum ozone (ppb) calculated with and without fire emissions in 2021: a) FINN2.5mod – No Fires, b) FINN2.5modvrs – No Fires. The bottom two panels show the annual average difference in $PM_{2.5}$ ($\mu g\ m^{-3}$): c) FINN2.5mod – No Fires, d) FINN2.5modvrs – No Fires.

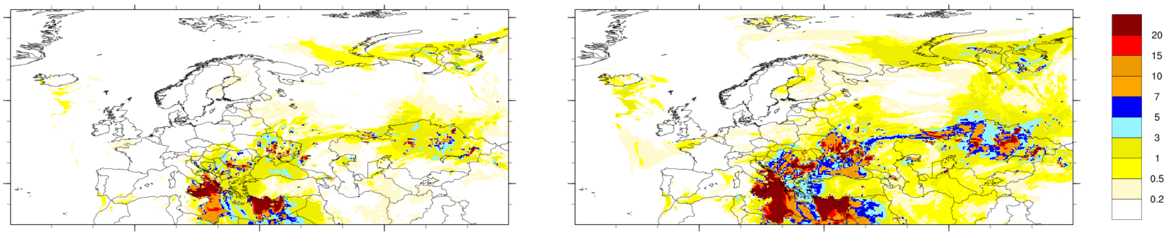

a) DMaxO3, FINN2.5mod – NoFire **b)** DMaxO3, FINN2.5modvrs – NoFire

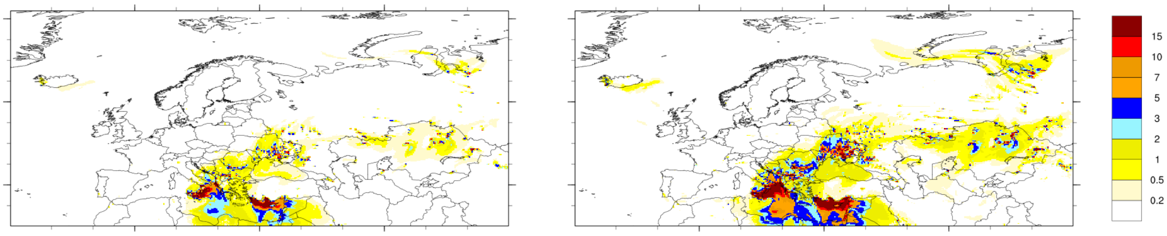

c) $PM_{2.5}$, FINN2.5mod – NoFire **d)** $PM_{2.5}$, FINN2.5modvrs – NoFire

Figure 9.3: The top panels show the difference in daily maximum ozone (ppb) on August 1 2021. calculated with and without fire emissions. a) FINN2.5mod – No Fires. b) FINN2.5modvrs – No Fires. The bottom two panels show the difference in $PM_{2.5}$ ($\mu g\ m^{-3}$) on August 1 2021. c) FINN2.5mod – No Fires. d) FINN2.5modvrs – No Fires.

1, 2021. This day, the calculated effects of fires was more than 20 ppb ozone and 15 ($\mu g\ m^{-3}$) $PM_{2.5}$ in southern Italy.

The fire in Sotalvo in central Spain started on August 14 and it was the biggest forest fire of that year in Spain. Even though it lasted only a few days, the devastated area was estimated to be as large as 21138 ha. The fire is also documented in San-Miguel-Ayanz et al.

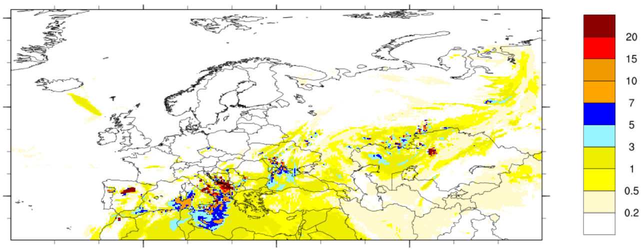

a) DMaxO3, FINN2.5mod – NoFire

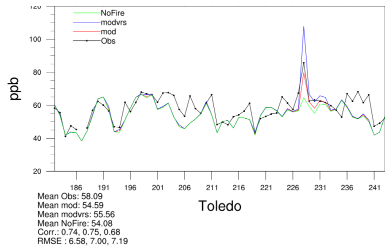

b) DMaxO3, July – August

Figure 9.4: The left panel shows the difference in DMaxO3 (ppb) on August 15 2021. calculated with and without FINN2.5mod emissions. The right panel shows measured against model calculated DMaxO3 at Toledo in Spain for July and August 2021.

(2022). Figure 9.4 a) shows the difference in DMaxO3 (FINN2.5mod – NoFire). Over central Spain a fire induced ozone plume is clearly visible. Figure 9.4 b) shows measured and model calculated DMaxO3 at Toledo for July and August. The calculations with and without fire emissions strongly suggest that this peak is caused by fires. At this site the calculations using FINN2.5modvrs overestimates the effects of fires. Figure 9.4 a) also shows that the fires in southern Italy and also in the Balkan countries had not died out two weeks later than the situation shown in Figure 9.3.

References

Jones, M. W., Abatzoglou, J. T., Veraverbeke, S., Andela, N., Lasslop, G., Forkel, M., Smith, A. J. P., Burton, C., Betts, R. A., van der Werf, G. R., Sitch, S., Canadell, J. G., Santín, C., Kolden, C., Doerr, S. H., and Le Quéré, C.: Global and Regional Trends and Drivers of Fire Under Climate Change, Reviews of Geophysics, 60, e2020RG000 726, doi:https://doi.org/10.1029/2020RG000726, URL https://agupubs.onlinelibrary.wiley.com/doi/abs/10.1029/2020RG000726, e2020RG000726 2020RG000726, 2022.

Rémy, S., Veira, A., Paugam, R., Sofiev, M., Kaiser, J. W., Marenco, F., Burton, S. P., Benedetti, A., Engelen, R. J., Ferrare, R., and Hair, J. W.: Two global data sets of daily fire emission injection heights since 2003, Atmospheric Chemistry and Physics, 17, 2921–2942, doi:10.5194/acp-17-2921-2017, URL https://acp.copernicus.org/articles/17/2921/2017/, 2017.

San-Miguel-Ayanz, J., Durrant, T., Boca, R., Maianti, P., G. Libertá, T. A., Oom, D., Branco, A., de Rigo, D., Ferrari, D., Pfeiffer, H., Grecchi, R., Onida, M., and Löffler, P.: Forest Fires in Europe, Middle East and North Africa 2021, Tech. rep., doi:10.2760/34094, URL file:///home/janeij/Downloads/JRC130846_01.pdf, 2022.

Val Martin, M. and Toska, M.: A Global Analysis of Wildfire Smoke Injection Heights Derived from Space-Based Multi-Angle Imaging., Remote Sens., 10, 1609, URL https://doi.org/10.3390/rs10101609, 2018.

Wiedinmyer, C., Akagi, S. K., Yokelson, R. J., Emmons, L. K., Al-Saadi, J. A., Orlando, J. J., and Soja, A. J.: The Fire INventory from NCAR (FINN): a high resolution global model to estimate the emissions from open burning, Geoscientific Model Dev., 4, 625–641, doi:10.5194/gmd-4-625-2011, 2011.

Wiedinmyer, C., Kimura, Y., McDonald-Buller, E. C., Emmons, L. K., Buchholz, R. R., Tang, W., Seto, K., Joseph, M. B., Barsanti, K. C., Carlton, A. G., and Yokelson, R.: The Fire Inventory from NCAR version 2.5: an updated global fire emissions model for climate and chemistry applications, Geoscientific Model Development, 16, 3873–3891, doi:10.5194/gmd-16-3873-2023, URL https://gmd.copernicus.org/articles/16/3873/2023/, 2023.

Part III

Technical EMEP Developments

CHAPTER 10

Updates to the EMEP MSC-W model, 2022–2023

David Simpson, Willem van Caspel, Anna Benedictow, Hilde Fagerli, Jan Eiof Jonson, Svetlana Tsyro, Alvaro Valdebenito and Peter Wind

Version v5.0 of the EMEP MSC-W model, as used for this report, has had a number of significant changes made since v4.45 used for EMEP Report 1/2022. Most notably, the photolysis schemes have been completely revised, but numerous other improvements have also been made. This chapter summarises the changes made since Simpson et al. (2022), and along with changes discussed in Simpson et al. (2013, 2015–2021) and Tsyro et al. (2014), updates the standard description given in Simpson et al. (2012). Table 10.4 summarises the changes made in the EMEP model since the version documented in Simpson et al. (2012), and these changes are discussed in more detail in Sect. 10.1-10.14, and in specific chapters mentioned therein.

10.1 Overview of changes

The major changes can be summarised:

- A new photolysis methodology (CloudJ) was introduced and the chemical scheme modified (to EmChem19rc) as part of this (Ch. 8, Sect. 10.2).
- The Isorropia_lite equilibrium module was implemented as an option (Sect. 10.3.1).
- The EQSAM equilibrium module was updated (Sect. 10.3.2).
- The possibility of using cloud liquid water directly from the NWP models was introduced (Sect.10.5).
- If present in the NWP meteorology, the mixing height from these NWP is now used directly by default (Sect. 10.6).

- The wildfire datasets and methodologies were updated (Sect. 10.7).
- The calculation of aerosol optical depth (AOD) has been revised and updated (Sect. 10.4).
- Soil NO emissions were updated to CAMS-GLOB-SOIL v2.4 (Sect. 10.8).
- CAMS-REG-TEMPO time-factors are used now by default (Sect. 10.9).
- The Local fractions methodology was expanded, with ozone included for the first time (Sect. 10.10).
- The CH_4 and H_2 boundary conditions were updated (sect. 10.11.1)
- The upper boundary conditions for ozone are now retrieved from ECMWF ERA5 data (Sect. 10.11.2).
- A mask was introduced to re-define some desert areas (Sect. 10.12).
- A new and simpler netcdf emissions format (denoted "CV" format) was introduced (Sect. 10.13).
- The basic chemical mechanism EmChem19a was thoroughly documented and compared with CRI and MCM schemes - see Bergström et al. (2022).

10.2 Cloud-J (and EmChem19rc)

As described in Chapter 8, the old tabulated photolysis rate system has been replaced with Cloud-J. The Cloud-J scheme takes into account radiative effects of aerosols and O_3 at model run-time, while also greatly improving the representation of modeled photolysis rates and their cloud-induced variability. In the default setup, Cloud-J is used to update photolysis rates every model hour using the Briegleb averaging scheme, increasing the total model run-time by at most 10%.

The Cloud-J scheme can be turned off using USES%CLOUDJ in config_emep.nml, reverting back to using the old tabulated scheme, while Cloud-J aerosol radiative effects can be turned off using USES%CLOUDJAEROSOL. The Cloud-J photolysis rates can be updated every model time-step rather than model hour by setting USES%HRLYCLOUDJ to false. Note that the latter does not apply to the tabulated scheme, which are always updated every model time-step. The use of monthly mean overhead stratospheric O_3 column measurements between 2002-2021 can be toggled on by setting USES%CLIMSTRATO3 to false. Climatological monthly mean stratospheric O_3 based on observation is used in the Cloud-J calculations as default, to avoid any possible issues with long-term trend analysis. Other default input files include the Cloud-J cross-sectional data ('FJX_spec.dat'), the J-value mapping to the cross-sectional data ('FJX_j2j.dat'), and aerosol and cloud optical properties ('FJX_scat-UMa.dat'). In addition, the old tabulated system was found to always use only clear-sky rates, which is part of what initiated the change to Cloud-J. To mimic the old behavior when the tabulated scheme is used, USES%CLEARSKYTAB is set to true as default. Setting this to false will make the tabulated scheme also include the effects of clouds.

To facilitate Cloud-J, a slight modification was made to the EmChem19a chemical mechanism (Bergström et al. 2022). The standard EmChem19a photolysis reaction for glyoxal combines the three photolysis channels into a single weighted reaction product, whereas Cloud-J calculates the photolysis rates of each of the channels explicitly. These explicit channels have been added to the EmChem19r chemical scheme (EmChem19a with residential heating), which is now named EmChem19rc. The EMEP model running with Cloud-J is nevertheless compatible also with older EmChem19a schemes. In such cases, the photolysis rates of the three glyoxal channels are summed up into a single reaction rate. EmChem19rc furthermore prescribes fixed background CH_4 and H_2 concentrations, as discussed in Section 10.11.1.

10.3 Thermodynamic modules

The EMEP model has three main options for the thermodynamic modules, which are denoted MARS, EQSAM and ISORROPIA in the model's config system. These modules calculate the gas-partitioning of especially the inorganic species, and also water uptake to aerosols. (These updated equilibrium modules also calculate aerosol acidity, but this parameter still needs more testing and verification.)

In principle we would have liked to update the default EMEP model to use ISORROPIA or EQSAM for the aerosol thermodynamics, together with improved cloud liquid water inputs (CLW, Sect. 10.5), but for reasons that we cannot yet explain, use of the updated CLW together with especially the EQSAM or ISORROPIA thermodynamic modules caused some instabilities in the source-receptor calculations. These calculations rely on the model results changing in an orderly manor when making even tiny changes in emissions from individual countries. Even the use of EQSAM or ISORROPIA with the older CLW method showed some issues, though of a lesser nature.

For these reasons, we have retained MARS for use in this report and for the source-receptor modelling. This decision will be re-visited in future once the newer thermodynamic codes have been more thoroughly tested.

10.3.1 ISORROPIA-lite

The old ISORROPIA-II thermodynamics module has been replaced by the new state of the art ISORROPIA-lite code, which in the EMEP model can be used for the partitioning between the gas and fine mode aerosol phase. ISORROPIA-lite assumes a liquid metastable equilibrium, i.e. no phase changes occur between the solid and liquid aerosol phase, which together with the use of pre-calculated activity coefficients leads to greatly reduced computational costs relative to ISSOROPIA-II (Kakavas et al. 2023, 2022). Additionally, ISORROPIA-lite includes the effects of water uptake by organic matter (OM). When ISORROPIA-lite is used for the fine-mode thermodynamics in the EMEP model, this by default assumes an internally mixed state for sea salt, allowing for water uptake by fine mode sea salt aerosol. The contribution of base cations from dust is also included by default. The internally mixed sea-salt and dust cation assumptions can be turned off by specifying AERO%CATIONS and AERO%INTERALMIXED in config_emep.nml, respectively. Since ISORROPIA-lite is intended for use in the troposphere, the module is only called for pressures greater than 200 hPa and temperatures greater than 250 Kelvin. The hygroscopic properties of OM are set using the default values provided with the ISORROPIA-lite code. These assume a single value of 0.15

for the hygroscopicity factor κ, and an organic aerosol density of 1.4 g/cm^3. The fine mode ammonium nitrate aerosol calculated by ISORROPIA-lite is comparable to that obtained from MARS, with an average annual increase of 0.02 µg m^{-3} across daily EBAS stations in Europe. Still, larger differences appear in the calculated $PM_{2.5}$ water (see Section 10.15.1.

The inclusion of fine mode dust cations has a negligibly small impact on the EMEP simulation results for Europe. Nevertheless, including these cations is important for the simulated aerosol properties over large desert areas such as the Sahara desert, where they can strongly impact the aerosol pH (Pye et al. 2020). Fine mode aerosol pH (pH_F) is a new optional EMEP model output, which has emerged as an important diagnostic for model performance, being a central component of aqueous chemistry (Paglione et al. 2021, Pye et al. 2020).

10.3.2 EQSAM v11

The EQSAM4clim (Equilibrium Simplified Aerosol Model) has been updated (from v10 to v11). In the EMEP MSC-W model, EQSAM is one of the options to calculate gas/aerosol partitioning and aerosol water (Metzger et al. 2012, 2016, 2018).

If selected in the model's config system, EQSAM will simulate a thermodynamic equilibrium for meta-stable aqueous aerosol system including SIA and sea salt (e.g. Na^+, Mg^2+, Ca^2+, K^+ cations). In principle, the EQSAM can calculate a full gas-liquid-solid partitioning, but the meta-stable aqueous aerosol approximation has been chosen as default.

The inclusion of sea salt can be turned on/off by setting AERO%INTERALMIXED to true/false in config_emep.nml, similar to for ISORROPIA. In the present version, EQSAM would only simulate equilibrium of aerosols in the fine fraction. For the same gas/aerosol system, i.e. excluding sea salt, the EQSAM calculates ammonium nitrate concentrations very close to those from MARS and ISORROPIA-lite. Accounting for sea salt cations leads to an additional formation of other nitrate salts and thus results in an increase of NO_3^- in particular over the seas and in the coastal regions. At the same time, NH_4^+ concentrations somewhat decrease due to less ammonia available for ammonium nitrate formation.

10.4 Aerosol Optical Depth

The calculation of Aerosol Optical Depth (AOD) has been revised, i.e. specific extinction efficiency and effective radius for SO_4^{2-} have been modified and assigned the value recommended by the OPAC database Hess et al. (1998) for 'soluble aerosol' (instead of the earlier value, more suitable for sulphuric acid aerosols). Consequently, the specific extinction efficiencies of fine NO_3^- and NH_4^+, which are assumed to be the same as for SO_4^{2-}, also changed. These modifications have resulted in somewhat lower AOD in western/central Europe (which used to be overestimated), but have only slightly affected AOD in the Mediterranean area (where mineral dust is often a dominating aerosol). On the other hand, some decrease in AOD in the southern parts of the domains is due to less mineral dust emitted, which is related to the changes in landuse data, namely some decrease of desert areas (see Section 10.12). The EMEP model underestimates by 32% the annual mean AOD observed at the AERONET sites in 2021, which is actually more consistent with the model underestimation of PM_{10}. The spatio-temporal correlation is as high as 0.81 (see Section D in Appendix).

10.5 Cloud liquid water and issues with source-receptor

In previous versions of the EMEP model, a fixed value was used for the cloud liquid water (CLW - volume H_2O per volume cloud air - set to 0.6e-6). This fixed value was used to avoid an over-reliance on the values predicted by NWP models, since early experience (back in the 1990s) suggested that such values could vary dramatically between NWP models.

However, the CLW values predicted by the current generation of NW models are believed to be more robust, and so the model can now make direct use of the NWP model's CLW, and this is done by setting the config flag `USES%FIXED_CLW` to be negative. (Otherwise the default value is +0.6e-6).

We had intended the new NWP-derived CLW values to be the new default for the EMEP model, but as noted above the use of these seems to worsen the stability of the source-receptor calculations. Until this issue is resolved, we retain the fixed CLW in the default EMEP configuration.

10.6 PBL height

In earlier EMEP model versions planetary boundary layer (PBL) height (also known as the mixing height) was calculated in the model based upon stability and other meteorology (Simpson et al. 2012). The new default (set with a config variable `PBL%HmixMethod='NWP'`) is to take this PBL height directly from the NWP model. If not available in the user's NWP, the older setting (`PBL%HmixMethod='JcRb_t2m'`) can be used.

10.7 Wildfires

The implementation of emissions from wildfires (or loosely called forest fires below) in the EMEP model is described in Ch. 9. In previous versions of the model, these emissions were dispersed though the lowest layers, up to 800 hPa height. Estimated injection heights from wildfires referred to in this chapter suggest that a majority of the fires emissions are released near the surface and subsequently mixed within the planetary boundary layer. A new method (config: USES%FFireDispMethod="PBL") has therefore been introduced for the vertical dispersion of Forest Fire (FF) emissions, dispersing the FF emissions between the surface and top of the boundary layer. This change had only marginal effects on model results. However, the new method seems scientifically more sound the than applying a fixed level of 800 hPa, as the top of the boundary layer to a large extent acts as a barrier for the exchange between the PBL and the free troposphere above.

10.8 Soil NO emissions

The default soil-NO emissions have now been set to v2.4 of the CAMS-GLOB-SOIL dataset (Simpson et al. 2023). As with previous CAMS-GLOB-SOIL datasets (versions v1.1–v2.3), the data consist of monthly fields of NO emissions from four main components (biome, fertilizer/manure, N-deposition and pulsing) with $0.5^\circ \times 0.5^\circ$ resolution. The model configuration allows the choice of using either 'Total' emissions (which uses all 4 components), or 'NoFert' (which uses just biome, N-deposition and pulsing). As discussed in Simpson and Darras

(2021) the NoFert option is used along with CEIP-based or ECLIPSE v6 inventories, and Total should be used for those inventories which do not already include agricultural soil-NO emissions (in particular, for CAMS-REG datasets).

Version v2.4 GLOB-SOIL-NO data have been calculated for the period 2000–2020, but as year-to-year variations are small (and uncertainties are large), we have chosen to use the climatological average of these emissions for each year.

There have been two main changes in the v2.4 calculations compared to earlier datasets, namely the direct use of ERA5 meteorology (ERA5 2023) (instead of meteorology from the EMEP system), and the use of soil temperatures. In v1.1, soil temperatures (T_s) were estimated from air temperatures (T_a) using simple empirical relationships, but some issues were found with the equations used. In v2.1–v2.3 we made the very simple assumption that $T_s = T_a$. In v2.4 we have used the upper (7 cm) soil temperature from the ERA5 meteorology. (Comparison of the use of T_a vs. T_s shows surprisingly little impact, however; usually emissions are within a few % with the two approaches.)

10.9 CAMS-REG-TEMPO time-factors

The new default time-factors (CAMS_TEMPO_CLIM) correspond to the CAMS-REG-TEMPO v3.2 simplified climatological temporal profiles (Guevara et al. 2021). For non-livestock agricultural emissions (GNFR Sector L) the monthly factors from CAMS-REG-TEMPO v4.1 are used after an error had been discovered in the v3.2 dataset.

10.10 Local Fractions

The range of applications of the Local Fraction method is continuously expanding. The most significant upgrade this year is that the method can be applied to non linear species such as ozone (see chapter 5). This allows to make standard SR matrices in a single run. Also new features can be addressed with the method, such as the contribution from stratospheric ozone, and the persistence of initial values. The Local Fraction runs are an extension of the standard model, in the sense that the reference concentrations will be identical and the chemical transformations used to compute the sensibilities to emission changes, are the same as in a standard run. Secondary inorganic aerosols are at present only available in the LF framework in an experimental branch of the model.

10.11 Updated boundary and initial conditions

10.11.1 CH_4 and H_2

The version of EmChem19 developed for use with Cloud-J (EmChem19rc, Section 10.2), also features fixed background concentrations of CH_4 and H_2. These species were allowed to degrade over time through the reaction with OH in earlier versions of EmChem19, leading to diminishing CH_4 and H_2 concentrations over the course of a simulation. This effect was most pronounced for global simulations, as CH_4 and H_2 are replenished through the boundary conditions in regional runs.

The (fixed) background CH_4 concentrations are read from a default input file containing annual mean global mean values. This file ('CH4_hist_CLE.txt') contains historical concentrations based on observations from 1960 up until 2019, and projected values up to 2050 made using the IIASA GP Review CLE emission scenario together with the box-model of Olivié et al. (2021). Alternatively, the default directory containing EMEP model input files also contains files with projected background concentrations from the Shared Socioeconomic Pathways (SSPs) scenarios discussed in CMIP6 AR6 Annex III (Intergovernmental Panel on Climate Change (IPCC) 2023).

In the EMEP model, the default behavior is that the iyr_trend CH_4 concentration, which is calculated in BoundaryConditions_mod.f90 based on the iyr_trend variable set in config_emep.nml, is replaced by the value read in from the CH_4 input file. The valid range of years for the input file is 1960-2050. If the input file is found, but a year of simulation outside of this range is chosen, the model stops. If BGND_CH4 is set to something greater than zero in config_emep.nml, this value overwrites all other CH_4 input values, i.e. also that of the input file.

A fixed global mean mixing ratio of 500 ppb is prescribed for H_2 regardless of the simulation year.

10.11.2 O_3 top boundary conditions

From the ECMWF ERA5 data set, a selection of 8 of the 137 model levels of ozone data at around 100 hPa, representative for the highest EMEP model level, is compiled for all years since 1990 and used as a top boundary condition. This ozone is computed with a relatively simple Cariolle stratospheric chemistry parametrisation (Cariolle D 2007) that is also applied in the troposphere (currently used for ECMWF's high resolution NWP model).

10.12 Desert mask

Previous model versions have frequently displayed excessive dust (and hence PM) formation in southern Spain (near Almeria), and also dust emissions on Greenland's coasts and some other Arctic regions. This was diagnosed as resulting from a mis-classification of barren land as desert in this region in the underlying EMEP/SEI map, with subsequent wind-blown dust from these desert grid-cells.

As described in Simpson et al. (2012), the standard EMEP model uses fine-scale (5 km resolution) European data which merges the CORINE land-cover maps (de Smet and Hettelingh 2001) with data and from the Stockholm Environment Institute at York (SEIY) which had more detail on agricultural land-cover (*ibid.*). The merged data-set was provided to MSC-W by the EMEP Coordinating Centre for Effects (Max Posch, CCE, pers. comm), and it is this data which features the regions of dust-producing deserts in Spain and elsewhere in Europe. As discussed in Simpson et al. (2017), land-cover outside of the CCE/SEI European domain is a merge of the 'GLC-2000' land-cover data-set (`http://bioval.jrc.ec.europa.eu/products/glc2000/glc2000.php`), and the Community Land Model (`http://www.cgd.ucar.edu/models/clm/`, Oleson et al. 2010, Lawrence et al. 2011).

A variety of methods were tested for removing the "false" deserts (e.g. through sediment supply maps: Parajuli and Zender 2017), but as an interim measure we have made use of data

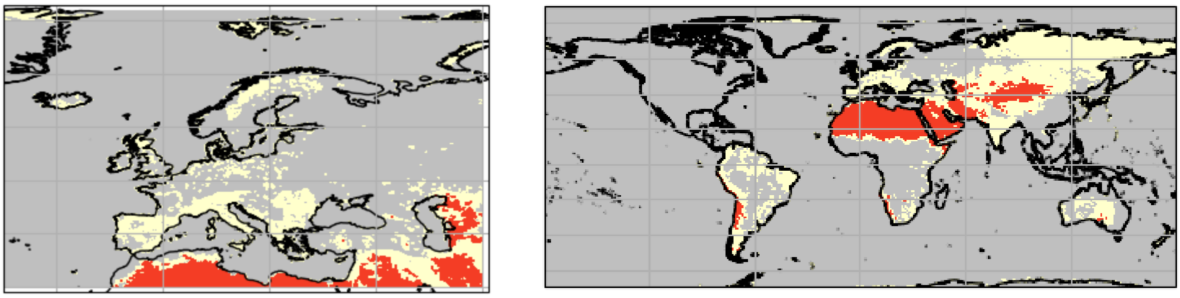

Figure 10.1: Revised desert mapping for the European domain (0.3° 0.2° lon/lat, left) and global scale (0.5°×0.5°). Red areas illustrate grid cells containing desert areas with new scheme; yellow areas show areas where desert fractions were re-defined as barren land. (Note that each grid cell usually contains many land-cover types; this plot gives no indication of the fractional coverage.)

from the Olson 2001 land-cover map (as processed for GEOS-Chem): `http://wiki.seas.harvard.edu/geos-chem/index.php/Olson_land_map`. We have retained desert areas from the EMEP maps only when the Olson map has the 'bare desert' category, and re-classified other areas as EMEP 'BARE'. Figure 10.1 illustrates the effect of the desert re-mapping on both European and global domains, with the yellow areas denoting grid cells where re-classification from desert to BARE took place.

10.13 New emissions CV-format

The standard main emission input files are now in a upgraded NetCDF format called CV-format. The format is more intuitive with one variable for each country and species (CV = country variables). The sector dependency is included through an extra dimension of the variable. Table 10.1 illustrates the format used for emissions used in this report, giving the example for Albanian (country code 'AL') SOx emissions and for the 13 GNFR sectors provided by CEIP.

Reading of the emission values by the EMEP model should now be faster. The emissions are also easily visualized, and addition or modifications of fields should be straightforward using standard tools.

10.14 Other

A number of smaller changes have been made:

- Bug-fixes include changes which modify the $PM_{2.5}$ fraction of coarse nitrate from 0.13 to 0.20, and a correction to the gravitational settling velocity of coarse particles (applying only to volcanic ash particles, when present in the simulation).

- Numerous small changes to make the code more flexible, and to improve memory and CPU usage.

Table 10.1: Extract of NetCDF attributes for new country variable ('CV') emission format

```
dimensions:
    lon = 1200 ;
    lat = 520 ;
    sector = 13 ;
    time = 1 ;
variables:
    float lon(lon) ;
            lon:standard_name = "longitude" ;
            lon:long_name = "longitude" ;
            lon:units = "degrees_east" ;
    float lat(lat) ;
            lat:long_name = "latitude" ;
            lat:units = "degrees_north" ;
            lat:standard_name = "latitude" ;
    int sector(sector) ;
            sector:long_name = "GNFR sector index" ;
    float time(time) ;
    float sox_AL(time, sector, lat, lon) ;
            sox_AL:units = "tonnes/year" ;
            sox_AL:species = "sox" ;
            sox_AL:molecular_weight = 64. ;
            sox_AL:molecular_weight_units = "g mole-1" ;
            sox_AL:country_ISO = "AL" ;
            sox_AL:countrycode = 1 ;
    ......
```

10.15 Impacts of selected model changes

This section presents results which illustrate the impact of some of the changes and options associated with model version rv5.0. Section 10.15.1 discusses the impact of the different thermodynamic modules on predicted aerosol liquid water in more detail. Section 10.15.2 discusses the impact of a forthcoming change to the IFS meteorological driver. In Sect. 10.15.3, we illustrate the changes in verification statistics associated with many of the modified variables and settings discussed above.

10.15.1 Aerosol liquid water

In the EMEP model, the thermodynamic modules calculate aerosol associated water at the ambient meteorological conditions and (at model layers) and at the relative humidity of 50% and temperature of 20°, which are required for the conditioning of particle sampling filters. The latter is diagnosed for surface PM_{10} and $PM_{2.5}$ for consistency with PM gravimetric measurements.

Due to accounting for the additional water uptake by OM, ISORROPIA-lite calculates somewhat more $PM_{2.5}$ water with respect to MARS. For the most direct comparison to MARS,

Fig. 10.2a and b show the annual mean MARS and ISORROPIA-lite $PM_{2.5}$ water, where ISORROPIA-lite does not include water uptake by sea salt and OM (as is also the case for MARS). Shown here is the $PM_{2.5}$ water calculated at 50% RH and 20°C, following standardized measurement guidelines. Comparing Fig. 10.2a and b finds that the inorganic water uptake follows the same geographical pattern between the two thermodynamics modules, being different only by about 0.2 µg m^{-3} over parts of Poland and Eastern Germany, and along the Western coast of Türkiye.

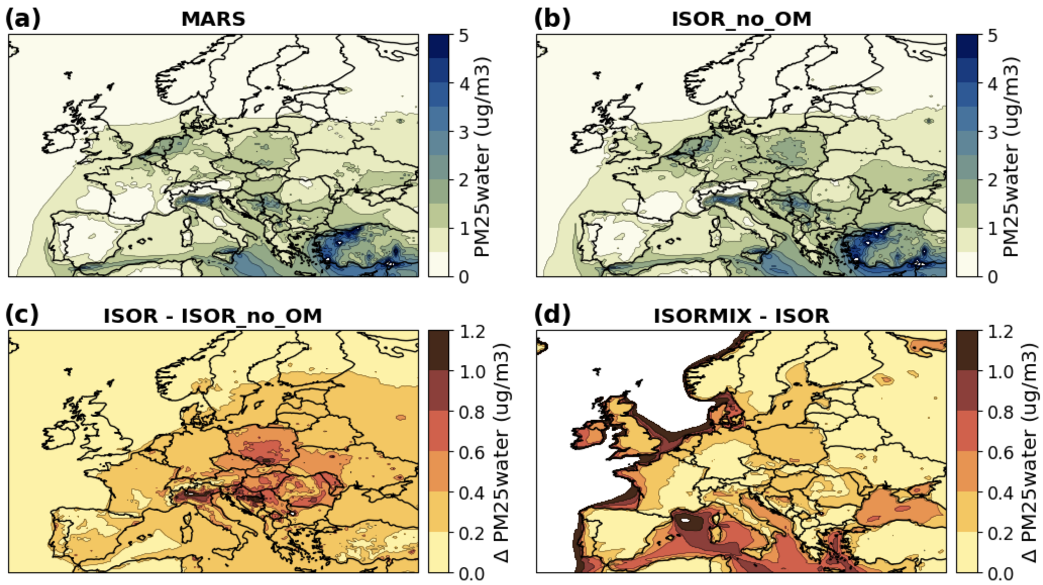

Figure 10.2: Annual mean surface $PM_{2.5}$ water (at 50% relative humidity) as calculated using the MARS **(a)** and ISORROPIA-lite **(b)** thermodynamics modules, where ISORROPIA-lite does not include the effects of sea-salt and OM (ISOR_no_OM). Panel **(c)** shows the difference in $PM_{2.5}$ water between ISORROPIA-lite with (ISOR) and without OM water uptake, while panel **(d)** shows the difference between ISORROPIA-lite with (ISORMIX) and without an internally mixed assumption for sea-salt. Values greater than 1.2 µg m^{-3} are not shown in panel **(d)**.

Fig. 10.2c shows the difference between ISORROPIA-lite with and without water uptake by OM. The water uptake by OM is greatest over regions with large primary OM emissions in Poland, Northern Italy, and the Balkans. The water uptake in the latter two peaks around 1.2 µg m^{-3}, constituting a roughly 50% local increase in total $PM_{2.5}$ water. Fig. 10.2d shows the difference between ISORROPIA-lite with both OM and sea-salt water uptake (ISORMIX), and with only OM water uptake. The water uptake by $PM_{2.5}$ sea-salt over the oceans is typically around 4 µg m^{-3}, but this has no impact on surface air quality over land. Nevertheless, Fig. 10.2d shows that water uptake by sea-salt can increase $PM_{2.5}$ water by 0.6-1.2 µg m^{-3} along the Western coast of Europe. The impact of water uptake by sea-salt quickly diminishes away from the coastal areas, however. Overall, annual mean $PM_{2.5}$ concentrations at the EBAS sites across Europe increase from 7.97 to 8.58 µg m^{-3} when OM and sea-salt water uptake are included in ISORROPIA-lite.

If only secondary inorganic aerosols are included (but not sea salt), the $PM_{2.5}$ water at 50% humidity calculated by EQSAM is quite close to that from MARS (10.3a), i.e. mostly 0.1 µg m^{-3} lower (up to 0.2 µg m^{-3} in eastern/south-eastern Europe and Türkiye). Accounting for sea salt cations in EQSAM results in an increase of PM water by 0.2-0.3 µg m^{-3} in the coastal areas and by 0.5-0.7 µg m^{-3} over the seas (10.3b).

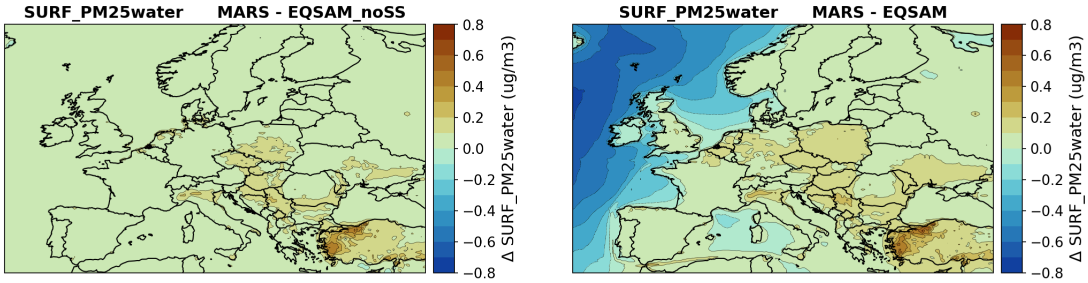

(a) (b)

Figure 10.3: Difference in annual mean surface $PM_{2.5}$ water (at 50% relative humidity) as calculated using the EQSAM and MARS thermodynamics modules, where EQSAM does not **(a)** and does **(b)** include the effects of sea-salt.

10.15.2 Changing IFS version - impact on model results

The model results presented for 2021 in this years EMEP Status report are driven by meteorology created by IFS Cycle 46r1 (in fact meteorology for years 2019-2021 is created from Cycle 46r1 simulations). This IFS version is no longer available, and from next year onward we will apply IFS Cycle 48r1 for meteorology. In order to know whether the change of version for the meteorological driver will impact the model results for air pollution, we created meteorology for 2021 with both IFS Cycle 46r1 and 48r1. These meteorological data have been used to drive two EMEP MSC-W model simulations for 2021.

The EMEP MSC-W model has been run with standard setup, as described in Chapter 2. However, these tests were done in an earlier phase of preparation of the EMEP Status Report 1/2021, using the officially reported emissions (in which GNFR C for PPM has not yet been replaced by Ref2 emissions), and CAMS day-to-day time-factors have been used (not adjusted for Covid-19). Thus the results themselves deviate somewhat from the status run for 2021 presented in Chapter 2. However, our main goal here was to see whether the change of version of the meteorological driver would introduce significant changes in our air pollution model results that would lead to artificial 'jumps' in our trend data series (e.g. artificial changes between year 2021 and 2022).

In Fig. 10.4 we present a comparison of the model results for 2021 (using Cycle rv46r1 and rv48r1, respectively) to EMEP data for 2021. The heat map shows the difference (normalized mean bias, in percent) of modelled versus observations for a range of components. Light blue or light red colours means small differences (negative or positive NMB, respectively), while the stronger colours indicate larger differences. The numbers in the table are the NMB (in percent) for each component. In general, the concentrations of most species are slightly higher when using IFS 48r1 compared to the model results using 46r1, so that in the cases where the model underestimated the concentrations the results improved with 48r1 meteorology (e.g. for $PM_{2.5}$), whereas the previously overestimation increased (e.g. for ozone). Still, in general the results are very similar. The largest differences are seen for sea salt aerosols, which are most sensitive to changes in the meteorological driver (as sea spray emissions have a very strongly dependency on the wind speed). Overall, the overestimation of sea salt in $PM_{2.5}$ increase from 34 to 44 %, and from 0 to 7% for sea salt in PM_{10}. Temporal correlation (daily) between observations and model change very little (by around 0.01 at most) for sea salt and other components (not shown).

Thus, our overall conclusion is that the change of IFS 46r1 to 48r1 will not cause artificial changes in concentration (except for sea salt where one needs to interpret trends with care).

Figure 10.4: Comparison of EMEP MSC-W model results to EMEP observations for 2021 using two different meteorological drivers (normalized mean bias (NMB) in %). Column '2023-DOY46r1' show the comparison for model results using IFS Cycle 46r1, whilst '2023-DOY48r1' show the comparison for model results using IFS Cycle 48r1.

Table 10.2: Setup of sensitivity runs. Model settings are default rv5.0, except where changes are indicated.

Run	Comment
Default	rv5.0 defaults. Uses Cloud-J, MARS, Hmix from the NWP, FINNv2.5, etc.
EQSAM	Use EQSAM v11 thermodynamics
ISORROPIA	ISORROPIA-lite thermodynamics
Hmix	Calculate mixing height (Hmix) in model, ie. not using NWP Hmix.
FINNV1.5	Use previous wildfire data.
BCs	Use previous boundary conditions for CH_4 and O_3.
CLW	Use cloud liquid water from NWP.
GENEMIS	Previous time-factors.
Jvals	Tabulated photolysis rates.
Retro	Uses old Hmix, Old (tabulated) J values, FINNv1.5, old BCs, and GENEMIS time-factors, plus MARS.

10.15.3 Sensitivity tests

In order to illustrate the impacts of some of the changes and options discussed above, we have run a series of sensitivity tests with $0.3° \times 0.2°$ resolution for 2018. The test runs are described in Table 10.2, and essentially involve using the model's configuration system to revert some aspect of the model setup from the default. For example, the 'EQSAM' run uses EQSAM (Sect. 10.3.2) instead of the default MARS thermodynamics model (although this uses the implemented EQSAM v11, not the v10 version used in rv4.45). We can also note that unlike MARS, both the EQSAM and ISORROPIA systems include sea-salt in the equilibrium calculations.

Table 10.3 presents verification statistics for some key outputs (as compared to EMEP/CCC data). We do not attempt to discuss all changes in detail, but rather just highlight some of the findings for each pollutant. The boundary condition (BCs) test has no impact on these statistics for any compound, so is omitted from Table 10.3. Indeed, in many cases the verification statistics hardly change at all with the individual modifications, although when several changes are made at the same time (the 'Retro' run) the verification changes are more noticeable. Where changes do occur, the run which gives an improvement for one compound often gives a worse performance for another. In general though, the combination of changes which are present in the new default run seem to out-perform the older model (as indicated by the Retro run)

As expected, the two thermodynamic tests (EQSAM, ISORROPIA) show little or no impact on mean of daily max. O_3 (MDmaxO3), NO_2, SO_2 or $SO_4{}^{2-}$. For NH_3 and and especially $NH_4{}^+$ the statistics are degraded with EQSAM, but there are only small changes for ISORROPIA. For $NO_3{}^-$ on the other hand, EQSAM causes little change, but bias (and to a lesser extent R^2) degrades with ISORROPIA. For $PM_{2.5}$ the net impact of EQSAM is similar to the default setup, whereas the ISORROPIA run produces better bias and IOA (partly because it simulates more aerosol water which reduces model underestimation). For PM_{10}, ISORROPIA has the best bias and lowest RMSE, and again EQSAM is similar to the defaults.

The Hmix test degrades the model results for most compounds. For example, for SO_2, NH_4^+ or $PM_{2.5}$. However, both bias and R^2 improve for NH_3. The use of FINNv1.5 instead of FINNv2.5 has little or no impact on these annual mean statistics, though of course forest-fires can have large impacts in particular regions and times (Sect. 9). The use of variable cloud liquid water (CLW) impacts most compounds to some extent. It gives the best statistics for SO_2, but worst statistics for SO_4^{2-}. The impacts on $PM_{2.5}$ and PM_{10} are small, but slightly worse than for our default run which uses fixed CLW values.

The use of GENEMIS monthly time-factors (rather than the updated CAMS-REG-TEMPO factors) has significant impacts on most compounds. For SO_2 statistics degrade (e.g. IOA from 0.78 to 0.74), but for SO_4^{2-} statistics improve. Similar features are seen for NH_3 (which degrades) and NH_4^+ (which improves). For $PM_{2.5}$ and PM_{10} the GENEMIS factors seem to provide better statistics than our new defaults. Of course, we are here presenting overall annual statistics, and such monthly factors are best investigated with comparison of monthly data, but this result is rather surprising given the age of the GENEMIS factors (which originated with data from the 1990s, Friedrich 1993, Friedrich and Reis 2004), and requires more evaluation.

The use of the old (tabulated) photolysis rates (test Jvals) degrades the bias and IOA statistics significantly for MDmaxO3. Somewhat degraded performance is also seen for SO_4^{2-}, $PM_{2.5}$ and PM_{10}. See Ch. 8 for more examples.

Finally, the Retro runs which combine most of the above tests give some indication of the net result of the many changes. The statistics for our new default are almost always better than for the retro tests, and in general significantly so.

Table 10.3: Verification statistics for sensitivity tests. Runs for 2018, with $0.3° \times 0.2°$ resolution.

Run	Ns	Obs	Mod	Bias	RMSE	R^2	IOA
Mean of Daily Max. Ozone (MDmaxO3, ppb)							
Default	117	42.60	42.76	0%	2.66	0.84	0.91
EQSAM	117	42.60	42.81	0%	2.66	0.84	0.91
ISORROPIA	117	42.60	42.72	0%	2.65	0.84	0.91
Hmix	117	42.60	43.95	3%	3.00	0.83	0.89
FINNv1.5	117	42.60	42.53	0%	2.65	0.84	0.91
CLW	117	42.60	42.85	1%	2.66	0.84	0.91
GENEMIS	117	42.60	42.22	-1%	2.63	0.84	0.91
Jvals	117	42.60	40.53	-5%	3.34	0.83	0.84
Retro	117	42.60	41.47	-3%	2.94	0.83	0.86
NO_2 in Air ($\mu g(N)\ m^{-3}$)							
Default	73	1.71	1.65	-4%	0.82	0.83	0.90
EQSAM	73	1.71	1.65	-4%	0.82	0.83	0.90
ISORROPIA	73	1.71	1.65	-4%	0.82	0.83	0.90
Hmix	73	1.71	1.53	-11%	0.83	0.82	0.90
FINNv1.5	73	1.71	1.65	-4%	0.82	0.83	0.90
CLW	73	1.71	1.65	-4%	0.82	0.83	0.90
GENEMIS	73	1.71	1.79	5%	0.89	0.83	0.89
Jvals	73	1.71	1.67	-3%	0.81	0.84	0.91
Retro	73	1.71	1.55	-10%	0.82	0.82	0.90

Notes: N_s= number of stations (from EMEP network, sites < 500 m altitude), Obs = observed values, Mod = modelled values, RMSE = root mean square error, R^2 = spatial correlation coefficient.

Continued on next page

Table 10.3 – continued from previous page

Run	Ns	Obs	Mod	Bias	RMSE	R^2	IOA
SO_2 in Air (μg(S) m^{-3})							
Default	57	0.30	0.28	-6%	0.21	0.62	0.78
EQSAM	57	0.30	0.28	-6%	0.21	0.62	0.78
ISORROPIA	57	0.30	0.29	-5%	0.21	0.62	0.78
Hmix	57	0.30	0.27	-12%	0.21	0.60	0.77
FINNv1.5	57	0.30	0.28	-6%	0.21	0.62	0.78
CLW	57	0.30	0.31	2%	0.21	0.63	0.79
GENEMIS	57	0.30	0.26	-13%	0.22	0.56	0.74
Jvals	57	0.30	0.29	-4%	0.21	0.62	0.78
Retro	57	0.30	0.27	-11%	0.21	0.61	0.77
Sulfate in Air (μg(S) m^{-3})							
Default	32	0.48	0.27	-44%	0.26	0.85	0.70
EQSAM	32	0.48	0.27	-45%	0.26	0.85	0.69
ISORROPIA	32	0.48	0.26	-45%	0.27	0.85	0.69
Hmix	32	0.48	0.26	-46%	0.27	0.84	0.68
FINNv1.5	32	0.48	0.27	-44%	0.26	0.85	0.70
CLW	32	0.48	0.24	-51%	0.29	0.84	0.65
GENEMIS	32	0.48	0.30	-39%	0.23	0.85	0.75
Jvals	32	0.48	0.25	-47%	0.28	0.85	0.67
Retro	32	0.48	0.25	-48%	0.28	0.84	0.66
Ammonia in Air (μg(N) m^{-3})							
Default	20	0.64	0.88	37%	0.49	0.91	0.88
EQSAM	20	0.64	0.90	41%	0.51	0.91	0.88
ISORROPIA	20	0.64	0.87	36%	0.48	0.91	0.89
Hmix	20	0.64	0.81	27%	0.42	0.91	0.91
FINNv1.5	20	0.64	0.87	36%	0.49	0.91	0.88
CLW	20	0.64	0.88	38%	0.50	0.91	0.88
GENEMIS	20	0.64	0.96	50%	0.63	0.91	0.84
Jvals	20	0.64	0.89	38%	0.50	0.91	0.88
Retro	20	0.64	0.82	27%	0.42	0.91	0.91
NH_4^+ in Air (μg m^{-3})							
Default	26	0.65	0.56	-13%	0.25	0.78	0.87
EQSAM	26	0.65	0.50	-22%	0.28	0.76	0.83
ISORROPIA	26	0.65	0.57	-12%	0.26	0.77	0.87
Hmix	26	0.65	0.53	-18%	0.26	0.77	0.85
FINNv1.5	26	0.65	0.56	-14%	0.25	0.78	0.87
CLW	26	0.65	0.54	-16%	0.26	0.78	0.86
GENEMIS	26	0.65	0.66	3%	0.26	0.77	0.88
Jvals	26	0.65	0.54	-16%	0.26	0.79	0.86
Retro	26	0.65	0.50	-22%	0.28	0.77	0.83
NO_3^- in Air (μg(N) m^{-3})							
Default	25	0.27	0.28	4%	0.10	0.83	0.91
EQSAM	25	0.27	0.27	1%	0.10	0.82	0.90
ISORROPIA	25	0.27	0.32	17%	0.11	0.84	0.89
Hmix	25	0.27	0.27	-2%	0.11	0.79	0.88
FINNv1.5	25	0.27	0.28	2%	0.10	0.83	0.91

Notes: N_s= number of stations (from EMEP network, sites < 500 m altitude), Obs = observed values, Mod = modelled values, RMSE = root mean square error, R^2 = spatial correlation coefficient.

Continued on next page

Table 10.3 – continued from previous page

Run	Ns	Obs	Mod	Bias	RMSE	R^2	IOA
CLW	25	0.27	0.29	7%	0.10	0.84	0.91
GENEMIS	25	0.27	0.34	25%	0.13	0.84	0.88
Jvals	25	0.27	0.28	2%	0.10	0.83	0.91
Retro	25	0.27	0.25	-7%	0.11	0.79	0.88
$PM_{2.5}$ ($\mu g\ m^{-3}$)							
Default	26	8.28	6.93	-16%	2.44	0.82	0.85
EQSAM	26	8.28	6.83	-18%	2.53	0.81	0.84
ISORROPIA	26	8.28	7.68	-7%	2.19	0.81	0.88
Hmix	26	8.28	6.75	-18%	2.61	0.80	0.83
FINNv1.5	26	8.28	6.83	-17%	2.51	0.81	0.84
CLW	26	8.28	6.80	-18%	2.52	0.82	0.84
GENEMIS	26	8.28	7.29	-12%	2.07	0.86	0.89
Jvals	26	8.28	6.69	-19%	2.58	0.82	0.83
Retro	26	8.28	6.39	-23%	2.88	0.79	0.80
PM_{10} ($\mu g\ m^{-3}$)							
Default	31	14.09	10.70	-24%	4.35	0.73	0.71
EQSAM	31	14.09	10.54	-25%	4.48	0.73	0.70
ISORROPIA	31	14.09	11.48	-19%	3.82	0.73	0.76
Hmix	31	14.09	10.40	-26%	4.59	0.72	0.69
FINNv1.5	31	14.09	10.58	-25%	4.49	0.71	0.69
CLW	31	14.09	10.56	-25%	4.48	0.72	0.69
GENEMIS	31	14.09	11.23	-20%	4.00	0.71	0.73
Jvals	31	14.09	10.39	-26%	4.58	0.73	0.69
Retro	31	14.09	9.94	-29%	5.00	0.71	0.65

Table 10.4: Summary of major EMEP MSC-W model versions from 2012–2023. Extends Table S1 of Simpson et al. 2012.

Version	Update	Ref$^{(a)}$
v5.0	Revised photolysis scheme and update of chemicals scheme to EmChem19rc, addition of ISORROPIA-lite, EQSAM v11, revisions in emissions of forest-fire, soil NO and dust, boundary conditions	This Report
v4.45	Improved and faster emissions handling; Updated soil NO to v2.3; New O_3 outputs	R2022
v4.44	Changed MMD of SS to 4.0μm; Bug fix on f_{SW} usage; Added extension "ZD_EmCso" for simulation of satellite observations.	R2022
v4.43	Updates to landcover and POD calculations; Much faster reading of netcdf emissions in new format.	R2022
v4.42	19-sector emissions system (GNFR-CAMS) introduced; Emissions for soil NO, DMS, and aircraft updated. Modified various parameters concerning fine/coarse fractions for sea-salt and nitrate; Added RH limits on Gerber functions; 'rnr' emission split and EmChem19r introduced; Revised global monthly emission factors produced; Changed default Kz; upgraded local fraction methods; cleaned up various config options.	R2021
rv4.36	Public domain (Nov. 2020); Updated NO_3 photolysis; Allow physical height and topography settings in sites/sondes output; better time resolution on Hmix outputs; allow hourly time-factors per country and species; Various emission coding improvements	
rv4.35	Various updates, including heavy refactoring of local-fraction code, bug-fixes in MARS module, and updates in chemical mechanisms, default PM and NMVOC speciation and GenChem systems	R2020
rv4.34	Public domain (Feb. 2020); EmChem19a, EmChem19p	R2020
rv4.33	Public domain (June 2019); EmChem19, PAR bug-fix, EQSAM4clim	R2019
rv4.32	Used for EMEP course, April 2019	
rv4.30	Moved to new GenChem-based system	
rv4.17a	Used for R2018. Small updates	R2018
rv4.17	Public domain (Feb. 2018); Corrections in global land-cover/deserts; added 'LOTOS' option for European NH_3 emissions; corrections to snow cover	R2018
rv4.16	New radiation scheme (Weiss&Norman); Added dry and wet deposition for N_2O_5; (Used for Stadtler et al. 2018, Mills et al. 2018b)	R2018
rv4.15	EmChem16 scheme; New global land-cover and BVOC	R2017
rv4.10	Public domain (Oct. 2016) (Used for Mills et al. 2018a)	R2016
rv4.9	Updates for GNFR sectors, DMS, sea-salt, dust, S_A and γ, N_2O_5	
rv4.8	Public domain (Oct. 2015); ShipNOx introduced. Used for EMEP HTAP2 model calculations, see special issue: `www.atmos-chem-phys.net/special_issue390.html`, and Jonson et al. (2017).	R2015
rv4.7	Used for reporting, summer 2015; New calculations of aerosol surface area; New gas-aerosol uptake and N_2O_5 hydrolysis rates; Added 3-D calculations of aerosol extinction and AODs; Emissions - new flexible mechanisms for interpolation and merging sources; Global - monthly emissions from ECLIPSE project; Global - LAI changes from LPJ-GUESS model; WRF meteorology (Skamarock and Klemp 2008) can now be used directly in EMEP model.	R2015
rv4.6	Used for Euro-Delta SOA runs Revised boundary condition treatments ; ISORROPIA capability added	R2015
rv4.5	Sixth open-source (Sep 2014) ; Improved dust, sea-salt, SOA modelling ; AOD and extinction coefficient calculations updated ; Data assimilation system added ; Hybrid vertical coordinates replace earlier sigma ; Flexibility of grid projection increased.	R2014
rv4.4	Fifth open-source (Sep 2013) ; Improved dust and sea-salt modelling ; AOD and extinction coefficient calculations added ; gfortran compatibility improved	R2014, R2013
rv4.3	Fourth public domain (Mar. 2013) ; Initial use of namelists ; Smoothing of MARS results ; Emergency module for volcanic ash and other events; Dust and road-dust options added as defaults ; Advection algorithm changed	R2013
rv4.0	Third public domain (Sep. 2012), as Simpson et al. (2012)	R2013

Notes: (a) R2018 refers to EMEP Status report 1/2018, etc.

References

Bergström, R., Hayman, G. D., Jenkin, M. E., and Simpson, D.: Update and comparison of atmospheric chemistry mechanisms for the EMEP MSC-W model system — EmChem19a, EmChem19X, CRIv2R5Em, CB6r2Em, and MCMv3.3Em, EMEP Technical Report 1/2022, The Norwegian Meteorological Institute, Oslo, Norway, 2022.

Cariolle D, T. H.: A revised linear ozone photochemistry parameterization for use in transport and general circulation models: multi-annual simulations, Atmospheric Chemistry and Physics, 7, 2183–2196, doi:https://doi.org/10.5194/acp-7-2183-2007, 2007.

de Smet, P. and Hettelingh, J.-P.: Intercomparison of Current Landuse/Land Cover Databases, in: Modelling and Mapping of Critical Thresholds in Europe. Status report 2001, edited by Posch, M., de Smet, P., Hettelingh, J.-P., and Downing, R., Coordination Centre for Effects, RIVM, Bilthoven, The Netherlands, 2001.

ERA5 2023: Copernicus Climate Change Service (C3S), ERA5: Fifth generation of ECMWF atmospheric reanalyses of the global climate., URL https://cds.climate.copernicus.eu/cdsapp#!/home.

Friedrich, R.: Generation of time-dependent emission data, in: Transport and Transformation of Pollutants in the Troposphere, Proceedings EUROTRAC symposium 1992, edited by et al., P. B., pp. 255–268, SPB Acad. Publish. bv., the Hague, Netherlands, 1993.

Friedrich, R. and Reis, S.: Emissions of Air Pollutants – Measurements, Calculation, Uncertainties - Results from the EUROTRAC-2 Subproject GENEMIS, Springer Publishers, Berlin, Heidelberg, Germany, 2004.

Guevara, M., Jorba, O., Tena, C., Denier van der Gon, H., Kuenen, J., Elguindi, N., Darras, S., Granier, C., and Pérez García-Pando, C.: Copernicus Atmosphere Monitoring Service TEMPOral profiles (CAMS-TEMPO): global and European emission temporal profile maps for atmospheric chemistry modelling, Earth System Science Data, 13, 367–404, doi:10.5194/essd-13-367-2021, URL https://essd.copernicus.org/articles/13/367/2021/, 2021.

Hess, M., Koepke, P., and Schult, I.: Optical properties of aerosols and clouds: The software package OPAC, Bulletin of the American meteorological society, 79, 831–844, 1998.

Intergovernmental Panel on Climate Change (IPCC): Annex III: Tables of Historical and Projected Well-mixed Greenhouse Gas Mixing Ratios and Effective Radiative Forcing of All Climate Forcers, p. 2139–2152, Cambridge University Press, doi:10.1017/9781009157896.017, 2023.

Jonson, J. E., Borken-Kleefeld, J., Simpson, D., Nyíri, A., Posch, M., and Heyes, C.: Impact of excess NOx emissions from diesel cars on air quality, public health and eutrophication in Europe, Environ. Res. Lett., 12, 094 017, URL http://stacks.iop.org/1748-9326/12/i=9/a=094017, 2017.

Kakavas, S., Pandis, S. N., and Nenes, A.: ISORROPIA-Lite: A Comprehensive Atmospheric Aerosol Thermodynamics Module for Earth System Models, Tellus B: Chemical and Physical Meteorology, doi:10.16993/tellusb.33, 2022.

Kakavas, S., Pandis, S., and Nenes, A.: Effects of Secondary Organic Aerosol Water on fine PM levels and composition over US, Atmospheric Chemistry and Physics Discussions, pp. 1–16, 2023.

Lawrence, D. M., Oleson, K. W., Flanner, M. G., Thornton, P. E., Swenson, S. C., Lawrence, P. J., Zeng, X., Yang, Z.-L., Levis, S., Sakaguchi, K., Bonan, G. B., and Slater, A. G.: Parameterization Improvements and Functional and Structural Advances in Version 4 of the Community Land Model, J. Adv. Modeling Earth Systems, 3, doi:10.1029/2011MS000045, 2011.

Metzger, S., Steil, B., Xu, L., Penner, J., and Lelieveld, J.: New representation of water activity based on a single solute specific constant to parameterize the hygroscopic growth of aerosols in atmospheric models, Atmospheric Chemistry and Physics, 12, 5429–5446, 2012.

Metzger, S., Steil, B., Abdelkader, M., Klingmüller, K., Xu, L., Penner, J. E., Fountoukis, C., Nenes, A., and Lelieveld, J.: Aerosol water parameterisation: a single parameter framework, Atmospheric Chemistry and Physics, 16, 7213–7237, 2016.

Metzger, S., Abdelkader, M., Steil, B., and Klingmüller, K.: Aerosol water parameterization: long-term evaluation and importance for climate studies, Atmospheric Chemistry and Physics, 18, 16 747–16 774, 2018.

Mills, G., Sharps, K., Simpson, D., Pleijel, H., Broberg, M., Uddling, J., Jaramillo, F., Davies, William, J., Dentener, F., Berg, M., Agrawal, M., Agrawal, S., Ainsworth, E. A., Büker, P., Emberson, L., Feng, Z., Harmens, H., Hayes, F., Kobayashi, K., Paoletti, E., and Dingenen, R.: Ozone pollution will compromise efforts to increase global wheat production, Global Change Biol., 24, 3560–3574, doi:10.1111/gcb.14157, URL https://onlinelibrary.wiley.com/doi/abs/10.1111/gcb.14157, 2018a.

Mills, G., Sharps, K., Simpson, D., Pleijel, H., Frei, M., Burkey, K., Emberson, L., Uddling, J., Broberg, M., Feng, Z., Kobayashi, K., and Agrawal, M.: Closing the global ozone yield gap: Quantification and cobenefits for multistress tolerance, Global Change Biol., doi:10.1111/gcb.14381, URL https://onlinelibrary.wiley.com/doi/abs/10.1111/gcb.14381, 2018b.

Oleson, K., Lawrence, D., Bonan, G., Flanner, M., Kluzek, E., Lawrence, P., Levis, S., Swenson, S., Thornton, P., Dai, A., Decker, M., Dickinson, R., Feddema, J., Heald, C., Hoffman, F., Lamarque, J., Mahowald, N., Niu, G., Qian, T., Randerson, J., Running, S., Sakaguchi, K., Slater, A., Stockli, R., Wang, A., Yang, Z., Zeng, X., and Zeng, X.: Technical Description of version 4.0 of the Community Land Model (CLM), NCAR Technical Note NCAR/TN-478+STR, National Center for Atmospheric Research, Boulder, CO, URL https://www.cesm.ucar.edu/models/cesm1.1/clm/CLM4_Tech_Note.pdf, iSSN Electronic Edition 2153-2400, 2010.

Olivié, D., Höglund-Isaksson, L., Klimont, Z., and von Salzen, K.: Calculation of future CH 4 mixing ratios for the ECLIPSE-v6b emission scenarios, Tech. rep., 2021.

Paglione, M., Decesari, S., Rinaldi, M., Tarozzi, L., Manarini, F., Gilardoni, S., Facchini, M. C., Fuzzi, S., Bacco, D., Trentini, A., et al.: Historical changes in seasonal aerosol acidity in the Po Valley (Italy) as inferred from fog water and aerosol measurements, Environmental science & technology, 55, 7307–7315, doi:10.1021/acs.est.1c00651, 2021.

Parajuli, S. P. and Zender, C. S.: Connecting geomorphology to dust emission through high-resolution mapping of global land cover and sediment supply, Aeolian Research, 27, 47–65, doi:https://doi.org/10.1016/j.aeolia.2017.06.002, URL https://www.sciencedirect.com/science/article/pii/S1875963717300642, 2017.

Pye, H. O. T., Nenes, A., Alexander, B., Ault, A. P., Barth, M. C., Clegg, S. L., Collett Jr., J. L., Fahey, K. M., Hennigan, C. J., Herrmann, H., Kanakidou, M., Kelly, J. T., Ku, I.-T., McNeill, V. F., Riemer, N., Schaefer, T., Shi, G., Tilgner, A., Walker, J. T., Wang, T., Weber, R., Xing, J., Zaveri, R. A., and Zuend, A.: The acidity of atmospheric particles and clouds, Atmospheric Chemistry and Physics, 20, 4809–4888, doi:10.5194/acp-20-4809-2020, URL https://acp.copernicus.org/articles/20/4809/2020/, 2020.

Simpson, D. and Darras, S.: Global soil NO emissions for Atmospheric Chemical Transport Modelling: CAMS-GLOB-SOIL v2.2, Earth System Sci. Data., in review, 1–35, doi:10.5194/essd-2021-221, URL https://essd.copernicus.org/preprints/essd-2021-221/, 2021.

Simpson, D., Benedictow, A., Berge, H., Bergström, R., Emberson, L. D., Fagerli, H., Hayman, G. D., Gauss, M., Jonson, J. E., Jenkin, M. E., Nyíri, A., Richter, C., Semeena, V. S., Tsyro, S., Tuovinen, J.-P., Valdebenito, A., and Wind, P.: The EMEP MSC-W chemical transport model – technical description, Atmos. Chem. Physics, 12, 7825–7865, doi:10.5194/acp-12-7825-2012, 2012.

Simpson, D., Tsyro, S., Wind, P., and Steensen, B. M.: EMEP model development, in: Transboundary acidification, eutrophication and ground level ozone in Europe in 2011. EMEP Status Report 1/2013, The Norwegian Meteorological Institute, Oslo, Norway, 2013.

Simpson, D., Tsyro, S., and Wind, P.: Updates to the EMEP/MSC-W model, in: Transboundary particulate matter, photo-oxidants, acidifying and eutrophying components. EMEP Status Report 1/2015, pp. 129–138, The Norwegian Meteorological Institute, Oslo, Norway, 2015.

Simpson, D., Nyíri, A., Tsyro, S., Valdebenito, Á., and Wind, P.: Updates to the EMEP/MSC-W model, in: Transboundary particulate matter, photo-oxidants, acidifying and eutrophying components. EMEP Status Report 1/2016, The Norwegian Meteorological Institute, Oslo, Norway, 2016.

Simpson, D., Bergström, R., Imhof, H., and Wind, P.: Updates to the EMEP MSC-W model, 2016-2017, in: Transboundary particulate matter, photo-oxidants, acidifying and eutrophying components. EMEP Status Report 1/2017, The Norwegian Meteorological Institute, Oslo, Norway, 2017.

Simpson, D., Wind, P., Bergström, R., Gauss, M., Tsyro, S., and Valdebenito, Á.: Updates to the EMEP/MSC-W model, 2017–2018, in: Transboundary particulate matter, photo-oxidants, acidifying and eutrophying components. EMEP Status Report 1/2018, pp. 109–116, The Norwegian Meteorological Institute, Oslo, Norway, 2018.

Simpson, D., Bergström, R., Tsyro, S., and Wind, P.: Updates to the EMEP MSC-W model, 2018-2019, in: Transboundary particulate matter, photo-oxidants, acidifying and eutrophying components. EMEP Status Report 1/2019, The Norwegian Meteorological Institute, Oslo, Norway, 2019.

Simpson, D., Bergström, R., and Wind, P.: Updates to the EMEP MSC-W model, 2019-2020, in: Transboundary particulate matter, photo-oxidants, acidifying and eutrophying components. EMEP Status Report 1/2020, The Norwegian Meteorological Institute, Oslo, Norway, 2020.

Simpson, D., Gauss, M., Mu, Q., Tsyro, S., Valdebenito, A., and Wind, P.: Updates to the EMEP MSC-W model, 2020-2021, in: Transboundary particulate matter, photo-oxidants, acidifying and eutrophying components. EMEP Status Report 1/2021, The Norwegian Meteorological Institute, Oslo, Norway, 2021.

Simpson, D., Gonzalez Fernandez, I., Segers, A., Tsyro, S., Valdebento, A., and Wind, P.: Updates to the EMEP/MSC-W model, 2021–2022, in: Transboundary particulate matter, photo-oxidants, acidifying and eutrophying components. EMEP Status Report 1/2022, pp. 133–146, The Norwegian Meteorological Institute, Oslo, Norway, available from www.emep.int, 2022.

Simpson, D., Benedictow, A., and Darras, S.: The CAMS soil emissions: CAMS-GLOB-SOIL, in: CAMS2_61 – Global and European emission inventories. Contribution to documentation of products provided by CAMS2_61, edited by Denier van der Gon, H., Gauss, M., and Granier, C., pp. 56–68, awaiting doi. Text available on request., 2023.

Skamarock, W. C. and Klemp, J. B.: A time-split nonhydrostatic atmospheric model for weather research and forecasting applications, J. Comp. Phys., 227, 3465–3485, doi:10.1016/j.jcp.2007.01.037, 2008.

Stadtler, S., Simpson, D., Schröder, S., Taraborrelli, D., Bott, A., and Schultz, M.: Ozone impacts of gas–aerosol uptake in global chemistry-transport models, Atmos. Chem. Physics, 18, 3147–3171, doi:10.5194/acp-18-3147-2018, URL `https://www.atmos-chem-phys.net/18/3147/2018/`, 2018.

Tsyro, S., Karl, M., Simpson, D., Valdebenito, A., and Wind, P.: Updates to the EMEP/MSC-W model, in: Transboundary particulate matter, photo-oxidants, acidifying and eutrophying components. EMEP Status Report 1/2014, pp. 143–146, The Norwegian Meteorological Institute, Oslo, Norway, 2014.

CHAPTER 11

Developments in the monitoring network, data quality and database infrastructure

Wenche Aas, Anne Hjellbrekke and Kjetil Tørseth

11.1 Compliance with the EMEP monitoring strategy

The monitoring obligations of EMEP were updated in 2019 and are defined by the Monitoring Strategy for 2020-2030 (UNECE (2019)).

The complexity in the monitoring program with respect to the number of variables and sites, whether parameters are at level 1 or level 2, and the required time resolution (hourly, daily, weekly), makes it challenging to assess whether a country is in compliance. CCC has developed an index to illustrate to what extent the Parties comply, how implementation compares with other countries, and how activities evolve with time.

The index is defined for level 1 parameters only, and is calculated based on the data reported in comparison with the expected. EMEP recommends one site per 50.000 km^2, but this target number is adjusted for very large countries (i.e. KZ, RU, TR and UA). The components and number of variables to be measured in accordance to the strategy are as follows: major inorganic ions in precipitation (10 variables), major inorganic components in air (13 variables), ozone (1 variable), PM mass (2 variables) and heavy metals in precipitation (7 variables). For heavy metals, the sampling frequency is weekly, and for the other components it is daily or hourly (ozone). Based on the relative implementation of the different variables, the index has been given the following relative weights: Inorganics in precipitation: 30%, inorganics in air: 30%, ozone: 20%, PM mass: 10%, heavy metals: 10%.

Figure 11.1 summarises implementation in 2021 compared to 2000, 2005 and 2010. The countries are sorted from left to right with increasing index for 2021. Slovakia, Estonia, The Netherlands, Denmark, and Switzerland have almost complete programs with an index of 90% or higher. Small countries generally comply better (due to more easily satisfying the site density requirements). Since 2010, 37% of the Parties have improved their monitoring

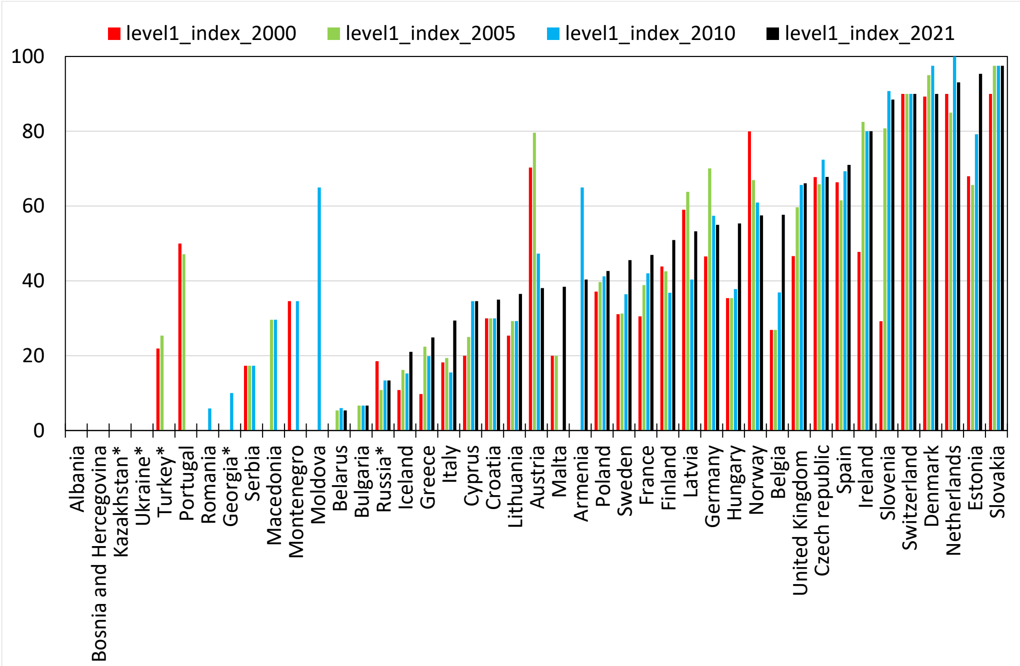

Figure 11.1: Index for implementation of the EMEP monitoring strategy, level 1 based on what has been reported for 2000, 2005, 2010 and 2021. * means adjusted land area.

programme, while 35% have a decrease. Improvements are seen in e.g. Belgium, Hungary and Sweden One Party, Malta, has reported data in 2021 and not in 2010, while Georgia, Macedonia, Moldova, Montenegro,Serbia, and Romania have stopped reporting/measuring. In addition Albania, Bosnia and Herzegovina, Kazakhstan, Portugal, Türkiye and Ukraine have not been reporting data for many years.

In Figure 2.4 in Ch 2.2, the geographical distribution of level 1 sites is shown for 2021. In large parts of Eastern Europe, implementation of the EMEP monitoring strategy is far from satisfactory.

For the level 2 parameters, an index has not been defined, but mapping the site distribution illustrate the compliance to the monitoring strategy. 57 sites from 20 different Parties reported at least one of the required aerosol component, 19 sites from 10 Parties measured volatile organic compounds(VOC), though only four sites with both hydrocarbons and carbonyls. One should note that some of these level 2 sites have been reporting data to ACTRIS (the European Research Infrastructure for the observation of Aerosol, Clouds and Trace Gases) and/or to the WMO Global Atmospheric Watch Programme (GAW) and not to EMEP. They have been included here in the overview since these observations are still comparable with those of EMEP. The sites with measurements of POPs and heavy metals are not included in this report but available in the EMEP/CCC data report (Aas et al. 2023).

Figure 11.2shows that level 2 measurements of aerosols have better spatial coverage than VOCs. 52 sites report data of either EC/OC or physical- and optical properties of aerosols. 15 of these sites report both. It should be noted that some of the EC/OC data from Spain and

France are not yet available in EBAS (http://ebas.nilu.no/) due to technical issues with e.g missing or wrong metadata, but will be included when these problems are solved.

Mineral dust is also a required level 2 component, 17 sites reported Al or Fe, which are used as tracers for mineral dust. Further, 6 sites reported measurements of organic and inorganic composition in non-refractory aerosols to EMEP and/or ACTRIS in 2021. In addition to various VOCs other oxidant precursors and gaseous short-lived climate pollutants are included as level 2 components in EMEP, i.e. methane and carbon monoxide. Data from 3 and 5 sites have reported respectively methane and carbon monoxide data to EMEP in 2021. However, there are much more measurement of these components conducted in Europe and data are available from ICOS, the European Integrated Carbon Observation System

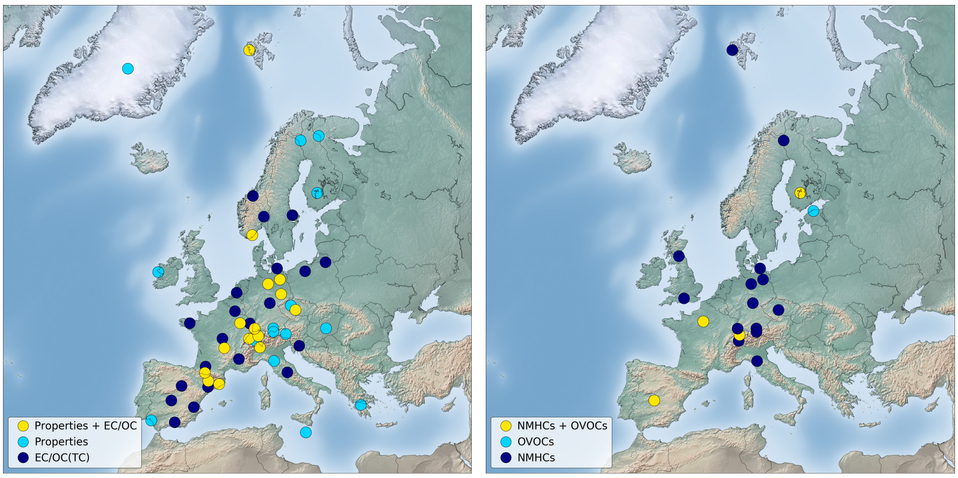

(a) Aerosols (b) VOCs

Figure 11.2: Sites measuring and reporting EMEP level 2 parameters for the year 2021.

11.2 Development in data reporting

Figureshows the status of the submission of data for 2021 and to what extent the data were reported in time. Of the 31 Parties reporting either level 1 and/or level 2 data, 58% reported within the deadline of 31 July 2022.

The time from reporting to available data in EBAS is usually 2-3 months depending on the quality of the data and the correctness of the data files submitted. Most of the Parties are now using the online data submission and validation tool (http://ebas-submit-tool.nilu.no) which has significantly improved the quality and timeliness of the reporting, though there are still a need for improvements for some Parties.

The EMEP data are extensively used. Figure 11.4 shows the access requests for EMEP data per year (Between 200-300 thousand annual datasets). The statistic counts how much data are downloaded, displayed or plotted. There was a big jump in 2013. This was the year when an automatic system for distributing all the data in EBAS to specific users was implemented. There seem to be somewhat less use of the the last couple of years. This is probably due to variations in how many global and regional studies are conducted for various assessments. I.e the work prior to the IPCC Sixth Assessment Report (AR6) included several studies were EMEP data were extensively used.

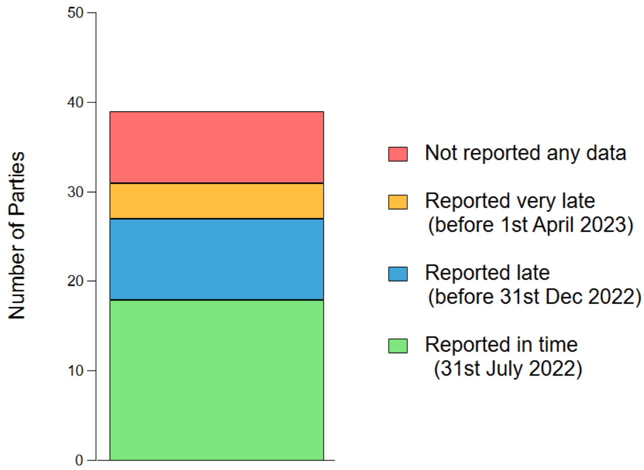

Figure 11.3: Submission of 2021 data to EMEP/CCC.

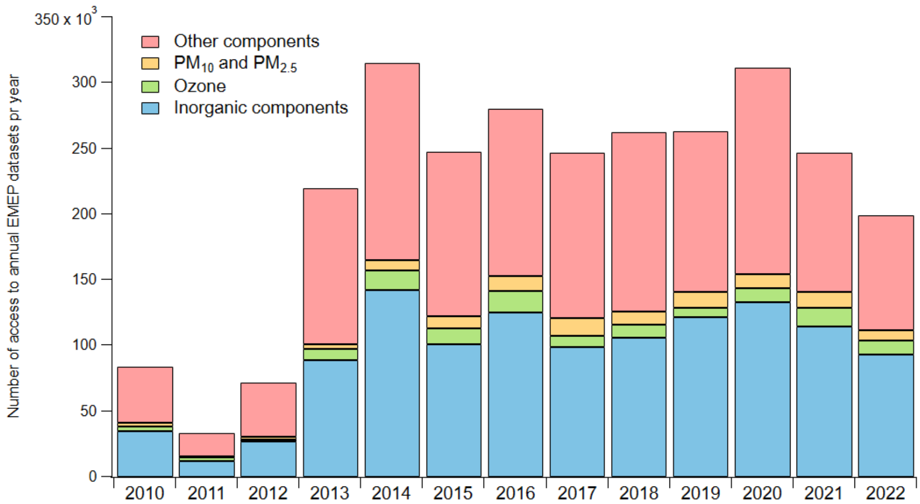

Figure 11.4: Access of EMEP data, number of annual datasets (compounds) per year.

EMEP observation data are made available through the research data infrastructure (EBAS, http://ebas.nilu.no). The most common way to access specific dataset is to search for data at https://ebas-data.nilu.no/ applying EMEP as "Framework" in the search interface. EMEP-CCC is continuously working to improve the so-called "FAIRness" of data, making them more easily Findable, Accessible, Interoperable and Reusable. Hereunder, work is ongoing in relation to vocabularies, machine readable data and metadata, persistent identificators of data (PIDs/DOIs). From 2023, EMEP data are made available under the Creative Commons CC by 4.0 license. Another achievement is that data can be accessed on the NILU THREDDS data server (https://thredds.nilu.no/thredds/catalog/ebas/catalog.html in NetCDF format. To facilitate data reporting, improved tools for data submissions are available (see e.g. services made available through the EU ATMO-ACCESS project (https://www.atmo-access.eu/virtual-access/#/ (specifically, the tool for homeless data, which also can be used for EMEP data reporting. Recently, also tutorials on data reporting has been made available on YouTube, see e.g.

https://www.youtube.com/watch?v=F18tegyCr-g&t=24s and https://www.youtube.com/watch?v=e9U6gbN3BOc.

These developments are made in harmonization with other ongoing efforts under ACTRIS, ENVRI-FAIR, WMO-GAW and other activities related to atmospheric composition data management.

References

Aas, W., Halvorsen, H. L., Hartz, W. F., Pfaffhuber, K. A., and Yttri, N.: Heavy metals and POP measurements 2021, Tech. Rep. EMEP/CCC Report 3/2023, NILU, Kjeller, Norway, 2023.

UNECE: Monitoring strategy for the Cooperative Programme for Monitoring and Evaluation of the Long-range Transmission of Air Pollutants in Europe for the period 2020–2029, Tech. Rep. ECE/EB.AIR/144/Add.1, UNECE, URL https://www.unece.org/fileadmin/DAM/env/documents/2019/AIR/EB_Decisions/Decision_2019_1.pdf, 2019.

Part IV

Appendices

APPENDIX A

National emissions for 2021 in the EMEP domain

This appendix contains the national emission data for 2021 used throughout this report for main pollutants and primary particle emissions in the new EMEP domain, which covers the geographic area between 30° N–82° N latitude and 30° W–90° E longitude. These are the emissions that are used as basis for the 2021 source-receptor calculations. Results of these source-receptor calculations are presented in Appendix C.

The land-based emissions for 2021 have been derived from the 2023 official data submissions to UNECE CLRTAP (Schindlbacher et al. 2023). This year, two different estimates for primary PM emissions have been available for the modeling: 1) EMEP emissions as prepared by CEIP based on the official data submissions for 2023, and 2) EMEP PM emissions where condensable organics from small-scale combustion are accounted for by using expert emission estimates for GNFR sector C from the CAMS-REG-AP v6.1.1 Ref2_v2.1 data set for 2021 (Simpson et al. 2022) for the following countries: Austria, Bosnia and Herzegovina, Belarus, Switzerland, Germany, Estonia, Georgia, Kazakhstan, Lithuania, Luxembourg, Montenegro, Moldova, Russian Federation and Ukraine. Please note that Kazakhstan and the Russian Federation is not fully included in the Ref2_v2.1 data set, thus only PM emissions from GNFR sector C in the areas west of 60° E longitude were replaced.

In this report (1) is referred to as EMEP and (2) is referred to as EMEPwRef2_v2.1C. National emission totals for both data sets are shown in Table A:2.

Emissions from international shipping occurring in different European seas within the EMEP domain are not reported to UNECE CLRTAP, but derived from other sources. This year's update uses the CAMS global shipping emissions (CAMS-GLOB-SHIP v3.2) (Granier et al. 2019) developed by FMI (Finnish Meteorological Institute).

Natural marine emissions of dimethyl sulfide (DMS) are calculated dynamically during the model run and vary with current meteorological conditions. SO_x emissions from passive degassing of Italian volcanoes (Etna, Stromboli and Vulcano) are reported by Italy (943.4 kt in total), while SO_x emissions from the eruption at Mt. Fagradalsfjall on the Reykjanes peninsula for the period of 19 March - 18 September 2021 are reported by Iceland (967 kt in total).

Note that emissions in this appendix are given in different units than used elsewhere in this report in order to keep consistency with the reported data.

References

Granier, C., Darras, S., Denier van der Gon, H., Doubalova, J., Elguindi, N., Galle, B., Gauss, M., Guevara, M., Jalkanen, J.-P., Kuenen, J., Liousse, C., Quack, B., Simpson, D., and Sindelarova, K.: The Copernicus Atmosphere Monitoring Service global and regional emissions (April 2019 version), doi:10.24380/d0bn-kx16, URL https://atmosphere.copernicus.eu/sites/default/files/2019-06/cams_emissions_general_document_apr2019_v7.pdf, 2019.

Schindlbacher, S., Ullrich, B., and Wankmüller, R.: Inventory review 2023. Review of emission data reported under the LRTAP Convention. Stage 1 and 2 review. Status of gridded and LPS data, EMEP/CEIP Technical Report 4/2023, CEIP Vienna, 2023.

Simpson, D., Kuenen, J., Fagerli, H., Heinesen, D., Benedictow, A., Denier van der Gon, H., Visschedijk, A., Klimont, Z., Aas, W., Lin, Y., Yttri, K. E., and Paunu, V.-V.: Revising $PM_{2.5}$ emissions from residential combustion, 2005–2019. Implications for air quality concentrations and trends, Temanord 2022:540, Nordic Council of Ministers, doi:10.6027/temanord2022-540, URL https://pub.norden.org/temanord2022-540, 2022.

Table A:1: National total emissions of main pollutants for 2021 in the EMEP domain. Unit: Gg. (Emissions of SO_x and NO_x are given as Gg(SO_2) and Gg(NO_2), respectively.)

Area/Pollutant	SO_x	NO_x	NH_3	NMVOC	CO
Albania	7	27	21	36	80
Armenia	8	44	15	17	47
Austria	11	123	66	111	523
Azerbaijan	86	351	81	381	653
Belarus	73	175	115	169	409
Belgium	23	142	68	122	290
Bosnia and Herzegovina	24	44	23	90	219
Bulgaria	51	94	43	87	267
Croatia	6	46	32	70	217
Cyprus	10	12	6	8	10
Czechia	69	159	67	187	790
Denmark	9	89	71	107	192
Estonia	12	23	10	27	109
Finland	23	105	31	83	338
France	89	756	547	1164	2707
Georgia	28	48	34	40	111
Germany	254	969	516	1044	2586
Greece	47	222	63	146	424
Hungary	14	110	77	114	345
Iceland	61	20	4	6	104
Ireland	12	100	125	115	123
Italy	79	611	351	868	2044
Kazakhstan	2247	557	110	572	1175
Kyrgyzstan	30	57	33	31	129
Latvia	4	34	16	37	102
Liechtenstein	0	0	0	0	0
Lithuania	11	52	38	48	112
Luxembourg	1	14	7	11	20
Malta	0	4	1	3	6
Moldova	4	30	20	58	122
Monaco	0	0	0	0	1
Montenegro	60	7	3	17	46
Netherlands	21	211	122	277	438
North Macedonia	89	21	8	21	53
Norway	15	141	31	145	427
Poland	392	591	289	715	2521
Portugal	39	137	61	152	285
Romania	66	214	159	234	964
Russian Federation	1337	3242	1260	3787	12255
Serbia	378	175	72	134	364
Slovakia	14	58	25	92	334
Slovenia	4	26	18	30	87
Spain	123	620	479	549	1637
Sweden	15	115	51	138	277
Switzerland	4	51	54	75	152
Tajikistan	136	65	36	111	686
Türkiye	976	823	930	413	1990
Turkmenistan	71	296	58	157	855
Ukraine	215	578	248	355	2888
United Kingdom	126	682	265	781	1274
Uzbekistan	331	334	218	415	1512
Asian areas	4390	4923	3560	5933	13356
North Africa	956	1400	427	1360	2450
Baltic Sea	9	268	0	3	26
Black Sea	13	81	0	1	7
Mediterranean Sea	177	1377	0	14	114
North Sea	21	562	0	6	61
North-East Atlantic Ocean	90	695	0	7	58
Natural marine emissions	2868	0	0	0	0
Volcanic emissions	1910	0	0	0	0
TOTAL	18137	22715	10964	21679	59374

Table A:2: National total emissions of particulate matter for 2021 in the EMEP domain. Unit: Gg.

Area/Pollutant	BC	$PM_{2.5}$ EMEP	PM_{co} EMEP	PM_{10} EMEP	$PM_{2.5}$ EMEPwRef2_v2.1C	PM_{co} EMEPwRef2_v2.1C	PM_{10} EMEPwRef2_v2.1C
Albania	2	14	3	17	14	3	17
Armenia	1	6	2	8	6	2	8
Austria	4	14	14	28	25	14	39
Azerbaijan	11	44	11	55	44	11	55
Belarus	8	58	18	75	63	18	81
Belgium	3	18	9	27	18	9	27
Bosnia and Herzegovina	6	39	7	46	49	7	56
Bulgaria	4	31	13	43	31	13	43
Croatia	4	28	23	51	28	23	51
Cyprus	0	1	1	2	1	1	2
Czechia	3	24	12	37	24	12	37
Denmark	2	12	10	22	12	10	22
Estonia	1	5	7	12	9	7	16
Finland	3	14	14	28	14	14	28
France	32	189	81	270	189	81	270
Georgia	7	22	5	27	19	8	28
Germany	10	83	101	184	106	101	207
Greece	8	36	22	57	36	22	57
Hungary	6	38	15	53	38	15	53
Iceland	0	1	1	2	1	1	2
Ireland	2	13	18	31	13	18	31
Italy	19	149	51	200	149	51	200
Kazakhstan	12	126	73	198	132	74	206
Kyrgyzstan	1	13	5	18	13	5	18
Latvia	2	18	11	29	18	11	29
Liechtenstein	0	0	0	0	0	0	0
Lithuania	1	7	18	25	15	18	34
Luxembourg	0	1	1	2	1	1	2
Malta	0	0	1	1	0	1	1
Moldova	3	20	6	26	17	4	21
Monaco	0	0	0	0	0	0	0
Montenegro	1	7	1	8	6	1	7
Netherlands	2	14	12	26	14	12	26
North Macedonia	1	9	4	13	9	4	13
Norway	3	25	10	34	25	10	34
Poland	18	297	91	388	297	91	388
Portugal	6	45	13	58	45	13	58
Romania	14	116	41	157	116	41	157
Russian Federation	44	314	428	742	428	434	862
Serbia	9	59	17	76	59	17	76
Slovakia	2	19	6	25	19	6	25
Slovenia	2	10	4	14	10	4	14
Spain	46	135	80	215	135	80	215
Sweden	2	16	19	35	16	19	35
Switzerland	1	6	8	14	6	8	14
Tajikistan	6	39	11	50	39	11	50
Türkiye	28	383	169	552	383	169	552
Turkmenistan	3	24	7	31	24	7	31
Ukraine	24	284	131	415	339	131	470
United Kingdom	16	83	61	144	83	61	144
Uzbekistan	10	70	21	90	70	21	90
Asian areas	220	1191	818	2008	1191	818	2008
North Africa	220	175	116	291	175	116	291
Baltic Sea	2	4	0	4	4	0	4
Black Sea	1	2	0	2	2	0	2
Mediterranean Sea	12	29	0	29	29	0	29
North Sea	4	9	0	9	9	0	9
North-East Atlantic Ocean	6	15	0	15	15	0	15
Natural marine emissions	0	0	0	0	0	0	0
Volcanic emissions	0	0	0	0	0	0	0
TOTAL	857	4404	2618	7021	4634	2629	7261

APPENDIX B

National emission trends

This appendix contains trends of national emission data for main pollutants and primary particle emissions for the years 1990–2021 in the EMEP domain, which covers the geographic area between 30° N–82° N latitude and 30° W–90° E longitude.

The land-based emissions for 1999–2021 have been derived from the 2023 official data submissions to UNECE CLRTAP (Schindlbacher et al. 2023). For primary PM in years 2005-2021, two different sets of emissions have been available: 1) EMEP emissions as prepared by CEIP based on the official data submissions for 2005-2021, and 2) EMEP PM emissions where condensable organics from small-scale combustion are accounted for by using expert emission estimates for GNFR sector C from the TNO Ref2 v2.1 emission data set (Simpson et al. 2022, Kuenen et al. 2022) for the following countries: Austria, Bosnia and Herzegovina, Belarus, Switzerland, Germany, Estonia, Georgia, Kazakhstan, Lithuania, Luxembourg, Montenegro, Moldova, Russian Federation and Ukraine. Please note that Kazakhstan and the Russian Federation is not fully included in the Ref2 v2.1 data set, thus only PM emissions from GNFR sector C in the areas west of 60° E longitude were replaced. In this report 1) is referred to as EMEP and 2) is referred to as EMEPwRef2_v2.1C. Please note that this year's trend calculations are based only on 2) EMEPwRef2_v2.1C emissions, which are also used in the status run (Ch 2 and in source-receptor calculations (Appendix C). These are the emissions which are shown in the emission tables in this appendix.

Emissions from international shipping occurring in different European seas within the EMEP domain are not reported to UNECE CLRTAP, but derived from other sources. This year, emissions for the sea regions for the years 2000 to 2021 are based on the most recent version of the CAMS global shipping emission data set (CAMS-GLOB-SHIP v3.2) (Granier et al. 2019, ECCAD 2019), developed by the Finish Meteorological Institute using AIS (Automatic Identification System) tracking data. Shipping emissions from 1990 to 1999 were estimated using the trend for global shipping from EDGAR v.4.3.2[1].

[1] https://edgar.jrc.ec.europa.eu

Natural marine emissions of dimethyl sulfide (DMS) are calculated dynamically during the model run and vary with current meteorological conditions.

SO_x emissions from passive degassing of Italian volcanoes (Etna, Stromboli and Vulcano) are those reported by Italy. SO_x and PM emission totals from volcanic eruptions of Icelandic volcanoes (Eyjafjallajökull in 2010, Grímsvötn in 2011, Barðarbunga in 2014-2015 and Fagradalsfjall in 2021) are reported by Iceland.

Note that emissions in this appendix are given in different units than used elsewhere in this report in order to keep consistency with the reported data.

References

ECCAD: Emissions of atmospheric Compounds and Compilation of Ancillary Data, URL https://eccad.aeris-data.fr, 2019.

Granier, C., Darras, S., Denier van der Gon, H., Doubalova, J., Elguindi, N., Galle, B., Gauss, M., Guevara, M., Jalkanen, J.-P., Kuenen, J., Liousse, C., Quack, B., Simpson, D., and Sindelarova, K.: The Copernicus Atmosphere Monitoring Service global and regional emissions (April 2019 version), doi:10.24380/d0bn-kx16, URL https://atmosphere.copernicus.eu/sites/default/files/2019-06/cams_emissions_general_document_apr2019_v7.pdf, 2019.

Kuenen, J., Visschedijk, A., Denier van der Gon, H., Klimont, Z., and Simpson, D.: Establishing a consistent PM emission inventory for small combustion at European level for 2005-2019, manuscript in preparation, 2022.

Schindlbacher, S., Ullrich, B., and Wankmüller, R.: Inventory review 2023. Review of emission data reported under the LRTAP Convention. Stage 1 and 2 review. Status of gridded and LPS data, EMEP/CEIP Technical Report 4/2023, CEIP Vienna, 2023.

Simpson, D., Kuenen, J., Fagerli, H., Heinesen, D., Benedictow, A., Denier van der Gon, H., Visschedijk, A., Klimont, Z., Aas, W., Lin, Y., Yttri, K. E., and Paunu, V.-V.: Revising $PM_{2.5}$ emissions from residential combustion, 2005–2019. Implications for air quality concentrations and trends, Temanord 2022:540, Nordic Council of Ministers, doi:10.6027/temanord2022-540, URL https://pub.norden.org/temanord2022-540, 2022.

Table B:1: National total emission trends of sulphur (1990-1999), as used for modelling at the MSC-W (Gg of SO_2 per year).

Area/Year	1990	1991	1992	1993	1994	1995	1996	1997	1998	1999
Albania	69	58	46	35	23	12	11	11	10	9
Armenia	40	33	26	19	12	5	4	4	3	2
Austria	74	71	54	53	47	47	44	40	36	34
Azerbaijan	181	188	195	201	208	215	215	215	214	214
Belarus	762	673	583	494	404	315	286	256	227	198
Belgium	365	366	357	332	290	258	248	226	212	173
Bosnia and Herzegovina	493	405	316	228	140	51	79	107	135	163
Bulgaria	1465	1242	1114	1558	1749	1698	1655	1619	1443	1090
Croatia	171	100	105	112	100	77	62	77	95	95
Cyprus	32	33	38	40	42	40	42	44	47	50
Czechia	1754	1650	1381	1302	1159	1059	914	694	425	232
Denmark	178	239	184	149	151	145	176	104	81	60
Estonia	278	252	193	156	151	117	125	118	107	99
Finland	249	206	156	138	123	105	109	101	93	92
France	1287	1378	1229	1069	995	938	925	782	813	716
Georgia	276	235	195	154	113	73	60	48	36	24
Germany	5464	3964	3237	2902	2416	1743	1476	1226	978	798
Greece	512	506	522	512	530	522	519	553	582	568
Hungary	829	832	715	719	629	613	612	625	565	557
Iceland	23	22	25	24	23	22	24	24	23	30
Ireland	183	183	171	162	177	163	150	169	180	161
Italy	1783	1672	1574	1471	1389	1322	1214	1138	1004	903
Kazakhstan	2500	2369	2239	2108	1977	1846	1777	1708	1638	1569
Kyrgyzstan	145	119	94	69	43	18	19	21	22	23
Latvia	100	82	70	66	67	49	56	44	40	32
Lithuania	218	244	121	113	110	86	84	75	91	68
Luxembourg	16	17	16	17	16	9	9	6	3	3
Malta	13	11	11	15	13	11	10	11	11	11
Moldova	149	124	104	72	57	31	32	16	12	6
Montenegro	45	46	37	35	28	3	40	37	49	47
Netherlands	198	184	174	163	150	137	125	110	101	95
North Macedonia	112	91	88	91	90	97	91	95	109	99
Norway	49	42	37	35	35	34	34	31	30	29
Poland	2553	2499	2230	2218	2114	2044	2077	1888	1703	1524
Portugal	318	308	367	310	288	322	263	275	322	331
Romania	819	700	697	700	665	696	699	614	494	475
Russian Federation	5705	5145	4585	4026	3466	2985	2911	2836	2762	2688
Serbia	577	509	491	458	419	499	502	541	549	418
Slovakia	140	135	132	127	123	121	118	117	118	115
Slovenia	203	188	194	191	185	125	116	120	110	96
Spain	2050	2071	2055	1955	1905	1767	1556	1623	1495	1509
Sweden	102	100	93	82	81	71	69	60	56	47
Switzerland	37	37	34	29	26	26	25	21	22	19
Tajikistan	64	63	44	34	24	20	14	14	13	11
Türkiye	1599	1647	1694	1742	1790	1837	1838	1839	1840	1841
Turkmenistan	83	71	73	47	46	36	35	33	37	41
Ukraine	4852	4387	3921	3456	2991	2525	2313	2100	1888	1676
United Kingdom	3580	3512	3417	3103	2814	2533	2155	1754	1753	1361
Uzbekistan	540	508	479	470	435	404	393	377	357	337
Asian areas	2241	2493	2745	2998	3250	3375	3247	3120	2992	2864
North Africa	731	733	735	737	739	743	751	758	766	774
Baltic Sea	157	163	176	171	176	182	186	190	196	205
Black Sea	34	36	39	38	39	40	41	42	43	45
Mediterranean Sea	641	668	719	702	720	744	760	778	800	840
North Sea	303	316	339	331	340	352	359	367	378	397
North-East Atlantic Ocean	410	427	459	448	460	476	485	497	511	537
Natural marine emissions	2899	2926	3042	2980	2969	2921	2898	2917	2880	2949
Volcanic emissions	8327	5119	6736	6226	5614	5266	5889	6739	6363	6000
TOTAL	58980	52398	50904	48193	45138	41971	40921	39955	37865	35353

Table B:2: National total emission trends of sulphur (2000-2010), as used for modelling at the MSC-W (Gg of SO_2 per year).

Area/Year	2000	2001	2002	2003	2004	2005	2006	2007	2008	2009	2010
Albania	9	10	12	13	14	16	14	12	10	9	7
Armenia	1	1	1	1	1	1	2	2	2	2	2
Austria	32	32	31	31	27	26	27	23	20	15	16
Azerbaijan	214	194	173	153	133	112	97	82	67	53	38
Belarus	169	151	133	116	98	80	80	79	78	78	77
Belgium	171	165	157	152	155	140	134	123	95	74	61
Bosnia and Herzegovina	192	198	205	211	218	225	235	245	256	266	277
Bulgaria	1102	1027	929	1007	966	955	948	1036	726	572	329
Croatia	60	59	63	64	52	59	55	60	54	56	35
Cyprus	48	45	45	47	40	38	31	29	22	18	22
Czechia	234	229	223	218	215	208	207	212	170	169	164
Denmark	33	30	29	35	29	26	31	28	21	16	16
Estonia	97	91	86	100	89	77	70	88	69	55	83
Finland	82	96	90	101	84	70	83	81	67	59	66
France	616	560	516	498	476	458	425	404	346	293	269
Georgia	11	10	9	7	6	5	5	6	6	6	7
Germany	643	622	559	532	492	473	474	457	451	393	403
Greece	558	574	557	566	568	585	544	529	456	400	233
Hungary	427	346	272	246	151	43	39	36	36	30	30
Iceland	35	39	41	38	33	40	40	59	75	69	74
Ireland	144	142	107	83	73	73	61	55	46	33	27
Italy	756	705	623	526	489	411	389	348	294	243	224
Kazakhstan	1499	1565	1631	1696	1762	1828	1908	1989	2070	2150	2231
Kyrgyzstan	25	25	25	25	25	26	28	31	33	36	38
Latvia	18	14	13	11	9	9	8	8	7	7	4
Lithuania	40	42	38	25	26	28	26	22	19	19	18
Luxembourg	4	4	3	3	3	3	3	2	2	2	2
Malta	9	12	11	12	12	12	12	13	10	7	8
Moldova	4	4	4	6	5	5	5	3	5	5	4
Montenegro	51	38	59	55	52	45	54	39	57	29	53
Netherlands	79	80	72	67	70	68	68	65	54	40	36
North Macedonia	106	108	96	95	96	95	93	99	77	103	86
Norway	27	25	23	23	25	23	21	19	20	15	18
Poland	1325	1282	1211	1169	1148	1129	1199	1110	877	758	825
Portugal	295	277	277	185	188	189	165	157	104	72	62
Romania	492	509	509	588	558	603	649	517	522	442	355
Russian Federation	2623	2605	2588	2570	2553	2527	2387	2247	2107	1981	1883
Serbia	463	459	484	508	518	444	460	469	480	432	401
Slovakia	117	123	99	102	93	86	85	69	68	63	68
Slovenia	93	63	63	60	50	40	17	14	12	10	10
Spain	1388	1330	1474	1222	1253	1207	1076	1047	385	286	245
Sweden	44	41	41	41	36	34	34	31	29	26	28
Switzerland	16	17	15	15	15	14	13	12	12	10	10
Tajikistan	9	13	15	15	18	19	24	37	41	46	53
Türkiye	1842	1805	1768	1731	1694	1657	1595	1532	1470	1407	1345
Turkmenistan	39	38	39	42	41	43	43	54	55	55	70
Ukraine	1464	1416	1369	1321	1273	1226	1279	1333	1386	1290	1216
United Kingdom	1296	1224	1103	1074	904	785	743	651	551	457	465
Uzbekistan	323	318	314	309	306	301	301	282	282	282	264
Asian areas	2842	2873	2904	2935	2967	3132	3297	3463	3628	3759	3823
North Africa	790	811	832	853	874	890	906	923	939	958	983
Baltic Sea	221	218	215	212	209	204	144	117	102	104	89
Black Sea	51	50	49	48	48	47	46	45	40	41	43
Mediterranean Sea	925	909	894	880	869	852	839	825	718	740	650
North Sea	420	413	406	400	395	387	287	240	215	219	181
North-East Atlantic Ocean	560	550	541	532	526	516	508	499	433	445	420
Natural marine emissions	2364	2318	2380	2232	2298	2338	2376	2352	2386	2356	2314
Volcanic emissions	5746	4279	5300	3556	2701	1205	1308	840	973	950	1070
TOTAL	33243	31185	31727	29363	28028	26137	25999	25149	23532	22507	21832

Table B:3: National total emission trends of sulphur (2011-2021), as used for modelling at the MSC-W (Gg of SO_2 per year).

Area/Year	2011	2012	2013	2014	2015	2016	2017	2018	2019	2020	2021
Albania	6	6	5	5	4	5	5	6	6	6	7
Armenia	2	2	3	3	3	3	4	5	6	6	8
Austria	15	15	14	15	14	13	13	12	11	10	11
Azerbaijan	43	49	54	59	65	68	72	75	79	77	86
Belarus	73	69	65	61	58	60	63	65	68	68	73
Belgium	53	47	43	41	41	34	32	32	30	24	23
Bosnia and Herzegovina	280	283	286	290	293	243	193	143	93	42	24
Bulgaria	655	323	163	154	135	94	93	79	72	69	51
Croatia	29	24	17	14	16	15	12	10	8	6	6
Cyprus	21	16	13	17	13	16	16	17	16	12	10
Czechia	168	160	145	134	129	115	110	97	80	67	69
Denmark	14	13	13	11	10	10	10	11	9	9	9
Estonia	73	43	42	44	36	35	39	31	19	11	12
Finland	60	50	48	44	41	40	35	33	30	23	23
France	219	216	199	157	150	131	127	121	98	89	89
Georgia	7	7	7	7	7	11	14	18	21	24	28
Germany	388	369	357	336	334	310	302	290	261	241	254
Greece	160	143	122	104	102	81	90	86	80	49	47
Hungary	34	30	29	26	24	23	28	23	17	16	14
Iceland	82	85	70	64	58	49	47	52	56	51	61
Ireland	25	23	23	17	16	15	15	14	11	11	12
Italy	202	181	150	134	128	123	119	113	112	85	79
Kazakhstan	2213	2195	2177	2159	2141	2158	2175	2192	2210	2149	2247
Kyrgyzstan	42	46	49	53	56	52	48	43	39	33	30
Latvia	4	4	4	4	4	3	4	4	4	4	4
Lithuania	19	17	15	13	15	15	13	13	12	11	11
Luxembourg	1	2	2	1	1	1	1	1	1	1	1
Malta	8	8	5	5	2	2	1	0	0	0	0
Moldova	5	4	4	4	4	3	4	4	5	4	4
Montenegro	60	56	59	58	62	54	56	64	62	66	60
Netherlands	35	35	31	30	31	29	27	25	23	20	21
North Macedonia	104	91	82	83	75	63	55	60	115	93	89
Norway	18	17	17	17	17	15	15	16	16	15	15
Poland	776	747	702	654	639	518	506	480	396	385	392
Portugal	57	52	48	43	45	45	46	45	44	38	39
Romania	327	257	208	181	149	98	78	71	86	61	66
Russian Federation	1870	1797	1764	1749	1739	1790	1586	1524	1478	1392	1337
Serbia	456	420	434	343	362	373	370	348	397	418	378
Slovakia	67	57	52	44	67	26	28	20	16	13	14
Slovenia	11	11	10	8	6	5	5	5	4	4	4
Spain	282	285	222	243	260	217	220	199	151	128	123
Sweden	25	25	22	20	17	17	17	17	16	15	15
Switzerland	8	9	8	7	6	5	5	5	4	4	4
Tajikistan	55	30	25	19	25	86	109	114	121	124	136
Türkiye	1317	1290	1262	1235	1207	1169	1130	1091	1052	1022	976
Turkmenistan	73	69	62	68	74	66	63	60	64	65	71
Ukraine	1320	1339	1422	922	854	948	801	654	508	350	215
United Kingdom	431	480	416	341	268	197	190	176	155	133	126
Uzbekistan	255	279	287	283	267	242	251	277	295	301	331
Asian areas	3886	3950	4013	3994	3933	3871	3810	3749	3972	4061	4390
North Africa	1008	1033	1058	1046	1017	987	957	928	954	886	956
Baltic Sea	77	76	74	75	9	9	9	9	10	8	9
Black Sea	42	42	41	42	41	40	42	41	44	12	13
Mediterranean Sea	700	692	679	627	669	667	695	706	709	138	177
North Sea	160	158	155	164	31	31	31	31	30	21	21
North-East Atlantic Ocean	452	447	439	459	485	475	493	508	490	91	90
Natural marine emissions	2446	2368	2434	2250	2454	2390	2394	2440	2926	3003	2868
Volcanic emissions	1243	943	943	11823	2070	943	943	943	943	943	1910
TOTAL	22464	21483	21097	30804	20778	19107	18620	18198	18534	17011	18137

Table B:4: National total emission trends of nitrogen oxides (1990-1999), as used for modelling at the MSC-W (Gg of NO_2 per year).

Area/Year	1990	1991	1992	1993	1994	1995	1996	1997	1998	1999
Albania	20	18	17	16	15	14	15	16	17	18
Armenia	88	74	60	45	31	16	16	17	17	17
Austria	219	228	217	208	200	199	217	203	215	207
Azerbaijan	186	171	157	142	128	113	110	108	105	102
Belarus	422	386	351	315	280	244	240	236	231	227
Belgium	422	421	422	417	416	410	395	381	383	357
Bosnia and Herzegovina	71	60	49	38	28	17	21	25	29	33
Bulgaria	306	232	202	210	206	211	207	175	174	158
Croatia	106	80	75	75	77	79	84	87	89	93
Cyprus	18	18	20	21	21	21	21	22	22	22
Czechia	760	721	677	552	459	391	373	345	328	303
Denmark	294	344	300	299	301	282	316	269	249	231
Estonia	75	67	45	41	45	48	52	52	50	45
Finland	307	304	288	293	294	273	278	272	258	253
France	2182	2227	2212	2099	2020	1982	1956	1889	1914	1875
Georgia	91	72	59	51	39	37	34	30	28	28
Germany	2843	2616	2466	2361	2229	2169	2085	2010	1981	1944
Greece	409	409	416	408	415	402	409	424	451	445
Hungary	247	216	195	194	193	191	194	197	197	201
Iceland	29	28	30	31	31	32	33	33	31	31
Ireland	169	171	180	172	172	171	174	169	178	179
Italy	2124	2191	2230	2127	2027	1988	1915	1837	1723	1628
Kazakhstan	1158	724	673	588	503	579	439	408	383	324
Kyrgyzstan	136	115	94	73	52	30	30	30	29	29
Latvia	99	95	78	68	58	53	53	50	46	45
Lithuania	151	159	99	73	68	74	76	82	80	73
Luxembourg	41	47	47	45	41	35	35	35	35	38
Malta	7	7	7	9	9	8	8	9	9	9
Moldova	115	96	71	55	42	37	35	31	27	20
Montenegro	1	1	1	1	1	1	1	1	1	1
Netherlands	680	669	655	637	596	581	570	542	522	515
North Macedonia	45	38	39	41	37	39	39	38	43	40
Norway	197	190	194	200	204	216	225	233	235	227
Poland	1121	1111	1111	1117	1101	1080	1112	1055	960	928
Portugal	260	274	296	286	285	297	279	281	294	306
Romania	474	400	412	372	373	376	421	403	354	307
Russian Federation	6090	5705	5321	4936	4552	4189	4086	3983	3879	3776
Serbia	183	168	157	130	137	152	159	169	169	132
Slovakia	136	120	112	110	111	112	112	112	112	108
Slovenia	75	70	69	73	76	75	77	78	68	61
Spain	1311	1351	1370	1308	1314	1320	1306	1327	1324	1327
Sweden	289	293	279	266	269	258	253	241	232	225
Switzerland	144	141	135	123	120	116	110	106	106	105
Tajikistan	42	37	28	20	13	12	10	11	10	9
Türkiye	831	859	887	915	944	972	983	994	1006	1017
Turkmenistan	177	132	117	108	117	114	109	109	117	136
Ukraine	2358	2155	1952	1750	1547	1344	1276	1207	1138	1069
United Kingdom	3049	2969	2927	2786	2731	2600	2520	2338	2260	2148
Uzbekistan	403	419	408	389	353	323	349	369	382	385
Asian areas	1936	2055	2175	2294	2414	2504	2537	2569	2601	2634
North Africa	549	564	579	594	608	624	642	660	678	696
Baltic Sea	263	274	294	287	295	305	311	319	328	344
Black Sea	74	77	83	81	83	86	88	90	92	97
Mediterranean Sea	1160	1209	1300	1269	1302	1347	1374	1407	1448	1519
North Sea	600	625	672	656	673	696	710	727	748	785
North-East Atlantic Ocean	773	805	866	845	868	897	915	937	964	1012
Natural marine emissions	0	0	0	0	0	0	0	0	0	0
Volcanic emissions	0	0	0	0	0	0	0	0	0	0
TOTAL	36318	35011	34176	32623	31527	30745	30399	29749	29351	28843

Table B:5: National total emission trends of nitrogen oxides (2000-2010), as used for modelling at the MSC-W (Gg of NO_2 per year).

Area/Year	2000	2001	2002	2003	2004	2005	2006	2007	2008	2009	2010
Albania	19	22	25	27	30	33	32	32	31	31	30
Armenia	17	17	18	18	19	19	21	24	26	28	30
Austria	213	223	231	242	242	248	238	232	219	205	206
Azerbaijan	99	105	110	116	121	127	130	133	136	139	142
Belarus	223	223	224	224	224	225	226	228	230	231	233
Belgium	359	348	338	334	345	329	315	306	280	249	250
Bosnia and Herzegovina	37	42	47	52	56	61	64	66	69	72	74
Bulgaria	164	163	177	186	184	187	164	162	163	153	138
Croatia	88	88	91	90	88	86	86	88	85	77	69
Cyprus	22	23	22	22	22	22	22	21	20	20	19
Czechia	311	309	302	305	305	302	293	292	274	258	255
Denmark	218	215	212	222	207	199	199	185	169	150	145
Estonia	44	49	48	49	45	42	40	45	42	36	42
Finland	241	245	243	249	237	208	224	211	194	177	187
France	1816	1776	1732	1682	1636	1587	1498	1429	1351	1281	1236
Georgia	28	24	24	25	25	27	29	33	30	34	36
Germany	1866	1810	1750	1708	1664	1616	1631	1585	1530	1439	1459
Greece	431	456	452	461	465	483	483	481	455	435	364
Hungary	189	189	181	185	183	179	172	168	162	151	148
Iceland	31	28	30	29	30	27	26	28	26	26	24
Ireland	181	180	173	172	174	175	171	167	152	127	120
Italy	1506	1476	1419	1398	1349	1290	1239	1173	1056	970	942
Kazakhstan	405	374	397	431	478	562	525	532	503	517	629
Kyrgyzstan	28	29	30	31	32	33	38	43	48	52	57
Latvia	43	47	45	47	47	46	48	48	44	41	42
Lithuania	63	63	64	62	62	64	63	64	63	54	57
Luxembourg	41	44	44	46	55	57	51	46	43	38	39
Malta	8	8	8	9	9	10	10	10	10	8	9
Moldova	19	21	22	23	26	26	25	25	26	26	29
Montenegro	1	3	4	6	7	9	9	10	10	10	11
Netherlands	496	482	466	461	450	440	433	417	406	367	360
North Macedonia	44	41	41	36	37	35	35	38	34	35	36
Norway	214	213	207	209	208	208	208	212	205	195	200
Poland	869	843	808	818	832	858	872	863	836	819	845
Portugal	301	298	304	279	282	283	262	252	234	221	204
Romania	316	330	336	341	344	333	333	313	308	262	248
Russian Federation	3691	3672	3652	3633	3613	3586	3478	3370	3262	3153	3042
Serbia	147	152	162	165	180	165	167	173	171	161	148
Slovakia	110	112	105	103	103	106	99	99	100	90	88
Slovenia	59	59	59	55	54	55	55	54	58	49	48
Spain	1335	1302	1325	1332	1346	1322	1292	1293	1105	989	936
Sweden	222	212	205	200	197	193	192	186	178	165	170
Switzerland	103	100	95	94	93	94	93	91	91	87	84
Tajikistan	8	9	9	9	10	10	11	13	12	12	12
Türkiye	1028	1024	1020	1017	1013	1009	1012	1014	1017	1019	1022
Turkmenistan	144	142	153	167	177	188	184	193	190	195	210
Ukraine	1000	996	993	990	986	983	957	931	905	878	852
United Kingdom	2065	2009	1914	1877	1819	1795	1732	1655	1481	1296	1269
Uzbekistan	398	398	388	374	362	351	350	336	335	326	307
Asian areas	2703	2791	2878	2966	3053	3186	3318	3451	3583	3702	3795
North Africa	721	749	776	804	832	881	930	979	1028	1075	1120
Baltic Sea	366	360	355	349	343	336	330	323	282	286	284
Black Sea	112	110	108	106	105	102	100	98	88	88	91
Mediterranean Sea	1685	1645	1613	1583	1554	1517	1479	1446	1261	1270	1217
North Sea	824	807	792	778	767	749	734	720	648	647	641
North-East Atlantic Ocean	1055	1027	1007	986	968	942	919	898	783	786	758
Natural marine emissions	0	0	0	0	0	0	0	0	0	0	0
Volcanic emissions	0	0	0	0	0	0	0	0	0	0	0
TOTAL	28730	28481	28232	28185	28095	28009	27647	27286	26048	25207	25011

Table B:6: National total emission trends of nitrogen oxides (2011-2021), as used for modelling at the MSC-W (Gg of NO_2 per year).

Area/Year	2011	2012	2013	2014	2015	2016	2017	2018	2019	2020	2021
Albania	30	30	30	30	30	30	29	29	28	26	27
Armenia	32	34	36	38	40	40	41	42	42	40	44
Austria	198	193	194	187	184	177	167	155	146	124	123
Azerbaijan	150	158	165	173	181	209	238	266	294	300	351
Belarus	230	228	225	223	220	213	205	198	190	178	175
Belgium	232	220	211	200	201	189	177	170	159	139	142
Bosnia and Herzegovina	73	71	69	68	66	62	59	55	51	46	44
Bulgaria	156	129	113	118	117	111	98	95	92	87	94
Croatia	66	58	57	54	54	54	55	50	49	46	46
Cyprus	21	21	15	16	14	14	13	13	14	12	12
Czechia	241	230	217	212	206	197	194	187	174	156	159
Denmark	137	127	122	113	109	109	107	101	97	89	89
Estonia	40	37	37	35	31	31	32	31	25	23	23
Finland	172	162	159	151	139	135	131	127	120	106	105
France	1179	1153	1134	1058	1035	986	956	902	849	737	756
Georgia	38	39	41	47	49	49	47	53	48	47	48
Germany	1438	1434	1437	1394	1368	1334	1279	1191	1107	976	969
Greece	326	286	274	269	263	262	268	259	250	222	222
Hungary	139	132	128	126	128	121	122	121	115	108	110
Iceland	22	22	21	21	22	20	20	21	20	18	20
Ireland	108	110	112	111	113	114	111	112	104	96	100
Italy	904	857	787	765	728	716	674	678	662	596	611
Kazakhstan	635	670	682	732	728	736	771	803	682	646	557
Kyrgyzstan	61	65	68	72	76	73	69	66	62	56	57
Latvia	39	40	39	38	38	36	36	37	35	33	34
Lithuania	56	56	53	56	57	57	56	56	55	53	52
Luxembourg	40	38	35	33	29	26	23	21	19	15	14
Malta	8	9	7	7	6	5	5	4	5	4	4
Moldova	30	28	30	30	29	32	34	36	37	34	30
Montenegro	10	10	9	9	8	8	8	8	8	7	7
Netherlands	347	327	311	285	282	267	258	253	238	216	211
North Macedonia	39	36	29	26	25	25	23	23	23	20	21
Norway	197	193	190	188	180	171	166	163	155	146	141
Poland	824	787	748	729	721	730	768	689	641	605	591
Portugal	187	174	170	167	170	162	165	160	155	135	137
Romania	259	251	230	222	221	211	220	222	218	205	214
Russian Federation	3075	3125	3145	3147	3124	3149	3179	3153	3182	3118	3242
Serbia	162	152	152	126	145	186	184	173	169	176	175
Slovakia	81	77	69	66	68	64	63	62	59	56	58
Slovenia	47	46	43	39	35	35	34	33	30	26	26
Spain	936	882	813	794	812	762	754	742	679	599	620
Sweden	163	156	153	151	147	144	139	134	125	117	115
Switzerland	80	80	81	77	73	71	67	64	61	53	51
Tajikistan	12	21	23	32	32	44	53	60	62	60	65
Türkiye	1035	1048	1061	1074	1087	1043	999	955	911	863	823
Turkmenistan	214	219	231	236	255	263	270	273	281	272	296
Ukraine	819	786	753	720	687	669	651	633	614	579	578
United Kingdom	1180	1203	1141	1065	1022	933	894	851	791	683	682
Uzbekistan	315	313	311	308	300	298	300	308	317	307	334
Asian areas	3888	3980	4073	4119	4140	4161	4183	4205	4455	4554	4923
North Africa	1165	1209	1254	1282	1301	1320	1339	1359	1398	1297	1400
Baltic Sea	291	284	275	269	268	267	268	274	288	250	268
Black Sea	88	86	83	85	83	79	83	80	86	78	81
Mediterranean Sea	1284	1250	1210	1106	1170	1133	1168	1176	1212	1027	1377
North Sea	647	633	614	627	645	621	629	624	601	564	562
North-East Atlantic Ocean	794	773	746	770	810	770	784	802	780	683	695
Natural marine emissions	0	0	0	0	0	0	0	0	0	0	0
Volcanic emissions	0	0	0	0	0	0	0	0	0	0	0
TOTAL	24942	24735	24413	24094	24076	23726	23669	23361	23073	21710	22715

Table B:7: National total emission trends of ammonia (1990-1999), as used for modelling at the MSC-W (Gg of NH_3 per year).

Area/Year	1990	1991	1992	1993	1994	1995	1996	1997	1998	1999
Albania	16	17	17	18	19	19	19	19	18	18
Armenia	11	10	10	10	10	9	9	9	9	9
Austria	69	70	68	68	68	68	67	67	67	66
Azerbaijan	45	44	44	43	42	42	43	44	45	47
Belarus	156	149	142	135	128	121	117	113	109	105
Belgium	105	106	106	106	106	106	104	102	100	97
Bosnia and Herzegovina	22	20	18	16	13	11	12	12	13	14
Bulgaria	113	94	99	71	63	52	53	50	42	46
Croatia	50	50	46	41	40	38	39	41	37	39
Cyprus	6	6	6	7	7	7	7	7	7	7
Czechia	136	125	112	100	91	87	89	87	84	83
Denmark	141	136	132	129	125	117	113	112	112	106
Estonia	21	19	16	12	11	10	8	9	9	8
Finland	36	34	33	34	35	35	36	37	37	39
France	675	672	666	658	650	656	661	657	656	655
Georgia	53	50	44	39	37	40	44	44	41	45
Germany	726	649	648	641	620	620	630	622	631	629
Greece	91	88	86	80	76	80	81	80	80	79
Hungary	138	112	95	85	81	81	80	79	82	83
Iceland	5	5	5	5	5	4	5	4	5	5
Ireland	111	113	116	115	116	117	121	124	128	126
Italy	469	475	463	468	458	454	448	459	459	465
Kazakhstan	151	149	147	145	144	142	129	116	103	90
Kyrgyzstan	31	30	28	27	26	24	24	24	24	24
Latvia	33	32	25	18	16	16	16	15	15	13
Lithuania	85	83	62	48	43	41	41	41	39	37
Luxembourg	6	6	6	6	6	6	7	7	7	7
Malta	2	2	2	2	2	2	2	2	2	2
Moldova	49	46	40	34	33	31	30	26	28	26
Montenegro	6	6	6	6	6	6	6	6	6	6
Netherlands	344	358	295	294	254	218	222	212	197	195
North Macedonia	16	15	15	15	15	15	14	14	13	13
Norway	31	31	32	30	29	30	30	29	30	31
Poland	495	433	410	380	382	375	354	358	366	362
Portugal	73	73	72	71	70	70	71	70	68	71
Romania	320	262	230	227	213	216	216	202	196	185
Russian Federation	2201	2069	1936	1803	1671	1544	1471	1399	1326	1254
Serbia	126	123	111	112	104	115	121	120	115	111
Slovakia	58	50	43	38	39	38	38	41	35	33
Slovenia	24	22	23	22	22	22	21	21	21	21
Spain	489	487	491	471	494	492	538	534	563	551
Sweden	60	58	59	61	62	61	61	62	62	60
Switzerland	69	68	67	66	66	66	64	62	62	62
Tajikistan	35	33	32	28	26	24	24	25	24	22
Türkiye	616	638	815	664	633	606	623	603	643	661
Turkmenistan	38	36	33	35	34	33	34	32	35	39
Ukraine	644	602	561	519	477	436	403	370	337	304
United Kingdom	306	310	296	292	298	292	299	309	309	302
Uzbekistan	203	189	176	162	147	134	131	132	130	126
Asian areas	1872	1954	2035	2116	2198	2266	2310	2354	2397	2441
North Africa	244	248	252	256	260	267	279	291	303	316
Baltic Sea	0	0	0	0	0	0	0	0	0	0
Black Sea	0	0	0	0	0	0	0	0	0	0
Mediterranean Sea	0	0	0	0	0	0	0	0	0	0
North Sea	0	0	0	0	0	0	0	0	0	0
North-East Atlantic Ocean	0	0	0	0	0	0	0	0	0	0
Natural marine emissions	0	0	0	0	0	0	0	0	0	0
Volcanic emissions	0	0	0	0	0	0	0	0	0	0
TOTAL	11823	11461	11273	10828	10570	10361	10365	10254	10225	10134

Table B:8: National total emission trends of ammonia (2000-2010), as used for modelling at the MSC-W (Gg of NH_3 per year).

Area/Year	2000	2001	2002	2003	2004	2005	2006	2007	2008	2009	2010
Albania	18	17	17	17	17	17	17	17	17	17	17
Armenia	9	10	10	10	11	11	11	12	12	13	13
Austria	64	64	63	63	63	63	63	64	64	65	65
Azerbaijan	50	51	54	58	61	63	66	66	67	69	70
Belarus	101	100	99	98	97	97	98	100	101	103	104
Belgium	95	93	90	86	81	80	79	76	74	74	75
Bosnia and Herzegovina	14	14	15	15	15	16	16	16	17	17	17
Bulgaria	45	41	42	43	44	43	39	39	38	38	37
Croatia	39	42	40	41	43	41	40	40	43	34	36
Cyprus	7	7	7	7	7	7	7	7	6	6	6
Czechia	80	80	80	78	74	74	73	73	72	68	66
Denmark	104	101	98	97	96	93	90	89	88	84	85
Estonia	8	9	8	9	9	10	11	10	11	10	11
Finland	36	37	38	39	39	40	39	39	38	37	38
France	669	663	649	633	627	627	614	613	626	617	606
Georgia	44	46	48	49	47	47	41	37	37	37	37
Germany	633	637	625	622	605	612	607	615	618	622	625
Greece	77	76	75	75	77	75	73	74	70	66	71
Hungary	87	86	86	87	85	80	80	80	73	70	70
Iceland	5	5	4	4	4	4	5	5	5	5	5
Ireland	121	121	121	121	119	120	122	115	117	117	115
Italy	457	456	445	444	439	421	417	418	408	392	379
Kazakhstan	76	80	84	88	92	96	98	99	101	102	104
Kyrgyzstan	24	24	25	25	26	26	27	28	28	29	30
Latvia	14	15	15	15	15	15	15	15	15	16	15
Lithuania	34	34	36	37	38	39	39	40	38	39	38
Luxembourg	7	7	6	6	6	6	6	6	6	6	6
Malta	2	2	2	2	2	2	2	2	2	2	2
Moldova	24	24	25	24	23	24	24	19	19	20	21
Montenegro	6	6	6	6	6	4	4	4	4	4	4
Netherlands	173	167	160	157	157	154	157	153	141	137	134
North Macedonia	13	13	12	12	12	11	11	11	11	10	11
Norway	30	30	31	32	32	32	32	32	32	32	32
Poland	350	338	330	316	306	323	326	333	322	310	300
Portugal	73	70	68	65	66	62	61	61	60	58	57
Romania	176	170	176	179	188	194	194	194	192	186	169
Russian Federation	1195	1192	1189	1186	1183	1190	1160	1129	1098	1068	1039
Serbia	107	102	106	103	110	107	105	106	96	101	92
Slovakia	33	34	36	34	31	32	29	30	29	28	28
Slovenia	22	22	23	22	20	21	21	21	20	20	20
Spain	573	574	566	572	544	509	504	510	460	457	456
Sweden	60	59	59	59	59	57	56	56	57	54	54
Switzerland	62	62	61	60	59	60	60	61	60	58	58
Tajikistan	21	23	24	25	26	28	28	29	32	35	34
Türkiye	645	585	578	601	620	637	649	616	580	582	592
Turkmenistan	41	47	56	62	65	66	68	64	66	64	63
Ukraine	271	262	252	243	233	224	227	230	233	236	239
United Kingdom	296	293	288	283	288	281	277	274	257	260	262
Uzbekistan	124	129	134	139	148	158	163	173	175	181	189
Asian areas	2501	2569	2637	2705	2773	2828	2883	2937	2992	3023	3007
North Africa	326	336	346	356	367	368	369	370	371	375	384
Baltic Sea	0	0	0	0	0	0	0	0	0	0	0
Black Sea	0	0	0	0	0	0	0	0	0	0	0
Mediterranean Sea	0	0	0	0	0	0	0	0	0	0	0
North Sea	0	0	0	0	0	0	0	0	0	0	0
North-East Atlantic Ocean	0	0	0	0	0	0	0	0	0	0	0
Natural marine emissions	0	0	0	0	0	0	0	0	0	0	0
Volcanic emissions	0	0	0	0	0	0	0	0	0	0	0
TOTAL	10043	10027	10047	10112	10158	10195	10201	10210	10100	10053	9989

Table B:9: National total emission trends of ammonia (2011-2021), as used for modelling at the MSC-W (Gg of NH_3 per year).

Area/Year	2011	2012	2013	2014	2015	2016	2017	2018	2019	2020	2021
Albania	17	17	17	17	17	18	19	19	20	20	21
Armenia	13	14	14	14	14	14	15	15	15	15	15
Austria	65	65	65	65	66	67	68	67	66	66	66
Azerbaijan	71	72	73	74	75	76	77	78	79	80	81
Belarus	105	106	107	108	109	110	111	112	113	114	115
Belgium	74	74	73	71	72	72	70	70	68	68	68
Bosnia and Herzegovina	17	18	18	19	19	20	20	21	22	22	23
Bulgaria	37	38	39	40	41	43	43	43	44	42	43
Croatia	37	36	29	28	31	29	32	33	31	32	32
Cyprus	6	6	6	6	5	5	5	5	5	6	6
Czechia	66	67	70	72	79	79	77	74	70	67	67
Denmark	82	80	78	78	79	80	81	80	76	79	71
Estonia	11	11	11	11	11	10	10	10	10	10	10
Finland	37	37	37	38	36	35	34	34	33	32	31
France	610	605	593	600	603	603	602	599	580	560	547
Georgia	37	40	43	37	37	36	34	33	33	34	34
Germany	628	633	640	647	644	637	619	591	570	530	516
Greece	70	68	68	65	64	64	64	63	63	64	63
Hungary	71	70	72	73	76	77	78	77	76	77	77
Iceland	5	4	4	5	5	5	5	5	4	4	4
Ireland	111	117	118	115	120	125	130	136	126	124	125
Italy	377	387	370	357	357	370	363	351	349	362	351
Kazakhstan	105	105	106	106	107	108	108	109	109	109	110
Kyrgyzstan	30	30	31	31	31	31	32	32	32	33	33
Latvia	15	16	16	16	16	16	16	16	16	16	16
Lithuania	37	37	37	39	40	39	39	38	39	40	38
Luxembourg	6	6	6	6	6	6	6	6	6	7	7
Malta	1	1	1	1	1	1	1	1	1	1	1
Moldova	20	18	17	19	17	18	21	22	21	20	20
Montenegro	3	3	4	4	4	4	4	3	3	3	3
Netherlands	132	126	124	127	129	130	132	130	125	123	122
North Macedonia	11	10	10	10	10	10	10	10	9	9	8
Norway	31	31	32	31	31	31	31	32	30	30	31
Poland	299	290	295	290	289	291	304	315	302	310	289
Portugal	57	56	55	57	58	58	59	59	60	61	61
Romania	168	163	165	165	170	166	164	162	159	156	159
Russian Federation	1063	1092	1096	1111	1153	1169	1191	1194	1244	1250	1260
Serbia	92	96	92	87	86	85	85	79	74	80	72
Slovakia	28	29	29	29	28	29	31	31	30	27	25
Slovenia	19	19	19	19	19	19	19	19	19	18	18
Spain	447	444	447	466	471	471	488	484	478	491	479
Sweden	54	53	54	54	54	52	53	53	52	52	51
Switzerland	57	56	56	56	55	55	55	54	54	53	54
Tajikistan	34	35	35	35	36	35	35	35	35	36	36
Türkiye	619	683	722	731	704	734	782	799	824	878	930
Turkmenistan	61	60	58	58	57	54	55	57	57	58	58
Ukraine	239	240	241	241	242	243	244	245	246	247	248
United Kingdom	261	260	256	267	269	271	274	270	269	260	265
Uzbekistan	193	196	200	202	205	211	213	213	215	217	218
Asian areas	2992	2976	2960	2967	2985	3004	3022	3040	3221	3293	3560
North Africa	394	403	412	415	415	415	415	414	426	396	427
Baltic Sea	0	0	0	0	0	0	0	0	0	0	0
Black Sea	0	0	0	0	0	0	0	0	0	0	0
Mediterranean Sea	0	0	0	0	0	0	0	0	0	0	0
North Sea	0	0	0	0	0	0	0	0	0	0	0
North-East Atlantic Ocean	0	0	0	0	0	0	0	0	0	0	0
Natural marine emissions	0	0	0	0	0	0	0	0	0	0	0
Volcanic emissions	0	0	0	0	0	0	0	0	0	0	0
TOTAL	10017	10100	10118	10181	10250	10332	10446	10440	10612	10679	10964

Table B:10: National total emission trends of non-methane volatile organic compounds (1990-1990), as used for modelling at the MSC-W (Gg of NMVOC per year).

Area/Year	1990	1991	1992	1993	1994	1995	1996	1997	1998	1999
Albania	42	42	42	42	42	43	41	39	37	35
Armenia	92	76	60	44	28	12	14	16	19	21
Austria	334	329	305	286	264	249	239	225	217	206
Azerbaijan	226	210	195	179	163	147	141	135	129	123
Belarus	421	388	356	323	291	258	254	250	246	241
Belgium	353	347	347	338	320	312	303	286	278	260
Bosnia and Herzegovina	139	129	119	109	99	89	83	77	70	64
Bulgaria	476	427	429	420	173	159	149	125	127	120
Croatia	172	137	104	102	99	120	122	109	108	107
Cyprus	13	13	13	13	14	14	14	14	13	14
Czechia	555	496	471	439	420	386	385	367	342	328
Denmark	212	221	221	212	214	210	212	200	191	183
Estonia	64	61	42	33	36	40	41	43	39	36
Finland	235	225	220	213	212	204	197	197	193	186
France	2928	2952	2884	2753	2596	2518	2467	2360	2312	2237
Georgia	54	54	51	56	32	39	52	45	39	38
Germany	3949	3427	3104	2916	2494	2363	2263	2206	2146	1982
Greece	321	322	317	317	319	307	313	311	318	319
Hungary	311	273	245	232	218	213	205	196	189	188
Iceland	10	10	10	10	10	9	9	9	9	9
Ireland	154	155	150	147	144	142	142	139	141	132
Italy	1982	2053	2124	2121	2072	2051	2001	1955	1868	1801
Kazakhstan	529	501	472	443	414	386	382	379	375	371
Kyrgyzstan	94	81	68	55	42	29	28	26	24	23
Latvia	86	83	74	68	64	63	63	60	57	55
Lithuania	128	132	108	95	88	88	89	88	80	71
Luxembourg	28	29	28	25	23	21	20	19	18	17
Malta	5	5	5	5	6	6	6	6	6	5
Moldova	106	90	67	54	50	48	49	47	40	34
Montenegro	15	15	15	15	15	15	13	11	9	7
Netherlands	607	572	526	503	468	436	415	379	378	361
North Macedonia	47	41	44	46	41	43	43	44	44	44
Norway	325	324	349	369	385	400	403	403	395	404
Poland	841	885	869	954	954	951	958	928	861	852
Portugal	249	252	256	242	241	236	237	238	239	237
Romania	395	328	301	278	283	290	339	344	319	289
Russian Federation	6135	5725	5315	4906	4496	4122	4034	3947	3859	3772
Serbia	191	167	162	148	147	145	148	153	156	138
Slovakia	255	236	223	198	183	171	164	151	152	144
Slovenia	65	63	61	62	63	63	66	63	58	56
Spain	1026	1030	1021	941	942	919	955	950	957	927
Sweden	367	351	331	299	293	277	272	252	241	232
Switzerland	302	288	265	240	226	210	199	186	175	167
Tajikistan	53	45	41	37	32	31	31	32	31	31
Türkiye	958	984	1009	1034	1060	1085	1055	1025	995	965
Turkmenistan	85	76	74	64	59	57	61	61	67	72
Ukraine	1331	1203	1075	947	819	692	675	659	643	626
United Kingdom	2905	2863	2779	2658	2502	2367	2322	2218	2110	1901
Uzbekistan	245	245	234	231	223	210	213	218	220	222
Asian areas	3791	3791	3790	3790	3789	3821	3917	4013	4108	4204
North Africa	1146	1193	1239	1285	1331	1395	1498	1600	1702	1804
Baltic Sea	2	2	2	2	2	2	3	3	3	3
Black Sea	1	1	1	1	1	1	1	1	1	1
Mediterranean Sea	9	9	9	10	10	10	10	11	11	11
North Sea	5	5	6	6	6	6	6	6	7	7
North-East Atlantic Ocean	6	6	6	6	6	6	7	7	7	7
Natural marine emissions	0	0	0	0	0	0	0	0	0	0
Volcanic emissions	0	0	0	0	0	0	0	0	0	0
TOTAL	35381	33968	32635	31325	29524	28487	28329	27829	27380	26690

Table B:11: National total emission trends of non-methane volatile organic compounds (2000-2010), as used for modelling at the MSC-W (Gg of NMVOC per year).

Area/Year	2000	2001	2002	2003	2004	2005	2006	2007	2008	2009	2010
Albania	33	34	34	34	35	35	35	34	34	33	33
Armenia	23	24	25	26	26	27	29	31	33	35	37
Austria	181	176	171	167	153	157	159	155	150	137	138
Azerbaijan	117	129	141	152	164	176	204	233	261	289	318
Belarus	237	237	237	236	236	236	236	237	238	238	239
Belgium	235	229	213	203	191	184	178	168	159	147	145
Bosnia and Herzegovina	57	55	52	49	46	43	43	44	44	44	45
Bulgaria	135	110	119	123	111	112	113	107	105	100	101
Croatia	104	102	105	108	113	114	114	110	108	94	91
Cyprus	13	13	14	15	15	16	15	15	14	13	13
Czechia	318	306	296	292	282	275	273	266	261	258	255
Denmark	181	172	166	163	158	154	149	147	144	134	131
Estonia	35	35	34	33	33	31	30	28	26	24	22
Finland	179	177	168	164	159	148	142	138	122	113	114
France	2149	2081	1965	1941	1848	1783	1695	1573	1514	1432	1465
Georgia	37	37	38	38	38	32	32	33	32	35	35
Germany	1814	1718	1625	1543	1538	1490	1486	1424	1361	1247	1363
Greece	313	311	324	335	345	338	315	292	264	253	219
Hungary	191	190	177	181	177	174	160	146	137	136	130
Iceland	9	8	8	8	8	7	7	7	7	6	6
Ireland	124	124	124	122	122	123	123	122	119	117	114
Italy	1625	1561	1466	1446	1343	1335	1300	1282	1260	1179	1113
Kazakhstan	368	386	405	424	442	461	488	515	542	570	597
Kyrgyzstan	21	23	25	27	29	32	34	36	39	41	44
Latvia	53	56	55	55	54	50	50	49	44	43	40
Lithuania	62	58	59	59	58	59	59	57	58	53	53
Luxembourg	16	16	16	15	16	15	14	12	14	12	12
Malta	5	5	5	4	4	4	4	4	4	4	4
Moldova	32	36	40	42	45	50	44	40	42	40	44
Montenegro	4	7	9	11	13	16	16	16	17	17	17
Netherlands	338	310	295	288	270	273	269	271	267	268	279
North Macedonia	46	39	38	37	37	25	26	27	27	25	26
Norway	414	424	381	334	297	249	219	213	180	164	167
Poland	826	798	807	774	802	797	855	834	857	808	776
Portugal	233	222	216	206	198	187	180	174	164	150	152
Romania	306	297	299	315	324	326	310	289	307	277	263
Russian Federation	3716	3716	3717	3718	3719	3703	3640	3578	3515	3455	3397
Serbia	149	146	147	151	153	149	146	150	145	144	136
Slovakia	144	146	133	132	133	141	135	129	126	117	117
Slovenia	55	55	51	51	49	48	46	46	44	40	40
Spain	887	858	844	780	761	729	701	683	640	609	601
Sweden	222	212	208	208	205	204	199	204	195	180	177
Switzerland	158	148	137	129	119	116	113	109	107	104	100
Tajikistan	31	32	32	32	34	36	37	40	41	43	44
Türkiye	934	885	836	787	737	688	672	657	641	626	610
Turkmenistan	74	76	81	84	86	86	85	87	89	87	92
Ukraine	610	616	623	629	635	641	623	604	585	566	547
United Kingdom	1762	1649	1536	1453	1347	1258	1195	1149	1059	948	914
Uzbekistan	226	225	221	219	216	216	221	224	227	233	234
Asian areas	4257	4288	4319	4350	4381	4405	4430	4455	4479	4502	4523
North Africa	1874	1927	1981	2034	2087	2049	2010	1971	1933	1895	1860
Baltic Sea	3	3	3	3	3	3	3	3	3	3	3
Black Sea	1	1	1	1	1	1	1	1	1	1	1
Mediterranean Sea	12	12	12	12	12	12	12	11	11	11	10
North Sea	7	7	7	7	7	7	7	7	6	6	6
North-East Atlantic Ocean	8	7	7	7	7	7	7	7	7	7	6
Natural marine emissions	0	0	0	0	0	0	0	0	0	0	0
Volcanic emissions	0	0	0	0	0	0	0	0	0	0	0
TOTAL	25968	25519	25047	24756	24426	24033	23691	23244	22807	22114	22018

Table B:12: National total emission trends of non-methane volatile organic compounds (2011-2021), as used for modelling at the MSC-W (Gg of NMVOC per year).

Area/Year	2011	2012	2013	2014	2015	2016	2017	2018	2019	2020	2021
Albania	32	32	31	31	30	31	32	33	34	35	36
Armenia	38	40	41	43	44	40	35	30	26	20	17
Austria	133	131	125	118	113	112	113	109	108	111	111
Azerbaijan	329	340	351	361	372	374	375	376	378	345	381
Belarus	228	218	208	197	187	184	181	178	175	168	169
Belgium	133	130	126	119	119	119	118	117	117	118	122
Bosnia and Herzegovina	60	75	89	104	119	115	110	105	100	95	90
Bulgaria	103	100	96	95	96	94	93	89	87	89	87
Croatia	86	80	75	69	70	72	69	69	74	70	70
Cyprus	9	9	7	7	7	8	9	8	8	7	8
Czechia	243	238	236	232	215	212	210	210	202	194	187
Denmark	125	120	121	113	115	111	109	108	103	106	107
Estonia	23	23	22	22	22	22	23	22	23	24	27
Finland	105	102	98	95	91	91	89	87	85	85	83
France	1352	1304	1296	1240	1211	1204	1203	1165	1129	1125	1164
Georgia	36	37	42	43	42	43	42	40	40	39	40
Germany	1274	1257	1213	1173	1147	1139	1143	1096	1066	1028	1044
Greece	204	196	179	176	169	160	155	149	149	141	146
Hungary	134	134	131	122	126	124	124	117	118	112	114
Iceland	6	6	6	6	6	6	6	7	6	6	6
Ireland	110	112	113	110	112	114	117	117	117	113	115
Italy	1022	1029	994	924	899	887	931	908	904	843	868
Kazakhstan	605	614	623	631	640	629	617	606	595	535	572
Kyrgyzstan	47	51	55	59	63	57	52	47	42	33	31
Latvia	40	40	39	39	36	34	35	40	36	36	37
Lithuania	50	51	50	49	50	49	52	50	49	46	48
Luxembourg	12	12	12	11	11	11	11	11	11	11	11
Malta	3	3	4	3	3	3	3	3	3	3	3
Moldova	44	42	41	48	52	55	59	62	69	69	58
Montenegro	17	17	16	16	16	16	16	17	17	17	17
Netherlands	272	264	262	245	253	248	249	242	238	270	277
North Macedonia	27	26	26	26	25	24	24	23	23	22	21
Norway	158	159	158	168	164	162	160	156	140	151	145
Poland	768	746	699	711	734	744	746	755	731	753	715
Portugal	143	137	136	142	142	139	140	143	142	152	152
Romania	257	256	244	242	239	232	235	231	233	232	234
Russian Federation	3437	3500	3493	3496	3532	3571	3635	3683	3717	3605	3787
Serbia	136	130	129	119	125	130	128	124	124	137	134
Slovakia	115	113	108	91	105	105	103	95	92	88	92
Slovenia	37	36	35	32	33	33	32	32	31	31	30
Spain	581	557	541	538	550	549	565	575	551	575	549
Sweden	175	167	160	156	157	150	143	139	139	138	138
Switzerland	96	93	90	86	82	80	79	77	76	74	75
Tajikistan	45	49	51	55	57	69	77	88	96	94	111
Türkiye	584	558	532	506	480	469	458	446	435	421	413
Turkmenistan	94	96	99	101	102	106	115	125	136	134	157
Ukraine	526	504	483	461	440	426	412	398	384	362	355
United Kingdom	888	871	841	824	823	807	818	841	823	798	781
Uzbekistan	237	238	239	240	242	274	303	330	358	354	415
Asian areas	4543	4564	4584	4659	4761	4863	4965	5066	5368	5488	5933
North Africa	1824	1789	1753	1681	1591	1500	1410	1320	1358	1260	1360
Baltic Sea	3	3	3	3	3	3	3	3	3	3	3
Black Sea	1	1	1	1	1	1	1	1	1	1	1
Mediterranean Sea	11	11	11	10	11	11	11	11	12	10	14
North Sea	6	6	6	6	7	6	7	7	6	6	6
North-East Atlantic Ocean	7	7	7	7	7	7	7	8	8	7	7
Natural marine emissions	0	0	0	0	0	0	0	0	0	0	0
Volcanic emissions	0	0	0	0	0	0	0	0	0	0	0
TOTAL	21574	21420	21129	20860	20846	20823	20955	20894	21093	20790	21679

Table B:13: National total emission trends of carbon monoxide (1990-1999), as used for modelling at the MSC-W (Gg of CO per year).

Area/Year	1990	1991	1992	1993	1994	1995	1996	1997	1998	1999
Albania	151	141	132	122	113	103	98	93	89	84
Armenia	495	405	315	225	135	45	57	69	82	94
Austria	1249	1257	1202	1142	1077	974	970	896	851	735
Azerbaijan	769	711	654	597	539	482	452	421	391	361
Belarus	1439	1302	1165	1028	892	755	753	752	751	749
Belgium	1506	1449	1453	1375	1312	1278	1231	1106	1050	983
Bosnia and Herzegovina	524	459	394	330	265	201	193	185	178	170
Bulgaria	936	552	639	709	623	642	588	439	504	451
Croatia	564	498	410	434	428	452	481	464	474	479
Cyprus	45	43	42	41	41	39	38	36	34	32
Czechia	2040	1940	1902	1693	1622	1546	1601	1479	1271	1144
Denmark	717	749	731	719	678	643	625	576	540	492
Estonia	246	236	145	137	168	215	251	249	215	197
Finland	764	736	715	700	687	662	657	651	646	630
France	10711	11043	10424	9870	9164	9027	8568	7993	7736	7307
Georgia	140	133	153	205	61	124	218	173	144	135
Germany	13319	11048	9528	8619	7586	7217	6646	6399	5885	5468
Greece	1239	1217	1162	1168	1150	1061	1063	1061	1066	1061
Hungary	1451	1335	1058	1124	1011	982	955	903	836	821
Iceland	56	55	55	53	51	49	46	46	51	55
Ireland	560	549	500	479	439	418	415	376	386	335
Italy	6794	7174	7277	7446	7033	7067	6777	6341	5906	5463
Kazakhstan	1878	1770	1663	1555	1447	1339	1335	1331	1326	1322
Kyrgyzstan	470	402	334	266	198	130	124	118	113	107
Latvia	405	370	327	328	311	292	294	275	260	257
Lithuania	385	435	247	227	198	219	233	231	227	201
Luxembourg	469	457	419	431	366	213	196	135	60	59
Malta	20	22	20	25	25	27	26	25	24	22
Moldova	375	308	189	118	114	110	115	120	99	76
Montenegro	33	33	33	33	34	34	30	25	21	17
Netherlands	1189	1096	1046	1019	964	953	952	885	843	810
North Macedonia	133	112	124	134	121	126	124	127	129	132
Norway	792	745	710	716	708	688	664	652	631	605
Poland	3659	4291	4287	4967	4639	4719	4881	4492	3892	3908
Portugal	792	803	833	804	809	815	788	769	739	706
Romania	1208	955	817	759	762	751	1099	1248	1185	1028
Russian Federation	19097	17930	16763	15596	14428	13333	13138	12943	12748	12553
Serbia	518	445	422	354	391	351	380	386	412	376
Slovakia	1033	953	897	799	723	655	615	560	571	545
Slovenia	290	276	272	287	280	280	289	265	233	215
Spain	4104	4173	4190	3875	3610	3116	3539	3366	3238	2975
Sweden	1094	1139	1076	976	994	936	909	826	776	713
Switzerland	818	780	719	628	575	532	511	480	459	444
Tajikistan	391	334	287	211	146	149	138	152	140	149
Türkiye	3405	3471	3537	3603	3670	3736	3679	3622	3566	3509
Turkmenistan	398	300	312	243	231	241	268	273	322	378
Ukraine	11357	9888	8418	6949	5479	4010	3934	3858	3781	3705
United Kingdom	8500	8614	8319	8047	7425	6822	6895	6458	6105	5712
Uzbekistan	1134	1145	1037	1039	974	817	871	921	954	958
Asian areas	9233	9463	9694	9924	10155	10346	10457	10569	10681	10792
North Africa	1744	1848	1953	2058	2162	2277	2414	2550	2687	2823
Baltic Sea	19	19	20	20	20	20	20	20	21	21
Black Sea	5	5	6	6	6	6	6	6	6	6
Mediterranean Sea	68	70	74	71	72	73	73	74	75	77
North Sea	50	52	55	53	53	54	54	55	55	57
North-East Atlantic Ocean	44	45	48	46	46	47	47	48	48	50
Natural marine emissions	0	0	0	0	0	0	0	0	0	0
Volcanic emissions	0	0	0	0	0	0	0	0	0	0
TOTAL	120828	115789	109211	104382	97213	92202	91783	88581	85516	82562

Table B:14: National total emission trends of carbon monoxide (2000-2010), as used for modelling at the MSC-W (Gg of CO per year).

Area/Year	2000	2001	2002	2003	2004	2005	2006	2007	2008	2009	2010
Albania	79	81	82	84	85	87	84	81	78	75	72
Armenia	106	106	107	107	107	108	109	111	112	113	115
Austria	729	700	668	669	651	627	627	604	586	566	582
Azerbaijan	330	350	369	388	408	427	450	474	497	520	543
Belarus	748	731	714	697	680	663	657	651	645	639	633
Belgium	996	924	962	916	863	801	742	616	621	427	497
Bosnia and Herzegovina	162	157	151	145	139	133	138	142	147	151	156
Bulgaria	413	376	419	436	385	372	388	362	348	321	334
Croatia	474	455	435	454	435	428	411	397	352	346	336
Cyprus	30	28	27	26	25	24	22	18	16	14	14
Czechia	1104	1069	1024	1042	1027	945	933	930	874	891	927
Denmark	472	463	438	441	423	423	410	415	394	358	348
Estonia	181	192	176	177	159	142	132	151	147	149	147
Finland	594	596	577	556	542	519	499	486	452	429	446
France	6710	6378	6213	6011	6142	5687	5131	4880	4717	4277	4707
Georgia	123	130	131	132	129	85	90	102	94	92	89
Germany	5130	4931	4630	4300	4084	3853	3822	3782	3758	3217	3529
Greece	1006	1010	962	927	913	864	881	824	754	691	612
Hungary	857	865	716	841	773	697	606	565	503	545	552
Iceland	53	53	53	52	52	50	56	70	107	110	109
Ireland	324	313	300	286	281	283	265	250	247	233	216
Italy	4728	4422	3825	3900	3360	3437	3296	3353	3486	3090	3054
Kazakhstan	1318	1328	1337	1347	1356	1366	1521	1676	1831	1986	2141
Kyrgyzstan	102	114	126	138	150	162	177	193	209	224	240
Latvia	240	247	240	241	234	212	214	199	185	192	154
Lithuania	183	180	181	175	173	175	180	179	176	165	159
Luxembourg	47	50	46	43	44	40	38	39	34	30	30
Malta	20	19	18	17	17	15	14	12	13	12	12
Moldova	61	63	59	71	70	73	72	66	73	66	70
Montenegro	13	28	44	59	74	90	83	76	69	63	56
Netherlands	772	774	758	757	763	747	758	744	742	680	709
North Macedonia	145	114	116	117	122	75	71	72	67	63	63
Norway	589	576	568	556	541	540	522	510	500	455	469
Poland	3359	3175	3178	3032	3051	3069	3311	3070	3165	3126	3407
Portugal	670	622	601	576	548	510	477	450	413	390	381
Romania	1059	1034	1038	1096	1199	1225	1137	1117	1159	1045	1051
Russian Federation	12393	12230	12066	11903	11739	11534	11330	11126	10922	10719	10518
Serbia	400	402	403	418	435	403	358	403	366	360	348
Slovakia	542	554	476	501	508	548	504	500	462	405	447
Slovenia	203	215	182	184	172	182	161	166	158	142	142
Spain	2628	2479	2257	2404	2168	1995	2004	1973	1826	1848	1861
Sweden	643	602	566	545	503	493	460	451	432	416	406
Switzerland	418	391	364	353	336	321	299	285	277	261	253
Tajikistan	183	192	175	177	206	215	226	251	241	241	239
Türkiye	3453	3309	3166	3023	2880	2737	2743	2750	2756	2762	2768
Turkmenistan	396	405	435	466	490	496	500	465	468	463	516
Ukraine	3629	3666	3704	3741	3778	3815	3640	3465	3290	3115	2940
United Kingdom	5174	4764	4209	3818	3574	3368	3160	3095	2587	2061	1946
Uzbekistan	976	962	951	922	872	861	856	874	891	905	864
Asian areas	10883	10963	11043	11123	11203	11164	11124	11085	11045	11029	11062
North Africa	2959	3095	3231	3366	3502	3461	3420	3378	3337	3303	3283
Baltic Sea	23	22	22	22	22	21	21	21	21	21	20
Black Sea	7	7	7	7	7	7	7	6	7	6	6
Mediterranean Sea	86	85	84	83	82	81	81	80	82	80	75
North Sea	60	59	58	58	58	57	57	56	57	56	53
North-East Atlantic Ocean	52	51	51	50	50	49	49	48	50	48	45
Natural marine emissions	0	0	0	0	0	0	0	0	0	0	0
Volcanic emissions	0	0	0	0	0	0	0	0	0	0	0
TOTAL	79038	77108	74743	73979	72594	70767	69323	68147	66842	63995	64749

Table B:15: National total emission trends of carbon monoxide (2011-2021), as used for modelling at the MSC-W (Gg of CO per year).

Area/Year	2011	2012	2013	2014	2015	2016	2017	2018	2019	2020	2021
Albania	71	70	70	69	69	71	73	75	77	76	80
Armenia	120	125	130	136	141	125	109	93	76	56	47
Austria	565	565	569	533	544	539	529	487	499	474	523
Azerbaijan	573	603	633	664	694	686	679	672	665	584	653
Belarus	604	575	547	518	489	475	462	449	435	416	409
Belgium	399	343	514	320	370	354	288	334	368	274	290
Bosnia and Herzegovina	182	209	235	261	288	276	265	253	242	228	219
Bulgaria	322	310	299	290	291	301	301	281	268	260	267
Croatia	311	293	282	249	270	260	254	232	219	217	217
Cyprus	13	12	12	12	11	12	12	11	11	10	10
Czechia	891	879	890	859	792	794	791	793	780	789	790
Denmark	307	290	276	253	257	248	237	221	205	191	192
Estonia	123	137	126	121	116	124	126	123	122	120	109
Finland	407	402	389	383	359	366	357	349	343	317	338
France	3860	3594	3655	3055	3035	3104	3025	2879	2819	2463	2707
Georgia	88	91	125	137	131	140	133	114	110	104	111
Germany	3448	3198	3161	2993	3094	2969	2976	2859	2754	2451	2586
Greece	593	637	547	556	533	477	490	467	460	422	424
Hungary	562	578	559	478	464	450	440	378	359	341	345
Iceland	106	107	109	108	110	109	112	111	105	104	104
Ireland	198	192	191	177	178	175	149	145	126	121	123
Italy	2414	2681	2488	2248	2259	2191	2262	2062	2080	1898	2044
Kazakhstan	2129	2118	2107	2096	2084	1928	1771	1615	1458	1178	1175
Kyrgyzstan	265	291	316	342	367	327	287	246	206	150	129
Latvia	156	156	138	131	107	105	112	116	112	99	102
Lithuania	153	148	139	131	125	124	122	124	117	111	112
Luxembourg	28	28	28	26	22	23	23	21	22	16	20
Malta	12	10	10	9	9	9	9	7	7	5	6
Moldova	75	69	71	94	99	103	125	175	160	155	122
Montenegro	53	51	48	45	43	43	44	44	45	45	46
Netherlands	670	641	611	567	572	555	548	535	517	449	438
North Macedonia	64	67	64	62	63	63	56	55	56	51	53
Norway	444	440	414	396	404	402	407	409	401	407	427
Poland	3089	3112	3001	2880	2844	2975	2955	3098	2717	2582	2521
Portugal	354	339	320	305	309	296	295	277	286	254	285
Romania	1009	978	955	959	914	935	942	943	950	910	964
Russian Federation	10821	11235	11427	11458	11492	11658	11810	11990	12078	11375	12255
Serbia	345	308	284	267	269	287	278	281	285	368	364
Slovakia	414	427	389	315	358	368	373	313	283	277	334
Slovenia	139	133	133	114	121	121	115	105	97	87	87
Spain	1847	1543	1854	1596	1736	1599	1595	1806	1534	1524	1637
Sweden	388	362	356	345	333	336	328	308	300	284	277
Switzerland	229	222	214	193	185	185	179	170	169	152	152
Tajikistan	214	254	247	255	281	400	455	535	585	578	686
Türkiye	2593	2418	2243	2068	1893	1909	1925	1942	1958	1979	1990
Turkmenistan	538	530	569	585	617	550	620	667	729	720	855
Ukraine	2898	2856	2813	2771	2729	2755	2782	2809	2835	2747	2888
United Kingdom	1798	1760	1713	1635	1566	1403	1431	1424	1335	1246	1274
Uzbekistan	885	871	858	852	813	985	1082	1179	1290	1274	1512
Asian areas	11094	11126	11158	11203	11253	11304	11354	11405	12084	12354	13356
North Africa	3264	3244	3224	3098	2917	2737	2557	2377	2445	2270	2450
Baltic Sea	20	20	20	20	20	20	20	21	25	23	26
Black Sea	6	6	6	6	6	6	7	6	7	7	7
Mediterranean Sea	77	76	75	74	78	75	78	79	89	77	114
North Sea	54	54	53	54	57	55	57	56	57	58	61
North-East Atlantic Ocean	46	46	45	46	48	46	48	51	58	53	58
Natural marine emissions	0	0	0	0	0	0	0	0	0	0	0
Volcanic emissions	0	0	0	0	0	0	0	0	0	0	0
TOTAL	62332	61833	61714	59420	59233	58935	58863	58577	58424	55780	59374

Table B:16: National total emission trends of fine particulate matter (1990-1999), as used for modelling at the MSC-W (Gg of $PM_{2.5}$ per year).

Area/Year	1990	1991	1992	1993	1994	1995	1996	1997	1998	1999
Albania	23	21	18	16	14	12	11	11	10	10
Armenia	15	13	11	9	7	5	4	4	4	4
Austria	27	27	27	26	26	26	26	25	25	25
Azerbaijan	23	21	20	18	16	14	15	15	15	16
Belarus	101	94	86	79	72	64	64	63	62	62
Belgium	55	54	53	52	51	50	48	46	44	42
Bosnia and Herzegovina	94	81	69	57	45	33	30	28	25	22
Bulgaria	43	36	33	36	33	31	34	31	36	32
Croatia	40	43	37	38	36	38	42	40	40	39
Cyprus	2	2	2	2	2	3	2	2	2	2
Czechia	299	234	192	175	137	121	122	96	70	52
Denmark	23	25	24	24	24	23	23	22	20	20
Estonia	34	31	28	25	22	19	18	16	14	12
Finland	47	43	39	35	35	32	31	30	28	28
France	468	520	501	484	442	443	463	423	420	401
Georgia	36	35	35	34	34	34	33	32	32	31
Germany	426	381	336	291	246	202	189	189	179	174
Greece	75	73	72	70	69	66	70	71	73	75
Hungary	95	84	73	62	52	41	42	44	45	47
Iceland	1	1	1	2	2	2	2	2	2	1
Ireland	29	28	25	25	23	21	22	20	22	19
Italy	238	265	239	239	236	237	225	222	223	219
Kazakhstan	191	180	169	158	147	136	132	128	124	120
Kyrgyzstan	24	21	18	15	11	8	8	8	8	8
Latvia	26	29	26	27	27	28	30	29	29	29
Lithuania	13	12	11	10	9	9	9	9	9	9
Luxembourg	16	16	14	16	13	8	8	5	2	2
Malta	1	1	1	1	1	1	1	1	1	1
Moldova	24	18	12	7	7	6	7	6	5	5
Montenegro	6	6	6	6	6	6	5	4	4	3
Netherlands	57	56	53	51	48	45	44	40	37	36
North Macedonia	33	29	35	31	29	30	33	32	36	31
Norway	41	38	37	40	43	43	44	48	44	42
Poland	422	440	418	512	460	455	458	406	352	341
Portugal	64	65	66	63	63	64	64	66	73	68
Romania	77	64	62	65	68	73	111	130	117	109
Russian Federation	1123	1002	880	759	638	524	516	507	498	490
Serbia	55	45	42	40	39	35	38	38	40	38
Slovakia	96	87	81	66	58	51	47	41	42	40
Slovenia	16	15	15	14	14	13	13	14	14	14
Spain	224	220	215	211	206	201	198	195	192	189
Sweden	46	46	44	44	43	42	42	39	36	34
Switzerland	17	17	16	15	15	14	14	13	13	12
Tajikistan	27	19	17	11	6	5	4	6	5	5
Türkiye	504	494	484	473	463	453	441	429	417	405
Turkmenistan	23	19	22	17	12	13	15	13	15	17
Ukraine	918	826	734	642	549	457	445	433	421	409
United Kingdom	254	253	245	226	217	196	189	179	168	164
Uzbekistan	84	83	72	72	71	59	59	61	60	60
Asian areas	643	662	682	701	721	735	738	741	745	748
North Africa	91	96	100	104	108	113	119	125	131	137
Baltic Sea	15	16	17	17	17	18	18	18	19	20
Black Sea	3	3	4	4	4	4	4	4	4	4
Mediterranean Sea	62	64	69	67	69	71	73	75	77	81
North Sea	31	32	34	33	34	35	36	37	38	40
North-East Atlantic Ocean	39	40	43	42	44	45	46	47	48	51
Natural marine emissions	0	0	0	0	0	0	0	0	0	0
Volcanic emissions	0	0	0	0	0	0	0	0	0	0
TOTAL	7458	7125	6667	6364	5880	5514	5523	5360	5216	5093

Table B:17: National total emission trends of fine particulate matter (2000-2010), as used for modelling at the MSC-W (Gg of $PM_{2.5}$ per year).

Area/Year	2000	2001	2002	2003	2004	2005	2006	2007	2008	2009	2010
Albania	9	10	10	10	11	11	11	11	11	11	11
Armenia	4	4	4	4	4	4	4	4	4	4	4
Austria	24	25	24	24	23	33	33	32	31	31	33
Azerbaijan	16	16	16	17	17	17	18	19	21	22	23
Belarus	61	61	61	61	61	65	64	64	63	63	62
Belgium	40	39	36	37	37	34	35	33	32	29	30
Bosnia and Herzegovina	19	20	21	22	23	51	52	52	52	53	53
Bulgaria	35	32	37	40	40	39	40	38	38	34	35
Croatia	36	39	38	44	42	44	40	38	38	37	38
Cyprus	2	2	2	2	2	2	2	2	2	2	2
Czechia	50	51	48	48	47	44	44	43	41	42	45
Denmark	20	20	20	21	21	21	22	24	23	21	21
Estonia	11	11	11	10	9	14	14	19	15	15	19
Finland	26	27	27	27	27	26	26	24	23	22	23
France	376	373	352	362	353	335	309	290	289	280	294
Georgia	31	29	27	25	23	15	16	17	17	17	16
Germany	165	159	153	146	141	162	164	162	160	144	154
Greece	66	70	69	68	69	68	67	67	64	61	47
Hungary	48	52	38	46	43	40	41	41	37	47	50
Iceland	2	2	2	2	2	2	2	2	2	2	2
Ireland	19	19	18	18	18	19	19	18	18	17	16
Italy	205	197	181	185	165	186	189	221	228	213	213
Kazakhstan	116	116	116	116	116	116	127	138	153	166	178
Kyrgyzstan	8	9	9	10	11	11	12	13	14	15	16
Latvia	27	28	28	29	30	27	27	26	25	27	21
Lithuania	9	9	9	9	9	18	19	18	19	18	18
Luxembourg	2	3	2	3	3	2	2	2	2	2	2
Malta	1	1	1	1	1	1	1	1	1	0	1
Moldova	5	4	5	5	5	15	15	15	15	15	16
Montenegro	2	3	5	7	9	11	11	10	10	10	9
Netherlands	35	33	32	31	30	29	28	26	25	23	23
North Macedonia	30	19	19	29	32	24	22	17	18	13	16
Norway	42	41	42	39	37	37	35	35	34	32	35
Poland	293	305	311	304	311	322	345	324	331	328	360
Portugal	66	63	63	60	60	58	56	54	52	50	50
Romania	106	87	90	106	119	120	115	113	132	125	129
Russian Federation	481	476	472	467	462	604	591	578	564	553	546
Serbia	40	40	41	42	42	40	37	41	37	43	43
Slovakia	44	43	32	32	30	36	32	28	26	23	26
Slovenia	14	16	14	15	14	16	15	16	16	14	15
Spain	185	178	172	188	173	167	171	171	157	164	161
Sweden	34	33	32	32	31	31	29	29	28	26	26
Switzerland	12	12	11	11	11	13	13	13	13	12	12
Tajikistan	6	6	7	7	8	9	9	11	11	11	11
Türkiye	393	388	382	377	372	367	382	398	413	429	444
Turkmenistan	19	18	19	20	19	20	21	17	18	18	19
Ukraine	397	401	404	408	411	451	430	409	389	368	347
United Kingdom	146	143	126	124	120	118	116	107	98	91	94
Uzbekistan	57	58	56	54	53	52	52	54	54	54	54
Asian areas	763	785	807	828	850	874	898	922	946	964	972
North Africa	143	150	156	163	169	170	170	171	172	173	174
Baltic Sea	21	21	21	20	20	20	16	14	12	12	11
Black Sea	5	5	5	5	5	5	5	5	4	4	4
Mediterranean Sea	89	88	86	85	84	83	82	80	68	71	64
North Sea	42	42	41	40	40	39	33	29	26	27	24
North-East Atlantic Ocean	53	52	51	51	50	49	48	48	40	42	40
Natural marine emissions	0	0	0	0	0	0	0	0	0	0	0
Volcanic emissions	0	0	0	0	0	0	0	0	0	0	1673
TOTAL	4955	4931	4863	4935	4915	5187	5173	5155	5130	5088	6827

Table B:18: National total emission trends of fine particulate matter (2011-2021), as used for modelling at the MSC-W (Gg of $PM_{2.5}$ per year).

Area/Year	2011	2012	2013	2014	2015	2016	2017	2018	2019	2020	2021
Albania	11	11	11	11	10	11	12	12	13	13	14
Armenia	6	7	8	10	11	10	10	9	8	7	6
Austria	31	31	31	27	28	27	27	25	25	24	25
Azerbaijan	23	24	25	25	26	29	32	35	38	39	44
Belarus	61	59	58	56	55	57	59	61	63	62	63
Belgium	25	25	25	21	22	22	20	19	18	17	18
Bosnia and Herzegovina	56	58	61	64	66	63	59	55	51	50	49
Bulgaria	38	37	34	34	34	31	31	30	30	31	31
Croatia	36	35	34	30	32	31	29	29	27	28	28
Cyprus	1	1	1	1	1	1	1	1	1	1	1
Czechia	44	44	44	42	31	30	30	29	27	25	24
Denmark	19	18	18	16	17	17	16	14	13	12	12
Estonia	22	14	15	13	11	10	11	10	9	9	9
Finland	20	20	20	19	17	18	17	17	16	14	14
France	243	256	260	217	220	223	212	200	195	172	189
Georgia	16	17	17	17	18	18	18	19	19	19	19
Germany	143	145	140	126	126	115	114	115	109	102	106
Greece	47	48	44	44	42	39	39	37	36	34	36
Hungary	56	58	58	49	51	49	47	41	38	37	38
Iceland	1	2	1	1	1	1	1	1	1	1	1
Ireland	14	14	14	14	14	14	13	14	13	13	13
Italy	168	185	180	161	169	162	170	156	151	144	149
Kazakhstan	175	172	170	167	165	159	154	148	143	133	132
Kyrgyzstan	17	17	17	17	18	17	16	15	14	13	13
Latvia	21	21	20	19	16	17	18	19	18	17	18
Lithuania	18	17	17	17	16	16	15	16	14	14	15
Luxembourg	2	1	1	1	1	1	1	1	1	1	1
Malta	1	1	0	1	0	0	1	0	0	0	0
Moldova	17	18	18	18	18	19	20	20	17	17	17
Montenegro	9	9	9	8	8	8	8	7	7	7	6
Netherlands	21	20	20	18	18	18	17	17	16	15	14
North Macedonia	22	21	24	17	15	13	9	9	9	9	9
Norway	32	32	28	26	26	25	25	25	23	24	25
Poland	335	339	326	301	297	307	300	373	324	307	297
Portugal	50	49	48	47	47	46	47	47	46	44	45
Romania	119	121	113	114	109	109	110	109	111	110	116
Russian Federation	539	543	531	525	502	476	468	461	449	435	428
Serbia	42	42	37	37	38	43	41	41	42	58	59
Slovakia	24	26	24	16	21	21	21	17	18	17	19
Slovenia	15	14	14	12	13	13	12	11	11	10	10
Spain	164	144	164	142	153	134	134	149	130	133	135
Sweden	26	24	23	20	19	19	19	18	18	17	16
Switzerland	11	11	10	10	9	9	8	8	7	7	6
Tajikistan	11	15	16	21	23	26	29	33	35	36	39
Türkiye	432	421	409	397	385	385	384	384	384	391	383
Turkmenistan	20	21	21	19	20	19	19	21	22	23	24
Ukraine	338	328	318	309	299	306	313	320	327	325	339
United Kingdom	88	88	90	87	85	83	84	87	83	79	83
Uzbekistan	54	52	52	51	49	55	58	59	63	65	70
Asian areas	980	988	996	1002	1005	1009	1013	1017	1077	1101	1191
North Africa	175	177	178	177	175	173	172	170	175	162	175
Baltic Sea	11	11	10	11	4	4	4	4	4	4	4
Black Sea	4	4	4	4	4	4	4	4	4	2	2
Mediterranean Sea	70	69	68	63	68	68	70	71	72	21	29
North Sea	23	23	23	24	11	10	11	11	10	9	9
North-East Atlantic Ocean	44	43	43	46	49	48	50	51	49	14	15
Natural marine emissions	0	0	0	0	0	0	0	0	0	0	0
Volcanic emissions	13185	0	0	0	0	0	0	0	0	0	0
TOTAL	18178	4992	4943	4743	4690	4639	4624	4672	4626	4474	4634

Table B:19: National total emission trends of particulate matter (1990-1999), as used for modelling at the MSC-W (Gg of PM_{10} per year).

Area/Year	1990	1991	1992	1993	1994	1995	1996	1997	1998	1999
Albania	33	29	25	21	17	14	13	13	12	12
Armenia	17	15	13	10	8	6	5	5	5	5
Austria	43	43	43	42	42	42	42	41	41	41
Azerbaijan	28	26	24	22	20	18	18	19	20	20
Belarus	146	135	125	115	105	95	93	90	88	86
Belgium	78	76	75	74	72	71	68	64	61	58
Bosnia and Herzegovina	172	146	119	93	67	41	40	39	37	36
Bulgaria	68	58	54	57	56	54	57	56	60	54
Croatia	60	60	50	53	53	55	60	59	58	54
Cyprus	4	4	4	4	4	4	4	5	5	5
Czechia	433	348	284	257	200	168	167	131	98	73
Denmark	35	37	35	35	35	35	35	34	32	31
Estonia	140	127	114	102	89	77	67	57	47	37
Finland	74	67	61	56	56	51	50	49	45	46
France	589	642	619	593	550	552	574	534	528	509
Georgia	48	46	43	41	39	37	36	36	35	35
Germany	886	778	670	562	455	347	330	336	323	318
Greece	162	155	150	143	139	130	132	133	135	136
Hungary	182	160	138	116	94	72	72	72	72	72
Iceland	3	3	3	3	3	3	3	3	3	3
Ireland	45	45	41	41	39	37	38	38	40	38
Italy	344	538	339	331	334	344	325	309	326	313
Kazakhstan	331	308	284	260	237	213	206	199	191	184
Kyrgyzstan	45	38	32	25	18	11	11	11	11	11
Latvia	31	34	31	32	31	33	34	34	34	34
Lithuania	40	37	35	32	29	26	27	27	27	27
Luxembourg	17	16	15	16	14	9	9	6	3	3
Malta	1	1	1	1	1	1	1	1	1	1
Moldova	32	25	18	12	11	9	10	9	8	7
Montenegro	7	7	7	7	7	7	6	5	4	3
Netherlands	80	78	74	71	66	62	60	55	51	51
North Macedonia	49	43	51	45	43	43	48	46	53	45
Norway	53	49	47	51	53	54	55	59	54	52
Poland	787	761	694	768	692	643	635	562	487	469
Portugal	80	81	83	80	80	82	81	84	151	107
Romania	133	108	101	106	108	114	153	169	153	141
Russian Federation	2295	2043	1790	1538	1286	1043	1032	1020	1009	997
Serbia	73	62	58	55	53	50	53	54	56	52
Slovakia	108	98	92	76	68	61	59	51	54	50
Slovenia	32	29	27	24	22	19	19	19	18	18
Spain	354	347	340	332	325	318	313	309	304	300
Sweden	67	66	65	65	64	62	62	58	56	53
Switzerland	25	25	25	24	23	22	22	21	20	20
Tajikistan	36	26	22	14	7	7	6	8	7	7
Türkiye	758	730	702	673	645	617	597	577	557	537
Turkmenistan	30	26	30	22	16	17	19	17	20	22
Ukraine	1610	1437	1264	1091	918	745	713	682	650	619
United Kingdom	395	393	373	343	325	298	294	276	259	252
Uzbekistan	113	112	96	96	93	77	78	80	79	79
Asian areas	1051	1081	1111	1141	1172	1195	1204	1213	1223	1232
North Africa	149	155	161	168	174	181	190	198	207	216
Baltic Sea	15	16	17	17	17	18	18	18	19	20
Black Sea	3	3	4	4	4	4	4	4	4	4
Mediterranean Sea	62	64	69	67	69	71	73	75	77	81
North Sea	31	32	34	33	34	35	36	37	38	40
North-East Atlantic Ocean	39	40	43	42	44	45	46	47	48	51
Natural marine emissions	0	0	0	0	0	0	0	0	0	0
Volcanic emissions	0	0	0	0	0	0	0	0	0	0
TOTAL	12522	11910	10826	10106	9224	8445	8402	8153	8006	7765

Table B:20: National total emission trends of particulate matter (2000-2010), as used for modelling at the MSC-W (Gg of PM_{10} per year).

Area/Year	2000	2001	2002	2003	2004	2005	2006	2007	2008	2009	2010
Albania	11	12	12	13	13	13	13	13	13	13	13
Armenia	5	5	5	5	5	5	5	5	5	6	6
Austria	40	40	39	39	39	48	47	47	46	45	47
Azerbaijan	21	21	21	22	22	22	23	25	26	28	29
Belarus	84	83	82	81	81	84	83	83	82	82	81
Belgium	55	53	50	50	50	46	46	43	43	38	40
Bosnia and Herzegovina	34	36	38	40	41	70	70	70	70	70	71
Bulgaria	63	53	64	66	67	69	67	62	60	51	49
Croatia	48	50	53	61	58	57	54	53	55	52	53
Cyprus	5	4	4	4	4	4	4	4	4	3	3
Czechia	70	70	65	65	65	61	62	61	58	58	60
Denmark	33	32	31	31	32	33	33	35	39	32	33
Estonia	27	27	23	21	20	24	21	31	24	23	30
Finland	43	44	44	45	44	42	43	41	38	37	38
France	481	476	452	463	454	431	402	381	378	363	379
Georgia	34	32	30	29	27	23	24	25	25	26	25
Germany	303	288	281	267	259	277	278	273	271	249	265
Greece	127	133	133	128	132	123	126	122	129	118	89
Hungary	72	77	61	72	74	71	63	61	64	75	71
Iceland	3	3	3	4	3	3	3	4	4	4	4
Ireland	39	40	39	41	42	43	43	43	41	39	36
Italy	293	290	402	270	279	290	263	363	315	308	341
Kazakhstan	177	177	177	178	178	178	192	206	224	241	256
Kyrgyzstan	11	12	13	14	14	15	17	18	19	21	22
Latvia	32	33	33	34	43	36	35	36	35	35	29
Lithuania	27	27	27	27	27	36	39	34	37	34	30
Luxembourg	3	3	3	4	3	3	3	3	3	2	2
Malta	1	1	1	1	2	2	2	2	1	1	1
Moldova	7	7	7	8	8	19	19	19	19	18	20
Montenegro	2	5	7	9	11	15	14	14	13	13	12
Netherlands	50	48	47	45	44	43	42	40	39	37	36
North Macedonia	44	28	29	42	46	37	34	28	28	22	28
Norway	52	51	52	48	46	47	45	46	44	41	45
Poland	406	418	423	413	419	435	466	440	445	438	473
Portugal	84	87	95	84	80	74	80	70	71	68	67
Romania	139	121	124	144	161	158	154	155	171	161	165
Russian Federation	987	982	977	972	966	1125	1098	1071	1044	1019	1000
Serbia	54	54	55	56	57	54	52	56	52	57	57
Slovakia	54	53	43	42	39	45	41	36	34	31	33
Slovenia	18	20	18	19	18	21	19	21	20	17	18
Spain	295	286	284	303	290	285	292	290	257	252	244
Sweden	53	51	51	51	50	51	49	49	46	44	44
Switzerland	19	19	18	18	18	20	21	21	21	20	20
Tajikistan	8	8	9	10	11	12	12	15	14	15	15
Türkiye	517	508	499	491	482	473	495	517	538	560	582
Turkmenistan	25	24	25	27	26	27	28	23	24	24	25
Ukraine	587	592	597	603	608	648	619	591	562	534	505
United Kingdom	235	238	209	221	203	197	192	178	161	150	162
Uzbekistan	77	78	75	72	71	69	69	72	72	73	72
Asian areas	1259	1295	1330	1366	1402	1444	1487	1529	1572	1605	1620
North Africa	226	237	248	258	269	270	270	271	271	273	276
Baltic Sea	21	21	21	20	20	20	16	14	12	12	11
Black Sea	5	5	5	5	5	5	5	5	4	4	4
Mediterranean Sea	89	88	86	85	84	83	82	80	68	71	64
North Sea	42	42	41	40	40	39	33	29	26	27	24
North-East Atlantic Ocean	53	52	51	51	50	49	48	48	40	42	40
Natural marine emissions	0	0	0	0	0	0	0	0	0	0	0
Volcanic emissions	0	0	0	0	0	0	0	0	0	0	5970
TOTAL	7552	7541	7613	7576	7602	7873	7842	7868	7779	7680	13737

Table B:21: National total emission trends of particulate matter (2011-2021), as used for modelling at the MSC-W (Gg of PM_{10} per year).

Area/Year	2011	2012	2013	2014	2015	2016	2017	2018	2019	2020	2021
Albania	13	13	13	13	13	13	14	15	15	16	17
Armenia	7	9	10	12	13	12	12	11	10	9	8
Austria	45	45	44	41	42	41	41	38	38	37	39
Azerbaijan	30	30	31	32	33	36	40	44	48	49	55
Belarus	79	78	76	74	73	75	77	79	81	79	81
Belgium	33	34	35	30	31	31	29	28	27	26	27
Bosnia and Herzegovina	74	77	80	83	86	80	74	68	62	58	56
Bulgaria	56	52	47	50	51	44	43	43	44	45	43
Croatia	48	48	49	45	40	44	38	42	35	51	51
Cyprus	3	2	2	2	2	2	2	2	2	2	2
Czechia	58	58	58	56	44	43	43	42	41	37	37
Denmark	30	29	29	28	27	27	26	26	23	22	22
Estonia	41	23	27	23	19	17	18	18	16	17	16
Finland	36	34	34	34	31	32	31	31	30	27	28
France	327	340	343	298	301	305	296	282	278	248	270
Georgia	24	24	25	25	26	26	26	27	27	27	28
Germany	257	258	256	241	239	219	222	230	215	203	207
Greece	77	75	70	74	68	67	65	59	58	56	57
Hungary	75	73	76	71	72	69	65	60	58	54	53
Iceland	3	3	3	2	2	3	2	2	2	2	2
Ireland	30	30	30	30	31	31	31	31	30	30	31
Italy	312	241	241	215	248	227	237	262	215	220	200
Kazakhstan	250	246	242	238	234	229	224	220	215	204	206
Kyrgyzstan	22	22	23	23	23	22	21	20	19	18	18
Latvia	31	31	29	28	27	26	27	28	28	26	29
Lithuania	36	31	35	35	38	31	31	38	33	35	34
Luxembourg	2	2	2	2	2	2	2	2	2	2	2
Malta	1	1	1	1	1	1	1	1	1	2	1
Moldova	21	21	22	22	22	22	24	25	22	23	21
Montenegro	12	12	11	11	11	10	10	9	8	8	7
Netherlands	35	34	33	32	32	31	31	31	30	28	26
North Macedonia	35	34	37	27	22	20	14	14	14	14	13
Norway	42	43	38	36	36	35	35	35	34	34	34
Poland	447	452	432	402	395	406	402	474	421	396	388
Portugal	73	69	62	58	58	58	57	58	58	57	58
Romania	157	160	150	151	145	143	143	146	151	149	157
Russian Federation	994	1002	984	979	948	916	909	900	885	871	862
Serbia	57	56	51	50	52	59	57	57	58	75	76
Slovakia	31	32	31	22	29	27	28	23	24	24	25
Slovenia	18	17	16	14	15	15	15	14	13	13	14
Spain	251	226	241	219	238	215	212	230	211	212	215
Sweden	45	42	43	38	37	38	39	38	37	35	35
Switzerland	19	19	18	18	17	16	16	16	15	14	14
Tajikistan	15	20	21	28	31	34	38	43	45	47	50
Türkiye	577	571	566	560	555	554	554	553	553	563	552
Turkmenistan	27	27	28	25	26	25	25	27	28	29	31
Ukraine	491	477	463	448	434	440	447	453	460	452	470
United Kingdom	150	144	153	148	146	147	153	151	147	134	144
Uzbekistan	73	69	69	67	65	72	76	77	82	85	90
Asian areas	1635	1650	1665	1676	1686	1695	1705	1714	1816	1857	2008
North Africa	279	282	285	286	285	284	283	282	290	269	291
Baltic Sea	11	11	10	11	4	4	4	4	4	4	4
Black Sea	4	4	4	4	4	4	4	4	4	2	2
Mediterranean Sea	70	69	68	63	68	68	70	71	72	21	29
North Sea	23	23	23	24	11	10	11	11	10	9	9
North-East Atlantic Ocean	44	43	43	46	49	48	50	51	49	14	15
Natural marine emissions	0	0	0	0	0	0	0	0	0	0	0
Volcanic emissions	47039	0	0	0	0	0	0	0	0	0	0
TOTAL	54674	7520	7478	7268	7234	7154	7151	7258	7198	7039	7261

Table B:22: National total emission trends of coarse particulate matter (1990-1999), as used for modelling at the MSC-W (Gg of PM$_{coarse}$ per year).

Area/Year	1990	1991	1992	1993	1994	1995	1996	1997	1998	1999
Albania	10	8	7	5	4	2	2	2	2	2
Armenia	2	2	2	1	1	1	1	1	1	1
Austria	16	16	16	16	16	16	16	16	16	16
Azerbaijan	5	5	4	4	4	3	4	4	4	5
Belarus	45	42	39	36	33	30	29	27	26	24
Belgium	23	23	22	21	21	20	19	18	17	16
Bosnia and Herzegovina	78	64	50	36	22	8	10	11	12	14
Bulgaria	26	22	21	21	23	23	23	24	24	23
Croatia	19	17	13	14	17	17	19	19	17	15
Cyprus	2	2	2	2	2	2	2	2	2	2
Czechia	134	113	92	82	63	47	46	35	27	21
Denmark	12	12	11	11	11	12	11	11	12	11
Estonia	106	96	87	77	67	57	49	41	33	25
Finland	27	24	22	21	21	19	19	19	17	17
France	121	123	118	109	109	109	111	110	108	108
Georgia	12	10	9	7	5	3	3	3	3	3
Germany	460	397	334	271	208	145	141	147	145	144
Greece	87	82	78	73	69	64	63	63	62	61
Hungary	88	76	65	54	43	32	30	28	27	25
Iceland	2	1	1	1	2	2	2	2	2	2
Ireland	16	16	16	16	16	15	16	18	18	19
Italy	106	273	101	92	98	107	100	87	103	94
Kazakhstan	140	128	115	102	90	77	74	71	67	64
Kyrgyzstan	21	18	14	10	7	3	3	3	3	3
Latvia	6	5	5	4	4	4	4	5	5	5
Lithuania	27	25	23	22	20	18	18	18	18	17
Luxembourg	1	1	1	1	1	1	1	1	1	1
Malta	0	0	0	0	0	0	0	0	0	0
Moldova	8	7	6	5	4	4	3	3	3	3
Montenegro	1	1	1	1	1	1	1	1	1	1
Netherlands	23	22	21	20	18	17	16	15	14	15
North Macedonia	16	14	16	14	13	14	15	15	17	14
Norway	12	10	11	10	11	10	11	11	11	11
Poland	365	321	276	256	232	188	177	156	135	127
Portugal	16	17	17	17	17	18	16	18	78	39
Romania	55	44	39	41	40	41	42	38	36	32
Russian Federation	1173	1041	910	779	648	519	516	513	510	508
Serbia	19	17	16	14	14	15	15	16	16	14
Slovakia	12	11	10	10	10	10	11	10	12	10
Slovenia	16	14	12	10	8	6	6	5	5	4
Spain	130	127	125	122	119	116	115	114	112	111
Sweden	21	21	21	20	21	20	20	19	20	19
Switzerland	9	9	9	8	8	8	8	8	8	7
Tajikistan	9	7	6	4	2	2	1	2	2	2
Türkiye	255	236	218	200	182	164	156	148	140	132
Turkmenistan	8	7	8	5	4	4	5	4	5	5
Ukraine	691	611	530	449	369	288	268	249	229	209
United Kingdom	141	140	128	116	108	102	104	97	91	88
Uzbekistan	29	29	24	24	22	18	18	19	19	20
Asian areas	409	419	430	441	451	460	466	472	478	484
North Africa	58	60	62	64	66	69	71	74	77	79
Baltic Sea	0	0	0	0	0	0	0	0	0	0
Black Sea	0	0	0	0	0	0	0	0	0	0
Mediterranean Sea	0	0	0	0	0	0	0	0	0	0
North Sea	0	0	0	0	0	0	0	0	0	0
North-East Atlantic Ocean	0	0	0	0	0	0	0	0	0	0
Natural marine emissions	0	0	0	0	0	0	0	0	0	0
Volcanic emissions	0	0	0	0	0	0	0	0	0	0
TOTAL	5065	4785	4159	3743	3345	2932	2879	2794	2791	2672

Table B:23: National total emission trends of coarse particulate matter (2000-2010), as used for modelling at the MSC-W (Gg of PM_{coarse} per year).

Area/Year	2000	2001	2002	2003	2004	2005	2006	2007	2008	2009	2010
Albania	2	2	2	2	2	2	2	2	2	2	2
Armenia	1	1	1	1	1	1	1	1	1	1	2
Austria	16	16	16	15	16	15	15	15	15	14	14
Azerbaijan	5	5	5	5	5	5	5	5	6	6	6
Belarus	23	22	22	21	20	19	19	19	19	19	19
Belgium	15	14	13	14	13	12	11	11	10	9	9
Bosnia and Herzegovina	15	16	17	17	18	19	18	18	18	18	18
Bulgaria	28	21	27	26	28	29	27	24	22	17	14
Croatia	12	11	15	17	16	13	14	15	17	14	14
Cyprus	2	2	2	2	2	2	2	2	2	1	1
Czechia	20	19	18	17	17	17	17	18	17	16	15
Denmark	12	12	12	11	11	12	11	11	16	11	12
Estonia	17	16	12	11	10	10	8	12	9	8	12
Finland	17	17	17	18	17	16	17	16	16	15	15
France	105	103	100	102	101	96	94	91	89	84	85
Georgia	3	3	3	3	3	8	8	8	8	8	8
Germany	138	129	128	120	118	115	114	111	111	105	110
Greece	61	62	64	60	63	55	59	55	65	57	42
Hungary	23	26	23	26	31	31	22	21	27	28	21
Iceland	2	2	2	3	2	1	1	1	2	2	2
Ireland	20	21	21	23	23	24	24	24	23	22	20
Italy	88	93	220	85	113	104	74	142	87	94	128
Kazakhstan	61	61	61	62	62	62	65	67	71	75	78
Kyrgyzstan	4	4	4	4	4	4	4	5	5	5	5
Latvia	5	5	5	5	12	8	9	10	10	8	8
Lithuania	17	17	17	17	17	18	20	16	18	16	13
Luxembourg	1	1	1	1	1	1	1	1	1	1	1
Malta	0	1	0	0	1	1	1	1	1	1	1
Moldova	2	3	3	2	3	4	4	4	4	3	4
Montenegro	1	1	2	2	3	4	3	3	3	3	3
Netherlands	15	15	15	14	14	14	13	14	14	13	13
North Macedonia	14	10	10	13	14	13	12	10	10	10	13
Norway	10	10	10	10	9	9	10	10	10	10	10
Poland	113	113	112	110	109	113	120	116	114	110	112
Portugal	18	24	32	24	20	16	24	16	18	18	17
Romania	33	34	34	38	42	38	39	41	39	35	36
Russian Federation	506	506	505	505	504	520	507	493	479	466	455
Serbia	14	14	14	14	15	15	15	15	15	14	14
Slovakia	11	10	10	10	9	9	9	8	8	8	7
Slovenia	4	4	4	4	4	4	4	5	5	2	4
Spain	110	108	112	115	117	118	121	119	100	88	83
Sweden	19	19	19	19	19	19	19	20	19	18	18
Switzerland	7	7	7	7	7	8	8	8	8	8	8
Tajikistan	2	2	2	2	3	3	3	4	4	4	4
Türkiye	124	120	117	113	110	106	113	119	125	132	138
Turkmenistan	6	6	6	7	6	7	7	6	6	6	6
Ukraine	190	191	193	195	197	197	189	181	174	166	158
United Kingdom	89	96	83	97	83	80	76	71	63	59	68
Uzbekistan	19	20	19	18	18	17	17	18	18	18	18
Asian areas	496	510	524	538	552	571	589	608	626	641	648
North Africa	83	87	92	96	100	100	100	100	100	101	102
Baltic Sea	0	0	0	0	0	0	0	0	0	0	0
Black Sea	0	0	0	0	0	0	0	0	0	0	0
Mediterranean Sea	0	0	0	0	0	0	0	0	0	0	0
North Sea	0	0	0	0	0	0	0	0	0	0	0
North-East Atlantic Ocean	0	0	0	0	0	0	0	0	0	0	0
Natural marine emissions	0	0	0	0	0	0	0	0	0	0	0
Volcanic emissions	0	0	0	0	0	0	0	0	0	0	4297
TOTAL	2597	2610	2750	2641	2688	2686	2670	2714	2650	2592	6911

Table B:24: National total emission trends of coarse particulate matter (2011-2021), as used for modelling at the MSC-W (Gg of PM_{coarse} per year).

Area/Year	2011	2012	2013	2014	2015	2016	2017	2018	2019	2020	2021
Albania	2	2	2	2	2	2	2	3	3	3	3
Armenia	2	2	2	2	2	2	2	2	2	2	2
Austria	14	13	13	14	14	14	14	14	14	13	14
Azerbaijan	6	6	7	7	7	8	8	9	10	10	11
Belarus	19	18	18	18	18	18	18	18	18	17	18
Belgium	9	9	9	9	9	9	9	9	9	9	9
Bosnia and Herzegovina	18	18	19	19	20	17	15	13	10	8	7
Bulgaria	18	14	13	16	17	12	12	13	15	13	13
Croatia	12	13	14	15	8	13	9	14	8	23	23
Cyprus	1	1	1	1	1	1	1	1	1	1	1
Czechia	15	15	14	14	14	13	13	13	13	12	12
Denmark	11	11	11	12	10	10	11	11	11	10	10
Estonia	19	9	11	10	8	7	7	8	7	8	7
Finland	15	14	15	14	14	14	13	13	13	13	14
France	85	85	84	80	81	82	84	82	83	76	81
Georgia	8	8	8	8	8	8	8	8	8	8	8
Germany	114	113	115	115	114	105	108	115	106	101	101
Greece	30	26	27	30	26	28	26	22	22	22	22
Hungary	19	15	18	22	21	20	18	19	19	17	15
Iceland	1	1	1	1	1	1	1	1	1	1	1
Ireland	15	16	16	16	16	17	18	17	18	18	18
Italy	144	56	61	53	79	64	67	106	64	76	51
Kazakhstan	75	74	72	71	70	70	71	72	72	70	74
Kyrgyzstan	5	5	5	5	5	5	5	5	5	5	5
Latvia	10	10	9	9	11	9	9	9	10	9	11
Lithuania	18	14	18	18	21	16	15	22	19	21	18
Luxembourg	1	1	1	1	1	1	1	1	1	1	1
Malta	1	1	1	1	1	1	1	1	1	1	1
Moldova	4	4	4	4	4	3	4	5	4	6	4
Montenegro	3	3	3	2	2	2	2	2	1	1	1
Netherlands	14	14	14	14	14	14	14	14	13	13	12
North Macedonia	14	13	13	10	8	7	5	6	5	5	4
Norway	10	10	10	10	10	10	10	10	10	10	10
Poland	111	114	106	101	97	99	102	100	97	89	91
Portugal	23	20	14	11	11	12	11	11	12	13	13
Romania	38	40	37	37	36	34	33	36	40	39	41
Russian Federation	456	460	453	454	446	440	441	439	436	436	434
Serbia	15	14	14	13	14	16	16	16	16	17	17
Slovakia	7	7	7	6	8	6	7	6	6	7	6
Slovenia	3	3	2	2	2	2	2	3	3	3	4
Spain	87	82	77	76	85	81	79	81	82	78	80
Sweden	20	18	19	18	18	19	19	19	19	18	19
Switzerland	8	8	8	8	8	8	8	8	8	8	8
Tajikistan	4	5	5	7	7	8	9	10	11	11	11
Türkiye	144	151	157	163	170	170	169	169	169	171	169
Turkmenistan	7	7	7	6	6	6	6	6	7	7	7
Ukraine	153	149	144	139	135	134	134	133	133	127	131
United Kingdom	62	57	63	61	60	64	69	65	64	55	61
Uzbekistan	18	17	17	16	16	17	18	18	19	19	21
Asian areas	655	662	669	675	681	687	693	698	740	756	818
North Africa	104	106	108	109	110	111	112	113	116	108	116
Baltic Sea	0	0	0	0	0	0	0	0	0	0	0
Black Sea	0	0	0	0	0	0	0	0	0	0	0
Mediterranean Sea	0	0	0	0	0	0	0	0	0	0	0
North Sea	0	0	0	0	0	0	0	0	0	0	0
North-East Atlantic Ocean	0	0	0	0	0	0	0	0	0	0	0
Natural marine emissions	0	0	0	0	0	0	0	0	0	0	0
Volcanic emissions	33854	0	0	0	0	0	0	0	0	0	0
TOTAL	36498	2529	2535	2526	2545	2516	2528	2588	2573	2566	2629

APPENDIX C

Source-receptor tables for 2021

The source-receptor tables in this appendix are calculated for the meteorological and chemical conditions of 2021, using the EMEP MSC-W model version rv5.0. The tables are calculated for the EMEP domain covering the geographic area between 30° N–82° N latitude and 30° W–90° E longitude, and are based on model runs driven by ECMWF-IFS(cy46r1) meteorology in $0.3° \times 0.2°$ longitude-latitude projection.

The source-receptor (SR) relationships give the change in air concentrations or depositions resulting from a change in emissions from each emitter country.

All tables in this appendix are based on source-receptor calculations with the 15% perturbation method using the EMEPwRef2_v2.1C emission data set as described in Chapter 3 and summarized in Appendix A. The perturbation method means that for each country, reductions in five different pollutants have been calculated separately, with an emission reduction of 15% for SO_x, NO_x, NH_3, NMVOC or PPM, respectively. Here, a reduction in PPM means that $PPM_{2.5}$ and PPM_{coarse} are reduced together in one simulation.

For year 2021, reductions in volcanic emissions are done both for passive SO_2 degassing of Italian volcanoes (Etna, Stromboli and Vulcano) and for SO_2 emissions from the Mt. Fagradalsfjall eruption in Iceland.

The deposition tables show the contribution from one country to another. They have been calculated adding the differences obtained by a 15% reduction for all emissions in one country multiplied by a factor of 100/15, in order to arrive at total estimates.

For the concentrations and indicator tables, the differences obtained by the 15% emission reduction of the relevant pollutants are given directly. Thus, the tables should be interpreted as estimates of this reduction scenario from the chemical conditions in 2021.

The SR tables in the following aim to respond to two fundamental questions about transboundary air pollution:

1. Where do the pollutants emitted by a country or region end up?

2. Where do the pollutants in a given country or region come from?

Each column answers the first question. The numbers within a column give the change in the value of each pollutant (or indicator) for each receiver country caused by the emissions in the country given at the top of the column.

Each row answers the second question. The numbers given in each row show which emitter countries were responsible for the change in pollutants in the country given at the beginning of each row.

A list of abbreviations of countries and regions is given in Table 1.2.

More information on aerosol components and SR tables in electronic format are available from the EMEP website www.emep.int.

Acidification and eutrophication

- Deposition of OXS (oxidised sulphur). The contribution from SO_x, NO_x, NH_3, PPM and VOC emissions have been summed up and scaled to a 100% reduction. Units: 100 Mg of S.

- Deposition of OXN (oxidised nitrogen). The contribution from SO_x, NO_x, NH_3, PPM and VOC emissions have been summed up and scaled to a 100% reduction. Units: 100 Mg of N.

- Deposition of RDN (reduced nitrogen). The contribution from SO_x, NO_x, NH_3, PPM and VOC emissions have been summed up and scaled to a 100% reduction. Units: 100 Mg of N.

Ground Level Ozone

- MM-AOT40f. Effect of a 15% reduction in NO_x emissions. Units: ppb.h

- MM-AOT40f. Effect of a 15% reduction in VOC emissions. Units: ppb.h

- SOMO35. Effect of a 15% reduction in NO_x emissions. Units: ppb.d

- SOMO35. Effect of a 15% reduction in VOC emissions. Units: ppb.d

- $MDA8_{AS}$. Effect of a 15% reduction in NO_x emissions. Units: ng/m^3

- $MDA8_{AS}$. Effect of a 15% reduction in VOC emissions. Units: ng/m^3

For ozone, we do not include the contributions from areas that are outside the EMEP domain. Until last year these had been included in the tables as BIC (Boundary and Initial Conditions) and were calculated by reducing NOx and NMVOC at the model boundary. However, the most important contributor to ozone from areas outside the EMEP domain is ozone itself, transported hemispherically accross the model boundary. Including the BIC contribution that is due (only) to NOx and NMVOC only would be misleading.

Particulate Matter

- $PM_{2.5}$. Effect of a 15% reduction in PPM emissions. Units: ng/m^3
- $PM_{2.5}$. Effect of a 15% reduction in SO_x emissions. Units: ng/m^3
- $PM_{2.5}$. Effect of a 15% reduction in NO_x emissions. Units: ng/m^3
- $PM_{2.5}$. Effect of a 15% reduction in NH_3 emissions. Units: ng/m^3
- $PM_{2.5}$. Effect of a 15% reduction in VOC emissions. Units: ng/m^3
- $PM_{2.5}$. Effect of a 15% reduction in all emissions. The contribution from a 15% reduction in PPM, SO_x, NO_x, NH_3 and VOC emissions have been summed up. Units: ng/m^3

Fine Elemental Carbon

- Fine EC. Effect of a 15% reduction in PPM emissions. Units: 0.1 ng/m^3

Coarse Elemental Carbon

- Coarse EC. Effect of a 15% reduction in PPM emissions. Units: 0.1 ng/m^3

Primary Particulate Matter

- $PPM_{2.5}$. Effect of a 15% reduction in PPM emissions. Units: ng/m^3

Table C.1: 2021 country-to-country blame matrices for **oxidised sulphur** deposition.
Units: 100 Mg of S. **Emitters →, Receptors ↓.**

	AL	AM	AT	AZ	BA	BE	BG	BY	CH	CY	CZ	DE	DK	EE	ES	FI	FR	GB	GE	GR	HR	HU	IE	IS	IT	KG	KZ	LT	LU	LV	MD	ME	
AL	15	0	0	0	1	0	0	0	0	0	0	0	0	0	1	0	0	0	0	1	0	0	0	0	3	0	0	0	0	0	0	5	AL
AM	0	13	0	17	0	0	0	0	0	0	0	0	0	0	0	0	0	0	3	0	0	0	0	0	0	0	2	0	0	0	0	0	AM
AT	0	0	23	0	0	0	0	0	1	0	9	28	0	0	1	0	2	1	0	0	1	1	0	0	3	0	0	0	0	0	0	0	AT
AZ	0	4	0	131	0	0	0	0	0	0	0	0	0	0	0	0	0	0	10	0	0	0	0	0	0	0	9	0	0	0	0	0	AZ
BA	0	0	1	0	42	0	1	0	0	0	3	3	0	0	1	0	1	0	0	0	1	1	0	0	4	0	0	0	0	0	0	13	BA
BE	0	0	0	0	0	27	0	0	0	0	0	12	0	0	1	0	11	4	0	0	0	0	0	0	0	0	0	0	0	0	0	0	BE
BG	1	0	0	0	2	0	80	1	0	0	2	2	0	0	1	0	0	0	0	9	0	1	0	0	2	0	1	0	0	0	0	7	BG
BY	0	0	1	1	1	0	2	121	0	0	7	14	0	1	1	1	1	1	0	1	0	1	0	0	1	0	5	3	0	1	1	2	BY
CH	0	0	0	0	0	0	0	0	8	0	0	5	0	0	1	0	5	0	0	0	0	0	0	0	4	0	0	0	0	0	0	0	CH
CY	0	0	0	0	0	0	0	0	0	3	0	0	0	0	0	0	0	0	0	0	0	0	0	0	0	0	0	0	0	0	0	0	CY
CZ	0	0	3	0	1	1	0	0	0	0	102	38	0	0	1	0	2	1	0	0	0	1	0	0	1	0	0	0	0	0	0	1	CZ
DE	0	0	5	0	0	17	0	2	3	0	31	530	2	0	5	0	32	19	0	0	0	0	1	1	3	0	1	0	1	0	0	1	DE
DK	0	0	0	0	0	1	0	0	0	0	1	14	8	0	0	0	2	3	0	0	0	0	0	0	0	0	0	0	0	0	0	0	DK
EE	0	0	0	0	0	0	0	3	0	0	1	3	0	6	0	2	0	1	0	0	0	0	0	0	0	0	1	1	0	1	0	0	EE
ES	0	0	0	0	0	1	0	0	0	0	0	4	0	0	233	0	6	2	0	0	0	0	0	0	2	0	0	0	0	0	0	1	ES
FI	0	0	0	0	0	0	0	6	0	0	2	8	1	6	1	44	1	2	0	0	0	0	0	1	0	0	7	2	0	1	0	1	FI
FR	0	0	1	0	0	11	0	0	2	0	2	46	0	0	57	0	188	23	0	0	0	0	1	0	9	0	0	0	1	0	0	1	FR
GB	0	0	0	0	0	3	0	0	0	0	1	11	0	0	2	0	7	220	0	0	0	0	6	1	0	0	0	0	0	0	0	0	GB
GE	0	4	0	31	0	0	0	0	0	1	0	0	0	0	0	0	0	0	75	1	0	0	0	0	0	0	7	0	0	0	0	1	GE
GL	0	0	0	0	0	0	0	0	0	0	0	0	0	0	0	0	0	0	0	0	0	0	0	1	0	0	0	0	0	0	0	0	GL
GR	2	0	0	0	1	0	9	0	0	0	1	1	0	0	1	0	0	0	0	53	0	0	0	0	4	0	0	0	0	0	0	5	GR
HR	0	0	1	0	5	0	1	0	0	0	3	3	0	0	1	0	2	0	0	0	10	1	0	0	6	0	0	0	0	0	0	3	HR
HU	0	0	3	0	4	0	2	0	0	0	8	7	0	0	1	0	1	0	0	1	2	26	0	0	3	0	0	0	0	0	0	6	HU
IE	0	0	0	0	0	0	0	0	0	0	0	2	0	0	0	0	1	7	0	0	0	0	21	0	0	0	0	0	0	0	0	0	IE
IS	0	0	0	0	0	0	0	0	0	0	0	0	0	0	0	0	0	1	0	0	0	0	0	60	0	0	0	0	0	0	0	0	IS
IT	1	0	2	0	3	0	1	0	1	0	3	6	0	0	11	0	12	0	0	1	3	1	0	0	133	0	0	0	0	0	0	7	IT
KG	0	0	0	1	0	0	0	0	0	0	0	0	0	0	0	0	0	0	0	0	0	0	0	0	0	63	166	0	0	0	0	0	KG
KZ	0	5	0	49	1	0	2	5	0	1	3	5	0	1	0	1	1	1	8	2	0	0	0	0	1	43	4439	0	0	0	0	4	KZ
LT	0	0	0	0	0	0	0	14	0	0	3	9	0	0	0	0	1	1	0	0	0	0	0	0	0	0	1	13	0	1	0	0	LT
LU	0	0	0	0	0	0	0	0	0	0	0	1	0	0	0	0	1	0	0	0	0	0	0	0	0	0	0	0	0	0	0	0	LU
LV	0	0	0	0	0	0	0	7	0	0	2	7	0	1	0	1	1	1	0	0	0	0	0	0	0	0	1	8	0	6	0	0	LV
MD	0	0	0	0	0	0	2	1	0	0	0	1	0	0	0	0	0	0	0	0	0	0	0	0	0	0	1	0	0	0	6	1	MD
ME	1	0	0	0	3	0	0	0	0	0	0	0	0	0	0	0	0	0	0	0	0	0	0	0	2	0	0	0	0	0	0	30	ME
MK	1	0	0	0	0	0	1	0	0	0	0	0	0	0	0	0	0	0	0	5	0	0	0	0	1	0	0	0	0	0	0	2	MK
MT	0	0	0	0	0	0	0	0	0	0	0	0	0	0	0	0	0	0	0	0	0	0	0	0	0	0	0	0	0	0	0	0	MT
NL	0	0	0	0	0	15	0	0	0	0	1	21	0	0	1	0	7	7	0	0	0	0	0	0	0	0	0	0	0	0	0	0	NL
NO	0	0	0	0	0	1	0	1	0	0	1	10	1	0	1	1	2	7	0	0	0	0	0	3	0	0	1	0	0	0	0	0	NO
PL	0	0	2	0	2	2	2	19	0	0	54	123	2	1	2	1	5	6	0	0	1	4	0	0	2	0	2	2	0	0	0	6	PL
PT	0	0	0	0	0	0	0	0	0	0	0	0	0	0	10	0	0	0	0	0	0	0	0	0	0	0	0	0	0	0	0	0	PT
RO	1	0	1	0	7	0	25	4	0	0	6	8	0	0	2	0	1	0	0	4	1	6	0	0	5	0	2	0	0	0	2	19	RO
RS	1	0	1	0	10	0	5	0	0	0	4	4	0	0	1	0	1	0	0	3	1	4	0	0	3	0	1	0	0	0	0	36	RS
RU	1	7	2	84	4	2	17	97	0	2	24	54	3	27	3	27	5	8	23	10	1	4	0	3	4	7	3428	10	0	4	2	18	RU
SE	0	0	1	0	0	2	1	6	0	0	6	28	4	2	1	7	3	6	0	0	0	0	0	1	1	0	3	2	0	1	0	1	SE
SI	0	0	1	0	0	0	0	0	0	0	1	2	0	0	1	0	1	0	0	0	2	0	0	0	4	0	0	0	0	0	0	0	SI
SK	0	0	1	0	2	0	1	0	0	0	11	6	0	0	1	0	1	0	0	0	1	5	0	0	1	0	0	0	0	0	0	3	SK
TJ	0	0	0	1	0	0	0	0	0	0	0	0	0	0	0	0	0	0	0	0	0	0	0	0	0	2	30	0	0	0	0	0	TJ
TM	0	1	0	10	0	0	0	0	0	0	0	0	0	0	0	0	0	0	1	0	0	0	0	0	0	0	48	0	0	0	0	0	TM
TR	1	4	0	6	1	0	12	2	0	6	1	2	0	0	1	0	1	0	3	14	0	0	0	0	3	0	4	0	0	0	0	5	TR
UA	1	1	1	7	5	1	18	37	0	0	13	23	1	1	2	1	2	2	3	6	1	5	0	0	4	0	23	2	0	0	4	14	UA
UZ	0	1	0	6	0	0	0	0	0	0	0	0	0	0	0	0	0	0	1	0	0	0	0	0	0	10	116	0	0	0	0	0	UZ
ATL	0	0	0	0	0	10	1	6	0	0	4	50	2	3	118	8	39	135	0	0	0	0	23	205	2	0	68	1	0	0	0	1	ATL
BAS	0	0	1	0	1	3	1	13	0	0	13	63	9	7	2	18	5	9	0	0	0	1	0	1	1	0	3	8	0	2	0	2	BAS
BLS	1	1	1	7	2	0	25	8	0	1	5	7	0	1	1	1	1	0	18	10	0	1	0	0	2	0	11	1	0	0	2	10	BLS
MED	7	0	4	0	16	1	25	1	1	14	13	26	0	0	91	0	50	3	0	68	6	2	0	0	156	0	1	0	0	0	0	56	MED
NOS	0	0	0	0	0	17	0	1	0	0	6	79	7	0	7	1	44	151	0	0	0	0	4	5	0	0	1	1	0	0	0	0	NOS
AST	0	3	0	104	0	0	1	1	0	5	1	1	0	0	0	0	0	0	6	3	0	0	0	0	1	20	617	0	0	0	0	1	AST
NOA	0	0	0	0	1	0	1	0	0	0	1	2	0	0	18	0	3	1	0	3	0	0	0	0	7	0	0	0	0	0	0	2	NOA
SUM	34	44	57	458	118	118	238	360	20	35	352	1276	43	58	582	115	448	627	153	198	33	70	59	281	381	145	9000	57	4	18	19	267	SUM
EXC	26	40	50	346	98	86	184	330	17	14	310	1047	25	47	345	87	306	327	129	114	26	65	31	71	211	126	8298	46	3	15	16	194	EXC
EU	5	0	44	1	30	79	123	64	9	3	251	912	20	17	331	57	281	86	1	70	21	47	24	3	180	0	21	30	3	10	3	63	EU
emis	35	39	54	429	118	117	254	366	19	50	345	1272	43	59	615	116	444	628	142	234	31	70	59	303	393	150	11236	57	4	18	19	299	emis
	AL	AM	AT	AZ	BA	BE	BG	BY	CH	CY	CZ	DE	DK	EE	ES	FI	FR	GB	GE	GR	HR	HU	IE	IS	IT	KG	KZ	LT	LU	LV	MD	ME	

Table C.1 Cont.: 2021 country-to-country blame matrices for **oxidised sulphur** deposition.
Units: 100 Mg of S. **Emitters →, Receptors ↓.**

	MK	MT	NL	NO	PL	PT	RO	RS	RU	SE	SI	SK	TJ	TM	TR	UA	UZ	ATL	BAS	BLS	MED	NOS	AST	NOA	BIC	DMS	VOL	SUM	EXC	EU	
AL	10	0	0	0	1	0	0	11	0	0	0	0	0	0	0	0	0	0	0	0	3	0	0	7	6	3	51	119	50	8	AL
AM	0	0	0	0	0	0	0	0	1	0	0	0	0	0	26	0	0	0	0	0	0	0	74	1	5	1	4	149	63	1	AM
AT	0	0	0	0	7	0	0	6	0	0	2	1	0	0	0	0	0	0	0	0	1	0	0	3	8	2	6	110	89	79	AT
AZ	0	0	0	0	0	0	0	0	8	0	0	0	0	2	25	1	1	0	0	0	0	0	123	2	8	1	6	329	190	1	AZ
BA	1	0	0	0	6	0	1	58	0	0	0	1	0	0	0	0	0	0	0	0	2	0	0	5	6	3	22	179	139	24	BA
BE	0	0	4	0	1	0	0	0	0	0	0	0	0	0	0	0	0	0	0	0	0	1	0	0	3	4	2	73	62	57	BE
BG	28	0	0	0	10	0	18	94	4	0	0	1	0	0	26	5	0	0	0	1	3	0	0	7	11	6	41	365	296	127	BG
BY	3	0	0	0	79	0	5	26	30	1	0	2	0	0	10	31	0	0	0	0	1	0	3	2	15	4	13	393	354	122	BY
CH	0	0	0	0	0	0	0	1	0	0	0	0	0	0	0	0	0	0	0	0	1	0	0	1	5	1	2	35	25	15	CH
CY	0	0	0	0	0	0	0	0	0	0	0	0	0	0	7	0	0	0	0	0	0	0	4	2	1	1	1	20	11	3	CY
CZ	1	0	0	0	31	0	1	18	1	0	1	3	0	0	0	0	0	0	0	0	1	0	0	2	7	2	5	228	211	187	CZ
DE	1	0	18	1	53	0	1	6	2	1	0	1	0	0	0	1	0	1	1	0	1	4	0	4	33	24	17	826	740	703	DE
DK	0	0	1	0	8	0	0	0	0	0	0	0	0	0	0	0	0	0	1	0	0	1	0	0	4	6	3	57	42	37	DK
EE	0	0	0	0	8	0	0	1	7	1	0	0	0	0	1	2	0	0	1	0	0	0	0	0	3	2	3	52	42	26	EE
ES	1	0	0	0	0	15	0	2	0	0	0	0	0	0	0	0	0	10	0	0	20	0	0	70	65	33	15	482	269	262	ES
FI	1	0	0	1	21	0	1	7	65	6	0	0	0	0	3	7	0	1	2	0	0	0	2	1	21	13	19	258	198	97	FI
FR	0	0	4	0	3	4	0	3	0	0	0	0	0	0	0	0	0	9	0	0	14	6	0	25	71	63	22	568	359	328	FR
GB	0	0	3	0	1	1	0	0	0	0	0	0	0	0	0	0	0	8	0	0	0	5	0	1	30	47	20	367	256	35	GB
GE	1	0	0	0	1	0	0	2	5	0	0	0	0	1	80	2	1	0	0	1	1	0	141	5	15	4	15	396	214	3	GE
GL	0	0	0	0	0	0	0	0	0	0	0	0	0	0	0	0	0	0	0	0	0	0	0	0	38	2	18	60	1	0	GL
GR	31	0	0	0	4	0	3	40	2	0	0	0	0	0	34	2	0	0	0	0	12	0	1	17	19	15	91	352	196	78	GR
HR	2	0	0	0	5	0	1	29	1	0	1	1	0	0	1	1	0	0	0	0	4	0	0	5	7	4	21	121	79	38	HR
HU	5	0	0	0	25	0	9	94	2	0	1	8	0	0	1	2	0	0	0	0	2	0	0	6	8	3	19	251	213	97	HU
IE	0	0	0	0	0	0	0	0	0	0	0	0	0	0	0	0	0	2	0	0	0	0	0	0	11	17	6	69	32	25	IE
IS	0	0	0	0	0	0	0	0	0	0	0	0	0	0	0	0	0	1	0	0	0	0	0	0	22	18	500	603	63	1	IS
IT	4	0	0	0	6	1	1	25	0	0	2	1	0	0	4	0	0	1	0	0	32	0	1	44	42	32	269	651	231	184	IT
KG	0	0	0	0	0	0	0	0	4	0	0	0	111	7	9	0	300	0	0	0	0	0	108	1	21	0	5	799	663	0	KG
KZ	6	0	0	0	15	0	3	16	417	0	0	1	90	59	118	44	442	0	0	1	2	0	809	11	154	6	68	6834	5784	37	KZ
LT	1	0	0	0	36	0	1	4	6	1	0	1	0	0	1	4	0	0	0	0	0	0	0	0	5	3	4	113	100	67	LT
LU	0	0	0	0	0	0	0	0	0	0	0	0	0	0	0	0	0	0	0	0	0	0	0	0	0	0	0	4	3	3	LU
LV	0	0	0	0	20	0	0	2	7	1	0	0	0	0	1	3	0	0	1	0	0	0	0	0	5	3	4	87	73	49	LV
MD	2	0	0	0	5	0	4	7	3	0	0	0	0	0	8	7	0	0	0	0	0	0	1	1	2	1	6	62	51	14	MD
ME	1	0	0	0	1	0	0	8	0	0	0	0	0	0	0	0	0	0	0	0	1	0	0	3	3	1	16	72	47	4	ME
MK	64	0	0	0	1	0	1	18	0	0	0	0	0	0	1	0	0	0	0	0	1	0	0	2	3	1	15	120	99	10	MK
MT	0	0	0	0	0	0	0	0	0	0	0	0	0	0	0	0	0	0	0	0	0	0	0	0	0	0	0	1	0	0	MT
NL	0	0	25	0	3	0	0	0	0	0	0	0	0	0	0	0	0	0	0	0	0	3	0	0	4	8	2	98	81	73	NL
NO	0	0	1	23	9	0	0	2	19	2	0	0	0	0	0	1	0	4	1	0	0	4	0	1	43	54	48	243	89	32	NO
PL	4	0	2	1	870	0	7	60	10	2	1	9	0	0	2	10	0	0	1	0	1	0	0	4	27	11	22	1285	1218	1095	PL
PT	0	0	0	0	0	46	0	0	0	0	0	0	0	0	0	0	0	6	0	0	2	0	0	10	14	10	3	102	58	57	PT
RO	28	0	0	0	38	0	145	197	10	0	0	3	0	0	32	16	0	0	0	1	4	0	1	13	21	8	59	674	567	247	RO
RS	36	0	0	0	13	0	9	410	3	0	0	2	0	0	2	3	0	0	0	0	2	0	0	6	9	3	34	610	555	54	RS
RU	28	0	2	4	198	0	24	118	4627	9	1	6	28	36	445	376	100	4	5	7	9	2	606	32	551	127	282	11503	9880	438	RU
SE	1	0	2	5	47	0	1	12	22	27	0	1	0	0	1	5	0	1	4	0	0	2	0	2	31	24	24	292	202	137	SE
SI	0	0	0	0	1	0	0	3	0	0	6	0	0	0	0	0	0	0	0	0	2	0	0	2	2	1	4	34	23	19	SI
SK	2	0	0	0	31	0	3	37	1	0	1	18	0	0	0	1	0	0	0	0	1	0	0	3	5	1	8	145	127	81	SK
TJ	0	0	0	0	0	0	0	0	2	0	0	0	242	9	4	0	78	0	0	0	0	0	90	0	16	0	3	477	367	0	TJ
TM	0	0	0	0	0	0	0	0	12	0	0	0	13	78	12	1	40	0	0	0	0	0	283	2	23	0	7	535	219	1	TM
TR	14	0	0	0	9	0	7	38	13	0	0	0	0	0	1878	14	0	0	0	5	25	0	873	71	105	39	177	3337	2042	59	TR
UA	19	0	1	0	139	0	34	126	127	1	1	5	0	1	148	367	1	0	1	4	6	0	33	16	45	17	77	1345	1146	260	UA
UZ	1	0	0	0	0	0	0	1	14	0	0	0	93	28	13	2	416	0	0	0	0	0	224	2	26	0	8	964	703	1	UZ
ATL	2	0	8	23	20	75	1	7	417	6	0	0	0	0	3	6	1	314	1	0	14	19	3	119	2907	4426	2985	12033	1246	371	ATL
BAS	2	0	3	2	126	0	2	15	40	17	0	2	0	0	3	10	0	1	22	0	1	2	1	2	30	50	18	511	384	284	BAS
BLS	19	0	0	0	35	0	25	87	83	0	0	1	0	1	527	96	0	0	0	37	10	0	122	25	45	128	96	1458	992	118	BLS
MED	65	1	1	0	32	6	13	168	7	0	2	3	0	0	599	11	0	7	0	3	560	1	282	646	305	790	1325	5370	1453	516	MED
NOS	0	0	26	12	28	1	0	2	3	3	0	0	0	0	0	0	0	10	2	0	1	53	0	4	94	338	95	999	403	226	NOS
AST	4	0	0	0	3	0	1	6	68	0	0	0	110	67	211	11	177	0	0	0	6	0	7384	57	590	14	72	9550	1426	18	AST
NOA	3	0	0	0	2	5	1	8	1	0	0	0	0	0	14	1	0	6	0	0	25	0	12	870	171	41	48	1248	76	45	NOA
SUM	391	1	107	75	1950	158	329	1780	6046	78	21	72	688	291	4249	1043	1557	386	46	62	774	105	11182	2117	5722	6418	6707	68019			SUM
EXC	297	0	68	38	1704	71	284	1486	5427	52	18	65	578	223	2892	908	1378	49	19	21	157	30	3378	394	1580	630	2068		28522	5277	EXC
EU	112	0	61	10	1226	69	194	643	142	38	16	48	0	0	112	60	0	32	13	3	101	19	11	222	429	297	670		5521	4155	EU
emis	443	1	104	73	1962	196	331	1891	6683	77	20	71	680	357	4880	1073	1654	449	46	63	883	105	21951	4780		14340	9552	90686	38518	7000	emis
	MK	MT	NL	NO	PL	PT	RO	RS	RU	SE	SI	SK	TJ	TM	TR	UA	UZ	ATL	BAS	BLS	MED	NOS	AST	NOA	BIC	DMS	VOL	SUM	EXC	EU	

Table C.2: 2021 country-to-country blame matrices for **oxidised nitrogen** deposition.
Units: 100 Mg of N. **Emitters →, Receptors ↓.**

	AL	AM	AT	AZ	BA	BE	BG	BY	CH	CY	CZ	DE	DK	EE	ES	FI	FR	GB	GE	GR	HR	HU	IE	IS	IT	KG	KZ	LT	LU	LV	MD	ME	
AL	16	0	1	0	1	0	1	0	0	0	1	1	0	0	2	0	1	0	0	3	1	1	0	0	12	0	0	0	0	0	0	1	AL
AM	0	26	0	40	0	0	0	0	0	0	0	0	0	0	0	0	0	0	3	0	0	0	0	0	0	0	0	0	0	0	0	0	AM
AT	0	0	93	0	1	3	0	0	9	0	16	80	1	0	5	0	17	4	0	0	3	3	0	0	33	0	0	0	0	0	0	0	AT
AZ	0	12	0	270	0	0	0	0	0	0	0	0	0	0	0	0	0	0	11	0	0	0	0	0	0	0	2	0	0	0	0	0	AZ
BA	1	0	6	0	28	1	1	0	1	0	6	11	0	0	4	0	4	1	0	1	7	8	0	0	23	0	0	0	0	0	0	1	BA
BE	0	0	0	0	0	40	0	0	0	0	0	18	1	0	2	0	34	17	0	0	0	0	1	0	0	0	0	0	1	0	0	0	BE
BG	3	0	2	0	2	1	77	1	0	0	4	8	0	0	3	0	2	1	0	19	1	8	0	0	9	0	0	0	0	0	2	1	BG
BY	0	0	4	1	1	3	2	108	1	0	11	41	4	2	2	3	8	8	0	1	1	7	1	0	5	0	1	13	0	5	3	0	BY
CH	0	0	2	0	0	2	0	0	39	0	0	17	0	0	5	0	26	2	0	0	0	0	0	0	21	0	0	0	0	0	0	0	CH
CY	0	0	0	0	0	0	0	0	0	3	0	0	0	0	0	0	0	0	0	1	0	0	0	0	0	0	0	0	0	0	0	0	CY
CZ	0	0	21	0	1	5	0	0	3	0	99	99	2	0	3	0	16	6	0	0	2	8	0	0	10	0	0	0	1	0	0	0	CZ
DE	0	0	29	0	0	64	0	2	25	0	40	880	18	0	16	2	181	91	0	0	1	3	6	0	19	0	0	2	11	1	0	0	DE
DK	0	0	0	0	0	5	0	0	0	0	2	32	21	0	1	0	9	16	0	0	0	0	1	0	0	0	0	0	0	0	0	0	DK
EE	0	0	0	0	0	1	0	5	0	0	1	10	2	7	0	5	2	3	0	0	0	0	0	0	0	0	0	3	0	4	0	0	EE
ES	0	0	1	0	0	3	0	0	1	0	0	12	0	0	625	0	49	10	0	0	0	0	1	0	8	0	0	0	0	0	0	0	ES
FI	0	0	1	1	0	3	0	10	1	0	3	23	6	7	2	87	6	10	0	0	0	2	1	0	2	0	1	5	0	5	0	0	FI
FR	0	0	4	0	0	45	0	0	15	0	4	132	3	0	146	1	788	103	0	0	1	1	10	0	48	0	0	0	6	0	0	0	FR
GB	0	0	0	0	0	10	0	0	0	0	1	29	2	0	5	0	30	363	0	0	0	0	32	0	0	0	0	0	1	0	0	0	GB
GE	0	15	0	91	0	0	0	0	0	0	0	1	0	0	1	0	0	0	55	1	0	0	0	0	1	0	1	0	0	0	0	0	GE
GL	0	0	0	0	0	0	0	0	0	0	0	0	0	0	0	0	0	1	0	0	0	0	0	0	0	0	0	0	0	0	0	0	GL
GR	5	0	2	0	2	0	14	1	0	0	2	4	0	0	4	0	3	1	0	108	1	3	0	0	14	0	0	0	0	0	1	1	GR
HR	1	0	11	0	9	1	1	0	1	0	7	15	0	0	5	0	8	1	0	1	23	11	0	0	41	0	0	0	0	0	0	0	HR
HU	1	0	22	0	6	2	2	1	2	0	16	29	1	0	6	0	9	2	0	1	9	64	0	0	28	0	0	0	0	0	0	0	HU
IE	0	0	0	0	0	2	0	0	0	0	0	5	0	0	1	0	6	21	0	0	0	0	39	0	0	0	0	0	0	0	0	0	IE
IS	0	0	0	0	0	0	0	0	0	0	0	1	0	0	0	0	1	4	0	0	0	0	1	9	0	0	0	0	0	0	0	0	IS
IT	2	0	20	0	6	2	1	0	10	0	7	27	1	0	45	0	59	3	0	3	12	6	0	0	631	0	0	0	0	0	0	1	IT
KG	0	1	0	4	0	0	0	0	0	0	0	0	0	0	0	0	0	0	0	0	0	0	0	0	0	63	25	0	0	0	0	0	KG
KZ	1	21	2	129	1	2	2	10	1	1	3	15	1	1	4	3	7	5	11	5	1	3	1	0	6	51	661	2	0	1	1	0	KZ
LT	0	0	1	0	0	2	0	12	0	0	5	25	4	1	1	2	4	6	0	0	0	1	0	0	1	0	0	21	0	4	0	0	LT
LU	0	0	0	0	0	1	0	0	0	0	0	2	0	0	0	0	3	1	0	0	0	0	0	0	0	0	0	0	2	0	0	0	LU
LV	0	0	1	0	0	2	0	10	0	0	3	19	4	2	0	3	3	5	0	0	0	1	0	0	1	0	0	10	0	15	0	0	LV
MD	0	0	1	0	0	0	2	2	0	0	1	3	0	0	1	0	1	0	0	1	0	1	0	0	2	0	0	0	0	0	10	0	MD
ME	2	0	0	0	1	0	0	0	0	0	0	1	0	0	1	0	1	0	0	0	0	1	0	0	7	0	0	0	0	0	0	4	ME
MK	2	0	0	0	1	0	2	0	0	0	1	1	0	0	1	0	1	0	0	9	0	1	0	0	3	0	0	0	0	0	0	0	MK
MT	0	0	0	0	0	0	0	0	0	0	0	0	0	0	0	0	0	0	0	0	0	0	0	0	0	0	0	0	0	0	0	0	MT
NL	0	0	0	0	0	18	0	0	0	0	1	31	2	0	2	0	23	29	0	0	0	0	2	0	0	0	0	0	0	0	0	0	NL
NO	0	0	1	0	0	5	0	2	0	0	1	28	11	1	2	5	12	36	0	0	0	0	3	1	1	0	0	1	0	1	0	0	NO
PL	0	0	19	0	3	18	2	16	4	0	74	262	18	1	6	2	35	34	0	1	5	23	2	0	16	0	0	9	2	4	1	0	PL
PT	0	0	0	0	0	0	0	0	0	0	0	1	0	0	37	0	3	1	0	0	0	0	0	0	1	0	0	0	0	0	0	0	PT
RO	4	0	10	1	9	2	27	6	2	0	12	28	1	0	8	0	9	3	0	9	5	30	0	0	32	0	0	1	0	1	11	1	RO
RS	5	0	6	0	9	1	9	1	1	0	9	16	1	0	5	0	4	1	0	6	4	18	0	0	19	0	0	0	0	0	0	2	RS
RU	3	27	15	223	5	17	15	187	5	1	32	155	23	25	15	92	44	53	28	22	5	23	6	1	32	7	518	42	2	30	11	1	RU
SE	0	0	4	0	0	10	0	7	1	0	9	79	28	3	4	21	20	35	0	0	1	3	3	0	3	0	0	5	1	4	0	0	SE
SI	0	0	10	0	1	0	0	0	1	0	2	7	0	0	3	0	4	0	0	0	5	2	0	0	23	0	0	0	0	0	0	0	SI
SK	0	0	10	0	2	1	1	0	1	0	16	21	1	0	3	0	5	2	0	0	3	18	0	0	10	0	0	0	0	0	0	0	SK
TJ	0	0	0	2	0	0	0	0	0	0	0	0	0	0	0	0	0	0	0	0	0	0	0	0	0	2	4	0	0	0	0	0	TJ
TM	0	4	0	34	0	0	0	0	0	0	0	1	0	0	0	0	0	0	2	0	0	0	0	0	0	1	12	0	0	0	0	0	TM
TR	2	12	2	24	1	1	14	3	1	5	2	7	0	0	7	0	4	1	5	45	1	3	0	0	12	0	1	0	0	0	3	0	TR
UA	2	2	11	18	5	5	17	70	2	0	21	67	5	1	8	3	15	11	4	14	5	26	1	0	25	0	4	9	1	4	20	1	UA
UZ	0	3	0	19	0	0	0	0	0	0	0	1	0	0	0	0	0	0	1	0	0	0	0	0	1	11	27	0	0	0	0	0	UZ
ATL	0	0	3	1	0	59	0	9	3	0	5	151	21	3	233	28	283	500	0	1	0	1	137	35	10	0	6	4	4	3	0	0	ATL
BAS	0	0	5	0	1	16	1	14	2	0	16	146	35	7	5	30	28	49	0	0	1	5	3	0	5	0	0	12	1	10	1	0	BAS
BLS	2	3	4	21	2	2	26	15	1	1	6	20	1	0	4	1	5	3	20	28	1	7	0	0	11	0	2	2	0	1	12	1	BLS
MED	22	0	41	1	27	13	34	3	15	10	22	95	2	0	333	1	256	25	0	229	31	22	2	0	597	0	0	1	2	0	3	6	MED
NOS	0	0	2	0	0	49	0	1	1	0	7	173	38	1	16	4	130	494	0	0	0	1	31	1	2	0	0	1	3	1	0	0	NOS
AST	1	16	1	225	1	0	2	2	0	6	1	5	0	0	3	1	4	2	9	12	0	1	0	0	6	22	103	0	0	0	1	0	AST
NOA	1	0	2	0	1	2	2	0	1	0	1	9	0	0	73	0	23	4	0	14	1	1	0	0	30	0	0	0	0	0	0	0	NOA
SUM	75	143	372	1106	128	418	259	500	152	28	474	2844	260	64	1659	296	2188	1969	152	542	134	319	286	50	1765	158	1369	149	42	96	84	21	SUM
EXC	49	123	314	859	96	278	194	455	128	11	414	2244	163	52	991	231	1460	894	123	258	98	281	112	13	1105	136	1258	127	32	80	67	15	EXC
EU	15	0	262	3	43	230	128	71	78	3	324	1849	114	22	928	124	1298	405	1	146	73	188	68	1	934	0	3	60	28	39	18	5	EU
emis	84	133	373	1069	135	432	287	533	156	37	485	2948	272	69	1888	320	2300	2075	145	677	139	334	304	60	1859	172	1696	158	44	103	93	22	emis
	AL	AM	AT	AZ	BA	BE	BG	BY	CH	CY	CZ	DE	DK	EE	ES	FI	FR	GB	GE	GR	HR	HU	IE	IS	IT	KG	KZ	LT	LU	LV	MD	ME	

Table C.2 Cont.: 2021 country-to-country blame matrices for **oxidised nitrogen** deposition.
Units: 100 Mg of N. **Emitters →, Receptors ↓.**

	MK	MT	NL	NO	PL	PT	RO	RS	RU	SE	SI	SK	TJ	TM	TR	UA	UZ	ATL	BAS	BLS	MED	NOS	AST	NOA	BIC	DMS	VOL	SUM	EXC	EU	
AL	2	0	0	0	1	0	1	9	0	0	0	0	0	0	1	0	0	0	0	0	15	0	0	8	3	0	0	82	55	26	AL
AM	0	0	0	0	0	0	0	0	1	0	0	0	0	1	15	0	0	0	0	0	1	0	41	1	3	0	0	134	88	1	AM
AT	0	0	4	0	8	0	1	2	1	0	7	2	0	0	0	1	0	1	2	0	8	6	0	4	3	0	0	320	297	279	AT
AZ	0	0	0	0	0	0	0	0	13	0	0	0	0	6	15	1	1	0	0	0	2	0	87	1	4	0	0	430	335	3	AZ
BA	0	0	1	0	7	0	2	15	1	0	1	3	0	0	0	1	0	1	1	0	16	1	0	7	3	0	0	164	135	86	BA
BE	0	0	14	1	1	0	0	0	0	0	0	0	0	0	0	0	0	3	1	0	1	24	0	0	3	0	0	164	132	114	BE
BG	4	0	1	0	12	0	38	32	8	0	0	3	0	0	27	13	0	1	1	6	21	1	0	9	5	0	0	328	285	190	BG
BY	0	0	6	2	91	0	11	5	89	5	1	5	0	1	6	72	0	2	16	2	4	11	2	2	5	0	0	573	530	231	BY
CH	0	0	2	0	0	0	0	0	0	0	0	0	0	0	0	0	0	1	0	0	3	3	0	1	2	0	0	128	117	76	CH
CY	0	0	0	0	0	0	0	0	0	0	0	0	0	0	5	0	0	0	0	0	4	0	3	1	1	0	0	19	10	5	CY
CZ	0	0	7	1	31	0	1	5	2	1	3	6	0	0	0	1	0	1	5	0	4	9	0	2	2	0	0	362	338	319	CZ
DE	0	0	94	7	43	2	1	1	8	8	1	2	0	0	0	2	0	14	35	0	8	132	0	5	17	0	0	1771	1560	1424	DE
DK	0	0	10	3	7	0	0	0	2	3	0	0	0	0	0	0	0	2	16	0	0	27	0	0	2	0	0	164	116	94	DK
EE	0	0	2	1	8	0	1	0	23	4	0	0	0	0	0	4	0	1	17	0	0	4	0	0	1	0	0	115	90	53	EE
ES	0	0	4	0	1	55	0	1	0	0	0	0	0	0	0	0	0	67	0	0	144	8	0	69	43	0	0	1107	775	761	ES
FI	0	0	5	9	23	0	2	1	105	23	0	1	0	1	1	11	0	6	52	0	2	15	1	1	13	0	0	452	362	210	FI
FR	0	0	40	2	4	13	0	1	3	2	1	0	0	0	0	1	0	65	4	0	88	120	0	32	44	0	0	1729	1376	1250	FR
GB	0	0	19	4	1	1	0	0	1	1	0	0	0	0	0	0	0	49	3	0	1	99	0	1	21	0	0	677	503	134	GB
GE	0	0	0	0	1	0	1	1	7	0	0	0	0	4	45	2	1	0	0	2	4	0	65	3	6	0	0	310	229	7	GE
GL	0	0	0	0	0	0	0	0	0	0	0	0	0	0	0	0	0	0	0	0	0	1	0	0	29	0	0	33	2	1	GL
GR	6	0	1	0	4	0	7	17	3	0	0	1	0	0	33	5	0	1	0	3	77	1	1	22	11	0	0	358	243	170	GR
HR	0	0	1	0	7	0	2	9	1	0	4	3	0	0	0	1	0	1	1	0	29	2	0	7	2	0	0	209	167	142	HR
HU	1	0	2	0	35	0	16	25	3	1	4	17	0	0	0	5	0	1	2	0	15	3	0	8	3	0	0	345	312	265	HU
IE	0	0	2	0	0	0	0	0	0	0	0	0	0	0	0	0	0	12	0	0	0	8	0	0	8	0	0	104	76	55	IE
IS	0	0	1	1	0	0	0	0	0	0	0	0	0	0	0	0	0	3	0	0	0	2	0	0	13	0	0	37	19	5	IS
IT	1	1	3	0	6	3	2	8	1	0	10	2	0	0	2	1	0	5	1	0	219	4	0	64	23	0	0	1196	878	843	IT
KG	0	0	0	0	0	0	0	0	4	0	0	0	25	10	5	0	158	0	0	0	1	0	88	1	9	0	0	395	297	2	KG
KZ	1	0	2	2	14	0	8	4	729	2	0	2	23	142	64	54	234	3	5	5	11	5	693	9	74	0	0	3037	2232	88	KZ
LT	0	0	4	1	39	0	2	1	18	4	0	1	0	0	1	9	0	1	15	0	1	8	0	0	2	0	0	198	170	121	LT
LU	0	0	1	0	0	0	0	0	0	0	0	0	0	0	0	0	0	0	0	0	0	1	0	0	0	0	0	11	10	9	LU
LV	0	0	3	2	23	0	1	0	25	5	0	1	0	0	1	7	0	1	20	0	1	7	0	0	2	0	0	181	149	98	LV
MD	0	0	0	0	7	0	9	2	6	0	0	1	0	0	5	19	0	0	1	2	3	1	0	1	1	0	0	86	77	30	MD
ME	0	0	0	0	1	0	0	4	0	0	0	0	0	0	0	0	0	0	0	0	7	0	0	4	1	0	0	39	27	15	ME
MK	11	0	0	0	1	0	1	12	1	0	0	0	0	0	2	0	0	0	0	0	4	0	0	3	1	0	0	62	53	23	MK
MT	0	0	0	0	0	0	0	0	0	0	0	0	0	0	0	0	0	0	0	0	0	0	0	0	0	0	0	1	0	0	MT
NL	0	0	64	1	2	0	0	0	1	1	0	0	0	0	0	0	0	4	2	0	1	44	0	0	4	0	0	232	178	146	NL
NO	0	0	10	70	8	0	0	0	12	13	0	0	0	0	0	1	0	20	19	0	1	59	0	1	25	0	0	352	227	104	NO
PL	0	0	30	6	551	1	15	12	30	11	3	23	0	0	1	29	0	5	54	0	8	48	0	5	9	0	0	1397	1269	1131	PL
PT	0	0	0	0	0	86	0	0	0	0	0	0	0	0	0	0	0	38	0	0	13	1	0	8	10	0	0	202	131	130	PT
RO	4	0	3	1	51	1	226	54	19	1	2	11	0	0	22	53	0	2	4	6	29	4	1	16	7	0	0	731	663	473	RO
RS	5	0	1	0	18	0	16	112	4	0	1	6	0	0	2	4	0	1	1	1	15	2	0	8	4	0	0	321	289	143	RS
RU	3	0	28	32	218	2	51	25	6163	47	3	14	6	94	222	505	66	41	133	37	51	63	451	25	316	-1	0	10258	9141	958	RU
SE	0	0	18	30	49	0	2	2	40	87	1	2	0	0	0	8	0	11	94	0	2	60	0	2	18	0	0	672	485	358	SE
SI	0	0	0	0	1	0	0	1	0	0	14	1	0	0	0	0	0	0	0	0	10	1	0	2	1	0	0	89	75	72	SI
SK	0	0	2	0	35	0	6	9	1	0	2	28	0	0	0	3	0	1	2	0	5	3	0	3	2	0	0	201	186	165	SK
TJ	0	0	0	0	0	0	0	0	2	0	0	0	56	13	2	0	45	0	0	0	0	0	75	0	6	0	0	209	127	1	TJ
TM	0	0	0	0	1	0	0	0	23	0	0	0	5	214	7	2	52	0	0	0	1	0	293	2	11	0	0	670	362	5	TM
TR	2	0	1	0	10	1	17	11	29	0	0	1	0	2	828	29	0	1	1	26	157	2	385	54	55	0	0	1770	1089	136	TR
UA	2	0	8	3	171	1	80	28	240	5	2	14	0	5	89	594	2	3	17	27	38	14	20	17	17	0	0	1773	1621	519	UA
UZ	0	0	0	0	1	0	0	0	29	0	0	0	27	57	8	2	244	0	0	0	1	0	209	1	11	0	0	658	434	5	UZ
ATL	0	0	78	124	21	122	2	1	310	29	0	1	0	1	2	10	0	1059	43	0	93	319	2	88	1792	3	0	5602	2202	1200	ATL
BAS	0	0	30	16	102	0	4	3	82	49	1	4	0	0	1	17	0	9	170	0	3	72	1	2	11	1	0	971	703	516	BAS
BLS	3	0	2	1	38	0	59	21	154	1	1	3	0	2	271	170	0	1	5	96	64	4	49	20	8	0	0	1176	928	226	BLS
MED	10	8	13	2	30	20	31	63	16	2	12	7	0	0	337	24	0	54	6	16	2096	27	137	749	118	1	3	5575	2367	1813	MED
NOS	0	0	91	75	24	3	0	0	9	17	0	1	0	0	0	1	0	77	46	0	4	439	0	4	53	3	1	1807	1180	595	NOS
AST	0	0	1	1	4	0	3	2	119	1	0	1	34	190	158	15	104	1	1	3	65	1	5473	45	385	0	0	7031	1056	54	AST
NOA	1	1	2	0	2	14	2	4	2	0	1	0	0	0	14	2	0	59	0	1	242	3	14	946	128	0	0	1607	215	184	NOA
SUM	58	11	613	402	1716	332	625	504	8339	328	78	171	176	743	2195	1679	908	1632	799	236	3593	1668	8093	2269	3350	6	5	58626			SUM
EXC	44	2	396	185	1494	171	523	410	7648	229	63	154	142	550	1412	1440	803	372	527	120	1025	803	2416	415	855	-2	1		28326	11478	EXC
EU	17	1	316	68	942	164	324	182	294	154	54	106	0	1	95	154	0	244	328	17	689	540	8	264	235	0	0		10335	8880	EU
emis	65	13	641	428	1800	416	652	532	9866	350	78	178	198	902	2506	1760	1018	2113	816	245	4192	1711	14984	4262				69128	40806	17159	emis
	MK	MT	NL	NO	PL	PT	RO	RS	RU	SE	SI	SK	TJ	TM	TR	UA	UZ	ATL	BAS	BLS	MED	NOS	AST	NOA	BIC	DMS	VOL	SUM	EXC	EU	

Table C.3: 2021 country-to-country blame matrices for **reduced nitrogen** deposition.
Units: 100 Mg of N. **Emitters →, Receptors ↓.**

	AL	AM	AT	AZ	BA	BE	BG	BY	CH	CY	CZ	DE	DK	EE	ES	FI	FR	GB	GE	GR	HR	HU	IE	IS	IT	KG	KZ	LT	LU	LV	MD	ME	
AL	69	0	0	0	1	0	0	0	0	0	0	1	0	0	4	0	1	0	0	3	1	1	0	0	11	0	0	0	0	0	0	1	AL
AM	0	47	0	28	0	0	0	0	0	0	0	0	0	0	0	0	0	0	5	0	0	0	0	0	0	0	0	0	0	0	0	0	AM
AT	0	0	283	0	1	2	0	0	19	0	21	119	1	0	10	0	13	2	0	0	5	7	0	0	58	0	0	0	0	0	0	0	AT
AZ	0	15	0	270	0	0	0	0	0	0	0	0	0	0	0	0	0	0	12	0	0	0	0	0	0	0	1	0	0	0	0	0	AZ
BA	1	0	5	0	80	0	0	0	1	0	4	8	0	0	8	0	3	0	0	0	19	12	0	0	30	0	0	0	0	0	0	1	BA
BE	0	0	0	0	0	183	0	0	0	0	0	17	1	0	4	0	80	13	0	0	0	0	2	0	1	0	0	0	4	0	0	0	BE
BG	5	0	2	0	2	0	158	1	0	0	3	5	0	0	6	0	1	0	0	23	2	9	0	0	11	0	1	0	0	0	2	0	BG
BY	0	0	5	1	1	1	1	442	2	0	9	32	4	1	3	1	7	4	0	1	2	11	1	0	6	0	2	25	0	5	6	0	BY
CH	0	0	2	0	0	1	0	0	252	0	0	24	0	0	9	0	27	1	0	0	0	0	0	0	34	0	0	0	0	0	0	0	CH
CY	0	0	0	0	0	0	0	0	0	10	0	0	0	0	0	0	0	0	0	0	0	0	0	0	0	0	0	0	0	0	0	0	CY
CZ	0	0	29	0	2	3	0	0	5	0	242	101	3	0	5	0	16	3	0	0	5	13	0	0	17	0	0	1	0	0	0	0	CZ
DE	0	0	46	0	0	70	0	1	58	0	37	2319	35	0	25	1	252	52	0	0	2	5	8	0	29	0	0	2	16	1	0	0	DE
DK	0	0	1	0	0	4	0	0	1	0	2	56	162	0	2	0	11	10	0	0	0	0	2	0	1	0	0	0	0	0	0	0	DK
EE	0	0	0	0	0	1	0	8	0	0	1	8	3	32	1	3	2	2	0	0	0	0	0	0	0	0	0	4	0	6	0	0	EE
ES	0	0	0	0	0	3	0	0	1	0	0	9	0	0	1953	0	66	6	0	0	0	0	1	0	8	0	0	0	0	0	0	0	ES
FI	0	0	2	1	0	2	0	15	1	0	4	22	7	6	3	142	7	5	0	0	1	4	1	0	3	0	2	8	0	4	1	0	FI
FR	0	0	3	0	0	58	0	0	36	0	2	93	5	0	307	0	2601	66	0	0	1	1	19	0	61	0	0	0	7	0	0	0	FR
GB	0	0	0	0	0	11	0	0	1	0	0	32	3	0	7	0	53	935	0	0	0	0	99	0	0	0	0	0	0	0	0	0	GB
GE	0	15	0	66	0	0	0	0	0	1	0	0	0	0	1	0	0	0	163	1	0	0	0	0	1	0	1	0	0	0	0	0	GE
GL	0	0	0	0	0	0	0	0	0	0	0	0	0	0	0	0	0	0	0	0	0	0	0	0	0	0	0	0	0	0	0	0	GL
GR	10	0	1	0	1	0	11	1	0	0	1	3	0	0	8	0	2	0	0	185	1	4	0	0	14	0	0	0	0	0	1	0	GR
HR	1	0	10	0	14	0	1	0	1	0	6	10	0	0	11	0	4	0	0	1	93	21	0	0	56	0	0	0	0	0	0	0	HR
HU	1	0	20	0	8	1	3	1	2	0	14	22	1	0	11	0	5	1	0	1	24	239	0	0	38	0	0	0	0	0	1	0	HU
IE	0	0	0	0	0	2	0	0	0	0	0	4	0	0	1	0	11	32	0	0	0	0	432	0	0	0	0	0	0	0	0	0	IE
IS	0	0	0	0	0	0	0	0	0	0	0	1	0	0	0	0	2	4	0	0	0	0	1	14	0	0	0	0	0	0	0	0	IS
IT	2	0	16	0	5	1	1	0	17	0	5	21	1	0	83	0	32	1	0	2	11	6	0	0	1675	0	0	0	0	0	0	0	IT
KG	0	0	0	3	0	0	0	0	0	0	0	0	0	0	0	0	0	0	0	0	0	0	0	0	0	152	36	0	0	0	0	0	KG
KZ	1	11	1	67	1	1	2	9	1	1	2	8	1	0	4	1	3	1	11	3	1	2	0	0	4	47	917	2	0	1	1	0	KZ
LT	0	0	1	0	0	1	0	30	0	0	3	22	5	1	1	1	5	4	0	0	0	2	1	0	1	0	0	126	0	7	1	0	LT
LU	0	0	0	0	0	3	0	0	0	0	0	3	0	0	0	0	8	0	0	0	0	0	0	0	0	0	0	0	11	0	0	0	LU
LV	0	0	1	0	0	1	0	19	0	0	2	17	5	3	1	1	4	4	0	0	0	1	1	0	1	0	0	24	0	53	1	0	LV
MD	0	0	0	0	0	0	2	2	0	0	0	2	0	0	1	0	0	0	0	1	0	1	0	0	2	0	0	0	0	0	43	0	MD
ME	3	0	0	0	2	0	0	0	0	0	0	1	0	0	2	0	1	0	0	0	1	1	0	0	7	0	0	0	0	0	0	8	ME
MK	6	0	0	0	0	0	1	0	0	0	0	1	0	0	2	0	0	0	0	10	0	1	0	0	4	0	0	0	0	0	0	0	MK
MT	0	0	0	0	0	0	0	0	0	0	0	0	0	0	0	0	0	0	0	0	0	0	0	0	0	0	0	0	0	0	0	0	MT
NL	0	0	0	0	0	51	0	0	0	0	1	76	3	0	3	0	39	21	0	0	0	0	2	0	0	0	0	0	1	0	0	0	NL
NO	0	0	1	0	0	4	0	3	0	0	1	29	15	1	3	3	14	19	0	0	0	1	4	0	1	0	0	2	0	1	0	0	NO
PL	0	0	19	0	4	10	2	32	7	0	69	242	31	1	10	1	42	18	0	0	9	40	2	0	24	0	1	17	1	3	2	0	PL
PT	0	0	0	0	0	0	0	0	0	0	0	1	0	0	69	0	4	0	0	0	0	0	0	0	1	0	0	0	0	0	0	0	PT
RO	5	0	8	0	10	1	35	7	2	0	10	21	1	0	15	0	5	1	0	9	9	59	0	0	39	0	1	2	0	0	17	1	RO
RS	7	0	5	0	12	0	9	1	1	0	6	11	1	0	9	0	3	0	0	6	11	31	0	0	22	0	0	0	0	0	0	2	RS
RU	3	19	12	139	4	8	13	214	6	2	24	116	23	18	22	44	35	26	48	14	5	26	6	0	28	8	467	47	1	25	14	1	RU
SE	0	0	6	0	1	7	1	13	3	0	11	87	46	3	7	12	24	20	0	0	2	6	4	0	6	0	1	9	1	4	1	0	SE
SI	0	0	13	0	1	0	0	0	1	0	2	6	0	0	5	0	2	0	0	0	7	3	0	0	37	0	0	0	0	0	0	0	SI
SK	0	0	11	0	3	0	1	1	1	0	17	17	1	0	5	0	4	1	0	0	7	37	0	0	16	0	0	0	0	0	0	0	SK
TJ	0	0	0	1	0	0	0	0	0	0	0	0	0	0	0	0	0	0	0	0	0	0	0	0	0	4	7	0	0	0	0	0	TJ
TM	0	1	0	11	0	0	0	0	0	0	0	0	0	0	0	0	0	0	1	0	0	0	0	0	0	1	5	0	0	0	0	0	TM
TR	3	12	1	15	1	0	14	3	0	6	1	4	0	0	16	0	2	0	7	29	1	3	0	0	15	0	1	0	0	0	3	0	TR
UA	3	2	8	12	6	2	21	78	2	0	13	46	5	1	14	1	9	4	8	10	7	40	1	0	31	0	5	11	0	2	43	1	UA
UZ	0	1	0	8	0	0	0	0	0	0	0	0	0	0	0	0	0	0	1	0	0	0	0	0	0	25	30	0	0	0	0	0	UZ
ATL	0	0	2	0	0	48	0	9	4	0	3	112	19	2	420	12	590	462	0	0	1	2	376	19	10	0	8	5	4	2	0	0	ATL
BAS	0	0	5	0	1	11	1	19	3	0	14	200	111	9	8	24	33	28	0	0	2	8	5	0	7	0	1	20	1	12	1	0	BAS
BLS	3	3	3	13	2	0	29	14	1	1	3	12	1	0	9	0	3	1	37	19	2	6	0	0	12	0	3	2	0	1	17	1	BLS
MED	31	0	25	0	18	6	22	3	17	11	13	63	3	0	483	0	184	10	0	124	29	21	2	0	553	0	0	1	1	0	3	1	MED
NOS	0	0	2	0	0	62	0	2	2	0	5	256	88	0	26	2	262	429	0	0	0	1	54	0	3	0	0	1	2	1	0	0	NOS
AST	1	8	0	99	0	0	1	2	0	4	0	2	0	0	4	0	1	0	8	4	0	1	0	0	3	31	78	0	0	0	0	0	AST
NOA	1	0	1	0	1	1	1	0	1	0	1	5	0	0	78	0	17	2	0	4	1	1	0	0	22	0	0	0	0	0	0	0	NOA
SUM	158	136	552	737	185	560	334	932	451	37	555	4265	588	79	3682	253	4491	2190	305	453	260	627	1028	36	2903	268	1568	312	53	128	159	20	SUM
EXC	122	125	514	624	163	431	280	883	423	20	516	3615	366	67	2654	213	3401	1259	259	301	226	588	590	16	2294	237	1478	283	46	113	137	18	EXC
EU	26	0	473	2	53	402	214	130	158	10	453	3300	313	46	2547	162	3241	262	2	222	178	458	477	0	2097	0	6	195	43	79	27	2	EU
emis	173	128	542	667	190	556	354	943	443	48	550	4248	583	80	3943	256	4504	2183	279	517	260	632	1027	36	2895	270	906	314	54	129	163	25	emis
	AL	AM	AT	AZ	BA	BE	BG	BY	CH	CY	CZ	DE	DK	EE	ES	FI	FR	GB	GE	GR	HR	HU	IE	IS	IT	KG	KZ	LT	LU	LV	MD	ME	

Table C.3 Cont.: 2021 country-to-country blame matrices for **reduced nitrogen** deposition.
Units: 100 Mg of N. **Emitters →, Receptors ↓.**

	MK	MT	NL	NO	PL	PT	RO	RS	RU	SE	SI	SK	TJ	TM	TR	UA	UZ	ATL	BAS	BLS	MED	NOS	AST	NOA	BIC	DMS	VOL	SUM	EXC	EU	
AL	0	0	0	0	1	0	1	5	1	0	0	0	0	0	0	0	0	0	0	0	0	0	0	4	2	0	-1	108	102	25	AL
AM	0	0	0	0	0	0	0	0	3	0	0	0	0	1	73	0	1	0	0	0	0	0	61	1	2	0	0	224	159	1	AM
AT	0	0	3	0	7	1	1	1	1	0	14	2	0	0	0	1	0	0	0	0	0	0	0	2	3	0	0	580	573	548	AT
AZ	0	0	0	0	0	0	0	0	34	0	0	0	0	4	55	0	3	0	0	0	0	0	130	1	3	0	0	529	395	2	AZ
BA	0	0	0	0	5	0	3	15	1	0	1	2	0	0	0	1	0	0	0	0	0	0	0	4	3	0	-1	208	202	102	BA
BE	0	0	36	0	1	0	0	0	0	0	0	0	0	0	0	0	0	0	0	0	0	-1	0	0	1	0	0	344	343	329	BE
BG	7	0	0	0	6	0	68	22	20	0	0	2	0	0	30	11	0	0	0	0	1	0	0	5	4	0	0	411	400	299	BG
BY	0	0	4	1	99	0	18	7	170	3	1	5	0	0	9	96	1	0	0	0	0	1	3	1	6	1	1	1003	990	248	BY
CH	0	0	1	0	0	1	0	0	0	0	0	0	0	0	0	0	0	0	0	0	0	0	0	1	2	0	0	358	354	101	CH
CY	0	0	0	0	0	0	0	0	0	0	0	0	0	0	6	0	0	0	0	0	0	0	3	1	0	0	0	21	17	10	CY
CZ	0	0	5	0	29	0	2	5	2	1	5	8	0	0	0	1	0	0	0	0	0	0	0	1	3	0	0	513	507	487	CZ
DE	0	0	189	3	47	1	1	1	9	6	2	2	0	0	0	2	0	1	-1	0	1	-4	0	3	13	1	-1	3239	3226	3099	DE
DK	0	0	11	1	11	0	0	0	2	4	0	0	0	0	0	0	0	0	-1	0	0	-1	0	0	2	0	0	283	283	268	DK
EE	0	0	1	1	8	0	1	0	26	4	0	0	0	0	1	4	0	0	0	0	0	0	0	0	1	0	0	121	118	76	EE
ES	0	0	3	0	0	57	0	0	0	0	0	0	0	0	0	0	0	0	0	0	-1	1	0	39	25	0	-1	2172	2111	2102	ES
FI	0	0	4	4	30	0	4	2	106	15	0	2	0	0	3	13	1	0	1	0	0	1	2	1	9	0	0	439	425	271	FI
FR	0	0	36	1	2	14	0	1	2	1	1	0	0	0	0	0	0	0	0	0	2	-5	0	18	28	0	-1	3363	3320	3213	FR
GB	0	0	20	1	1	1	0	0	0	1	0	0	0	0	0	0	0	-2	0	0	0	-2	0	1	12	-2	-2	1171	1166	229	GB
GE	0	0	0	0	0	0	1	1	20	0	0	0	0	3	176	1	2	0	0	0	0	0	87	3	6	1	0	553	454	6	GE
GL	0	0	0	0	0	0	0	0	0	0	0	0	0	0	0	0	0	0	0	0	0	0	0	0	23	0	0	23	1	0	GL
GR	4	0	0	0	3	0	8	10	8	0	0	1	0	0	34	4	0	0	0	0	0	0	1	10	8	0	-3	331	315	243	GR
HR	0	0	0	0	5	0	3	10	2	0	11	3	0	0	1	1	0	0	0	0	0	0	0	4	3	0	0	274	267	236	HR
HU	1	0	1	0	19	1	36	31	8	0	9	26	0	0	1	6	0	0	0	0	0	0	0	4	3	0	0	538	530	471	HU
IE	0	0	2	0	0	0	0	0	0	0	0	0	0	0	0	0	0	-1	0	0	0	-1	0	0	5	-2	-1	485	485	453	IE
IS	0	0	1	0	0	0	0	0	0	0	0	0	0	0	0	0	0	0	0	0	0	0	0	0	10	0	0	34	24	6	IS
IT	0	0	1	0	5	3	2	5	1	0	9	1	0	0	3	1	0	0	0	0	-2	0	0	34	17	1	-3	1960	1912	1877	IT
KG	0	0	0	0	0	0	0	0	15	0	0	0	41	5	15	0	188	0	0	0	0	0	257	1	9	0	0	724	457	1	KG
KZ	1	0	1	0	10	0	7	3	1203	1	0	1	36	69	176	28	350	0	0	0	1	0	1751	7	59	1	2	4809	2987	55	KZ
LT	0	0	3	1	54	0	3	1	36	4	0	1	0	0	1	11	0	0	0	0	0	0	0	0	2	0	0	330	327	241	LT
LU	0	0	1	0	0	0	0	0	0	0	0	0	0	0	0	0	0	0	0	0	0	0	0	0	0	0	0	27	27	26	LU
LV	0	0	3	1	25	0	1	1	35	5	0	1	0	0	1	8	0	0	0	0	0	0	0	0	2	0	0	221	217	148	LV
MD	0	0	0	0	3	0	26	2	18	0	0	0	0	0	9	27	0	0	0	0	0	0	1	1	1	0	0	146	144	41	MD
ME	0	0	0	0	1	0	0	3	0	0	0	0	0	0	0	0	0	0	0	0	0	0	0	2	1	0	0	35	32	15	ME
MK	20	0	0	0	1	0	1	8	2	0	0	0	0	0	2	0	0	0	0	0	0	0	0	1	1	0	0	65	63	24	MK
MT	0	1	0	0	0	0	0	0	0	0	0	0	0	0	0	0	0	0	0	0	0	0	0	0	0	0	0	1	1	1	MT
NL	0	0	375	0	3	0	0	0	1	1	0	0	0	0	0	0	0	0	0	0	0	-3	0	0	1	0	0	576	577	555	NL
NO	0	0	8	124	11	0	1	1	10	12	0	0	0	0	0	2	0	0	1	0	0	1	0	1	19	0	0	293	270	110	NO
PL	0	0	23	3	1287	1	27	15	59	11	6	23	0	0	1	41	0	0	0	0	0	1	0	3	12	1	1	2104	2085	1902	PL
PT	0	0	0	0	0	172	0	0	0	0	0	0	0	0	0	0	0	0	0	0	0	0	0	5	6	0	0	259	249	248	PT
RO	3	0	1	0	28	1	652	52	53	1	2	11	0	0	32	58	0	0	0	0	1	0	1	9	9	1	0	1174	1153	909	RO
RS	4	0	1	0	10	0	29	223	15	0	1	5	0	0	3	4	0	0	0	0	0	0	0	4	4	0	-1	442	434	160	RS
RU	4	0	17	10	205	1	65	25	15994	26	3	11	11	51	562	380	139	1	3	1	3	4	933	19	253	5	8	20155	18924	799	RU
SE	0	0	15	18	65	0	5	4	38	218	1	3	0	0	1	12	0	0	0	0	0	2	0	2	13	1	0	672	654	542	SE
SI	0	0	0	0	1	0	0	0	0	0	63	0	0	0	0	0	0	0	0	0	0	0	0	1	1	0	0	146	144	141	SI
SK	0	0	1	0	22	0	12	11	3	0	4	69	0	0	0	4	0	0	0	0	0	0	0	2	2	0	0	257	252	226	SK
TJ	0	0	0	0	0	0	0	0	5	0	0	0	130	6	6	0	71	0	0	0	0	0	232	0	6	0	0	470	231	0	TJ
TM	0	0	0	0	0	0	0	0	34	0	0	0	3	158	19	1	100	0	0	0	0	0	450	1	8	0	0	796	337	2	TM
TR	1	0	0	0	6	1	23	7	73	0	0	1	0	1	3961	24	1	0	0	0	-2	0	397	40	42	0	-8	4708	4239	125	TR
UA	2	0	4	1	133	1	162	31	686	4	2	11	0	3	168	1054	4	0	0	0	2	1	27	11	18	2	4	2718	2654	538	UA
UZ	0	0	0	0	0	0	0	0	39	0	0	0	31	26	21	1	657	0	0	0	0	0	361	1	9	0	0	1215	844	2	UZ
ATL	0	0	61	37	19	151	3	2	194	13	0	1	0	0	3	8	1	-9	2	0	1	7	5	54	1444	-18	2	4096	2608	1857	ATL
BAS	0	0	27	7	135	0	6	3	86	75	1	4	0	0	2	19	0	0	-6	0	0	-1	1	1	12	-2	-1	894	890	719	BAS
BLS	2	0	1	0	22	0	85	14	428	1	1	2	0	1	632	161	2	0	0	-3	1	0	55	13	18	-2	1	1634	1551	216	BLS
MED	3	8	6	0	15	16	32	24	36	1	11	5	0	0	454	20	0	1	0	0	-26	2	167	461	123	-24	-13	2949	2258	1634	MED
NOS	0	0	153	44	28	3	0	0	7	14	0	1	0	0	0	1	0	0	0	0	0	-9	0	3	37	-4	-1	1477	1450	964	NOS
AST	0	0	0	0	2	0	2	2	290	0	0	0	37	91	310	7	167	0	0	0	0	0	35229	82	253	0	-5	36716	1157	26	AST
NOA	0	0	1	0	1	11	2	2	2	0	0	0	0	0	13	1	0	-1	0	0	-3	0	11	1140	75	-3	-4	1389	174	149	NOA
SUM	55	10	1021	259	2366	442	1295	551	19781	424	153	207	289	420	6783	2019	1689	-8	0	-1	-18	-1	40169	2004	2635	-40	-28	110783			SUM
EXC	49	2	771	170	2143	260	1164	503	18738	320	140	194	252	327	5370	1801	1519	0	4	2	9	-1	4699	250	674	12	-6		55984	21512	EXC
EU	17	1	714	33	1657	254	827	173	413	272	130	156	0	1	114	180	2	0	-1	0	3	-6	9	144	174	4	-9		20520	18921	EU
emis	68	12	1004	253	2382	505	1306	595	10374	420	152	207	296	480	7659	2045	1799	0	0	0	0	0	29319	3518				90291	57454	27478	emis
	MK	MT	NL	NO	PL	PT	RO	RS	RU	SE	SI	SK	TJ	TM	TR	UA	UZ	ATL	BAS	BLS	MED	NOS	AST	NOA	BIC	DMS	VOL	SUM	EXC	EU	

Table C.4: 2021 country-to-country blame matrices for **MM-AOT40f**.
Units: ppb.h per 15% emis. red. of NO_x. **Emitters →, Receptors ↓.**

	AL	AM	AT	AZ	BA	BE	BG	BY	CH	CY	CZ	DE	DK	EE	ES	FI	FR	GB	GE	GR	HR	HU	IE	IS	IT	KG	KZ	LT	LU	LV	MD	
AL	730	0	29	1	67	2	44	7	8	0	19	46	3	1	97	5	87	15	1	106	46	56	4	1	336	0	1	2	0	2	1	AL
AM	1	15	2	552	1	0	6	4	1	4	2	8	1	0	15	2	10	3	101	11	1	2	1	0	11	0	28	1	0	1	2	AM
AT	1	0	494	0	8	3	3	5	76	0	95	379	5	1	69	7	240	24	0	1	40	42	9	1	261	0	1	3	2	2	0	AT
AZ	1	28	2	188	1	1	5	6	1	1	2	9	1	1	10	4	10	3	56	6	1	2	1	0	9	0	65	1	0	1	2	AZ
BA	10	0	88	0	633	2	23	8	12	0	56	113	4	1	104	6	114	20	0	12	191	135	5	1	315	0	1	4	1	3	1	BA
BE	0	0	2	0	0	-375	0	2	3	0	6	-48	8	1	33	8	257	62	0	0	0	0	19	2	5	0	0	1	10	1	0	BE
BG	20	0	26	2	27	3	794	24	5	0	28	59	5	2	41	7	44	13	2	81	17	59	4	1	76	0	2	6	0	4	17	BG
BY	0	0	8	1	3	2	2	315	2	0	21	78	9	7	8	17	37	24	0	1	4	16	5	1	10	0	4	40	1	20	7	BY
CH	0	0	32	0	2	3	1	3	452	0	14	209	4	1	99	4	523	31	0	1	8	4	9	1	269	0	1	2	1	1	0	CH
CY	9	3	9	10	9	2	42	14	3	458	7	23	2	1	47	3	35	8	6	246	6	11	2	0	70	0	4	3	0	2	6	CY
CZ	0	0	116	0	10	2	4	7	18	0	328	403	10	1	30	8	195	29	0	1	25	63	9	1	48	0	1	6	3	3	0	CZ
DE	0	0	37	0	1	-3	0	4	24	0	50	299	12	1	31	9	239	47	0	0	3	6	12	2	20	0	1	3	6	2	0	DE
DK	0	0	3	0	0	-1	0	8	1	0	9	69	-71	2	11	21	58	114	0	0	1	3	15	3	3	0	1	9	1	7	0	DK
EE	0	0	2	1	0	3	0	73	1	0	7	60	13	107	4	64	26	27	0	0	1	4	6	1	2	0	2	32	1	67	1	EE
ES	0	0	3	0	1	3	1	2	3	0	2	17	1	0	1294	1	177	24	0	1	1	1	7	1	19	0	0	0	1	0	0	ES
FI	0	0	1	1	0	2	0	17	0	0	3	24	6	12	2	136	12	14	0	0	0	1	4	1	1	0	1	8	0	9	0	FI
FR	0	0	7	0	1	-3	1	3	20	0	5	73	4	1	145	5	933	60	0	1	3	2	18	1	54	0	1	1	3	1	0	FR
GB	0	0	0	0	0	-4	0	1	0	0	1	17	7	0	4	6	32	-18	0	0	0	0	34	2	1	0	0	1	1	1	0	GB
GE	2	40	3	441	2	1	9	12	1	1	4	12	1	1	14	3	13	4	572	12	2	4	1	0	15	0	26	3	0	2	4	GE
GL	0	0	0	0	0	0	0	0	0	0	0	0	0	0	0	0	0	0	0	0	0	0	0	0	0	0	0	0	0	0	0	GL
GR	83	0	20	2	29	3	220	15	5	0	17	44	3	2	70	5	62	14	2	725	19	35	4	1	189	0	2	4	0	3	9	GR
HR	7	0	155	0	199	3	17	8	16	0	76	166	5	1	95	7	158	24	0	9	537	174	7	1	342	0	1	4	1	3	1	HR
HU	2	0	135	1	45	3	19	16	13	0	109	183	9	2	44	7	111	25	0	2	102	499	8	2	133	0	1	6	2	4	3	HU
IE	0	0	0	0	0	-5	0	1	0	0	1	11	3	0	4	3	42	95	0	0	0	0	-9	2	1	0	0	0	1	0	0	IE
IS	0	0	0	0	0	1	0	0	0	0	0	7	4	0	1	5	6	23	0	0	0	0	6	13	0	0	0	0	0	0	0	IS
IT	5	0	81	1	32	4	9	4	32	0	28	90	3	1	164	4	303	24	0	14	60	25	7	1	806	0	1	2	1	1	1	IT
KG	1	4	3	19	1	1	2	2	1	0	2	8	0	0	17	2	13	2	3	3	1	2	1	0	11	454	232	1	0	0	0	KG
KZ	1	2	3	9	1	1	2	8	1	0	3	11	1	1	11	9	12	7	2	2	1	3	2	1	9	14	289	2	0	2	1	KZ
LT	0	0	5	1	1	3	1	136	2	0	16	98	17	10	5	23	38	34	0	0	2	9	7	1	4	0	2	181	1	46	3	LT
LU	0	0	5	0	0	20	0	3	5	0	9	42	7	1	44	8	413	53	0	0	1	1	15	1	10	0	1	2	-234	1	0	LU
LV	0	0	3	1	1	3	1	108	1	0	10	75	15	22	5	39	32	31	0	0	1	6	6	1	3	0	2	85	1	137	2	LV
MD	2	0	11	2	10	2	32	63	3	0	26	63	7	3	20	9	36	19	1	5	8	26	4	1	32	0	5	12	1	6	214	MD
ME	82	0	41	1	176	3	38	8	8	0	28	65	4	1	108	6	92	17	1	25	71	89	4	1	331	0	1	3	0	2	1	ME
MK	192	0	28	2	40	3	134	11	6	0	22	52	4	1	87	5	60	13	1	274	25	67	4	1	197	0	1	3	0	2	3	MK
MT	15	0	34	1	34	5	23	4	10	0	18	56	3	1	149	3	210	27	0	60	28	20	7	1	393	0	2	2	1	1	1	MT
NL	0	0	1	0	0	-44	0	2	1	0	3	-47	12	1	17	10	101	64	0	0	0	0	16	2	2	0	0	2	2	2	0	NL
NO	0	0	1	0	0	3	0	7	0	0	2	19	9	3	2	19	14	40	0	0	0	1	7	2	1	0	0	5	0	4	0	NO
PL	1	0	21	1	7	1	4	31	5	0	84	191	21	3	13	12	78	43	0	1	10	41	8	2	20	0	2	17	2	9	3	PL
PT	0	0	1	0	0	2	0	1	1	0	1	10	1	0	533	1	73	27	0	0	0	0	9	1	5	0	0	0	0	0	0	PT
RO	5	0	27	2	26	3	77	32	4	0	39	70	6	2	33	7	50	17	1	7	18	91	4	1	66	0	3	9	1	5	25	RO
RS	46	0	60	1	99	3	102	13	8	0	54	94	5	2	64	6	71	18	1	23	58	155	5	1	158	0	1	4	1	3	3	RS
RU	0	1	1	8	1	1	2	16	1	0	2	12	1	3	4	12	7	6	3	1	1	2	2	0	3	0	26	4	0	3	1	RU
SE	0	0	2	0	0	3	0	11	0	0	5	35	16	7	4	31	21	33	0	0	0	2	6	2	1	0	0	8	0	9	0	SE
SI	2	0	299	0	30	3	8	5	21	0	72	200	4	1	86	7	168	22	0	4	261	73	8	1	436	0	1	4	1	2	1	SI
SK	2	0	97	1	25	3	12	16	11	0	177	183	11	1	34	6	104	30	0	1	45	264	7	2	84	0	2	8	2	4	3	SK
TJ	1	4	2	17	1	0	1	1	1	0	2	6	0	0	15	1	10	1	3	3	1	1	0	0	10	42	97	0	0	0	0	TJ
TM	1	7	3	44	1	1	2	4	1	0	3	9	1	1	13	5	11	3	7	3	1	3	1	0	9	5	157	1	0	1	1	TM
TR	5	13	7	44	6	1	40	18	2	8	8	23	2	1	35	3	24	7	24	59	4	10	2	0	39	0	6	4	0	2	10	TR
UA	1	0	10	4	7	2	16	77	2	0	21	53	6	3	14	10	31	18	2	5	7	24	4	1	22	0	8	14	1	8	25	UA
UZ	1	4	3	19	1	1	2	4	1	0	3	9	1	1	13	5	11	4	4	3	1	2	1	0	9	23	226	1	0	1	1	UZ
ATL	0	0	0	0	0	0	0	0	0	0	0	0	0	0	1	0	2	1	0	0	0	0	0	0	0	0	0	0	0	0	0	ATL
BAS	0	0	1	0	0	1	0	10	0	0	3	28	6	7	2	21	15	22	0	0	0	2	4	1	1	0	0	8	0	9	0	BAS
BLS	1	0	1	3	1	0	9	8	0	0	2	6	1	0	2	2	4	2	7	3	1	2	0	0	3	0	2	2	0	1	5	BLS
MED	4	0	6	1	6	1	14	2	2	1	4	10	1	0	28	1	40	4	0	25	8	5	1	0	35	0	0	1	0	0	1	MED
NOS	0	0	0	0	0	-2	0	0	0	0	0	1	2	0	1	2	6	9	0	0	0	0	4	1	0	0	0	0	0	0	0	NOS
AST	1	3	2	19	1	0	3	2	1	6	1	5	0	0	12	1	8	1	3	12	1	1	0	0	9	15	54	0	0	0	1	AST
NOA	3	0	5	0	4	1	7	1	3	1	3	12	0	0	123	0	50	5	0	24	4	3	1	0	55	0	0	0	0	0	1	NOA
EXC	3	2	11	12	6	0	12	18	4	1	11	35	3	3	56	12	62	13	5	11	7	12	4	1	32	8	67	5	0	4	3	EXC
EU	4	0	35	1	11	-2	35	15	11	1	33	100	7	4	215	21	227	35	0	28	21	34	8	1	101	0	1	10	2	7	3	EU
	AL	AM	AT	AZ	BA	BE	BG	BY	CH	CY	CZ	DE	DK	EE	ES	FI	FR	GB	GE	GR	HR	HU	IE	IS	IT	KG	KZ	LT	LU	LV	MD	

Table C.4 Cont.: 2021 country-to-country blame matrices for **MM-AOT40f**.
Units: ppb.h per 15% emis. red. of NO_x. **Emitters →, Receptors ↓.**

	ME	MK	MT	NL	NO	PL	PT	RO	RS	RU	SE	SI	SK	TJ	TM	TR	UA	UZ	ATL	BAS	BLS	MED	NOS	AST	NOA	DMS	VOL	EXC	EU	
AL	63	55	1	3	6	58	9	47	251	36	7	6	22	0	0	16	23	0	25	10	5	315	11	2	135	0	0	2319	1036	AL
AM	0	1	0	1	2	9	2	11	4	114	2	0	1	0	90	291	23	21	5	2	15	21	2	660	27	0	0	1356	104	AM
AT	0	0	0	0	11	67	8	8	9	26	12	91	15	0	0	1	9	0	39	14	0	53	15	1	26	0	0	2030	1858	AT
AZ	0	1	0	1	3	10	1	10	3	284	3	0	2	0	171	95	29	42	5	4	13	12	2	357	15	0	0	1073	94	AZ
BA	17	2	0	3	9	93	10	45	120	37	11	17	41	0	0	4	19	0	29	14	2	171	15	1	91	0	0	2295	1398	BA
BE	0	0	0	-132	28	11	5	1	0	25	19	0	0	0	0	0	3	0	60	8	0	9	-103	0	4	0	0	-39	-166	BE
BG	7	26	0	3	10	83	4	329	174	153	11	5	25	0	1	54	161	0	20	15	48	53	12	2	51	0	0	2415	1716	BG
BY	0	0	0	3	21	210	1	26	6	323	32	2	12	0	1	2	158	1	21	43	2	4	20	2	3	0	0	1440	571	BY
CH	0	0	0	1	8	18	12	4	3	26	7	6	2	0	0	1	6	0	51	7	0	56	14	1	24	0	0	1768	1233	CH
CY	2	8	0	2	4	31	5	47	32	130	4	2	6	0	3	898	89	1	12	6	33	827	6	59	86	0	0	2304	1065	CY
CZ	0	0	0	-5	16	177	3	15	17	37	18	18	65	0	0	1	14	0	38	24	1	14	15	1	9	0	0	1702	1546	CZ
DE	0	0	0	-25	26	56	4	2	1	31	21	3	5	0	0	1	5	0	49	13	0	10	-3	0	7	0	0	936	794	DE
DK	0	0	0	-15	67	79	2	2	1	48	53	1	2	0	0	0	8	0	61	-33	0	2	28	0	2	0	0	516	264	DK
EE	0	0	0	3	28	65	1	4	1	275	63	0	3	0	1	1	38	0	24	120	1	1	25	1	1	0	0	990	540	EE
ES	0	0	0	1	3	4	220	2	1	8	2	1	1	0	0	1	3	0	152	1	0	157	12	2	107	0	0	1806	1757	ES
FI	0	0	0	2	17	36	0	1	0	137	40	0	1	0	0	1	12	0	16	54	0	0	12	0	0	0	0	505	303	FI
FR	0	0	0	-12	13	11	13	2	2	30	10	2	1	0	0	1	5	0	96	6	0	72	4	1	21	0	0	1420	1282	FR
GB	0	0	0	-16	33	4	1	0	0	14	11	0	0	0	0	0	1	0	67	7	0	1	-22	0	1	0	0	137	103	GB
GE	1	2	0	1	4	19	2	22	6	256	4	1	3	0	83	216	65	20	7	5	73	17	4	207	22	0	0	1908	151	GE
GL	0	0	0	0	0	0	0	0	0	0	0	0	0	0	0	0	0	0	0	0	0	0	0	0	0	0	0	2	1	GL
GR	9	55	1	4	7	60	6	114	138	108	7	4	16	0	1	107	90	1	21	11	30	336	12	3	126	0	0	2316	1635	GR
HR	5	2	0	3	11	97	9	39	75	38	13	72	41	0	0	3	18	0	34	15	2	235	17	1	62	0	0	2444	2034	HR
HU	2	1	0	3	15	216	4	142	95	61	17	35	155	0	0	3	65	0	29	23	2	52	19	1	31	0	0	2299	1949	HU
IE	0	0	0	-9	17	3	1	0	0	11	5	0	0	0	0	0	1	0	53	3	0	1	6	0	1	0	0	180	52	IE
IS	0	0	0	1	16	2	0	0	0	7	8	0	0	0	0	0	1	0	23	6	0	0	12	0	0	0	0	102	42	IS
IT	3	2	1	3	7	37	13	14	21	25	8	37	10	0	0	4	9	0	45	9	1	399	15	2	125	0	0	1899	1726	IT
KG	0	1	0	1	1	6	2	3	2	107	2	1	1	191	62	37	7	717	6	2	1	8	1	374	22	0	0	1925	82	KG
KZ	0	0	0	1	7	12	2	5	3	577	6	1	2	2	16	15	20	29	11	6	2	5	4	55	8	0	0	1110	104	KZ
LT	0	0	0	3	24	193	1	11	3	183	57	1	7	0	1	1	78	0	26	89	1	2	31	1	1	0	0	1211	740	LT
LU	0	0	0	-30	21	16	6	1	0	27	15	0	1	0	0	1	5	0	57	9	0	15	-1	0	8	0	0	472	354	LU
LV	0	0	0	3	24	106	1	7	2	216	63	1	5	0	1	1	56	0	23	103	1	1	27	1	1	0	0	1073	628	LV
MD	1	2	0	4	13	169	2	206	22	220	14	3	15	0	2	16	444	1	18	20	27	18	15	3	13	0	0	1754	714	MD
ME	435	8	1	3	8	84	10	43	237	41	9	7	33	0	0	9	22	0	26	13	3	250	13	1	125	0	0	2159	1102	ME
MK	17	346	0	3	7	74	8	102	411	65	8	5	28	0	1	36	46	0	23	13	9	128	11	2	127	0	0	2398	1198	MK
MT	7	5	-775	7	7	39	10	21	39	27	7	11	10	0	1	16	15	0	37	8	6	-142	17	2	236	0	0	558	346	MT
NL	0	0	0	-638	40	17	3	1	0	27	21	0	0	0	0	0	3	0	53	9	0	4	-192	0	2	0	0	-375	-517	NL
NO	0	0	0	2	101	17	0	1	0	34	35	0	1	0	0	0	4	0	37	22	0	0	41	0	0	0	0	335	146	NO
PL	0	0	0	0	23	581	2	35	14	88	33	5	45	0	0	1	68	0	32	53	1	7	27	1	4	0	0	1526	1237	PL
PT	0	0	0	1	3	2	947	1	1	4	1	0	0	0	0	0	1	0	309	1	0	45	10	1	51	0	0	1631	1590	PT
RO	4	3	0	4	12	143	3	797	82	144	14	6	43	0	1	12	205	1	21	18	19	32	14	2	27	0	0	2104	1525	RO
RS	30	20	0	3	10	108	6	172	482	72	11	11	52	0	0	7	54	0	24	17	6	76	14	1	66	0	0	2096	1229	RS
RU	0	0	0	1	6	16	1	4	2	536	7	0	1	0	5	7	28	3	8	9	4	2	5	9	2	0	0	742	92	RU
SE	0	0	0	3	48	37	1	2	1	57	108	0	2	0	0	0	8	0	29	55	0	1	30	0	1	0	0	464	303	SE
SI	1	1	0	1	9	75	8	16	21	30	11	522	19	0	0	2	11	0	35	13	1	178	14	1	47	0	0	2449	2289	SI
SK	1	1	0	4	16	355	3	100	48	61	18	22	424	0	1	3	72	0	28	25	2	29	21	1	19	0	0	2265	1972	SK
TJ	0	0	0	0	1	4	2	2	2	70	1	1	1	838	152	38	5	585	4	1	1	9	1	563	26	0	0	1922	65	TJ
TM	0	0	0	1	4	9	2	5	3	276	3	1	2	13	432	40	15	295	7	4	3	8	2	195	15	0	0	1399	90	TM
TR	2	4	0	2	4	34	4	58	21	194	5	1	6	0	7	867	112	2	12	7	62	115	6	200	67	0	0	1732	383	TR
UA	1	1	0	3	15	153	2	85	15	412	20	2	16	0	4	14	479	2	17	24	25	12	14	4	10	0	0	1616	529	UA
UZ	0	0	0	1	4	9	2	5	2	283	4	1	2	52	79	30	13	392	7	3	2	7	2	118	13	0	0	1232	88	UZ
ATL	0	0	0	0	1	0	1	0	0	1	0	0	0	0	0	0	0	0	4	0	0	0	0	0	0	0	0	8	5	ATL
BAS	0	0	0	-1	16	39	0	2	1	41	41	0	1	0	0	0	8	0	15	-7	0	0	14	0	0	0	0	292	192	BAS
BLS	0	0	0	1	2	14	0	19	3	93	3	0	1	0	1	16	69	0	2	3	45	3	2	2	2	0	0	292	78	BLS
MED	1	2	0	1	1	9	3	12	10	17	1	2	2	0	0	25	13	0	9	2	6	106	3	-2	25	0	0	301	212	MED
NOS	0	0	0	-9	9	3	0	0	0	4	4	0	0	0	0	0	0	0	13	1	0	0	-26	0	0	0	0	38	14	NOS
AST	0	1	0	0	1	5	1	5	3	71	1	0	1	25	114	120	10	81	3	1	3	39	1	1307	25	0	0	605	78	AST
NOA	1	1	1	1	1	6	32	7	7	8	1	1	2	0	0	19	6	0	63	1	2	182	3	0	788	0	0	404	342	NOA
EXC	1	2	0	-1	12	40	13	25	11	354	12	3	7	10	21	49	46	35	22	13	7	28	7	40	16	0	0	1063	378	EXC
EU	1	3	0	-9	18	95	52	69	22	64	28	11	20	0	0	9	34	0	61	25	4	83	12	1	37	0	0	1386	1153	EU
	ME	MK	MT	NL	NO	PL	PT	RO	RS	RU	SE	SI	SK	TJ	TM	TR	UA	UZ	ATL	BAS	BLS	MED	NOS	AST	NOA	DMS	VOL	EXC	EU	

Table C.5: 2021 country-to-country blame matrices for **MM-AOT40f**.
Units: ppb.h per 15% emis. red. of VOC. **Emitters →, Receptors ↓.**

	AL	AM	AT	AZ	BA	BE	BG	BY	CH	CY	CZ	DE	DK	EE	ES	FI	FR	GB	GE	GR	HR	HU	IE	IS	IT	KG	KZ	LT	LU	LV	MD	
AL	122	0	9	1	17	5	8	2	4	0	13	54	5	1	20	1	51	25	0	14	10	17	3	0	110	0	1	1	0	1	1	AL
AM	0	86	1	411	1	1	2	3	1	1	3	14	1	0	4	1	10	6	33	3	1	2	1	0	9	0	11	1	0	1	2	AM
AT	0	0	112	0	2	9	1	2	34	0	38	213	6	0	15	1	106	28	0	0	10	8	4	0	127	0	0	1	1	1	0	AT
AZ	0	6	1	918	1	1	2	5	1	0	3	17	2	1	4	1	11	8	25	2	1	2	1	0	9	0	20	1	0	1	2	AZ
BA	3	0	18	1	111	6	4	2	7	0	25	91	5	0	20	1	58	26	0	2	18	22	3	0	98	0	0	1	1	1	1	BA
BE	0	0	2	0	0	159	0	1	2	0	5	170	10	0	9	1	167	78	0	0	0	0	6	0	5	0	0	0	4	0	0	BE
BG	2	0	7	2	6	6	69	6	3	0	20	65	6	1	9	2	34	22	0	10	4	15	3	0	30	0	1	2	1	1	6	BG
BY	0	0	3	1	1	5	1	38	2	0	12	49	5	1	3	2	27	22	0	0	1	4	2	0	7	0	1	4	0	2	2	BY
CH	0	0	13	0	1	9	0	1	184	0	10	185	6	0	18	1	156	28	0	0	4	2	3	0	181	0	0	1	1	0	0	CH
CY	3	1	5	15	5	4	12	9	3	41	11	49	4	1	13	2	35	21	2	34	4	8	2	0	47	0	3	2	0	1	5	CY
CZ	0	0	25	0	3	16	1	2	12	0	204	235	12	0	8	1	103	34	0	0	6	13	4	0	31	0	0	1	2	1	0	CZ
DE	0	0	15	0	0	28	0	1	15	0	25	378	14	0	8	1	124	55	0	0	1	2	5	0	16	0	0	1	3	1	0	DE
DK	0	0	1	0	0	18	0	2	1	0	6	104	80	1	3	2	57	83	0	0	0	1	6	0	3	0	0	2	1	1	0	DK
EE	0	0	1	1	0	6	0	9	1	0	3	39	7	6	1	5	25	26	0	0	0	1	3	0	2	0	1	3	0	4	0	EE
ES	0	0	1	0	0	7	0	1	2	0	2	34	2	0	232	0	81	27	0	0	1	1	3	0	15	0	0	0	1	0	0	ES
FI	0	0	0	1	0	2	0	3	0	0	1	16	3	1	1	6	11	13	0	0	0	0	2	0	1	0	0	1	0	1	0	FI
FR	0	0	3	0	1	23	0	1	9	0	5	109	6	0	29	1	258	63	0	0	2	1	6	0	41	0	0	1	2	0	0	FR
GB	0	0	0	0	0	12	0	0	0	0	1	45	5	0	1	1	30	209	0	0	0	0	10	0	1	0	0	0	0	0	0	GB
GE	0	7	2	300	1	2	2	5	1	0	4	20	2	0	4	1	13	9	85	3	1	2	1	0	10	0	10	1	0	1	3	GE
GL	0	0	0	0	0	0	0	0	0	0	0	0	0	0	0	0	0	0	0	0	0	0	0	0	0	0	0	0	0	0	0	GL
GR	11	0	8	3	9	6	21	5	4	0	15	59	5	1	15	2	45	27	0	124	6	13	3	0	71	0	1	2	0	1	4	GR
HR	2	0	31	0	37	8	4	3	11	0	35	136	6	1	21	2	81	32	0	2	57	24	4	0	136	0	1	1	1	1	1	HR
HU	1	0	35	1	9	8	4	4	12	0	53	154	9	1	11	1	76	32	0	1	12	93	4	0	60	0	1	2	1	1	2	HU
IE	0	0	0	0	0	11	0	0	0	0	1	24	2	0	1	0	29	105	0	0	0	0	31	0	2	0	0	0	0	0	0	IE
IS	0	0	0	0	0	1	0	0	0	0	0	6	3	0	0	0	4	15	0	0	0	0	1	0	0	0	0	0	0	0	0	IS
IT	2	0	23	1	9	8	2	2	14	0	19	94	6	0	37	1	116	34	0	3	17	8	4	0	629	0	1	1	1	1	1	IT
KG	0	1	1	17	0	1	1	2	1	0	2	9	1	0	4	1	8	5	1	1	1	1	1	0	8	42	67	0	0	0	1	KG
KZ	0	0	1	9	1	1	1	3	1	0	2	14	2	0	3	1	10	10	1	1	1	1	1	0	7	2	53	1	0	1	1	KZ
LT	0	0	2	1	0	6	0	16	1	0	8	52	10	1	2	2	29	27	0	0	1	3	3	0	3	0	1	15	0	4	1	LT
LU	0	0	4	0	0	43	0	1	2	0	9	226	9	0	11	1	160	51	0	0	0	1	4	0	8	0	0	1	36	1	0	LU
LV	0	0	1	1	0	5	0	12	1	0	5	43	8	1	2	2	26	24	0	0	0	2	3	0	2	0	1	6	0	10	1	LV
MD	0	0	4	2	2	7	5	11	2	0	17	64	7	1	6	1	33	31	0	2	2	7	4	0	18	0	1	3	1	1	62	MD
ME	16	0	10	1	24	5	6	2	5	0	15	57	5	0	21	1	48	23	0	5	9	17	2	0	97	0	1	1	0	1	1	ME
MK	17	0	8	2	10	5	14	3	4	0	15	54	5	1	16	1	36	21	0	30	6	17	2	0	59	0	1	1	0	1	2	MK
MT	5	0	14	1	13	9	6	3	7	0	18	83	7	1	43	2	110	41	0	16	11	10	5	0	289	0	1	1	1	1	1	MT
NL	0	0	1	0	0	65	0	1	1	0	3	194	12	0	5	1	100	100	0	0	0	0	9	0	2	0	0	1	1	0	0	NL
NO	0	0	0	0	0	3	0	1	0	0	1	15	4	0	1	1	10	22	0	0	0	0	2	0	1	0	0	1	0	0	0	NO
PL	0	0	7	1	2	11	1	5	3	0	41	125	15	1	4	1	50	45	0	0	3	10	5	0	13	0	1	2	1	1	1	PL
PT	0	0	1	0	0	6	0	0	1	0	1	23	1	0	101	0	54	25	0	0	0	0	3	0	5	0	0	0	0	0	0	PT
RO	1	0	8	2	5	6	12	6	4	0	23	67	7	1	8	1	37	24	0	2	3	18	3	0	28	0	1	2	1	1	9	RO
RS	6	0	17	1	24	7	13	4	6	0	31	92	7	1	13	1	47	26	0	4	11	36	3	0	55	0	1	1	1	1	2	RS
RU	0	0	1	7	0	1	0	3	0	0	2	10	1	0	1	1	6	6	0	0	0	1	1	0	3	0	4	1	0	1	1	RU
SE	0	0	1	0	0	5	0	2	0	0	2	27	8	1	1	1	17	23	0	0	0	1	2	0	1	0	0	1	0	1	0	SE
SI	1	0	54	0	6	8	2	2	14	0	34	153	5	0	20	2	85	30	0	1	38	12	4	0	236	0	0	1	1	1	0	SI
SK	1	0	26	1	5	8	2	3	9	0	67	137	10	0	8	1	69	32	0	0	7	40	4	0	44	0	1	2	1	1	1	SK
TJ	0	1	1	18	0	1	0	1	1	0	1	7	1	0	4	0	7	4	1	1	0	1	0	0	7	6	38	0	0	0	0	TJ
TM	0	1	2	45	1	1	1	4	1	0	3	16	1	0	4	1	12	9	2	1	1	2	1	0	9	1	38	1	0	1	1	TM
TR	1	3	3	33	2	3	7	7	2	1	8	34	3	1	8	1	21	14	5	10	2	4	2	0	22	0	3	2	0	1	5	TR
UA	0	0	4	5	2	4	3	14	2	0	13	49	6	1	4	1	26	23	0	1	2	6	3	0	13	0	2	3	0	2	8	UA
UZ	0	1	1	19	1	1	1	3	1	0	3	13	1	0	4	1	10	8	1	1	1	1	1	0	9	8	58	1	0	1	1	UZ
ATL	0	0	0	0	0	0	0	0	0	0	0	1	0	0	1	0	1	1	0	0	0	0	0	0	0	0	0	0	0	0	0	ATL
BAS	0	0	0	0	0	4	0	2	0	0	2	29	12	1	1	2	15	19	0	0	0	1	2	0	1	0	0	1	0	2	0	BAS
BLS	0	0	1	3	0	1	2	3	0	0	2	8	1	0	1	0	4	3	2	1	0	1	0	0	2	0	1	1	0	0	2	BLS
MED	1	0	2	1	2	2	2	1	1	0	3	15	1	0	10	0	20	7	0	9	2	2	1	0	33	0	0	0	0	0	1	MED
NOS	0	0	0	0	0	3	0	0	0	0	0	11	2	0	0	0	10	19	0	0	0	0	1	0	0	0	0	0	0	0	0	NOS
AST	0	1	1	25	1	1	1	2	1	1	2	9	1	0	3	0	7	4	1	3	1	1	1	0	8	1	16	0	0	0	1	AST
NOA	1	0	2	1	2	2	1	1	2	0	3	20	1	0	29	0	30	10	0	4	2	2	1	0	32	0	0	0	0	0	0	NOA
EXC	1	0	3	14	1	4	2	4	2	0	6	36	3	0	11	1	28	18	1	2	1	3	2	0	21	1	13	1	0	1	1	EXC
EU	1	0	10	1	3	13	4	3	6	0	18	103	8	1	41	2	88	37	0	5	4	7	4	0	69	0	0	1	1	1	1	EU
	AL	AM	AT	AZ	BA	BE	BG	BY	CH	CY	CZ	DE	DK	EE	ES	FI	FR	GB	GE	GR	HR	HU	IE	IS	IT	KG	KZ	LT	LU	LV	MD	

Table C.5 Cont.: 2021 country-to-country blame matrices for **MM-AOT40f**.
Units: ppb.h per 15% emis. red. of VOC. **Emitters →, Receptors ↓.**

	ME	MK	MT	NL	NO	PL	PT	RO	RS	RU	SE	SI	SK	TJ	TM	TR	UA	UZ	ATL	BAS	BLS	MED	NOS	AST	NOA	DMS	VOL	EXC	EU	
AL	15	7	0	13	3	36	3	14	49	21	3	2	8	0	0	3	7	0	0	0	0	2	0	1	28	0	0	679	401	AL
AM	0	0	0	3	1	13	1	6	2	66	1	0	1	0	12	34	10	5	0	0	0	0	0	178	7	0	0	767	82	AM
AT	0	0	0	16	3	37	2	3	3	12	4	15	9	0	0	0	3	0	0	0	0	0	1	0	7	0	0	831	741	AT
AZ	0	0	0	4	2	16	1	6	2	140	2	0	2	0	22	15	14	10	0	0	0	0	0	138	6	0	0	1282	90	AZ
BA	3	1	0	14	3	48	3	12	31	17	4	4	11	0	0	1	5	0	0	0	0	1	0	0	21	0	0	682	471	BA
BE	0	0	0	142	8	9	1	0	0	12	6	0	0	0	0	0	2	0	0	0	0	0	3	0	1	0	0	802	698	BE
BG	1	2	0	14	3	57	1	56	27	56	4	1	10	0	0	12	29	0	0	0	0	1	0	1	12	0	0	607	428	BG
BY	0	0	0	11	4	69	0	7	2	63	5	1	4	0	0	1	22	0	0	0	0	0	0	1	1	0	0	382	223	BY
CH	0	0	0	20	3	16	3	2	1	14	3	3	2	0	0	0	3	0	0	0	0	0	1	0	6	0	0	877	639	CH
CY	1	2	0	10	3	41	2	23	14	90	4	1	5	0	1	159	35	1	0	0	0	5	0	50	25	0	0	733	362	CY
CZ	0	0	0	29	5	117	1	4	6	16	6	5	19	0	0	0	5	0	0	0	0	0	1	0	3	0	0	933	847	CZ
DE	0	0	0	63	7	35	1	1	1	12	6	1	3	0	0	0	2	0	0	0	0	0	2	0	2	0	0	825	730	DE
DK	0	0	0	60	19	40	1	1	1	15	15	0	1	0	0	0	3	0	0	2	0	0	3	0	1	0	0	529	404	DK
EE	0	0	0	15	5	21	0	2	0	62	8	0	1	0	0	0	7	0	0	1	0	0	0	0	1	0	0	267	155	EE
ES	0	0	0	13	2	6	31	1	1	6	1	0	1	0	0	0	1	0	1	0	0	2	0	1	29	0	0	474	434	ES
FI	0	0	0	6	2	11	0	0	0	25	4	0	0	0	0	0	2	0	0	0	0	0	0	0	0	0	0	116	69	FI
FR	0	0	0	42	4	11	4	1	1	16	4	1	1	0	0	0	2	0	0	0	0	1	1	0	6	0	0	650	552	FR
GB	0	0	0	35	5	3	0	0	0	5	2	0	0	0	0	0	0	0	0	0	0	0	2	0	0	0	0	369	149	GB
GE	0	0	0	4	2	20	1	9	2	100	2	0	2	0	9	24	18	4	0	0	0	0	0	67	6	0	0	691	110	GE
GL	0	0	0	0	0	0	0	0	0	0	0	0	0	0	0	0	0	0	0	0	0	0	0	0	0	0	0	1	0	GL
GR	2	6	0	15	3	49	2	29	29	52	4	2	8	0	0	25	22	0	0	0	0	3	0	1	28	0	0	710	505	GR
HR	2	1	0	17	4	54	3	12	23	19	5	12	12	0	0	1	6	0	0	0	0	1	0	0	16	0	0	805	664	HR
HU	1	0	0	20	5	115	2	35	26	26	6	6	40	0	0	1	13	0	0	0	0	0	1	0	9	0	0	883	750	HU
IE	0	0	0	23	3	2	0	0	0	4	1	0	0	0	0	0	0	0	0	0	0	0	1	0	0	0	0	243	129	IE
IS	0	0	0	3	1	1	0	0	0	1	1	0	0	0	0	0	0	0	0	0	0	0	0	0	0	0	0	40	22	IS
IT	1	1	1	17	4	31	4	6	8	17	4	13	5	0	0	1	5	0	0	0	0	3	0	1	31	0	0	1153	1053	IT
KG	0	0	0	2	1	6	1	2	1	44	1	0	1	67	8	5	4	359	0	0	0	0	0	83	5	0	0	678	52	KG
KZ	0	0	0	3	2	10	1	2	1	96	2	0	1	2	2	3	6	17	0	0	0	0	0	19	3	0	0	277	68	KZ
LT	0	0	0	13	5	62	0	3	1	45	8	0	3	0	0	0	13	0	0	1	0	0	0	0	1	0	0	341	229	LT
LU	0	0	0	66	5	13	2	1	0	14	5	0	1	0	0	0	3	0	0	0	0	0	1	0	2	0	0	680	602	LU
LV	0	0	0	13	5	38	0	2	1	47	8	0	2	0	0	0	10	0	0	1	0	0	0	0	1	0	0	286	184	LV
MD	0	0	0	14	4	87	1	42	6	68	5	1	6	0	0	6	62	0	0	0	0	0	0	1	5	0	0	596	336	MD
ME	75	2	0	12	3	38	3	11	36	19	3	2	9	0	0	2	6	0	0	0	0	1	0	1	27	0	0	593	379	ME
MK	3	45	0	12	3	45	2	20	59	29	3	2	10	0	0	5	10	0	0	0	0	1	0	1	24	0	0	576	364	MK
MT	3	2	121	21	5	42	4	11	14	28	5	6	7	0	0	5	9	0	0	0	0	17	0	1	66	0	0	980	841	MT
NL	0	0	0	282	9	14	1	0	0	11	7	0	0	0	0	0	2	0	0	0	0	0	5	0	1	0	0	825	700	NL
NO	0	0	0	9	15	7	0	0	0	7	3	0	0	0	0	0	1	0	0	0	0	0	1	0	0	0	0	105	59	NO
PL	0	0	0	27	6	294	1	10	5	28	7	1	13	0	0	1	12	0	0	1	0	0	1	0	2	0	0	752	643	PL
PT	0	0	0	11	1	3	179	0	0	4	1	0	0	0	0	0	1	0	2	0	0	1	0	0	15	0	0	425	392	PT
RO	1	1	0	13	4	78	1	131	16	50	5	1	12	0	0	4	32	0	0	0	0	0	0	1	8	0	0	629	469	RO
RS	5	4	0	16	4	64	2	35	148	29	5	3	17	0	0	2	11	0	0	0	0	1	0	0	15	0	0	755	483	RS
RU	0	0	0	3	1	9	0	2	1	86	1	0	1	0	1	1	6	1	0	0	0	0	0	3	1	0	0	165	45	RU
SE	0	0	0	13	6	14	0	1	0	13	9	0	1	0	0	0	2	0	0	0	0	0	1	0	0	0	0	152	106	SE
SI	0	0	0	15	3	40	3	5	8	16	4	89	7	0	0	0	4	0	0	0	0	1	0	0	13	0	0	907	820	SI
SK	0	0	0	20	5	176	1	22	12	24	5	4	78	0	0	1	13	0	0	0	0	0	1	0	6	0	0	841	734	SK
TJ	0	0	0	2	1	5	1	2	1	39	1	0	1	236	15	6	3	217	0	0	0	0	0	93	5	0	0	632	44	TJ
TM	0	0	0	4	2	12	1	3	2	103	2	0	1	7	77	7	9	83	0	0	0	0	0	64	5	0	0	472	80	TM
TR	0	1	0	8	2	32	1	18	6	85	3	1	3	0	1	130	27	1	0	0	0	1	0	50	15	0	0	527	199	TR
UA	0	0	0	10	4	72	1	18	4	126	5	1	6	0	0	4	94	0	0	0	0	0	0	2	4	0	0	544	254	UA
UZ	0	0	0	3	2	10	1	3	1	86	2	0	1	33	11	5	6	303	0	0	0	0	0	39	4	0	0	617	70	UZ
ATL	0	0	0	0	0	0	0	0	0	0	0	0	0	0	0	0	0	0	0	0	0	0	0	0	0	0	0	5	4	ATL
BAS	0	0	0	11	4	18	0	1	0	17	8	0	1	0	0	0	2	0	0	1	0	0	0	0	0	0	0	157	112	BAS
BLS	0	0	0	2	1	10	0	5	1	37	1	0	1	0	0	8	14	0	0	0	0	0	0	1	1	0	0	121	45	BLS
MED	0	0	0	4	1	8	1	4	3	10	1	1	1	0	0	11	4	0	0	0	0	2	0	3	16	0	0	168	124	MED
NOS	0	0	0	10	3	2	0	0	0	1	1	0	0	0	0	0	0	0	0	0	0	0	1	0	0	0	0	65	41	NOS
AST	0	0	0	2	1	7	1	3	2	36	1	0	1	6	13	18	5	26	0	0	0	0	0	449	8	0	0	215	55	AST
NOA	0	0	0	5	1	8	9	3	2	7	1	1	1	0	0	4	3	0	0	0	0	2	0	4	169	0	0	195	160	NOA
EXC	0	0	0	9	3	22	2	6	3	68	3	1	2	4	3	8	10	18	0	0	0	0	0	12	4	0	0	347	173	EXC
EU	0	0	0	27	4	51	9	13	5	21	5	3	6	0	0	2	7	0	0	0	0	1	1	1	10	0	0	585	493	EU
	ME	MK	MT	NL	NO	PL	PT	RO	RS	RU	SE	SI	SK	TJ	TM	TR	UA	UZ	ATL	BAS	BLS	MED	NOS	AST	NOA	DMS	VOL	EXC	EU	

Table C.6: 2021 country-to-country blame matrices for **SOMO35**.
Units: ppb.d per 15% emis. red. of NO_x. **Emitters →, Receptors ↓.**

	AL	AM	AT	AZ	BA	BE	BG	BY	CH	CY	CZ	DE	DK	EE	ES	FI	FR	GB	GE	GR	HR	HU	IE	IS	IT	KG	KZ	LT	LU	LV	MD	
AL	64	0	3	0	7	0	4	1	1	0	2	5	0	0	10	0	9	1	0	12	5	5	0	0	33	0	0	0	0	0	0	AL
AM	0	-32	0	43	0	0	1	0	0	0	0	1	0	0	2	0	1	0	9	2	0	0	0	0	2	0	2	0	0	0	0	AM
AT	0	0	36	0	1	0	1	1	7	0	8	31	0	0	7	1	21	2	0	0	4	4	1	0	24	0	0	0	0	0	0	AT
AZ	0	2	0	-10	0	0	1	1	0	0	0	1	0	0	1	0	1	0	6	1	0	0	0	0	1	0	6	0	0	0	0	AZ
BA	1	0	8	0	55	0	2	1	1	0	5	9	0	0	10	0	11	2	0	2	19	12	0	0	30	0	0	0	0	0	0	BA
BE	0	0	0	0	0	-53	0	0	0	0	0	-9	1	0	4	1	26	5	0	0	0	0	2	0	1	0	0	0	0	0	0	BE
BG	2	0	3	0	3	0	75	2	1	0	3	5	0	0	5	1	4	1	0	10	2	5	0	0	8	0	0	1	0	0	2	BG
BY	0	0	1	0	0	0	0	25	0	0	2	6	1	1	1	2	3	2	0	0	0	2	1	0	1	0	0	4	0	2	1	BY
CH	0	0	4	0	0	0	0	0	36	0	1	15	0	0	10	0	52	3	0	0	1	0	1	0	26	0	0	0	0	0	0	CH
CY	1	0	1	1	1	0	4	1	0	47	1	3	0	0	5	0	4	1	1	22	1	1	0	0	7	0	0	0	0	0	0	CY
CZ	0	0	11	0	1	0	1	1	2	0	25	31	1	0	3	1	17	3	0	0	2	5	1	0	5	0	0	1	0	0	0	CZ
DE	0	0	3	0	0	-1	0	0	2	0	4	11	1	0	3	1	23	4	0	0	0	0	1	0	2	0	0	0	0	0	0	DE
DK	0	0	0	0	0	0	0	1	0	0	1	4	-10	0	1	2	5	8	0	0	0	0	1	0	0	0	0	1	0	1	0	DK
EE	0	0	0	0	0	0	0	6	0	0	1	5	1	7	0	6	2	2	0	0	0	0	1	0	0	0	0	3	0	6	0	EE
ES	0	0	0	0	0	0	0	0	0	0	0	1	0	0	134	0	16	2	0	0	0	0	1	0	3	0	0	0	0	0	0	ES
FI	0	0	0	0	0	0	0	1	0	0	0	2	1	1	0	13	1	1	0	0	0	0	0	0	0	0	0	1	0	1	0	FI
FR	0	0	1	0	0	-1	0	0	2	0	0	5	0	0	16	1	87	5	0	0	0	0	2	0	6	0	0	0	0	0	0	FR
GB	0	0	0	0	0	0	0	0	0	0	0	1	1	0	1	1	4	-14	0	0	0	0	3	0	0	0	0	0	0	0	0	GB
GE	0	3	1	36	0	0	1	1	0	0	0	2	0	0	2	0	2	1	52	2	0	1	0	0	2	0	2	0	0	0	0	GE
GL	0	0	0	0	0	0	0	0	0	0	0	0	0	0	0	0	0	0	0	0	0	0	0	0	0	0	0	0	0	0	0	GL
GR	8	0	2	0	3	0	20	1	1	0	2	4	0	0	7	0	6	1	0	68	2	3	0	0	18	0	0	0	0	0	1	GR
HR	1	0	14	0	19	0	2	1	1	0	6	12	0	0	9	1	14	2	0	1	46	16	1	0	32	0	0	0	0	0	0	HR
HU	0	0	12	0	4	0	2	1	1	0	9	14	1	0	4	1	10	2	0	0	11	44	1	0	12	0	0	1	0	0	0	HU
IE	0	0	0	0	0	0	0	0	0	0	0	1	0	0	1	0	5	8	0	0	0	0	-13	0	0	0	0	0	0	0	0	IE
IS	0	0	0	0	0	0	0	0	0	0	0	1	0	0	0	1	1	3	0	0	0	0	1	2	0	0	0	0	0	0	0	IS
IT	1	0	8	0	3	0	1	0	3	0	2	8	0	0	15	0	27	2	0	2	6	2	1	0	69	0	0	0	0	0	0	IT
KG	0	1	0	3	0	0	0	0	0	0	0	1	0	0	2	0	1	0	0	1	0	0	0	0	1	44	20	0	0	0	0	KG
KZ	0	0	0	2	0	0	0	1	0	0	0	1	0	0	1	1	1	1	0	0	0	0	0	0	1	2	31	0	0	0	0	KZ
LT	0	0	0	0	0	0	0	11	0	0	1	7	1	1	1	2	3	3	0	0	0	1	1	0	1	0	0	11	0	4	0	LT
LU	0	0	1	0	0	-3	0	0	0	0	1	-4	1	0	5	1	42	5	0	0	0	0	1	0	2	0	0	0	-33	0	0	LU
LV	0	0	0	0	0	0	0	9	0	0	1	5	1	2	1	4	3	2	0	0	0	1	1	0	0	0	0	7	0	9	0	LV
MD	0	0	1	0	1	0	3	6	0	0	2	5	1	0	2	1	3	2	0	1	1	3	0	0	3	0	1	1	0	1	18	MD
ME	8	0	4	0	19	0	4	1	1	0	3	6	0	0	11	0	10	1	0	4	7	8	0	0	31	0	0	0	0	0	0	ME
MK	21	0	3	0	4	0	12	1	1	0	2	5	0	0	9	0	6	1	0	27	2	5	0	0	20	0	0	0	0	0	0	MK
MT	1	0	3	0	3	0	2	0	1	0	2	5	0	0	17	0	21	2	0	7	3	2	1	0	40	0	0	0	0	0	0	MT
NL	0	0	0	0	0	-7	0	0	0	0	0	-6	1	0	2	1	10	5	0	0	0	0	2	0	0	0	0	0	0	0	0	NL
NO	0	0	0	0	0	0	0	1	0	0	0	1	1	0	1	3	2	4	0	0	0	0	1	0	0	0	0	0	0	0	0	NO
PL	0	0	2	0	1	0	0	3	0	0	7	15	2	0	1	1	7	4	0	0	1	4	1	0	2	0	0	1	0	1	0	PL
PT	0	0	0	0	0	0	0	0	0	0	0	1	0	0	63	0	7	2	0	0	0	0	1	0	1	0	0	0	0	0	0	PT
RO	1	0	3	0	3	0	8	3	0	0	4	6	1	0	3	1	5	2	0	1	2	9	0	0	7	0	0	1	0	1	2	RO
RS	4	0	5	0	10	0	10	1	1	0	5	8	0	0	6	1	7	2	0	2	6	14	0	0	15	0	0	0	0	0	0	RS
RU	0	0	0	1	0	0	0	2	0	0	0	1	0	0	0	1	1	1	0	0	0	0	0	0	0	0	3	0	0	0	0	RU
SE	0	0	0	0	0	0	0	1	0	0	0	3	1	1	1	4	2	3	0	0	0	0	1	0	0	0	0	1	0	1	0	SE
SI	0	0	28	0	3	0	1	0	2	0	6	15	0	0	8	1	15	2	0	1	24	6	1	0	38	0	0	0	0	0	0	SI
SK	0	0	9	0	2	0	1	1	1	0	15	14	1	0	3	1	10	2	0	0	4	26	1	0	8	0	0	1	0	0	0	SK
TJ	0	1	0	2	0	0	0	0	0	0	0	1	0	0	2	0	1	0	0	0	0	0	0	0	1	3	8	0	0	0	0	TJ
TM	0	1	0	7	0	0	0	1	0	0	0	1	0	0	2	1	2	0	1	1	0	0	0	0	1	1	18	0	0	0	0	TM
TR	1	1	1	3	1	0	4	2	0	1	1	2	0	0	4	0	3	1	2	7	0	1	0	0	4	0	0	0	0	0	1	TR
UA	0	0	1	1	1	0	2	7	0	0	2	4	1	0	1	1	3	2	0	1	1	2	0	0	2	0	1	1	0	1	2	UA
UZ	0	1	0	3	0	0	0	1	0	0	0	1	0	0	2	1	1	0	1	0	0	0	0	0	1	2	26	0	0	0	0	UZ
ATL	0	0	0	0	0	0	0	0	0	0	0	0	0	0	4	0	4	3	0	0	0	0	1	0	0	0	0	0	0	0	0	ATL
BAS	0	0	0	0	0	0	0	2	0	0	1	6	2	2	1	6	4	5	0	0	0	1	1	0	0	0	0	2	0	2	0	BAS
BLS	0	0	1	2	1	0	7	5	0	0	1	3	1	0	2	1	2	1	5	3	1	2	0	0	3	0	1	1	0	1	3	BLS
MED	2	0	3	0	3	0	5	1	1	1	2	5	0	0	19	0	25	2	0	14	3	2	1	0	27	0	0	0	0	0	0	MED
NOS	0	0	0	0	0	-1	0	0	0	0	0	0	1	0	2	2	3	4	0	0	0	0	3	1	0	0	0	0	0	0	0	NOS
AST	0	1	0	2	0	0	0	0	0	1	0	1	0	0	1	0	1	0	0	1	0	0	0	0	1	2	6	0	0	0	0	AST
NOA	1	0	1	0	1	0	1	0	1	0	0	2	0	0	18	0	8	1	0	5	1	1	0	0	9	0	0	0	0	0	0	NOA
EXC	0	0	1	1	1	0	1	2	0	0	1	3	0	0	6	1	6	1	1	1	1	1	0	0	3	1	7	1	0	0	0	EXC
EU	0	0	3	0	1	-1	3	1	1	0	3	7	1	0	23	2	21	3	0	3	2	3	1	0	9	0	0	1	0	1	0	EU
	AL	AM	AT	AZ	BA	BE	BG	BY	CH	CY	CZ	DE	DK	EE	ES	FI	FR	GB	GE	GR	HR	HU	IE	IS	IT	KG	KZ	LT	LU	LV	MD	

Table C.6 Cont.: 2021 country-to-country blame matrices for **SOMO35**.
Units: ppb.d per 15% emis. red. of NO_x. **Emitters →, Receptors ↓.**

	ME	MK	MT	NL	NO	PL	PT	RO	RS	RU	SE	SI	SK	TJ	TM	TR	UA	UZ	ATL	BAS	BLS	MED	NOS	AST	NOA	DMS	VOL	EXC	EU	
AL	7	6	0	0	1	6	1	5	22	3	1	1	2	0	0	2	2	0	3	1	1	36	1	0	16	0	0	223	106	AL
AM	0	0	0	0	0	1	0	1	1	11	0	0	0	0	7	41	3	2	1	0	2	5	0	67	4	0	0	103	14	AM
AT	0	0	0	-1	1	5	1	1	1	3	1	9	1	0	0	0	1	0	4	1	0	6	1	0	3	0	0	175	157	AT
AZ	0	0	0	0	0	1	0	1	1	29	0	0	0	0	16	14	3	4	1	0	2	2	0	35	2	0	0	84	11	AZ
BA	2	0	0	0	1	8	1	4	12	3	1	2	4	0	0	1	2	0	3	1	0	18	1	0	10	0	0	212	132	BA
BE	0	0	0	-17	3	1	1	0	0	3	2	0	0	0	0	0	0	0	6	1	0	2	-13	0	1	0	0	-27	-39	BE
BG	1	3	0	0	1	8	0	32	18	13	1	1	2	0	0	5	14	0	2	1	4	7	1	0	6	0	0	233	166	BG
BY	0	0	0	0	2	19	0	3	1	29	3	0	1	0	0	0	14	0	2	4	0	1	2	0	0	0	0	127	52	BY
CH	0	0	0	-1	1	2	1	0	0	4	1	1	0	0	0	0	1	0	5	1	0	7	1	0	4	0	0	163	116	CH
CY	0	1	0	0	0	3	0	4	3	10	0	0	1	0	0	83	7	0	2	1	3	80	1	9	9	0	0	215	104	CY
CZ	0	0	0	-1	2	12	0	1	2	4	2	2	5	0	0	0	1	0	4	2	0	2	1	0	1	0	0	140	125	CZ
DE	0	0	0	-4	3	5	0	0	0	4	2	0	0	0	0	0	1	0	5	1	0	1	-1	0	1	0	0	69	55	DE
DK	0	0	0	-2	6	6	0	0	0	6	5	0	0	0	0	0	1	0	6	-4	0	0	0	0	0	0	0	39	18	DK
EE	0	0	0	0	3	6	0	0	0	27	6	0	0	0	0	0	4	0	3	9	0	0	2	0	0	0	0	87	45	EE
ES	0	0	0	0	0	0	21	0	0	1	0	0	0	0	0	0	0	0	15	0	0	15	1	0	14	0	0	184	180	ES
FI	0	0	0	0	3	3	0	0	0	15	5	0	0	0	0	0	1	0	3	5	0	0	1	0	0	0	0	51	29	FI
FR	0	0	0	-2	1	1	1	0	0	3	1	0	0	0	0	0	1	0	9	0	0	8	-1	0	4	0	0	134	122	FR
GB	0	0	0	-2	3	0	0	0	0	1	1	0	0	0	0	0	0	0	8	1	0	0	-3	0	0	0	0	2	11	GB
GE	0	0	0	0	0	2	0	3	1	28	0	0	0	0	7	32	7	2	1	1	8	4	1	24	4	0	0	195	21	GE
GL	0	0	0	0	0	0	0	0	0	0	0	0	0	0	0	0	0	0	0	0	0	0	0	0	0	0	0	0	0	GL
GR	1	6	0	0	1	5	1	11	13	8	1	0	1	0	0	10	8	0	2	1	3	38	1	0	15	0	0	217	154	GR
HR	1	0	0	0	1	8	1	4	7	3	1	7	4	0	0	0	2	0	3	1	0	23	1	0	7	0	0	219	179	HR
HU	0	0	0	0	2	16	0	13	9	6	2	3	14	0	0	0	6	0	3	2	0	5	2	0	3	0	0	203	170	HU
IE	0	0	0	-1	2	0	0	0	0	1	0	0	0	0	0	0	0	0	8	0	0	0	0	0	0	0	0	5	-7	IE
IS	0	0	0	0	1	0	0	0	0	1	1	0	0	0	0	0	0	0	3	1	0	0	1	0	0	0	0	13	6	IS
IT	0	0	0	0	1	3	1	1	2	2	1	3	1	0	0	1	1	0	4	1	0	40	1	0	14	0	0	172	155	IT
KG	0	0	0	0	0	1	0	0	0	10	0	0	0	22	7	5	1	61	1	0	0	2	0	63	3	0	0	185	9	KG
KZ	0	0	0	0	1	1	0	1	0	67	1	0	0	0	3	2	3	4	1	1	0	1	0	7	1	0	0	130	12	KZ
LT	0	0	0	0	2	16	0	1	0	18	5	0	1	0	0	0	7	0	3	7	0	0	2	0	0	0	0	102	58	LT
LU	0	0	0	-5	2	2	1	0	0	3	2	0	0	0	0	0	1	0	5	1	0	2	-1	0	2	0	0	24	13	LU
LV	0	0	0	0	3	9	0	1	0	22	6	0	0	0	0	0	5	0	2	8	0	0	2	0	0	0	0	94	52	LV
MD	0	0	0	0	1	14	0	21	2	18	2	0	1	0	0	1	39	0	2	2	2	2	1	0	1	0	0	159	68	MD
ME	38	1	0	0	1	8	1	4	23	3	1	1	3	0	0	1	2	0	3	1	0	28	1	0	14	0	0	208	107	ME
MK	2	30	0	0	1	7	1	10	39	5	1	1	2	0	0	3	4	0	3	1	1	15	1	0	14	0	0	229	115	MK
MT	1	1	-72	1	1	4	1	2	4	2	1	1	1	0	0	2	1	0	5	1	1	-2	1	0	37	0	0	61	41	MT
NL	0	0	0	-74	4	2	0	0	0	3	3	0	0	0	0	0	0	0	5	1	0	1	-22	0	0	0	0	-52	-65	NL
NO	0	0	0	0	12	1	0	0	0	5	4	0	0	0	0	0	0	0	5	2	0	0	4	0	0	0	0	38	15	NO
PL	0	0	0	-1	2	42	0	3	1	8	3	1	4	0	0	0	6	0	3	4	0	1	2	0	1	0	0	123	97	PL
PT	0	0	0	0	0	0	95	0	0	0	0	0	0	0	0	0	0	0	34	0	0	6	1	0	8	0	0	173	169	PT
RO	0	0	0	0	1	13	0	74	8	13	2	1	4	0	0	1	19	0	2	2	2	4	1	0	3	0	0	201	145	RO
RS	3	2	0	0	1	10	1	16	36	6	1	1	5	0	0	1	5	0	3	1	1	9	1	0	7	0	0	187	114	RS
RU	0	0	0	0	1	2	0	1	0	54	1	0	0	0	1	1	3	0	1	1	0	0	0	1	0	0	0	77	10	RU
SE	0	0	0	0	6	3	0	0	0	7	10	0	0	0	0	0	1	0	4	5	0	0	3	0	0	0	0	49	30	SE
SI	0	0	0	0	1	6	1	2	2	3	1	39	2	0	0	0	1	0	3	1	0	17	1	0	6	0	0	212	195	SI
SK	0	0	0	0	2	24	0	9	4	6	2	2	30	0	0	0	6	0	3	2	0	3	2	0	2	0	0	189	162	SK
TJ	0	0	0	0	0	0	0	0	0	7	0	0	0	84	15	4	1	44	1	0	0	1	0	93	3	0	0	177	7	TJ
TM	0	0	0	0	0	1	0	1	0	38	0	0	0	2	59	6	3	35	1	1	1	2	0	36	2	0	0	187	13	TM
TR	0	1	0	0	0	3	0	6	2	16	0	0	1	0	1	89	10	0	2	1	6	15	1	23	8	0	0	170	40	TR
UA	0	0	0	0	2	13	0	8	1	37	2	0	2	0	0	1	40	0	2	2	2	1	1	1	1	0	0	145	49	UA
UZ	0	0	0	0	1	1	0	1	0	43	0	0	0	6	12	5	3	33	1	1	0	1	0	23	2	0	0	148	12	UZ
ATL	0	0	0	0	1	0	2	0	0	2	1	0	0	0	0	0	0	0	20	0	0	1	1	0	1	0	0	21	14	ATL
BAS	0	0	0	-1	5	10	0	1	0	14	13	0	0	0	0	0	2	0	5	-10	0	0	3	0	0	0	0	81	50	BAS
BLS	0	0	0	0	1	9	0	15	3	60	2	0	1	0	1	9	42	0	2	2	37	3	1	2	3	0	0	192	55	BLS
MED	1	1	0	0	1	4	2	4	5	5	1	1	1	0	0	14	4	0	6	1	2	94	1	0	23	0	0	161	122	MED
NOS	0	0	0	-5	7	2	0	0	0	3	3	0	0	0	0	0	0	0	12	1	0	0	-25	0	0	0	0	26	11	NOS
AST	0	0	0	0	0	1	0	1	0	11	0	0	0	3	12	12	1	8	1	0	0	4	0	152	3	0	0	70	9	AST
NOA	0	0	0	0	0	1	4	1	1	1	0	0	0	0	0	3	1	0	8	0	0	28	1	0	125	0	0	63	53	NOA
EXC	0	0	0	0	1	4	1	3	1	37	1	0	1	1	3	5	4	4	3	1	1	3	1	6	2	0	0	108	36	EXC
EU	0	0	0	-1	2	7	5	6	2	6	3	1	2	0	0	1	3	0	6	2	0	9	1	0	5	0	0	128	105	EU
	ME	MK	MT	NL	NO	PL	PT	RO	RS	RU	SE	SI	SK	TJ	TM	TR	UA	UZ	ATL	BAS	BLS	MED	NOS	AST	NOA	DMS	VOL	EXC	EU	

Table C.7: 2021 country-to-country blame matrices for **SOMO35**.
Units: ppb.d per 15% emis. red. of VOC. **Emitters →, Receptors ↓.**

	AL	AM	AT	AZ	BA	BE	BG	BY	CH	CY	CZ	DE	DK	EE	ES	FI	FR	GB	GE	GR	HR	HU	IE	IS	IT	KG	KZ	LT	LU	LV	MD	
AL	15	0	1	0	2	1	1	0	1	0	2	7	1	0	2	0	5	3	0	2	1	2	0	0	13	0	0	0	0	0	0	AL
AM	0	13	0	42	0	0	0	0	0	0	0	2	0	0	1	0	1	1	4	0	0	0	0	0	1	0	1	0	0	0	0	AM
AT	0	0	13	0	0	1	0	0	4	0	4	26	1	0	2	0	11	3	0	0	1	1	0	0	16	0	0	0	0	0	0	AT
AZ	0	1	0	109	0	0	0	1	0	0	0	2	0	0	0	0	1	1	4	0	0	0	0	0	1	0	2	0	0	0	0	AZ
BA	0	0	2	0	15	1	1	0	1	0	3	11	1	0	2	0	6	3	0	0	2	3	0	0	12	0	0	0	0	0	0	BA
BE	0	0	0	0	0	17	0	0	0	0	1	19	1	0	1	0	22	9	0	0	0	0	1	0	1	0	0	0	0	0	0	BE
BG	0	0	1	0	1	1	9	1	0	0	2	7	1	0	1	0	4	2	0	2	1	2	0	0	4	0	0	0	0	0	1	BG
BY	0	0	0	0	0	0	0	4	0	0	1	5	1	0	0	0	3	2	0	0	0	1	0	0	1	0	0	0	0	0	0	BY
CH	0	0	2	0	0	1	0	0	25	0	1	24	1	0	2	0	19	3	0	0	0	0	0	0	23	0	0	0	0	0	0	CH
CY	0	0	1	1	1	0	1	1	0	4	1	5	0	0	1	0	3	2	0	3	0	1	0	0	5	0	0	0	0	0	0	CY
CZ	0	0	3	0	0	2	0	0	1	0	21	26	1	0	1	0	10	3	0	0	1	2	0	0	4	0	0	0	0	0	0	CZ
DE	0	0	2	0	0	3	0	0	2	0	3	41	1	0	1	0	14	6	0	0	0	0	1	0	2	0	0	0	0	0	0	DE
DK	0	0	0	0	0	2	0	0	0	0	1	10	7	0	0	0	6	8	0	0	0	0	1	0	0	0	0	0	0	0	0	DK
EE	0	0	0	0	0	1	0	1	0	0	0	4	1	1	0	1	3	3	0	0	0	0	0	0	0	0	0	0	0	0	0	EE
ES	0	0	0	0	0	1	0	0	0	0	0	4	0	0	26	0	9	3	0	0	0	0	0	0	3	0	0	0	0	0	0	ES
FI	0	0	0	0	0	0	0	0	0	0	0	2	0	0	0	1	1	1	0	0	0	0	0	0	0	0	0	0	0	0	0	FI
FR	0	0	0	0	0	2	0	0	1	0	1	12	1	0	4	0	30	7	0	0	0	0	1	0	6	0	0	0	0	0	0	FR
GB	0	0	0	0	0	1	0	0	0	0	0	5	0	0	0	0	4	22	0	0	0	0	1	0	0	0	0	0	0	0	0	GB
GE	0	1	0	30	0	0	0	1	0	0	1	3	0	0	1	0	2	1	12	0	0	0	0	0	1	0	1	0	0	0	0	GE
GL	0	0	0	0	0	0	0	0	0	0	0	0	0	0	0	0	0	0	0	0	0	0	0	0	0	0	0	0	0	0	0	GL
GR	1	0	1	0	1	1	2	1	0	0	2	6	1	0	2	0	5	3	0	15	1	1	0	0	8	0	0	0	0	0	0	GR
HR	0	0	4	0	5	1	1	0	1	0	4	14	1	0	2	0	8	3	0	0	7	3	0	0	18	0	0	0	0	0	0	HR
HU	0	0	4	0	1	1	0	0	1	0	6	15	1	0	1	0	7	3	0	0	2	11	0	0	7	0	0	0	0	0	0	HU
IE	0	0	0	0	0	1	0	0	0	0	0	3	0	0	0	0	3	11	0	0	0	0	3	0	0	0	0	0	0	0	0	IE
IS	0	0	0	0	0	0	0	0	0	0	0	1	0	0	0	0	1	3	0	0	0	0	0	0	0	0	0	0	0	0	0	IS
IT	0	0	3	0	1	1	0	0	2	0	2	11	1	0	4	0	12	3	0	1	2	1	0	0	78	0	0	0	0	0	0	IT
KG	0	0	0	2	0	0	0	0	0	0	0	1	0	0	0	0	1	1	0	0	0	0	0	0	1	9	7	0	0	0	0	KG
KZ	0	0	0	2	0	0	0	0	0	0	0	2	0	0	0	0	1	1	0	0	0	0	0	0	1	0	8	0	0	0	0	KZ
LT	0	0	0	0	0	1	0	1	0	0	1	6	1	0	0	0	3	3	0	0	0	0	0	0	1	0	0	1	0	0	0	LT
LU	0	0	0	0	0	5	0	0	1	0	1	24	1	0	1	0	20	6	0	0	0	0	0	0	2	0	0	0	4	0	0	LU
LV	0	0	0	0	0	1	0	1	0	0	1	5	1	0	0	0	3	2	0	0	0	0	0	0	0	0	0	1	0	1	0	LV
MD	0	0	0	0	0	1	1	1	0	0	2	6	1	0	1	0	3	3	0	0	0	1	0	0	2	0	0	0	0	0	6	MD
ME	2	0	1	0	4	1	1	0	1	0	2	7	0	0	2	0	5	2	0	1	1	2	0	0	11	0	0	0	0	0	0	ME
MK	3	0	1	0	2	1	2	0	0	0	2	6	1	0	2	0	4	2	0	5	1	2	0	0	7	0	0	0	0	0	0	MK
MT	1	0	1	0	1	1	1	0	1	0	2	8	1	0	5	0	12	4	0	2	1	1	0	0	31	0	0	0	0	0	0	MT
NL	0	0	0	0	0	7	0	0	0	0	0	19	1	0	1	0	11	10	0	0	0	0	1	0	0	0	0	0	0	0	0	NL
NO	0	0	0	0	0	0	0	0	0	0	0	2	0	0	0	0	2	3	0	0	0	0	0	0	0	0	0	0	0	0	0	NO
PL	0	0	1	0	0	1	0	1	0	0	5	14	1	0	0	0	5	4	0	0	0	1	0	0	2	0	0	0	0	0	0	PL
PT	0	0	0	0	0	1	0	0	0	0	0	3	0	0	12	0	6	3	0	0	0	0	0	0	1	0	0	0	0	0	0	PT
RO	0	0	1	0	1	1	2	1	0	0	3	7	1	0	1	0	4	2	0	0	0	2	0	0	4	0	0	0	0	0	1	RO
RS	1	0	2	0	3	1	2	0	1	0	3	10	1	0	1	0	5	3	0	1	1	4	0	0	7	0	0	0	0	0	0	RS
RU	0	0	0	1	0	0	0	0	0	0	0	1	0	0	0	0	1	1	0	0	0	0	0	0	0	0	1	0	0	0	0	RU
SE	0	0	0	0	0	1	0	0	0	0	0	3	1	0	0	0	2	3	0	0	0	0	0	0	0	0	0	0	0	0	0	SE
SI	0	0	7	0	1	1	0	0	2	0	4	17	1	0	2	0	9	3	0	0	5	2	0	0	34	0	0	0	0	0	0	SI
SK	0	0	3	0	1	1	0	0	1	0	8	15	1	0	1	0	7	3	0	0	1	6	0	0	6	0	0	0	0	0	0	SK
TJ	0	0	0	2	0	0	0	0	0	0	0	1	0	0	0	0	1	0	0	0	0	0	0	0	1	1	4	0	0	0	0	TJ
TM	0	0	0	10	0	0	0	1	0	0	0	2	0	0	1	0	2	1	1	0	0	0	0	0	1	0	5	0	0	0	0	TM
TR	0	0	0	3	0	0	1	1	0	0	1	4	0	0	1	0	2	1	0	1	0	1	0	0	3	0	0	0	0	0	0	TR
UA	0	0	0	1	0	0	0	2	0	0	2	5	1	0	0	0	3	2	0	0	0	1	0	0	2	0	0	0	0	0	1	UA
UZ	0	0	0	4	0	0	0	0	0	0	0	2	0	0	1	0	1	1	0	0	0	0	0	0	1	2	7	0	0	0	0	UZ
ATL	0	0	0	0	0	0	0	0	0	0	0	2	0	0	1	0	3	3	0	0	0	0	0	0	0	0	0	0	0	0	0	ATL
BAS	0	0	0	0	0	1	0	1	0	0	1	8	3	0	0	1	4	6	0	0	0	0	1	0	0	0	0	0	0	0	0	BAS
BLS	0	0	1	3	0	1	2	2	0	0	2	6	1	0	1	0	3	2	2	1	0	1	0	0	2	0	0	0	0	0	1	BLS
MED	1	0	2	0	1	1	1	0	1	0	2	9	1	0	7	0	14	4	0	4	1	1	0	0	24	0	0	0	0	0	0	MED
NOS	0	0	0	0	0	2	0	0	0	0	0	9	2	0	1	0	7	18	0	0	0	0	1	0	0	0	0	0	0	0	0	NOS
AST	0	0	0	5	0	0	0	0	0	0	0	1	0	0	0	0	1	1	0	0	0	0	0	0	1	0	2	0	0	0	0	AST
NOA	0	0	0	0	0	0	0	0	0	0	1	3	0	0	4	0	5	2	0	1	0	0	0	0	6	0	0	0	0	0	0	NOA
EXC	0	0	0	2	0	0	0	0	0	0	1	4	0	0	1	0	3	2	0	0	0	0	0	0	3	0	2	0	0	0	0	EXC
EU	0	0	1	0	0	1	0	0	1	0	2	11	1	0	5	0	10	4	0	1	1	1	0	0	9	0	0	0	0	0	0	EU
	AL	AM	AT	AZ	BA	BE	BG	BY	CH	CY	CZ	DE	DK	EE	ES	FI	FR	GB	GE	GR	HR	HU	IE	IS	IT	KG	KZ	LT	LU	LV	MD	

Table C.7 Cont.: 2021 country-to-country blame matrices for **SOMO35**.
Units: ppb.d per 15% emis. red. of VOC. **Emitters →, Receptors ↓.**

	ME	MK	MT	NL	NO	PL	PT	RO	RS	RU	SE	SI	SK	TJ	TM	TR	UA	UZ	ATL	BAS	BLS	MED	NOS	AST	NOA	DMS	VOL	EXC	EU	
AL	2	1	0	1	0	5	0	2	6	3	0	0	1	0	0	1	1	0	0	0	0	0	0	0	4	0	0	83	48	AL
AM	0	0	0	0	0	2	0	1	0	8	0	0	0	0	1	6	1	1	0	0	0	0	0	30	1	0	0	91	12	AM
AT	0	0	0	2	0	4	0	0	1	2	1	2	1	0	0	0	0	0	0	0	0	0	0	0	1	0	0	98	87	AT
AZ	0	0	0	0	0	2	0	1	0	17	0	0	0	0	2	2	2	1	0	0	0	0	0	19	1	0	0	154	11	AZ
BA	1	0	0	2	0	7	0	1	4	2	1	0	2	0	0	0	1	0	0	0	0	0	0	0	3	0	0	85	57	BA
BE	0	0	0	15	1	1	0	0	0	2	1	0	0	0	0	0	0	0	0	0	0	0	0	0	0	0	0	93	80	BE
BG	0	0	0	1	0	7	0	6	3	6	0	0	1	0	0	1	3	0	0	0	0	0	0	0	2	0	0	70	50	BG
BY	0	0	0	1	0	8	0	1	0	8	0	0	1	0	0	0	2	0	0	0	0	0	0	0	0	0	0	43	25	BY
CH	0	0	0	2	0	2	0	0	0	2	0	0	0	0	0	0	0	0	0	0	0	0	0	0	1	0	0	114	81	CH
CY	0	0	0	1	0	4	0	2	2	8	0	0	1	0	0	16	3	0	0	0	0	0	0	13	4	0	0	72	36	CY
CZ	0	0	0	3	1	12	0	1	1	2	1	1	2	0	0	0	1	0	0	0	0	0	0	0	0	0	0	101	92	CZ
DE	0	0	0	7	1	3	0	0	0	2	1	0	0	0	0	0	0	0	0	0	0	0	0	0	0	0	0	92	81	DE
DK	0	0	0	6	2	4	0	0	0	2	2	0	0	0	0	0	0	0	0	0	0	0	0	0	0	0	0	52	39	DK
EE	0	0	0	2	1	2	0	0	0	7	1	0	0	0	0	0	1	0	0	0	0	0	0	0	0	0	0	29	17	EE
ES	0	0	0	1	0	1	3	0	0	1	0	0	0	0	0	0	0	0	0	0	0	0	0	0	4	0	0	54	49	ES
FI	0	0	0	1	0	1	0	0	0	3	0	0	0	0	0	0	0	0	0	0	0	0	0	0	0	0	0	13	7	FI
FR	0	0	0	4	1	1	0	0	0	2	0	0	0	0	0	0	0	0	0	0	0	0	0	0	1	0	0	75	64	FR
GB	0	0	0	3	1	0	0	0	0	1	0	0	0	0	0	0	0	0	0	0	0	0	0	0	0	0	0	40	17	GB
GE	0	0	0	1	0	3	0	1	0	13	0	0	0	0	1	4	2	0	0	0	0	0	0	11	1	0	0	82	14	GE
GL	0	0	0	0	0	0	0	0	0	0	0	0	0	0	0	0	0	0	0	0	0	0	0	0	0	0	0	0	0	GL
GR	0	1	0	1	0	5	0	3	3	5	0	0	1	0	0	3	2	0	0	0	0	0	0	0	4	0	0	77	56	GR
HR	0	0	0	2	0	7	0	1	3	2	1	2	2	0	0	0	1	0	0	0	0	0	0	0	2	0	0	94	78	HR
HU	0	0	0	2	1	14	0	4	3	3	1	1	5	0	0	0	1	0	0	0	0	0	0	0	1	0	0	98	83	HU
IE	0	0	0	3	0	0	0	0	0	1	0	0	0	0	0	0	0	0	0	0	0	0	0	0	0	0	0	27	15	IE
IS	0	0	0	1	0	0	0	0	0	1	0	0	0	0	0	0	0	0	0	0	0	0	0	0	0	0	0	8	4	IS
IT	0	0	0	2	0	4	0	1	1	2	0	2	1	0	0	0	1	0	0	0	0	0	0	0	4	0	0	136	124	IT
KG	0	0	0	0	0	1	0	0	0	5	0	0	0	10	1	1	0	49	0	0	0	0	0	15	1	0	0	91	6	KG
KZ	0	0	0	0	0	1	0	0	0	14	0	0	0	1	1	0	1	4	0	0	0	0	0	5	0	0	0	42	8	KZ
LT	0	0	0	1	0	8	0	0	0	6	1	0	0	0	0	0	1	0	0	0	0	0	0	0	0	0	0	38	26	LT
LU	0	0	0	7	1	2	0	0	0	2	1	0	0	0	0	0	0	0	0	0	0	0	0	0	1	0	0	78	69	LU
LV	0	0	0	1	0	5	0	0	0	5	1	0	0	0	0	0	1	0	0	0	0	0	0	0	0	0	0	31	20	LV
MD	0	0	0	1	0	10	0	6	1	8	1	0	1	0	0	1	6	0	0	0	0	0	0	0	1	0	0	66	38	MD
ME	10	0	0	1	0	6	0	1	5	3	0	0	1	0	0	0	1	0	0	0	0	0	0	0	4	0	0	76	47	ME
MK	0	6	0	1	0	6	0	2	8	3	0	0	1	0	0	1	1	0	0	0	0	0	0	0	3	0	0	73	45	MK
MT	0	0	9	2	0	4	1	1	1	3	1	1	1	0	0	1	1	0	0	0	0	2	0	0	12	0	0	99	85	MT
NL	0	0	0	26	1	2	0	0	0	1	1	0	0	0	0	0	0	0	0	0	0	0	0	0	0	0	0	84	70	NL
NO	0	0	0	1	2	1	0	0	0	1	0	0	0	0	0	0	0	0	0	0	0	0	0	0	0	0	0	14	8	NO
PL	0	0	0	3	1	31	0	1	1	3	1	0	2	0	0	0	1	0	0	0	0	0	0	0	0	0	0	83	71	PL
PT	0	0	0	1	0	0	20	0	0	0	0	0	0	0	0	0	0	0	0	0	0	0	0	0	3	0	0	50	46	PT
RO	0	0	0	1	0	10	0	16	2	6	1	0	2	0	0	0	3	0	0	0	0	0	0	0	1	0	0	75	56	RO
RS	1	1	0	2	0	9	0	4	17	3	1	0	2	0	0	0	1	0	0	0	0	0	0	0	2	0	0	88	56	RS
RU	0	0	0	0	0	1	0	0	0	14	0	0	0	0	0	0	1	0	0	0	0	0	0	1	0	0	0	23	5	RU
SE	0	0	0	1	1	2	0	0	0	2	1	0	0	0	0	0	0	0	0	0	0	0	0	0	0	0	0	18	12	SE
SI	0	0	0	2	0	5	0	1	1	2	1	10	1	0	0	0	1	0	0	0	0	0	0	0	2	0	0	113	101	SI
SK	0	0	0	2	1	23	0	3	2	3	1	1	10	0	0	0	1	0	0	0	0	0	0	0	1	0	0	103	90	SK
TJ	0	0	0	0	0	1	0	0	0	4	0	0	0	64	2	1	0	28	0	0	0	0	0	14	1	0	0	113	5	TJ
TM	0	0	0	1	0	2	0	1	0	16	0	0	0	3	17	1	1	15	0	0	0	0	0	23	1	0	0	84	13	TM
TR	0	0	0	1	0	4	0	2	1	8	0	0	0	0	0	17	3	0	0	0	0	0	0	12	2	0	0	58	22	TR
UA	0	0	0	1	0	9	0	2	0	16	1	0	1	0	0	1	9	0	0	0	0	0	0	0	0	0	0	62	29	UA
UZ	0	0	0	0	0	2	0	0	0	14	0	0	0	7	3	1	1	46	0	0	0	0	0	10	1	0	0	97	10	UZ
ATL	0	0	0	1	0	0	1	0	0	1	0	0	0	0	0	0	0	0	0	0	0	0	0	0	1	0	0	15	10	ATL
BAS	0	0	0	3	1	7	0	0	0	7	3	0	0	0	0	0	1	0	0	0	0	0	0	0	0	0	0	51	35	BAS
BLS	0	0	0	1	1	8	0	5	1	28	1	0	1	0	0	8	9	0	0	0	0	0	0	2	1	0	0	95	37	BLS
MED	0	0	0	2	0	5	1	2	2	4	0	1	1	0	0	5	2	0	0	0	0	1	0	4	14	0	0	101	79	MED
NOS	0	0	0	6	2	1	0	0	0	1	1	0	0	0	0	0	0	0	0	0	0	0	1	0	0	0	0	54	32	NOS
AST	0	0	0	0	0	1	0	0	0	6	0	0	0	1	2	2	1	3	0	0	0	0	0	83	1	0	0	31	7	AST
NOA	0	0	0	1	0	1	1	1	1	1	0	0	0	0	0	1	0	0	0	0	0	0	0	1	26	0	0	34	27	NOA
EXC	0	0	0	1	0	3	0	1	0	10	0	0	0	1	1	1	1	3	0	0	0	0	0	3	1	0	0	45	20	EXC
EU	0	0	0	3	0	6	1	2	1	3	1	0	1	0	0	0	1	0	0	0	0	0	0	0	1	0	0	67	56	EU
	ME	MK	MT	NL	NO	PL	PT	RO	RS	RU	SE	SI	SK	TJ	TM	TR	UA	UZ	ATL	BAS	BLS	MED	NOS	AST	NOA	DMS	VOL	EXC	EU	

Table C.8: 2021 country-to-country blame matrices for $\mathbf{MDA8}_{\mathrm{AS}}$.
Units: ng/m^3 per 15% emis. red. of NO_x. **Emitters →, Receptors ↓.**

	AL	AM	AT	AZ	BA	BE	BG	BY	CH	CY	CZ	DE	DK	EE	ES	FI	FR	GB	GE	GR	HR	HU	IE	IS	IT	KG	KZ	LT	LU	LV	MD	
AL	569	0	25	0	60	2	26	6	7	0	18	42	2	1	79	3	72	13	0	61	40	44	3	0	290	0	0	2	0	1	1	AL
AM	1	50	2	443	1	0	4	3	1	2	2	6	0	0	10	1	7	2	74	8	1	2	1	0	8	0	16	1	0	1	1	AM
AT	0	0	425	0	7	2	3	6	70	0	87	356	5	2	56	7	192	21	0	1	38	38	7	1	244	0	1	3	2	2	0	AT
AZ	1	25	2	274	1	0	4	5	1	1	2	7	1	1	9	3	8	3	51	5	1	2	1	0	7	0	52	1	0	1	1	AZ
BA	8	0	76	0	487	2	16	7	11	0	46	91	3	1	83	5	97	17	0	6	175	119	4	1	272	0	0	3	1	2	1	BA
BE	0	0	3	0	0	-624	0	3	4	0	6	-85	13	1	38	11	340	71	0	0	0	1	25	4	5	0	1	2	10	2	0	BE
BG	17	0	24	1	24	2	664	20	4	0	25	50	4	2	33	6	36	12	1	82	15	48	3	1	62	0	1	5	0	3	15	BG
BY	0	0	9	1	3	2	3	294	2	0	22	69	10	9	8	24	34	25	0	1	4	18	5	2	11	0	5	48	1	25	6	BY
CH	0	0	31	0	2	-1	1	4	441	0	11	197	3	1	86	4	502	29	0	1	6	3	7	1	260	0	1	2	1	1	0	CH
CY	7	1	6	5	6	1	30	9	2	396	5	17	1	1	34	2	26	6	4	185	4	8	2	0	44	0	2	2	0	1	4	CY
CZ	0	0	120	0	9	2	2	7	18	0	320	368	8	2	26	9	171	29	0	0	22	56	9	2	50	0	1	7	3	4	0	CZ
DE	0	0	35	0	1	-13	0	5	27	0	48	222	13	2	32	12	253	52	0	0	2	5	14	3	20	0	1	5	6	4	0	DE
DK	0	0	3	0	0	-3	0	8	1	0	11	79	-91	6	13	24	60	116	0	0	1	3	17	6	2	0	1	8	1	7	0	DK
EE	0	0	2	1	0	1	0	62	1	0	5	54	21	80	4	89	28	35	0	0	1	5	9	4	2	0	3	37	1	66	1	EE
ES	0	0	2	0	1	2	0	1	2	0	1	14	1	0	1136	1	134	21	0	0	1	1	6	1	15	0	0	0	0	0	0	ES
FI	0	0	1	1	0	1	0	17	0	0	4	32	11	14	3	204	19	26	0	0	0	2	8	7	2	0	2	8	0	10	1	FI
FR	0	0	6	0	1	-6	1	3	20	0	4	75	4	1	145	6	954	66	0	1	3	2	22	2	50	0	1	2	3	1	0	FR
GB	0	0	1	0	0	-4	0	1	1	0	2	22	9	1	8	8	51	-89	0	0	0	0	77	8	1	0	0	1	1	1	0	GB
GE	2	37	3	368	2	1	10	10	1	1	3	12	1	1	11	3	12	4	507	10	2	4	1	0	13	0	17	2	0	1	4	GE
GL	0	0	0	0	0	0	0	0	0	0	0	1	0	0	0	0	0	2	0	0	0	0	1	2	0	0	0	0	0	0	0	GL
GR	67	0	18	1	24	2	169	10	4	0	15	38	2	1	54	4	49	12	1	596	16	28	3	0	149	0	1	3	0	2	7	GR
HR	6	0	144	0	168	2	12	7	14	0	65	133	3	1	77	6	131	20	0	5	447	154	5	1	329	0	1	4	1	2	1	HR
HU	2	0	135	0	40	2	13	15	12	0	99	157	7	2	38	7	99	22	0	2	97	497	7	2	123	0	1	6	1	4	2	HU
IE	0	0	0	0	0	-2	0	1	1	0	1	13	4	1	9	5	62	173	0	0	0	0	21	8	2	0	1	1	1	1	0	IE
IS	0	0	0	0	0	1	0	1	0	0	1	12	6	0	2	7	20	44	0	0	0	0	16	74	1	0	0	1	0	1	0	IS
IT	3	0	68	0	25	3	6	3	30	0	22	79	2	1	126	4	247	19	0	7	48	19	5	1	774	0	1	2	1	1	0	IT
KG	0	3	2	10	1	0	1	1	1	0	1	5	0	0	11	1	8	1	2	2	1	1	0	0	7	333	159	0	0	0	0	KG
KZ	1	2	3	10	1	1	2	8	1	0	3	11	1	1	11	9	12	7	3	2	1	3	2	1	9	12	285	2	0	2	1	KZ
LT	0	0	5	1	1	1	1	135	2	0	17	90	18	12	6	30	38	34	0	0	2	10	8	2	6	0	2	156	1	57	2	LT
LU	0	0	7	0	0	-33	0	4	7	0	9	27	8	1	42	10	549	60	0	0	1	1	17	2	12	0	1	3	-293	2	0	LU
LV	0	0	3	1	1	3	1	104	1	0	9	75	18	31	5	51	34	33	0	0	1	7	8	3	4	0	3	83	1	113	2	LV
MD	2	0	10	2	8	2	30	63	2	0	23	56	7	3	17	9	31	19	1	5	7	27	4	1	28	0	3	13	1	7	191	MD
ME	68	0	34	0	140	2	24	6	8	0	21	51	2	1	80	4	80	14	0	15	60	65	3	1	272	0	0	2	0	2	1	ME
MK	176	0	23	1	36	2	88	8	6	0	17	41	2	1	70	4	48	11	1	224	21	49	3	0	160	0	1	2	0	2	2	MK
MT	11	0	24	0	27	4	16	3	8	0	15	45	2	1	122	3	199	23	0	35	20	14	7	1	369	0	1	1	1	1	1	MT
NL	0	0	1	0	0	-92	0	3	2	0	4	-69	24	1	21	13	136	78	0	0	0	1	29	4	2	0	1	3	2	2	0	NL
NO	0	0	1	0	0	3	0	7	0	0	3	24	13	3	4	33	20	61	0	0	0	1	13	9	1	0	1	5	0	4	0	NO
PL	0	0	21	0	6	-1	3	36	5	0	86	182	19	3	13	14	74	43	0	0	10	39	8	2	21	0	1	19	2	10	2	PL
PT	0	0	1	0	0	1	0	1	1	0	0	9	1	0	442	1	62	23	0	0	0	0	7	2	4	0	0	0	0	0	0	PT
RO	5	0	24	1	24	2	77	30	4	0	37	61	6	2	28	7	43	16	0	7	17	92	4	1	58	0	1	8	1	5	24	RO
RS	42	0	51	0	88	2	75	11	8	0	45	76	5	1	52	5	61	16	0	15	53	144	4	1	137	0	1	3	1	3	2	RS
RU	0	1	2	8	1	1	2	19	1	0	3	15	3	4	4	25	10	12	2	1	1	2	3	2	4	0	38	6	0	5	1	RU
SE	0	0	2	0	0	3	0	13	1	0	5	46	22	8	6	63	30	53	0	0	1	3	11	7	2	0	1	10	1	10	0	SE
SI	1	0	269	0	26	2	6	5	19	0	60	164	3	1	71	6	144	19	0	2	236	61	5	1	478	0	1	3	1	2	1	SI
SK	1	0	105	0	22	3	8	15	12	0	161	165	8	2	29	8	93	23	0	1	44	271	6	2	80	0	1	8	1	4	2	SK
TJ	0	2	2	9	1	0	1	1	1	0	1	4	0	0	9	1	6	1	2	2	1	1	0	0	6	30	61	0	0	0	0	TJ
TM	1	8	3	49	1	1	2	5	1	0	3	10	1	1	13	5	12	3	8	3	1	3	1	0	10	5	149	1	0	1	1	TM
TR	4	9	5	26	5	1	34	13	2	6	6	17	1	1	26	2	18	5	15	45	3	8	1	0	28	0	3	3	0	2	7	TR
UA	1	0	10	4	6	2	15	76	2	0	21	48	6	3	13	12	28	18	2	5	6	25	4	1	20	0	7	15	1	8	24	UA
UZ	1	5	3	21	1	1	2	5	1	0	3	10	1	1	13	5	12	4	5	3	1	3	1	0	10	20	217	1	0	1	1	UZ
ATL	0	0	0	0	0	0	0	1	0	0	0	7	3	1	26	7	47	48	0	0	0	0	21	11	1	0	1	1	0	1	0	ATL
BAS	0	0	3	0	1	2	0	26	1	0	10	96	27	20	6	80	43	61	0	0	1	6	12	5	3	0	1	24	1	27	1	BAS
BLS	3	2	8	15	6	2	68	48	2	0	14	37	5	2	13	9	21	11	32	19	5	16	3	1	21	0	5	9	0	5	31	BLS
MED	14	0	26	1	27	4	42	6	8	3	15	48	2	1	151	3	223	20	1	110	29	18	5	1	251	0	1	2	1	1	4	MED
NOS	0	0	1	0	0	-8	0	3	0	0	4	20	20	2	7	20	48	142	0	0	0	1	39	13	1	0	0	3	1	3	0	NOS
AST	1	2	2	21	1	0	3	2	1	4	1	4	0	0	9	1	6	1	3	8	1	1	0	0	7	13	52	0	0	0	1	AST
NOA	4	0	6	0	6	1	11	2	3	0	3	13	1	0	116	1	47	5	0	38	4	4	1	0	66	0	0	0	0	0	1	NOA
EXC	3	2	10	11	5	-1	10	19	4	0	10	33	4	3	49	20	61	16	5	9	6	11	6	3	30	6	69	6	0	5	3	EXC
EU	3	0	32	0	9	-6	30	15	11	1	31	90	8	5	190	31	220	39	0	23	18	32	10	3	95	0	1	10	1	8	3	EU
	AL	AM	AT	AZ	BA	BE	BG	BY	CH	CY	CZ	DE	DK	EE	ES	FI	FR	GB	GE	GR	HR	HU	IE	IS	IT	KG	KZ	LT	LU	LV	MD	

Table C.8 Cont.: 2021 country-to-country blame matrices for **MDA8**$_{\rm AS}$.
Units: ng/m^3 per 15% emis. red. of NO$_x$. **Emitters** →, **Receptors** ↓.

	ME	MK	MT	NL	NO	PL	PT	RO	RS	RU	SE	SI	SK	TJ	TM	TR	UA	UZ	ATL	BAS	BLS	MED	NOS	AST	NOA	DMS	VOL	EXC	EU	
AL	54	38	1	3	5	47	7	37	219	25	5	5	17	0	0	9	16	0	18	7	2	272	9	1	98	0	0	1857	834	AL
AM	0	1	0	1	1	7	1	8	3	72	1	0	1	0	56	215	17	12	3	2	9	17	2	490	21	0	0	1044	74	AM
AT	0	0	0	-5	12	54	6	7	8	33	12	93	14	0	0	1	8	0	29	13	0	49	11	1	20	0	0	1818	1650	AT
AZ	0	1	0	1	3	9	1	9	3	240	3	0	1	0	145	80	25	34	4	3	10	10	2	307	13	0	0	1024	80	AZ
BA	11	1	0	2	9	75	8	38	112	32	10	15	32	0	0	3	16	0	22	11	1	134	12	1	65	0	0	1898	1182	BA
BE	0	0	0	-252	39	13	6	1	0	38	26	0	1	0	0	1	5	0	86	11	0	10	-204	0	4	0	0	-291	-457	BE
BG	6	24	0	2	8	71	3	295	163	118	9	5	23	0	0	54	131	0	15	13	39	44	10	1	39	0	0	2073	1470	BG
BY	0	0	0	2	26	219	1	29	7	367	39	2	14	0	1	4	158	1	25	53	3	5	20	2	3	0	0	1512	608	BY
CH	0	0	0	-5	8	17	10	3	3	34	7	5	2	0	0	2	6	0	38	7	1	48	10	1	21	0	0	1689	1157	CH
CY	2	7	0	1	2	22	3	32	25	83	3	1	4	0	1	581	60	0	8	4	21	567	4	18	51	0	0	1638	832	CY
CZ	0	0	0	-7	19	151	3	10	13	45	20	17	54	0	0	1	11	0	33	21	0	15	15	1	8	0	0	1582	1426	CZ
DE	0	0	0	-53	33	57	4	1	1	48	26	3	4	0	0	1	6	0	53	12	0	11	-11	0	7	0	0	879	702	DE
DK	0	0	0	-26	97	79	3	3	1	79	70	0	2	0	0	0	9	0	72	-40	0	2	48	0	2	0	0	593	273	DK
EE	0	0	0	0	50	66	1	5	1	367	93	1	3	0	1	1	36	0	42	144	1	1	32	1	1	0	0	1137	574	EE
ES	0	0	0	1	3	3	192	1	1	7	1	1	0	0	0	1	2	0	136	1	0	135	10	1	95	0	0	1554	1513	ES
FI	0	0	0	2	59	40	1	3	1	257	86	0	2	0	1	1	16	0	63	77	0	1	24	1	1	0	0	841	453	FI
FR	0	0	0	-14	15	11	13	2	1	32	10	2	1	0	0	1	5	0	120	6	0	67	-3	1	20	0	0	1447	1298	FR
GB	0	0	0	-17	43	6	2	0	0	19	14	0	0	0	0	0	1	0	144	9	0	1	-15	0	2	0	0	169	184	GB
GE	1	2	0	1	3	17	1	20	7	209	3	1	2	0	61	173	54	13	6	4	65	16	3	172	20	0	0	1611	136	GE
GL	0	0	0	0	1	0	0	0	0	1	0	0	0	0	0	0	0	0	3	0	0	0	1	0	0	0	0	9	3	GL
GR	8	46	1	3	5	44	5	87	110	68	5	3	12	0	0	96	62	0	15	8	18	277	9	1	90	0	0	1831	1309	GR
HR	4	1	0	1	10	81	7	32	68	34	12	67	35	0	0	2	16	0	26	12	1	198	13	1	44	0	0	2107	1754	HR
HU	1	1	0	-2	16	180	4	116	86	56	17	35	147	0	0	3	55	0	25	20	2	47	16	1	25	0	0	2105	1791	HU
IE	0	0	0	-10	28	3	1	0	0	16	8	0	0	0	0	0	1	0	161	5	0	2	23	0	2	0	0	353	122	IE
IS	0	0	0	2	23	5	1	0	0	15	13	0	0	0	0	0	2	0	77	9	0	1	19	0	0	0	0	251	90	IS
IT	2	1	1	3	6	30	10	10	17	22	7	32	7	0	0	2	6	0	32	7	1	338	12	1	91	0	0	1652	1512	IT
KG	0	0	0	0	1	4	1	2	1	67	1	0	1	126	38	23	5	556	3	1	1	5	1	214	14	0	0	1379	52	KG
KZ	0	0	0	1	8	12	2	6	3	593	7	1	2	2	19	17	23	31	12	6	2	6	4	57	8	0	0	1134	105	KZ
LT	0	0	0	-1	37	202	1	10	3	247	75	1	8	0	1	2	70	0	35	113	1	3	31	1	1	0	0	1295	753	LT
LU	0	0	0	-82	27	17	6	1	0	39	21	0	1	0	0	1	6	0	66	11	0	16	-14	0	7	0	0	476	329	LU
LV	0	0	0	2	45	115	1	7	2	327	91	1	4	0	1	1	51	0	37	143	1	2	35	1	1	0	0	1242	669	LV
MD	1	2	0	3	15	152	2	209	21	209	16	2	15	0	1	16	441	1	18	21	23	15	15	2	11	0	0	1677	680	MD
ME	296	6	0	3	6	60	7	32	204	30	7	7	24	0	0	6	17	0	19	8	2	212	10	1	83	0	0	1666	861	ME
MK	15	273	0	2	5	54	6	75	377	44	6	5	21	0	0	25	33	0	16	8	5	99	8	1	91	0	0	1938	925	MK
MT	5	4	-423	6	6	32	9	13	27	17	5	8	8	0	0	8	8	0	30	6	2	17	14	1	206	0	0	688	537	MT
NL	0	0	0	-1016	55	24	4	1	0	49	34	0	1	0	0	0	5	0	85	14	0	5	-349	0	2	0	0	-675	-874	NL
NO	0	0	0	3	178	20	1	1	0	84	51	0	1	0	0	0	5	0	93	27	0	1	61	0	1	0	0	552	205	NO
PL	0	0	0	-5	29	526	2	27	12	106	39	5	41	0	0	2	60	0	33	57	1	8	25	1	4	0	0	1463	1158	PL
PT	0	0	0	1	3	1	878	1	0	3	1	0	0	0	0	0	1	0	346	0	0	43	8	0	54	0	0	1445	1411	PT
RO	4	3	0	2	12	133	3	741	83	120	15	5	41	0	1	12	188	0	18	18	16	27	14	1	23	0	0	1946	1418	RO
RS	24	18	0	1	9	95	5	147	454	55	10	10	44	0	0	5	43	0	19	14	4	63	12	1	52	0	0	1826	1047	RS
RU	0	0	0	1	19	21	1	5	2	789	15	0	2	0	5	7	31	3	31	17	4	3	8	10	3	0	0	1079	137	RU
SE	0	0	0	3	108	43	1	2	1	115	154	0	2	0	0	0	11	0	71	71	0	1	50	0	1	0	0	739	427	SE
SI	1	0	0	1	9	59	7	12	18	29	12	406	16	0	0	1	9	0	26	12	1	165	12	1	34	0	0	2166	2025	SI
SK	1	1	0	0	17	291	3	76	44	57	19	21	313	0	0	2	55	0	23	23	1	26	17	1	13	0	0	1974	1718	SK
TJ	0	0	0	0	1	2	1	2	1	43	1	0	1	594	92	23	3	416	2	0	1	5	0	322	16	0	0	1323	41	TJ
TM	0	1	0	1	3	9	2	6	3	287	4	1	2	9	537	43	17	292	7	4	3	8	2	207	16	0	0	1519	96	TM
TR	1	3	0	1	3	27	3	46	17	125	3	1	4	0	4	629	80	1	8	5	44	86	4	139	48	0	0	1245	294	TR
UA	1	1	0	2	17	148	1	84	14	404	22	2	16	0	3	15	443	2	18	26	24	12	14	5	8	0	0	1558	514	UA
UZ	0	1	0	1	4	10	2	6	3	326	4	1	2	44	90	32	17	413	7	4	2	7	2	110	13	0	0	1306	96	UZ
ATL	0	0	0	-2	26	3	17	0	0	46	8	0	0	0	0	0	2	0	264	5	0	3	16	0	5	0	0	280	142	ATL
BAS	0	0	0	-3	72	130	1	4	2	179	161	1	4	0	0	0	20	0	60	-49	0	2	48	0	1	0	0	1029	659	BAS
BLS	1	3	0	3	13	90	2	144	23	553	15	2	10	0	3	88	417	1	14	18	368	18	12	10	13	0	0	1783	523	BLS
MED	5	7	1	4	5	32	18	35	38	44	5	9	8	0	0	105	33	0	40	6	12	812	12	2	136	0	0	1369	1049	MED
NOS	0	0	0	-46	100	19	2	1	0	40	35	0	0	0	0	0	3	0	148	17	0	1	-195	0	1	0	0	475	172	NOS
AST	0	1	0	0	1	4	1	4	2	84	1	0	1	18	88	83	10	61	3	1	3	24	1	1037	18	0	0	505	61	AST
NOA	1	3	1	1	1	8	29	10	10	10	1	1	2	0	0	23	7	0	55	1	2	196	3	1	823	0	0	445	367	NOA
EXC	1	1	0	-3	21	40	11	24	11	458	19	3	6	8	24	38	45	33	36	17	6	24	9	34	13	0	0	1158	374	EXC
EU	1	3	0	-18	31	87	47	62	19	84	39	10	17	0	0	8	30	0	73	29	3	72	10	1	31	0	0	1334	1073	EU
	ME	MK	MT	NL	NO	PL	PT	RO	RS	RU	SE	SI	SK	TJ	TM	TR	UA	UZ	ATL	BAS	BLS	MED	NOS	AST	NOA	DMS	VOL	EXC	EU	

Table C.9: 2021 country-to-country blame matrices for **MDA8**$_{AS}$.
Units: ng/m^3 per 15% emis. red. of VOC. **Emitters →, Receptors ↓.**

	AL	AM	AT	AZ	BA	BE	BG	BY	CH	CY	CZ	DE	DK	EE	ES	FI	FR	GB	GE	GR	HR	HU	IE	IS	IT	KG	KZ	LT	LU	LV	MD	
AL	86	0	8	1	14	4	4	2	4	0	11	46	4	0	16	1	42	21	0	7	8	13	2	0	93	0	0	1	0	1	0	AL
AM	0	63	1	299	1	1	1	2	1	0	2	10	1	0	3	1	7	4	26	2	1	1	1	0	6	0	7	1	0	0	1	AM
AT	0	0	93	0	2	9	0	2	33	0	34	213	6	0	12	1	93	26	0	0	9	7	3	0	120	0	0	1	1	1	0	AT
AZ	0	4	1	834	1	1	1	4	1	0	3	14	1	0	3	1	9	7	20	2	1	2	1	0	8	0	17	1	0	1	2	AZ
BA	2	0	16	0	70	5	2	2	6	0	20	81	4	0	16	1	48	20	0	1	16	18	2	0	84	0	0	1	1	1	0	BA
BE	0	0	3	0	0	196	0	1	2	0	5	210	14	0	10	2	250	121	0	0	0	1	10	0	4	0	0	1	4	1	0	BE
BG	2	0	7	1	6	5	50	5	3	0	17	57	5	1	7	1	28	19	0	10	4	12	2	0	24	0	0	2	0	1	5	BG
BY	0	0	3	1	1	5	1	39	2	0	13	53	7	1	3	2	26	25	0	0	1	5	3	0	7	0	1	5	0	2	2	BY
CH	0	0	11	0	1	11	0	1	159	0	8	189	5	0	16	1	147	26	0	0	3	2	3	0	169	0	0	1	1	0	0	CH
CY	2	0	3	6	3	3	8	6	2	29	7	33	3	1	9	1	25	15	1	26	2	5	2	0	31	0	1	1	0	1	4	CY
CZ	0	0	24	0	2	16	1	2	11	0	174	247	11	1	7	2	98	34	0	0	5	11	4	0	33	0	0	1	2	1	0	CZ
DE	0	0	13	0	0	35	0	2	15	0	23	409	16	1	8	2	138	71	0	0	1	2	6	0	14	0	0	1	3	1	0	DE
DK	0	0	1	0	0	20	0	2	1	0	7	113	86	1	4	2	65	108	0	0	0	1	9	0	2	0	0	2	1	1	0	DK
EE	0	0	1	1	0	10	0	7	1	0	3	50	10	7	2	8	35	37	0	0	0	2	4	0	2	0	1	3	1	5	0	EE
ES	0	0	1	0	0	5	0	1	1	0	1	26	2	0	174	0	60	21	0	0	0	0	3	0	11	0	0	0	0	0	0	ES
FI	0	0	1	1	0	4	0	3	0	0	2	26	6	1	1	8	18	24	0	0	0	1	4	0	1	0	1	1	0	1	0	FI
FR	0	0	3	0	0	25	0	1	8	0	4	105	6	0	28	1	256	72	0	0	1	1	7	0	30	0	0	1	2	0	0	FR
GB	0	0	1	0	0	16	0	0	1	0	2	61	7	0	2	1	48	328	0	0	0	0	21	0	2	0	0	0	1	0	0	GB
GE	0	5	2	234	1	2	2	5	1	0	4	19	2	0	3	1	11	7	69	2	1	2	1	0	9	0	7	1	0	1	2	GE
GL	0	0	0	0	0	0	0	0	0	0	0	0	0	0	0	0	0	1	0	0	0	0	0	0	0	0	0	0	0	0	0	GL
GR	9	0	6	1	7	4	15	4	3	0	12	47	4	1	12	1	34	22	0	95	5	10	2	0	56	0	0	1	0	1	3	GR
HR	1	0	28	0	26	7	2	2	10	0	31	120	5	0	17	1	70	27	0	1	42	19	3	0	129	0	0	1	1	1	1	HR
HU	0	0	34	0	8	8	2	3	11	0	50	145	8	1	9	1	68	29	0	0	11	79	4	0	56	0	0	2	1	1	1	HU
IE	0	0	0	0	0	11	0	0	1	0	1	33	4	0	2	1	39	163	0	0	0	0	48	0	2	0	0	0	0	0	0	IE
IS	0	0	0	0	0	3	0	0	0	0	1	12	5	0	0	1	12	34	0	0	0	0	4	2	0	0	0	0	0	0	0	IS
IT	1	0	18	0	6	6	1	2	12	0	14	76	5	0	29	1	96	27	0	1	13	6	3	0	545	0	0	1	1	1	0	IT
KG	0	0	1	10	0	1	0	1	1	0	1	6	0	0	3	0	5	3	1	0	0	1	0	0	5	29	47	0	0	0	0	KG
KZ	0	0	1	10	1	1	1	3	1	0	2	14	2	0	3	1	10	10	1	1	1	1	1	0	7	1	49	1	0	1	1	KZ
LT	0	0	2	1	1	7	0	16	1	0	10	58	11	1	2	2	31	35	0	0	1	3	4	0	4	0	1	15	1	5	1	LT
LU	0	0	5	0	0	58	0	2	4	0	7	243	12	1	10	2	217	74	0	0	0	1	6	0	7	0	0	1	34	1	0	LU
LV	0	0	1	1	0	7	0	11	1	0	6	51	9	2	2	3	31	34	0	0	0	2	4	0	3	0	1	6	1	11	1	LV
MD	0	0	4	2	2	6	4	11	2	0	17	62	7	1	5	2	29	30	0	1	2	7	4	0	15	0	1	3	1	2	52	MD
ME	10	0	8	1	19	4	3	1	4	0	11	45	4	0	16	1	38	18	0	2	7	12	2	0	78	0	0	1	0	1	0	ME
MK	17	0	7	1	9	4	8	2	3	0	11	42	4	0	12	1	28	16	0	24	5	12	2	0	48	0	0	1	0	1	1	MK
MT	3	0	10	1	9	7	3	2	5	0	13	64	5	0	36	1	96	33	0	6	8	6	4	0	233	0	0	1	1	1	1	MT
NL	0	0	1	0	0	96	0	1	2	0	5	251	18	1	7	2	156	172	0	0	0	0	16	0	3	0	0	1	2	1	0	NL
NO	0	0	0	0	0	5	0	1	0	0	2	22	6	0	1	1	16	34	0	0	0	0	4	0	1	0	0	1	0	1	0	NO
PL	0	0	7	1	2	14	1	6	3	0	42	142	15	1	4	2	52	50	0	0	2	9	5	0	13	0	0	3	1	2	1	PL
PT	0	0	0	0	0	6	0	0	1	0	1	20	1	0	78	0	46	22	0	0	0	0	3	0	4	0	0	0	0	0	0	PT
RO	1	0	8	1	5	6	10	6	3	0	23	66	6	1	7	1	33	23	0	1	3	19	3	0	24	0	1	2	1	1	8	RO
RS	5	0	16	1	21	6	8	3	6	0	28	85	7	1	11	1	41	22	0	2	10	31	2	0	48	0	0	1	1	1	1	RS
RU	0	0	1	7	0	2	0	4	0	0	2	14	2	1	1	2	9	12	0	0	0	1	2	0	3	0	6	1	0	1	1	RU
SE	0	0	1	0	0	7	0	2	0	0	3	37	12	1	2	3	25	37	0	0	0	1	4	0	1	0	0	1	0	1	0	SE
SI	0	0	46	0	5	8	1	2	12	0	28	133	4	0	18	1	74	27	0	0	31	9	3	0	250	0	0	1	1	1	0	SI
SK	0	0	29	0	4	9	2	3	9	0	65	136	9	1	7	1	63	27	0	0	7	38	4	0	41	0	0	2	1	1	1	SK
TJ	0	0	1	11	0	0	0	1	0	0	1	5	0	0	2	0	4	2	1	0	0	1	0	0	5	4	25	0	0	0	0	TJ
TM	0	1	2	50	1	2	1	4	1	0	3	17	2	1	5	1	12	9	2	1	1	2	1	0	10	1	35	1	0	1	1	TM
TR	1	2	2	19	2	2	5	5	1	1	6	25	2	1	6	1	15	10	3	7	1	3	1	0	15	0	1	1	0	1	3	TR
UA	0	0	4	4	2	4	2	15	2	0	14	50	5	1	4	2	24	23	0	1	2	6	3	0	12	0	2	3	0	2	7	UA
UZ	0	1	2	19	1	1	1	3	1	0	3	14	1	0	4	1	11	8	1	1	1	2	1	0	9	5	50	1	0	1	1	UZ
ATL	0	0	0	0	0	5	0	0	0	0	1	15	3	0	7	1	29	38	0	0	0	0	5	0	1	0	0	0	0	0	0	ATL
BAS	0	0	1	0	0	13	0	6	1	0	6	87	36	4	2	9	45	61	0	0	0	2	6	0	3	0	0	4	1	5	0	BAS
BLS	1	0	4	15	3	5	12	15	2	0	13	54	6	1	5	2	23	21	6	6	2	7	2	0	16	0	2	4	0	2	12	BLS
MED	4	0	10	1	9	8	7	3	5	0	13	70	5	1	48	1	105	34	0	28	9	8	4	0	163	0	0	1	1	1	2	MED
NOS	0	0	1	0	0	20	0	1	1	0	3	96	20	1	2	2	67	212	0	0	0	0	16	0	1	0	0	1	1	1	0	NOS
AST	0	0	1	28	0	1	1	2	1	0	1	7	1	0	3	0	6	3	1	2	0	1	0	0	6	1	14	0	0	0	1	AST
NOA	1	0	2	0	2	2	2	1	2	0	3	22	1	0	25	0	28	11	0	7	2	2	1	0	35	0	0	0	0	0	1	NOA
EXC	0	0	3	12	1	5	1	4	2	0	6	38	4	1	9	2	29	23	1	2	1	3	3	0	18	1	13	1	0	1	1	EXC
EU	1	0	9	0	2	14	3	3	6	0	17	107	9	1	32	2	87	44	0	4	3	6	5	0	60	0	0	1	1	1	1	EU
	AL	AM	AT	AZ	BA	BE	BG	BY	CH	CY	CZ	DE	DK	EE	ES	FI	FR	GB	GE	GR	HR	HU	IE	IS	IT	KG	KZ	LT	LU	LV	MD	

Table C.9 Cont.: 2021 country-to-country blame matrices for **MDA8**$_{AS}$.
Units: ng/m^3 per 15% emis. red. of VOC. **Emitters →, Receptors ↓.**

	ME	MK	MT	NL	NO	PL	PT	RO	RS	RU	SE	SI	SK	TJ	TM	TR	UA	UZ	ATL	BAS	BLS	MED	NOS	AST	NOA	DMS	VOL	EXC	EU	
AL	12	4	0	12	2	28	2	9	38	13	3	2	7	0	0	1	4	0	0	0	0	1	0	0	20	0	0	526	324	AL
AM	0	0	0	2	1	9	0	4	1	45	1	0	1	0	8	23	7	3	0	0	0	0	0	127	5	0	0	550	57	AM
AT	0	0	0	19	4	31	2	2	2	14	4	14	8	0	0	0	3	0	0	0	0	0	1	0	5	0	0	771	685	AT
AZ	0	0	0	3	2	13	1	5	2	121	2	0	1	0	19	13	12	8	0	0	0	0	0	114	5	0	0	1144	77	AZ
BA	2	0	0	13	3	39	2	10	24	13	4	4	9	0	0	0	4	0	0	0	0	1	0	0	15	0	0	546	399	BA
BE	0	0	0	201	12	9	2	0	0	18	8	0	1	0	0	0	2	0	0	0	0	0	4	0	2	0	0	1089	932	BE
BG	1	2	0	12	3	49	1	48	24	43	4	1	9	0	0	11	23	0	0	0	0	0	0	1	10	0	0	505	357	BG
BY	0	0	0	12	5	79	0	7	2	70	6	1	5	0	0	1	22	0	0	0	0	0	0	1	1	0	0	419	246	BY
CH	0	0	0	23	3	13	3	1	1	16	3	2	1	0	0	0	2	0	0	0	0	0	1	0	5	0	0	826	615	CH
CY	1	1	0	7	2	29	1	15	10	54	2	1	3	0	0	92	23	0	0	0	0	3	0	8	14	0	0	471	250	CY
CZ	0	0	0	30	6	101	1	3	4	17	7	4	16	0	0	0	3	0	0	0	0	0	1	0	2	0	0	880	799	CZ
DE	0	0	0	79	8	34	2	1	1	18	8	1	2	0	0	0	2	0	0	1	0	0	2	0	2	0	0	919	801	DE
DK	0	0	0	69	25	40	1	1	1	22	19	0	1	0	0	0	3	0	0	2	0	0	4	0	1	0	0	611	449	DK
EE	0	0	0	25	7	25	1	2	0	89	11	0	1	0	0	0	7	0	0	1	0	0	1	0	1	0	0	358	208	EE
ES	0	0	0	11	1	3	25	0	0	5	1	0	0	0	0	0	1	0	1	0	0	2	0	0	25	0	0	358	327	ES
FI	0	0	0	10	5	14	0	1	0	42	6	0	1	0	0	0	3	0	0	0	0	0	0	0	0	0	0	187	108	FI
FR	0	0	0	45	5	9	4	1	1	16	4	1	1	0	0	0	2	0	0	0	0	1	2	0	5	0	0	642	535	FR
GB	0	0	0	45	7	4	0	0	0	7	3	0	0	0	0	0	1	0	1	0	0	0	3	0	1	0	0	559	215	GB
GE	0	0	0	4	2	17	1	8	2	83	2	0	2	0	7	18	15	3	0	0	0	0	0	52	5	0	0	559	96	GE
GL	0	0	0	0	0	0	0	0	0	0	0	0	0	0	0	0	0	0	0	0	0	0	0	0	0	0	0	3	1	GL
GR	2	5	0	11	2	36	2	21	22	31	3	1	6	0	0	15	15	0	0	0	0	2	0	1	20	0	0	527	387	GR
HR	1	0	0	16	3	47	2	9	16	15	5	11	10	0	0	0	4	0	0	0	0	1	0	0	12	0	0	687	580	HR
HU	0	0	0	21	5	109	1	26	20	23	6	6	37	0	0	1	10	0	0	0	0	0	1	0	7	0	0	802	688	HU
IE	0	0	0	32	5	2	0	0	0	6	2	0	0	0	0	0	1	0	1	0	0	0	1	0	1	0	0	357	180	IE
IS	0	0	0	7	3	3	0	0	0	4	3	0	0	0	0	0	1	0	0	0	0	0	0	0	0	0	0	99	53	IS
IT	1	0	1	15	3	24	3	4	5	13	4	10	3	0	0	0	3	0	0	0	0	3	0	0	23	0	0	958	882	IT
KG	0	0	0	1	1	4	0	1	1	27	1	0	0	47	5	3	2	271	0	0	0	0	0	46	3	0	0	483	33	KG
KZ	0	0	0	3	2	10	1	2	1	97	2	0	1	1	2	3	7	13	0	0	0	0	0	17	3	0	0	271	68	KZ
LT	0	0	0	16	6	70	0	3	1	54	9	0	3	0	0	0	12	0	0	1	0	0	1	0	1	0	0	389	261	LT
LU	0	0	0	107	8	13	2	1	0	18	8	0	1	0	0	0	3	0	0	0	0	0	2	0	2	0	0	845	735	LU
LV	0	0	0	15	6	47	0	2	1	61	11	0	2	0	0	0	9	0	0	1	0	0	1	0	1	0	0	343	218	LV
MD	0	0	0	13	4	93	1	39	5	68	5	1	7	0	0	6	59	0	0	0	0	0	0	1	4	0	0	572	329	MD
ME	43	1	0	10	2	28	2	8	27	12	3	2	6	0	0	1	3	0	0	0	0	1	0	0	18	0	0	435	293	ME
MK	3	36	0	10	2	34	2	14	49	19	3	1	7	0	0	3	7	0	0	0	0	1	0	0	17	0	0	449	280	MK
MT	2	1	63	17	4	31	4	6	9	13	4	4	5	0	0	1	4	0	0	0	0	13	0	1	54	0	0	717	630	MT
NL	0	0	0	347	14	20	1	1	0	21	10	0	1	0	0	0	2	0	0	0	0	0	7	0	1	0	0	1152	938	NL
NO	0	0	0	12	23	8	0	0	0	11	4	0	0	0	0	0	1	0	0	0	0	0	1	0	0	0	0	159	87	NO
PL	0	0	0	32	6	289	1	8	4	34	8	1	13	0	0	1	11	0	0	1	0	0	1	0	1	0	0	783	664	PL
PT	0	0	0	11	1	2	162	0	0	3	1	0	0	0	0	0	1	0	2	0	0	0	0	0	14	0	0	365	336	PT
RO	1	0	0	14	3	77	1	112	15	43	5	1	13	0	0	5	28	0	0	0	0	0	0	1	6	0	0	580	437	RO
RS	4	3	0	14	3	60	2	28	119	22	4	3	15	0	0	1	8	0	0	0	0	0	0	0	12	0	0	644	425	RS
RU	0	0	0	4	2	11	0	2	1	110	2	0	1	0	1	1	7	1	0	0	0	0	0	3	1	0	0	216	63	RU
SE	0	0	0	18	10	17	0	1	0	21	12	0	1	0	0	0	3	0	0	1	0	0	1	0	0	0	0	223	148	SE
SI	0	0	0	15	3	34	2	4	5	14	4	61	5	0	0	0	3	0	0	0	0	1	0	0	10	0	0	808	736	SI
SK	0	0	0	23	5	189	1	17	10	23	5	4	56	0	0	1	10	0	0	0	0	0	1	0	4	0	0	807	712	SK
TJ	0	0	0	1	0	3	0	1	1	23	0	0	0	147	8	3	2	144	0	0	0	0	0	53	3	0	0	401	27	TJ
TM	0	0	0	4	2	12	1	3	2	108	2	0	1	4	65	8	9	62	0	0	0	0	0	63	5	0	0	449	84	TM
TR	0	1	0	6	1	24	1	13	5	54	2	1	2	0	1	86	19	0	0	0	0	1	0	31	10	0	0	360	146	TR
UA	0	0	0	11	4	80	1	17	4	124	5	1	6	0	0	4	91	0	0	0	0	0	0	2	3	0	0	543	261	UA
UZ	0	0	0	3	2	10	1	3	1	95	2	0	1	23	9	5	7	221	0	0	0	0	0	36	4	0	0	529	75	UZ
ATL	0	0	0	11	3	2	4	0	0	6	2	0	0	0	0	0	1	0	0	0	0	0	1	0	2	0	0	136	87	ATL
BAS	0	0	0	34	14	62	1	2	1	64	28	0	2	0	0	0	5	0	0	4	0	0	1	0	1	0	0	507	354	BAS
BLS	0	1	0	11	4	67	1	38	8	211	6	1	6	0	1	48	79	0	0	0	1	1	0	4	6	0	0	723	294	BLS
MED	2	1	3	18	3	33	6	12	12	28	4	4	5	0	0	26	11	0	0	0	0	9	0	5	69	0	0	713	569	MED
NOS	0	0	0	75	27	14	1	0	0	12	9	0	0	0	0	0	1	0	0	0	0	0	6	0	0	0	0	588	332	NOS
AST	0	0	0	2	1	6	0	2	1	34	1	0	1	5	9	12	5	20	0	0	0	0	0	300	5	0	0	181	43	AST
NOA	0	0	0	6	1	9	8	3	3	7	1	1	1	0	0	4	3	0	0	0	0	2	0	2	152	0	0	202	165	NOA
EXC	0	0	0	11	3	23	2	5	3	77	3	1	2	3	3	6	10	13	0	0	0	0	0	10	4	0	0	351	174	EXC
EU	0	0	0	31	5	49	8	11	4	23	6	2	5	0	0	1	6	0	0	0	0	1	1	0	8	0	0	571	473	EU
	ME	MK	MT	NL	NO	PL	PT	RO	RS	RU	SE	SI	SK	TJ	TM	TR	UA	UZ	ATL	BAS	BLS	MED	NOS	AST	NOA	DMS	VOL	EXC	EU	

Table C.10: 2021 country-to-country blame matrices for **PM2.5**.
Units: ng/m^3 per 15% emis. red. of PPM. **Emitters →, Receptors ↓.**

	AL	AM	AT	AZ	BA	BE	BG	BY	CH	CY	CZ	DE	DK	EE	ES	FI	FR	GB	GE	GR	HR	HU	IE	IS	IT	KG	KZ	LT	LU	LV	MD	
AL	163	0	1	0	8	0	2	0	0	0	1	1	0	0	1	0	1	0	0	6	3	2	0	0	8	0	0	0	0	0	0	AL
AM	0	80	0	22	0	0	0	0	0	0	0	0	0	0	0	0	0	0	9	0	0	0	0	0	0	0	0	0	0	0	0	AM
AT	0	0	160	0	3	0	0	0	2	0	9	14	0	0	0	0	4	0	0	0	7	7	0	0	13	-0	0	0	0	0	0	AT
AZ	0	6	0	203	0	0	0	0	0	0	0	0	0	0	0	0	0	0	13	0	0	0	0	0	0	0	1	0	0	0	0	AZ
BA	1	0	3	0	512	0	1	0	0	0	2	2	0	0	0	0	2	0	0	0	30	7	0	0	8	0	0	0	0	0	0	BA
BE	0	0	0	0	0	162	0	0	1	0	1	25	0	0	1	0	71	10	0	0	0	0	1	0	1	0	0	0	2	0	0	BE
BG	1	0	1	0	4	0	167	1	0	0	1	1	0	0	0	0	1	0	0	6	2	3	0	0	2	0	0	0	0	0	3	BG
BY	0	0	1	0	1	0	0	117	0	0	2	3	1	0	0	0	1	1	0	0	1	2	0	0	1	0	0	4	0	2	1	BY
CH	0	0	6	0	0	0	0	0	92	0	1	17	0	0	1	0	25	0	0	0	0	0	0	0	19	0	0	0	0	0	0	CH
CY	0	0	0	0	0	0	1	0	0	18	0	0	0	0	0	0	0	0	0	3	0	0	0	0	1	0	0	0	0	0	0	CY
CZ	0	0	16	0	3	1	0	0	1	0	190	24	0	0	0	0	6	1	0	0	5	10	0	0	3	-0	0	0	0	0	0	CZ
DE	0	0	9	0	0	4	0	0	3	-0	7	149	1	0	1	0	19	4	0	0	0	1	0	0	2	-0	0	0	1	0	0	DE
DK	0	0	0	0	0	2	0	0	0	-0	1	15	74	0	0	0	5	6	0	0	0	1	0	0	0	0	0	0	0	0	0	DK
EE	0	0	0	0	0	0	0	5	0	0	1	2	1	55	0	2	1	1	0	0	0	0	0	0	0	0	0	3	0	11	0	EE
ES	0	0	0	0	0	0	0	0	0	0	0	0	0	0	108	0	4	0	0	0	0	0	0	0	1	-0	0	0	0	0	0	ES
FI	0	0	0	0	0	0	0	1	0	0	0	1	0	1	0	17	0	0	0	0	0	0	0	0	0	0	0	0	0	1	0	FI
FR	0	0	1	0	0	3	0	0	2	0	1	8	0	0	4	0	158	3	0	0	0	0	0	0	4	-0	0	0	0	0	0	FR
GB	0	-0	0	-0	0	2	0	0	0	-0	0	3	0	0	0	0	6	99	-0	0	0	0	3	0	0	-0	-0	0	0	0	0	GB
GE	0	8	0	18	0	0	0	0	0	0	0	0	0	0	0	0	0	0	126	0	0	0	0	0	0	0	0	0	0	0	0	GE
GL	0	0	0	0	0	0	0	0	0	0	0	0	0	0	0	0	0	0	0	0	0	0	0	0	0	0	0	0	0	0	0	GL
GR	4	0	0	0	3	0	10	1	0	0	0	0	0	0	0	0	1	0	0	99	1	1	0	0	4	0	0	0	0	0	1	GR
HR	0	0	8	0	101	0	1	0	0	0	4	4	0	0	1	0	2	0	0	0	242	20	0	0	21	0	0	0	0	0	0	HR
HU	0	0	13	0	16	0	2	1	0	-0	7	5	0	0	0	0	2	0	0	0	27	245	0	0	7	-0	0	0	0	0	1	HU
IE	0	-0	0	-0	0	0	0	0	0	0	0	1	0	0	0	0	3	12	-0	0	0	0	51	0	0	0	0	0	0	0	0	IE
IS	0	0	0	0	0	0	0	0	0	0	0	0	0	0	0	0	0	0	0	0	0	0	0	2	0	0	0	0	0	0	0	IS
IT	0	0	3	0	4	0	0	0	1	0	1	1	0	0	2	0	6	0	0	0	5	2	0	0	327	0	0	0	0	0	0	IT
KG	0	0	0	0	0	0	0	0	0	0	0	0	0	0	0	0	0	0	0	0	0	0	0	0	0	34	5	0	0	0	0	KG
KZ	0	0	0	0	0	0	0	0	0	0	0	0	0	0	0	0	0	0	0	0	0	0	0	0	0	1	33	0	0	0	0	KZ
LT	0	0	1	0	1	0	0	21	0	0	2	4	1	1	0	0	1	1	0	0	0	1	0	0	0	0	0	70	0	8	1	LT
LU	0	0	1	0	0	19	0	0	1	0	2	50	0	0	1	0	87	4	0	0	0	0	0	0	2	0	0	0	61	0	0	LU
LV	0	0	0	0	0	0	0	11	0	0	1	3	1	3	0	1	1	1	0	0	0	1	0	0	0	0	0	13	0	75	0	LV
MD	0	0	1	0	1	0	3	3	0	0	1	2	0	0	0	0	0	0	0	1	1	2	0	0	1	0	0	0	0	0	272	MD
ME	11	0	1	0	27	0	1	0	0	0	1	1	0	0	0	0	1	0	0	1	4	3	0	0	5	0	0	0	0	0	0	ME
MK	11	0	1	0	5	0	9	0	0	0	1	1	0	0	0	0	1	0	0	15	2	3	0	0	3	0	0	0	0	0	1	MK
MT	1	0	0	0	3	0	1	0	0	0	0	0	0	0	3	0	4	0	0	1	1	1	0	0	23	0	0	0	0	0	0	MT
NL	0	0	0	0	0	37	0	0	0	0	1	45	1	0	1	0	26	14	0	0	0	0	1	0	0	0	-0	0	0	0	0	NL
NO	0	0	0	0	0	0	0	0	0	0	0	0	0	0	0	0	0	1	0	0	0	0	0	0	0	0	0	0	0	0	0	NO
PL	0	0	2	0	2	1	0	4	0	-0	15	14	1	0	0	0	3	2	0	0	2	6	0	0	1	0	0	1	0	1	0	PL
PT	0	0	0	-0	0	0	0	0	0	0	0	0	0	0	27	0	2	0	0	0	0	0	0	0	0	0	0	0	0	0	0	PT
RO	0	0	1	0	4	0	12	1	0	0	1	1	0	0	0	0	1	0	0	1	2	9	0	0	2	0	0	0	0	0	7	RO
RS	4	0	2	0	39	0	9	1	0	0	2	2	0	0	0	0	1	0	0	2	12	17	0	0	4	0	0	0	0	0	1	RS
RU	0	0	0	0	0	0	0	1	0	0	0	0	0	0	0	0	0	0	0	0	0	0	0	0	0	0	3	0	0	0	0	RU
SE	0	0	0	0	0	0	0	0	0	0	0	2	2	0	0	1	1	1	0	0	0	0	0	0	0	0	0	0	0	0	0	SE
SI	0	0	35	0	8	0	0	0	0	0	4	4	0	0	0	0	3	0	0	0	61	9	0	0	47	-0	0	0	0	0	0	SI
SK	0	0	9	0	6	0	1	1	0	-0	16	6	0	0	0	0	2	1	0	0	7	50	0	0	4	0	0	0	0	0	0	SK
TJ	0	0	0	0	0	0	0	0	0	0	0	0	0	0	0	0	0	0	0	0	0	0	0	0	0	2	1	0	0	0	0	TJ
TM	0	0	0	2	0	0	0	0	0	0	0	0	0	0	0	0	0	0	0	0	0	0	0	0	0	0	4	0	0	0	0	TM
TR	0	1	0	1	0	0	1	0	0	0	0	0	0	0	0	0	0	0	1	1	0	0	0	0	0	0	0	0	0	0	0	TR
UA	0	0	0	0	1	0	1	8	0	0	1	2	0	0	0	0	1	0	0	0	1	2	0	0	1	0	1	1	0	0	8	UA
UZ	0	0	0	0	0	0	0	0	0	0	0	0	0	0	0	0	0	0	0	0	0	0	0	0	0	5	9	0	0	0	0	UZ
ATL	0	0	0	0	0	0	0	0	0	0	0	0	0	0	1	0	1	1	0	0	0	0	0	0	0	0	0	0	0	0	0	ATL
BAS	0	0	0	0	0	1	0	2	0	0	1	7	6	2	0	3	2	2	0	0	0	1	0	0	0	0	0	2	0	3	0	BAS
BLS	0	0	0	1	1	0	5	2	0	0	0	0	0	0	0	0	0	0	8	1	0	1	0	0	0	0	0	0	0	0	3	BLS
MED	1	0	1	0	4	0	1	0	0	0	0	1	0	0	7	0	6	0	0	6	3	1	0	0	21	0	0	0	0	0	0	MED
NOS	0	0	0	0	0	2	0	0	0	0	0	5	2	0	0	0	8	16	0	0	0	0	1	0	0	0	0	0	0	0	0	NOS
AST	0	0	0	1	0	0	0	0	0	0	0	0	0	0	0	0	0	0	0	0	0	0	0	0	0	0	1	0	0	0	0	AST
NOA	0	0	0	0	1	0	0	0	0	0	0	0	0	0	3	0	1	0	0	1	0	0	0	0	2	0	0	0	0	0	0	NOA
EXC	0	0	1	1	2	1	1	2	0	0	2	4	0	0	3	0	6	2	1	1	1	2	0	0	6	1	6	0	0	1	1	EXC
EU	0	0	6	0	3	2	6	1	1	0	6	17	1	1	15	2	25	2	0	3	5	8	1	0	26	0	0	2	0	2	1	EU
	AL	AM	AT	AZ	BA	BE	BG	BY	CH	CY	CZ	DE	DK	EE	ES	FI	FR	GB	GE	GR	HR	HU	IE	IS	IT	KG	KZ	LT	LU	LV	MD	

Table C.10 Cont.: 2021 country-to-country blame matrices for **PM2.5**.
Units: ng/m^3 per 15% emis. red. of PPM. **Emitters →, Receptors ↓.**

	ME	MK	MT	NL	NO	PL	PT	RO	RS	RU	SE	SI	SK	TJ	TM	TR	UA	UZ	ATL	BAS	BLS	MED	NOS	AST	NOA	BIC	DMS	VOL	EXC	EU	
AL	16	13	0	0	0	3	0	4	46	0	0	0	1	0	0	0	2	0	0	0	0	1	0	0	1	0	0	0	282	32	AL
AM	0	0	0	0	0	0	0	0	0	1	0	0	0	0	0	21	1	0	0	0	0	0	0	8	0	0	0	0	134	1	AM
AT	0	0	0	0	0	7	0	2	2	0	0	10	2	-0	0	0	2	0	0	0	0	0	0	0	0	0	0	0	244	235	AT
AZ	0	0	0	0	0	0	0	0	0	8	0	0	0	0	1	5	2	1	0	0	0	0	0	9	0	0	0	0	241	1	AZ
BA	5	0	0	0	0	6	0	5	27	0	0	1	1	0	0	0	2	0	0	0	0	0	0	0	0	0	0	0	621	71	BA
BE	0	0	0	17	0	3	0	0	0	0	0	0	0	0	0	0	1	0	0	0	0	0	6	0	0	0	0	0	299	287	BE
BG	1	2	0	0	0	5	0	35	22	2	0	0	1	0	0	6	13	0	0	0	0	0	0	0	0	0	0	0	279	224	BG
BY	0	0	0	0	0	40	0	3	1	8	0	0	1	0	0	1	31	0	0	0	0	0	0	0	0	0	0	0	225	63	BY
CH	0	0	0	0	0	1	0	0	0	0	0	0	0	0	0	0	0	0	0	0	0	0	0	0	0	0	0	0	164	70	CH
CY	0	0	0	0	0	1	0	1	1	1	0	0	0	0	0	83	4	0	0	0	0	3	0	9	2	0	0	0	116	26	CY
CZ	0	0	0	1	0	45	0	3	4	1	0	2	8	-0	0	0	2	0	0	0	0	0	0	0	0	0	0	0	329	315	CZ
DE	0	0	0	5	0	13	0	0	0	0	0	0	0	-0	0	0	1	0	0	0	0	0	1	0	0	0	0	0	223	214	DE
DK	0	0	0	3	2	12	0	0	0	1	2	0	0	0	0	0	1	0	0	2	0	0	2	0	0	0	0	0	127	116	DK
EE	0	0	0	0	1	12	0	1	0	7	2	0	0	0	0	0	5	0	0	1	0	0	0	0	0	0	0	0	112	91	EE
ES	0	0	0	0	0	0	8	0	0	0	0	0	0	0	0	0	0	0	1	0	0	1	0	0	2	0	0	0	124	123	ES
FI	0	0	0	0	1	3	0	0	0	5	2	0	0	0	0	0	2	0	0	0	0	0	0	0	0	0	0	0	36	26	FI
FR	0	0	0	1	0	1	0	0	0	0	0	0	0	-0	0	0	0	0	0	0	0	0	1	0	0	0	0	0	190	183	FR
GB	0	0	0	2	0	2	0	0	0	0	0	0	0	-0	-0	0	0	-0	1	0	0	0	2	-0	0	0	0	0	118	18	GB
GE	0	0	0	0	0	0	0	0	0	4	0	0	0	0	0	11	2	0	0	0	0	0	0	2	0	0	0	0	171	1	GE
GL	0	0	0	0	0	0	0	0	0	0	0	0	0	0	0	0	0	0	0	0	0	0	0	0	0	0	0	0	0	0	GL
GR	1	6	0	0	0	3	0	6	10	1	0	0	0	0	0	9	7	0	0	0	0	2	0	0	1	0	0	0	171	128	GR
HR	1	0	0	0	0	9	0	6	30	0	0	15	2	-0	0	0	3	0	0	0	0	1	0	0	0	0	0	0	473	336	HR
HU	0	0	0	0	0	24	0	38	39	1	0	6	20	-0	0	0	9	0	0	0	0	0	0	0	0	0	0	0	465	397	HU
IE	0	0	0	0	0	1	0	0	0	0	0	0	0	0	0	0	0	0	1	0	0	0	0	0	0	0	0	0	70	58	IE
IS	0	0	0	0	0	0	0	0	0	0	0	0	0	0	0	0	0	0	0	0	0	0	0	0	0	0	0	0	3	0	IS
IT	0	0	0	0	0	2	0	2	2	0	0	4	0	0	0	0	1	0	0	0	0	2	0	0	2	0	0	0	365	355	IT
KG	0	0	0	0	0	0	0	0	0	0	0	0	0	8	0	0	0	17	0	0	0	0	0	10	0	0	0	0	65	0	KG
KZ	0	0	0	0	0	0	0	0	0	11	0	0	0	1	1	0	2	4	0	0	0	0	0	6	0	0	0	0	54	1	KZ
LT	0	0	0	0	1	49	0	2	1	8	1	0	1	0	0	0	11	0	0	1	0	0	0	0	0	0	0	0	189	145	LT
LU	0	0	0	2	0	3	0	0	0	0	0	0	0	0	0	0	1	0	0	0	0	0	1	0	0	0	0	0	236	230	LU
LV	0	0	0	0	1	22	0	1	0	6	1	0	1	0	0	0	8	0	0	1	0	0	0	0	0	0	0	0	153	125	LV
MD	0	0	0	0	0	15	0	70	3	5	0	0	1	0	0	4	63	0	0	0	0	0	0	0	0	0	0	0	453	100	MD
ME	212	1	0	0	0	4	0	4	33	0	0	0	1	0	0	0	2	0	0	0	0	0	0	0	0	0	0	0	315	28	ME
MK	1	172	0	0	0	4	0	6	61	0	0	0	1	0	0	1	3	0	0	0	0	0	0	0	0	0	0	0	303	47	MK
MT	1	0	38	0	0	1	0	1	2	0	0	0	0	0	0	0	1	0	0	0	0	21	0	0	11	0	0	0	85	76	MT
NL	0	0	0	132	0	6	0	0	0	0	0	0	0	0	0	0	1	0	0	0	0	0	10	0	0	0	0	0	266	250	NL
NO	0	0	0	0	20	1	0	0	0	1	1	0	0	0	0	0	0	0	0	0	0	0	0	0	0	0	0	0	25	3	NO
PL	0	0	0	1	0	439	0	4	3	3	0	1	8	0	0	0	12	0	0	0	0	0	0	0	0	0	0	0	527	500	PL
PT	0	0	0	0	0	0	170	0	0	0	0	0	0	0	0	0	0	0	2	0	0	0	0	0	1	0	0	0	201	200	PT
RO	0	0	0	0	0	11	0	314	16	2	0	0	2	0	0	3	18	0	0	0	0	0	0	0	0	0	0	0	411	358	RO
RS	8	7	0	0	0	9	0	28	453	1	0	1	2	0	0	0	5	0	0	0	0	0	0	0	0	0	0	0	613	93	RS
RU	0	0	0	0	0	2	0	0	0	40	0	0	0	0	0	0	6	0	0	0	0	0	0	0	0	0	0	0	56	4	RU
SE	0	0	0	0	3	4	0	0	0	1	13	0	0	0	0	0	1	0	0	1	0	0	0	0	0	0	0	0	32	24	SE
SI	0	0	0	0	0	7	0	3	4	0	0	237	1	-0	0	0	2	0	0	0	0	1	0	0	0	0	0	0	427	411	SI
SK	0	0	0	0	0	60	0	14	11	1	0	2	146	-0	0	0	11	0	0	0	0	0	0	0	0	0	0	0	350	318	SK
TJ	0	0	0	0	0	0	0	0	0	0	0	0	0	127	2	0	0	18	0	0	0	0	0	21	0	0	0	0	151	0	TJ
TM	0	0	0	0	0	0	0	0	0	4	0	0	0	3	34	1	2	15	0	0	0	0	0	6	0	0	0	0	65	1	TM
TR	0	0	0	0	0	1	0	2	1	2	0	0	0	0	0	229	6	0	0	0	0	1	0	6	0	0	0	0	246	6	TR
UA	0	0	0	0	0	22	0	14	2	15	0	0	1	0	0	4	251	0	0	0	0	0	0	0	0	0	0	0	339	48	UA
UZ	0	0	0	0	0	0	0	0	0	4	0	0	0	15	7	0	2	94	0	0	0	0	0	3	0	0	0	0	137	1	UZ
ATL	0	0	0	0	0	0	2	0	0	0	0	0	0	0	0	0	0	0	1	0	0	0	0	0	0	0	0	0	7	6	ATL
BAS	0	0	0	1	1	25	0	1	0	5	6	0	0	0	0	0	3	0	0	5	0	0	1	0	0	0	0	0	76	62	BAS
BLS	0	0	0	0	0	4	0	9	2	17	0	0	0	0	0	72	48	0	0	0	3	0	0	1	0	0	0	0	178	22	BLS
MED	1	0	0	0	0	2	1	2	3	1	0	1	0	0	0	21	3	0	0	0	0	8	0	2	10	0	0	0	87	53	MED
NOS	0	0	0	3	4	2	0	0	0	0	0	0	0	0	0	0	0	0	0	0	0	0	7	0	0	0	0	0	47	26	NOS
AST	0	0	0	0	0	0	0	0	0	1	0	0	0	1	1	8	1	1	0	0	0	0	0	235	0	0	0	0	16	0	AST
NOA	0	0	0	0	0	0	1	0	0	0	0	0	0	0	0	1	1	0	0	0	0	1	0	1	47	0	0	0	15	11	NOA
EXC	0	0	0	1	1	11	1	6	3	19	0	1	1	2	1	10	13	4	0	0	0	0	0	2	0	0	0	0	121	51	EXC
EU	0	0	0	2	1	40	5	21	4	1	2	2	3	0	0	1	4	0	0	0	0	1	0	0	0	0	0	0	222	204	EU
	ME	MK	MT	NL	NO	PL	PT	RO	RS	RU	SE	SI	SK	TJ	TM	TR	UA	UZ	ATL	BAS	BLS	MED	NOS	AST	NOA	BIC	DMS	VOL	EXC	EU	

Table C.11: 2021 country-to-country blame matrices for **PM2.5**.
Units: ng/m^3 per 15% emis. red. of SO_x. **Emitters →, Receptors ↓.**

	AL	AM	AT	AZ	BA	BE	BG	BY	CH	CY	CZ	DE	DK	EE	ES	FI	FR	GB	GE	GR	HR	HU	IE	IS	IT	KG	KZ	LT	LU	LV	MD	
AL	35	0	1	0	11	0	7	1	0	0	3	4	0	0	1	0	1	0	0	9	1	1	0	0	8	0	1	0	0	0	0	AL
AM	0	41	0	90	0	0	0	0	0	0	0	0	0	0	0	0	0	0	13	0	0	0	0	0	0	0	10	0	0	0	0	AM
AT	0	0	28	0	2	1	0	1	1	0	11	29	0	0	1	0	4	1	0	0	2	2	0	0	5	0	0	0	0	0	0	AT
AZ	0	4	0	173	0	0	0	0	0	0	0	0	0	0	0	0	0	0	12	0	0	0	0	0	0	0	35	0	0	0	0	AZ
BA	1	0	2	0	87	0	3	1	0	0	7	10	0	0	1	0	2	1	0	0	3	3	0	0	6	0	1	0	0	0	0	BA
BE	0	0	0	0	0	41	0	0	0	0	3	41	0	0	3	0	35	15	0	0	0	0	1	0	1	0	0	0	1	0	0	BE
BG	1	0	1	0	4	0	76	3	0	0	3	4	0	0	0	0	1	0	0	6	0	2	0	0	2	0	3	0	0	0	1	BG
BY	0	0	0	0	1	0	1	35	0	0	3	10	1	1	0	1	1	2	0	0	0	1	0	0	0	0	6	2	0	0	0	BY
CH	0	0	2	0	0	1	0	0	22	0	2	19	0	0	1	0	11	2	0	0	0	0	0	0	8	0	0	0	0	0	0	CH
CY	0	0	0	0	1	0	3	1	0	34	0	1	0	0	0	0	0	0	0	13	0	0	0	0	2	0	1	0	0	0	0	CY
CZ	0	0	8	0	3	1	1	1	1	0	76	54	0	0	1	0	5	3	0	0	1	3	0	0	2	0	0	0	0	0	0	CZ
DE	0	0	5	0	0	5	0	1	2	0	10	100	1	0	1	0	12	9	0	0	0	0	0	0	1	0	0	0	0	0	0	DE
DK	0	0	0	0	0	3	0	1	0	0	2	26	12	0	1	0	4	12	0	0	0	0	0	1	0	0	1	0	0	0	0	DK
EE	0	0	0	0	0	0	0	5	0	0	1	5	1	4	0	3	1	2	0	0	0	0	0	0	0	0	3	2	0	1	0	EE
ES	0	0	0	0	0	0	0	0	0	0	0	2	0	0	63	0	3	1	0	0	0	0	0	0	2	0	0	0	0	0	0	ES
FI	0	0	0	0	0	0	0	1	0	0	0	2	0	1	0	9	0	1	0	0	0	0	0	0	0	0	2	0	0	0	0	FI
FR	0	0	1	0	0	3	0	0	1	0	2	15	0	0	9	0	31	7	0	0	0	0	0	0	3	0	0	0	0	0	0	FR
GB	0	-0	0	0	0	1	0	0	0	0	1	6	0	0	1	0	4	69	0	0	0	0	3	1	0	0	0	0	0	0	0	GB
GE	0	4	0	56	0	0	0	0	0	0	0	0	0	0	0	0	0	0	81	0	0	0	0	0	0	0	12	0	0	0	0	GE
GL	0	0	0	0	0	0	0	0	0	0	0	0	0	0	0	0	0	0	0	0	0	0	0	0	0	0	0	0	0	0	0	GL
GR	2	0	0	0	4	0	22	1	0	0	2	3	0	0	1	0	1	0	0	39	0	1	0	0	6	0	1	0	0	0	0	GR
HR	0	0	4	0	28	0	2	1	0	0	10	16	0	0	1	0	3	1	0	0	13	4	0	0	11	0	1	0	0	0	0	HR
HU	0	0	4	0	9	1	3	2	0	0	13	19	0	0	1	0	2	1	0	0	3	27	0	0	5	0	1	0	0	0	0	HU
IE	0	0	0	0	0	1	0	0	0	0	0	4	0	0	1	0	2	18	0	0	0	0	20	1	0	0	0	0	0	0	0	IE
IS	0	0	0	0	0	0	0	0	0	0	0	0	0	0	0	0	0	1	0	0	0	0	0	33	0	0	0	0	0	0	0	IS
IT	0	0	2	0	5	0	1	0	1	0	3	6	0	0	4	0	6	1	0	0	2	1	0	0	53	0	1	0	0	0	0	IT
KG	0	0	-0	0	0	0	0	0	-0	0	0	0	0	0	-0	0	-0	-0	0	0	-0	0	-0	0	0	39	57	0	-0	0	0	KG
KZ	0	0	0	1	0	0	0	1	0	0	0	0	0	0	0	0	0	0	0	0	0	0	0	0	0	2	208	0	0	0	0	KZ
LT	0	0	0	0	0	1	0	13	0	0	3	11	1	1	0	1	1	3	0	0	0	1	0	0	0	0	4	10	0	1	0	LT
LU	0	0	1	0	0	9	0	0	1	0	4	62	0	0	3	0	39	9	0	0	0	0	0	0	1	0	0	0	10	0	0	LU
LV	0	0	0	0	0	1	0	8	0	0	2	7	1	1	0	2	1	3	0	0	0	0	0	0	0	0	4	7	0	4	0	LV
MD	0	0	0	1	2	0	7	7	0	0	4	7	0	0	0	0	1	1	0	1	0	2	0	0	1	0	6	1	0	0	15	MD
ME	3	0	1	0	27	0	4	0	0	0	4	5	0	0	1	0	1	0	0	1	1	1	0	0	5	0	1	0	0	0	0	ME
MK	6	0	0	0	6	0	17	1	0	0	3	4	0	0	1	0	1	0	0	16	0	2	0	0	3	0	1	0	0	0	0	MK
MT	1	0	0	0	5	0	3	0	0	0	1	3	0	0	7	0	4	1	0	3	1	1	0	0	30	0	1	0	0	0	0	MT
NL	0	0	0	0	0	33	0	0	0	0	2	53	0	0	2	0	21	21	0	0	0	0	1	0	0	0	0	0	0	0	0	NL
NO	0	0	0	0	0	0	0	0	0	0	0	1	0	0	0	0	0	2	0	0	0	0	0	0	0	0	1	0	0	0	0	NO
PL	0	0	1	0	1	1	1	5	0	0	16	33	1	0	1	1	3	4	0	0	0	2	0	0	1	0	2	1	0	0	0	PL
PT	0	0	0	0	0	0	0	0	0	0	0	2	0	0	31	0	2	1	0	0	0	0	0	0	0	0	0	0	0	0	0	PT
RO	0	0	1	0	4	0	14	3	0	0	4	7	0	0	0	0	1	1	0	2	0	4	0	0	1	0	3	0	0	0	1	RO
RS	1	0	1	0	20	0	15	1	0	0	6	9	0	0	1	0	1	1	0	3	1	5	0	0	3	0	2	0	0	0	0	RS
RU	0	0	0	1	0	0	0	2	0	0	0	1	0	0	0	1	0	0	0	0	0	0	0	0	0	0	32	0	0	0	0	RU
SE	0	0	0	0	0	0	0	1	0	0	1	4	1	0	0	1	1	3	0	0	0	0	0	0	0	0	2	0	0	0	0	SE
SI	0	0	8	0	6	1	1	0	0	0	9	17	0	0	1	0	3	1	0	0	10	2	0	0	23	0	1	0	0	0	0	SI
SK	0	0	3	0	4	1	2	2	0	0	19	20	0	0	0	0	2	2	0	0	1	13	0	0	3	0	1	0	0	0	0	SK
TJ	0	0	-0	1	0	0	0	0	-0	0	0	0	0	0	0	0	0	0	0	0	-0	0	0	0	0	4	36	0	0	0	0	TJ
TM	0	0	0	6	0	0	0	0	0	0	0	0	0	0	0	0	0	0	1	0	0	0	0	0	0	1	96	0	0	0	0	TM
TR	0	1	0	3	0	0	3	1	0	1	0	1	0	0	0	0	0	0	2	3	0	0	0	0	1	0	1	0	0	0	0	TR
UA	0	0	0	2	1	0	3	9	0	0	3	7	0	0	0	0	1	1	1	1	0	1	0	0	1	0	12	1	0	0	1	UA
UZ	0	0	0	2	0	0	0	1	0	0	0	0	0	0	0	0	0	0	0	0	0	0	0	0	0	7	136	0	0	0	0	UZ
ATL	0	0	0	0	0	0	0	0	0	0	0	1	0	0	2	0	1	2	0	0	0	0	0	1	0	0	1	0	0	0	0	ATL
BAS	0	0	0	0	0	1	0	2	0	0	2	12	2	1	0	3	2	5	0	0	0	0	0	0	0	0	2	1	0	0	0	BAS
BLS	0	1	0	6	1	0	6	4	0	0	1	2	0	0	0	0	0	0	8	2	0	0	0	0	0	0	7	0	0	0	1	BLS
MED	1	0	0	0	4	0	5	1	0	1	2	3	0	0	9	0	5	1	0	8	1	1	0	0	17	0	1	0	0	0	0	MED
NOS	0	0	0	0	0	2	0	0	0	0	1	7	1	0	1	0	4	17	0	0	0	0	1	1	0	0	0	0	0	0	0	NOS
AST	0	0	0	3	0	0	0	0	0	1	0	0	0	0	0	0	0	0	0	0	0	0	0	0	0	1	26	0	0	0	0	AST
NOA	0	0	0	0	1	0	1	0	0	0	0	1	0	0	6	0	1	0	0	2	0	0	0	0	4	0	0	0	0	0	0	NOA
EXC	0	0	0	2	1	0	1	2	0	0	2	5	0	0	2	1	2	2	1	1	0	0	0	0	1	1	51	0	0	0	0	EXC
EU	0	0	2	0	2	2	4	1	0	0	6	19	1	0	10	1	7	4	0	2	1	2	1	0	6	0	1	1	0	0	0	EU
	AL	AM	AT	AZ	BA	BE	BG	BY	CH	CY	CZ	DE	DK	EE	ES	FI	FR	GB	GE	GR	HR	HU	IE	IS	IT	KG	KZ	LT	LU	LV	MD	

Table C.11 Cont.: 2021 country-to-country blame matrices for **PM2.5**.
Units: ng/m^3 per 15% emis. red. of SO_x. **Emitters →, Receptors ↓.**

	ME	MK	MT	NL	NO	PL	PT	RO	RS	RU	SE	SI	SK	TJ	TM	TR	UA	UZ	ATL	BAS	BLS	MED	NOS	AST	NOA	BIC	DMS	VOL	EXC	EU	
AL	33	67	0	0	0	10	0	5	122	1	0	0	1	0	0	7	4	0	0	0	0	6	0	1	6	8	6	29	335	52	AL
AM	0	0	0	0	0	0	0	0	1	6	0	0	0	0	2	76	2	1	0	0	0	0	0	156	2	9	1	6	245	2	AM
AT	1	0	0	0	0	17	0	2	15	2	0	4	2	0	0	1	3	0	0	0	0	1	0	0	1	8	3	2	134	106	AT
AZ	0	0	0	0	0	1	0	0	1	26	0	0	0	0	7	31	7	2	0	0	0	0	0	150	1	8	1	3	303	2	AZ
BA	24	3	0	0	0	20	0	5	110	2	0	1	2	0	0	2	4	0	0	0	0	3	0	0	3	8	4	12	302	66	BA
BE	0	0	0	7	0	6	0	0	1	1	0	0	0	0	0	0	1	0	2	0	0	1	4	0	1	10	19	1	161	141	BE
BG	6	16	0	0	0	17	0	22	102	8	0	0	1	0	0	23	22	0	0	0	1	2	0	1	3	8	7	8	326	137	BG
BY	1	1	0	1	0	48	0	2	9	17	1	0	1	0	0	8	20	0	0	1	0	0	0	1	1	7	5	1	174	74	BY
CH	0	0	0	0	0	3	0	1	2	1	0	0	0	0	0	1	1	0	0	0	0	1	0	0	2	9	3	2	78	50	CH
CY	2	5	0	0	0	2	0	1	9	7	0	0	0	0	0	603	9	0	0	0	1	16	0	75	17	11	39	35	695	58	CY
CZ	1	1	0	1	0	49	0	2	24	2	0	2	5	0	0	1	3	0	0	0	0	1	1	0	1	8	6	1	255	213	CZ
DE	0	0	0	5	0	19	0	1	3	2	0	0	0	0	0	1	2	0	1	0	0	0	2	0	1	9	12	1	181	162	DE
DK	0	0	0	3	1	16	0	0	2	2	1	0	0	0	0	1	1	0	1	2	0	0	3	0	0	8	21	0	94	72	DK
EE	0	0	0	0	1	14	0	1	3	12	2	0	0	0	0	4	6	0	0	1	0	0	0	0	0	6	7	0	73	37	EE
ES	1	0	0	0	0	1	8	0	2	0	0	0	0	0	0	0	0	0	5	0	0	8	0	0	19	14	17	5	86	80	ES
FI	0	0	0	0	1	4	0	0	1	18	2	0	0	0	0	2	2	0	0	1	0	0	0	0	0	5	7	0	50	21	FI
FR	1	0	0	1	0	3	0	1	4	1	0	0	0	0	0	0	1	0	2	0	0	3	1	0	3	11	18	4	87	71	FR
GB	0	0	0	1	0	4	0	0	0	0	0	0	0	0	0	0	0	0	3	0	0	0	2	0	0	10	28	0	92	20	GB
GE	0	1	0	0	0	1	0	1	2	15	0	0	0	0	2	73	6	1	0	0	1	0	0	67	1	7	4	4	258	3	GE
GL	0	0	0	0	0	0	0	0	0	0	0	0	0	0	0	0	0	0	0	0	0	0	0	0	0	23	1	0	0	0	GL
GR	8	37	0	0	0	10	0	8	71	5	0	0	1	0	0	55	13	0	0	0	1	10	0	1	6	8	14	34	294	93	GR
HR	7	2	0	0	0	25	0	7	98	2	0	3	2	0	0	1	4	0	0	0	0	5	0	0	2	8	5	10	250	103	HR
HU	5	4	0	0	0	55	0	19	111	3	0	2	8	0	0	3	6	0	0	0	0	1	0	0	1	8	4	5	312	165	HU
IE	0	0	0	1	0	2	0	0	0	0	0	0	0	0	0	0	0	0	3	0	0	0	1	0	0	11	33	0	51	32	IE
IS	0	0	0	0	0	0	0	0	0	0	0	0	0	0	0	0	0	0	0	0	0	0	0	0	0	11	18	0	35	0	IS
IT	4	3	0	0	0	8	0	2	24	1	0	1	1	0	0	2	3	0	0	0	0	13	0	0	9	8	13	51	136	92	IT
KG	0	0	0	0	0	0	0	0	0	2	0	-0	0	13	3	3	0	121	0	0	0	0	0	42	0	7	0	1	240	0	KG
KZ	0	0	0	0	0	2	0	0	0	41	0	0	0	1	2	3	5	15	0	0	0	0	0	20	0	9	1	1	283	3	KZ
LT	1	1	0	1	1	47	0	1	6	12	1	0	1	0	0	5	9	0	0	1	0	0	1	1	0	7	8	1	139	84	LT
LU	0	0	0	3	0	7	0	0	1	1	0	0	0	0	0	1	1	0	1	0	0	1	2	0	2	9	13	1	156	140	LU
LV	0	0	0	1	1	23	0	1	4	11	1	0	0	0	0	5	8	0	0	1	0	0	0	0	0	6	8	1	98	53	LV
MD	3	3	0	0	0	36	0	21	25	15	0	0	1	0	0	29	46	0	0	0	2	1	0	1	1	9	5	4	239	84	MD
ME	131	12	0	0	0	11	0	4	114	1	0	0	1	0	0	4	3	0	0	0	0	3	0	1	3	8	4	16	339	41	ME
MK	15	164	0	0	0	12	0	8	151	2	0	0	1	0	0	10	5	0	0	0	0	2	0	1	4	8	4	13	430	69	MK
MT	7	6	2	0	0	5	1	2	25	1	0	0	0	0	0	3	3	0	1	0	0	51	0	0	43	10	48	171	116	64	MT
NL	0	0	0	28	0	11	0	0	0	1	0	0	0	0	0	0	1	0	2	0	0	0	6	0	1	9	21	0	179	154	NL
NO	0	0	0	0	5	3	0	0	0	6	1	0	0	0	0	1	1	0	1	0	0	0	1	0	0	7	14	0	24	7	NO
PL	1	1	0	1	0	155	0	3	17	5	1	0	3	0	0	3	6	0	0	1	0	0	1	0	1	8	8	1	270	225	PL
PT	0	0	0	0	0	1	47	0	0	0	0	0	0	0	0	0	0	0	13	0	0	3	0	0	13	15	25	2	86	84	PT
RO	5	7	0	0	0	32	0	64	67	7	0	0	2	0	0	18	20	0	0	0	1	1	0	1	2	8	4	6	270	134	RO
RS	28	28	0	0	0	27	0	18	344	3	0	0	2	0	0	4	7	0	0	0	0	2	0	0	3	8	3	10	536	95	RS
RU	0	0	0	0	0	4	0	0	1	63	0	0	0	0	0	4	7	1	0	0	0	0	0	3	0	8	4	0	119	7	RU
SE	0	0	0	0	3	6	0	0	1	6	4	0	0	0	0	1	2	0	1	1	0	0	1	0	0	5	9	0	38	21	SE
SI	1	1	0	0	0	20	0	4	38	2	0	25	2	0	0	1	4	0	0	0	0	4	0	0	1	7	4	6	182	126	SI
SK	3	2	0	1	0	75	0	8	52	3	0	1	21	0	0	3	5	0	0	0	0	1	0	0	1	7	4	3	248	172	SK
TJ	0	0	0	0	0	0	0	0	0	3	0	-0	0	79	13	5	0	91	0	0	0	0	0	50	0	9	0	1	232	0	TJ
TM	0	0	0	0	0	1	0	0	1	21	0	0	0	4	45	8	6	40	0	0	0	0	0	79	0	10	1	2	233	2	TM
TR	1	3	0	0	0	3	0	2	9	9	0	0	0	0	0	533	12	0	0	0	2	3	0	88	5	11	10	15	590	14	TR
UA	1	2	0	0	0	34	0	6	14	29	0	0	1	0	1	25	64	0	0	0	1	1	0	3	1	8	4	3	225	61	UA
UZ	0	0	0	0	0	1	0	0	0	22	0	0	0	14	15	5	5	161	0	0	0	0	0	35	0	10	1	1	371	2	UZ
ATL	0	0	0	0	0	1	1	0	0	4	0	0	0	0	0	0	0	0	3	0	0	0	0	0	3	17	34	0	15	7	ATL
BAS	0	0	0	1	1	18	0	0	3	8	3	0	0	0	0	2	3	0	0	3	0	0	1	0	0	6	12	0	75	48	BAS
BLS	1	3	0	0	0	11	0	5	13	40	0	0	0	0	1	134	49	0	0	0	9	1	0	12	1	7	18	5	298	30	BLS
MED	6	7	0	0	0	6	1	3	26	4	0	0	0	0	0	101	7	0	1	0	1	30	0	11	31	10	38	85	218	61	MED
NOS	0	0	0	2	1	4	0	0	0	1	0	0	0	0	0	0	0	0	2	0	0	0	4	0	0	9	30	0	45	22	NOS
AST	0	0	0	0	0	0	0	0	1	5	0	0	0	1	7	46	2	7	0	0	0	1	0	297	3	15	2	5	101	2	AST
NOA	2	2	0	0	0	1	2	1	7	1	0	0	0	0	0	17	2	0	2	0	0	9	0	3	121	18	17	33	52	19	NOA
EXC	1	1	0	0	0	9	0	2	8	35	0	0	0	1	2	28	8	9	0	0	0	1	0	13	1	9	6	3	184	30	EXC
EU	2	3	0	1	1	24	2	6	19	4	1	1	1	0	0	6	4	0	1	0	0	3	1	0	4	9	12	7	145	98	EU
	ME	MK	MT	NL	NO	PL	PT	RO	RS	RU	SE	SI	SK	TJ	TM	TR	UA	UZ	ATL	BAS	BLS	MED	NOS	AST	NOA	BIC	DMS	VOL	EXC	EU	

Table C.12: 2021 country-to-country blame matrices for **PM2.5**.
Units: ng/m^3 per 15% emis. red. of NO_x. **Emitters →, Receptors ↓.**

	AL	AM	AT	AZ	BA	BE	BG	BY	CH	CY	CZ	DE	DK	EE	ES	FI	FR	GB	GE	GR	HR	HU	IE	IS	IT	KG	KZ	LT	LU	LV	MD	
AL	53	0	1	0	3	0	2	0	0	0	1	2	0	0	1	0	1	0	0	6	2	1	0	0	9	0	0	0	0	0	0	AL
AM	0	66	0	77	0	0	0	0	0	0	0	0	0	0	0	0	0	0	8	0	0	0	0	0	0	0	0	0	0	0	0	AM
AT	0	0	89	0	1	2	0	0	8	0	14	60	0	0	1	0	10	2	0	0	5	6	0	0	29	0	0	0	0	0	0	AT
AZ	0	11	0	219	0	0	0	0	0	0	0	0	0	0	0	0	0	0	11	0	0	0	0	0	0	0	2	0	0	0	0	AZ
BA	0	0	7	0	43	1	1	0	1	0	4	11	0	0	1	0	3	1	0	0	11	8	0	0	10	-0	0	0	0	0	0	BA
BE	0	0	1	0	0	42	0	0	3	0	3	87	2	0	5	0	102	42	0	0	0	0	3	0	3	0	0	0	3	0	0	BE
BG	0	0	1	0	1	0	41	1	0	0	1	2	0	0	0	0	1	0	0	4	1	2	0	0	1	0	0	0	0	0	2	BG
BY	0	0	1	0	0	1	0	33	0	0	3	13	1	0	0	1	2	3	0	0	0	2	0	0	1	0	0	5	0	1	1	BY
CH	0	0	11	0	0	2	0	0	125	0	2	64	0	0	1	0	36	4	0	0	0	0	0	0	33	0	0	0	0	0	0	CH
CY	0	0	0	0	0	0	0	0	0	20	0	0	0	-0	0	-0	0	0	0	9	0	0	0	0	1	0	0	0	0	-0	0	CY
CZ	0	0	31	0	1	3	0	1	5	0	73	86	1	0	1	0	14	5	0	0	4	11	0	0	7	0	0	0	1	0	0	CZ
DE	0	0	15	0	0	12	0	0	11	0	9	181	3	0	2	0	34	19	0	0	0	1	1	0	3	0	0	0	2	0	0	DE
DK	0	0	1	0	0	9	0	1	1	0	3	81	35	0	1	1	15	25	0	0	0	0	1	0	0	0	0	1	1	0	0	DK
EE	0	0	0	0	0	1	0	5	0	0	1	6	1	4	0	2	1	2	0	0	0	0	0	0	0	0	0	4	0	4	0	EE
ES	0	0	0	0	0	0	0	0	0	0	0	1	0	0	84	0	5	1	0	0	0	0	0	0	1	-0	-0	0	0	0	0	ES
FI	0	0	0	0	0	0	0	1	0	0	0	2	1	0	0	5	0	1	0	0	0	0	0	0	0	0	0	0	0	0	0	FI
FR	0	0	2	0	0	9	0	0	5	0	2	32	0	0	8	0	88	14	0	0	0	0	1	0	6	0	0	0	1	0	0	FR
GB	0	0	0	0	0	6	0	0	0	0	1	19	2	0	1	0	16	89	0	0	0	0	7	0	1	0	0	0	0	0	0	GB
GE	0	8	0	53	0	0	0	0	0	0	0	0	0	0	0	0	0	0	43	0	0	0	0	0	0	0	0	0	0	0	0	GE
GL	0	-0	0	0	0	0	0	-0	-0	-0	0	0	0	0	-0	0	0	0	0	0	0	0	0	0	0	0	0	-0	0	-0	0	GL
GR	2	0	0	0	1	0	6	0	0	0	0	0	0	-0	0	-0	1	0	0	40	0	0	0	0	3	0	0	0	0	0	0	GR
HR	0	0	18	0	19	1	1	0	1	0	8	17	0	0	1	0	5	1	0	0	39	16	0	0	40	0	0	0	0	0	0	HR
HU	0	0	23	0	7	1	2	1	2	0	14	26	0	0	1	0	5	2	0	0	15	84	0	0	18	0	0	0	0	0	0	HU
IE	0	0	0	0	0	4	0	0	0	0	1	12	1	0	1	0	10	58	0	0	0	0	46	0	0	0	0	0	0	0	0	IE
IS	0	0	-0	0	0	0	0	0	0	0	0	0	0	0	0	0	0	1	0	0	0	0	0	-0	0	0	0	0	0	0	0	IS
IT	0	0	9	0	2	1	0	0	4	0	2	9	0	0	3	0	9	1	0	0	4	2	0	0	246	0	0	0	0	0	0	IT
KG	0	0	0	0	0	0	0	-0	0	0	0	0	0	-0	0	-0	0	0	0	0	0	0	0	0	0	24	2	-0	0	-0	0	KG
KZ	0	0	0	0	0	0	0	0	0	0	0	0	0	0	0	0	0	0	0	0	0	0	0	0	0	1	9	0	0	0	0	KZ
LT	0	0	1	0	0	2	0	13	0	0	4	20	3	1	0	1	3	5	0	0	0	2	0	0	1	0	0	19	0	3	0	LT
LU	0	0	3	0	0	31	0	0	5	0	3	113	1	0	3	0	91	21	0	0	0	0	1	0	4	0	0	0	9	0	0	LU
LV	0	0	1	0	0	1	0	10	0	0	2	10	2	1	0	1	2	4	0	0	0	1	0	0	0	0	0	11	0	7	0	LV
MD	0	0	1	0	0	0	4	5	0	0	3	8	0	0	0	0	1	1	0	1	0	3	0	0	1	0	0	1	0	0	31	MD
ME	4	0	1	0	7	0	1	0	0	0	1	2	0	0	0	0	1	0	0	1	2	1	0	0	5	0	0	0	0	0	0	ME
MK	5	0	0	0	1	0	6	0	0	0	0	1	0	0	0	0	1	0	0	14	0	1	0	0	2	0	0	0	0	0	0	MK
MT	0	0	0	0	1	0	0	-0	0	0	0	0	0	-0	2	-0	3	0	0	1	1	0	0	0	18	0	-0	-0	0	-0	0	MT
NL	0	0	1	0	0	34	0	0	2	0	3	111	4	0	4	0	64	59	0	0	0	0	4	0	1	0	0	0	2	0	0	NL
NO	0	0	0	0	0	0	0	0	0	0	0	2	1	0	0	0	0	1	0	0	0	0	0	0	0	0	0	0	0	0	0	NO
PL	0	0	5	0	1	2	0	4	1	0	21	53	3	0	1	1	7	6	0	0	1	6	0	0	3	0	0	2	0	1	0	PL
PT	0	0	0	0	0	0	0	0	0	0	0	1	0	0	31	-0	2	1	0	0	0	0	0	0	0	0	0	0	0	0	0	PT
RO	0	0	2	0	1	0	10	2	0	0	3	6	0	0	0	0	2	1	0	1	1	9	0	0	2	0	0	0	0	0	3	RO
RS	3	0	7	0	12	1	8	1	1	0	6	11	0	0	1	0	3	1	0	2	6	19	0	0	7	-0	0	0	0	0	1	RS
RU	0	0	0	1	0	0	0	2	0	0	0	1	0	0	0	0	0	0	0	0	0	0	0	0	0	0	3	0	0	0	0	RU
SE	0	0	0	0	0	1	0	0	0	0	0	9	3	0	0	1	2	3	0	0	0	0	0	0	0	0	0	0	0	0	0	SE
SI	0	0	49	0	4	1	0	0	3	0	9	24	0	0	1	0	7	2	0	0	29	9	0	0	118	0	0	0	0	0	0	SI
SK	0	0	14	0	2	1	1	1	1	0	17	22	0	0	0	0	5	2	0	0	5	35	0	0	9	0	0	0	0	0	0	SK
TJ	0	0	0	0	0	0	0	-0	0	0	-0	0	0	-0	0	-0	0	0	0	0	0	0	0	0	0	3	2	-0	0	-0	0	TJ
TM	0	0	0	2	0	0	0	0	0	0	0	0	0	0	0	0	0	0	0	0	0	0	0	0	0	0	7	0	0	0	0	TM
TR	0	3	0	2	0	0	1	0	0	0	0	1	0	0	0	0	0	0	1	3	0	0	0	0	1	0	0	0	0	0	0	TR
UA	0	0	1	1	0	0	1	7	0	0	2	7	0	0	0	0	1	1	0	0	0	3	0	0	1	0	1	1	0	0	4	UA
UZ	0	0	0	1	0	0	0	0	0	0	0	0	0	0	0	0	0	0	0	0	0	0	0	0	0	4	13	0	0	0	0	UZ
ATL	0	0	0	0	0	0	0	0	0	0	0	1	0	0	1	0	2	2	0	0	0	0	1	0	0	0	0	0	0	0	0	ATL
BAS	0	0	1	0	0	2	0	1	0	0	2	23	5	0	0	1	4	6	0	0	0	0	0	0	0	0	0	1	0	1	0	BAS
BLS	0	0	0	1	0	0	2	1	0	0	0	0	0	0	0	-0	0	0	3	1	0	0	0	0	0	0	0	0	0	0	1	BLS
MED	1	0	0	0	1	0	1	0	0	0	0	0	0	-0	4	-0	3	0	0	4	1	0	0	0	16	0	0	-0	0	-0	0	MED
NOS	0	0	0	0	0	5	0	0	0	0	1	21	3	0	1	0	14	23	0	0	0	0	1	0	0	0	0	0	0	0	0	NOS
AST	0	0	0	2	0	0	0	0	0	0	0	0	0	-0	0	-0	0	0	0	0	0	0	0	0	0	0	2	0	0	0	0	AST
NOA	0	0	0	0	0	0	0	-0	0	0	0	0	0	-0	3	-0	1	0	0	1	0	0	0	0	2	0	-0	-0	0	-0	0	NOA
EXC	0	0	2	2	0	1	1	1	1	0	1	9	0	0	3	0	5	3	0	1	0	1	0	0	5	1	3	0	0	0	0	EXC
EU	0	0	6	0	1	4	2	1	3	0	6	34	2	0	13	1	19	7	0	2	2	4	1	0	22	0	0	1	1	0	0	EU
	AL	AM	AT	AZ	BA	BE	BG	BY	CH	CY	CZ	DE	DK	EE	ES	FI	FR	GB	GE	GR	HR	HU	IE	IS	IT	KG	KZ	LT	LU	LV	MD	

Table C.12 Cont.: 2021 country-to-country blame matrices for **PM2.5**.
Units: ng/m^3 per 15% emis. red. of NO$_x$. **Emitters →, Receptors ↓.**

	ME	MK	MT	NL	NO	PL	PT	RO	RS	RU	SE	SI	SK	TJ	TM	TR	UA	UZ	ATL	BAS	BLS	MED	NOS	AST	NOA	BIC	DMS	VOL	EXC	EU	
AL	5	7	0	0	0	1	0	2	25	0	0	0	0	0	0	1	1	0	0	0	0	11	0	0	1	4	0	0	125	29	AL
AM	0	0	0	0	0	0	0	0	0	1	0	0	0	0	1	19	1	0	0	0	0	0	0	50	0	4	0	0	175	1	AM
AT	0	0	0	2	0	8	0	1	1	1	0	9	2	0	0	0	1	0	1	1	0	2	3	0	0	4	0	0	255	239	AT
AZ	0	0	0	0	0	0	0	0	0	11	0	0	0	0	4	6	1	1	0	0	1	0	0	56	0	5	0	0	269	1	AZ
BA	2	0	0	1	0	6	0	3	11	1	0	1	2	0	0	0	2	0	0	1	0	4	1	0	1	4	0	0	131	70	BA
BE	0	0	0	52	2	5	0	0	0	1	1	0	1	0	0	0	1	0	6	2	0	2	57	0	0	11	0	0	360	310	BE
BG	0	1	0	0	0	4	0	23	11	3	0	0	1	0	0	5	9	0	0	0	3	2	0	0	1	4	0	0	116	81	BG
BY	0	0	0	2	1	38	0	3	1	18	1	0	2	0	0	1	19	0	1	5	0	0	4	0	0	3	0	0	156	78	BY
CH	0	0	0	2	0	1	0	0	0	0	0	1	0	0	0	0	0	0	1	0	0	2	3	0	0	5	0	0	286	156	CH
CY	0	0	0	0	0	0	0	0	0	1	-0	0	0	0	0	43	1	0	0	0	1	30	0	9	2	6	0	0	78	32	CY
CZ	0	0	0	4	0	28	0	2	2	2	1	3	9	0	0	0	2	0	1	2	0	1	6	0	0	5	0	0	298	280	CZ
DE	0	0	0	26	1	10	0	0	0	2	2	0	1	0	0	0	1	0	3	7	0	1	30	0	0	7	0	0	339	305	DE
DK	0	0	0	22	5	12	0	0	0	2	6	0	0	0	0	0	1	0	3	31	0	0	59	0	0	6	0	0	224	189	DK
EE	0	0	0	1	1	9	0	0	0	12	3	0	0	0	0	0	2	0	0	9	0	0	3	0	0	2	0	0	61	37	EE
ES	0	0	0	0	0	0	6	0	0	0	0	0	0	0	0	0	0	0	6	0	0	12	1	0	3	5	0	0	100	99	ES
FI	0	0	0	1	1	2	0	0	0	4	2	0	0	0	0	0	1	0	0	4	0	0	1	0	0	1	0	0	23	16	FI
FR	0	0	0	8	0	1	0	0	0	1	0	0	0	0	0	0	0	0	5	1	0	4	20	0	1	5	0	0	182	161	FR
GB	0	0	0	14	1	3	0	0	0	1	1	0	0	0	0	0	0	0	9	3	0	0	41	0	0	6	0	0	163	72	GB
GE	0	0	0	0	0	0	0	0	0	5	0	0	0	0	1	11	1	0	0	0	1	0	0	11	0	3	0	0	124	1	GE
GL	0	0	-0	0	0	0	-0	0	0	0	0	0	0	-0	-0	0	0	0	0	0	0	0	0	0	-0	5	0	0	0	0	GL
GR	0	4	0	0	0	1	0	2	5	1	-0	0	0	0	0	6	2	0	0	0	1	13	0	0	1	4	0	0	78	56	GR
HR	0	0	0	1	0	8	0	4	12	1	0	9	3	0	0	0	2	0	0	1	0	11	2	0	0	4	0	0	209	170	HR
HU	0	0	0	2	0	24	0	31	28	2	0	6	18	0	0	0	6	0	1	1	0	4	2	0	0	5	0	0	322	272	HU
IE	0	0	0	7	1	2	0	0	0	0	0	0	0	0	0	0	0	0	15	2	0	0	21	0	0	5	0	0	142	83	IE
IS	0	0	0	0	0	0	0	0	0	0	0	0	0	0	0	0	0	0	0	0	0	0	0	0	0	1	0	0	1	0	IS
IT	0	0	0	1	0	2	0	1	2	0	0	6	1	0	0	0	1	0	1	0	0	33	1	0	2	6	0	0	308	296	IT
KG	0	0	0	0	0	0	0	0	0	-0	-0	0	0	4	0	0	0	26	0	-0	0	0	0	18	0	2	0	0	57	0	KG
KZ	0	0	0	0	0	0	0	0	0	18	0	0	0	0	1	0	0	2	0	0	0	0	0	16	0	4	0	0	33	1	KZ
LT	0	0	0	4	1	47	0	1	0	13	3	0	2	0	0	0	7	0	1	14	0	0	7	0	0	3	0	0	160	118	LT
LU	0	0	0	20	1	2	0	0	0	1	1	0	0	0	0	0	0	0	4	1	0	2	25	0	0	7	0	0	314	286	LU
LV	0	0	0	2	1	19	0	1	0	11	2	0	1	0	0	0	4	0	1	10	0	0	5	0	0	3	0	0	95	64	LV
MD	0	0	0	1	0	19	0	48	3	9	0	0	2	0	0	4	57	0	0	1	4	1	1	0	0	4	0	0	207	95	MD
ME	25	0	0	0	0	1	0	2	14	0	0	0	0	0	0	0	1	0	0	0	0	5	0	0	1	4	0	0	72	19	ME
MK	1	18	0	0	0	1	0	3	25	0	0	0	0	0	0	2	1	0	0	0	0	3	0	0	1	4	0	0	84	30	MK
MT	0	0	1	0	0	0	0	0	1	-0	-0	0	0	0	0	0	0	0	1	-0	0	60	0	0	11	5	0	0	31	28	MT
NL	0	0	0	91	2	12	0	0	0	2	2	0	0	0	0	0	1	0	8	6	0	1	95	0	1	15	0	0	403	337	NL
NO	0	0	0	1	3	0	0	0	0	1	1	0	0	0	0	0	0	0	1	1	0	0	3	0	0	1	0	0	11	6	NO
PL	0	0	0	6	1	120	0	3	1	5	2	1	6	0	0	0	8	0	1	9	0	1	8	0	0	5	0	0	272	244	PL
PT	0	0	0	0	0	0	48	0	0	0	0	0	0	0	0	0	0	0	17	0	0	2	0	0	2	4	0	0	83	82	PT
RO	0	0	0	1	0	12	0	92	11	3	0	0	3	0	0	2	16	0	0	1	2	2	1	0	0	4	0	0	187	146	RO
RS	3	3	0	1	0	11	0	20	85	1	0	1	4	0	0	1	4	0	1	1	0	3	1	0	1	5	0	0	223	108	RS
RU	0	0	0	0	0	2	0	0	0	48	0	0	0	0	0	0	3	0	0	1	0	0	0	1	0	2	0	0	62	5	RU
SE	0	0	0	2	1	3	0	0	0	1	5	0	0	0	0	0	0	0	1	7	0	0	5	0	0	2	0	0	32	26	SE
SI	0	0	0	2	0	7	0	2	4	1	0	68	2	0	0	0	2	0	1	1	0	16	2	0	0	5	0	0	346	330	SI
SK	0	0	0	2	0	26	0	10	6	2	0	3	31	0	0	0	6	0	1	1	0	2	2	0	0	4	0	0	203	182	SK
TJ	0	0	0	0	0	-0	0	0	0	-0	-0	-0	0	36	3	0	0	23	0	-0	0	0	0	24	0	2	0	0	67	0	TJ
TM	0	0	0	0	0	0	0	0	0	5	-0	0	0	1	27	0	0	18	0	0	0	0	0	21	0	4	0	0	61	0	TM
TR	0	0	0	0	0	1	0	1	1	4	0	0	0	0	0	91	3	0	0	0	3	8	0	16	1	6	0	0	115	9	TR
UA	0	0	0	1	0	20	0	11	1	24	0	0	2	0	0	3	65	0	0	2	3	1	2	1	0	4	0	0	164	54	UA
UZ	0	0	0	0	0	0	0	0	0	7	0	0	0	5	7	0	0	46	0	0	0	0	0	9	0	5	0	0	85	1	UZ
ATL	0	0	0	1	0	0	0	0	0	0	0	0	0	0	0	0	0	0	3	0	0	0	2	0	0	2	0	0	9	6	ATL
BAS	0	0	0	5	1	12	0	0	0	4	4	0	0	0	0	-0	1	0	1	14	0	0	10	0	0	3	0	0	77	64	BAS
BLS	0	0	0	0	0	1	0	4	1	15	0	0	0	0	0	19	10	0	0	0	13	3	0	1	0	3	0	0	62	10	BLS
MED	0	0	0	0	0	0	0	0	1	0	-0	0	0	0	0	5	1	0	1	0	0	31	0	1	5	4	0	0	41	32	MED
NOS	0	0	0	12	1	3	0	0	0	1	1	0	0	0	0	0	0	0	3	4	0	0	24	0	0	4	0	0	88	62	NOS
AST	0	0	0	0	0	0	0	0	0	1	-0	0	0	1	3	4	0	1	0	0	0	1	0	152	0	5	0	0	14	1	AST
NOA	0	0	0	0	0	0	1	0	0	0	-0	0	0	0	0	1	0	0	2	0	0	9	0	1	26	5	0	0	10	8	NOA
EXC	0	0	0	2	0	5	0	2	1	23	0	0	1	1	1	4	5	2	1	1	0	2	3	5	0	3	0	0	92	42	EXC
EU	0	0	0	6	1	15	2	7	2	2	1	1	2	0	0	1	3	0	3	3	0	6	10	0	1	4	0	0	174	153	EU
	ME	MK	MT	NL	NO	PL	PT	RO	RS	RU	SE	SI	SK	TJ	TM	TR	UA	UZ	ATL	BAS	BLS	MED	NOS	AST	NOA	BIC	DMS	VOL	EXC	EU	

Table C.13: 2021 country-to-country blame matrices for **PM2.5**.
Units: ng/m^3 per 15% emis. red. of NH_3. **Emitters →, Receptors ↓.**

	AL	AM	AT	AZ	BA	BE	BG	BY	CH	CY	CZ	DE	DK	EE	ES	FI	FR	GB	GE	GR	HR	HU	IE	IS	IT	KG	KZ	LT	LU	LV	MD	
AL	66	0	1	0	1	0	1	0	0	-0	1	2	0	0	1	0	0	0	0	5	1	3	0	-0	5	0	-0	0	0	0	0	AL
AM	0	125	0	45	0	0	0	0	0	-0	0	0	0	0	0	0	0	0	9	0	0	0	0	-0	0	0	-0	0	0	0	0	AM
AT	0	0	68	0	1	1	0	0	3	-0	8	21	0	0	1	0	3	1	0	0	4	8	0	0	11	-0	-0	0	0	0	0	AT
AZ	0	11	0	206	0	0	0	0	0	-0	0	0	0	0	0	0	0	-0	8	0	0	0	0	-0	0	0	0	0	0	0	0	AZ
BA	1	0	4	0	89	0	1	0	1	0	3	7	0	0	1	0	2	1	0	0	15	9	0	0	8	-0	-0	0	0	0	0	BA
BE	-0	0	0	0	0	106	0	0	1	-0	1	38	1	0	2	0	38	17	0	-0	0	0	2	0	2	-0	-0	0	2	0	0	BE
BG	1	0	1	0	1	0	76	1	0	0	1	2	0	0	0	0	1	0	0	4	1	5	0	-0	3	0	-0	0	0	0	1	BG
BY	0	0	1	0	0	1	0	57	0	0	4	14	2	0	0	0	2	2	0	0	1	3	0	0	1	0	0	3	0	1	1	BY
CH	-0	0	2	0	0	1	0	0	62	-0	0	15	0	0	1	0	9	1	0	-0	0	0	0	-0	15	0	-0	0	0	0	0	CH
CY	0	0	0	0	-0	0	0	0	0	36	0	0	0	-0	0	0	0	0	0	-0	0	0	0	-0	0	-0	-0	0	0	0	0	CY
CZ	0	0	15	0	1	2	0	0	2	-0	97	51	2	0	1	0	8	3	0	0	4	15	0	0	5	-0	-0	0	0	0	0	CZ
DE	0	0	6	0	0	9	0	0	4	-0	9	154	2	0	1	0	19	9	0	0	0	1	1	0	2	0	0	0	1	0	0	DE
DK	0	0	1	0	0	4	0	0	0	-0	4	54	70	0	1	0	9	15	0	0	0	2	2	0	0	0	0	0	0	0	0	DK
EE	0	0	0	0	0	1	0	9	0	-0	2	10	2	18	0	1	2	2	0	0	0	1	0	0	0	0	0	7	0	7	0	EE
ES	-0	0	0	-0	-0	0	0	0	0	-0	0	0	0	0	53	0	3	0	0	0	0	0	0	0	1	-0	-0	0	0	0	0	ES
FI	0	0	0	0	0	0	0	3	0	-0	0	4	1	1	0	13	1	1	0	0	0	0	0	-0	0	0	0	1	0	1	0	FI
FR	0	0	1	0	0	5	0	0	2	-0	1	11	0	0	5	0	60	6	0	0	0	0	1	0	5	-0	-0	0	0	0	0	FR
GB	0	-0	0	-0	0	6	0	0	0	-0	0	14	2	0	1	0	13	98	-0	-0	0	0	4	0	1	-0	-0	0	0	0	0	GB
GE	0	9	0	30	0	0	0	0	0	-0	0	0	0	0	0	0	0	0	55	0	0	0	0	-0	0	0	-0	0	0	0	0	GE
GL	-0	0	0	0	-0	0	-0	0	0	-0	-0	0	-0	-0	0	-0	-0	-0	0	-0	-0	-0	-0	-0	0	0	0	-0	0	-0	0	GL
GR	2	0	0	0	0	0	5	0	0	0	1	1	0	0	0	0	0	0	0	47	1	2	0	-0	2	0	-0	0	0	0	0	GR
HR	0	0	7	0	20	0	1	0	1	-0	5	9	0	0	1	0	2	1	0	0	69	14	0	-0	32	-0	-0	0	0	0	0	HR
HU	0	0	9	0	4	1	2	0	1	-0	10	14	1	0	1	0	2	1	0	0	14	124	0	0	12	-0	-0	0	0	0	0	HU
IE	0	-0	0	-0	0	2	0	0	0	0	0	7	1	0	0	0	9	23	-0	0	0	0	36	0	0	0	-0	0	0	0	0	IE
IS	-0	0	0	-0	-0	0	-0	0	0	-0	-0	0	0	-0	0	-0	0	0	0	-0	0	-0	0	1	0	0	0	0	0	-0	0	IS
IT	0	0	3	0	1	0	0	0	1	-0	1	2	0	0	2	0	2	0	0	0	2	1	0	-0	140	-0	-0	0	0	0	0	IT
KG	-0	0	0	0	-0	0	-0	0	0	-0	0	0	0	0	0	0	0	-0	0	-0	-0	0	-0	-0	0	32	2	0	0	0	0	KG
KZ	-0	0	0	0	0	0	0	0	0	-0	0	0	0	0	0	0	0	0	0	-0	0	0	0	-0	0	1	20	0	0	0	0	KZ
LT	0	0	1	0	0	2	0	16	1	-0	4	22	4	0	1	0	4	3	0	0	1	3	1	0	1	0	0	43	0	2	0	LT
LU	-0	0	1	0	-0	24	0	0	2	-0	1	67	1	0	2	0	42	8	0	-0	0	0	1	0	3	0	-0	0	37	0	0	LU
LV	0	0	1	0	0	1	0	14	0	-0	3	15	3	1	0	0	3	3	0	0	0	2	0	0	1	0	0	21	0	25	0	LV
MD	0	0	1	0	0	0	2	2	0	0	2	6	0	0	0	0	1	0	0	1	1	4	0	0	1	0	0	0	0	0	44	MD
ME	7	0	2	0	8	0	1	0	0	0	2	4	0	0	1	0	1	0	0	1	3	6	0	0	5	0	0	0	0	0	0	ME
MK	9	0	1	0	2	0	5	0	0	-0	2	3	0	0	1	0	1	0	0	15	2	7	0	0	4	0	0	0	0	0	0	MK
MT	0	0	0	0	0	0	0	0	0	0	0	1	0	0	3	0	1	0	0	0	0	1	0	0	12	0	-0	0	0	0	0	MT
NL	-0	0	0	0	-0	34	-0	0	1	-0	1	58	2	0	2	0	24	30	0	-0	0	0	3	0	1	-0	-0	0	1	0	0	NL
NO	0	0	0	0	0	0	0	0	0	-0	0	2	1	0	0	0	1	1	0	0	0	0	0	-0	0	0	0	0	0	0	0	NO
PL	0	0	4	0	1	2	0	2	1	-0	21	46	3	0	1	0	7	3	0	0	2	10	1	0	3	0	0	1	0	0	0	PL
PT	-0	-0	0	-0	-0	0	-0	0	0	-0	0	0	0	0	14	0	1	0	-0	-0	0	0	0	0	0	0	-0	0	0	0	0	PT
RO	0	0	1	0	1	0	5	1	0	0	2	4	0	0	0	0	1	0	0	1	1	9	0	-0	3	0	0	0	0	0	2	RO
RS	3	0	4	0	8	0	10	0	1	-0	4	7	0	0	1	0	1	0	0	2	7	19	0	0	6	-0	-0	0	0	0	1	RS
RU	0	0	0	0	0	0	0	2	0	-0	0	1	0	0	0	0	0	0	0	0	0	0	0	-0	0	0	2	0	0	0	0	RU
SE	0	0	0	0	0	1	0	1	0	-0	1	11	5	0	0	1	2	2	0	0	0	0	0	-0	0	0	0	0	0	0	0	SE
SI	0	0	18	0	2	0	0	0	1	-0	5	10	0	0	1	0	2	1	0	0	19	6	0	0	78	-0	-0	0	0	0	0	SI
SK	0	0	8	0	2	1	1	0	1	-0	18	21	1	0	1	0	3	1	0	0	6	54	0	0	9	-0	0	0	0	0	0	SK
TJ	-0	0	0	0	-0	0	-0	-0	0	-0	0	0	0	-0	-0	-0	-0	-0	-0	-0	-0	-0	-0	-0	0	3	0	0	0	-0	0	TJ
TM	-0	0	0	1	-0	0	-0	0	0	-0	0	0	0	0	0	0	0	-0	0	-0	0	0	0	-0	0	1	3	0	0	0	0	TM
TR	0	1	0	0	0	0	1	0	0	0	0	0	0	0	0	0	0	0	0	1	0	0	0	-0	0	0	-0	0	0	0	0	TR
UA	0	0	1	0	0	0	1	5	0	0	3	9	1	0	0	0	1	1	0	0	1	4	0	0	1	0	1	1	0	0	3	UA
UZ	-0	0	0	0	-0	0	-0	0	0	-0	0	0	0	0	-0	0	0	0	0	-0	0	0	0	-0	0	5	8	0	0	0	0	UZ
ATL	0	0	0	0	0	0	0	0	0	-0	0	1	0	0	1	-0	2	2	0	0	0	0	1	-0	0	0	-0	0	0	0	0	ATL
BAS	0	0	1	0	0	2	0	3	0	-0	4	37	14	1	1	2	6	5	0	0	0	1	1	0	0	0	0	3	0	2	0	BAS
BLS	0	0	0	1	0	0	3	1	0	0	0	1	0	0	0	0	0	0	4	1	0	1	0	-0	1	0	0	0	0	0	1	BLS
MED	1	0	0	0	0	0	1	0	0	0	0	1	0	0	6	0	1	0	0	3	1	1	0	-0	9	0	-0	0	0	0	0	MED
NOS	0	0	0	0	0	9	0	0	0	-0	1	27	8	0	1	0	20	40	0	0	0	0	3	-0	0	0	-0	0	0	0	0	NOS
AST	0	0	0	1	-0	0	0	0	0	0	0	0	0	0	0	0	0	0	0	0	0	0	0	-0	0	0	0	0	0	0	0	AST
NOA	0	0	0	0	0	0	0	0	0	0	0	0	0	0	1	0	0	0	0	0	0	0	0	-0	0	0	-0	0	0	0	0	NOA
EXC	0	0	1	1	0	1	1	2	0	0	1	7	1	0	2	0	3	2	0	0	1	2	0	0	3	1	4	1	0	0	0	EXC
EU	0	0	3	0	1	3	3	1	1	0	5	25	2	0	8	1	12	3	0	2	2	6	1	0	13	0	0	1	0	1	0	EU
	AL	AM	AT	AZ	BA	BE	BG	BY	CH	CY	CZ	DE	DK	EE	ES	FI	FR	GB	GE	GR	HR	HU	IE	IS	IT	KG	KZ	LT	LU	LV	MD	

Table C.13 Cont.: 2021 country-to-country blame matrices for **PM2.5**.
Units: ng/m^3 per 15% emis. red. of NH_3. **Emitters →, Receptors ↓.**

	ME	MK	MT	NL	NO	PL	PT	RO	RS	RU	SE	SI	SK	TJ	TM	TR	UA	UZ	ATL	BAS	BLS	MED	NOS	AST	NOA	BIC	DMS	VOL	EXC	EU	
AL	1	2	0	0	0	2	0	3	26	0	0	0	1	-0	0	0	1	0	0	0	0	0	0	-0	0	0	0	0	126	27	AL
AM	0	0	-0	0	0	0	0	0	-0	1	0	0	0	-0	0	32	0	0	0	0	0	0	0	28	0	1	0	0	212	0	AM
AT	0	0	0	1	0	3	0	2	3	0	0	5	2	-0	-0	0	0	0	0	0	0	0	0	-0	0	0	0	0	148	139	AT
AZ	0	0	-0	0	0	0	-0	0	0	8	0	0	0	0	2	9	0	1	0	0	0	0	0	31	0	0	0	0	246	0	AZ
BA	2	0	0	1	0	4	0	6	39	1	0	1	2	-0	0	0	1	0	0	0	0	0	0	-0	-0	0	0	0	197	64	BA
BE	-0	-0	0	32	0	1	0	0	-0	0	0	0	0	-0	0	0	0	0	0	0	0	0	0	-0	-0	1	0	0	246	227	BE
BG	0	1	0	0	0	2	0	32	20	1	0	0	1	-0	0	10	5	0	0	0	0	0	0	0	0	0	0	0	175	133	BG
BY	0	0	0	2	0	41	0	3	1	11	1	0	2	0	0	1	21	0	0	0	0	0	0	1	0	0	0	0	178	82	BY
CH	-0	-0	0	1	0	0	0	0	0	0	0	0	0	0	0	0	0	0	0	0	0	0	0	-0	-0	0	0	0	108	45	CH
CY	-0	-0	-0	0	0	-0	-0	0	-0	1	0	0	0	-0	0	47	0	-0	0	0	0	0	0	2	1	0	0	0	84	36	CY
CZ	0	0	0	4	0	20	0	4	7	1	0	3	9	-0	-0	0	1	0	0	0	0	0	0	0	0	1	0	0	258	242	CZ
DE	0	0	0	16	0	7	0	0	0	0	1	0	1	-0	-0	0	0	0	0	0	0	0	0	0	0	0	0	0	244	229	DE
DK	0	0	0	14	1	15	0	1	1	1	3	0	1	0	0	0	1	0	0	0	0	0	0	0	0	1	0	0	200	181	DK
EE	0	0	0	2	0	18	0	1	0	12	3	0	1	0	0	1	4	0	0	0	0	0	0	0	0	0	0	0	106	76	EE
ES	-0	-0	0	0	0	0	2	0	-0	0	0	0	0	-0	-0	-0	0	-0	0	0	0	0	0	-0	-0	0	0	0	60	59	ES
FI	0	0	0	1	0	4	0	0	0	9	2	0	0	0	0	1	2	0	0	0	0	0	0	0	0	0	0	0	45	30	FI
FR	0	-0	0	4	0	0	0	0	0	0	0	0	0	-0	0	0	0	0	0	0	0	0	0	-0	-0	0	0	0	102	94	FR
GB	0	-0	0	11	0	1	0	0	0	0	0	0	0	-0	-0	-0	0	-0	0	0	0	0	0	-0	0	1	0	0	152	54	GB
GE	0	0	-0	0	0	0	0	0	0	4	0	0	0	0	0	16	0	0	0	0	0	0	0	4	0	0	0	0	115	1	GE
GL	-0	-0	-0	0	-0	-0	0	-0	-0	0	-0	0	-0	-0	0	0	0	0	0	0	0	0	0	-0	-0	7	0	0	-0	-0	GL
GR	0	2	0	0	0	1	0	5	6	1	0	0	0	0	0	16	2	0	0	0	0	0	0	0	0	0	0	0	95	65	GR
HR	0	0	0	1	0	5	0	7	36	1	0	6	2	-0	0	0	1	0	0	0	0	0	0	-0	0	0	0	0	224	164	HR
HU	0	0	0	2	0	17	0	30	40	0	0	4	13	-0	-0	1	2	0	0	0	0	0	0	0	0	0	0	0	307	255	HU
IE	0	-0	0	3	0	1	0	0	0	0	0	0	0	0	-0	-0	0	-0	0	0	0	0	0	-0	0	1	0	0	83	59	IE
IS	-0	-0	0	0	0	0	-0	-0	-0	-0	0	0	-0	0	-0	-0	0	0	0	0	0	0	0	0	-0	0	0	0	2	0	IS
IT	0	0	0	0	0	1	0	1	1	0	0	2	0	-0	0	0	0	0	0	0	0	0	0	-0	0	0	0	0	162	158	IT
KG	-0	-0	-0	0	0	0	0	0	-0	0	0	0	0	3	0	0	0	18	0	0	0	0	0	6	-0	0	0	0	56	0	KG
KZ	-0	-0	-0	0	0	0	0	0	-0	27	0	0	0	0	1	0	1	6	0	0	0	0	0	20	-0	0	0	0	57	1	KZ
LT	0	0	0	4	0	61	0	2	1	11	2	0	2	0	0	1	9	0	0	0	0	0	0	1	0	0	0	0	201	158	LT
LU	-0	-0	0	13	0	1	0	0	-0	0	0	0	0	0	-0	0	0	0	0	0	0	0	0	-0	0	0	0	0	203	192	LU
LV	0	0	0	3	0	31	0	1	1	10	3	0	1	0	0	1	6	0	0	0	0	0	0	1	0	0	0	0	152	116	LV
MD	0	0	0	1	0	11	0	30	2	8	0	0	2	0	0	4	39	0	0	0	0	0	0	1	0	0	0	0	165	64	MD
ME	33	0	0	0	0	3	0	4	32	1	0	0	1	0	0	0	1	0	0	0	0	0	0	0	0	0	0	0	119	35	ME
MK	0	50	0	0	0	3	0	7	45	0	0	0	2	0	0	1	1	0	0	0	0	0	0	0	0	0	0	0	162	52	MK
MT	0	0	59	0	0	1	0	0	0	-0	0	0	0	0	0	0	0	0	0	0	0	0	0	-0	0	0	0	0	80	79	MT
NL	-0	-0	0	156	0	2	0	0	-0	0	0	0	0	-0	0	0	0	0	0	0	0	0	0	-0	-0	1	0	0	315	283	NL
NO	0	0	0	1	4	1	0	0	0	0	1	0	0	0	0	0	0	0	0	0	0	0	0	0	0	-0	0	0	13	7	NO
PL	0	0	0	4	0	158	0	5	4	2	1	1	8	0	0	1	6	0	0	0	0	0	0	0	0	1	0	0	302	281	PL
PT	-0	-0	0	0	0	0	44	0	-0	0	0	0	0	0	-0	-0	0	-0	0	0	0	0	0	-0	-0	0	0	0	61	61	PT
RO	0	0	0	0	0	6	0	104	11	1	0	0	2	0	0	3	8	0	0	0	0	0	0	0	0	0	0	0	171	141	RO
RS	2	4	0	1	0	7	0	30	226	1	0	1	3	-0	0	1	2	0	0	0	0	0	0	0	0	0	0	0	352	103	RS
RU	0	0	0	0	0	2	0	0	0	60	0	0	0	0	0	1	3	0	0	0	0	0	0	2	0	0	0	0	75	6	RU
SE	0	0	0	2	1	6	0	0	0	1	13	0	0	0	0	0	1	0	0	0	0	0	0	0	0	0	0	0	50	43	SE
SI	0	0	0	1	0	3	0	2	5	0	0	72	1	-0	-0	0	0	0	0	0	0	0	0	-0	0	0	0	0	229	220	SI
SK	0	0	0	2	0	39	0	18	18	1	0	3	81	-0	-0	1	4	0	0	0	0	0	0	0	0	1	0	0	298	267	SK
TJ	-0	-0	-0	-0	-0	-0	-0	-0	-0	-0	0	0	0	25	0	-0	-0	17	0	0	0	0	0	5	-0	0	0	0	46	-0	TJ
TM	-0	-0	-0	0	0	0	-0	0	-0	2	0	0	0	1	28	0	0	20	0	0	0	0	0	15	-0	0	0	0	56	0	TM
TR	0	0	0	0	0	0	0	1	0	2	0	0	0	0	0	160	1	0	0	0	0	0	0	4	0	0	0	0	170	4	TR
UA	0	0	0	1	0	21	0	9	2	25	0	0	2	0	0	6	95	1	0	0	0	0	0	1	0	0	0	0	196	57	UA
UZ	-0	-0	-0	0	0	0	-0	0	-0	4	0	0	0	5	2	0	0	72	0	0	0	0	0	6	-0	0	0	0	97	0	UZ
ATL	0	-0	0	0	0	0	0	0	0	0	0	0	0	-0	0	0	0	0	0	0	0	0	0	0	0	-1	0	0	9	7	ATL
BAS	0	0	0	6	1	32	0	1	1	6	10	0	1	0	0	1	3	0	0	0	0	0	0	0	0	0	0	0	145	125	BAS
BLS	0	0	0	0	0	2	0	9	1	20	0	0	0	0	0	57	15	0	0	0	0	0	0	1	0	0	0	0	123	21	BLS
MED	0	0	0	0	0	0	0	1	1	1	0	0	0	0	0	23	1	0	0	0	0	0	0	2	2	0	0	0	52	25	MED
NOS	0	0	0	22	2	3	0	0	0	0	1	0	0	0	0	0	0	0	0	0	0	0	0	0	0	-0	0	0	138	96	NOS
AST	-0	-0	0	0	0	0	0	0	-0	1	0	0	0	0	1	4	0	0	0	0	0	0	0	91	1	1	0	0	8	0	AST
NOA	-0	0	-0	0	0	0	0	0	0	0	0	0	0	0	0	2	0	0	0	0	0	0	0	0	16	1	0	0	5	3	NOA
EXC	0	0	0	1	0	6	0	3	2	29	1	0	1	0	1	8	5	4	0	0	0	0	0	5	0	0	0	0	97	36	EXC
EU	0	0	0	5	0	17	1	9	4	2	2	1	2	0	0	1	2	0	0	0	0	0	0	0	0	0	0	0	142	127	EU
	ME	MK	MT	NL	NO	PL	PT	RO	RS	RU	SE	SI	SK	TJ	TM	TR	UA	UZ	ATL	BAS	BLS	MED	NOS	AST	NOA	BIC	DMS	VOL	EXC	EU	

Table C.14: 2021 country-to-country blame matrices for **PM2.5**.
Units: ng/m^3 per 15% emis. red. of VOC. **Emitters →, Receptors ↓.**

	AL	AM	AT	AZ	BA	BE	BG	BY	CH	CY	CZ	DE	DK	EE	ES	FI	FR	GB	GE	GR	HR	HU	IE	IS	IT	KG	KZ	LT	LU	LV	MD	
AL	1	0	0	0	1	0	0	0	0	0	1	2	0	0	1	0	1	1	0	1	1	1	0	0	5	0	0	0	0	0	0	AL
AM	0	5	0	6	0	0	0	0	0	0	0	0	0	0	0	0	0	0	1	0	0	0	0	0	0	0	0	0	0	0	0	AM
AT	0	0	1	0	0	0	0	0	0	0	0	1	0	0	0	0	1	1	0	0	1	0	0	0	3	0	0	0	0	0	0	AT
AZ	0	1	0	23	0	0	0	0	0	0	0	1	0	0	0	0	0	0	1	0	0	0	0	0	0	0	1	0	0	0	0	AZ
BA	0	0	1	0	4	0	0	0	0	0	1	2	0	0	1	0	1	1	0	0	1	1	0	0	4	-0	0	0	0	0	0	BA
BE	0	0	0	0	0	3	0	0	1	0	1	9	0	0	1	0	4	4	0	0	0	0	0	0	2	0	0	0	0	0	0	BE
BG	0	0	0	0	1	0	1	0	0	0	1	2	0	0	0	0	1	1	0	1	0	0	0	0	2	0	0	0	0	0	0	BG
BY	0	0	0	0	0	0	0	0	0	0	0	1	0	0	0	0	0	1	0	0	0	0	0	0	1	0	0	-0	0	0	0	BY
CH	0	0	0	0	0	0	0	0	-1	0	0	-0	0	0	0	0	1	0	0	0	0	0	0	-0	2	0	0	0	0	0	0	CH
CY	0	0	0	0	0	0	0	0	0	-0	0	1	0	0	1	0	1	0	0	2	0	0	0	0	2	0	0	0	0	0	0	CY
CZ	0	0	1	0	0	0	0	0	0	0	1	4	0	0	0	0	1	1	0	0	0	1	0	0	2	0	0	0	0	0	0	CZ
DE	0	0	1	0	0	1	0	0	1	0	1	6	0	0	1	0	2	2	0	0	0	0	0	0	2	0	0	0	0	0	0	DE
DK	0	0	0	0	0	0	0	0	0	0	0	2	-0	0	0	0	1	1	0	0	0	0	0	0	0	0	0	0	0	0	0	DK
EE	0	0	0	0	0	0	0	0	0	0	0	1	0	0	0	0	0	0	0	0	0	0	0	0	0	0	0	-0	0	0	0	EE
ES	0	0	0	0	0	0	0	0	0	0	0	1	0	0	4	0	1	1	0	0	0	0	0	0	2	0	0	0	0	0	0	ES
FI	0	0	0	0	0	0	0	0	0	0	0	0	0	0	0	0	0	0	0	0	0	0	0	0	0	0	0	0	0	0	0	FI
FR	0	0	0	0	0	0	0	0	0	0	0	2	0	0	1	0	1	1	0	0	0	0	0	0	2	0	0	0	-0	0	0	FR
GB	0	0	0	0	0	0	0	0	0	0	0	2	-0	0	0	0	1	2	0	0	0	0	-0	0	1	0	0	0	0	0	0	GB
GE	0	1	0	5	0	0	0	0	0	0	0	0	0	0	0	0	0	0	1	0	0	0	0	0	0	0	0	0	0	0	0	GE
GL	0	0	0	0	0	0	0	0	0	0	0	0	0	0	0	0	0	0	0	0	0	0	0	0	0	0	0	0	0	0	0	GL
GR	0	0	0	0	1	0	1	0	0	0	1	2	0	0	1	0	1	1	0	3	0	0	0	0	3	0	0	0	0	0	0	GR
HR	0	0	1	0	2	0	0	0	0	0	1	3	0	0	1	0	2	1	0	0	2	1	0	0	7	0	0	0	0	0	0	HR
HU	0	0	1	0	2	0	0	0	0	0	1	4	0	0	0	0	1	1	0	0	1	2	0	0	3	0	0	0	0	0	0	HU
IE	0	0	0	0	0	-0	0	0	0	0	0	0	0	0	0	0	-0	-1	0	0	0	0	-1	0	0	0	0	0	-0	0	0	IE
IS	0	0	0	0	0	0	0	0	0	0	0	0	-0	0	0	0	0	0	0	0	0	0	-0	0	0	0	0	0	0	0	0	IS
IT	0	0	1	0	0	0	0	0	1	0	1	3	0	0	2	0	3	1	0	0	1	0	0	0	39	0	0	0	0	0	0	IT
KG	0	0	0	0	0	0	0	0	0	0	0	0	0	0	0	0	0	0	0	0	0	0	0	0	0	2	1	0	0	0	0	KG
KZ	0	0	0	0	0	0	0	0	0	0	0	0	0	0	0	0	0	0	0	0	0	0	0	0	0	0	2	0	0	0	0	KZ
LT	0	0	0	0	0	0	0	0	0	0	0	1	-0	0	0	0	0	1	0	0	0	0	0	0	0	0	0	-0	0	0	0	LT
LU	0	0	1	0	0	0	0	0	1	0	1	7	0	0	1	0	3	1	0	0	0	0	0	0	2	0	0	0	-0	0	0	LU
LV	0	0	0	0	0	0	0	0	0	0	0	1	0	0	0	0	0	1	0	0	0	0	0	0	0	0	0	-0	0	0	0	LV
MD	0	0	0	0	0	0	0	0	0	0	1	1	0	0	0	0	1	0	0	0	0	0	0	0	1	0	0	0	0	0	1	MD
ME	0	0	0	0	1	0	0	0	0	0	1	2	0	0	1	0	1	0	0	0	1	0	0	0	4	0	0	0	0	0	0	ME
MK	0	0	0	0	1	0	1	0	0	0	1	2	0	0	0	0	1	1	0	1	0	1	0	0	3	0	0	0	0	0	0	MK
MT	0	0	1	0	1	0	0	0	0	0	1	3	0	0	2	0	3	1	0	0	1	0	0	0	10	0	0	0	0	0	0	MT
NL	0	0	0	0	0	3	0	0	1	0	1	11	0	0	1	0	5	5	0	0	0	0	0	0	2	0	0	0	0	0	0	NL
NO	0	0	0	0	0	0	0	0	0	0	0	0	0	0	0	0	0	0	0	0	0	0	0	0	0	0	0	0	0	0	0	NO
PL	0	0	0	0	0	0	0	0	0	0	1	3	0	0	0	0	1	1	0	0	0	1	0	0	2	0	0	0	0	0	0	PL
PT	0	0	0	0	0	0	0	0	0	0	0	1	0	0	2	0	1	1	0	0	0	0	0	0	1	0	0	0	0	0	0	PT
RO	0	0	0	0	1	0	0	0	0	0	1	2	0	0	0	0	1	1	0	0	0	0	0	0	2	0	0	0	0	0	0	RO
RS	0	0	1	0	2	0	1	0	0	0	1	3	0	0	1	0	1	1	0	0	1	1	0	0	4	-0	0	0	0	0	0	RS
RU	0	0	0	0	0	0	0	0	0	0	0	0	0	0	0	0	0	0	0	0	0	0	0	0	0	0	0	0	0	0	0	RU
SE	0	0	0	0	0	0	0	0	0	0	0	0	0	0	0	0	0	0	0	0	0	0	0	0	0	0	0	0	0	0	0	SE
SI	0	0	1	0	1	0	0	0	0	0	1	3	0	0	1	0	2	1	0	0	2	0	0	0	10	0	0	0	0	0	0	SI
SK	0	0	1	0	1	0	0	0	0	0	1	3	0	0	0	0	1	1	0	0	0	1	0	0	2	0	0	0	0	0	0	SK
TJ	0	0	0	0	0	0	0	0	0	0	0	0	0	0	0	0	0	0	0	0	0	0	0	0	0	1	1	0	0	0	0	TJ
TM	0	0	0	1	0	0	0	0	0	0	0	0	0	0	0	0	0	0	0	0	0	0	0	0	0	0	1	0	0	0	0	TM
TR	0	0	0	0	0	0	0	0	0	0	0	1	0	0	0	0	0	0	0	0	0	0	0	0	1	0	0	0	0	0	0	TR
UA	0	0	0	0	0	0	0	0	0	0	0	1	0	0	0	0	0	0	0	0	0	0	0	0	1	0	0	0	0	0	0	UA
UZ	0	0	0	0	0	0	0	0	0	0	0	0	0	0	0	0	0	0	0	0	0	0	0	0	0	1	2	0	0	0	0	UZ
ATL	0	0	0	0	0	0	0	0	0	0	0	0	0	0	0	0	0	0	0	0	0	0	-0	0	0	0	0	0	0	0	0	ATL
BAS	0	0	0	0	0	0	0	0	0	0	0	1	0	0	0	0	0	1	0	0	0	0	0	0	0	0	0	0	0	0	0	BAS
BLS	0	0	0	1	0	0	0	0	0	0	0	1	0	0	0	0	0	0	0	0	0	0	0	0	1	0	0	0	0	0	0	BLS
MED	0	0	0	0	1	0	0	0	0	0	1	2	0	0	2	0	2	1	0	1	1	0	0	0	8	0	0	0	0	0	0	MED
NOS	0	0	0	0	0	1	0	0	0	0	0	2	0	0	0	0	1	2	0	0	0	0	0	0	0	0	0	0	0	0	0	NOS
AST	0	0	0	1	0	0	0	0	0	0	0	0	0	0	0	0	0	0	0	0	0	0	0	0	0	0	0	0	0	0	0	AST
NOA	0	0	0	0	0	0	0	0	0	0	0	1	0	0	2	0	1	0	0	0	0	0	0	0	3	0	0	0	0	0	0	NOA
EXC	0	0	0	0	0	0	0	0	0	0	0	1	0	0	0	0	0	0	0	0	0	0	0	0	1	0	0	0	0	0	0	EXC
EU	0	0	0	0	0	0	0	0	0	-0	0	2	0	0	1	0	1	1	0	0	0	0	0	0	4	0	0	0	0	0	0	EU
	AL	AM	AT	AZ	BA	BE	BG	BY	CH	CY	CZ	DE	DK	EE	ES	FI	FR	GB	GE	GR	HR	HU	IE	IS	IT	KG	KZ	LT	LU	LV	MD	

Table C.14 Cont.: 2021 country-to-country blame matrices for **PM2.5**.
Units: ng/m^3 per 15% emis. red. of VOC. **Emitters →, Receptors ↓.**

	ME	MK	MT	NL	NO	PL	PT	RO	RS	RU	SE	SI	SK	TJ	TM	TR	UA	UZ	ATL	BAS	BLS	MED	NOS	AST	NOA	BIC	DMS	VOL	EXC	EU	
AL	0	0	0	0	0	2	0	1	1	1	0	0	0	0	0	0	0	0	0	0	0	0	0	0	1	-3	0	0	23	16	AL
AM	0	0	0	0	0	0	0	0	0	4	0	0	0	0	0	1	0	0	0	0	0	0	0	23	0	-2	0	0	20	2	AM
AT	0	0	0	0	0	1	0	0	0	1	0	0	0	0	0	0	0	0	0	0	0	0	0	0	0	-4	0	0	13	10	AT
AZ	0	0	0	0	0	1	0	0	0	10	0	0	0	0	1	1	1	1	0	0	0	0	0	38	0	1	0	0	45	4	AZ
BA	0	0	0	0	0	2	0	1	1	1	0	0	1	-0	0	0	0	0	0	0	0	0	0	0	1	-3	0	0	23	15	BA
BE	0	0	0	6	0	2	0	0	0	1	0	0	0	0	0	0	0	0	0	0	0	0	0	0	0	2	0	0	33	28	BE
BG	0	0	0	0	0	2	0	2	0	3	0	0	0	0	0	1	1	0	0	0	0	0	0	0	0	-3	0	0	20	13	BG
BY	0	0	0	0	0	1	0	0	0	3	0	0	0	0	0	0	1	0	0	0	0	0	0	0	0	-3	0	0	11	5	BY
CH	0	0	0	0	0	0	0	0	0	0	0	0	0	0	0	0	0	0	0	0	0	0	0	0	0	-6	0	0	4	4	CH
CY	0	0	0	0	0	1	0	1	0	5	0	0	0	0	0	5	1	0	0	0	0	0	0	7	2	-3	0	0	24	10	CY
CZ	0	0	0	0	0	1	0	0	0	1	0	0	1	0	0	0	0	0	0	0	0	0	0	0	0	-4	0	0	18	14	CZ
DE	0	0	0	1	0	1	0	0	0	1	0	0	0	0	0	0	0	0	0	0	0	0	0	0	0	-2	0	0	20	16	DE
DK	0	0	0	1	0	1	0	0	0	1	0	0	0	0	0	0	0	0	0	0	0	0	0	0	0	-2	0	0	9	6	DK
EE	0	0	0	0	0	0	0	0	0	2	0	0	0	0	0	0	0	0	0	0	0	0	0	0	0	-2	0	0	6	3	EE
ES	0	0	0	0	0	0	1	0	0	0	0	0	0	0	0	0	0	0	0	0	0	0	0	0	1	-1	0	0	12	10	ES
FI	0	0	0	0	0	0	0	0	0	1	0	0	0	0	0	0	0	0	0	0	0	0	0	0	0	-1	0	0	3	1	FI
FR	0	0	0	1	0	0	0	0	0	0	0	0	0	0	0	0	0	0	0	0	0	0	0	0	0	-2	0	0	10	8	FR
GB	0	0	0	1	0	0	0	0	0	0	0	0	0	0	0	0	0	0	0	0	0	0	0	0	0	-1	0	0	8	6	GB
GE	0	0	0	0	0	0	0	0	0	5	0	0	0	0	0	1	1	0	0	0	0	0	0	10	0	-2	0	0	16	2	GE
GL	0	0	0	0	0	0	0	0	0	0	0	0	0	0	0	0	0	0	0	0	0	0	0	0	0	0	0	0	0	0	GL
GR	0	0	0	0	0	2	0	1	1	3	0	0	0	0	0	1	1	0	0	0	0	0	0	0	1	-2	0	0	24	16	GR
HR	0	0	0	0	0	2	0	1	1	1	0	1	1	0	0	0	0	0	0	0	0	0	0	0	0	-3	0	0	29	22	HR
HU	0	0	0	0	0	3	0	2	2	1	0	0	1	0	0	0	1	0	0	0	0	0	0	0	0	-3	0	0	29	22	HU
IE	0	0	0	-0	0	-0	0	0	0	0	0	0	0	0	0	0	0	0	0	0	0	0	0	0	0	-3	0	0	-2	-1	IE
IS	0	0	0	0	0	0	0	0	0	0	0	0	0	0	0	0	0	0	0	0	0	0	0	0	0	-0	0	0	0	0	IS
IT	0	0	0	0	0	1	0	0	0	1	0	1	0	0	0	0	0	0	0	0	0	0	0	0	1	-2	0	0	58	54	IT
KG	0	0	0	0	0	0	0	0	0	1	0	0	0	1	0	0	0	7	0	0	0	0	0	4	0	-2	0	0	13	0	KG
KZ	0	0	0	0	0	0	0	0	0	4	0	0	0	0	0	0	0	1	0	0	0	0	0	3	0	-3	0	0	10	1	KZ
LT	0	0	0	0	0	1	0	0	0	2	0	0	0	0	0	0	0	0	0	0	0	0	0	0	0	-3	0	0	8	4	LT
LU	0	0	0	1	0	1	0	0	0	0	0	0	0	0	0	0	0	0	0	0	0	0	0	0	0	-2	0	0	20	16	LU
LV	0	0	0	0	0	1	0	0	0	2	0	0	0	0	0	0	0	0	0	0	0	0	0	0	0	-2	0	0	7	3	LV
MD	0	0	0	0	0	2	0	2	0	4	0	0	0	0	0	1	1	0	0	0	0	0	0	1	0	-4	0	0	19	10	MD
ME	-0	0	0	0	0	1	0	1	1	1	0	0	0	0	0	0	0	0	0	0	0	0	0	0	1	-3	0	0	16	12	ME
MK	0	2	0	0	0	2	0	1	1	1	0	0	0	0	0	0	1	0	0	0	0	0	0	0	1	-3	0	0	22	14	MK
MT	0	0	1	0	0	1	0	1	0	1	0	0	0	0	0	0	0	0	0	0	0	0	0	0	4	-1	0	0	31	26	MT
NL	0	0	0	9	0	2	0	0	0	1	0	0	0	0	0	0	0	0	0	0	0	0	0	0	0	4	0	0	43	36	NL
NO	0	0	0	0	0	0	0	0	0	0	0	0	0	0	0	0	0	0	0	0	0	0	0	0	0	-0	0	0	2	1	NO
PL	0	0	0	1	0	3	0	0	0	1	0	0	1	0	0	0	0	0	0	0	0	0	0	0	0	-3	0	0	19	15	PL
PT	0	0	0	0	0	0	3	0	0	0	0	0	0	0	0	0	0	0	0	0	0	0	0	0	1	0	0	0	10	9	PT
RO	0	0	0	0	0	2	0	4	1	2	0	0	0	0	0	0	1	0	0	0	0	0	0	0	0	-3	0	0	20	14	RO
RS	0	1	0	0	0	3	0	2	4	1	0	0	1	0	0	0	1	0	0	0	0	0	0	0	1	-3	0	0	31	19	RS
RU	0	0	0	0	0	0	0	0	0	4	0	0	0	0	0	0	0	0	0	0	0	0	0	1	0	-2	0	0	6	1	RU
SE	0	0	0	0	0	0	0	0	0	1	0	0	0	0	0	0	0	0	0	0	0	0	0	0	0	-1	0	0	3	2	SE
SI	0	0	0	0	0	1	0	0	0	1	0	2	0	0	0	0	0	0	0	0	0	0	0	0	0	-4	0	0	28	24	SI
SK	0	0	0	0	0	3	0	1	1	1	0	0	1	0	0	0	0	0	0	0	0	0	0	0	0	-3	0	0	21	16	SK
TJ	0	0	0	0	0	0	0	0	0	2	0	0	0	4	1	0	0	8	0	0	0	0	0	5	0	-2	0	0	17	0	TJ
TM	0	0	0	0	0	0	0	0	0	5	0	0	0	0	2	0	0	2	0	0	0	0	0	16	0	-2	0	0	15	2	TM
TR	0	0	0	0	0	1	0	0	0	4	0	0	0	0	0	-1	1	0	0	0	0	0	0	7	1	-5	0	0	10	5	TR
UA	0	0	0	0	0	1	0	1	0	5	0	0	0	0	0	0	1	0	0	0	0	0	0	1	0	-3	0	0	15	7	UA
UZ	0	0	0	0	0	0	0	0	0	4	0	0	0	2	1	0	0	16	0	0	0	0	0	9	0	-2	0	0	29	1	UZ
ATL	0	0	0	0	0	0	0	0	0	0	0	0	0	0	0	0	0	0	0	0	0	0	0	0	0	-0	0	0	1	1	ATL
BAS	0	0	0	0	0	1	0	0	0	2	0	0	0	0	0	0	0	0	0	0	0	0	0	0	0	-1	0	0	7	4	BAS
BLS	0	0	0	0	0	1	0	1	0	9	0	0	0	0	0	2	2	0	0	0	0	0	0	2	0	-2	0	0	24	7	BLS
MED	0	0	0	0	0	1	0	1	0	2	0	0	0	0	0	1	1	0	0	0	0	0	0	1	3	-1	0	0	29	22	MED
NOS	0	0	0	2	0	1	0	0	0	0	0	0	0	0	0	0	0	0	0	0	0	0	0	0	0	0	0	0	10	8	NOS
AST	0	0	0	0	0	0	0	0	0	2	0	0	0	0	0	1	0	1	0	0	0	0	0	46	0	-2	0	0	7	1	AST
NOA	0	0	0	0	0	0	0	0	0	1	0	0	0	0	0	0	0	0	0	0	0	0	0	0	5	-1	0	0	12	9	NOA
EXC	0	0	0	0	0	0	0	0	0	3	0	0	0	0	0	0	0	1	0	0	0	0	0	2	0	-2	0	0	11	5	EXC
EU	0	0	0	0	0	1	0	0	0	1	0	0	0	0	0	0	0	0	0	0	0	0	0	0	0	-2	0	0	17	13	EU
	ME	MK	MT	NL	NO	PL	PT	RO	RS	RU	SE	SI	SK	TJ	TM	TR	UA	UZ	ATL	BAS	BLS	MED	NOS	AST	NOA	BIC	DMS	VOL	EXC	EU	

Table C.15: 2021 country-to-country blame matrices for **PM2.5**.
Units: ng/m^3 per 15% emis. red. of PPM, SO_x, NO_x, NH_3 and VOC. **Emitters →, Receptors ↓.**

	AL	AM	AT	AZ	BA	BE	BG	BY	CH	CY	CZ	DE	DK	EE	ES	FI	FR	GB	GE	GR	HR	HU	IE	IS	IT	KG	KZ	LT	LU	LV	MD	
AL	318	0	3	0	25	0	13	1	1	0	6	10	0	0	4	0	5	1	0	27	7	8	0	0	35	0	1	0	0	0	1	AL
AM	0	317	0	239	0	0	0	0	0	0	0	1	0	0	0	0	0	0	39	1	0	0	0	0	1	0	11	0	0	0	0	AM
AT	0	0	346	0	7	3	1	1	14	0	43	126	1	0	2	0	22	6	0	0	18	23	0	0	61	0	0	0	1	0	0	AT
AZ	0	33	0	823	0	0	1	1	0	0	0	1	0	0	0	0	0	0	46	0	0	0	0	0	1	0	39	0	0	0	0	AZ
BA	2	0	16	0	734	2	6	1	2	0	17	32	1	0	3	0	9	3	0	1	59	27	0	0	37	-0	1	0	0	0	1	BA
BE	0	0	3	0	0	354	0	1	6	0	9	201	4	0	11	1	250	88	0	0	0	1	6	0	9	0	0	0	9	0	0	BE
BG	2	0	3	0	11	1	361	6	1	0	6	11	1	0	1	0	3	2	0	21	4	12	0	0	9	0	3	1	0	0	7	BG
BY	0	0	3	1	2	2	1	244	1	0	13	41	4	2	1	2	6	7	0	1	2	7	1	0	4	0	7	15	0	4	3	BY
CH	0	0	21	0	0	3	0	0	301	0	6	114	0	0	4	0	82	7	0	0	1	1	0	0	77	0	0	0	1	0	0	CH
CY	1	0	0	1	1	0	4	1	0	107	1	2	0	0	2	0	2	1	1	27	0	1	0	0	7	0	1	0	0	0	1	CY
CZ	0	0	71	0	9	7	1	3	9	0	438	219	3	0	3	0	35	13	0	0	15	41	1	0	19	0	0	1	1	0	1	CZ
DE	0	0	36	0	1	31	0	1	21	0	35	590	7	0	6	1	86	42	0	0	1	3	3	0	9	0	0	1	4	0	0	DE
DK	0	0	3	0	1	18	0	2	2	0	11	177	191	0	3	1	34	58	0	0	1	3	4	1	1	0	1	1	1	1	0	DK
EE	0	0	1	0	0	2	0	24	0	0	4	23	5	82	1	8	5	8	0	0	0	2	1	0	1	0	4	15	0	24	1	EE
ES	0	0	0	0	1	1	0	0	0	0	1	5	0	0	312	0	17	3	0	0	0	0	0	0	6	0	0	0	0	0	0	ES
FI	0	0	0	0	0	1	0	6	0	0	1	9	2	3	0	44	2	3	0	0	0	0	0	0	0	0	3	2	0	2	0	FI
FR	0	0	4	0	1	20	0	0	11	0	5	69	1	0	27	0	337	31	0	0	1	1	3	0	19	0	0	0	2	0	0	FR
GB	0	0	1	0	0	15	0	0	1	0	2	43	4	0	3	0	40	357	0	0	0	0	17	1	2	0	0	0	1	0	0	GB
GE	0	30	0	162	0	0	1	1	0	0	0	1	0	0	0	0	0	0	306	1	0	0	0	0	1	0	13	0	0	0	0	GE
GL	0	0	0	0	0	0	0	0	0	0	0	0	0	0	0	0	0	0	0	0	0	0	0	0	0	0	0	0	0	0	0	GL
GR	11	0	2	0	8	0	44	3	0	0	4	6	0	0	3	0	3	1	0	228	3	5	0	0	18	0	1	0	0	0	3	GR
HR	1	0	37	0	170	2	5	1	3	0	28	49	1	0	4	0	14	4	0	1	366	55	0	0	111	0	1	0	0	0	1	HR
HU	1	0	50	0	38	3	9	3	3	0	46	68	2	0	2	0	13	6	0	1	59	482	1	0	44	0	1	1	0	0	2	HU
IE	0	0	0	0	0	7	0	0	0	0	1	23	2	0	2	0	23	109	0	0	0	0	151	1	1	0	0	0	0	0	0	IE
IS	0	0	0	0	0	0	0	0	0	0	0	0	0	0	0	0	0	2	0	0	0	0	0	37	0	0	0	0	0	0	0	IS
IT	1	0	17	0	11	1	2	1	9	0	7	22	0	0	13	0	26	3	0	1	13	6	0	0	805	0	1	0	0	0	0	IT
KG	0	0	0	1	0	0	0	0	0	0	0	0	0	0	0	0	0	0	0	0	0	0	0	0	0	131	67	0	0	0	0	KG
KZ	0	0	0	2	0	0	0	1	0	0	0	1	0	0	0	0	0	0	0	0	0	0	0	0	0	6	271	0	0	0	0	KZ
LT	0	0	4	0	2	4	1	64	1	0	13	59	10	3	1	3	9	14	0	0	2	6	1	0	3	0	4	142	0	14	1	LT
LU	0	0	6	0	0	84	0	1	10	0	10	299	2	0	9	0	261	44	0	0	0	1	4	0	13	0	0	0	117	0	0	LU
LV	0	0	2	0	1	3	0	43	1	0	7	36	7	7	1	4	6	11	0	0	1	3	1	0	2	0	4	52	0	112	1	LV
MD	1	0	3	1	4	1	17	18	1	0	11	24	1	1	1	1	4	3	1	4	2	11	0	0	5	0	7	2	0	1	363	MD
ME	26	0	5	0	71	1	7	1	1	0	8	14	1	0	3	0	5	2	0	4	11	12	0	0	24	0	1	0	0	0	1	ME
MK	33	0	3	0	15	0	38	2	1	0	6	10	0	0	3	0	4	1	0	63	5	12	0	0	16	0	1	0	0	0	1	MK
MT	2	0	2	0	9	1	4	0	1	0	3	7	0	0	18	0	15	2	0	5	4	3	0	0	93	0	1	0	0	0	0	MT
NL	0	0	3	0	0	140	0	1	4	0	7	277	7	0	10	1	140	129	0	0	0	0	9	1	5	0	0	1	4	0	0	NL
NO	0	0	0	0	0	1	0	1	0	0	1	6	2	0	0	1	2	5	0	0	0	0	0	0	0	0	1	0	0	0	0	NO
PL	0	0	14	0	5	7	2	15	3	0	74	149	8	1	3	1	21	16	0	0	6	25	1	0	10	0	2	5	1	2	1	PL
PT	0	0	0	0	0	1	0	0	0	0	0	4	0	0	106	0	7	4	0	0	0	0	0	0	1	0	0	0	0	0	0	PT
RO	1	0	6	0	11	1	41	7	1	0	10	20	1	0	1	0	5	2	0	4	5	32	0	0	11	0	3	1	0	0	15	RO
RS	11	0	15	0	80	1	43	3	2	0	19	31	1	0	3	0	8	3	0	9	26	61	0	0	24	-0	2	1	0	0	3	RS
RU	0	0	0	3	0	0	0	7	0	0	1	3	1	1	0	1	1	1	1	0	0	0	0	0	0	0	40	1	0	1	0	RU
SE	0	0	1	0	0	2	0	2	0	0	2	26	11	1	1	3	6	8	0	0	0	1	1	0	0	0	2	1	0	1	0	SE
SI	0	0	111	0	21	2	1	1	5	0	27	59	1	0	4	0	16	4	0	0	121	27	0	0	276	0	1	0	0	0	1	SI
SK	0	0	35	0	15	3	4	4	3	0	70	72	2	0	2	0	13	6	0	1	19	153	1	0	26	0	1	1	0	1	1	SK
TJ	0	0	0	1	0	0	0	0	0	0	0	0	0	0	0	0	0	0	0	0	0	0	0	0	0	13	40	0	0	0	0	TJ
TM	0	1	0	11	0	0	0	1	0	0	0	1	0	0	0	0	0	0	1	0	0	0	0	0	0	3	110	0	0	0	0	TM
TR	0	5	0	7	1	0	6	2	0	2	1	2	0	0	1	0	1	1	3	8	0	1	0	0	3	0	2	0	0	0	1	TR
UA	0	0	3	4	3	1	6	30	1	0	10	25	2	1	1	1	4	4	2	2	2	11	0	0	4	0	15	3	0	1	16	UA
UZ	0	0	0	3	0	0	0	1	0	0	0	1	0	0	0	0	0	0	0	0	0	0	0	0	0	23	168	0	0	0	0	UZ
ATL	0	0	0	0	0	1	0	0	0	0	0	3	0	0	6	0	6	7	0	0	0	0	2	1	0	0	1	0	0	0	0	ATL
BAS	0	0	2	0	1	6	1	8	1	0	9	81	27	5	2	8	14	19	0	0	1	2	1	0	1	0	2	7	0	6	0	BAS
BLS	0	2	1	11	2	0	17	8	0	0	2	6	0	0	1	0	1	1	24	5	1	2	0	0	2	0	8	1	0	0	6	BLS
MED	4	0	2	0	10	1	7	1	1	2	3	7	0	0	28	0	17	2	0	22	6	3	0	0	70	0	1	0	0	0	1	MED
NOS	0	0	1	0	0	18	0	1	1	0	3	62	14	0	3	0	47	98	0	0	0	0	6	1	2	0	0	0	1	0	0	NOS
AST	0	1	0	8	0	0	0	0	0	1	0	0	0	0	0	0	0	0	1	1	0	0	0	0	0	2	29	0	0	0	0	AST
NOA	1	0	0	0	2	0	2	0	0	0	1	2	0	0	14	0	5	1	0	5	1	1	0	0	11	0	0	0	0	0	0	NOA
EXC	1	1	4	7	4	3	4	8	2	0	6	26	2	1	11	2	16	9	2	3	3	6	1	0	17	3	65	2	0	1	2	EXC
EU	1	0	18	0	7	11	14	5	5	0	23	97	5	2	46	4	66	16	0	8	10	20	4	0	71	0	1	4	1	3	1	EU
	AL	AM	AT	AZ	BA	BE	BG	BY	CH	CY	CZ	DE	DK	EE	ES	FI	FR	GB	GE	GR	HR	HU	IE	IS	IT	KG	KZ	LT	LU	LV	MD	

Table C.15 Cont.: 2021 country-to-country blame matrices for **PM2.5**.
Units: ng/m^3 per 15% emis. red. of PPM, SO_x, NO_x, NH_3 and VOC. **Emitters →, Receptors ↓.**

	ME	MK	MT	NL	NO	PL	PT	RO	RS	RU	SE	SI	SK	TJ	TM	TR	UA	UZ	ATL	BAS	BLS	MED	NOS	AST	NOA	BIC	DMS	VOL	EXC	EU	
AL	55	89	0	1	0	18	0	14	221	3	0	1	3	0	0	8	8	0	0	0	0	18	0	1	8	10	6	29	891	157	AL
AM	0	1	0	0	0	1	0	1	2	12	0	0	0	0	4	149	4	1	0	0	1	1	0	265	3	11	1	6	786	6	AM
AT	1	0	0	4	1	35	0	6	22	4	1	28	9	0	0	1	6	0	1	1	0	3	3	0	2	8	3	2	795	730	AT
AZ	0	0	0	0	0	2	0	1	2	62	0	0	0	0	16	52	12	6	0	0	1	1	0	284	2	14	1	3	1104	9	AZ
BA	33	4	0	2	0	39	0	20	189	5	1	4	7	0	0	3	9	0	0	1	0	8	1	1	5	9	4	12	1273	285	BA
BE	0	0	0	112	2	18	1	1	1	3	2	0	1	0	0	1	2	0	8	2	0	2	67	0	2	23	19	1	1099	993	BE
BG	7	21	0	1	0	30	0	114	155	16	0	1	4	0	0	45	50	0	0	1	4	4	1	1	4	8	7	8	915	587	BG
BY	1	1	0	5	1	168	0	11	12	58	3	1	5	0	0	11	91	1	1	6	0	1	4	2	1	7	5	1	743	302	BY
CH	0	0	0	3	0	5	0	2	2	2	0	1	1	0	0	1	2	0	1	1	0	3	3	0	2	8	3	2	640	325	CH
CY	2	5	0	0	0	4	0	4	10	15	0	0	0	0	0	780	15	0	0	0	2	49	0	103	24	15	39	35	997	162	CY
CZ	1	1	0	10	1	143	0	10	38	6	2	10	32	0	0	2	9	0	1	3	0	2	7	0	1	10	6	1	1157	1064	CZ
DE	0	0	0	52	2	49	1	2	4	5	3	1	2	0	0	1	4	0	4	7	0	2	33	0	2	14	12	1	1007	926	DE
DK	0	0	0	43	9	55	0	1	3	7	12	0	2	0	0	1	4	0	4	35	0	1	65	0	1	13	21	0	654	565	DK
EE	0	0	0	4	3	54	0	2	3	46	9	0	1	0	0	5	18	0	1	12	0	0	4	1	0	7	7	0	358	244	EE
ES	1	0	0	1	0	1	25	1	3	0	0	0	0	0	0	0	0	0	11	0	0	21	1	0	24	18	17	5	382	372	ES
FI	0	0	0	1	3	13	0	1	1	38	8	0	0	0	0	2	7	0	1	5	0	0	2	1	0	6	7	0	157	94	FI
FR	1	0	0	14	1	7	1	2	5	2	1	1	1	0	0	1	2	0	7	1	0	7	22	0	5	14	18	4	571	517	FR
GB	0	0	0	29	2	10	0	0	0	2	1	0	0	0	0	0	1	0	13	3	0	0	45	0	1	15	28	0	534	170	GB
GE	0	1	0	0	0	2	0	1	2	32	0	0	0	0	4	112	10	1	0	0	2	0	0	95	2	8	4	4	685	8	GE
GL	0	0	0	0	0	0	0	0	0	0	0	0	0	0	0	0	0	0	0	0	0	0	0	0	0	34	1	0	0	0	GL
GR	10	50	0	1	0	16	0	23	93	11	0	1	2	0	0	87	25	0	0	0	2	25	0	1	10	10	14	34	662	358	GR
HR	9	3	0	3	0	48	0	24	178	5	1	34	10	0	0	2	10	0	1	1	0	16	2	0	4	9	5	10	1185	795	HR
HU	6	5	0	5	1	124	0	120	220	8	1	18	60	0	0	5	24	0	1	2	0	6	3	1	2	10	4	5	1435	1112	HU
IE	0	0	0	11	1	6	0	0	0	1	1	0	0	0	0	0	0	0	19	2	0	0	23	0	0	13	33	0	344	231	IE
IS	0	0	0	0	0	0	0	0	0	0	0	0	0	0	0	0	0	0	1	0	0	0	0	0	0	12	18	0	41	2	IS
IT	5	3	0	1	0	14	1	6	30	3	0	15	2	0	0	2	5	0	1	0	0	48	1	0	15	12	13	51	1029	955	IT
KG	0	0	0	0	0	0	0	0	0	3	0	0	0	29	4	4	0	189	0	0	0	0	0	79	0	8	0	1	430	1	KG
KZ	0	0	0	0	0	3	0	0	1	101	0	0	0	2	4	4	9	28	0	0	0	0	0	66	0	10	1	1	436	7	KZ
LT	1	1	0	9	2	204	0	7	8	46	7	1	5	0	0	7	36	0	1	16	0	0	8	2	1	7	8	1	696	508	LT
LU	0	0	0	39	1	13	1	1	1	3	2	1	1	0	0	1	2	0	5	1	0	3	27	0	3	15	13	1	929	864	LU
LV	0	0	0	6	2	96	0	4	5	40	8	1	3	0	0	6	26	0	1	12	0	0	5	1	0	7	8	1	505	362	LV
MD	3	4	0	2	1	83	0	171	33	40	1	1	6	0	0	42	207	1	0	2	6	2	2	3	2	9	5	4	1083	353	MD
ME	400	14	0	1	0	21	0	14	193	4	0	1	4	0	0	5	7	0	0	0	0	8	0	1	5	9	4	16	861	135	ME
MK	17	405	0	1	0	21	0	24	282	4	0	1	4	0	0	14	11	0	0	0	1	5	0	1	6	9	4	13	1000	212	MK
MT	7	7	101	1	0	9	2	4	28	2	0	1	1	0	0	4	5	0	1	0	0	132	0	0	69	14	48	171	344	274	MT
NL	0	0	0	415	3	33	1	0	0	4	3	0	1	0	0	0	3	0	10	7	0	2	112	0	2	29	21	0	1205	1060	NL
NO	0	0	0	1	33	5	0	0	0	8	3	0	0	0	0	1	2	0	2	1	0	0	4	0	0	8	14	0	76	24	NO
PL	1	1	0	13	2	874	0	16	26	16	4	3	26	0	0	4	33	0	2	10	0	1	9	1	1	11	8	1	1390	1265	PL
PT	0	0	0	1	0	1	313	0	0	0	0	0	0	0	0	0	0	0	32	0	0	5	1	0	16	20	25	2	441	436	PT
RO	6	8	0	2	1	62	0	578	106	15	1	2	9	0	0	26	64	0	0	1	3	3	1	1	3	8	4	6	1059	793	RO
RS	41	43	0	2	0	56	0	99	1112	7	1	3	13	0	0	7	20	0	1	1	0	5	2	1	5	10	3	10	1753	418	RS
RU	0	0	0	0	0	9	0	1	1	215	1	0	0	0	1	5	19	2	0	1	0	0	0	7	0	9	4	0	319	23	RU
SE	0	0	0	5	8	19	0	1	1	10	36	0	0	0	0	1	4	0	1	8	0	0	5	0	0	6	9	0	155	117	SE
SI	2	1	0	3	1	38	0	12	50	5	1	404	6	0	0	1	9	0	1	1	0	21	3	0	2	7	4	6	1213	1112	SI
SK	3	2	0	5	1	203	0	51	88	8	1	9	280	0	0	4	27	0	1	1	0	3	3	1	1	9	4	3	1119	955	SK
TJ	0	0	0	0	0	0	0	0	0	5	0	0	0	272	18	6	1	157	0	-0	0	0	0	105	0	9	0	1	513	1	TJ
TM	0	0	0	0	0	2	0	0	1	36	0	0	0	10	136	10	9	95	0	0	0	0	0	137	1	13	1	2	430	5	TM
TR	1	3	0	0	0	5	0	6	11	21	0	0	0	0	0	1011	23	0	0	0	5	12	0	122	8	13	10	15	1132	38	TR
UA	2	2	0	2	1	99	0	40	18	98	1	1	6	0	1	38	477	1	0	2	4	2	2	6	2	9	4	3	939	227	UA
UZ	0	0	0	0	0	2	0	0	0	40	0	0	0	41	32	6	8	389	0	0	0	0	0	62	0	13	1	1	719	5	UZ
ATL	0	0	0	1	1	1	4	0	0	5	0	0	0	0	0	0	0	0	7	0	0	1	2	0	4	17	34	0	41	26	ATL
BAS	0	0	0	13	4	88	0	3	4	23	23	0	2	0	0	3	10	0	1	22	0	0	12	1	0	8	12	0	381	303	BAS
BLS	1	3	0	1	0	19	0	29	17	100	0	0	1	0	1	284	125	1	0	0	25	5	0	16	2	9	18	5	684	91	BLS
MED	7	8	0	1	0	9	2	8	31	8	0	2	1	0	0	150	12	0	2	0	1	69	0	16	52	13	38	85	427	192	MED
NOS	0	0	0	40	9	12	0	0	1	3	3	0	0	0	0	0	1	0	5	4	0	0	35	0	0	13	30	0	328	213	NOS
AST	0	0	0	0	0	1	0	0	1	10	0	0	0	3	12	62	3	11	0	0	0	2	0	821	5	19	2	5	147	5	AST
NOA	2	2	0	0	0	2	4	2	8	2	0	0	0	0	0	22	3	0	4	0	0	20	0	5	215	24	17	33	93	50	NOA
EXC	1	2	0	4	1	32	2	13	15	108	2	1	3	4	6	50	30	20	1	1	1	3	3	27	2	11	6	3	505	163	EXC
EU	2	3	0	14	2	96	10	44	29	11	6	5	9	0	0	9	13	0	4	4	0	9	11	1	6	12	12	7	700	594	EU

ME MK MT NL NO PL PT RO RS RU SE SI SK TJ TM TR UA UZ ATL BAS BLS MED NOS AST NOA BIC DMS VOL EXC EU

Table C.16: 2021 country-to-country blame matrices for **fine EC**.
Units: 0.1 ng/m^3 per 15% emis. red. of PPM. **Emitters →, Receptors ↓.**

	AL	AM	AT	AZ	BA	BE	BG	BY	CH	CY	CZ	DE	DK	EE	ES	FI	FR	GB	GE	GR	HR	HU	IE	IS	IT	KG	KZ	LT	LU	LV	MD	
AL	261	0	1	0	9	0	2	0	0	0	1	1	0	0	2	0	1	0	0	7	3	3	0	0	11	0	0	0	0	0	0	AL
AM	0	153	0	76	0	0	0	0	0	0	0	0	0	0	0	0	0	0	19	0	0	0	0	0	0	0	0	0	0	0	0	AM
AT	0	0	170	0	2	0	0	0	2	0	11	23	0	0	1	0	6	1	0	0	6	8	0	0	16	0	0	0	0	0	0	AT
AZ	0	14	0	665	0	0	0	0	0	0	0	0	0	0	0	0	0	0	36	0	0	0	0	0	0	0	0	0	0	0	0	AZ
BA	2	0	5	0	553	0	2	0	0	0	4	4	0	0	2	0	2	0	0	1	35	11	0	0	11	0	0	0	0	0	0	BA
BE	0	0	0	0	0	283	0	0	0	0	1	35	1	0	1	0	100	14	0	0	0	0	1	0	1	0	0	0	2	0	0	BE
BG	2	0	1	0	4	0	199	1	0	0	1	2	0	0	1	0	1	0	0	8	2	4	0	0	2	0	0	0	0	0	3	BG
BY	0	0	0	0	0	0	0	146	0	0	2	4	1	1	0	1	1	1	0	0	0	2	0	0	1	0	0	8	0	4	2	BY
CH	0	0	6	0	0	0	0	0	99	0	1	25	0	0	1	0	37	1	0	0	0	0	0	0	21	0	0	0	0	0	0	CH
CY	0	0	0	0	1	0	1	0	0	37	0	0	0	0	1	0	0	0	0	5	0	0	0	0	2	0	0	0	0	0	0	CY
CZ	0	0	13	0	2	1	1	0	1	0	195	39	1	0	0	0	8	1	0	0	4	11	0	0	3	0	0	0	0	0	0	CZ
DE	0	0	8	0	0	7	0	0	3	0	7	221	2	0	1	0	26	4	0	0	0	1	0	0	2	0	0	0	1	0	0	DE
DK	0	0	0	0	0	3	0	0	0	0	1	22	92	0	0	0	7	8	0	0	0	0	1	0	0	0	0	0	0	0	0	DK
EE	0	0	0	0	0	0	0	6	0	0	1	2	1	73	0	4	1	1	0	0	0	1	0	0	0	0	0	5	0	13	0	EE
ES	0	0	0	0	0	0	0	0	0	0	0	1	0	0	155	0	9	1	0	0	0	0	0	0	1	0	0	0	0	0	0	ES
FI	0	0	0	0	0	0	0	1	0	0	0	1	0	1	0	26	0	0	0	0	0	0	0	0	0	0	0	1	0	1	0	FI
FR	0	0	1	0	0	6	0	0	2	0	0	14	0	0	5	0	247	6	0	0	0	0	1	0	5	0	0	0	1	0	0	FR
GB	0	0	0	0	0	1	0	0	0	0	0	3	0	0	1	0	5	147	0	0	0	0	5	0	0	0	0	0	0	0	0	GB
GE	0	7	0	50	0	0	0	0	0	0	0	0	0	0	0	0	0	0	244	0	0	0	0	0	0	0	0	0	0	0	0	GE
GL	0	0	0	0	0	0	0	0	0	0	0	0	0	0	0	0	0	0	0	0	0	0	0	0	0	0	0	0	0	0	0	GL
GR	8	0	1	0	4	0	11	0	0	0	1	1	0	0	1	0	1	0	0	119	1	2	0	0	6	0	0	0	0	0	1	GR
HR	2	0	11	0	112	0	2	0	0	0	6	6	0	0	1	0	3	0	0	1	266	26	0	0	21	0	0	0	0	0	0	HR
HU	0	0	17	0	14	0	2	1	0	0	12	9	0	0	1	0	3	1	0	0	26	292	0	0	8	0	0	0	0	0	1	HU
IE	0	0	0	0	0	1	0	0	0	0	0	1	0	0	0	0	3	18	0	0	0	0	94	0	0	0	0	0	0	0	0	IE
IS	0	0	0	0	0	0	0	0	0	0	0	0	0	0	0	0	0	0	0	0	0	0	0	6	0	0	0	0	0	0	0	IS
IT	1	0	4	0	5	0	0	0	1	0	1	2	0	0	3	0	10	0	0	0	5	2	0	0	387	0	0	0	0	0	0	IT
KG	0	0	0	0	0	0	0	0	0	0	0	0	0	0	0	0	0	0	0	0	0	0	0	0	0	45	0	0	0	0	0	KG
KZ	0	0	0	1	0	0	0	0	0	0	0	0	0	0	0	0	0	0	0	0	0	0	0	0	0	1	0	0	0	0	0	KZ
LT	0	0	0	0	0	0	0	22	0	0	2	5	1	1	0	1	2	1	0	0	0	2	0	0	1	0	0	116	0	14	1	LT
LU	0	0	1	0	0	39	0	0	1	0	1	70	1	0	1	0	104	6	0	0	0	0	0	0	2	0	0	0	66	0	0	LU
LV	0	0	0	0	0	0	0	13	0	0	1	4	1	5	0	1	1	1	0	0	0	1	0	0	0	0	0	22	0	89	0	LV
MD	0	0	0	0	1	0	5	5	0	0	1	2	0	0	0	0	1	0	0	1	0	2	0	0	1	0	0	1	0	1	290	MD
ME	22	0	1	0	30	0	2	0	0	0	1	2	0	0	2	0	1	0	0	1	4	5	0	0	9	0	0	0	0	0	0	ME
MK	22	0	1	0	6	0	9	0	0	0	1	1	0	0	1	0	1	0	0	21	2	4	0	0	5	0	0	0	0	0	0	MK
MT	1	0	1	0	4	0	0	0	0	0	1	1	0	0	4	0	6	0	0	2	2	1	0	0	29	0	0	0	0	0	0	MT
NL	0	0	0	0	0	57	0	0	0	0	1	51	1	0	1	0	36	17	0	0	0	0	1	0	1	0	0	0	0	0	0	NL
NO	0	0	0	0	0	0	0	0	0	0	0	0	0	0	0	0	0	1	0	0	0	0	0	0	0	0	0	0	0	0	0	NO
PL	0	0	2	0	1	1	1	5	0	0	14	21	1	0	0	0	4	2	0	0	1	6	0	0	2	0	0	2	0	1	1	PL
PT	0	0	0	0	0	0	0	0	0	0	0	1	0	0	39	0	4	1	0	0	0	0	0	0	0	0	0	0	0	0	0	PT
RO	1	0	1	0	4	0	16	1	0	0	2	2	0	0	0	0	1	0	0	1	2	12	0	0	2	0	0	0	0	0	10	RO
RS	6	0	3	0	43	0	11	1	0	0	4	4	0	0	1	0	2	0	0	2	14	26	0	0	6	0	0	0	0	0	1	RS
RU	0	0	0	1	0	0	0	2	0	0	0	0	0	0	0	0	0	0	0	0	0	0	0	0	0	0	0	0	0	0	0	RU
SE	0	0	0	0	0	0	0	0	0	0	0	2	2	0	0	1	1	1	0	0	0	0	0	0	0	0	0	0	0	0	0	SE
SI	0	0	43	0	7	0	1	0	1	0	4	7	0	0	1	0	4	0	0	0	61	11	0	0	47	0	0	0	0	0	0	SI
SK	0	0	10	0	4	0	1	1	0	0	23	9	0	0	0	0	3	1	0	0	5	51	0	0	4	0	0	0	0	0	0	SK
TJ	0	0	0	0	0	0	0	0	0	0	0	0	0	0	0	0	0	0	0	0	0	0	0	0	0	3	0	0	0	0	0	TJ
TM	0	0	0	6	0	0	0	0	0	0	0	0	0	0	0	0	0	0	1	0	0	0	0	0	0	0	0	0	0	0	0	TM
TR	0	2	0	2	0	0	2	0	0	0	0	0	0	0	0	0	0	0	1	2	0	0	0	0	1	0	0	0	0	0	0	TR
UA	0	0	0	1	1	0	2	12	0	0	1	2	0	0	0	0	1	0	0	0	0	2	0	0	1	0	0	1	0	1	10	UA
UZ	0	0	0	2	0	0	0	0	0	0	0	0	0	0	0	0	0	0	0	0	0	0	0	0	0	5	0	0	0	0	0	UZ
ATL	0	0	0	0	0	0	0	0	0	0	0	0	0	0	2	0	2	2	0	0	0	0	1	0	0	0	0	0	0	0	0	ATL
BAS	0	0	0	0	0	1	0	2	0	0	1	10	8	4	0	4	2	2	0	0	0	1	0	0	0	0	0	3	0	4	0	BAS
BLS	0	0	0	2	1	0	6	3	0	0	0	1	0	0	0	0	0	0	12	2	0	1	0	0	1	0	0	0	0	0	5	BLS
MED	2	0	1	0	4	0	2	0	0	0	1	1	0	0	11	0	10	0	0	10	3	1	0	0	27	0	0	0	0	0	0	MED
NOS	0	0	0	0	0	3	0	0	0	0	0	6	2	0	1	0	10	24	0	0	0	0	1	0	0	0	0	0	0	0	0	NOS
AST	0	0	0	5	0	0	0	0	0	0	0	0	0	0	0	0	0	0	0	0	0	0	0	0	0	0	0	0	0	0	0	AST
NOA	0	0	0	0	1	0	0	0	0	0	0	0	0	0	6	0	2	0	0	1	0	0	0	0	3	0	0	0	0	0	0	NOA
EXC	1	0	1	4	3	1	2	3	0	0	2	6	0	0	5	1	9	3	1	1	1	2	0	0	7	1	0	1	0	1	1	EXC
EU	0	0	6	0	3	4	7	1	1	0	7	26	2	1	21	2	39	2	0	4	6	10	2	0	31	0	0	3	0	2	1	EU
	AL	AM	AT	AZ	BA	BE	BG	BY	CH	CY	CZ	DE	DK	EE	ES	FI	FR	GB	GE	GR	HR	HU	IE	IS	IT	KG	KZ	LT	LU	LV	MD	

Table C.16 Cont.: 2021 country-to-country blame matrices for **fine EC**.
Units: 0.1 ng/m^3 per 15% emis. red. of PPM. **Emitters →, Receptors ↓.**

	ME	MK	MT	NL	NO	PL	PT	RO	RS	RU	SE	SI	SK	TJ	TM	TR	UA	UZ	ATL	BAS	BLS	MED	NOS	AST	NOA	BIC	DMS	VOL	EXC	EU	
AL	15	11	0	0	0	7	0	3	63	0	0	0	1	0	0	1	2	0	0	0	0	2	0	0	2	0	0	0	407	45	AL
AM	0	0	0	0	0	0	0	0	0	0	0	0	0	0	1	31	0	0	0	0	0	0	0	0	0	0	0	0	282	1	AM
AT	0	0	0	0	0	14	0	2	3	0	0	9	3	0	0	0	2	0	0	0	0	0	0	0	0	0	0	0	281	271	AT
AZ	0	0	0	0	0	0	0	0	0	0	0	0	0	0	2	8	1	1	0	0	0	0	0	0	0	0	0	0	728	1	AZ
BA	5	0	0	0	0	16	0	4	28	0	0	1	2	0	0	0	2	0	0	0	0	1	0	0	2	0	0	0	693	101	BA
BE	0	0	0	30	1	3	0	0	0	0	0	0	0	0	0	0	1	0	0	0	0	0	18	0	0	0	0	0	474	459	BE
BG	1	2	0	0	0	15	0	42	25	0	0	0	1	0	0	6	20	0	0	0	0	0	0	0	1	0	0	0	344	281	BG
BY	0	0	0	0	0	101	0	5	1	0	0	0	1	0	0	0	37	0	0	1	0	0	0	0	0	0	0	0	320	132	BY
CH	0	0	0	0	0	1	0	0	0	0	0	0	0	0	0	0	0	0	0	0	0	0	0	0	0	0	0	0	194	93	CH
CY	0	0	0	0	0	2	0	2	1	0	0	0	0	0	0	69	4	0	0	0	0	5	0	0	2	0	0	0	128	51	CY
CZ	0	0	0	1	0	116	0	4	4	0	0	2	9	0	0	0	3	0	0	0	0	0	1	0	0	0	0	0	422	409	CZ
DE	0	0	0	8	1	29	0	1	1	0	0	0	0	0	0	0	1	0	0	1	0	0	4	0	0	0	0	0	326	316	DE
DK	0	0	0	3	5	24	0	0	0	0	2	0	0	0	0	0	1	0	0	8	0	0	7	0	0	0	0	0	173	159	DK
EE	0	0	0	0	1	23	0	1	0	0	2	0	0	0	0	0	7	0	0	4	0	0	0	0	0	0	0	0	143	127	EE
ES	0	0	0	0	0	0	9	0	0	0	0	0	0	0	0	0	0	0	1	0	0	2	0	0	3	0	0	0	176	175	ES
FI	0	0	0	0	1	5	0	0	0	0	1	0	0	0	0	0	2	0	0	1	0	0	0	0	0	0	0	0	43	38	FI
FR	0	0	0	2	0	2	0	0	0	0	0	0	0	0	0	0	0	0	0	0	0	1	3	0	1	0	0	0	293	284	FR
GB	0	0	0	2	0	0	0	0	0	0	0	0	0	0	0	0	0	0	1	0	0	0	6	0	0	0	0	0	165	18	GB
GE	0	0	0	0	0	0	0	0	0	0	0	0	0	0	1	14	1	0	0	0	0	0	0	0	0	0	0	0	320	1	GE
GL	0	0	0	0	0	0	0	0	0	0	0	0	0	0	0	0	0	0	0	0	0	0	0	0	0	0	0	0	0	0	GL
GR	1	5	0	0	0	6	0	7	13	0	0	0	1	0	0	12	8	0	0	0	0	4	0	0	3	0	0	0	209	157	GR
HR	2	0	0	0	0	20	0	6	28	0	0	16	3	0	0	0	3	0	0	0	0	1	0	0	1	0	0	0	538	389	HR
HU	0	0	0	0	0	74	0	47	33	0	0	5	29	0	0	0	14	0	0	0	0	0	0	0	1	0	0	0	592	527	HU
IE	0	0	0	1	0	0	0	0	0	0	0	0	0	0	0	0	0	0	1	0	0	0	1	0	0	0	0	0	118	100	IE
IS	0	0	0	0	0	0	0	0	0	0	0	0	0	0	0	0	0	0	0	0	0	0	0	0	0	0	0	0	7	0	IS
IT	0	0	0	0	0	4	0	1	2	0	0	4	0	0	0	0	1	0	0	0	0	4	0	0	3	0	0	0	437	426	IT
KG	0	0	0	0	0	0	0	0	0	0	0	0	0	13	0	1	0	32	0	0	0	0	0	0	0	0	0	0	92	0	KG
KZ	0	0	0	0	0	1	0	0	0	0	0	0	0	1	1	0	3	7	0	0	0	0	0	0	0	0	0	0	17	1	KZ
LT	0	0	0	0	1	127	0	3	1	0	1	0	1	0	0	0	14	0	0	2	0	0	1	0	0	0	0	0	317	278	LT
LU	0	0	0	7	1	5	0	0	0	0	0	0	0	0	0	0	1	0	0	0	0	0	3	0	0	0	0	0	305	298	LU
LV	0	0	0	0	1	50	0	2	0	0	1	0	1	0	0	0	10	0	0	2	0	0	0	0	0	0	0	0	208	182	LV
MD	0	0	0	0	0	47	0	93	3	0	0	0	1	0	0	4	114	0	0	0	0	0	0	0	0	0	0	0	577	159	MD
ME	213	1	0	0	0	10	0	3	42	0	0	0	1	0	0	0	2	0	0	0	0	1	0	0	2	0	0	0	353	43	ME
MK	1	171	0	0	0	10	0	6	76	0	0	0	1	0	0	1	4	0	0	0	0	1	0	0	2	0	0	0	348	65	MK
MT	1	0	152	0	0	3	0	1	3	0	0	0	0	0	0	0	1	0	0	0	0	35	0	0	14	0	0	0	214	204	MT
NL	0	0	0	207	1	7	0	0	0	0	0	0	0	0	0	0	1	0	0	0	0	0	31	0	0	0	0	0	385	365	NL
NO	0	0	0	0	28	1	0	0	0	0	1	0	0	0	0	0	0	0	0	0	0	0	1	0	0	0	0	0	33	4	NO
PL	0	0	0	1	1	1221	0	8	2	0	1	0	9	0	0	0	20	0	0	2	0	0	1	0	0	0	0	0	1328	1295	PL
PT	0	0	0	0	0	0	178	0	0	0	0	0	0	0	0	0	0	0	3	0	0	1	0	0	2	0	0	0	224	223	PT
RO	1	1	0	0	0	34	0	389	16	0	0	0	3	0	0	2	35	0	0	0	0	0	0	0	1	0	0	0	540	468	RO
RS	8	8	0	0	0	28	0	32	480	0	0	1	4	0	0	0	8	0	0	0	0	0	0	0	1	0	0	0	694	139	RS
RU	0	0	0	0	0	4	0	0	0	0	0	0	0	0	0	0	8	0	0	0	0	0	0	0	0	0	0	0	19	6	RU
SE	0	0	0	0	4	8	0	0	0	0	13	0	0	0	0	0	1	0	0	2	0	0	1	0	0	0	0	0	38	31	SE
SI	0	0	0	0	0	12	0	3	4	0	0	243	1	0	0	0	2	0	0	0	0	1	0	0	1	0	0	0	455	439	SI
SK	0	0	0	0	0	184	0	19	8	0	0	2	169	0	0	0	17	0	0	0	0	0	0	0	0	0	0	0	515	483	SK
TJ	0	0	0	0	0	0	0	0	0	0	0	0	0	215	2	1	0	31	0	0	0	0	0	0	0	0	0	0	252	0	TJ
TM	0	0	0	0	0	0	0	0	0	0	0	0	0	5	53	1	2	27	0	0	0	0	0	0	0	0	0	0	97	1	TM
TR	0	0	0	0	0	2	0	2	1	0	0	0	0	0	0	207	6	0	0	0	0	1	0	0	1	0	0	0	230	10	TR
UA	0	0	0	0	0	60	0	18	1	0	0	0	1	0	0	4	328	0	0	0	0	0	0	0	0	0	0	0	451	93	UA
UZ	0	0	0	0	0	1	0	0	0	0	0	0	0	24	6	1	2	161	0	0	0	0	0	0	0	0	0	0	203	1	UZ
ATL	0	0	0	0	0	0	2	0	0	0	0	0	0	0	0	0	0	0	1	0	0	0	0	0	1	0	0	0	10	8	ATL
BAS	0	0	0	1	2	58	0	1	0	0	7	0	0	0	0	0	4	0	0	16	0	0	1	0	0	0	0	0	119	107	BAS
BLS	0	0	0	0	0	11	0	14	2	0	0	0	0	0	0	53	69	0	0	0	4	1	0	0	0	0	0	0	184	37	BLS
MED	1	0	0	0	0	4	1	2	3	0	0	1	0	0	0	19	3	0	0	0	0	14	0	0	16	0	0	0	110	76	MED
NOS	0	0	0	4	7	3	0	0	0	0	0	0	0	0	0	0	0	0	0	1	0	0	19	0	0	0	0	0	63	31	NOS
AST	0	0	0	0	0	0	0	0	0	0	0	0	0	3	2	7	1	2	0	0	0	0	0	0	0	0	0	0	21	1	AST
NOA	0	0	0	0	0	1	1	1	1	0	0	0	0	0	0	2	1	0	0	0	0	2	0	0	92	0	0	0	21	17	NOA
EXC	0	0	0	1	1	29	1	7	4	0	0	1	1	3	2	10	17	6	0	0	0	0	0	0	0	0	0	0	141	82	EXC
EU	0	0	0	3	1	109	5	26	4	0	2	2	4	0	0	1	6	0	0	1	0	1	1	0	1	0	0	0	345	324	EU
	ME	MK	MT	NL	NO	PL	PT	RO	RS	RU	SE	SI	SK	TJ	TM	TR	UA	UZ	ATL	BAS	BLS	MED	NOS	AST	NOA	BIC	DMS	VOL	EXC	EU	

Table C.17: 2021 country-to-country blame matrices for **coarse EC**.
Units: 0.1 ng/m^3 per 15% emis. red. of PPM. **Emitters →, Receptors ↓.**

	AL	AM	AT	AZ	BA	BE	BG	BY	CH	CY	CZ	DE	DK	EE	ES	FI	FR	GB	GE	GR	HR	HU	IE	IS	IT	KG	KZ	LT	LU	LV	MD	
AL	12	0	0	0	1	0	0	0	0	0	0	0	0	0	0	0	0	0	0	1	0	0	0	0	0	0	0	0	0	0	0	AL
AM	0	10	0	4	0	0	0	0	0	0	0	0	0	0	0	0	0	0	2	0	0	0	0	0	0	0	0	0	0	0	0	AM
AT	0	0	14	0	0	0	0	0	2	0	1	3	0	0	0	0	0	0	0	0	1	0	0	0	0	0	0	0	0	0	0	AT
AZ	0	1	0	35	0	0	0	0	0	0	0	0	0	0	0	0	0	0	4	0	0	0	0	0	0	0	0	0	0	0	0	AZ
BA	0	0	0	0	57	0	0	0	0	0	1	1	0	0	0	0	0	0	0	0	4	1	0	0	0	0	0	0	0	0	0	BA
BE	0	0	0	0	0	22	0	0	0	0	0	8	0	0	0	0	4	1	0	0	0	0	0	0	0	0	0	0	0	0	0	BE
BG	0	0	0	0	1	0	17	0	0	0	0	0	0	0	0	0	0	0	0	1	0	0	0	0	0	0	0	0	0	0	0	BG
BY	0	0	0	0	0	0	0	7	0	0	0	1	0	0	0	0	0	0	0	0	0	0	0	0	0	0	0	2	0	0	0	BY
CH	0	0	0	0	0	0	0	0	103	0	0	4	0	0	0	0	1	0	0	0	0	0	0	0	1	0	0	0	0	0	0	CH
CY	0	0	0	0	0	0	0	0	0	5	0	0	0	0	0	0	0	0	0	1	0	0	0	0	0	0	0	0	0	0	0	CY
CZ	0	0	1	0	0	0	0	0	0	0	25	7	0	0	0	0	0	0	0	0	1	1	0	0	0	0	0	0	0	0	0	CZ
DE	0	0	1	0	0	0	0	0	2	0	2	38	0	0	0	0	1	0	0	0	0	0	0	0	0	0	0	0	0	0	0	DE
DK	0	0	0	0	0	0	0	0	0	0	0	4	5	0	0	0	0	1	0	0	0	0	0	0	0	0	0	0	0	0	0	DK
EE	0	0	0	0	0	0	0	0	0	0	0	0	0	8	0	1	0	0	0	0	0	0	0	0	0	0	0	2	0	1	0	EE
ES	0	0	0	0	0	0	0	0	0	0	0	0	0	0	9	0	0	0	0	0	0	0	0	0	0	0	0	0	0	0	0	ES
FI	0	0	0	0	0	0	0	0	0	0	0	0	0	0	0	6	0	0	0	0	0	0	0	0	0	0	0	0	0	0	0	FI
FR	0	0	0	0	0	0	0	0	1	0	0	2	0	0	0	0	10	0	0	0	0	0	0	0	0	0	0	0	0	0	0	FR
GB	0	0	0	0	0	0	0	0	0	0	0	0	0	0	0	0	0	14	0	0	0	0	0	0	0	0	0	0	0	0	0	GB
GE	0	0	0	2	0	0	0	0	0	0	0	0	0	0	0	0	0	0	37	0	0	0	0	0	0	0	0	0	0	0	0	GE
GL	0	0	0	0	0	0	0	0	0	0	0	0	0	0	0	0	0	0	0	0	0	0	0	0	0	0	0	0	0	0	0	GL
GR	0	0	0	0	0	0	1	0	0	0	0	0	0	0	0	0	0	0	0	16	0	0	0	0	0	0	0	0	0	0	0	GR
HR	0	0	1	0	8	0	0	0	0	0	1	1	0	0	0	0	0	0	0	0	25	1	0	0	1	0	0	0	0	0	0	HR
HU	0	0	1	0	2	0	0	0	0	0	1	1	0	0	0	0	0	0	0	0	2	14	0	0	0	0	0	0	0	0	0	HU
IE	0	0	0	0	0	0	0	0	0	0	0	0	0	0	0	0	0	2	0	0	0	0	7	0	0	0	0	0	0	0	0	IE
IS	0	0	0	0	0	0	0	0	0	0	0	0	0	0	0	0	0	0	0	0	0	0	0	0	0	0	0	0	0	0	0	IS
IT	0	0	0	0	0	0	0	0	1	0	0	0	0	0	0	0	0	0	0	0	1	0	0	0	13	0	0	0	0	0	0	IT
KG	0	0	0	0	0	0	0	0	0	0	0	0	0	0	0	0	0	0	0	0	0	0	0	0	0	5	0	0	0	0	0	KG
KZ	0	0	0	0	0	0	0	0	0	0	0	0	0	0	0	0	0	0	0	0	0	0	0	0	0	0	0	0	0	0	0	KZ
LT	0	0	0	0	0	0	0	1	0	0	0	1	0	0	0	0	0	0	0	0	0	0	0	0	0	0	0	35	0	1	0	LT
LU	0	0	0	0	0	3	0	0	0	0	0	12	0	0	0	0	4	0	0	0	0	0	0	0	0	0	0	0	11	0	0	LU
LV	0	0	0	0	0	0	0	1	0	0	0	1	0	1	0	0	0	0	0	0	0	0	0	0	0	0	0	13	0	4	0	LV
MD	0	0	0	0	0	0	1	0	0	0	0	0	0	0	0	0	0	0	0	0	0	0	0	0	0	0	0	0	0	0	13	MD
ME	1	0	0	0	4	0	0	0	0	0	0	0	0	0	0	0	0	0	0	0	1	0	0	0	0	0	0	0	0	0	0	ME
MK	1	0	0	0	1	0	1	0	0	0	0	0	0	0	0	0	0	0	0	4	0	0	0	0	0	0	0	0	0	0	0	MK
MT	0	0	0	0	0	0	0	0	0	0	0	0	0	0	0	0	0	0	0	0	0	0	0	0	2	0	0	0	0	0	0	MT
NL	0	0	0	0	0	4	0	0	0	0	0	10	0	0	0	0	1	1	0	0	0	0	0	0	0	0	0	0	0	0	0	NL
NO	0	0	0	0	0	0	0	0	0	0	0	0	0	0	0	0	0	0	0	0	0	0	0	0	0	0	0	0	0	0	0	NO
PL	0	0	0	0	0	0	0	0	0	0	2	4	0	0	0	0	0	0	0	0	0	0	0	0	0	0	0	1	0	0	0	PL
PT	0	0	0	0	0	0	0	0	0	0	0	0	0	0	2	0	0	0	0	0	0	0	0	0	0	0	0	0	0	0	0	PT
RO	0	0	0	0	1	0	1	0	0	0	0	0	0	0	0	0	0	0	0	0	0	1	0	0	0	0	0	0	0	0	0	RO
RS	0	0	0	0	6	0	1	0	0	0	0	1	0	0	0	0	0	0	0	0	1	1	0	0	0	0	0	0	0	0	0	RS
RU	0	0	0	0	0	0	0	0	0	0	0	0	0	0	0	0	0	0	0	0	0	0	0	0	0	0	0	0	0	0	0	RU
SE	0	0	0	0	0	0	0	0	0	0	0	0	0	0	0	0	0	0	0	0	0	0	0	0	0	0	0	0	0	0	0	SE
SI	0	0	3	0	1	0	0	0	0	0	1	1	0	0	0	0	0	0	0	0	8	0	0	0	2	0	0	0	0	0	0	SI
SK	0	0	1	0	1	0	0	0	0	0	3	1	0	0	0	0	0	0	0	0	1	3	0	0	0	0	0	0	0	0	0	SK
TJ	0	0	0	0	0	0	0	0	0	0	0	0	0	0	0	0	0	0	0	0	0	0	0	0	0	1	0	0	0	0	0	TJ
TM	0	0	0	0	0	0	0	0	0	0	0	0	0	0	0	0	0	0	0	0	0	0	0	0	0	0	0	0	0	0	0	TM
TR	0	0	0	0	0	0	0	0	0	0	0	0	0	0	0	0	0	0	0	0	0	0	0	0	0	0	0	0	0	0	0	TR
UA	0	0	0	0	0	0	0	0	0	0	0	0	0	0	0	0	0	0	0	0	0	0	0	0	0	0	0	0	0	0	0	UA
UZ	0	0	0	0	0	0	0	0	0	0	0	0	0	0	0	0	0	0	0	0	0	0	0	0	0	1	0	0	0	0	0	UZ
ATL	0	0	0	0	0	0	0	0	0	0	0	0	0	0	0	0	0	0	0	0	0	0	0	0	0	0	0	0	0	0	0	ATL
BAS	0	0	0	0	0	0	0	0	0	0	0	2	0	0	0	1	0	0	0	0	0	0	0	0	0	0	0	1	0	0	0	BAS
BLS	0	0	0	0	0	0	1	0	0	0	0	0	0	0	0	0	0	0	1	0	0	0	0	0	0	0	0	0	0	0	0	BLS
MED	0	0	0	0	0	0	0	0	0	0	0	0	0	0	1	0	0	0	0	1	0	0	0	0	1	0	0	0	0	0	0	MED
NOS	0	0	0	0	0	0	0	0	0	0	0	1	0	0	0	0	0	2	0	0	0	0	0	0	0	0	0	0	0	0	0	NOS
AST	0	0	0	0	0	0	0	0	0	0	0	0	0	0	0	0	0	0	0	0	0	0	0	0	0	0	0	0	0	0	0	AST
NOA	0	0	0	0	0	0	0	0	0	0	0	0	0	0	0	0	0	0	0	0	0	0	0	0	0	0	0	0	0	0	0	NOA
EXC	0	0	0	0	0	0	0	0	0	0	0	1	0	0	0	0	0	0	0	0	0	0	0	0	0	0	0	0	0	0	0	EXC
EU	0	0	0	0	0	0	1	0	0	0	1	4	0	0	1	0	2	0	0	1	1	0	0	0	1	0	0	1	0	0	0	EU
	AL	AM	AT	AZ	BA	BE	BG	BY	CH	CY	CZ	DE	DK	EE	ES	FI	FR	GB	GE	GR	HR	HU	IE	IS	IT	KG	KZ	LT	LU	LV	MD	

Table C.17 Cont.: 2021 country-to-country blame matrices for **coarse EC**.
Units: 0.1 ng/m^3 per 15% emis. red. of PPM. **Emitters** →, **Receptors** ↓.

	ME	MK	MT	NL	NO	PL	PT	RO	RS	RU	SE	SI	SK	TJ	TM	TR	UA	UZ	ATL	BAS	BLS	MED	NOS	AST	NOA	BIC	DMS	VOL	EXC	EU	
AL	1	1	0	0	0	1	0	0	4	0	0	0	0	0	0	0	0	0	0	0	0	0	0	0	0	0	0	0	24	4	AL
AM	0	0	0	0	0	0	0	0	0	0	0	0	0	0	0	5	0	0	0	0	0	0	0	0	0	0	0	0	21	0	AM
AT	0	0	0	0	0	2	0	0	0	0	0	1	0	0	0	0	0	0	0	0	0	0	0	0	0	0	0	0	27	24	AT
AZ	0	0	0	0	0	0	0	0	0	0	0	0	0	0	0	1	0	0	0	0	0	0	0	0	0	0	0	0	42	0	AZ
BA	0	0	0	0	0	2	0	0	4	0	0	0	0	0	0	0	0	0	0	0	0	0	0	0	0	0	0	0	71	9	BA
BE	0	0	0	3	0	0	0	0	0	0	0	0	0	0	0	0	0	0	0	0	0	0	0	0	0	0	0	0	39	38	BE
BG	0	0	0	0	0	1	0	3	3	0	0	0	0	0	0	2	2	0	0	0	0	0	0	0	0	0	0	0	33	24	BG
BY	0	0	0	0	0	6	0	0	0	0	0	0	0	0	0	0	5	0	0	0	0	0	0	0	0	0	0	0	23	10	BY
CH	0	0	0	0	0	0	0	0	0	0	0	0	0	0	0	0	0	0	0	0	0	0	0	0	0	0	0	0	110	7	CH
CY	0	0	0	0	0	0	0	0	0	0	0	0	0	0	0	28	0	0	0	0	0	0	0	0	0	0	0	0	34	6	CY
CZ	0	0	0	0	0	17	0	0	1	0	0	0	1	0	0	0	0	0	0	0	0	0	0	0	0	0	0	0	56	54	CZ
DE	0	0	0	1	0	2	0	0	0	0	0	0	0	0	0	0	0	0	0	0	0	0	0	0	0	0	0	0	48	45	DE
DK	0	0	0	0	1	2	0	0	0	0	1	0	0	0	0	0	0	0	0	0	0	0	0	0	0	0	0	0	13	12	DK
EE	0	0	0	0	0	2	0	0	0	0	0	0	0	0	0	0	1	0	0	0	0	0	0	0	0	0	0	0	16	15	EE
ES	0	0	0	0	0	0	0	0	0	0	0	0	0	0	0	0	0	0	0	0	0	0	0	0	0	0	0	0	10	10	ES
FI	0	0	0	0	0	0	0	0	0	0	0	0	0	0	0	0	0	0	0	0	0	0	0	0	0	0	0	0	7	7	FI
FR	0	0	0	0	0	0	0	0	0	0	0	0	0	0	0	0	0	0	0	0	0	0	0	0	0	0	0	0	16	14	FR
GB	0	0	0	0	0	0	0	0	0	0	0	0	0	0	0	0	0	0	0	0	0	0	0	0	0	0	0	0	15	1	GB
GE	0	0	0	0	0	0	0	0	0	0	0	0	0	0	0	3	0	0	0	0	0	0	0	0	0	0	0	0	42	0	GE
GL	0	0	0	0	0	0	0	0	0	0	0	0	0	0	0	0	0	0	0	0	0	0	0	0	0	0	0	0	0	0	GL
GR	0	2	0	0	0	1	0	1	1	0	0	0	0	0	0	5	1	0	0	0	0	0	0	0	0	0	0	0	29	20	GR
HR	0	0	0	0	0	2	0	0	4	0	0	1	0	0	0	0	0	0	0	0	0	0	0	0	0	0	0	0	47	34	HR
HU	0	0	0	0	0	9	0	3	6	0	0	0	3	0	0	0	1	0	0	0	0	0	0	0	0	0	0	0	47	37	HU
IE	0	0	0	0	0	0	0	0	0	0	0	0	0	0	0	0	0	0	0	0	0	0	0	0	0	0	0	0	9	7	IE
IS	0	0	0	0	0	0	0	0	0	0	0	0	0	0	0	0	0	0	0	0	0	0	0	0	0	0	0	0	0	0	IS
IT	0	0	0	0	0	0	0	0	0	0	0	0	0	0	0	0	0	0	0	0	0	0	0	0	1	0	0	0	18	16	IT
KG	0	0	0	0	0	0	0	0	0	0	0	0	0	2	0	0	0	3	0	0	0	0	0	0	0	0	0	0	10	0	KG
KZ	0	0	0	0	0	0	0	0	0	0	0	0	0	0	0	0	0	1	0	0	0	0	0	0	0	0	0	0	2	0	KZ
LT	0	0	0	0	0	8	0	0	0	0	0	0	0	0	0	0	2	0	0	0	0	0	0	0	0	0	0	0	49	46	LT
LU	0	0	0	1	0	0	0	0	0	0	0	0	0	0	0	0	0	0	0	0	0	0	0	0	0	0	0	0	32	31	LU
LV	0	0	0	0	0	3	0	0	0	0	0	0	0	0	0	0	1	0	0	0	0	0	0	0	0	0	0	0	26	23	LV
MD	0	0	0	0	0	4	0	4	0	0	0	0	0	0	0	1	13	0	0	0	0	0	0	0	0	0	0	0	38	10	MD
ME	10	0	0	0	0	1	0	0	4	0	0	0	0	0	0	0	0	0	0	0	0	0	0	0	0	0	0	0	23	4	ME
MK	0	15	0	0	0	1	0	1	6	0	0	0	0	0	0	0	0	0	0	0	0	0	0	0	0	0	0	0	32	8	MK
MT	0	0	37	0	0	0	0	0	0	0	0	0	0	0	0	0	0	0	0	0	0	0	0	0	2	0	0	0	42	41	MT
NL	0	0	0	20	0	0	0	0	0	0	0	0	0	0	0	0	0	0	0	0	0	0	0	0	0	0	0	0	38	36	NL
NO	0	0	0	0	3	0	0	0	0	0	0	0	0	0	0	0	0	0	0	0	0	0	0	0	0	0	0	0	4	0	NO
PL	0	0	0	0	0	90	0	1	0	0	0	0	1	0	0	0	2	0	0	0	0	0	0	0	0	0	0	0	103	100	PL
PT	0	0	0	0	0	0	9	0	0	0	0	0	0	0	0	0	0	0	0	0	0	0	0	0	0	0	0	0	12	12	PT
RO	0	0	0	0	0	3	0	25	2	0	0	0	0	0	0	0	4	0	0	0	0	0	0	0	0	0	0	0	40	32	RO
RS	0	1	0	0	0	3	0	4	46	0	0	0	1	0	0	0	1	0	0	0	0	0	0	0	0	0	0	0	68	14	RS
RU	0	0	0	0	0	0	0	0	0	0	0	0	0	0	0	0	1	0	0	0	0	0	0	0	0	0	0	0	2	1	RU
SE	0	0	0	0	0	0	0	0	0	0	4	0	0	0	0	0	0	0	0	0	0	0	0	0	0	0	0	0	7	6	SE
SI	0	0	0	0	0	1	0	0	1	0	0	17	0	0	0	0	0	0	0	0	0	0	0	0	0	0	0	0	36	33	SI
SK	0	0	0	0	0	27	0	1	1	0	0	0	15	0	0	0	2	0	0	0	0	0	0	0	0	0	0	0	56	52	SK
TJ	0	0	0	0	0	0	0	0	0	0	0	0	0	21	0	0	0	3	0	0	0	0	0	0	0	0	0	0	25	0	TJ
TM	0	0	0	0	0	0	0	0	0	0	0	0	0	0	5	0	0	2	0	0	0	0	0	0	0	0	0	0	8	0	TM
TR	0	0	0	0	0	0	0	0	0	0	0	0	0	0	0	77	1	0	0	0	0	0	0	0	0	0	0	0	79	1	TR
UA	0	0	0	0	0	5	0	1	0	0	0	0	0	0	0	1	52	0	0	0	0	0	0	0	0	0	0	0	61	7	UA
UZ	0	0	0	0	0	0	0	0	0	0	0	0	0	2	1	0	0	14	0	0	0	0	0	0	0	0	0	0	18	0	UZ
ATL	0	0	0	0	0	0	0	0	0	0	0	0	0	0	0	0	0	0	0	0	0	0	0	0	0	0	0	0	1	1	ATL
BAS	0	0	0	0	0	3	0	0	0	0	2	0	0	0	0	0	1	0	0	0	0	0	0	0	0	0	0	0	12	10	BAS
BLS	0	0	0	0	0	1	0	1	0	0	0	0	0	0	0	20	9	0	0	0	0	0	0	0	0	0	0	0	34	3	BLS
MED	0	0	0	0	0	0	0	0	0	0	0	0	0	0	0	9	0	0	0	0	0	0	0	0	3	0	0	0	16	5	MED
NOS	0	0	0	0	1	0	0	0	0	0	0	0	0	0	0	0	0	0	0	0	0	0	0	0	0	0	0	0	5	2	NOS
AST	0	0	0	0	0	0	0	0	0	0	0	0	0	0	0	2	0	0	0	0	0	0	0	0	0	0	0	0	3	0	AST
NOA	0	0	0	0	0	0	0	0	0	0	0	0	0	0	0	1	0	0	0	0	0	0	0	0	19	0	0	0	2	1	NOA
EXC	0	0	0	0	0	2	0	0	0	0	0	0	0	0	0	3	3	1	0	0	0	0	0	0	0	0	0	0	16	7	EXC
EU	0	0	0	0	0	9	0	2	1	0	1	0	0	0	0	0	1	0	0	0	0	0	0	0	0	0	0	0	29	26	EU
	ME	MK	MT	NL	NO	PL	PT	RO	RS	RU	SE	SI	SK	TJ	TM	TR	UA	UZ	ATL	BAS	BLS	MED	NOS	AST	NOA	BIC	DMS	VOL	EXC	EU	

Table C.18: 2021 country-to-country blame matrices for **PPM2.5**
Units: ng/m^3 per 15% emis. red. of PPM. **Emitters** →, **Receptors** ↓.

	AL	AM	AT	AZ	BA	BE	BG	BY	CH	CY	CZ	DE	DK	EE	ES	FI	FR	GB	GE	GR	HR	HU	IE	IS	IT	KG	KZ	LT	LU	LV	MD	
AL	152	0	1	0	8	0	2	0	0	0	1	1	0	0	1	0	1	0	0	6	3	2	0	0	8	0	0	0	0	0	0	AL
AM	0	74	0	21	0	0	0	0	0	0	0	0	0	0	0	0	0	0	8	0	0	0	0	0	0	0	0	0	0	0	0	AM
AT	0	0	143	0	3	0	0	0	2	0	8	13	0	0	0	0	4	0	0	0	6	7	0	0	12	0	0	0	0	0	0	AT
AZ	0	6	0	190	0	0	0	0	0	0	0	0	0	0	0	0	0	0	12	0	0	0	0	0	0	0	1	0	0	0	0	AZ
BA	1	0	3	0	491	0	1	0	0	0	2	2	0	0	1	0	2	0	0	0	29	7	0	0	8	0	0	0	0	0	0	BA
BE	0	0	0	0	0	149	0	0	0	0	1	21	0	0	1	0	64	8	0	0	0	0	0	0	1	0	0	0	2	0	0	BE
BG	1	0	1	0	4	0	155	1	0	0	1	1	0	0	0	0	1	0	0	5	2	3	0	0	2	0	0	0	0	0	3	BG
BY	0	0	1	0	1	0	0	109	0	0	2	3	0	0	0	0	1	1	0	0	1	2	0	0	1	0	0	4	0	2	1	BY
CH	0	0	5	0	0	0	0	0	82	0	1	15	0	0	1	0	22	0	0	0	0	0	0	0	18	0	0	0	0	0	0	CH
CY	0	0	0	0	0	0	1	0	0	17	0	0	0	0	0	0	0	0	0	3	0	0	0	0	1	0	0	0	0	0	0	CY
CZ	0	0	14	0	3	1	0	1	1	0	174	22	0	0	0	0	6	1	0	0	5	9	0	0	3	0	0	0	0	0	0	CZ
DE	0	0	8	0	0	4	0	0	3	0	6	134	1	0	1	0	17	3	0	0	0	1	0	0	1	0	0	0	1	0	0	DE
DK	0	0	0	0	0	1	0	0	0	0	1	13	69	0	0	0	4	5	0	0	0	1	0	0	0	0	0	0	0	0	0	DK
EE	0	0	0	0	0	0	0	5	0	0	1	2	1	50	0	2	1	1	0	0	0	0	0	0	0	0	0	2	0	10	0	EE
ES	0	0	0	0	0	0	0	0	0	0	0	0	0	0	99	0	4	0	0	0	0	0	0	0	1	0	0	0	0	0	0	ES
FI	0	0	0	0	0	0	0	1	0	0	0	1	0	1	0	16	0	0	0	0	0	0	0	0	0	0	0	0	0	1	0	FI
FR	0	0	1	0	0	3	0	0	2	0	1	7	0	0	4	0	144	3	0	0	0	0	0	0	4	0	0	0	0	0	0	FR
GB	0	0	0	0	0	1	0	0	0	0	0	3	0	0	0	0	5	92	0	0	0	0	3	0	0	0	0	0	0	0	0	GB
GE	0	8	0	18	0	0	0	0	0	0	0	0	0	0	0	0	0	0	119	0	0	0	0	0	0	0	0	0	0	0	0	GE
GL	0	0	0	0	0	0	0	0	0	0	0	0	0	0	0	0	0	0	0	0	0	0	0	0	0	0	0	0	0	0	0	GL
GR	4	0	0	0	3	0	9	1	0	0	1	0	0	0	1	0	1	0	0	91	1	1	0	0	4	0	0	0	0	0	1	GR
HR	0	0	7	0	96	0	1	0	0	0	4	4	0	0	1	0	2	0	0	0	227	19	0	0	20	0	0	0	0	0	0	HR
HU	0	0	11	0	15	0	2	1	0	0	6	5	0	0	0	0	2	1	0	0	25	227	0	0	7	0	0	0	0	0	1	HU
IE	0	0	0	0	0	0	0	0	0	0	0	1	0	0	0	0	3	11	0	0	0	0	48	0	0	0	0	0	0	0	0	IE
IS	0	0	0	0	0	0	0	0	0	0	0	0	0	0	0	0	0	0	0	0	0	0	0	2	0	0	0	0	0	0	0	IS
IT	0	0	3	0	4	0	0	0	1	0	1	1	0	0	2	0	6	0	0	0	5	2	0	0	297	0	0	0	0	0	0	IT
KG	0	0	0	0	0	0	0	0	0	0	0	0	0	0	0	0	0	0	0	0	0	0	0	0	0	33	5	0	0	0	0	KG
KZ	0	0	0	0	0	0	0	0	0	0	0	0	0	0	0	0	0	0	0	0	0	0	0	0	0	1	32	0	0	0	0	KZ
LT	0	0	1	0	1	0	0	20	0	0	2	4	1	1	0	0	1	1	0	0	0	1	0	0	0	0	0	64	0	7	0	LT
LU	0	0	1	0	0	17	0	0	1	0	2	44	0	0	1	0	78	4	0	0	0	0	0	0	2	0	0	0	58	0	0	LU
LV	0	0	0	0	0	0	0	10	0	0	1	3	1	3	0	1	1	1	0	0	0	1	0	0	0	0	0	12	0	69	0	LV
MD	0	0	1	0	1	0	3	3	0	0	1	2	0	0	0	0	1	0	0	1	1	2	0	0	1	0	0	0	0	0	256	MD
ME	11	0	1	0	26	0	1	0	0	0	1	1	0	0	0	0	1	0	0	1	4	3	0	0	6	0	0	0	0	0	0	ME
MK	11	0	1	0	5	0	8	0	0	0	1	1	0	0	0	0	1	0	0	15	2	3	0	0	3	0	0	0	0	0	1	MK
MT	1	0	0	0	3	0	1	0	0	0	0	1	0	0	4	0	4	0	0	1	2	1	0	0	23	0	0	0	0	0	0	MT
NL	0	0	0	0	0	32	0	0	0	0	1	38	1	0	1	0	22	12	0	0	0	0	1	0	1	0	0	0	0	0	0	NL
NO	0	0	0	0	0	0	0	0	0	0	0	0	0	0	0	0	0	1	0	0	0	0	0	0	0	0	0	0	0	0	0	NO
PL	0	0	2	0	2	1	0	4	0	0	13	13	1	0	0	0	3	1	0	0	2	5	0	0	2	0	0	1	0	1	0	PL
PT	0	0	0	0	0	0	0	0	0	0	0	0	0	0	25	0	2	0	0	0	0	0	0	0	0	0	0	0	0	0	0	PT
RO	0	0	1	0	4	0	11	1	0	0	1	1	0	0	0	0	1	0	0	1	2	8	0	0	2	0	0	0	0	0	7	RO
RS	4	0	2	0	37	0	9	1	0	0	2	2	0	0	0	0	1	0	0	2	11	16	0	0	4	0	0	0	0	0	1	RS
RU	0	0	0	0	0	0	0	1	0	0	0	0	0	0	0	0	0	0	0	0	0	0	0	0	0	0	3	0	0	0	0	RU
SE	0	0	0	0	0	0	0	0	0	0	0	2	1	0	0	1	1	1	0	0	0	0	0	0	0	0	0	0	0	0	0	SE
SI	0	0	31	0	8	0	0	0	0	0	3	4	0	0	1	0	3	0	0	0	57	8	0	0	44	0	0	0	0	0	0	SI
SK	0	0	8	0	6	0	1	1	0	0	14	5	0	0	0	0	2	1	0	0	6	46	0	0	4	0	0	0	0	0	0	SK
TJ	0	0	0	0	0	0	0	0	0	0	0	0	0	0	0	0	0	0	0	0	0	0	0	0	0	2	1	0	0	0	0	TJ
TM	0	0	0	2	0	0	0	0	0	0	0	0	0	0	0	0	0	0	0	0	0	0	0	0	0	0	4	0	0	0	0	TM
TR	0	1	0	1	0	0	1	0	0	0	0	0	0	0	0	0	0	0	1	1	0	0	0	0	0	0	0	0	0	0	0	TR
UA	0	0	0	0	1	0	1	8	0	0	1	2	0	0	0	0	1	0	0	0	1	2	0	0	1	0	1	1	0	0	8	UA
UZ	0	0	0	0	0	0	0	0	0	0	0	0	0	0	0	0	0	0	0	0	0	0	0	0	0	4	9	0	0	0	0	UZ
ATL	0	0	0	0	0	0	0	0	0	0	0	0	0	0	1	0	1	1	0	0	0	0	0	0	0	0	0	0	0	0	0	ATL
BAS	0	0	0	0	0	1	0	2	0	0	1	7	5	2	0	2	2	2	0	0	0	0	0	0	0	0	0	2	0	3	0	BAS
BLS	0	0	0	1	1	0	5	2	0	0	0	0	0	0	0	0	0	0	8	1	0	1	0	0	0	0	0	0	0	0	3	BLS
MED	1	0	1	0	4	0	1	0	0	0	0	1	0	0	7	0	6	0	0	6	3	1	0	0	21	0	0	0	0	0	0	MED
NOS	0	0	0	0	0	2	0	0	0	0	0	4	1	0	0	0	7	15	0	0	0	0	1	0	0	0	0	0	0	0	0	NOS
AST	0	0	0	1	0	0	0	0	0	0	0	0	0	0	0	0	0	0	0	0	0	0	0	0	0	0	1	0	0	0	0	AST
NOA	0	0	0	0	1	0	0	0	0	0	0	0	0	0	3	0	1	0	0	1	0	0	0	0	2	0	0	0	0	0	0	NOA
EXC	0	0	1	1	2	1	1	2	0	0	1	4	0	0	3	0	5	2	1	1	1	2	0	0	6	1	6	0	0	1	1	EXC
EU	0	0	5	0	3	2	5	1	1	0	6	16	1	1	13	1	23	2	0	3	5	8	1	0	24	0	0	1	0	1	1	EU
	AL	AM	AT	AZ	BA	BE	BG	BY	CH	CY	CZ	DE	DK	EE	ES	FI	FR	GB	GE	GR	HR	HU	IE	IS	IT	KG	KZ	LT	LU	LV	MD	

Table C.18 Cont.: 2021 country-to-country blame matrices for **PPM2.5**
Units: ng/m^3 per 15% emis. red. of PPM. **Emitters →, Receptors ↓.**

	ME	MK	MT	NL	NO	PL	PT	RO	RS	RU	SE	SI	SK	TJ	TM	TR	UA	UZ	ATL	BAS	BLS	MED	NOS	AST	NOA	BIC	DMS	VOL	EXC	EU	
AL	15	12	0	0	0	3	0	4	44	0	0	0	1	0	0	1	2	0	0	0	0	1	0	0	1	0	0	0	269	33	AL
AM	0	0	0	0	0	0	0	0	0	1	0	0	0	0	0	19	1	0	0	0	0	0	0	8	0	0	0	0	126	1	AM
AT	0	0	0	0	0	7	0	2	2	0	0	9	2	0	0	0	2	0	0	0	0	0	0	0	0	0	0	0	222	213	AT
AZ	0	0	0	0	0	0	0	0	0	7	0	0	0	0	1	5	3	1	0	0	0	0	0	9	0	0	0	0	227	1	AZ
BA	5	0	0	0	0	7	0	5	27	0	0	1	1	0	0	0	3	0	0	0	0	0	0	0	0	0	0	0	598	70	BA
BE	0	0	0	13	0	3	0	0	0	0	0	0	0	0	0	0	0	0	0	0	0	0	5	0	0	0	0	0	267	258	BE
BG	1	2	0	0	0	5	0	33	21	2	0	0	1	0	0	6	13	0	0	0	0	0	0	0	0	0	0	0	265	211	BG
BY	0	0	0	0	0	37	0	3	1	8	0	0	1	0	0	1	29	0	0	0	0	0	0	0	0	0	0	0	211	59	BY
CH	0	0	0	0	0	1	0	0	0	0	0	0	0	0	0	0	0	0	0	0	0	0	0	0	0	0	0	0	147	64	CH
CY	0	0	0	0	0	1	0	1	1	2	0	0	0	0	0	87	4	0	0	0	0	3	0	9	2	0	0	0	120	25	CY
CZ	0	0	0	1	0	42	0	2	4	1	0	2	8	0	0	0	2	0	0	0	0	0	0	0	0	0	0	0	303	290	CZ
DE	0	0	0	5	0	12	0	0	0	0	0	0	0	0	0	0	1	0	0	0	0	0	1	0	0	0	0	0	201	192	DE
DK	0	0	0	2	2	11	0	0	0	1	1	0	0	0	0	0	1	0	0	2	0	0	2	0	0	0	0	0	117	107	DK
EE	0	0	0	0	1	12	0	1	0	7	2	0	0	0	0	0	5	0	0	1	0	0	0	0	0	0	0	0	104	84	EE
ES	0	0	0	0	0	0	8	0	0	0	0	0	0	0	0	0	0	0	1	0	0	1	0	0	2	0	0	0	115	114	ES
FI	0	0	0	0	1	3	0	0	0	5	2	0	0	0	0	0	2	0	0	0	0	0	0	0	0	0	0	0	33	24	FI
FR	0	0	0	1	0	1	0	0	0	0	0	0	0	0	0	0	0	0	0	0	0	0	1	0	0	0	0	0	174	168	FR
GB	0	0	0	1	0	2	0	0	0	0	0	0	0	0	0	0	0	0	1	0	0	0	2	0	0	0	0	0	109	16	GB
GE	0	0	0	0	0	0	0	0	0	4	0	0	0	0	0	11	2	0	0	0	0	0	0	2	0	0	0	0	164	1	GE
GL	0	0	0	0	0	0	0	0	0	0	0	0	0	0	0	0	0	0	0	0	0	0	0	0	0	0	0	0	0	0	GL
GR	1	6	0	0	0	3	0	6	10	1	0	0	0	0	0	9	7	0	0	0	0	2	0	0	1	0	0	0	163	120	GR
HR	1	0	0	0	0	9	0	6	29	1	0	14	2	0	0	0	3	0	0	0	0	1	0	0	0	0	0	0	448	317	HR
HU	0	0	0	0	0	24	0	36	37	1	0	5	18	0	0	0	8	0	0	0	0	0	0	0	0	0	0	0	435	370	HU
IE	0	0	0	0	0	1	0	0	0	0	0	0	0	0	0	0	0	0	1	0	0	0	0	0	0	0	0	0	66	55	IE
IS	0	0	0	0	0	0	0	0	0	0	0	0	0	0	0	0	0	0	0	0	0	0	0	0	0	0	0	0	3	0	IS
IT	0	0	0	0	0	2	0	2	2	0	0	4	0	0	0	0	1	0	0	0	0	2	0	0	2	0	0	0	335	325	IT
KG	0	0	0	0	0	0	0	0	0	0	0	0	0	8	0	0	0	17	0	0	0	0	0	10	0	0	0	0	64	0	KG
KZ	0	0	0	0	0	0	0	0	0	10	0	0	0	1	1	0	2	4	0	0	0	0	0	6	0	0	0	0	53	1	KZ
LT	0	0	0	0	1	45	0	2	1	8	1	0	1	0	0	1	10	0	0	1	0	0	0	0	0	0	0	0	176	134	LT
LU	0	0	0	2	0	3	0	0	0	0	0	0	0	0	0	0	1	0	0	0	0	0	1	0	0	0	0	0	215	209	LU
LV	0	0	0	0	1	20	0	1	0	6	1	0	1	0	0	0	8	0	0	1	0	0	0	0	0	0	0	0	143	116	LV
MD	0	0	0	0	0	15	0	65	3	5	0	0	1	0	0	4	60	0	0	0	0	0	0	0	0	0	0	0	429	95	MD
ME	200	1	0	0	0	4	0	4	32	0	0	0	1	0	0	0	2	0	0	0	0	1	0	0	0	0	0	0	302	28	ME
MK	1	163	0	0	0	4	0	6	58	0	0	0	1	0	0	1	3	0	0	0	0	0	0	0	0	0	0	0	291	46	MK
MT	1	0	37	0	0	1	0	1	2	0	0	0	0	0	0	0	1	0	0	0	0	20	0	0	11	0	0	0	86	77	MT
NL	0	0	0	119	0	5	0	0	0	0	0	0	0	0	0	0	0	0	0	0	0	0	9	0	0	0	0	0	234	220	NL
NO	0	0	0	0	19	1	0	0	0	1	1	0	0	0	0	0	0	0	0	0	0	0	0	0	0	0	0	0	24	3	NO
PL	0	0	0	1	0	411	0	4	3	3	0	1	8	0	0	0	12	0	0	0	0	0	0	0	0	0	0	0	495	469	PL
PT	0	0	0	0	0	0	161	0	0	0	0	0	0	0	0	0	0	0	2	0	0	0	0	0	1	0	0	0	190	190	PT
RO	0	0	0	0	0	11	0	293	15	2	0	0	2	0	0	3	18	0	0	0	0	0	0	0	0	0	0	0	388	336	RO
RS	8	7	0	0	0	9	0	27	430	1	0	1	2	0	0	1	5	0	0	0	0	0	0	0	0	0	0	0	585	91	RS
RU	0	0	0	0	0	2	0	0	0	37	0	0	0	0	0	0	6	0	0	0	0	0	0	0	0	0	0	0	53	4	RU
SE	0	0	0	0	3	4	0	0	0	1	12	0	0	0	0	0	1	0	0	1	0	0	0	0	0	0	0	0	30	23	SE
SI	0	0	0	0	0	7	0	3	4	0	0	217	1	0	0	0	2	0	0	0	0	1	0	0	0	0	0	0	395	380	SI
SK	0	0	0	0	0	57	0	14	10	1	0	2	136	0	0	0	11	0	0	0	0	0	0	0	0	0	0	0	328	297	SK
TJ	0	0	0	0	0	0	0	0	0	0	0	0	0	122	2	0	0	17	0	0	0	0	0	20	0	0	0	0	146	0	TJ
TM	0	0	0	0	0	0	0	0	0	4	0	0	0	3	31	1	2	14	0	0	0	0	0	6	0	0	0	0	63	1	TM
TR	0	0	0	0	0	1	0	2	1	2	0	0	0	0	0	223	6	0	0	0	0	1	0	6	0	0	0	0	242	6	TR
UA	0	0	0	0	0	21	0	13	2	14	0	0	1	0	0	4	240	0	0	0	0	0	0	0	0	0	0	0	325	46	UA
UZ	0	0	0	0	0	0	0	0	0	4	0	0	0	14	6	0	2	89	0	0	0	0	0	3	0	0	0	0	131	1	UZ
ATL	0	0	0	0	0	0	2	0	0	0	0	0	0	0	0	0	0	0	1	0	0	0	0	0	0	0	0	0	7	5	ATL
BAS	0	0	0	1	1	23	0	1	0	4	6	0	0	0	0	0	3	0	0	5	0	0	0	0	0	0	0	0	71	57	BAS
BLS	0	0	0	0	0	4	0	9	2	17	0	0	0	0	0	72	48	0	0	0	3	0	0	1	0	0	0	0	176	22	BLS
MED	1	0	0	0	0	2	1	2	3	1	0	1	0	0	0	21	3	0	0	0	0	8	0	2	10	0	0	0	88	52	MED
NOS	0	0	0	3	4	2	0	0	0	0	0	0	0	0	0	0	0	0	0	0	0	0	6	0	0	0	0	0	42	23	NOS
AST	0	0	0	0	0	0	0	0	0	1	0	0	0	1	1	8	1	1	0	0	0	0	0	224	0	0	0	0	17	1	AST
NOA	0	0	0	0	0	0	1	0	1	0	0	0	0	0	0	2	1	0	0	0	0	1	0	1	45	0	0	0	15	11	NOA
EXC	0	0	0	0	1	10	1	5	3	17	0	0	1	2	1	10	12	3	0	0	0	0	0	2	0	0	0	0	115	48	EXC
EU	0	0	0	2	1	38	5	20	4	1	2	2	3	0	0	1	4	0	0	0	0	1	0	0	0	0	0	0	206	188	EU
	ME	MK	MT	NL	NO	PL	PT	RO	RS	RU	SE	SI	SK	TJ	TM	TR	UA	UZ	ATL	BAS	BLS	MED	NOS	AST	NOA	BIC	DMS	VOL	EXC	EU	

APPENDIX D

Model evaluation

The EMEP MSC-W model is regularly evaluated against various kinds of measurements, including ground-based, airborne and satellite measurements. As the main application of the model within the LRTAP Convention is to assess the status of air quality on regional scales and to quantify long-range transboundary air pollution, the emphasis of the evaluation performed for the EMEP status reports has traditionally been put on the EMEP measurement sites.

A detailed evaluation against measurements from the EMEP network (available from the EBAS data base as described in Section 2.2 and Chapter 11) can be found at the AeroVal webpage that has been developed for the evaluation of EMEP MSC-W model output (due to some quality issues with data from the European Environment Agency's (EEA) Air Quality e-Reporting Database, the observations from 2021 observations are currently not shown):

https://aeroval.met.no/evaluation.php?project=emep&exp_name=2023-reporting

On this page, the user can select the set of measurement data, the station or country of interest, and view a large number of statistical parameters (bias, correlation, root mean square error, etc.). AeroVal is flexible and allows using all available observations, including irregular and non-standard-frequency measurements. For temporal averaging, 75% data coverage in a hierarchical manner is required for most of components, i.e. at least 18 hourly measurement values to calculate a daily mean, at least 21 daily values to calculate a monthly mean, and at least 9 months for an annual mean. The coverage requirement for daily values was lowered for size-resolved aerosols (in $PM_{2.5}$ and PM_{10}) because of a lower sampling frequency (e.g. every 4th or 6th day); for these components at least 4 daily values are required for calculating a monthly mean. Most of the observational data is collocated with model results on a daily basis (EBAS-d dataset), then monthly, seasonally and yearly mean statistics are calculated. The dataset EBAS-m is based on monthly averaged data in order to incorporate observations with coarser resolutions (e.g. every 4th or 6th day, weekly, 15-daily, monthly) and thus, includes more sites than the EBAS-d. For NO_2 and ozone, model results are also evaluated with hourly observations.

The web interface displays co-located observational and model datasets and contains:

- daily and monthly time series for each station, averaged per country, or the whole area covered by the model and the measurement network (labeled 'ALL');
- statistics and scatter plots calculated for each station and country;
- an overall evaluation of the results using statistics calculated for each country or the whole area covered by the model and the measurement network (so-called Heatmaps and Taylor Diagrams).

The different types of visualization (bar charts, line charts, tables, etc.) are available both for viewing and for downloading.

Table D:1 summarizes common statistical measures of model performance for 2021 with respect to EMEP observations. The flexibility of AeroVal allows including more observational data with different sampling resolution and duration with respect to what was included in the earlier EMEP reports. The statistics provided in Table D:1 are based the yearly averaged observations and model results.

Table D:1: Comparison of model results and observations for 2021. Annual averages over all EMEP sites with measurements. N_{stat}= number of stations, wd=wet deposition, Corr. = spatial correlation coefficient, RMSE = root mean square error. The numbers are taken from AeroVal (last updated 17 August 2023).

Component	N_{stat}	Obs.	Mod.	Bias (%)	RMSE	Corr.
NO_2 (µg(N) m^{-3})	82	1.24	1.150	-8	0.52	0.88
PM_{10} (µg m^{-3})	63	11.17	8.44	-24	3.90	0.75
$PM_{2.5}$ (µg m^{-3})	51	6.84	6.06	-11	1.96	0.75
Ozone daily max (ppb)	120	39.9	41.83	5.1	3.42	0.82
Ozone daily mean (ppb)	120	31.38	33.77	7.6	4.34	0.74
SO_2 (µg(S) m^{-3})	71	0.28	0.24	-14	0.56	0.29
HNO_3 (µg(N) m^{-3})	25	0.06	0.06	2	0.04	0.57
${NO_3}^-$ +HNO_3 (µg(N) m^{-3})	36	0.30	0.30	-1	0.12	0.75
NH_3 (µg(N) m^{-3})	35	0.91	1.22	34	1.19	0.77
NH_3 +${NH_4}^+$ (µg(N) m^{-3})	38	00.99	0.91	-8	0.71	0.75
${SO_4}^{2-}$, including sea salt (µg m^{-3})	53	1.08	0.64	-41	0.5	0.80
${SO_4}^{2-}$, sea salt corrected (µg m^{-3})	41	0.93	0.62	-34	0.48	0.83
${SO_4}^{2-}$ in PM_{10} (µg m^{-3})	56	1.01	0.63	-37	0.51	0.82
${SO_4}^{2-}$ in $PM_{2.5}$ (µg m^{-3})	21	0.96	0.68	-29	0.32	0.69
${NO_3}^-$ in PM_{10} (µg m^{-3})	56	1.04	1.19	14	0.51	0.84
${NO_3}^-$ in $PM_{2.5}$ (µg m^{-3})	22	0.76	1.22	61	0.56	0.89
${NH_4}^+$ in PM_{10} (µg m^{-3})	51	0.58	0.51	-13	0.33	0.66
${NH_4}^+$ in $PM_{2.5}$ (µg m^{-3})	22	0.52	0.60	15	0.16	0.8
EC in PM_{10} (μg(C) m^{-3})	7	0.19	0.17	-12	0.06	0.92
EC in $PM_{2.5}$ (μg(C) m^{-3})	16	0.24	0.23	-3	0.08	0.91
OC in $PM_{2.5}$ (μg(C) m^{-3})	16	1.92	1.37	-29	1.04	0.60
Sea salt in PM_{10} (μg(C) m^{-3})	39	1.70	1.75	3	0.71	0.95
Sea salt in $PM_{2.5}$ (μg(C) m^{-3})	25	0.37	0.44	19	0.37	0.61
SO_4^{2-} wd (mg(S)$m^{-2}d^{-1}$)	83	0.34	0.24	-30	0.17	0.54
NO_3^- wd (mg(N)$m^{-2}d^{-1}$)	87	0.41	0.46	12	0.19	0.79
NH_4^+ wd (mg(N)$m^{-2}d^{-1}$)	86	0.63	0.65	3	0.39	0.72
Precipitation (mm)	102	2.31	2.61	13	0.63	0.85
AOD	104	0.15	0.10	-33	0.06	0.90

APPENDIX E

EMEP intensive measurement period, summer 2022

To better understand the formations of ozone during heat waves, the EMEP Task Force on Measurement and Modelling (TFMM) organized an intensive measurement period (IMP) in summer 2022. One week of observations of VOCs relevant as ozone precursors was conducted between 12-19 July 2022. The IMP was conducted in close cooperation with the European infrastructures ACTRIS and RI-Urbans.

Table E:1 below gives an overview of which compounds were measured where. More than 120 different VOCs were measured as listed in Table E:2.

Table E:1: Sites participating in the EMEP intensive measurement period (12-19 July 2022), which type of measurements were conducted and their sampling methods

Code	Name	Latitude	Longitude	altitude	Ozone	NO2	OVOCs	NMHCs	terpenes	tracers	EC/OC
AT0002R	Illmitz	47.767	16.767	117.0m	monitor	monitor	DNPH	Canister	Tenax	$PM_{2.5}$	$PM_{2.5}$
BE0007R	TMNT09 Vielsalm	50.304	6.001	496.0m			DNPH TR-ToF-MS	Canister PTR-ToF-MS	Tenax PTR-ToF-MS	$PM_{2.5}$	$PM_{2.5}$
CH0010U	Zürich-Kaserne	47.378	8.53	409.0m	monitor	monitor	GC/FID	GC/FID	GC/FID		PM_{10} and $PM_{2.5}$
CH0053R	Beromünster	47.19	8.175	797.0m	monitor		GC/FID	GC/FID	GC/FID		PM_{10}
CY0002R	Agia Marina Xyliatou (CAO)	35.038	33.058	520.0m	monitor	monitor	PTR-ToF-MS	PTR-ToF-MS	PTR-ToF-MS		TCA08
CZ0003R	Kosetice (NAOK)	49.573	15.08	535.0m			DNPH	Canister (CZ)	Tenax	?	
DE0007R	Neuglobsow	53.167	13.033	62.0m			DNPH	Canister (UBA)	Tenax	$PM_{2.5}$	$PM_{2.5}$
DE0008R	Schmücke	50.65	10.767	937.0m			DNPH	Canister (UBA)	Tenax	$PM_{2.5}$	$PM_{2.5}$
DE0043G	Hohenpeissenberg	47.801	11.01	975.0m	monitor	monitor	GC/FID	GC/FID			
DE0044R	Melpitz	51.526	12.928	86.0m				Canister	Tenax	PM_{10}	
ES	Huelva Region							dosimeters	dosimeters		
ES0019U	Barcelona	41.387	2.115	80.0m	monitor	monitor	PTR-MS	PTR-MS	PTR-MS	PM_{10}	PM_{10}
ES0021U	Madrid	40.456	-3.726	669.0m			DNPH	Canister	Tenax	?	
ES0025U	Bilbao	43.259	-2.946	None	monitor	monitor		GC/FID			
ES1778R	Montseny	41.767	2.35	700.0m	monitor	monitor	PTR-MS	PTR-MS	PTR-MS	PM_{10}	PM_{10}
FI0050R	Hyytiälä	61.85	24.283	181.0m	monitor	monitor	PTR-MS	PTR-MS			
FR0008R	Donon	48.5	7.133	775.0m	monitor	monitor	DNPH	Canister	Tenax	$PM_{2.5}$	$PM_{2.5}$
FR0013R	Peyrusse Vieille	43.617	0.183	200.0m	monitor	monitor	GC/FID	GC/FID	Tenax	$PM_{2.5}$	$PM_{2.5}$
FR0018R	La Coulonche	48.633	-0.45	309.0m	monitor	monitor	DNPH	Canister	Tenax	$PM_{2.5}$	$PM_{2.5}$
FR0020R	SIRTA	48.709	2.159	162.0m	monitor		PTR-MS	PTR-MS /GC	PTR-MS	PM_{10}	PM_{10}
FR0027U	Villeneuve d'Ascq	50.611	3.14	70.0m	monitor	monitor	DNPH	Canister	Tenax		
FR0030R	Puy de Dôme	45.772	2.965	1465.0m	monitor		DNPH			$PM_{2.5}$	$PM_{2.5}$
FR0035U	Marseille Longchamp	43.305	5.395	73.0m						PM_{10}	
FR0038U	Grenoble Frenes	45.162	5.736	214.0m						PM_{10}	
FR0041U	Paris Chatelet	48.862	2.345	35.0m						$PM_{2.5}$	
GB0048R	Auchencorth Moss	55.792	-3.243	260.0m			DNPH		Tenax	$PM_{2.5}$	$PM_{2.5}$
GB1055R	Chilbolton	51.15	-1.438	78.0m			DNPH		Tenax	$PM_{2.5}$	$PM_{2.5}$
IE0031R	Mace Head	53.326	-9.899	5.0m			DNPH	Canister	Tenax		
IT0004R	Ispra	45.8	8.633	209.0m			DNPH	GC/MS	Tenax	$PM_{2.5}$	
IT0009R	Monte Cimone	44.193	10.701	2165.0m	monitor	monitor	DNPH	GC/MS	Tenax	PM_{10}	
NO0002R	Birkenes II	58.389	8.252	219.0m	monitor	KI sinters	DNPH	Canister	Tenax	PM_{10}	PM_{10} and $PM_{2.5}$

Table E:2: List of volatile organic compounds (VOCs) measured during the EMEP intensive measurement period (12-19 July 2022) and which sampling methods have been used

Component	VOC	Sampling methods
2-2-4-trimethylpentane	alkane	Canister, GC-MS
2-2-dimethylbutane	alkane	Canister
2-3-dimethylbutane	alkane	Canister, GC-MS
2-3-dimethylpentane	alkane	Canister, GC-MS
2-4-dimethylpentane	alkane	Canister
2-methylbutane	alkane	Canister, GC-MS
2-methylhexane	alkane	Canister, GC-MS
2-methylpentane	alkane	Canister, GC-MS
2-methylpropane	alkane	Canister, GC-MS
3-methylheptane	alkane	Canister, GC-MS
3-methylhexane	alkane	Canister
3-methylpentane	alkane	Canister, GC-MS
cyclo-hexane	alkane	Canister
ethane	alkane	Canister, GC-MS
isoheptanes	alkane	GC-MS
isohexanes	alkane	GC-MS
methyl-cyclohexane	alkane	Canister, GC-MS
methyl-cyclopentane	alkane	GC-MS
n-butane	alkane	Canister, GC-MS
n-decane	alkane	Canister, Tenax
n-dodecane	alkane	Canister, Tenax
n-heptane	alkane	Canister, GC-MS
n-hexane	alkane	Canister, GC-MS
n-nonane	alkane	Canister, Tenax, GC-MS
n-octane	alkane	Canister, Tenax, GC-MS
n-pentadecane	alkane	Tenax
n-pentane	alkane	Canister, GC-MS
n-tetradecane	alkane	Tenax
n-tridecane	alkane	Tenax
n-undecane	alkane	Canister, Tenax
propane	alkane	Canister, GC-MS
1-3-butadiene	alkene	Canister, GC-MS
1-butene	alkene	Canister, GC-MS
1-hexene	alkene	GC-MS
1-pentene	alkene	GC-MS
2-methyl-2-butene	alkene	Canister
butenes	alkene	GC-MS
cis-2-butene	alkene	Canister, GC-MS
ethene	alkene	Canister, GC-MS
isoprene	alkene	Canister,PTR-MS, GC-MS
mass_69_organic_compounds	alkene	PTR-MS
pentenes	alkene	Canister, GC-MS
propene	alkene	Canister, GC-MS
trans-2-butene	alkene	Canister, GC-MS
trans-2-pentene	alkene	GC-MS
ethyne	alkyne	Canister, GC-MS
propyne	alkyne	Canister, GC-MS
1-2-3-trimethylbenzene	aromatic	Canister, Tenax, GC-MS
1-2-4-trimethylbenzene	aromatic	Tenax, GC-MS
1-3-5-triethylbenzene	aromatic	Tenax
1-3-5-trimethylbenzene	aromatic	Canister, Tenax, GC-MS
1-ethyl-3-methylbenzene	aromatic	Tenax
1-ethyl-4-methylbenzene	aromatic	Tenax
benzene	aromatic	Canister, Tenax, PTR-MS, GC-MS
chlorobenzene	aromatic	PTR-MS
ethylbenzene	aromatic	Canister, Tenax, GC-MS
m-p-xylene	aromatic	Canister, Tenax, GC-MS
n-propylbenzene	aromatic	Canister, Tenax
o-xylene	aromatic	Canister, Tenax, GC-MS
styrene	aromatic	Canister, Tenax, PTR-MS
toluene	aromatic	Canister, Tenax, PTR-MS, GC-MS
1-2-3-4-tetramethylbenzene	aromatic	Tenax
1-2-4-5-tetramethylbenzene	aromatic	Tenax
1-3-diethylbenzene	aromatic	Tenax
1-4-diethylbenzene	aromatic	Tenax
1-ethyl-2-methylbenzene	aromatic	Tenax

Continued on next page

Table E:2 – continued from previous page

Component	VOC	Sampling methods
1-methyl-2-propylbenzene	aromatic	Tenax
2-ethyl-p-xylene	aromatic	Tenax
mass_107_organic_compounds	aromatic	PTR-MS
mass_107.086_organic_compounds	aromatic	PTR-MS
mass_121_organic_compounds	aromatic	PTR-MS
tert-butylbenzene	aromatic	Tenax
acenaphthene	PAH	Tenax
acenaphthylene	PAH	Tenax
anthracene	PAH	Tenax
fluorene	PAH	Tenax
naphthalene	PAH	Canister, Tenax
3-carene	terpene	Tenax
alpha-humulene	terpene	Tenax
alpha-phellandrene	terpene	Canister
alpha-pinene	terpene	Canister, Tenax, GC-MS
beta-caryophyllene	terpene	Tenax
beta-farnesene	terpene	Tenax
beta-pinene	terpene	Canister, Tenax
camphene	terpene	Tenax
eucalyptol	terpene	Tenax
iso-longifolene	terpene	Tenax
limonene	terpene	Canister, Tenax, GC-MS
linalool	terpene	Tenax
longicyclene	terpene	Tenax
monoterpenes	terpene	PTR-MS
myrcene	terpene	Canister, Tenax
p-cymene	terpene	Tenax
sabinene	terpene	Canister, Tenax
terpinolene	terpene	Tenax
bornylacetate	terpene, o-voc	Tenax
nopinone	terpene, o-voc	Tenax
2-methylphenol	o-voc	Tenax
2-methylpropenal	o-voc	DNPH, Canister
2-methylpropene	o-voc	Canister, GC-MS
2-oxopropanal	o-voc	DNPH
2-propanol	o-voc	Canister
3-buten-2-one	o-voc	DNPH, Canister
4-methylphenol	o-voc	Tenax
acetonitrile	o-voc	PTR-MS, GC-MS
benzaldehyde	o-voc	Canister
butanales	o-voc	DNPH
butanone	o-voc	DNPH, Canister, GC-MS
ethanal	o-voc	DNPH, PTR-MS, GC-MS
ethanedial	o-voc	DNPH
ethanol	o-voc	Canister, PTR-MS, GC-MS
furfural	o-voc	Tenax
hexanal	o-voc	Canister
mass_59_organic_compounds	o-voc	PTR-MS
mass_71_organic_compounds	o-voc	PTR-MS
mass_73_organic_compounds	o-voc	PTR-MS
mass_73.065_organic_compounds	o-voc	PTR-MS
methanal	o-voc	DNPH, PTR-MS
methanol	o-voc	Canister, PTR-MS, GC-MS
methyl_acetate	o-voc	PTR-MS
n-butanal	o-voc	Canister
n-propanol	o-voc	Canister, GC-MS
pentanal	o-voc	Canister
phenylmethanol	o-voc	Tenax
propanal	o-voc	DNPH
propanone	o-voc	DNPH, Canister, GC-MS

APPENDIX F

Trend simulation done in 2023

Trend runs with the EMEP MSC-W model (version rv5.0) have been performed this year at 0.1°×0.1° longitude/latitude resolution for the 32-year period from 1990 to 2021, using meteorological data and emissions for each respective year (IFS version cy40r1 for 1990–2018 and cy46r1 for 2019–2021).

Land-based emissions for 1990–2021 were derived from the 2023 official data submissions to UNECE CLRTAP (Schindlbacher et al. 2023), as documented in Ch 3. For the period 2005–2021, the officially submitted PM_{10} and $PM_{2.5}$ emissions from residential combustion (GNFR sector C) have been used for the countries which emissions seemed to include condensable organics. For other countries, updated TNO Ref2_v2.1 emission data (or gap-filled data by CEIP) were used, as described in Ch 3.3 (see Simpson et al. (2022) for more details). For the years before 2005, condensables were not taken into account, as reliable information on condensable emissions before 2005 is not available.

The effects of socio-economic activity restrictions due to the COVID-19 pandemic on emission temporal profiles for 2020 and 2021 were implemented according to Guevara et al. (2022).

Forest fire emissions were taken from the Fire INventory from NCAR (FINN) (Wiedinmyer et al. 2011), version FINN2.5, based on MODIS data (see section 9.2.1) for the 2002–2021 period (daily resolution), whereas for the 1990–2001 period (unavailable from FINN), monthly averages over the 2010–2020 period were used.

Natural marine emissions of dimethyl sulfide (DMS) are calculated dynamically during the model run and vary with current meteorological conditions.

SO_x emissions from passive degassing of Italian volcanoes (Etna, Stromboli and Vulcano) are those reported by Italy. SO_x and PM emissions from volcanic eruptions of Icelandic volcanoes (Eyjafjallajökull in 2010, Grímsvötn in 2011, Barðarbunga in 2014-2015 and Fagradalsfjall in 2021) are reported by Iceland.

The boundary conditions for the main gaseous and aerosol species were based on climatological observed values with prescribed trends in trans-Atlantic fluxes, while ozone levels have been corrected based on annual measurements at Mace Head in Ireland (c.f. Simpson et al. 2012) and, at the model top, on 3-hourly resolved stratospheric ozone from the ERA-5 reanalysis. Boundary conditions for natural particles of sea salt and mineral dust were the same as in the status run, i.e. 5-year monthly average concentrations, derived from EMEP MSC-W global runs and kept invariable over the calculation period.

References

Guevara, M., Petetin, H., Jorba, O., Denier van der Gon, H., Kuenen, J., Super, I., Jalkanen, J.-P., Majamäki, E., Johansson, L., Peuch, V.-H., and Pérez García-Pando, C.: European primary emissions of criteria pollutants and greenhouse gases in 2020 modulated by the COVID-19 pandemic disruptions, Earth System Science Data, 14, 2521–2552, doi:10.5194/essd-14-2521-2022, URL https://essd.copernicus.org/articles/14/2521/2022/, 2022.

Schindlbacher, S., Ullrich, B., and Wankmüller, R.: Inventory review 2023. Review of emission data reported under the LRTAP Convention. Stage 1 and 2 review. Status of gridded and LPS data, EMEP/CEIP Technical Report 4/2023, CEIP Vienna, 2023.

Simpson, D., Benedictow, A., Berge, H., Bergström, R., Emberson, L. D., Fagerli, H., Hayman, G. D., Gauss, M., Jonson, J. E., Jenkin, M. E., Nyíri, A., Richter, C., Semeena, V. S., Tsyro, S., Tuovinen, J.-P., Valdebenito, A., and Wind, P.: The EMEP MSC-W chemical transport model – technical description, Atmos. Chem. Physics, 12, 7825–7865, doi:10.5194/acp-12-7825-2012, 2012.

Simpson, D., Kuenen, J., Fagerli, H., Heinesen, D., Benedictow, A., Denier van der Gon, H., Visschedijk, A., Klimont, Z., Aas, W., Lin, Y., Yttri, K. E., and Paunu, V.-V.: Revising $PM_{2.5}$ emissions from residential combustion, 2005–2019. Implications for air quality concentrations and trends, Temanord 2022:540, Nordic Council of Ministers, doi:10.6027/temanord2022-540, URL https://pub.norden.org/temanord2022-540, 2022.

Wiedinmyer, C., Akagi, S. K., Yokelson, R. J., Emmons, L. K., Al-Saadi, J. A., Orlando, J. J., and Soja, A. J.: The Fire INventory from NCAR (FINN): a high resolution global model to estimate the emissions from open burning, Geoscientific Model Dev., 4, 625–641, doi:10.5194/gmd-4-625-2011, 2011.

APPENDIX G

Temporal profiles for 2021

The effects of socio-economic activity restrictions due to the COVID-19 pandemic on emission temporal profiles for 2020 were estimated in Guevara et al. (2022). Following the same methodology, the authors also created daily adjustment factors to the 2021 emissions and combined them with CAMS-REG-TEMPO v3.2 temporal profiles (Guevara et al. 2021) in order to estimate temporal profiles for year 2021. For non-livestock agricultural emissions (GNFR Sector L) the monthly factors from CAMS-REG-TEMPO v4.1 were used after an error had been discovered in the v3.2 dataset.

The COVID-19 adjustment factors for 2021 are summarised in Table G:1 and Table G:2. The adjusted CAMS-REG-TEMPO temporal profiles for 2021 are summarised in Table G:3

Table G:1: Adjustment factors by pollutant and sector for 2021 following Guevara et al. 2022 methodology.

GNFR Sector	CO	NH_3	NMVOC	NO_x	PM_{10}	$PM_{2.5}$	SO_x	CH_4
F1 - RoadTranspExhGas	same profile for all species							
F2 - RoadTranspExhDis	X	X	X	X	X	X	X	X
F3 - RoadTranspExhLPG	same profile for all species							
F4 - RoadTranspNonExh			X		X	X		
H - Aviation	same profile for all species							

Table G:2: Adjustment factors by country and sector for 2021 following Guevara et al. 2022 methodology.

GNFR Sector	Countries
H - Aviation	AL, AM, AT, BA, BE, BG, CH, CY, CZ, DE, DK, EE, ES, FI, FR, GB, GR, HR, HU, IE, IL, IT, LT, LU, LV, MA, MD, ME, MT, NL, NO, PL, PT, RO, RS, SE, SK, TR, UA
F1 - RoadTranspExhGas	AT, BA, BE, BG, BY, CH, CZ, DE, DK, EE, EG, ES, FI, FR, GB, GE, GR, HR, HU, IE, IL, IQ, IT, JO, KW, KZ, LB, LT, LU, LV, LY, MA, MD, MK, MT, NL, NO, PL, PT, RO, RS, RU, SA, SE, SI, SK, TR, UA
F2 - RoadTranspExhDis	AT, BA, BE, BG, BY, CH, CZ, DE, DK, EE, ES, FI, FR, GB, GR, HR, HU, IE, IT, LT, LU, LV, MD, MK, MT, NL, NO, PL, PT, RO, RS, RU, SE, SI, SK, TR, UA
F3 - RoadTranspExhLPG	AT, BA, BE, BG, BY, CH, CZ, DE, DK, EE, EG, ES, FI, FR, GB, GE, GR, HR, HU, IE, IL, IQ, IT, JO, KW, KZ, LB, LT, LU, LV, LY, MA, MD, MK, MT, NL, NO, PL, PT, RO, RS, RU, SA, SE, SI, SK, TR, UA
F4 - RoadTranspNonExh	AT, BA, BE, BG, BY, CH, CZ, DE, DK, EE, ES, FI, FR, GB, GR, HR, HU, IE, IT, LT, LU, LV, MD, MK, MT, NL, NO, PL, PT, RO, RS, RU, SE, SI, SK, TR, UA
H - Aviation	AM, AT, BE, BG, CH, CY, CZ, DE, DK, EE, ES, FI, FR, GB, GE, GR, HR, HU, IE, IL, IT, LT, LU, LV, MA, MD, MK, MT, NL, NO, PL, PT, RO, RS, SE, SI, SK, TR

Table G:3: CAMS-REG-TEMPO temporal profiles for 2021.

GNFR Sector	Monthly Factors	Weekly factors	Daily Factors	Hourly factors
A - PublicPower	X	X		X
B - Industry	X	X		X
C - OtherStationaryComb			X	X
D - Fugitive	X	X		X
E - Solvents	X	X		X
F1 - RoadTranspExhGas			X	X
F2 - RoadTranspExhDis			X	X
F3 - RoadTranspExhLPG			X	X
F4 - RoadTranspNonExh			X	X
G - Shipping	X	X		X
H - Aviation			X	X
I - OffRoadTransp	X	X		X
J - Waste	X	X		X
K - AgriLivestock	SO_x, CO, NMVOC, PM_{10}, $PM_{2.5}$		NO_x, NH_3	X
L - AgriOther	SO_x, CO, NMVOC, PM_{10}, $PM_{2.5}$, NO_x		NH_3	X

References

Guevara, M., Jorba, O., Tena, C., Denier van der Gon, H., Kuenen, J., Elguindi, N., Darras, S., Granier, C., and Pérez García-Pando, C.: Copernicus Atmosphere Monitoring Service TEMPOral profiles (CAMS-TEMPO): global and European emission temporal profile maps for atmospheric chemistry modelling, Earth System Science Data, 13, 367–404, doi:10.5194/essd-13-367-2021, URL `https://essd.copernicus.org/articles/13/367/2021/`, 2021.

Guevara, M., Petetin, H., Jorba, O., Denier van der Gon, H., Kuenen, J., Super, I., Jalkanen, J.-P., Majamäki, E., Johansson, L., Peuch, V.-H., and Pérez García-Pando, C.: European primary emissions of criteria pollutants and greenhouse gases in 2020 modulated by the COVID-19 pandemic disruptions, Earth System Science Data, 14, 2521–2552, doi:10.5194/essd-14-2521-2022, URL `https://essd.copernicus.org/articles/14/2521/2022/`, 2022.

APPENDIX H

Explanatory note on country reports for 2021

The country reports issued by EMEP MSC-W (Klein et al. 2023) focus on chemical species that are relevant to eutrophication, acidification and ground level ozone, but information on particulate matter is given as well. The country reports provide for each country:

- horizontal maps of emissions, and modelled air concentrations and depositions in 2021;
- time series of emissions in the years 1990 to 2021;
- time series of modelled air concentrations and depositions in the years 1990 to 2021;
- maps and charts on transboundary air pollution in 2021, visualizing the effect of the country on its surroundings, and vice versa;
- frequency analysis of air concentrations and depositions, based on measurements and model results for 2021, along with a statistical analysis of model performance;
- maps on the risk of damage from ozone and particulate matter in 2021.

EMEP MSC-W produces these country reports for 47 Parties to the Convention, and for Tajikistan, Turkmenistan and Uzbekistan. For the Russian Federation the country report includes only the territory which is within the EMEP domain (see Figure 1.1).

All 50 country reports are written in English. For the 12 EECCA countries, the reports are made available also in Russian. All country reports can be downloaded in pdf format from the MSC-W report page on the EMEP website:

`https://emep.int/mscw/mscw_publications.html#2023`

This year, the country reports are found under the header *MSC-W Data Note 1/2023 Individual Country Reports*. The reports for each country can be selected from a drop-down menu.

References

Klein, H., Gauss, M., Tsyro, S., and Nyiri, A.: Transboundary air pollution by sulphur, nitrogen, ozone and particulate matter in 2021, Country Reports, Tech. Rep. EMEP MSC-W Note 1/2023 Individual Country Reports, The Norwegian Meteorological Institute, Oslo, Norway, available at www.emep.int/mscw/mscw_publications.html, 2023.

emep

Meteorological Synthesizing Centre – West
Norwegian Meteorological Institute
P.O.Box 43 – Blindern, NO-0313 Oslo, Norway

ccc
NILU
Norwegian Institute for Air Research
P.O. Box 100
NO-2027 Kjeller
Norway
Phone: +47 63 89 80 00
Fax: +47 63 89 80 50
E-mail: kjetil.torseth@nilu.no
Internet: www.nilu.no

ciam
International Institute for Applied Systems Analysis (IIASA)
Schlossplatz 1
A-2361 Laxenburg
Austria
Phone: +43 2236 807 0
Fax: +43 2236 71 313
E-mail: amann@iiasa.ac.at
Internet: www.iiasa.ac.at

ceip
Umweltbundesamt GmbH
Spittelauer Lände 5
1090 Vienna
Austria
Phone: +43-(0)1-313 04
Fax: +43-(0)1-313 04/5400
E-mail: emep.emissions@umweltbundesamt.at
Internet: http://www.umweltbundesamt.at/

msc-e
Meteorological Synthesizing Centre-East
2nd Roshchinsky proezd, 8/5, room 207
115419 Moscow
Russia
Phone +7 926 906 91 78
Fax: +7 495 956 19 44
E-mail: msce@msceast.org
Internet: www.msceast.org

msc-w
Norwegian Meteorological Institute (MET Norway)
P.O. Box 43 Blindern
NO-0313 OSLO
Norway
Phone: +47 22 96 30 00
Fax: +47 22 96 30 50
E-mail: emep.mscw@met.no
Internet: www.emep.int